2016
Atomic, Molecular, and Optical Sciences Research PI Meeting

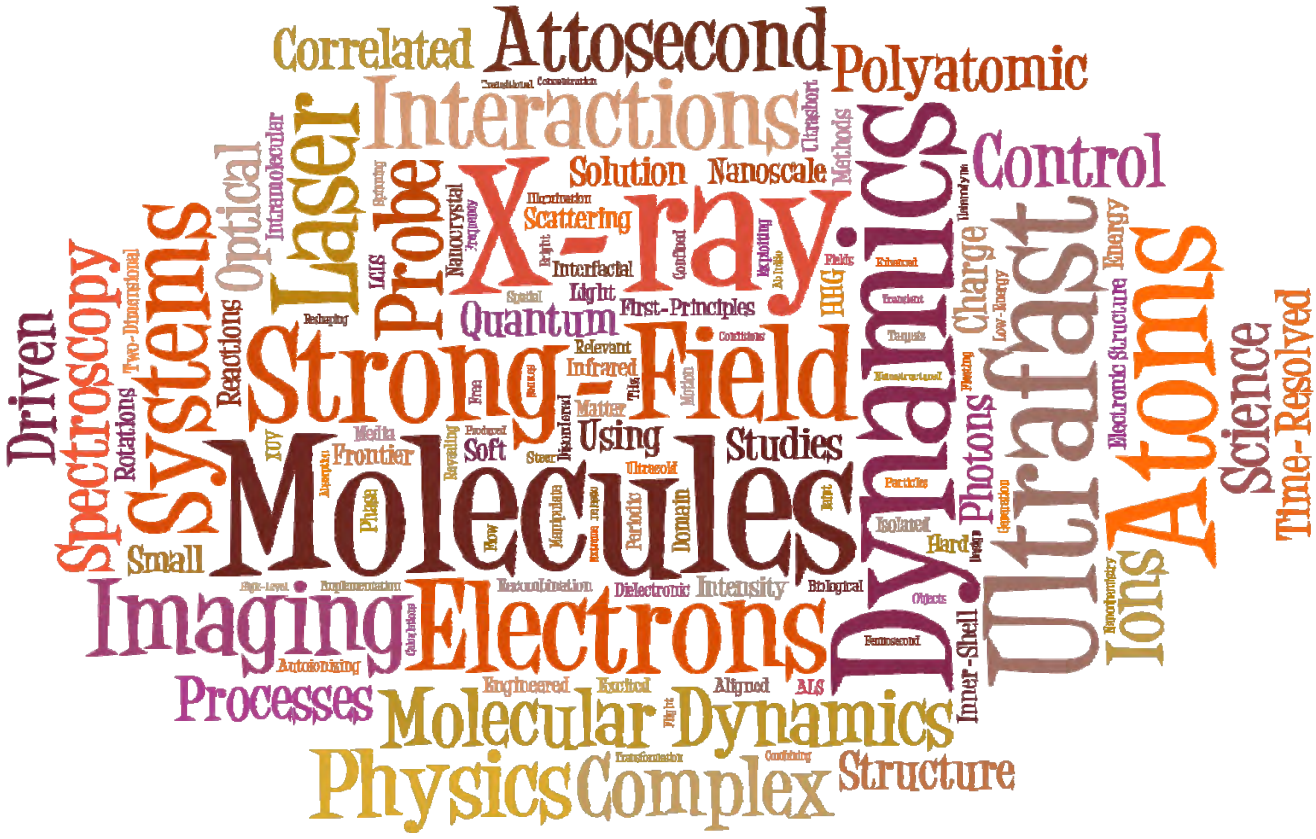

Gaithersburg Marriott Washingtonian Center
Gaithersburg, Maryland
October 23-26, 2016

U.S. DEPARTMENT OF ENERGY | Office of Science

Office of Basic Energy Sciences
Chemical Sciences, Geosciences & Biosciences Division

Page is intentionally blank.

Program and Abstracts

2016
Atomic, Molecular, and Optical Sciences Research PI Meeting

Gaithersburg Marriott Washingtonian Center
Gaithersburg, Maryland
October 23–26, 2016

Chemical Sciences, Geosciences, and Biosciences Division
Office of Basic Energy Sciences
Office of Science
U.S. Department of Energy

Cover Graphics: The input for the Tagxedo (http://www.tagxedo.com) cover art is based on the titles of the abstracts for this year's meeting. The font is Duality.

The research grants and contracts described in this document are supported by the U.S. DOE Office of Science, Office of Basic Energy Sciences, Chemical Sciences, Geosciences and Biosciences Division

Page is intentionally blank.

FOREWARD

This volume summarizes the 36th annual Research Meeting of the Atomic, Molecular and Optical Sciences (AMOS) Program sponsored by the U. S. Department of Energy (DOE), Office of Basic Energy Sciences (BES), and comprises descriptions of the current research sponsored by the AMOS program. The participants of this meeting include the DOE laboratory and university principal investigators (PIs) within the BES AMOS Program. The purpose is to facilitate scientific interchange among the PIs and to promote a sense of program identity.

The BES/AMOS program is vigorous and innovative, and enjoys strong support within the Department of Energy. This is due entirely to our scientists, the outstanding research they perform, and the relevance of this research to DOE missions. The AMOS community continues to explore new scientific frontiers relevant to the DOE mission and the strategic challenges facing our nation and the world.

We are deeply indebted to the members of the scientific community who have contributed their valuable time toward the review of proposals and programs, either by mail review of grant applications, panel reviews, or on-site reviews of our multi-PI programs. These thorough and thoughtful reviews are central to the continued vitality of the AMOS program.

We are privileged to serve in the management of this research program. In performing these tasks, we learn from the achievements and share the excitement of the research of the scientists and students whose work is summarized in the abstracts published on the following pages.

Many thanks to the staff of the Oak Ridge Institute for Science and Education (ORISE), in particular Connie Lansdon and Tim Ledford, and to the Gaithersburg Marriott Washingtonian Center for assisting with the meeting. We also thank Diane Marceau, Gwen Johnson, and Michaelena Kyler-Leon in the Chemical Sciences, Geosciences, and Biosciences Division for their indispensable behind-the-scenes efforts in support of the BES/AMOS program.

Thomas B. Settersten
Jeffrey L. Krause
Chemical Sciences, Geosciences, and Biosciences Division
Office of Basic Energy Sciences
Office of Science
US Department of Energy

Page is intentionally blank.

Agenda

Page is intentionally blank.

2016 Atomic, Molecular and Optical Sciences Research PI Meeting

Office of Basic Energy Sciences
U. S. Department of Energy

Gaithersburg Marriott Washingtonian Center, Gaithersburg, Maryland
October 23–26, 2016

Sunday, October 23

3:00 – 6:00 pm	**** Registration ****
6:00 pm	**** Reception (No Host, Lobby Lounge) ****
6:30 pm	**** Dinner (on your own) ****

Monday, October 24

7:30 am	**** Breakfast (Salons A-C) ****
	All presentations held in Salons D-G
8:00 am	*Welcome and Introductory Remarks* **Thomas B. Settersten**, DOE BES
Session I	Chair: **Anthony F. Starace**, University of Nebraska
8:30 am	*Structure and Dynamics of Atoms, Ions, Molecules, and Surfaces: Molecular Dynamics with Ion and Laser Beams* **Itzik Ben-Itzhak,** Kansas State University
9:00 am	*Finding Conical Intersections with Simultaneous Hard X-Ray Scattering and Spectroscopy* **Kelly J. Gaffney**, SLAC Accelerator National Laboratory
9:30 am	*Strong and Weak Field Ionization: Probes of Molecular Structure and Dynamics* **Thomas C. Weinacht**, Stony Brook University
10:00 am	**** Break ****
10:30 am	*Noncollinear Four-Wave Mixing Attosecond Dynamics* **Stephen R. Leone**, Lawrence Berkeley National Laboratory
11:00 am	*Nonlinear X-ray Science* **David A. Reis**, SLAC Accelerator National Laboratory
11:30 am	*X-rays with Femtosecond Duration and Angstrom Wavelength from a Laser Synchrotron* **Donald Umstadter**, University of Nebraska
12:00 pm	**** Lunch (Salons A-C) ****
1:00 – 4:00 pm	Free/Discussion Time

Session II	Chair: **Thomas K. Allison**, Stony Brook University
4:30 pm	*Extended Numerical Detector Theory and Tunneling-Exit Momentum* **Joseph H. Eberly**, University of Rochester
5:00 pm	*Ion Fragmentation of Small Molecules Absorbing One or Two X-Rays* **Stephen H. Southworth**, Argonne National Laboratory
5:30 pm	*Electron and Photon Driven Dynamics in Molecules* **Daniel S. Slaughter**, Lawrence Berkeley National Laboratory
6:00 pm	**** Reception (No Host, Lobby Lounge) ****
6:30 pm	**** Dinner (Salons A-C) ****

Tuesday, October 25

7:30 am	**** Breakfast (Salons A-C) ****
Session III	Chair: **Amy Cordones-Hahn**, SLAC National Accelerator Laboratory
8:30 am	*Recent Development in Laser-Induced Electron Diffraction and Attosecond Electron Dynamics* **Chii-Dong Lin**, Kansas State University
9:00 am	*Attosecond Dynamics in Molecules Driven by Ultrashort Laser Pulses* **Andreas Becker**, University of Colorado
9:30 am	*Strong Field Spectroscopy with Higher-Order Harmonic Generation* **Carlos A. Trallero**, Kansas State University
10:00 am	**** Break ****
10:30 am	*Probing Complexity Using the LCLS and the ALS* **Nora Berrah**, University of Connecticut
11:00 am	*Large-scale Atomistic Calculations of Intense X-ray Laser Dynamics in Nanoclusters* **Phay J. Ho**, Argonne National Laboratory
11:30 am	*Complexity and Correlated Motion of Electrons in Free and Confined Atomic Systems* **Steven T. Manson**, Georgia State University
12:00 pm	**** Lunch (Salons A-C) ****
1:00 – 4:00 pm	Free/Discussion Time

Session IV	Chair: **James Cryan**, SLAC National Accelerator Laboratory
4:30 pm	*Quantum Dots with Engineered Auger Interactions for Lasers and LEDs* **Victor I. Klimov**, Los Alamos National Laboratory
5:00 pm	*Optical Two-Dimensional Spectroscopy of Semiconductor Quantum Wells and Quantum Dots* **Steven T. Cundiff**, University of Michigan
5:30 pm	*Algorithms for X-Ray Imaging of Single Particles* **Veit Elser**, Cornell University
6:00 pm	**** Reception (No Host, Lobby Lounge) ****
6:30 pm	**** Dinner (on your own) ****

Wednesday, October 26

7:30 am	**** Breakfast (Salons A-C) ****
Session V	Chair: **Matthias Fuchs**, University of Nebraska
8:30 am	*The Electronic and Nonadiabatic Nuclear Dynamics of Electron Attachment and X-ray Photoionization of Polyatomic Molecules* **C. William McCurdy**, LBNL/University of California, Davis
9:00 am	*Low-Energy Electron Interactions with Complex Targets* **Thomas M. Orlando**, Georgia Tech
9:30 am	*Electron/Photon Interactions with Atoms/Ions* **Alfred Z. Msezane**, Clark Atlanta University
10:00 am	**** Break ****
10:30 am	*Studies of Autoionizing States Relevant to Dielectronic Recombination* **Thomas F. Gallagher**, University of Virginia
11:00 am	*Phonon Second Harmonic Generation in Aqueous Solution Measured by UXAFS* **Christoph Rose-Petruck**, Brown University
11:30 am	*Closing Remarks* **Thomas B. Settersten**, DOE BES Adjourn

Page is intentionally blank.

Table of Contents

Page is intentionally blank.

TABLE OF CONTENTS

Lawrence Berkeley National Laboratory

Los Alamos National Laboratory

SLAC National Accelerator Laboratory

University Research Summaries (by PI)

Page is intentionally blank.

Laboratory Research Summaries
(by institution)

Page is intentionally blank.

AMO Physics at Argonne National Laboratory

Christoph Bostedt, Gilles Doumy, Robert Dunford, Phay Ho, Elliot Kanter,
Anne Marie March, Steve Southworth, Linda Young
Argonne National Laboratory, Argonne, IL 60439
cbostedt@anl.gov, gdoumy@aps.anl.gov, dunford@anl.gov, pho@anl.gov, kanter@anl.gov,
amarch@anl.gov, southworth@anl.gov, young@anl.gov

1 Overview

The Argonne AMO physics program is focused on exploring the frontiers of x-ray physics and laying the foundation for ultrafast x-ray applications in other scientific domains. The program takes unique advantage of the existing and upcoming accelerator-based light sources, primarily the Advanced Photon Source (APS) Synchrotron at Argonne and the Linac Coherent Light Source (LCLS) x-ray free-electron laser (XFEL) at SLAC.

In the high intensity limit accessible at XFELs we aim for a quantitative and predictive understanding of x-ray interactions with matter in a combined experimental and theoretical approach. In previous work, we have largely achieved this goal for the ionization dynamics of isolated atoms, and our current work extends our efforts to complex systems, including molecules, clusters, and nanoparticles. Our computational capabilities are greatly enhanced by developing massively parallel codes that run on the MIRA supercomputer at the Argonne Leadership Computing Facility (ALCF).

At the ultrafast time resolution frontier, we employ novel optical/x-ray and x-ray/x-ray pump-probe techniques to explore electronic and nuclear dynamics as well as ultrafast charge migration and transfer mechanisms in molecules and clusters in real time. Corresponding theoretical and computational approaches are being developed to simulate and understand ultrafast processes.

At APS we develop instrumentation and methods to measure electronic and geometric changes of photo-excited molecules in liquid solutions. These studies include transition-metal-centered molecular complexes whose photo-induced transitions are important to understand in order to develop solar fuels and other applications. We are currently developing advanced laser-pump/x-ray-probe techniques, such as double-pulse excitation from one or two lasers, to measure, and ultimately guide, the complex electronic and structural dynamics of solvated molecules. In cooperation with the broad community of users of time-resolved x rays, we are contributing to plans for beamlines and end station upgrades at APS.

2 X-ray Physics at the Intensity Frontier

Ultraefficient ionization dynamics of atoms, molecules, and clusters by intense hard x-ray radiation

P. J. Ho, E. P. Kanter, C. Bostedt, L. Young, S. H. Southworth, C. S. Lehman, B. Krässig, C. Knight,[1] A. Rudenko,[2] D. Rolles,[2] , S.-K. Son,[3] R. Santra[3] and other collaborators

XFELs deliver femtosecond x-ray pulses of unprecedented intensity to explore a new regime of light-matter interactions. In the high-intensity regime where the single-photon saturation fluence is exceeded, early experiments at LCLS established that multiphoton x-ray ionization via sequential

single photon absorption is the dominant interaction [46] and that "hidden" inner-shell resonances could vastly alter the ionization dynamics in rare gas atoms [47, 48, 49]. In the past year, we have furthered understanding of intense x-ray interactions with matter in increasingly complex systems, from atoms, molecules to clusters, through complementary theoretical and experimental efforts.

For atoms, we have developed a Monte-Carlo rate equation (MCRE) approach [7], which systematically incorporates bound-bound resonances to model multiphoton ionization dynamics induced by high-fluence, high-intensity XFEL pulses. We showed that these resonances are responsible for ionization far beyond the sequential single photon absorption limit and are central to a quantitative understanding of atomic ionization dynamics in XFEL pulses. We have investigated multiphoton ionization dynamics for Kr and Xe atoms in XFEL pulses for a variety of conditions, to compare and quantify the effects of bandwidth, pulse duration, pulse fluence and photon energy [21]. This comprehensive computational investigation reveals that resonant transitions can be critically important, and the resulting ionization dynamics with narrow and broadband x-ray pulses can be drastically different, as shown in Fig.1(a).

Experimentally, we have extended our exploration from the soft x-ray regime to the hard x-ray regime and from atoms to molecules in collaboration with the Kansas State University group. Experiments at extreme intensities (10^{19}W/cm^2) were performed at the Coherent X-ray Imaging (CXI) beamline of the LCLS using the broad bandwidth x-ray pulses generated by the self-amplified spontaneous emission (SASE) scheme and the narrow bandwidth self-seeded x-ray pulses to study rare gas atoms (Xe, Kr, Ar) and small polyatomic molecules (CH_3I, C_6H_5I). Our analysis of the molecular fragmentation dynamics reveals an efficient ultrafast charge transfer mechanism from the absorbing heavy atom to the neighboring atoms of the molecules, leading to a higher ionization level than in the corresponding atom - a qualitative difference from previous observations in the soft x-ray regime. A publication is being prepared.

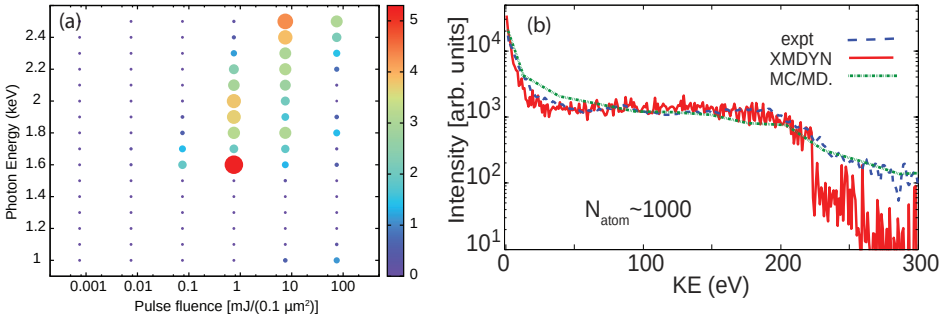

Figure 1: Left: The difference between the average charge state of Kr ions exposed to a broad bandwidth SASE pulse (BW= 1%) and a seeded pulse (BW=0.01%) as a function of x-ray photon energies and pulse energy. [21]. Right: Electron kinetic energy distribution between experimental and calculated data using MC/MD method for argon clusters with 1000 atoms are in excellent agreement.

For clusters, we have used the comprehensive atomic codes (including resonance behavior)[7, 21] in combination with classical molecular dynamics to track electron and ion dynamics over on ultrafast timescales in complex systems. This method, a hybrid quantum Monte Carlo and classical molecular dynamics (MC/MD), incorporates all multiphoton ionization features of atoms and molecules, and was extended to include electron collision dynamics that are important in more complex systems. The processes included are photoionization, Auger, fluorescence, elastic scattering, Compton scattering, electron-impact ionization and recombination processes. The MC/MD code is highly parallel and has been shown to achieve good scalability on the MIRA, a massively parallel

supercomputer at ALCF. We have validated our codes and method by reproducing the previously published [50] intensity averaged experimental electron spectra of Ar_{1000} clusters in intense XFEL pulses, as shown in Fig. 1(b) [44].

An ongoing effort is to use the MC/MD method to study XFEL dynamics of both homogeneous and heterogeneous clusters with larger sizes and heavier (Xe) elements under realistic experimental pulse conditions, including x-ray/x-ray pump/probe setup enabled by two-color XFEL pulses. The results will provide insight into an unexpected ultrafast, collective compression of the Xe cluster observed in our recent experiment [24]. Also, we will investigate the feasibility of manipulating the x-ray scattering response via resonant excitation in the x-ray regime by extending the MC/MD method. The anticipated results will complement our experimental efforts of strongly pumped clusters described below. For that work we have received a 2016 ASCR Leadership Computing Challenge (ALCC) award with 10-million core-hours to carry out these calculations.

Time-resolved x-ray imaging of optically excited clusters

M. Bucher, P. J. Ho, L. Young, C. Bostedt, T. Gorkhover,[4] O. Gessner,[5] A. Vilesov,[6] T. Fennel,[7] A. Rudenko,[2] M. Kling,[8] D. Rupp,[9] T. Möller,[9] and other collaborators

Single-shot imaging with intense x-ray pulses from XFELs opens the opportunity to probe the non-equilibrium dynamics in highly excited nanoclusters with femtosecond time and nanometer spatial resolution. We have performed the first femtosecond time-resolved coherent x-ray diffractive imaging experiment at LCLS, following the evolution of individual xenon clusters with 15-30 nm radii after exposure to near-infrared laser pump pulses [23]. The delay between the optical and x-ray pulses was varied in the femtosecond to picosecond regime. During the ionizing laser pulse excitation, electrons are rapidly injected into the surrounding vacuum and charge the nanosample early in the pulse. The growing positive space charge confines the electrons and forms a non-equilibrium nanoplasma. Although charge states up to Xe^{20+} are created, fewer than 1% of the delocalized electrons can escape from the cluster and are bound to the cluster Coulomb potential. Subsequently, the confined electrons initiate expansion of the cluster as they transfer kinetic energy to the ions. We were able to correlate time-dependent changes in the x-ray diffraction patterns to the ultrafast structural changes in the cluster electron density profile, see Fig. 2. More specifically, a characteristic loss of higher-order information in the x-ray diffraction patterns show that the nanoplasma expansion starts with a softening of the outermost surface that rapidly evolves towards the inner particle core [23].

We expanded this initial work on Xe clusters and used ultrafast diffractive imaging to monitor the local ignition and growth of a nanoplasma inside an optically transparent He matrix. He droplets with diameters of 200-1000 nm are doped with a few (20) Xe atoms and illuminated with a strong near-infrared laser pulse. While the He matrix is transparent to the near-infrared light, the minute amount of Xe atoms will provide a seed for the formation of an anisotropic nanoplasma that becomes a resonant IR absorber and leads to strong ionization of the droplet within the duration of the pulse. The experiments showed some strong anisotropies in the plasma expansion and provided a first glimpse on the effect of photon-induced anisotropies in the plasma expansion of nominally isotropic systems.

In another recent investigation we aim at real-time imaging of light-induced electron density modulations and ultrafast anisotropic expansion from monodisperse particles. An intense infrared femtosecond pump pulse is again used to ionize the particles. Our experiments hold promise that, due to greatly improved timing between the x-ray and optical lasers, the goal of measuring light-induced electron density modulations is within reach.

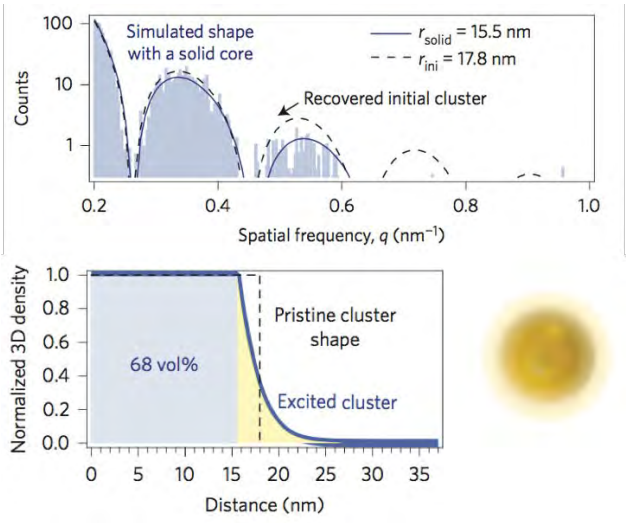

Figure 2: Top: radially averaged scattering profile from a single-shot diffraction image of a cluster, 100 fsec after NIR laser pumping. The higher order information fades due to rapid expansion of the surface atoms. Bottom: reconstructed cluster density profile and depiction of the cluster.

Imaging x-ray induced charge transfer processes in Xe - He core-shell systems
M. Bucher, P. J. Ho, L. Young, C. Bostedt, O. Gessner,[5] A. Vilesov,[6] T. Gorkhover,[4] D. Rupp,[9] T. Möller,[9] and other collaborators

One potential strategy for overcoming rapid sample damage in single-shot coherent imaging applications at XFELs is to embed the sample in sacrificial layers. We have used superfluid He droplets as a host matrix for Xe clusters in order to investigate ultrafast charge transfer processes from the strongly absorbing Xe core to the He shell. The superfluid He droplets with sizes up to 1 μm in diameter are generated in a free nozzle beam expansion of liquid He in vacuum. Earlier imaging experiments on pristine droplets showed the formation of a wide variety of shapes from spherical to strongly deformed droplets as evidenced by large anisotropies and intensity anomalies (streaks) in the obtained diffraction images. Light doping of the superfluid He droplets with Xe atoms allowed imaging of quantum vortices inside the droplet due to the large signal contrast between the heavy Xe and light He atoms. For the lightly doped He droplets the droplet itself can provide phase information for the image reconstruction and the quantum vortices can be directly visualized [22]. In such lightly doped systems symmetric arrangements of quantum vortices are found which exhibit unexpectedly large distances of the vortices from the droplet center (∼0.7-0.8 droplet radii) [28]. The data show that the Xe dopant atoms contribute to the total angular momentum of the droplets leading to the stabilization of widely spaced vortex configurations. When the doping level is increased the coherent diffractive images are dominated by the dopants, leading to very complex scattering patterns. Recent improvements in the experimental system and data analysis allowed us to combine multiple detector planes into one scattering pattern and reconstruct single shot images of the Xe structures inside a He droplet as demonstrated in Fig. 3.

A novel x-ray pump x-ray probe scheme was used to investigate charge transfer processes in heavily doped He nanodroplets. The ultrafast scattering information from these systems indicate a rapid charge transfer from the He shell to the strongly x-ray absorbing Xe core structure. Delay dependent images from pristine Xe clusters show a degradation of the scattering signal from the

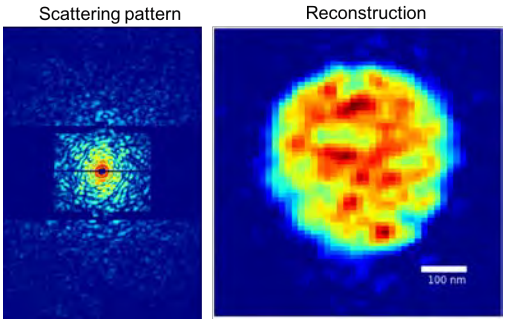

Figure 3: Left: Coherent diffractive image of a He droplet strongly doped with Xe atoms stitched together from two detector planes. The scattering pattern is dominated by the information from the Xe dopant atoms. Right: When using the full information from all detector planes the He-Xe structure can be reconstructed with phase retrieval algorithms. The reconstructed image shows a complex Xe structure in the He droplet.

probe pulse. For Xe clusters embedded in He droplets the x-ray contrast from the core is maintained over a long delay window up to 900 femtoseconds indicating strongly reduced x-ray radiation damage. Simultaneously recorded time-of-flight ion spectra show a delay–dependent kinetic energy release from the shell ions supporting the hypothesis of efficient charge transfer mechanisms inside the nanoplasma. The MC/MD is being developed to model the results and to investigate the ionization dynamics in helium droplets.

Transient structural changes in nanoparticles probed with hard x-ray scattering
M. Bucher, P.J. Ho, L. Young, C. Bostedt, K.R. Ferguson,[4] K. Nagaya,[10] H. Fukuzawa,[11] K. Ueda[11] and other collaborators

For any sample in strong fields, the ionization and electron redistribution within the sample leads to strong changes in its interatomic potential energy landscape. In finite, nanoscale systems these sudden changes can lead to a strong structural response that is competing with the nanoparticle expansion and disintegration dynamics. The internal atomic arrangement of small nanoparticles can be investigated with few femtosecond, hard x-ray bursts from XFELs with Ångstrom resolution. The information from ultrafast hard x-ray scattering is complementary to the single-shot imaging approach which yields information about the overall particle shape and form factor.

In a first x-ray pump/x-ray probe experiment, single large van der Waals clusters were isochorically heated to a nanoplasma state with an intense 10-fs x-ray pump pulse and the structural evolution of the sample was probed with a second x-ray pulse [24]. The data show systematic contraction of the cluster within 80 fs and indications for rapid electronic damage within 10 fs after the pump pulse (Fig. 4). The unexpected and fast compression of the cluster is attributed to the massive electronic excitation that induces a collective change in bond character as depicted in Fig. 4. This process can be described as an x-ray induced "metallization' of the van-der-Waals cluster leading to a transient bond contraction prior to Coulomb expansion.

Current and future efforts focus on optical excitation of the cluster nanoplasma. In contrast to x-ray ionization, strong optical fields couple to the electrons in the outer valence levels. Tuning the laser intensity will allow controlling the electron mobility in the cluster, yielding deeper insight into the transient bond contraction mechanism strongly excited nanoscale systems.

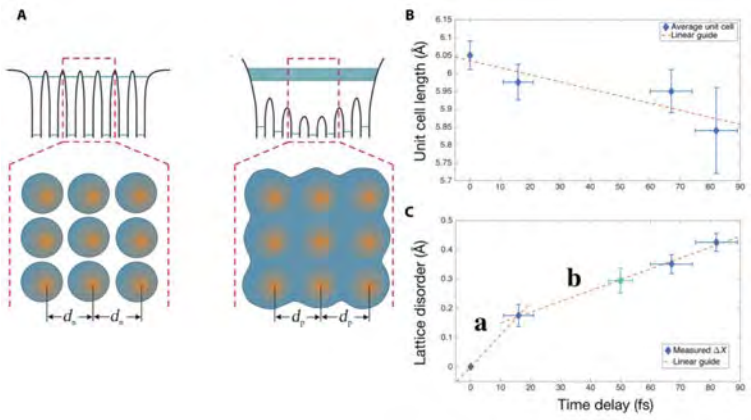

Figure 4: Panel A) Electrons are highly localized in the initial van der Waals cluster, forming an ordered crystal lattice with a well-defined neutral atomic spacing (dn). During the nanoplasma transition, the highly excited electrons become delocalized in the deep Coulomb potential, affecting the overall lattice geometry with a new plasma spacing (dp). Panel B) The average unit cell lengths measured from the q value for the (111) and (220) fcc reflection planes show a consistent decrease with increasing delay. Panel C) Apparent lattice disorder summarizing electronic and structural damage. Two distinct regimes show a fast disorder (region a) on the same time scale as electronic responses, and a slower change (region b) indicative of lattice distortion.

Atomistic 3D coherent imaging of non-biological systems with high-intensity XFEL pulses

P. J. Ho, C. Knight,[1] M. Tegze,[12] G. Faigel,[12] C. Bostedt, and L. Young

XFELs have opened exploration of a new regime of light-matter interactions and provided a potential route to single particle 3D-imaging with atomic scale resolution. Very recently, 3D images were obtained after the procedure of classification, orientation and reconstruction of a set of 2D images, at ∼125 nm resolution. The attained resolution is rather distant from the desired 3 Å, highlighting the importance of understanding fundamental processes of electronic and nuclear dynamics (see Fig. 5) and imaging holistically. Using our recently developed hybrid quantum Monte Carlo and classical molecular dynamics method [42, 44], we address 3D-imaging of a non-biological system at atomic resolution. In particular, we investigate the scattering response of Ar clusters as a function of size and XFEL pulse parameters (pulse duration, wavelength, fluence) in the intense-field regime and the changing roles of inelastic vs. elastic scattering vs. photoabsorption at the extreme intensities and short wavelengths required for imaging, 10^{20} W/cm^2 at 1.5 Å. Since this MC/MD method treats both the electrons and atoms/ions on equal footing, we could explore the limitations of the previously employed frozen lattice approximation over a wide range of pulse parameters. We showed that atomistic reconstruction with resolution reaching 2 Å can be achieved in the face of severe electronic damage with an R-factor as high as 0.466. Also, we examined the particle size required to achieve successful 3D-orientation by quantifying the number of scattered photons per Shannon pixel with the inclusion of reduced scattering strength at high fluence. We found that Compton scattering effects, which play a deleterious role in bio-molecular systems at high Q, are less important in heavy systems. Although free-electron scattering represents a significant background, we find that recovery of the original structure is in principle possible with 3 Å resolution for particles of 11-nm diameter. A manuscript describing these recent findings has been submitted [42].

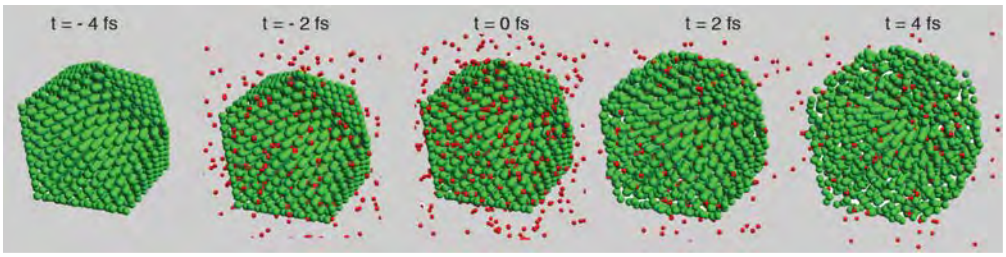

Figure 5: Snapshots of ionization dynamics of a 7-shell Ar cluster (1415 nuclei + 25470 electrons) induced by an 8-keV, 10^{14} photons/μ^2 pulse with 2-fs duration. The larger green and smaller red particles represent argon atoms/ions and electrons, respectively.

So far, our results associated with the impact of ultrafast ionization were obtained by assuming that the entire 3D Q-space scattering pattern is available for reconstruction of the initial structure. However, a realistic representation of an experiment would feature a collection of noisy 2D scattering patterns, from which orientation would first be required to generate the 3D Q-space distribution from which solution of the phase problem and reconstruction would then proceed. We plan to undertake these efforts on heterogeneous systems, focusing on quantifying the impact of heterogeneity, Compton scattering and pulse parameters on the scattering response.

High-resolution in-flight holography with clusters as reference scatterers
T. Gorkhover,[4] M. Bucher, G. Doumy, A. Al-Haddad, P. J. Ho, L. Young, C. Bostedt, J. Hajdu,[13] T. Möller[9] and other collaborators

Iterative phasing can reconstruct objects from their diffraction patterns alone, but it requires solving a non-convex high-dimensional minimization. Holography provides a way to immediately obtain an image of the sample that can then be used as the starting point for the iterative algorithm. So far, holography approaches have been limited to fixed targets with fixed reference scatterers. We have developed a method to obtain in-flight X-ray Fourier holograms of biological nanoparticles using single Xe clusters as reference scatterers in the gas phase. First experiments show that we can recover asymmetric shape projections via a simple two-dimensional inverse Fourier transformation. The proposed in-flight holography method has the potential to significantly reduce the complexity of structure determination and can be used as a tool for single shot imaging of injected objects in the gas phase. Ongoing efforts focus on increasing the resolution and obtaining basic 3D information by using multiple reference scatterers.

3 Ultrafast Inner-Shell Induced Molecular Dynamics

Ultrafast site-selective molecular dynamics of x-ray absorption
A. Picón, C. S. Lehmann, S. H. Southworth, C. Bostedt, G. Doumy, P. J. Ho, E. P. Kanter, B. Krässig, A. M. March, D. Moonshiram, L. Young, S. T. Pratt,[14] A. Rudenko,[2] D. Rolles,[2] and other collaborators

Dynamical processes in molecules typically involve the flow of charge and energy from one atomic site to another on the femtosecond time scale. The LCLS and other XFELs are developing methods to generate two intense, femtosecond x-ray pulses with two colors and controlled delay [51]. Using the atomic site specificity of x-ray absorption, this opens the opportunity to trigger

dynamics at one atomic site and track the response at other sites. We used this capability to study the ionization and dissociation of XeF_2 molecules induced by x-ray absorption [29]. As illustrated

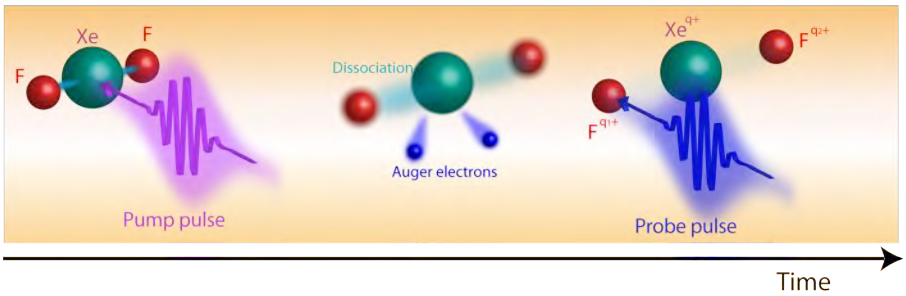

Figure 6: Illustration of "hetero-site-specific x-ray pump-probe spectroscopy" to study molecular dynamics in progress [29]. The technique uses two ultrafast x-ray pulses with two colors and controlled delay to trigger dynamics at one atomic site and follow the response at another site.

in Fig. 6, an x-ray photon from the pump pulse was absorbed by a Xe 3d electron and triggered a decay process in which several Auger electrons were ejected, and the molecule dissociated into atomic Xe and F ions. After a delay between 4-54 fs, an x-ray photon from the probe pulse was absorbed by one of the emerging F ions and increased its charge state. The separated ions were detected in coincidence with an ion momentum imaging spectrometer to measure the charge states and momentum distributions of the fragment ions in each breakup channel. Time-dependent pump-probe effects were recorded in two channels, and the pathways leading to those products were identified. A theoretical simulation was developed to model the process and explain the underlying mechanism. By studying this process in small molecules, insight is gained to the mechanisms responsible for x-ray damage in biomolecules and materials.

Ultrafast x-ray-induced nuclear dynamics in N_2 molecules using femtosecond x-ray pump-probe spectroscopy

C. S. Lehmann, A. Picón, S. H. Southworth, C. Bostedt, G. Doumy, P. J. Ho, E. P. Kanter, B. Krässig, A. M. March, D. Moonshiram, L. Young, S. T. Pratt,[14] A. Rudenko,[2] D. Rolles,[2] and other collaborators

We used two ∼10-fs, ∼700-eV x-ray pulses with controlled delay generated at the LCLS for a pump-probe study of the x-ray ionization and fragmentation of N_2 molecules [34]. X-ray absorption produces a core-hole state that mainly decays by an Auger process leaving two holes in the valence shell. A manifold of two-hole states of N_2^{2+} are produced, and some are dissociative (leading to N^+–N^+ separated ions) while others are quasibound (producing long-lived N_2^{2+} ions). While the nuclear wave packets evolve on the N_2^{2+} potential curves, an x-ray photon from the probe pulse is absorbed and projects the ions onto the N^+-N^{3+} breakup channel. The ions were detected in coincidence and time-dependent features were observed in the kinetic energy release (KER) spectra. A quantum mechanical model was developed to treat K-shell photoionization by the x-ray pump pulse, Auger decay, propagation of nuclear wave packets on the N_2^{2+} potential energy curves, and the time-dependent KERs in the N^+-N^{3+} breakup channel induced by the probe pulse. The measured and calculated KERs for the N^+-N^{3+} breakup channel are shown in Fig. 7. A peak in the measured KER is observed to shift to lower energy at increasing time delay. This is attributed to the dissociative intermediate states, i.e., the measurements recorded snapshots of the breakup of the two N^+ ions. The broad structure centered near 40 eV is also observed in the pump-only

measurements and is largely attributed to two-photon or one-photon processes that do not display a time dependence. However, the simulated pump-probe results show both a shifting low-energy peak due to dissociative intermediate states and structures near 38 eV from quasibound states. Future XFEL capabilities with shorter pulses and high repetition rate will enable the possibility to select specific intermediate states and to explore the role of Auger processes in the coherent evolution of the nuclear wave packets. The further development of the theoretical methods in our group will also yield insight into the non-adiabatic effects of x-ray induced molecular dynamics that can be experimentally investigated with femtosecond x-ray-pump/x-ray-probe spectroscopy.

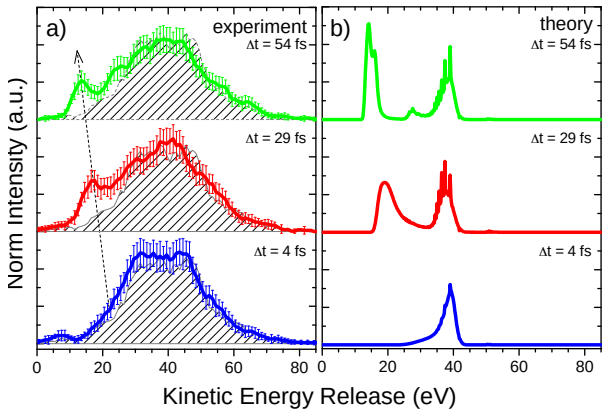

Figure 7: Kinetic energy release (a) measurements and (b) theory for the N^+-N^{3+} breakup channel of N_2 molecules in an x-ray-pump–x-ray-probe experiment. The shaded areas in (a) are the pump-only measurements, and the peak shifting to lower energy with increasing time delay is due to dissociative N_2^{2+} intermediate states. This feature is observed in the theoretical simulation (b) at 29 fs and 54 fs. The calculated structures near 38 eV at 29 fs and 54 fs are due to quasibound N_2^{2+} intermediate states. The dissociative and quasibound states are unresolved in the 4-fs calculation.

Mapping the electronic to nuclear relaxation of a molecular core-hole state with time-resolved photoelectron spectroscopy

A. Picón, A. Al-Haddad, G. Doumy, L. Young, S. H. Southworth, C. Bostedt, R. Shepard,[14] S. T. Pratt,[14] and other collaborators

We are developing a combined experimental and theoretical approach for directly mapping the transient electronic configurations during electronic and nuclear relaxation of core-excited molecules on the femtosecond time scale. We plan to employ time-resolved, high-resolution, core-level photoemission spectroscopy at the AMO endstation at LCLS. Photoemission responds instantly to changes in the electronic environment as compared with Auger, fluorescence, and ion spectroscopies that are ultimately limited by the core-hole lifetime. As a target, we will begin by using CO as a simple hetero-nuclear molecule. In our x-ray-pump/x-ray-probe experiment, the first pulse will preferentially photoionize the O 1s electron and trigger Auger decay and dissociation of the molecular ion. The second pulse will photoionize a C 1s electron and its energy spectrum will be recorded as a function of time delay. Time-dependent energy shifts and structures in the C 1s spectrum will be sensitive to the transient chemical environment, see Fig. 8.

Concurrently, we are developing a theoretical formalism for time-dependent core-level binding energy calculations including inner-vacancy decay processes and time-dependent nuclear dynamics.

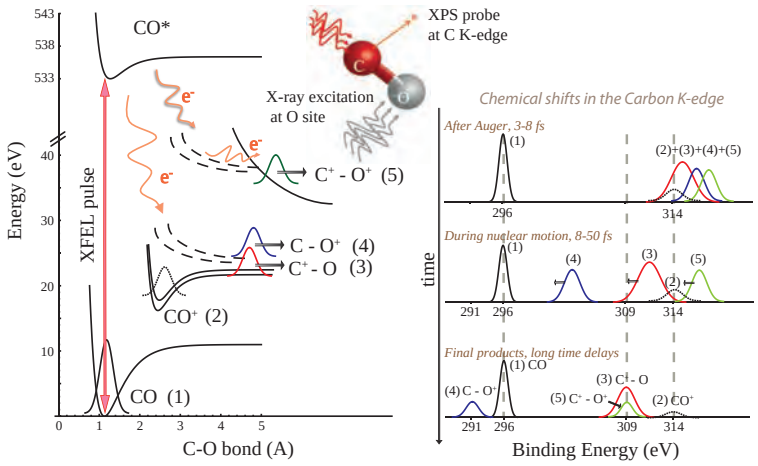

Figure 8: Left: Relaxation channels after core-hole decay of the O 1s→1π^* (CO*) state. Right: Time-dependent core-levels shifts.

The formalism allows us to follow electronic relaxation during Auger decay and nuclear relaxation processes on their natural femtosecond time scales. Our theoretical time-dependent approach will be flexible but also fully integrated in a quantum chemistry code in order to calculate the required electronic and nuclear properties. We will be able to calculate the continuum orbitals and the corresponding transition elements involving those orbitals, such as Auger or photoionization transitions. So far, our time-dependent model enables the study of small molecules interacting with short x-ray pulses with time durations comparable to Auger processes, as for example in CO. In the future, it can also be integrated in other quantum chemistry frameworks, such as DFT-type calculations, to study larger molecules and other complex systems.

Stimulated emission in atoms, clusters, and thin solid films of noble gases
A. Al-Haddad, M. Bucher, C. Bostedt, N. Rohringer,[15] T. Möller,[9] and other collaborators

Understanding stimulated emission processes is an essential ingredient for the development of novel non-linear spectroscopy techniques in the short wavelength regime [36]. We aim at exploring stimulated emission processes in atoms, clusters, and thin films of noble gases involving inner-shell levels. In the first experiments, the focus of our studies was on lasing in atoms and nanoclusters. We were able to show that it is possible to stimulate emission lines from Xe and Kr clusters, and that the lasing signal exhibits striking differences with its gaseous counterpart. We plan to complement the previous experiments with investigations of thin solid films to further study the effects of condensation, neighbor interactions, and plasma formation in the sample on the stimulated emission processes.

Site-selective photochemistry via localized inner-shell excitation
L. Young, S. H. Southworth, C. Bostedt, G. Doumy, A. Picón, S. L. Sorensen[16], M. Simon[17], M. Patanen[18] and collaborators)

Earlier work in our group investigated the femtosecond molecular response to site-specific inner-shell excitation in simple systems, XeF_2, with x-ray pump/x-ray probe techniques. Here we extend this theme to more complex molecules, where an initially localized inner-shell hole can be created

in several distinct chemical environments. For low Z-elements the decay of the hole is dominated by Auger decay to form two valence holes, which may remain localized and lead to preferential bond breakage around the initial hole site. For non-resonant excitation, the degree of selectivity is governed by the competition between double hole transfer and Coulomb explosion, the former of which can be induced on femtosecond timescales by small nuclear displacements [52]. Site selective photochemistry was first observed in early synchrotron radiation studies [53], where excitation into near edge resonance features was shown to create fragmentation localized to the atom initially excited. We plan to study these phenomena in the textbook ESCA molecule, ethyl-trifluoroacetate (CF_3-CO-O-CH_2-CH_3), where the four different carbon sites differ in binding energy by approximately 10 eV. Using the PLEIADES beamline at SOLEIL (10-1000 eV, 20000-100000 resolving power, complete polarization control) equipped with an electron-ion coincidence spectrometer (EPICEA) we will be able to measure photoelectron-ion-ion coincidences and thus isolate the ion fragmentation pattern resulting from an initially localized core excitation. With photoelectron/Auger-electron/ion coincidence measurements, we would be able to investigate the selectivity as a function of the internal energy of the doubly ionized molecule. Taking advantage of the distinctive molecular framework, we expect this investigation to shed light on the competition between various ultrafast energy transfer pathways (Auger emission, hole migration, molecular dissociation). Beamtime in December 2016 has been awarded.

Molecular response to x-ray absorption and vacancy cascades
R. W. Dunford, S. H. Southworth, G. Doumy, E. P. Kanter, B. Krässig, L. Young

This program utilizes the APS to study cascade decay and Coulomb explosion in molecules following ionization of deep inner shells of heavy atoms in selected molecules. In earlier studies of molecular effects in vacancy cascades of the molecule XeF_2, we found evidence that the total charge produced in the XeF_2 molecule was larger than that produced in an isolated Xe atom [54]. The experimental results combined with a theoretical analysis further indicated that the F atoms participate in the decay cascade during the fragmentation process. This lowers the kinetic energy release (KER) in comparison to a model in which the KER is estimated based on the ground state Xe-F intramolecular distance. An improved apparatus has been used in more recent experiments; first doing a more detailed study of the XeF_2 molecule and then moving on to other species such as IBr, and $IBrCH_2$. Recently, the analysis of the new data has concentrated on determining the probabilities for the various breakup modes of XeF_2. One of the challenges is that the highly charged ions produced in these experiments have large cross sections for electron pickup in the molecular beam. Charge exchange distorts the observed ion distributions following photoionization and adds additional ions (from background gas) unrelated to the ions from the molecular breakup we are studying. Further complications include the variation of detection efficiency with charge state and dead time in the coincidence electronics. To understand these issues and be able to make corrections and more reliably estimate uncertainties, we have developed a Monte-Carlo code to model these experiments. The code not only allows us to quantify systematic effects in our current data, but will be useful in guiding the choice of future experiments. Results of the new XeF_2 measurements are being prepared for publication.

Stimulated Raman adiabatic passage with two-color x-ray pulses
A. Picón, C. Bostedt, S. H. Southworth, L. Young, C. Callegari[19], K. Prince[19], J. Mompart[20], and collaborators

Seeding techniques for XFELs allow the generation of highly coherent, intense x-ray pulses

with durations on the order of femtoseconds. In the optical regime, in which lasers have achieved a high-degree of spatio-temporal coherence several decades ago, we find many quantum control techniques for atoms and molecules based on coherence. We recently proposed a theoretical scheme to transfer some of the coherent control techniques to the x-ray regime and perform stimulated Raman adiabatic passage (STIRAP) involving inner-hole excited states [17].

So far, studies with intense XFEL pulses show a complex multiphoton response driven by strong electron correlation. When matter is illuminated by high-fluence XFEL pulses, the inner-shell hole-decay processes proceed concurrently with the absorption of additional x-ray photons [46, 55, 48]. Hence, the typical response to XFEL pulses is to produce highly charged final states, and the extension of coherent quantum control techniques to the x-ray regime is not trivial.

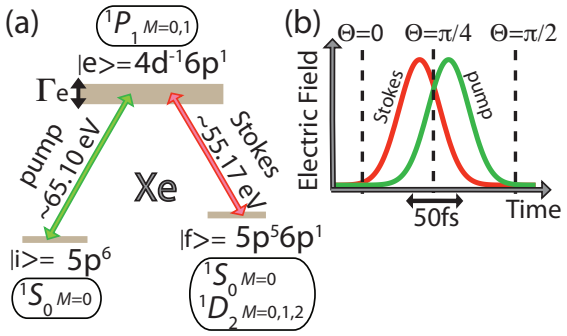

Figure 9: (a) STIRAP scheme for xenon with the three main states shown. (b) Typical scheme for STIRAP where the Stokes pulse arrives before the pump pulse.

Considering the most recent developments in seeding techniques at FELs that have significantly increased the quality of the pulse temporal coherence, we have expanded our theoretical approach for STIRAP in the short wavelength regime. Numerical results in two well-known systems, the neon atom and the carbon monoxide molecule, show that a robust control of population transfer is possible and we have developed an experimental scheme to demonstrate STIRAP at the FERMI FEL. Using the 4d core-hole state in Xe, we can use a three-level system as shown in Fig. 9, in which $|i\rangle$ is the ground state of Xe atom, $|e\rangle$ is the core-hole state $4d^{-1}6p$, and $|f\rangle$ is the excited final state $5p^56p$. Preliminary calculations show that a maximum transfer of 6% is possible to reach with the experimental conditions at FERMI, which is a significant and experimentally measureable effect.

4 X-ray Probes of Photo-excited Dynamics in Solution

Probing transient valence orbital changes with picosecond valence-to-core x-ray emission spectroscopy

A. M. March, G. Doumy, S. H. Southworth, L. Young, W. Gawelda,[21] M. Harder,[21] A. Galler,[21] Z. Németh,[12] G. Vankó,[12] and collaborators

We have performed a complete, simultaneous characterization of the electronic structure of an optically-excited state of a spin-crossover complex, $[Fe(terpy)_2]^{2+}$, by measuring, in the same setup, the Fe K-edge x-ray absorption spectrum (XAS) and the full Fe 1s x-ray emission (XES) spectrum, including core-to-core XES ($K\alpha$ and $K\beta$) as well as valence-to-core XES (vtc-XES) [45]. This allowed access not only to the geometric structure around the metal center and spin state, but also to the molecular valence orbitals responsible for chemical bonding in the complex.

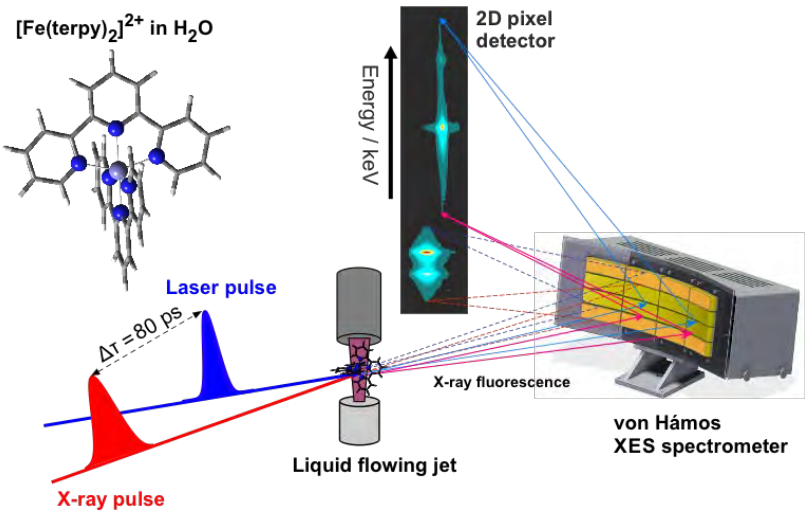

Figure 10: The experimental setup showing the 16-crystal von Hamos spectrometer installed at APS 7ID-D in a pump-probe geometry. Two different sets of 8 Si analyzer crystals were used to collect both $K\alpha$ and $K\beta$ plus vtc x-ray emission simultaneously. The detector image shown is a cropped actual image from the Pilatus 100k pixel detector recorded during the experiment. On the left the molecular structure of the $[Fe(terpy)_2]^{2+}$ complex is shown.

In order to capture the very weak vtc-XES lines, efficient use of the incident x-ray flux and efficient detection of the fluorescence were required. This was realized using pump-probe cycling at the MHz repetition rate of the x rays and by implementing a new XES spectrometer designed by JJ X-ray for the FXE instrument at the European XFEL. Fig. 10 depicts the experimental XES setup. Using a total of 16 crystals in a von Hamos geometry (8 for $K\alpha$, 8 for $K\beta$+vtc), we were able to obtain a full transient spectrum using an accumulated x-ray dose of 10^{17} x-ray photons. The XES spectrum was recorded with a single, position-sensitive, time-gateable detector, and the measurements were made at beamline 7ID at the APS.

Towards combining complex laser excitation with time-resolved x-ray spectroscopies: pump-repump-probe study of photo-excited $FeCN_6$

A. M. March, G. Doumy, S. H. Southworth, L. Young, C. Bostedt, M. N. Diez,[21] Z. Németh,[12] D. Szemes[12] and collaborators

The increased measurement efficiency we have achieved with our setup at the APS allowed us to incorporate flux demanding x-ray probe techniques, but it also opens the possibility of expanding the laser pump parameter space that can be explored. This in turn enables exploration of photochemical reactions that are more complex than those that have been studied with x rays so far. In the typical experiments carried out to date, a single transform-limited laser pulse initiates a reaction and x-ray spectra at one or more time delays are recorded. Studies have focused on reactions where only one intermediate state or photoproduct dominates, since it is easiest in this case to separate the signal of the photoinduced intermediate/product from the residual ground state component, assuming an estimate for the excited state fraction can be obtained. Extraction of the signals for reactions where more than one intermediate/product are present can, in principle, be done if the spectra of the intermediates/products are known. But this is often not the case since most intermediates/products are short lived and it is their spectra that one sets out to obtain in doing

the measurement. Theoretical modeling can help, but the most characteristic portions of the XAS spectrum, XANES and the pre-edge, are difficult to model with the accuracy required for fitting the data. By using multiple laser pulse excitations it should be possible to modify the ratios of the intermediate or product states in a controlled way and allow for separation of the signals. One of the simplest implementations is the so-called pump-repump-probe scheme, where the repump pulse, with varying delay/intensity, is used to influence the outcome of the reaction. Another possible implementation is 2D spectroscopy. In this natural extension of traditional transient absorption spectroscopy, the pump wavelength is a variable parameter in addition to the usual probe wavelength and pump/probe time delay.

We have performed a first experimental attempt at the pump-repump-probe concept using a pair of 343 nm pulses to pump and repump $FeCN_6$, and followed the evolution of the XAS transient. This first attempt required significant development of the laser optics and timing controls, but we succeeded in recording our first data sets. A follow up experiment is planned with more versatile control of the pump and repump pulses.

Improving measurement efficiency for the high-repetition-rate pump-probe setup at 7ID-D at the APS

A. M. March, G. Doumy, S. H. Southworth, A. Al-Haddad, M.-F. Tu, L. Young and C. Bostedt

During our latest APS experiment, we implemented several improvements to our setup to increase the efficiency with which we are able to collect x-ray absorption and x-ray emission data for samples that require a refreshed sample volume between each pump-probe cycle. Improvements include the addition of a new fast-flowing liquid jet. Our previous jet speed was ≈ 7 m/s, which, given our laser and x-ray spot sizes at the jet, allowed for refresh of the sample for pump-probe cycles with repetition rates up to ≈ 300 kHz. The fast jet (see Fig. 11), capable of speeds up to 100 m/s, allowed us to use ≈ 1 MHz pump-probe rate, fully exploiting the high synchrotron x-ray flux for samples that require a fresh sample volume for each pump-probe cycle.

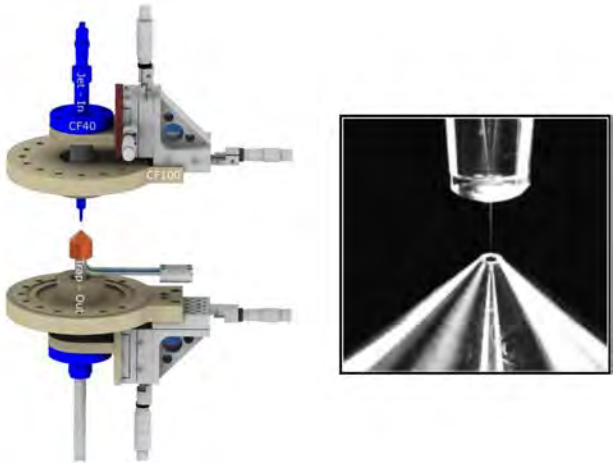

Figure 11: The liquid microjet system consists of an injector unit (top) and a beam capture assembly (bottom), both with motorized position controls, and is compatible with vacuum operation. The liquid pump can generate jets below 100 μm at flow speeds up to 100 m/s [56].

Another improvement was the addition of multiple photon detection capability, to complement the single photon detection scheme we had been using. Single photon counting detection is sufficient

for our x-ray emission spectroscopy measurements since the signal strength is small. However, for x-ray absorption measurements, where a much larger solid angle can be used to collect the signal, the ability to detect more than one photon in a given shot enhances the speed at which XANES and EXAFS data can be collected. We implemented a new MHz digital boxcar averager that digitizes the analog signal from the avalanche photodiode detectors and allows for pulse height and pulse area measurements. This capability is particularly important when measuring x-ray absorption spectra of samples that damage or that produce irreversible photoproducts with repetitive laser exposure.

Reversible photoswitching of magnetic properties

G. Doumy, A. M. March, S. H. Southworth, A. Al-Haddad, M.-F. Tu, L. Young, C. Bostedt, G. Subramanian[22], M. Khusniyarov[23] and collaborators

Spin-crossover (SCO) metal complexes are a very interesting class of bistable molecular systems, the properties of which can be reversibly switched by several means, and in particular by irradiation with light. Understanding the mechanisms at play in the photoswitching process is crucial for future use of these systems as building blocks for molecular electronics and spintronics, as well as for high-density magnetic memory. The most common SCO complexes are pseudo octahedral d^6 complexes of iron(II), which offer the opportunity to switch between a diamagnetic low-spin (S=0) state and a paramagnetic high-spin (S=2) state. Controlling the state via light irradiation is very attractive because of the expected very high switching speed and relative ease in selectively addressing via wavelength control. Indeed, photoswitching in SCO systems is well documented (e.g. in our previous work [12] on $[Fe(bipy)_3]^{2+}$ and $[Fe(terpy)_2]^{2+}$), for those involving a light-induced excited spin-state trapping (LIESST) effect. A very new class of systems is represented by metal complexes with one or more of the ligands exhibiting photochromic properties; upon light absorption, the ligand photoisomerizes, in turn inducing a modification of the ligand field, which results in a change of the spin state. Dubbed ligand-driven light-induced spin change (LD-LISC), this process can be accomplished at room temperature and, like LIESST, promises spin state control at the single-molecule level. Due to their novelty, these systems have been scarcely studied, and the mechanism behind the ligand field modification is still unclear. In addition, no data are available concerning the dynamics of the photoswitching effect.

We have begun to study one such very promising complex, developed by Dr. Khusniyarov's group, using time-resolved XAS and XES. Direct characterization of the metal center's environment and electronic properties would allow for a better understanding of the mechanism at play, and a determination of the characteristics relevant for the efficiency of the complex would illuminate future avenues for synthesizing even better complexes.

Probing ultrafast electron (de)localization dynamics in mixed valence complexes using time-resolved x-ray spectroscopies

A. M. March, G. Doumy, S. H. Southworth, M. Khalil,[24] R. Schoenlein,[4] A. Cordones-Hahn,[4] J. H. Lee,[5] T. Kim[25] and collaborators

Cyanide-bridged transition metal mixed-valence complexes are a class of molecules that exhibit unique redox, spectroscopic, and charge transfer properties by virtue of bearing oxidizing and reducing moieties. They are widely studied for their applications in magnetism and photo-chemical energy conversion, and they serve as model systems to probe the coupling between electronic and vibrational motions during photo-induced ultrafast electron transfer reactions using equilibrium and transient spectroscopic techniques. A central question in the field of transition metal mixed-valence

complexes is the precise nature and extent of electron delocalization. X-ray absorption spectroscopy (XAS) and x-ray emission spectroscopy (XES), including resonant inelastic x-ray scattering (RIXS) maps, can probe changes in the local electronic structure following metal-to-metal charge transfer (MMCT) excitation with atomic specificity, tracking time-evolving spin-orbit couplings, solvent rearrangement and metal-ligand interactions. Using crystal optics for a von Hamos dispersive geometry developed in house by the APS Optics Group, we measured simultaneously the K_α and K_β portions of the emission spectrum (including the valence-to-core transitions) at both the Fe K-edge and the Cr K-edge. For the two Fe-containing complexes, only static measurements were performed since the back electron transfer rates are known to be too fast (100 fs) to be followed at a synchrotron, but represent a crucial building block for an upcoming XFEL time-resolved measurement. In contrast, the covalently linked electron acceptor Cr(III) in a Ru-Cr-Ru mixed valence complex leads to remarkably long-lived charge-separated intermediates, attributed to the existence of electronic states of different spin multiplicity that effectively inhibit back electron transfer. Transient XAS measurements identified the production of a unique photoproduct with a lifetime around 35 ns. Time-resolved XES spectra were recorded at a repetition rate of 1.3 MHz, and the K_β spectrum exhibits a small transient signal consistent with the spin change associated with the MMCT. DFT calculations, including molecular dynamics to take into account the effect of the solvent, are in progress to complete the interpretation.

Time-resolved x-ray absorption spectroscopy of cobalt-based hydrogen evolution systems for artificial photosynthesis

D. Moonshiram, C. Gimbert-Suriñach[26], A. Guda[27], A. Picón, C. S. Lehmann, S. H. Southworth, G. Doumy, A. M. March, X. Zhang[28], A. Llobet[26], and collaborators

Solar hydrogen fuel technology based on artificial photosynthesis will only be feasible if it can be performed efficiently and at low cost. An important element for the optimum performance and competitive cost of solar fuel cells is the hydrogen evolving catalyst of the reductive half-cell, which is responsible for the H-H bond formation. While metallic platinum is well known to catalyze the water reduction efficiently near the thermodynamic potential, the high cost of this precious metal has prompted the scientific community to search for alternative catalysts based on earth-abundant materials. In this context, the use of molecular cobalt-based catalysts has proven to be a good alternative given the high turnover numbers and stability achieved under catalytic conditions. Time resolved x-ray absorption spectroscopy (tr-XAS) was used to study the light induced hydrogen evolution reaction catalyzed by a stable earth-abundant cobalt complex, $[Ru(bpy)_3]^{2+}$ photosensitizer and an equimolar mixture of sodium ascorbate/ascorbic acid electron donor in pure water. XANES and EXAFS analysis of a binary mixture of the octahedral Co(III) pre-catalyst and a $[Ru(bpy)_3]^{2+}$ after illumination revealed in-situ formation of a Co(II) intermediate with significantly distorted geometry and electron transfer kinetics of 51 ns. On the other hand, tr-XAS experiments of the complete photocatalytic system in the presence of the electron donor showed the formation of a square planar Co(I) intermediate species within a few nanoseconds followed by its decay in the microsecond timescales. The experimental x-ray absorption spectra of the molecular species formed along the catalytic cycle were modeled using a combination of molecular orbital DFT (DFT-MO) and Finite Difference Method (FDM) calculations. These findings allowed us to assign the full mechanistic pathway followed by the catalyst as well as to determine the rate limiting step of the process, which consists of the protonation of the Co(I) species. This study provided a complete kinetics scheme for the hydrogen evolution reaction by a cobalt catalyst, revealing unique information for the development of better catalysts for the reductive side of hydrogen fuel cells [33].

Mechanistic evaluation of a nickel-based proton reduction catalyst using time-resolved x-ray absorption spectroscopy

D. Moonshiram, A. Guda[27], L. Kohler[14], A. Picón, C. S. Lehmann, S. H. Southworth, X. Zhang[28], K. L. Mulfort[14], and collaborators

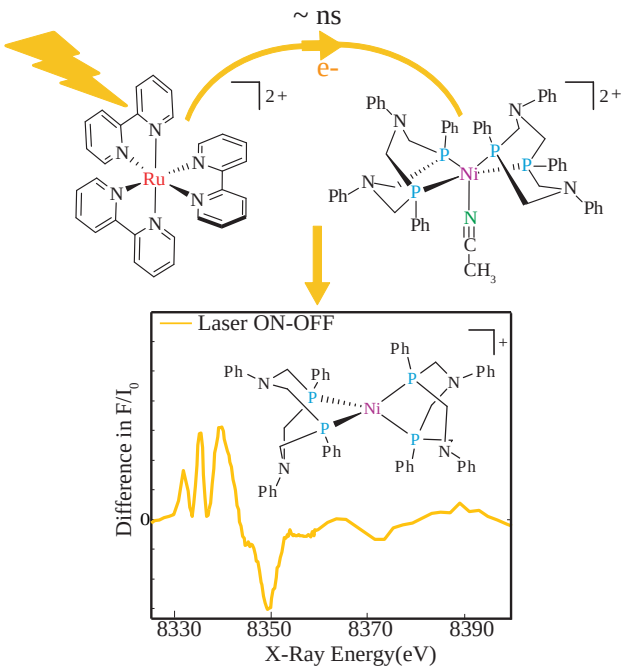

Figure 12: Time-resolved x-ray absorption spectrum upon laser excitation of a photocatalytic system consisting of the $Ni(P_2^{Ph}N_2^{Ph})_2(CH_3CN)]^{2+}$ catalyst, $[Ru(bpy)_3]^{2+}$ photosensitizer and ascorbic acid electron donor. In the graph the difference of fluorescence yield absorption spectra with pump laser on and pump laser off are shown.

The prospect of using molecular hydrogen as fuel has motivated the discovery and development of molecular catalysts for photo-induced water oxidation, proton reduction and their integration in catalyst-photosensitizer systems. In particular, a family of highly stable and tunable molecular electrocatalysts based on nickel(II) diphosphine coordination complexes with the general formula $[Ni(P_2^RN_2^{R'})]^{2+}$ (where $P_2^RN_2^{R'}$ denotes 1,5-R'-3,7-R-1,5-diaza-3,7-diphosphacyclooctane groups with substituent R and R' groups covalently bound to phosphorous and nitrogen atoms respectively) has been developed. We have studied the light-induced electronic and geometric changes taking place in a multimolecular $[Ru(bpy)_3]^{2+}/Ni(P_2^{Ph}N_2^{Ph})_2(CH_3CN)]^{2+}$/ascorbic acid photocatalytic system with tr-XAS in the ns to s time regime [35]. Tr-XAS allowed us to observe the diffusion-governed electron transfer between the excited photosensitizer and the nickel(II) proton reduction catalyst on the nanosecond timescale followed by formation of a transient distorted tetrahedral Ni(I) intermediate, see Fig. 12. A 50 fold increase in the decay lifetime of the Ni(I) species, in the presence of the electron donor, shows that the favored catalytic pathway occurs through reductive quenching of the excited photosensitizer followed by electron transfer to the catalyst. Our study is supported by molecular orbital Density Functional Theory (DFT-MO) calculations. It provides relevant information for ongoing synthetic efforts on Du Bois-type nickel complexes.

5 Affiliations of collaborators

[1]Argonne Leadership Computing Facility, Argonne National Laboratory, Argonne, IL
[2]Kansas State University, Manhattan, KS
[3]Center for Free-Electron Laser Science, DESY, Hamburg, Germany
[4]SLAC National Accelerator Laboratory, Menlo Park, CA
[5]Lawrence Berkeley National Laboratory, Berkeley, CA
[6]University of Southern California, Los Angeles, CA
[7]Universität Rostock, Germany
[8]Ludwig Maximilian Universität München, Germany
[9]Technische Universität Berlin, Germany
[10]Kyoto University, Japan
[11]Tohoku University, Japan
[12]Wigner Research Centre for Physics, Hungarian Academy Sciences, Budapest, Hungary
[13]Uppsala University, Sweden
[14]Chemical Sciences and Engineering Division, Argonne National Laboratory, Argonne, IL
[15]Max Planck Institute for the Structure and Dynamics of Matter, Hamburg, Germany
[16]Lund University, Lund, Sweden
[17]Université Pierre et Marie Curie, Paris, France
[18]University of Oulu, Oulu, Finland
[19]Elettra-Sincrotrone Trieste, Area Science Park, Trieste, Italy
[20]Universitat Autònoma de Barcelona, Barcelona, Spain
[21]European XFEL, Hamburg, Germany
[22]Arizona State University, Phoenix, AZ
[23]University of Erlangen-Nuremberg, Germany
[24]University of Washington, Seattle, WA
[25]Pusan National University, South Korea
[26]Institute of Chemical Research of Catalonia, Tarragona, Spain
[27]Southern Federal University, Rostov, Russia
[28]X-Ray Science Division, Argonne National Laboratory, Argonne, IL

References

Publications 2014–2016

[1] Z. Yan, Y. Bao, U. Manna, R. A Shah, N. F. Scherer, "Enhancing nano particle electrodynamics with gold nanoplate mirrors, Supporting Information," Nano Lett. **14**, 2436 (2014).

[2] L. Young, "Ultraintense X-ray interactions at the Linac Coherent Light Source," Chapter 15, 529-556. In Attosecond and XUV Physics, Editors: Thomas Schultz and Marc Vrakking, Wiley (2014).

[3] R. Reininger, E. M. Dufresne, M. Borland, M. Beno, L. Young, P. G. Evans, "A short-pulse X-ray beamline for spectroscopy and scattering," J. Synchrotron Rad. **21**, 1194 (2014).

[4] L. Young, "Understanding ultraintense x-ray interactions with matter," Advances in Chemical Physics, Volume 157: Proceedings of the 240 Conference: Science's Great Challenges, First Edition, p. 183-194 (2015).

[5] C. Bressler, W. Gawelda, A. Galler, M. M. Nielsen, V. Sundström, G. Doumy, A. M. March, S. H. Southworth, L. Young, and G. Vankó, "Solvation dynamics monitored by combined X-ray spectroscopies and scattering: photoinduced spin transition in aqueous $[Fe(bpy)_3]^{2+}$, Faraday Discuss. **171**, 169 (2014).

[6] Y. Pushkar, D. Moonshiram, V. Purohit, L. Yan, and I. Alperovich, "Spectroscopic analysis of catalytic water oxidation by $[Ru^{II}(bpy)(tpy)H_2O]^{2+}$ suggests that Ru^{V}=O is not a rate-limiting intermediate," J. Am. Chem. Soc. **136**, 11938 (2014).

[7] P. J. Ho, C. Bostedt, S. Schorb, and L. Young, "Theoretical tracking of resonance-enhanced multiple ionization pathways in x-ray free-electron laser pulses," Phys. Rev. Lett. **113**, 253001 (2014).

[8] Z. Yan, M. Sajjin, N. F. Scherer, "Tailoring nano particle dynamics with optical phase," in preparation (2014).

[9] U. Manna, Z. Yan, Y. Bao, J. Jureller, N. F. Scherer, "Meso-scale dipolar interactions in synthetic photonic metal nanoparticle lattices," in preparation (2014).

[10] W. Helml, A. R. Maier, W. Schweinberger, I. Grguras, P. Radcliffe, G. Doumy, C. Roedig, J. Gagnon, M. Messerschmidt, S. Schorb, C. Bostedt, G. Grüner, L. F. DiMauro, D. Cubaynes, J. D. Bozek, Th. Tschentscher, J. T. Costello, M. Meyer, R. Coffee, S. Düsterer, A. L. Cavalieri, and R. Kienberger, "Measuring the temporal structure of few-femtosecond free-electron laser x-ray pulses directly in the time domain," Nature Photon. **8**, 950 (2014).

[11] Y. Li, Z. Jiang, X.-M. Lin, H. Wen, D. A. Walko, S. A. Deshmukh, R. Subbaraman, S. K. R. S. Sankaranarayanan, S. K. Gray, and P. J. Ho, "Femtosecond laser pulse driven melting in gold nanorod aqueous colloidal suspension: identification of a transition from stretched to exponential kinetics," Scientific Reports **5**, 8146 (2015).

[12] G. Vankó, A. Bordage, M. Pápai, K. Haldrup, P. Glatzel, A. M. March, G. Doumy, A. Britz, A. Galler, T. Assefa, D. Cabaret, A. Juhin, T. B. van Driel, K. S. Kjær, A. Dohn, K. B. Møller, H. T. Lemke, E. Gallo, M. Rovezzi, Z. Németh, E. Rozsályi, T. Rozgonyi, J. Uhlig, V. Sundström, M. M. Nielsen, L. Young, S. H. Southworth, C. Bressler, and W. Gawelda, "Detailed characterization of a nanosecond-lived excited state: x-ray and theoretical investigation of the quintet state in photoexcited $[Fe(terpy)_2]^{2+}$, J. Phys. Chem C **119**, 5888 (2015).

[13] A. M. March, T. A. Assefa, C. Bressler, G. Doumy, A. Galler, W. Gawelda, E. P. Kanter, Z. Németh, M. Pápai, S. H. Southworth, L. Young, and G. Vankó, Feasibility of valence-to-core x-ray emission spectroscopy for tracking transient species," J. Phys. Chem. C **119**, 14571 (2015).

[14] R. Reininger, Z. Liu, G. Doumy, and L. Young, "A simple optical system delivering a tunable micrometer pink beam that can compensate for heat-induced deformations," J. Synchrotron Rad. **22**, 930 (2015).

[15] B. Zimmermann, V. McKoy, S. H. Southworth, E. P. Kanter, B. Krässig, and R. Wehlitz, "Dipole and nondipole photoionization of molecular hydrogen," Phys. Rev. A **91**, 053410 (2015).

[16] S. H. Southworth, R. Wehlitz, A. Picón, C. S. Lehmann, L. Cheng, and J. F. Stanton, "Inner-shell photoionization and core-hole decay of Xe and XeF_2," J. Chem. Phys. **142**, 224302 (2015).

[17] A. Picón, J. Mompart, and S. H. Southworth, "Stimulated Raman adiabatic passage with two-color x-ray pulses," New J. Phys. **17**, 083038 (2015).

[18] C. Hernández-García, L. Plaja, J. San Román, and A. Picón, "Quantum-path signatures in attosecond helical beams driven by optical vortices", New J. Phys. **17**, 093029 (2015).

[19] R. Santra and L. Young, "Interaction of intense X-ray beams with atoms," in "Synchrotron Light Sources and Free-Electron Lasers: Accelerator Physics, Instrumentation and Science Applications," Editors: E. Jaeschke, S. Khan, J.R. Schneider, and J.B. Hastings (Springer, Heidelberg), p 1-24 (2015).

[20] L. Young, "A stable narrow-band X-ray laser," (Invited News & Views article for Nature), Nature **524**, 424 (2015).

[21] P. J. Ho, E. P. Kanter, and L. Young, "Resonance-mediated atomic ionization dynamics induced by ultraintense x-ray pulses," Phys. Rev. A **92**, 063430 (2015).

[22] R.M.P. Tanyag, C. Bernando, C.F. Jones, C. Bacellar, K.R. Ferguson, D. Anielski, R. Boll, S. Carron, J.P. Cryan, L. Englert, S.W. Epp, B. Erk, L. Foucar, L.F. Gomez, R. Hartmann, D.M. Neumark, D. Rolles, B. Rudek, A. Rudenko, K.R. Siefermann, J. Ullrich, F. Weise, C. Bostedt, O. Gessner, and A. Vilesov, "X-ray coherent diffractive imaging by immersion in nanodroplets," Struc. Dyn. **2**, 051102 (2015).

[23] T. Gorkhover, S. Schorb, R. Coffee, M. Adolph, L. Foucar, D. Rupp, A. Aquila, J. D. Bozek, S. W. Epp, B. Erk, L. Gumprecht, L. Holmegaard, A. Hartmann, R. Hartmann, G. Hauser, P. Holl, A. Hömke, N. Kimmel, K.-U. Kühnel, P. Johnsson, M. Messerschmidt, C. Reich, A. Rouzée, B. Rudek, C. Schmidt, J. Schulz, H. Soltau, S. Stern, G. Weidenspointner, B. White, J. Küpper, L. Strüder, I. Schlichting, J. Ullrich, D. Rolles, A. Rudenko, T. Möller, and C. Bostedt, "Femtosecond and nanometer visualisation of structural dynamics in superheated nanoparticles," Nature Photonics **10**, 93 (2016).

[24] K. R. Ferguson, M. Bucher, T. Gorkhover, S. Boutet, H. Fukuzawa, J. E. Koglin, Y. Kumagai, A. Lutman, A. Marinelli, M. Messerschmidt, K. Nagaya, J. Turner, K. Ueda, G. J. Williams, P. H. Bucksbaum, and C. Bostedt, "Transient lattice compression in the solid-to-plasma transition," Science Advances **2**, 1500837 (2016).

[25] C. Bostedt, S. Boutet, D. M. Fritz, Z. Huang, H. J. Lee, H. T. Lemke, A. Robert, W. F. Schlotter, J. J. Turner, and G. J. Williams, "The Linac Coherent Light Source: The First Five Years," Rev. Mod. Phys. **88**, 015007 (2016).

[26] E. M. Dufresne, R. W. Dunford, E. P. Kanter, Y. Gao, S. Moon, D. A. Walko, and X. Zhang, "Pink-beam focusing with a one-dimensional compound refractive lens," J. Synchrotron Rad. **23**, 1082 (2016).

[27] L. Flückiger, D. Rupp, M. Adolph, T. Gorkhover, M. Krikunova, M. Müller, T. Oelze, Y. Ovcharenko, M. Sauppe, S. Schorb, C. Bostedt, S. Düsterer, M. Harmand, H. Redlin, R. Treusch, T. Möller, "Time-resolved x-ray imaging of a laser-induced nanoplasma and its neutral residuals," New J. Phys. **18**, 043017 (2016).

[28] C.F. Jones, C. Bernando, R.M.P. Tanyag, C. Bacellar, K.R. Ferguson, L.F. Gomez, D. Anielski, A. Belkacem, R. Boll, J.D. Bozek, S. Carron, J. Cryan, L. Englert, S.W. Epp, B. Erk, L. Foucar, R. Hartmann, D. Neumark, D. Rolles, A. Rudenko, K.R. Siefermann, F. Weise, B. Rudek, F.P. Sturm, J. Ullrich, C. Bostedt, O. Gessner, A.F.

Vilesov, "Coupled motion of Xe clusters and quantum vortices in He nanodroplets," Phys. Rev. B **93**, 180510 (2016).

[29] A. Picón, C. S. Lehmann, C. Bostedt, A. Rudenko, A. Marinelli, T. Osipov, D. Rolles, N. Berrah, C. Bomme, M. Bucher, G. Doumy, B. Erk, K. Ferguson, T. Gorkhover, P. J. Ho, E. P. Kanter, B. Krässig, J. Krzywinski, A. A. Lutman, A. M. March, D. Moonshiram, D. Ray, L. Young, S. T. Pratt, and S. H. Southworth, "Hetero-site-specific ultrafast intramolecular dynamics," Nature Comm. **7**, 11652 (2016).

[30] R. Boll, B. Erk, R. Coffee, S. Trippel, T. Kierspel, C. Bomme, J.D. Bozek, M. Burkett, S. Carron, K.R. Ferguson, L. Foucar, J. Kpper, T. Marchenko, C. Miron, M. Patanen, T. Osipov, S. Schorb, M. Simon, M. Swiggers, S. Techert, K. Ueda, C. Bostedt, D. Rolles, A. Rudenko, "Charge transfer in dissociating iodomethane and fluoromethane molecules ionized by intense femtosecond X-ray pulses," Struc. Dyn. **3**, 043207 (2016).

[31] D.A. Walko, B.W. Adams, G. Doumy, E.M. Dufresne, Y. Li, A.M. March, A.R. Sandy, J. Wang, H. Wen, and Y. Zhu, "Developments in Time-Resolved X-ray Research at APS Beamline 7ID," 12th International Conference on Synchrotron Radiation Instrumentation, AIP Conf. Proc., **1741**, 030048 (2016).

[32] Y. Gao, R. Harder, S. Southworth, J. Guest, N. Scherer, Z. Yan, L. Ocola, M. Pelton, and L. Young, "Bragg diffraction from sub-micron particles isolated by optical tweezers," AIP Conf. Proc. **1741**, 050010 (2016).

[33] D. Moonshiram, C. Gimbert-Suriñach, A. Guda, A. Picon, C.S. Lehmann, X. Zhang, G. Doumy, A.M. March, J. Benet-Buchholz, A. Soldatov, A. Llobet, and S.H. Southworth "Tracking the Structural and Electronic Configurations of a Cobalt Proton Reduction Catalyst in Water," J. Am. Chem. Soc. **138**, 10586 (2016).

[34] C. S. Lehmann, A. Picón, C. Bostedt, A. Rudenko, A. Marinelli, D. Moonshiram, T. Osipov, D. Rolles, N. Berrah, C. Bomme, M. Bucher, G. Doumy, B. Erk, K. Ferguson, T. Gorkhover, P. J. Ho, E. P. Kanter, B. Krässig, J. Krzywinski, A. A. Lutman, A. M. March, D. Ray, L. Young, S. T. Pratt, and S. H. Southworth, "Ultrafast measurements of molecular nuclear dynamics using two x-ray pulses," Phys. Rev. A **94**, 013426 (2016).

[35] D. Moonshiram, A. Guda, L. Kohler, A. Picon, S. Guda, C.S. Lehmann, X. Zhang, S.H. Southworth, and K.L. Mulfort, "Mechanistic Evaluation of a Nickel Proton Reduction Catalyst Using Time-Resolved X-ray Absorption Spectroscopy," J. Phys. Chem. C, DOI: 10.1021/acs.jpcc.6b06883 (2016).

[36] V. Kimberg, A. Sanchez-Gonzalez, L. Mercadier, C. Weninger, A. Lutman, D. Ratner, R. Coffee, M. Bucher, M. Mucke, M. Agaker, C. Sathe, C. Bostedt, J. Nordgren, J.-E. Rubensson and N. Rohringer, "Stimulated X-ray Raman scattering a critical assessment of the building block of nonlinear X-ray spectroscopy", Faraday Disc., DOI: 10.1039/c6fd00103c (2016).

[37] D. Rupp, L. Flückiger, M. Adolph, T. Gorkhover,M. Krikunova, J.P. Muüller, M. Muüller, T. Oelze, Y. Ovcharenko, B. Röben, M. Sauppe, S. Schorb, D. Wolter, R. Mitzner, M. Wöstmann, S. Roling, M. Harmand, R. Treusch, M. Arbeiter, T. Fennel, C. Bostedt, and T. Möller, "Observation of recombination-enhanced surface expansion of clusters in intense soft x-ray laser pulses", Phys. Rev. Lett, in press (2016).

[38] C. Suriñach, D. Moonshiram, L. Francas, N. Planas, F. Bozoglian, A. Guda, L. Mognon, I. Lopez, C.J. Cramer, L. Gagliardi, and A. Llobet, "Structural and Spectroscopic Characterization of Reaction Intermediates involved in a Dinuclear Co-Hbpp Water Oxidation Catalyst", under review, J. Am. Chem. Soc. (2016).

[39] D. Moonshiram, Y. Pineda-Galvan, D. Erdman, M. Palenik. R. Thummel, and Y. Pushkar, "Spectroscopic analysis of catalytic water oxidation by Ru complex - uncovering the facility of oxygen atom transfer", under review, J. Am. Chem. Soc. (2016).

[40] J. Creus, R. Matheu, I. Penafiel , D. Moonshiram, J. Benet-Buchholtz, J. Garcia-Anton, X. Sala, C. Godard, and A. Llobet, "A Million Turnover Molecular Anode for Catalytic Water Oxidation", under review, Angew. Chem. Int. Ed. (2016).

[41] R. Sullivan, J. Jia, A. Vázquez-Mayagoitia, and A. Picón, "Normal Auger processes with ultrashort x-ray pulses in Neon," under review, Phys. Rev. A (2016).

[42] Phay J. Ho, Chris Knight, Miklos Tegze, Gyula Faigel, C. Bostedt, and L. Young, "Atomistic 3D coherent X-ray imaging of non-biological systems," under review, Phys. Rev. X (2016).

[43] D. Moonshiram, A. Picón, M.-F. Tu, X. Zhang, A. Aukauloo, and F. Avenier, "Studying the photo-assisted activation of oxygen in artificial analogues of methane monooxygenase enzymes through time-resolved X-ray absorption spectroscopy", to be submitted to Inorg. Chem. (2016).

[44] Phay J. Ho, and Chris Knight, "Large-scale atomistic calculations of cluster in intense x-ray pulses," to be submitted J. Phys. B (2016).

[45] A. M. March, T. A. Assefa, C. Boemer, C. Bressler, A. Britz, G. Doumy, A. Galler, M. Harder, D. Khakhulin, Z. Németh, S. Schulz, S. H. Southworth, H. Yavas, L. Young, W. Gawelda, and G. Vankó, "Probing transient valence orbital changes with picosecond valence-to-core x-ray emission spectroscopy," to be submitted J. Phys. Chem. Lett. (2016).

Other cited references

[46] L. Young, E. P. Kanter, B. Krässig, Y. Li, A. M. March, S. T. Pratt, R. Santra, S. H. Southworth, N. Rohringer, L. F. DiMauro, G. Doumy, C. A. Roedig, N. Berrah, L. Fang, M. Hoener, P. H. Bucksbaum, J. P. Cryan, S.

Ghimire, J. M. Glownia, D. A. Reis, J. D. Bozek, C. Bostedt, and M. Messerschmidt, "Femtosecond electronic response of atoms to ultra-intense x-rays," Nature **466**, 56 (2010).

[47] E. P. Kanter, B. Krässig, Y. Li, A. M. March, P. Ho, N. Rohringer, R. Santra, S. H. Southworth, L. F. DiMauro, G. Doumy, C. A. Roedig, N. Berrah, L. Fang, M. Hoener, P. H. Bucksbaum, S. Ghimire, D. A. Reis, J. D. Bozek, C. Bostedt, M. Messerschmidt, and L. Young, "Unveiling and driving hidden resonances with high-fluence, high-intensity x-ray pulses," Phys. Rev. Lett. **107**, 233001 (2011).

[48] S. Schorb, D. Rupp, M. L. Swiggers, R. N. Coffee, M. Messerschmidt, G. Williams, J. D. Bozek, S.-I. Wada, O. Kornilov, T. Möller, and C. Bostedt, "Size-dependent ultrafast ionization dynamics of nanoscale samples in intense femtosecond x-ray free-electron-laser pulses," Phys. Rev. Lett. **108**, 233401 (2012).

[49] B. Rudek, S.-K. Son, L. Foucar, S. W. Epp, B. Erk, *et al.*, "Ultra-efficient ionization of heavy atoms by intense X-ray free-electron laser pulses," Nat. Photon. **6**, 858 (2012).

[50] T. Tachibana, et al., Nanoplasma formation by high intensity hard x-rays, Scientific Reports **5**, 10977 (2015).

[51] A. A. Lutman, R. Coffee, Y. Ding, Z. Huang, J. Krzywinski, T. Maxwell, M. Messerschmidt, and H.-D. Nuhn, "Experimental demonstration of femtosecond two-color x-ray free-electron lasers," Phys. Rev. Lett. **110**, 134801 (2013).

[52] Z. Li, O. Vendrell, and R. Santra, "Ultrafast Charge Transfer of a Valence Double Hole in Glycine Driven Exclusively by Nuclear Motion," Phys. Rev. Lett. **115** 143002 (2015).

[53] W. Eberhardt,T.K. Sham, R. Carr, S. Krummacher, M. Strongin, S. L. Weng, and D. Wesner, "Site-Specific Fragmentation of Small Molecules Following Soft-X-Ray Excitation," Phys. Rev. Lett. **50**, 1038 (1983).

[54] R. W. Dunford, S. H. Southworth, D. Ray, E. P. Kanter, B. Krässig, L. Young, D. A. Arms, E. M. Dufresne, D. A. Walko, O. Vendrell, S.-K. Son, and R. Santra, "Evidence for interatomic Coulombic decay in Xe K-shell-vacancy decay of XeF_2," Phys. Rev. A **86**, 033401 (2012).

[55] M. Hoener, L. Fang, O. Kornilov, O. Gessner, S. T. Pratt, M. Gühr, E. P. Kanter, C. Blaga, C. Bostedt, J. D. Bozek, P. H. Bucksbaum, C. Buth, M. Chen, R. Coffee, J. Cryan, L. DiMauro, M. Glownia, E. Hosler, E. Kukk, S. R. Leone, B. McFarland, M. Messerschmidt, B. Murphy, V. Petrovic, D. Rolles, and N. Berrah, "Ultraintense x-ray induced ionization, dissociation, and frustrated absorption in molecular nitrogen," Phys. Rev. Lett. **104**, 253002 (2010).

[56] The graphics are taken from http://www.microliquids.com/.

Page is intentionally blank.

J.R. Macdonald Laboratory Overview

The J.R. Macdonald Laboratory (JRML) focuses on the interaction of intense laser pulses with matter for the purpose of understanding and even controlling the resulting ultrafast dynamics. The timescales involved range from attoseconds, necessary for studying electronic motion in matter, to femtoseconds and picoseconds for molecular vibration and rotation, respectively. We continue to harness the expertise within the Lab to further our progress in both understanding and control. The synergy afforded by the close interaction of theory and experiment within the Lab serves as a significant multiplier for this effort. To achieve our goals, we are advancing theoretical modeling and computational approaches as well as experimental techniques, such as particle imaging (COLTRIMS, VMI, etc.), molecular alignment, and high-harmonic generation.

Most of our research projects are associated with one of four themes: "Attosecond Physics", "Extending and enhancing harmonic generation", "Imaging dynamics in large molecules" and "Strong field control of small molecules". These themes serve as broad outlines only, as the boundary between them is not always well defined. Similarly, in many cases it is hard to distinguish between improving theoretical and experimental "tools" and the resulting science discovery. A few examples are briefly mentioned below, while further details are provided in the individual abstracts of the PIs: I. Ben-Itzhak, B.D. Esry, V. Kumarappan, C.D. Lin, D. Rolles, A. Rudenko, U. Thumm, and C.A. Trallero.

Attosecond physics: Attosecond science is motivated by the idea of observing electronic motion in atoms and molecules on its natural timescale. Given this time scale, attosecond time delays, which have attracted particular attention in recent years, have been attributed to electronic processes. However, our theoretical treatment of dissociation without electronic excitation by strong laser fields indicates that attosecond time delays can also be caused by nuclear motion. This prediction is supported by our measurements of dissociation of specific vibrational levels of D_2^+.

Extending and enhancing harmonic generation: High harmonic generation (HHG) is usually used to produce attosecond pulses. Our recent theoretical and experimental work focuses on increasing the HHG efficiency to enable the use of high harmonics in pump-probe studies. The harmonics are also a source of high-energy photons, enabling population of specific molecular states. In addition, they provide information on the microscopic and macroscopic laser-driven processes involved in their generation. We employ HHG spectroscopy to retrieve the harmonic amplitude and phase.

Imaging dynamics in large molecules: Our work on this topic ranges from theoretical treatment of laser-induced electron diffraction (LIED) to experiments employing this technique as well as to pump-probe measurements of molecular dynamics. The latter technique has been employed to image nuclear wave packets in aligned or randomly oriented polyatomic molecules, such as CO_2 and halomethanes.

Strong field control of small molecules: Methods for controlling the motion of heavy particles in small molecules continue to be developed. Work in the Lab has also led to the imaging of structural rearrangement in small polyatomic molecules and to theoretical treatment of nuclear-dynamics imaging. Related work on charge transfer following multiphoton ionization by X-rays has been conducted at the LCLS. Employing impulsive alignment techniques, we have measured the ionization rate of asymmetric top molecules as a function of their alignment.

A significant fraction of JRML research is done in collaboration with others. For example, E. Wells from Augustana University and R.R. Lucchese from Texas A&M University take advantage of data measured at JRML. Similarly, some of us conduct experiments at free electron lasers, such as LCLS and FLASH, and at other facilities. Our group is well connected through such collaborations with many AMO groups across the world (ALS, ANL, Århus, FLASH, Univ. of Frankfurt, ICFO Barcelona, Univ. of Jena, LBNL, LCLS, Max-Planck Institutes for Quantum Optics and Kernphysik, the Ohio State Univ., Texas A&M Univ., Tokyo Univ., Weizmann Institute, and others).

Finally, it is worth mentioning the laser facilities available to researchers at JRML. Our high-repetition rate laser, PULSAR, and the high-power, tunable long wavelength laser, HITS, are the main laser systems, while the old workhorse laser, KLS, is still yielding high-quality results. On the personnel side, Daniel Rolles, who joined us in early 2015, is in the process of building new apparatus in the lab, while performing experiments at JRML using existing equipment and at FELs as a natural continuation of his previous work. Combining the experimental and theoretical expertise within the Lab with our large spectrum of laser and imaging capabilities continues to produce exciting physics.

Structure and Dynamics of Atoms, Ions, Molecules, and Surfaces: Molecular Dynamics with Ion and Laser Beams

Itzik Ben-Itzhak, J. R. Macdonald Laboratory, Physics Department, Kansas State University, Manhattan, KS 66506; ibi@phys.ksu.edu

Scope: *The goal of this part of the JRML program is to study and control molecular dynamics under the influence of ultrashort intense laser pulses. To this end, we typically study molecular ion beams and have a close collaboration between theory and experiment.*[1]

Pump-probe studies of fragmentation of a fast HD^+ beam

M. Zohrabi, B. Berry, T. Severt, Bethany Jochim, Peyman Feizollah, Kanaka Raju P., Jyoti Rajput, K.D. Carnes, Youliang Yu, B.D. Esry, and I. Ben-Itzhak

Studies of fast molecular ion beams in strong-field ultrafast lasers are of particular interest for benchmark molecules such as H_2^+, H_3^+ and HeH^+. However, the low target density of a typical ion beam puts severe limits on studies of time evolution through the implementation of the pump-probe technique. We have recently conducted a first-of-its-kind NIR-pump—NIR-probe measurement on a few-keV HD^+ beam target.

Specifically, in our measurements the first pulse initiated the dissociation of the HD^+, while the second ionized the molecule during its dissociation. We have observed enhancement in the ionization yield of the dissociating wave packet at about 24 and 200 fs, as shown in Fig. 1, corresponding to internuclear distances estimated classically to be about 15 and 60 a.u., respectively. The enhancement around 15 a.u. is consistent with previous predictions [1] and observations [2-5] of enhanced ionization in hydrogen. In contrast, the enhancement at very large internuclear separation is surprising given the fact that the interaction between the ionic and atomic fragments is extremely weak (i.e. the potentials are practically flat).

Based on a model proposed a while back by Esry *et al*. [6], it is likely that this enhancement is due to 10-photon ionization that becomes resonant around this distance. Time-dependent Schrödinger equation (TDSE) calculations, conducted recently by Esry's group using a 1-D H_2^+ model, qualitatively reproduce the experimentally observed ionization enhancement at large internuclear distance.

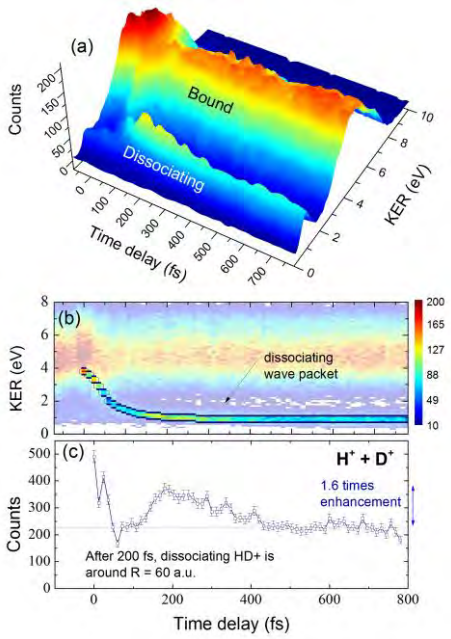

Figure 1. Measured ionization yield, $H^+ + D^+$, by a 3.3×10^{14} W/cm^2 probe pulse following dissociation of HD^+ by a 7.6×10^{13} W/cm^2 pump pulse, both 23 fs and 790 nm. The yield as a function of pump-probe time delay and kinetic energy release (KER), shown as (a) 3D plot and (b) density map. (c) The ionization yield of the dissociating wave packet as a function of time delay.

References

1. T. Zuo and A.D. Bandrauk, Phys. Rev. A **52**, R2511 (1995)
2. G.N. Gibson *et al*., Phys. Rev. Lett. **79**, 2022 (1997)
3. Th. Ergler *et al*., Phys. Rev. Lett. **95**, 093001 (2005)
4. A.S. Alnaser *et al*., J. Phys. B **39**, S485 (2006)
5. I. Ben-Itzhak *et al*., Phys. Rev. A **78**, 063419 (2008)
6. B.D. Esry *et al*., Phys. Rev. Lett. **97**, 013003 (2006)

Imaging three-body fragmentation – Sequential and concerted breakup mechanisms

Jyoti Rajput, M. Zohrabi, U. Ablikim, Bethany Jochim, Ben Berry, Peyman Feizollah, T. Severt, Farzaneh Ziaee, Balram Kaderiya, Kanaka Raju P., Daniel Rolles, Artem Rudenko, K.D. Carnes, B.D. Esry, and I. Ben-Itzhak

Advances in imaging techniques have led to better understanding of molecular fragmentation induced by photons or collisions. The experimental differentiation between concerted and sequential (sometimes called "stepwise") fragmentation mechanisms in polyatomic molecules is a long-standing goal. Key to its achievement is the coincidence detection of all fragments, although alternatives without coincidence detection have been suggested [1].

The sequential breakup of triply-charged triatomic molecules may involve an intermediate dication – later undergoing unimolecular dissociation, for example

$$OCS^{3+} \rightarrow S^{+} + CO^{2+}$$
$$\hookrightarrow C^{+} + O^{+}.$$

In particular we focus on metastable dication states which survive much longer than their rotational period, i.e. $\tau \gg T_R$. This "delayed" sequential breakup has been invoked to explain a circular feature in a Newton diagram showing the momenta of the three final fragments measured in coincidence [2-4]. This example demonstrates the strong link between the method used to visualize the multi-parameter data and the conclusions one can draw from it about the underlying fragmentation mechanism.

We further explore the identity of these metastable states by analyzing the coincidence three-dimensional momentum imaging data of the three fragment ions in two frames of reference associated with each of the breakup steps. This method allows the clear identification of sequential breakup of states with $\tau \gg T_R$, separating them from the other competing breakup mechanisms, and thus providing branching ratios. More importantly, the evaluated kinetic energy release (KER) during each step opens the door to pinpointing the specific electronic, or with improved resolution, vibrational states. Our method is demonstrated using ionization of OCS and CO_2^+ targets by ultrashort intense laser pulses. However, it is applicable for other processes leading to three-body breakup as long as the momenta for the three fragments are detected in coincidence.

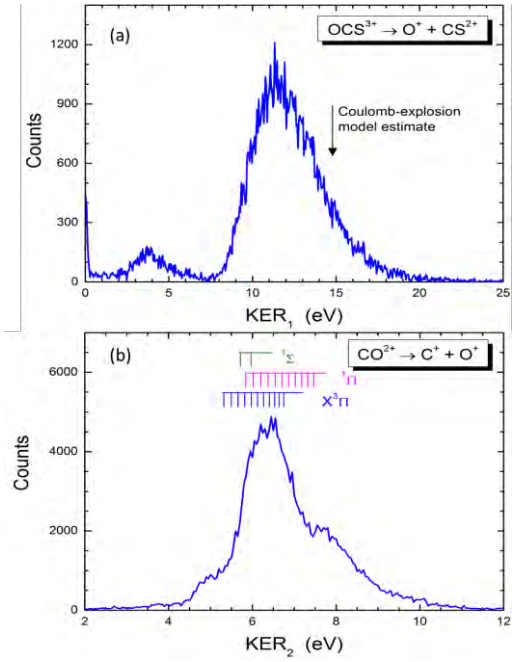

Figure 2. Kinetic energy release distribution for the first step (top) and second step (bottom) of OCS^{3+} fragmentation. The tic marks indicate the expected KER for unimolecular dissociation of CO^{2+} based on measured values reported by Lundqvist *et al.* [5].

References

1. C.E.M. Strauss and P.L. Houston, J. Chem. Phys. **94**, 8751 (1990)
2. N. Neumann *et al.*, Phys. Rev. Lett. **104**, 103201 (2010)
3. C. Wu *et al.*, Phys. Rev. Lett. **110**, 103601 (2013)
4. B. Wales *et al.*, J. Elec. Spec. Rel. Phenom. **195**, 332 (2014)
5. Lundqvist *et al.*, Phys. Rev. Lett. **75**, 1058 (1995)

Future plans: We will continue to probe molecular-ion beams in a strong laser field, specifically exploring challenging two-color, pump-probe and CEP-dependence experiments. We will carry on our studies of more complex systems, including simple polyatomic molecules focusing first on three-body breakup, as well as isomerization processes.

In addition, we have recently initiated similar coincidence 3D momentum imaging measurements of molecular anion beams in ultrafast intense laser pulses using our upgraded setup. For example, we have observed F_2^- fragmentation into $F^- + F$, $F + F$, $F^+ + F$, and $F^+ + F^+$. The data analysis of these measurements is in progress.

Further down the line we intend to photo-detach the anion beam and study the response of neutral molecular beams to similar laser pulses.

Publications of DOE sponsored research in the last 3 years:

24. "Complete characterization of single-cycle double-ionization of argon from the non-sequential to the sequential ionization regime", M. Kübel, C. Burger, Nora G. Kling, T. Pischke, Lucas Beaufore, I. Ben-Itzhak, G.G. Paulus, J. Ullrich, T. Pfeifer, R. Moshammer, M. F. Kling, and B. Bergues, Phys. Rev. A **93**, 053422 (2016).
23. "Steering proton migration in hydrocarbons using intense few-cycle laser fields", M. Kübel, R. Siemering, C. Burger, Nora G. Kling, H. Li, A.S. Alnaser, B. Bergues, S. Zherebtsov, A.M. Azzeer, I. Ben-Itzhak, R. Moshammer, R. de Vivie-Riedle, and M.F. Kling, Phys. Rev. Lett. **116**, 193001 (2016).
22. "Molecular frame photoelectron angular distributions for core ionization of ethane, carbon tetrafluoride and 1,1-difluoroethylene", A. Menssen, C.S. Trevisan, M.S. Schöffler., T. Jahnke, I. Bocharova, F. Sturm, N. Gehrken, B. Gaire, H. Gassert, S. Zeller, J. Voigtsberger, A. Kuhlins, F. Trinter, A. Gatton, J. Sartor, D. Reedy, C. Nook, B. Berry, M. Zohrabi, A. Kalinin, I. Ben-Itzhak, A. Belkacem, R. Dörner, T. Weber, A.L. Landers, T.N. Rescigno, C.W. McCurdy, and J.B. Williams, J. Phys. B **49**, 055203 (2016).
21. "Long term carrier-envelope-phase stabilization of a terawatt-class Ti:Sapphire laser", A. M. Summers, B. Langdon, J. Garlick, X. Ren, D. Wilson, S. Zigo, M. Kling, S. Lei, C. Elles, E. Wells, E. Poliakoff, K. Carnes, V. Kumarappan, I. Ben-Itzhak, and C. Trallero-Herrero, in Frontiers in Optics 2015, OSA Technical Digest (online) (Optical Society of America, 2015), paper FTu3F.2.
20. "Quantum control of photodissociation using intense, femtosecond pulses shaped with third order dispersion", Uri Lev, L. Graham, C.B. Madsen, I. Ben-Itzhak, B.D. Bruner, B.D. Esry, H. Frostig, O. Heber, A. Natan, V.S. Prabhudesai, D. Schwalm, Y. Silberberg, D. Strasser, I.D. Williams, and D. Zajfman, J. Phys. B **48**, 201001 (2015) – Fast Track Communication – IOP Select.
19. "Auger decay and subsequent fragmentation pathways of ethylene following *K*-shell ionization" B. Gaire, D.J. Haxton, F.P. Sturm, J. Williams, A. Gatton, I. Bocharova, N. Gehrken, M. Schöffler, H. Gassert, S. Zeller, J. Voigtsberger, T. Jahnke, M. Zohrabi, D. Reedy, C. Nook, A.L. Landers, A. Belkacem, C.L. Cocke, I. Ben-Itzhak, R. Dörner, and Th. Weber, Phys. Rev. A **92**, 013408 (2015).
18. "Note: Determining the detection efficiency of excited neutral atoms by a microchannel plate detector", Ben Berry, M. Zohrabi, D. Hayes, U. Ablikim, Bethany Jochim, T. Severt, K.D. Carnes, and I. Ben-Itzhak, Rev. Sci. Instrum. **86**, 046103 (2015).
17. "Coherent electronic wave packet motion in C_{60} controlled by the waveform and polarization of few-cycle laser fields", H. Li, B. Mignolet, G. Wachter, S. Skruszewicz, S. Zherebtsov, F. Süßmann, A. Kessel, S.A. Trushin, Nora G. Kling, M. Kübel, B. Ahn, D. Kim, I. Ben-Itzhak, C.L. Cocke, T. Fennel, J. Tiggesbäumker, K.-H. Meiwes-Broer, C. Lemell, J. Burgdörfer, R.D. Levine, F. Remacle, and M.F. Kling, Phys. Rev. Lett. **114**, 123004 (2015).
16. "Identification of a previously unobserved dissociative ionization pathway in time-resolved photospectroscopy of the deuterium molecule", Wei Cao, Guillaume Laurent, Itzik Ben-Itzhak and C. Lewis Cocke, Phys. Rev. Lett., **114**, 113001 (2015) – *Editors' Suggestion*.
15. "A carrier-envelope-phase stabilized terawatt class laser at 1 kHz with a wavelength tunable option", Benjamin Langdon, Jonathan Garlick, Xiaoming Ren, Derrek J. Wilson, Adam M. Summers, Stefan Zigo, Matthias F. Kling, Shuting Lei, Christopher G. Elles, Eric Wells, Erwin D. Poliakoff, Kevin D. Carnes, Vinod Kumarappan, Itzik Ben-Itzhak, and Carlos A. Trallero-Herrero, Opt. Exp. **23**, 4563 (2015). *Featured in Nature Photonics* http://www.nature.com/nphoton/journal/v9/n4/pdf/nphoton.2015.47.pdf.

14. "Fragmentation of CD^+ induced by intense ultrashort laser pulses", L. Graham, M. Zohrabi, B. Gaire, U. Ablikim, B. Jochim, B. Berry, T. Severt, A.M. Summers, U. Lev, O. Heber, D. Zajfman, I.D. Williams, K.D. Carnes, B.D. Esry, and I. Ben-Itzhak, Phys. Rev. A **91**, 023414 (2015).
13. "Attosecond control of electron emission in two-color ionization of atoms", G. Laurent, W. Cao, I. Ben-Itzhak, and C.L. Cocke, *Ultrafast Phenomena XIX* – Proceedings of the 19th International Conference, Okinawa, Japan, July 2014, edited by Kaoru Yamanouchi, Steven Cundiff, Regina de Vivie-Riedle, Makoto Kuwata-Gonokami, and Louis DiMauro, Springer Proceedings in Physics, Vol. **162** (2015) p. 3.
12. "Note: Position dependence of time signals picked of a microchannel plate detector", U. Ablikim, M. Zohrabi, Bethany Jochim, B. Berry, T. Severt, K.D. Carnes, and I. Ben-Itzhak, Rev. Sci. Instrum. **86**, 016111 (2015).
11. "Incorporating real time velocity map image reconstruction into closed-loop coherent control", C.E. Rallis, T.G. Burwitz, P.R. Andrews, M. Zohrabi, R. Averin, S. De, B. Bergues, Bethany Jochim, A.V. Voznyuk, Neal Gregerson, B. Gaire, I. Znakovskaya, J. Mckenna, K.D. Carnes, M.F. Kling, I. Ben-Itzhak, and E. Wells, Rev. Sci. Instrum. **85**, 113105 (2014).
10. "Thick-lens velocity-map imaging spectrometer with high resolution for high-energy charged particles", N.G. Kling, D. Paul, A. Gura, G. Laurent, S. De, H. Li, Z. Wang, B. Ahn, C.H. Kim, T.K. Kim, I.V. Litvinyuk, C.L. Cocke, I. Ben-Itzhak, D. Kim, and M.F. Kling, Journal of Instrumentation **9,** P05005 (2014).
9. "Subfemtosecond steering of hydrocarbon deprotonation through superposition of vibrational modes", A.S. Alnaser, M. Kübel, R. Siemering, B. Bergues, Nora G. Kling, K.J. Betsch, Y. Deng, J. Schmidt, Z.A. Alahmed, A.M. Azzeer, J. Ullrich, I. Ben-Itzhak, R. Moshammer, U. Kleineberg, F. Krausz, R. de Vivie-Riedle, and M.F. Kling, Nature Communications **5**, 3800 (2014).
8. "Multielectron effects in strong-field dissociative ionization of molecules", X. Gong, M. Kunitski, K.J. Betsch, Q. Song, L.Ph.H. Schmidt, T. Jahnke, Nora G. Kling, O. Herrwerth, B. Bergues, A. Senftleben, J. Ullrich, R. Moshammer, G.G. Paulus, I. Ben-Itzhak, M. Lezius, M.F. Kling, H. Zeng, R.R. Jones, and J. Wu, Phys. Rev. A **89**, 043429 (2014).
7. "Hydrogen and fluorine migration in photo-double-ionization of 1,1-difluoroethylene (1,1-$C_2H_2F_2$) near and above threshold", B. Gaire, I. Bocharova, F.P. Sturm, N. Gehrken, J. Rist, H. Sann, M. Kunitski, J. Williams, M.S. Schöffler, T. Jahnke, B. Berry, M. Zohrabi, M. Keiling, A. Moradmand, A.L. Landers, A. Belkacem, R. Dörner, I. Ben-Itzhak, and Th. Weber, Phys. Rev. A **89**, 043423 (2014).
6. "Attosecond Control of electron emission from atoms", G. Laurent, W. Cao, I. Ben-Itzhak, and C.L. Cocke, Journal of Physics: Conference Series **488**, 012008 (2014) – ICPEAC 2013 proceedings – invited talk.
5. "Non-sequential double ionization of Ar: from the single- to the many-cycle regime", M. Kübel, K.J. Betsch, Nora G. Kling, A.S. Alnaser, J. Schmidt, U. Kleineberg, Y. Deng, I. Ben-Itzhak, G.G. Paulus, T. Pfeifer, J. Ullrich, R. Moshammer, M.F. Kling, and B. Bergues, New J. Phys. **16**, 033008 (2014).
4. "Elucidating isotopic effects in intense ultrafast laser-driven D_2H^+ fragmentation", A.M. Sayler, J. McKenna, B. Gaire, Nora G. Johnson, K.D. Carnes, B.D. Esry, and I. Ben-Itzhak, J. Phys. B: At. Mol. Opt. Phys. **47**, 031001 (2014) – Fast Track Communication – IOP Select (see also LabTalk).
3. "Photo-double-ionization of ethylene and acetylene near threshold", B. Gaire, S.Y. Lee, D. J. Haxton, P.M. Pelz, I. Bocharova, F.P. Sturm, N. Gehrken, M. Honig, M. Pitzer, D. Metz, H-K. Kim, M. Schöffler, R. Dörner, H. Gassert, S. Zeller, J. Voigtsberger, W. Cao, M. Zohrabi, J. Williams, A. Gatton, D. Reedy, C. Nook, Thomas Müller, A.L. Landers, C.L. Cocke, I. Ben-Itzhak, T. Jahnke, A. Belkacem, and Th. Weber, Phys. Rev. A **89**, 013403 (2014) – Editors' suggestion.
2. "Adaptive strong-field control of chemical dynamics guided by three-dimensional momentum imaging", E. Wells, C.E. Rallis, M. Zohrabi, R. Siemering, B. Jochim, P.R. Andrews, U. Ablikim, B. Gaire, S. De, K.D. Carnes, B. Bergues, R. de Vivie-Riedle, M.F. Kling, and I. Ben-Itzhak, Nature Communications **4**, 2895 (2013).
1. "Carrier-envelope phase control over pathway interference in strong-field dissociation of H_2^+", Nora G. Kling, K.J. Betsch, M. Zohrabi, S. Zeng, F. Anis, U. Ablikim, Bethany Jochim, Z. Wang, M. Kübel, M.F. Kling, K.D. Carnes, B.D. Esry, and I. Ben-Itzhak, Phys. Rev. Lett. **111**, 163004 (2013).

[i] In addition to the close collaboration with the theory group of *Brett Esry*, some of our studies are done in collaboration with others at JRML and elsewhere.

Strong-field dynamics of few-body atomic and molecular systems

B.D. Esry
J. R. Macdonald Laboratory, Kansas State University, Manhattan, KS 66506
esry@phys.ksu.edu

Program Scope

A main component of my program is to quantitatively understand the behavior of simple benchmark systems in ultrashort, intense laser pulses. As we gain this understanding, we will work to transfer it to more complicated systems. The other main component of my program is to develop novel analytical and numerical tools to more efficiently and more generally treat these systems and to provide rigorous, self-consistent pictures within which their non-perturbative dynamics can be understood. The ultimate goal is to uncover the simplest picture that can explain the most — ideally, without heavy computation being necessary.

"Attosecond time delays" in molecular dissociation

Recent progress

Many groups have been studying "attosecond time delays" in atomic ionization since their first measurement in Ref. [R1], with theoretical papers (see, for example, Refs. [R1–R9]) far outnumbering experimental ones [R1, R10–R13]. Nevertheless, there has been considerable confusion in the field on this topic with many — often subtly — different interpretations of the results [R14]. Part of the confusion stems from the paucity of experiments due to their difficulty and part from the difficulties theory has had reproducing the experimental results that are available. Using molecular analogs of atomic systems [R15] can largely remove both of these difficulties, thus paving the way towards a clear demonstration of what these measurements tell us about the dynamics.

In the molecular analogs we study, alkali-hydride cations and similar heteronuclear diatomic molecules, the time-dependent nuclear motion substitutes for the one-electron dynamics in an atom. This analogy is possible because these molecules possess a key structural feature — namely, their ground-state potential curve is well-separated energetically from other states [R15]. In this case, the laser field interacts with the molecule via the permanent dipole moment so that the time-dependent Schrödinger equation (TDSE) for the nuclear motion in a strong field can thus be mapped directly onto that for the electronic motion in an atom (in atomic units):

$$i\frac{\partial}{\partial t}\Psi(\mathbf{R},t) = \left[-\frac{1}{2\mu}\nabla^2 + U(R) - q_{\rm eff}\,\boldsymbol{\mathcal{E}}(t)\cdot\mathbf{R}\right]\Psi(\mathbf{R},t). \quad (1)$$

In this equation, $U(R)$ is the single relevant Born-Oppenheimer potential; $\boldsymbol{\mathcal{E}}(t)$, the laser's electric field; μ, the reduced mass; and $q_{\rm eff}$, the effective charge,

$$q_{\rm eff} = \frac{m_A}{m_A+m_B}, \quad (2)$$

assuming the AB^+ molecule dissociates to $A+B^+$. There is an additional, species-dependent, short-range correction to the dipole moment not indicated in Eq. (1), but this is typically a small correction. These molecular proxy systems thus provide a "heavy electron" with mass μ and charge $q_{\rm eff}$ — both of which can be tuned somewhat by the choice of isotope.

Our calculations, shown in Fig. 1, indicate that a RABITT-like scheme [R16] for dissociation of HeH^+ is feasible. Specifically, dissociation of different initial vibrational states, $HeH^+(v)$, with a combination of ω, 2ω, and 4ω pulses produces variation of the 3ω peak as a function of the delay τ of the fundamental (at 3200 nm) with respect to the harmonics. The τ dependence is that expected for RABITT [R16]: $P(\tau) = \alpha + \beta\cos[2\omega(\tau - \tau_{vv'})]$ with $\tau_{vv'}$ the delay of interest for attosecond physics. It would reasonably be expected that $\tau_{vv'}$ is on the order of femtoseconds for the purely nuclear dynamics at play in the dissociation of HeH^+.

The results, however, yield the surprising result that the delays are on the attosecond timescale: fitting $P(\tau)$ to the traces in Figs. 1(c) and 1(d) gives

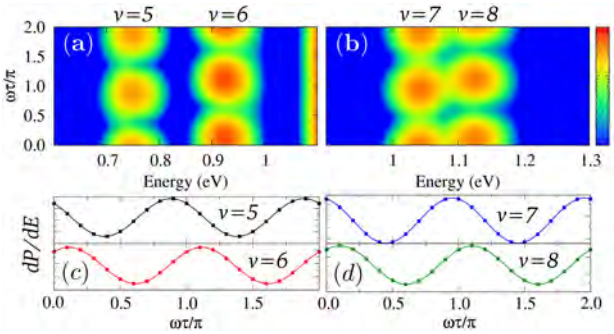

Figure 1: Nuclear RABITT for strong-field dissociation of HeH^+: (a)–(b) show the energy-dependence of the 3ω peak as a function of delay, and (c)–(d) show the delay dependence at the maximum of the 3ω peak from which the time delays $\tau_{vv'}$ are extracted. (Adapted from Ref. [R17].)

$\tau_{vv'}$ in the range 75–550 as. One significant implication of this outcome is that care must be taken in applying RABITT to molecules if the goal is to extract information about the electronic dynamics — more sophisticated analyses might be required to disentangle possible nuclear contributions. Another significant implication of these results is that attosecond-scale measurements can be done with femtosecond-scale pulses given that the pulse lengths of the three colors were 60 fs, 42 fs, and 30 fs, respectively. In this case, only the delay needs to be controlled at the attosecond timescale, which is generally much easier.

There is, however, a much simpler route to an experimentally realizable scenario. The fact that RABITT is a special case of our photon-phase analysis (see Ref. [R18]) suggests that all that is required to see a "delay" is an interferometric measurement. In other words, a simple two-color experiment should yield delays with similar underlying physics.

Two-color experiments with ion targets like HeH^+ are feasible. For instance, Fig. 2 shows a measurement of strong-field, two-color D_2^+ dissociation [R17]. In fact, because the experiment had sufficient resolution to resolve vibrational states, we were able to isolate two-color dissociation from v=7–9 and plot their normalized spatial asymmetry,

$$\mathcal{A} = \frac{P_{\rm up} - P_{\rm down}}{P_{\rm up} + P_{\rm down}}, \qquad (3)$$

as a function of the two-color delay. The probabilities $P_{\rm up}$ and $P_{\rm down}$ in Eq. (3) are the dissociation probabilities for each vibrational state in the up or down direction relative to the laser polarization (obtained by integrating the measured spectrum over a KER range). Fitting $\mathcal{A}$ to the result predicted from our photon-phase analysis yields delays $\tau_{vv'}$ in the 10–100 as range — consistent with our nuclear RABITT calculations.

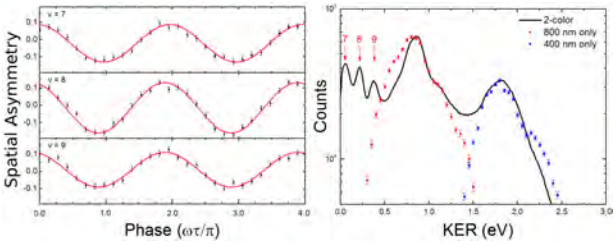

Figure 2: Normalized spatial asymmetry for dissociation of D_2^+ as a function of the delay τ between 800-nm and 400-nm pulses. The solid curves are sinusoidal fits (ω refers to the 800-nm pulse). The KER distributions are also shown for all combinations of the two pulses with the 400-nm and 800-nm distributions normalized to the corresponding two-color peaks. (Adapted from Ref. [R17].)

Future plans

Determining whether delays like this involving nuclear dynamics are generally on the order of attoseconds — and understanding why — will be one focus of our future effort. Using atomic-analog molecules that dissociate only via permanent dipole transitions will allow us to separate nuclear from electronic dynamics in a way not possible in a system like D_2^+. If purely nuclear dynamics can lead to delays of attoseconds, then this clearly has consequences for the notion that attosecond time delays automatically imply electronic dynamics and will thus be important for anyone wanting to apply an attosecond-time-delay technique to molecules.

Quantitative design of an optimal complex absorbing potential for strong-field problems

Recent Progress

To theoretically describe highly nonperturbative interactions, such as strong-field physics, in a fully quantitative manner, the best option is usually to numerically solve the TDSE. One of the most popular such approaches represents the wave function on a finite grid large enough so that there are no reflections from the boundaries which behave as infinitely hard walls. Otherwise, the reflections might lead to unphysical changes in the observables. Given a maximum energy that the grid must represent, the total number of grid points required is proportional to the box size. Thus, the larger the box, the more expensive the calculation. In fact, the large grids required to describe current experiments have become a key bottleneck to improving the numerical efficiency of solving the TDSE, especially as laser wavelengths push beyond 800 nm.

Fortunately, if the wave function at large distances can be easily reconstructed or is not of interest, it can be absorbed at a sufficiently large distance that it does not affect the dynamics at small distances. Applying such absorbing techniques, one can generally reduce the box size significantly. The absorb-and-reconstruct strategy was probably first developed by Heather and Metiu [R19] which they demonstrated for strong-field dissociation. Their work has been adopted in hundreds of papers since. A new implementation [R20] has proven similarly effective.

Among the various methods to effect absorption at the boundary, the most widely used—and prob-

ably the simplest—method is the complex absorbing potential (CAP) [R21–R25] or the closely related masking function [R26]. Another increasingly popular absorbing boundary technique is exterior complex scaling [R27–R30], where one rotates the coordinate at large distances into the complex plane.

We have focused on optimizing the CAP due to its popularity and the simplicity of its implementation. While CAPs are simple, previous implementations have required a relatively large spatial range to be effective, especially at low energies. The portion of the grid devoted to absorption has thus been non-negligible, consuming computational resources for this unphysical part of the calculation. Our goal was thus to minimize the absorbing range x_R (defined by $|V(x_R)| = 10^{-4}$ a.u.) while maintaining a minimum level of absorption over a predetermined energy range. We used the reflection coefficient R to quantify a potential's performance. In the end, we were able to find an optimized CAP with a factor of 3–4 reduction in x_R compared to some widely-used CAPs [R21, R24–R26].

To be useful for absorbing an ionized electron in the strong-field problem, we need $R(E) \leqslant R_0$ over a large energy range. Specifically, our targeted energy range is $0.006 \leqslant E \leqslant 3$ a.u. ($0.11 \leqslant k \leqslant 2.45$ a.u., $E = k^2/2$), which corresponds to $0.1\hbar\omega \leqslant E \leqslant 14U_\mathrm{p}$ for an 800-nm laser pulse at 10^{14} W/cm^2 (U_p is the pondermotive energy, $U_p = I/(4m\omega^2)$, and ω is the laser frequency).

After some experimentation (and reading the literature [R22]), we found that the smallest x_R is obtained by superposing a real potential over the imaginary absorbing potential. The real potential should have a longer range than the imaginary potential so that it accelerates the wavepacket before the absorption region, thereby shortening its longest wavelength. Potentials that are continuous in all derivatives also tend to give the best performance.

To satisfy these conditions, and to provide an analytical result, we chose our potential to have the form (in SI units)

$$V(x) = -\frac{\hbar^2\alpha_1^2}{2m}e^{-x/2\beta} - i\frac{\hbar^2\alpha_2^2}{2m}e^{-x/\beta}. \qquad (4)$$

Its reflection coefficient is

$$R = \left| \frac{{}_1F_1(\tfrac{1}{2} - e^{i\pi/4}\frac{\lambda_1^2}{\lambda_2} + 2iK, 1 + 4iK, -4e^{3i\pi/4}\lambda_2)}{{}_1F_1(\tfrac{1}{2} - e^{i\pi/4}\frac{\lambda_1^2}{\lambda_2} - 2iK, 1 - 4iK, -4e^{3i\pi/4}\lambda_2)} \right|^2$$

where $K = k\beta$, $\lambda_1 = \alpha_1\beta$, and $\lambda_2 = \alpha_2\beta$. Figure 3 summarizes the results for several different values of the minimum absorption parameter R_0. We have verified that our CAP performs as expected in the TDSE as well.

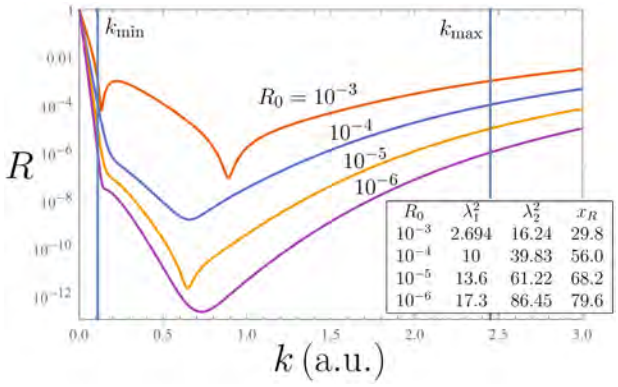

Figure 3: Reflection coefficient for the CAP in Eq. (4) as a function of electron momentum k. The table inset gives the potential parameters and absorption range for each minimum absorption parameter R_0. (Adapted from Ref. [R31].)

Future Plans

Having an analytical expression for R greatly simplifies re-optimizing our CAP for different energy ranges or absorption goals. We will spend some time working to parametrize R to make the process even simpler, but we do not expect to spend any further significant effort on this development. Rather, we will utilize this CAP in our TDSE codes.

References

[R1] M. Schultze, M. Fieß, N. Karpowicz, J. Gagnon, M. Korbman, M. Hofstetter, S. Neppl, A. L. Cavalieri, Y. Komninos, Th. Mercouris, C. A. Nicolaides, R. Pazourek, S. Nagele, J. Feist, J. Burgdörfer, A. M. Azzeer, R. Ernstorfer, R. Kienberger, U. Kleineberg, E. Goulielmakis, F. Krausz, and V. S. Yakovlev, Science **328**, 1658 (2010).

[R2] J. Su, H. Ni, A. Becker, and A. Jaroń-Becker, Phys. Rev. A **89**, 013404 (2014).

[R3] M. Ivanov and O. Smirnova, Phys. Rev. Lett. **107**, 213605 (2011).

[R4] C. H. Zhang and U. Thumm, Phys. Rev. A **84**, 065403 (2011).

[R5] I. A. Ivanov, Phys. Rev. A **83**, 023421 (2011).

[R6] J. M. Dahlström and E. Lindroth, J. Phys. B **47**, 124012 (2014).

[R7] R. Pazourek, J. Feist, S. Nagele, and J. Burgdörfer, Phys. Rev. Lett. **108**, 163001 (2012).

[R8] J. Wätzel, A. S. Moskalenko, Y. Pavlyukh, and J. Berakdar, J. Phys. B **48**, 025602 (2015).

[R9] M. D. Śpiewanowski and L. B. Madsen, Phys. Rev. A **86**, 045401 (2012).

[R10] K. Klünder, J. M. Dahlström, M. Gisselbrecht, T. Fordell, M. Swoboda, D. Guénot, P. Johnsson, J. Caillat, J. Mauritsson, A. Maquet, R. Taïeb, and A. L'Huillier, Phys. Rev. Lett. **106**, 143002 (2011).

[R11] D. Guénot, K. Klünder, C. L. Arnold, D. Kroon, J. M. Dahlström, M. Miranda, T. Fordell, M. Gisselbrecht, P. Johnsson, J. Mauritsson, E. Lindroth, A. Maquet, R. Taïeb, A. L'Huillier, and A. S. Kheifets, Phys. Rev. A **85**, 053424 (2012).

[R12] D. Guénot, D. Kroon, E. Balogh, E. W. Larsen, M. Kotur, M. Miranda, T. Fordell, P. Johnsson, J. Mauritsson, M. Gisselbrecht, K. Varjù, C. L. Arnold, T. Carette, A. S. Kheifets, E. Lindroth, A. L'Huillier, and J. M. Dahlström, J. Phys. B **47**, 245602 (2014).

[R13] C. Palatchi, J. M. Dahlström, A. S. Kheifets, I. A. Ivanov, D. M. Canaday, P. Agostini, and L. F. DiMauro, J. Phys. B **47**, 245003 (2014).

[R14] A. Maquet, J. Caillat, and R. Taïeb, J. Phys. B **47**, 204004 (2014).

[R15] D. Ursrey, F. Anis, and B. D. Esry, Phys. Rev. A **85**, 023429 (2012).

[R16] P. M. Paul, E. S. Toma, P. Breger, G. Mullot, F. Augé, H. G. M. Ph. Balcou, and P. Agostini, Science **292**, 1689 (2001).

[R17] G. S. J. Armstrong, J. McKenna, D. Ray, B. Gaire, M. Zohrabi, T. Severt, B. Berry, P. Feizollah, R. P. Kanaka, B. Jochim, F. Anis, D. Ursrey, J. V. Hernández, K. D. Carnes, I. Ben-Itzhak, and B. D. Esry (in preparation).

[R18] J. V. Hernández and B. D. Esry arXiv:0911.2693.

[R19] R. Heather and H. Metiu, J. Chem. Phys. **86**, 5009 (1987).

[R20] L. Tao and A. Scrinzi, New J. Phys. **14**, 013021 (2012).

[R21] U. V. Riss and H. Meyer, J. Chem. Phys. **105**, 1409 (1996).

[R22] J. Muga, J. Palao, B. Navarro, and I. Egusquiza, Phys. Rep. **395**, 357 (2004).

[R23] M. Tarana and C. H. Greene, Phys. Rev. A **85**, 013411 (2012).

[R24] R. Kosloff and D. Kosloff, J. Comp. Phys. **63**, 363 (1986).

[R25] A. Vibok and G. G. Balint-Kurti, J. Chem. Phys. **96**, 7615 (1992).

[R26] J. L. Krause, K. J. Schafer, and K. C. Kulander, Phys. Rev. A **45**, 4998 (1992).

[R27] T. N. Rescigno, M. Baertschy, W. A. Isaacs, and C. W. McCurdy, Science **286**, 2474 (1999).

[R28] F. He, C. Ruiz, and A. Becker, Phys. Rev. A **75**, 053407 (2007).

[R29] L. Tao, W. Vanroose, B. Reps, T. N. Rescigno, and C. W. McCurdy, Phys. Rev. A **80**, 063419 (2009).

[R30] A. Scrinzi, Phys. Rev. A **81**, 053845 (2010).

[R31] Y. Yu and B. D. Esry (in preparation).

Publications of DOE-sponsored research in the last 3 years

[P1] N. G. Kling, K. J. Betsch, M. Zohrabi, S. Zeng, F. Anis, U. Ablikim, B. Jochim, Z. Wang, M. Kübel, M. F. Kling, K. D. Carnes, B. D. Esry, and I. Ben-Itzhak, "Carrier-envelope phase control over pathway interference in strong-field dissociation of H_2^+," Phys. Rev. Lett. **111**, 163004 (2013).

[P2] T. Rathje, A. M. Sayler, S. Zeng, P. Wustelt, H. Figger, B. D. Esry, and G. G. Paulus, "Coherent control at its most fundamental: Carrier-envelope-phase-dependent electron localization in photodissociation of a H_2^+ molecular ion beam target," Phys. Rev. Lett. **111**, 093002 (2013).

[P3] J. Wu, M. Kunitski, M. Pitzer, F. Trinter, L. P. H. Schmidt, T. Jahnke, M. Magrakvelidze, C. B. Madsen, L. B. Madsen, U. Thumm, and R. Dörner, "Electron-nuclear energy sharing in above-threshold multiphoton dissociative ionization of H_2," Phys. Rev. Lett. **111**, 023002 (2013), although my name does not appear, C.B. Madsen was a postdoc in my group.

[P4] A. M. Sayler, J. McKenna, B. Gaire, N. G. Kling, K. D. Carnes, B. D. Esry, and I. Ben-Itzhak, "Elucidating isotopic effects in intense ultrafast laser-driven D_2H^+ fragmentation," J. Phys. B **47**, 031001(FTC) (2014).

[P5] L. Graham, M. Zohrabi, B. Gaire, U. Ablikim, B. Jochim, B. Berry, T. Severt, K. J. Betsch, A. M. Summers, U. Lev, O. Heber, D. Zajfman, I. D. Williams, K. Carnes, B. D.Esry, and I. Ben-Itzhak, "Fragmentation of CD^+ induced by intense ultrashort laser pulses," Phys. Rev. A **91**, 023414 (2015).

[P6] U. Lev, L. Graham, C. B. Madsen, I. Ben-Itzhak, B. D. Bruner, B. D. Esry, H. Frostig, O. Heber, A. Natan, V. S. Prabhudesai, D. Schwalm, Y. Silberberg, D. Strasser, I. D. Williams, and D. Zajfman, "Quantum control of photodissociation using intense, femtosecond pulses shaped with third order dispersion," J. Phys. B **48**, 201001(FTC) (2015).

[P7] Y. Yu, S. Zeng, J. V. Hernández, Y. Wang, and B. D. Esry, "Influence of the initial angular distribution on strong-field molecular dissociation," Phys. Rev. A **94**, 023423 (2016).

Controlling rotations of asymmetric top molecules: methods and applications

Vinod Kumarappan
James R. Macdonald Laboratory, Department of Physics
Kansas State University, Manhattan, KS 66506
vinod@phys.ksu.edu

Program Scope

The goal of this program is to improve molecular alignment methods, especially for asymmetric top molecules, and then use well-aligned molecules for further experiments in ultrafast molecular physics. We use multi-pulse sequences for 1D alignment and orientation and 3D alignment of molecules. We have identified a single metric for 3D alignment of molecules and used it to experimentally demonstrate a multi-pulse scheme for 3D alignment of asymmetric top molecules [P2]. By using two-pulse alignment and cold molecules for high harmonic generation, we have shown that a Cooper minimum and shape resonance in nitrogen can clearly be identified in the HHG spectrum of nitrogen [P1]. In this experiment we were able to extract the complete angle-dependence of the photo-ionization cross section of the molecule over a range of ∼20-65 eV. We have also demonstrated experimentally a multi-pulse technique (proposed by Zhang *et al.* [1]) for orienting polar molecules [P3]. Our main focus now is to further develop our method for extracting orientation-resolved information from rotational wavepacket dynamics, particularly for asymmetric top molecules. We are particularly interested in applying this method to obtain molecular frame photoelectron angular distributions.

Strong field ionization and fragmentation of sulphur dioxide:

In the past few years we have shown that the rotational wave packet dynamics induced by impulsive alignment of a molecule can be exploited to obtain the orientation dependence of probe-driven processes as well as the time evolution of the molecular axis distribution. Briefly, the angle-dependence of the measured signal is expressed as an expansion in a Wigner function basis, and the delay-dependent signal as a convolution of the time-dependent molecular axis distribution and the angle dependence of the probe process. The algorithm uses TDSE calculations of the rotational wavepacket and linear regression to deconvolve the two functions. In the case of asymmetric top molecules, this method (which we call Orientation Resolution from Rotational Coherence Spectroscopy, or ORRCS) can extract the dependence of probe-driven processes as a function of the two Euler angles that are necessary to specify the orientation of the molecule relative to a linearly polarized field. In many cases— non-dissociative ionization by an ultrashort laser pulse, for instance—this method is unique in this capability.ORRCS is also the only method available for determining the full 2dD rotational wavepacket dynamics in asymmetric tops. We are currently using this method to study angle-resolved strong field ionization in asymmetric tops and developing new measurement techniques based on ORRCS.

Continuing our experiments on measuring orientation-resolved strong-field ionization of asymmetric top molecules, we measured the delay-dependent ionization yields of SO_2. Using the ORRCS algorithm, we found the ionization occurs predominantly when the laser polarization is along the molecule's B axis, as would be expected from the HOMO orbital of the molecule [2]. The measured delay-dependence of the yield of the molecular ion, the fit to the data and the angle dependence of ionization extracted using ORRCS are shown in Fig. 1. Compared to our measurements of the

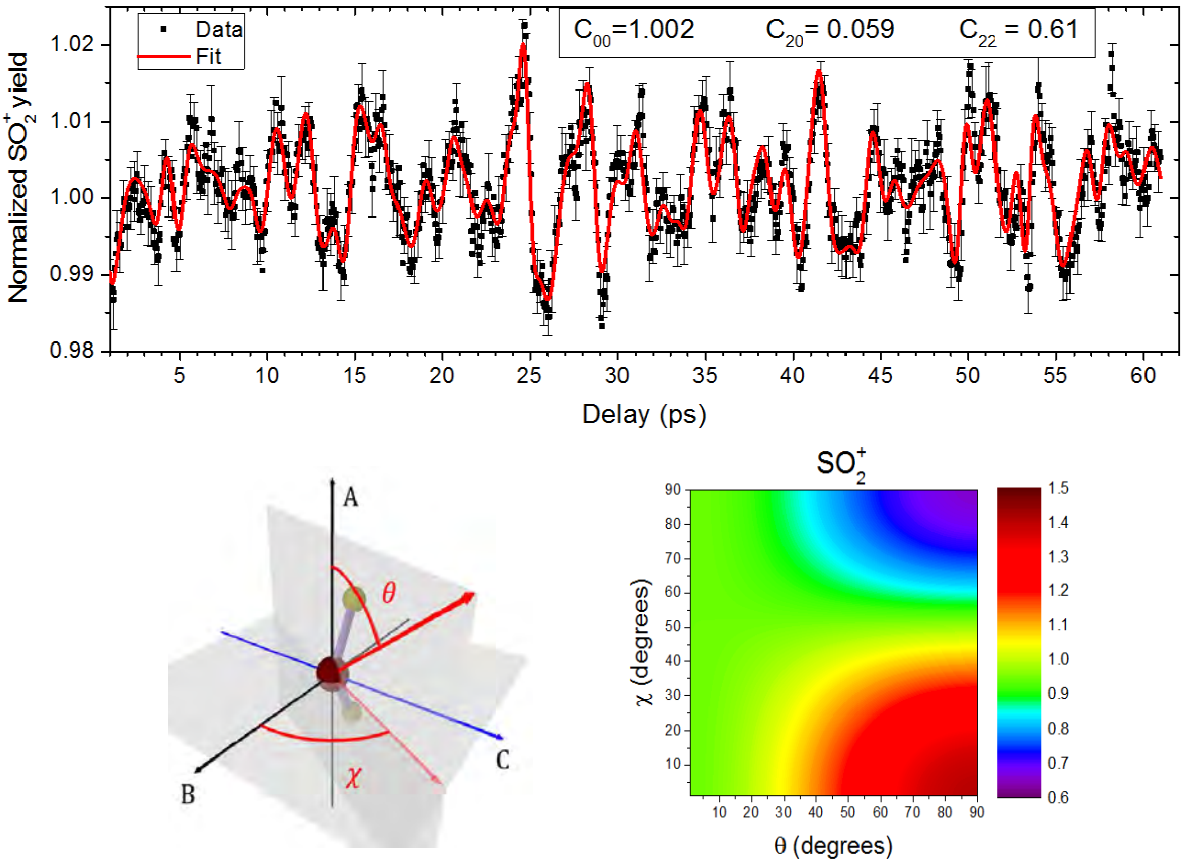

Figure 1: Top: Measured angle-integrated yield of SO_2^+ as a function of delay after an impulsive alignment pulse at zero delay. The solid red line is the best fit obtained using the ORRCS algorithm. Bottom left: The angular coordinates of the laser polarization in the molecular frame. Bottom right: The angle dependence of strong field ionization extracted using ORRCS. This dependence is consistent with expectations from the shape of the HOMO of the molecule, which has a large lobe along the B axis of the molecule [2].

ionization of ethylene, the variation of the ion yield with delay is significantly smaller, resulting in noisier data and extraction of only the lowest order angular parameters.

The yield of the SO^+ fragment ion, measured with higher probe intensity, shows a much stronger but simpler modulation. ORRCS analysis shows that this fragment is produced most efficiently when the laser is polarized along the A axis of the molecule. We see no dependence of the production of this fragment on the Euler angle χ.

We have also measured the delay-dependence of strong-field ionization of thiophene; the analysis of this data is in progress.

Strong-field-induced wave packet dynamics in carbon dioxide molecule:

In a collaboration lead by Artem Rudenko, we studied the wavepacket launched by an ionizing pump in carbon dioxide molecules using a probe pulse that further ionized the molecules. In these experiments, the pump and probe were both either 8 fs or 30 fs long. In each case, both the pump and the probe were intense enough to ionize the molecules and we measured the yield of the

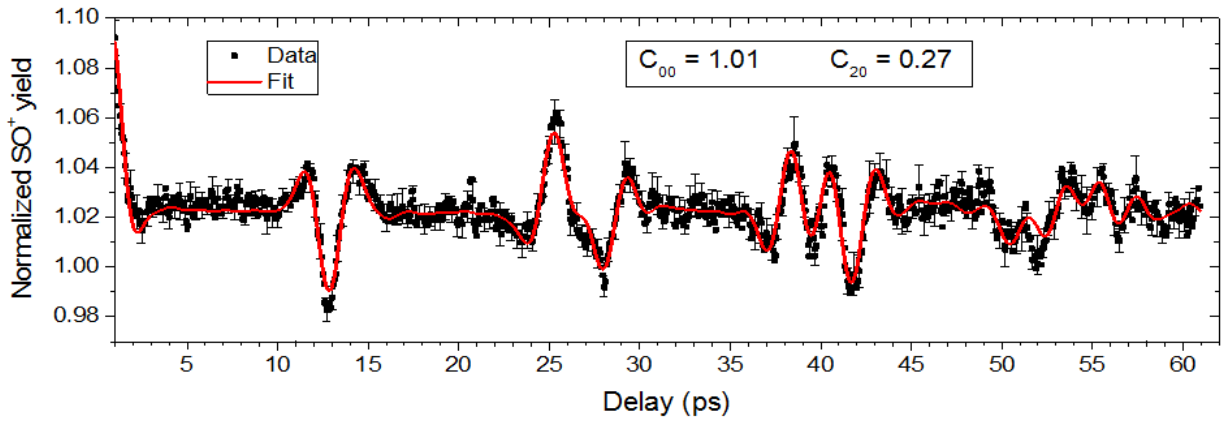

Figure 2: Measured delay-dependent SO^+ ion yield from SO_2 and the ORRCS fit to the data. The angle dependence is determined by $\langle \cos^2 \theta \rangle$ alone. This dependence on the most polarizible axis of the molecule leads simpler time evolution of the signal with stronger modulation than is seem in SO_2^+. The probe pulse in this experiment was 35 fs, 500 TW/cm^2.

molecular dication (CO_2^{2+}) as a function of pump probe delay. By Fourier analyzing of the time dependent signal, we were able construct a picture of the dynamics induced by the pump pulse. In the experiment with 8 fs pulses, the bandwidth of the pump pulse was broad enough to launch a vibrational wave packet in the neutral molecule via non-resonant Raman transitions. Realizing this turned out to be critical for interpreting the 8 fs data. But these pulses are too short to excite significant rotational motion. On the other hand, the 30 fs pulses are too narrow in bandwidth and too broad in time to excite a coherent vibrational wave packet, but do excite rotational motion. In both cases, we find clear evidence of a spin-orbit wave packet in the singly charged cation produced by the pump. An article has been accepted for publication in Faraday Discussions [P6].

Future plans:

We are building a fifth harmonic setup based on four-wave difference frequency mixing [3], which requires generating the third harmonic as an intermediate step. The third and the fifth harmonic sources will both be used for low-order multi-photon ionization of molecules. We will impulsively align molecules and measure the lab-frame photoelectron angular distributions as a function of delay between the 800 nm alignment pulse and the harmonic pulse. We will then attempt to obtain molecular frame photo-electron angular distributions from the delay dependence of the lab frame distributions.

We have also replaced our gated integrator setup with a high-speed digitizer. This not only allows us to simultaneously measure the delay-dependence of all the ionic fragments simultaneously, we also expect to be able to use ORRCS with covariance mapping to extract the orientation dependence of various fragmentation channels.

Publications from DOE-funded research:

[P1] X. Ren, V. Makhija, A.-T. Le, J. Troß, S. Mondal, C. Jin, V. Kumarappan and C. Trallero-Herrero, "Measuring the angle-dependent photoionization cross section of nitrogen using high-harmonic generation", Physical Review A 88, 043421 (2013).

[P2] X. Ren, V. Makhija, V. Kumarappan, "Multipulse Three-Dimensional Alignment of Asymmetric Top Molecules", Physical Review Letters 112, 173602 (2014).
[P3] X. Ren, V. Makhija, H. Li, M. F. Kling, V. Kumarappan, "Alignment-assisted field-free orientation of rotationally cold CO molecules", Physical Review A 90, 013419 (2014).
[P4] J. Yang, V. Makhija, V. Kumarappan, M. Centurion, "Reconstruction of three-dimensional molecular structure from diffraction of laser-aligned molecules", Structural Dynamics 1, 044101 (2014).
[P5] Benjamin Langdon, Jonathan Garlick, Xiaoming Ren, Derrek J. Wilson, Adam M. Summers, Stefan Zigo, Matthias F. Kling, Shuting Lei, Christopher G. Elles, Eric Wells, Erwin D. Poliakoff, Kevin D. Carnes, Vinod Kumarappan, Itzik Ben-Itzhak, and Carlos A. Trallero-Herrero, "Carrier-envelope-phase stabilized terawatt class laser at 1 kHz with a wavelength tunable option," Opt. Express 23, 4563-4572 (2015).
[P6] Artem Rudenko, Varun Makhija, Aram Vajdi, Thorsten Ergler, Markus Schuerholz, Robert Moshammer, Joachim Ullrich, and Vinod Kumapparan, "Strong-field-induced wave packet dynamics in carbon dioxide molecule", Faraday Discuss. 2016, (accepted).

References:

[1] S. Zhang *et al.*, Phys. Rev. A **83**, 043410 (2011).
[2] L. S. Spector *et al.* Nature Communications **5**, 3190 (2014).
[3] M. Beutler, M. Ghotbi, F. Noack, and I.V. Hertel, Opt. Lett. 35, 1491-1493 (2010)

Strong field rescattering physics and attosecond physics

C. D. Lin
J. R. Macdonald Laboratory, Kansas State University
Manhattan, KS 66506
e-mail: cdlin@phys.ksu.edu

Program Scope:
We investigated the interaction of ultrafast intense laser pulses, and of attosecond pulses, with atoms and molecules. Most notable accomplishments in the past year are: (1) Extracting bond lengths of C_2H_2 molecules at equilibrium and of $C_2H_2^{++}$ at the breakup using laser-induced electron diffraction method; (2) Developing new methods of retrieving the XUV, the IR or the atomic dipole phase in attosecond streaking measurements; (3) Work with experimental group to demonstrate the buildup of Fano resonances in the time domain; (4) Developing inner-shell photoelectron diffraction method for dynamic imaging; and (5) Optimization of phase matching conditions for high-order harmonic generation. Additional results and plans for the coming year will also be summarized.

1. Laser-induced electron diffraction (LIED) from aligned polyatomic molecules

Recent progress
In the last grant period four publications (A1, A4, A11, and A13) have been published on LIED to determine the bond lengths of small molecules at equilibrium distances, and another which measures bond lengths 9 fs later after an electron is removed. This is possible because of the 160 kHz, 3.1 micron laser at Barcelona (Biegert's group) is available for LIED experiment. Molecules are either aligned or not aligned. Two methods have been used to extract information from the photoelectrons. One is the fitting method and the other is the Fourier transform method. With LIED, we showed that the C-C and C-H bond lengths for hydrocarbon molecules can both be accurately retrieved. In (B1) the change of C-H and C-C bond length in the dissociative ionization of $C_2H_2^{++}$ dication 9 fs after ionization have also been derived from the photoelectron spectra in coincidence with the C_2H^+ and H^+ breakup channel. The extracted bond lengths are consistent with results from quantum chemistry calculations. We also worked with Ueda's group in Sendai to extract C-C and C-H bond lengths from the benzene molecule.

Future plan
We are extending LIED to larger asymmetric polyatomic molecules. If the molecules are partially 1D aligned, it was shown in [A11] that it is possible to extract 2D bond length information. We continue collaborating with Biegert's group where LIED experiments are being carried out. LIED as a powerful tool for dynamic imaging of molecules has now been shown by three different experimental groups. The method is especially useful for dynamics of light atoms in a molecule.

2. Observation of buildup of Fano resonances in the time domain

Recent progress
In a 2010 paper we predicted the buildup of a Fano resonance in the time domain. The prediction has now been verified by Thomas Pfeifer's group at Heidelberg using transient absorption spectroscopy method. They did the XUV-IR experiment near 60 eV, in photon energy range around the 2s2p state state of helium. The IR used was intense such that it is capable of quickly ionizing the "bound" 2s2p part of the resonance to stop further decay. By analyzing the

transient absorption spectra versus different time delays, the gradual buildup of the resonance in the time domain can be directly observed from the experimental data. This work has been submitted for publication.

3. Retrieval of XUV, IR or atomic dipole phase in attosecond streaking experiments

Recent progress

To determine the pulse duration of an XUV attosecond pulse the standard approach is to measure photoelectron spectra of the XUV in the presence of a time delayed IR. Using the so-called FROG-CRAB method, the phase of the XUV pulse can be retrieved. The same method has been also used to obtain the phase of the atomic dipole transition matrix element, or equivalently, the so-called time delay. The photoionization time delay difference of 21-as between the 2p and 2s states of Ne reported by the MPQ group had been shown to be much larger than any theoretical calculations. Over the past five years this discrepancy has been investigated thoroughly by theorists. We looked into how the 21-as was derived from the experimental data, and concluded that the source of the discrepancy is due to the retrieval method used in the experiment, partly by the central momentum approximation and partly due to the inaccuracy of the FROG-CRAB retrieval algorithm. This work was reported in [A5].

We have since developed a new retrieval method.

Ongoing projects and future plan

The retrieval method we developed is more accurate and stable than FROG-CRAB and can retrieve the IR pulse accurately as well. Our method also does not rely on the central momentum approximation. In our ongoing work, we showed that our new method can be used to characterize broadband single attosecond pulses in the water-window region. The method also can be used to characterize short IR pulses including synthesized multi-color waveforms. We are hoping to use the algorithm to enable *in situ* characterization of both the XUV and the IR pulses in attosecond experiments where such information has not been available.

4. Retrieving bond lengths using inner-shell photoelectron diffraction method

Recent progress

The so-called inner-shell photoelectron diffraction (ISPD) method has been used to probe the interatomic distances of a molecule. An inner-shell electron from a known atom in the molecule can be ionized by a hard X-ray, the emitted electron can go directly to the detector, or scattered by other atoms in the molecule before arriving at the detector. The interference in the photoelectron angular distributions contain interatomic separation information. The method works well if the molecule is fixed in space. We looked into this problem for gas-phase molecules and found that the diffraction image is readily destroyed if the molecules have rotational motion, thus making ISPD not useful for gas-phase molecules. However, we did find another way to salvage the method. We showed in [A7] that we are able to retrieve the change of bond lengths using ISPD if the molecules are partially 1D aligned and that the diffraction images are taken from a few different directions of the light polarizations with respect to the alignment axis of the molecule. We anticipate that this method be implemented at XFEL light sources for the dynamic imaging studies.

In another related photoelectron imaging project we mention that it is well known that standard photoelectron spectra are not very sensitive to the small change of the geometry of a molecule. The situation changes if there exists a shape resonance in the energy range of interest. In [A3] we found that we can take advantage of this situation to probe small change of bond

length in the SF_6 molecule. For specific cases this may also afford a new method of studying dynamics of molecules using lower energy photoelectrons where ISPD is not possible.

5. Optimization of phase matching to generate low-divergence soft X-rays harmonics

Recent progress

We continue to collaborate with my former student Cheng Jin who now teaches in Nanjing University of Science and Technology in China on waveform synthesis and macroscopic effects of high-order harmonic generation, focusing on the optimization of extending the cutoff energy, the enhancement of harmonic yields and on favorable macroscopic phase matching. In [A12] we studied the pressure and the radius of a hollow core fiber that would generate low-divergence soft X-ray harmonics such that it would not require further focusing of the beam for applications. We also investigated harmonics generated under high laser intensity and high gas pressure situations, and perform analysis that would explain how phase matching occurs under the optimized conditions. These works have been submitted for publications at this writing.

Additional items

Recent progress

During the past grant period, we published a Tutorial Article [A9] in Journal of Physics B, on the strong field approximation for harmonic generation at mid-infrared lasers. We also have re-examined the PPT theory so that it can be used to calibrate the laser intensities by experimentalists, see [A8], one paper [A10] on sequential double ionization of helium with rigorous quantum simulation, and a collaboration to study the effect of nonadiabatic ionization in strong field photoelectron holography [A2].

Publications

A. Published and accepted papers (2015- present)

A1. Michael G. Pullen, Benjamin Wolter, Anh-Thu Le , Matthias Baudisch, Michele Sclafani, Hugo Pires, Claus Dieter Schröter, Joachim Ullrich, Robert Moshammer , Thomas Pfeifer , C. D. Lin , and Jens Biegert, " Influence of orbital symmetry on diffraction imaging with rescattering electron wave packets", Nature Communications, 7, 11922 (2016).

A2. Xiaohong Song, Cheng Lin, Zhihao Sheng, Peng Liu, Zhangjin Chen, Weifeng Yang, Shilin Hu, C. D. Lin, and Jing Chen, "Unraveling nonadiabatic ionization and Coulomb potential effect in strong-field photoelectron holography", Scientific reports, 6, 28392 (2016).

A3. Ngoc-Ty Nguyen, R. R. Lucchese, C. D. Lin and Anh Thu Le, "Probing and extracting structure of vibrating SF_6 molecules with inner-shell photoelectrons", Phys. Rev. A93, 063419 (2016).

A4. Yuta Ito, Chuncheng Wang, Anh-Thu Le, Misaki Okunishi, Dajun Ding, C. D. Lin, and Kiyoshi Ueda, "Extracting conformational structure information of benzene molecules via laser-induced electron Diffraction", Structure Dynamics, 3, 034303 (2016)

A5. Hui Wei and C. D. Lin, "Critical evaluation of attosecond time delays retrieved from photoelectron streaking measurements", Phys. Rev. A93, 053412 (2016)

A6. M. Reduzzi, W.-C. Chu, C. Feng, A. Dubrouil, J Hummert, F. Calegari, F. Frassetto, L. Poletto, O. Komilov, M. Nisoli, C.-D. Lin, G. Sansone, "Observation of autoionization dynamics and sub-cycle quantum beating in electronic molecular wave packets", J. Phys. B49, 065102 (2016).

A7. Xu Wang , Anh-Thu Le , Chao Yu , R. R. Lucchese, and C. D. Lin, " Retrieving transient conformational molecular structure information from inner-shell photoionization of laser-aligned molecules", Scientific Reports, 6, 23655 (2016).

A8. Song-Feng Zhao, Anh-Thu le, Cheng Jin and C. D. Lin, "Calibrating laser intensity in experiments using an analytical ionization model", Phys. Rev. A93, 023413 (2016).

A9. Anh-Thu Le, Hui Wei, Cheng Jin, and C. D. Lin, "Strong field approximation in high-order harmonic generation with mid-infrared lasers", J. Phys. B49, 053001 (2016) (Tutorial)

A10. Zhangjin Chen, Yanyan Zheng, Weifeng Yang, Xiaohong Song, J. L. Xu, L. F. DiMauro, O. Zatsarinny, K. Bartschat, T. Morishita, S. F. Zhao, and C. D. Lin, "Numerical simulation of the ratio between double and single ionization of He in strong laser field", Phys. Rev. A92, 063427 (2015)

A11. Chao Yu, Hui Wei, Xu Wang Anh Thu Le , Ruifeng Lu, and C. D. Lin, "Reconstruction of two-dimensional molecular structure with laser-induced electron diffraction from laser-aligned polyatomic molecules", Scientific Reports, 5, 15753 (2015).

A12. Cheng Jin, Gregory J. Stein, Kyung-Han Hong and C. D. Lin," Generation of Bright, Spatially Coherent Soft X-Ray High Harmonics in a Hollow Waveguide Using Two-Color Synthesized Laser Pulses", Phys. Rev. Lett. 115, 043901 (2015).

A13. Michael Pullen , Benjamin Wolter, Anh-Thu Le, Matthias Baudisch, Michaël Hemmer, Arne Senftleben, Claus Dieter Schröter, Joachim Ullrich, Robert Moshammer, C. D. Lin, Jens Biegert, " Imaging an aligned polyatomic molecule with laser-induced electron diffraction", Nature Comms. 6, 7262 (2015).

A14. Hui Wei, Anh-Thu Le, Toru Morishita, Chao Yu, and C. D. Lin " Benchmarking accurate spectral phase retrieval of single attosecond pulses" , Phys. Rev. A 91, 023407 (2015).

B. Papers accepted for Publications

B1. Cheng Jin and C. D. Lin, "Optimization of multi-color laser waveform for high-order harmonic Generation", Chinese Phys. B, (A review)

Imaging Ultrafast Dynamics in Polyatomic Molecules

Daniel Rolles
J.R. Macdonald Laboratory, Physics Department, Kansas State University,
Manhattan, KS 66506, rolles@phys.ksu.edu

Program Scope: *This program focuses on imaging nuclear and electronic dynamics during photochemical reactions by means of femtosecond pump-probe experiments with laboratory-based laser sources complemented by experiments with free-electron lasers and 3rd generation synchrotrons. The aim of these experiments is to study exemplary reactions in gas-phase molecules with the goal of clarifying their reaction mechanisms and pathways.*

Recent Progress: In my second year as an assistant professor in the Physics Department at Kansas State University, I have continued setting up new experimental capabilities at the J.R. Macdonald Laboratory while simultaneously pursuing an active research program using the existing experimental facilities at JRML as well as various external user facilities. My main focus was on (i) studying ultrafast nuclear wave-packet dynamics and charge transfer processes in halomethanes by performing pump-probe experiments using ultrafast ultraviolet and near-infrared lasers, free-electron lasers, and high harmonic generation sources; and (ii) on investigating the photoionization and fragmentation dynamics of structural isomers using photoelectron-ion-ion coincidence experiments. These projects were performed in close collaboration with other experimentalists at JRML and with outside collaborators.

(i) Ultrafast nuclear wave-packet dynamics and charge transfer in halomethanes, *F. Ziaee, Y. Malakar, B. Kaderiya, S. Pathak, W.L. Pearson, K.R. Pandiri, I. Ben-Itzhak, A. Rudenko, D. Rolles, E. Savelyev[1], R. Boll[1], C. Bomme[1], B. Erk[1], S. Techert[1], J. Küpper[1], T. Laarmann[1], M. Brouard[2], A. Rouzee[3], T. Marchenko[4], M. Simon[4], H. Stapelfeldt[5], J. Rothhardt[6], S. Hädrich[6], J. Limpert[6], A. Tünnermann[6]; [1]DESY, Hamburg, Germany; [2]Oxford University, UK; [3]Max-Born-Institut, Berlin, Germany; [4]UPMC/CNRS, Paris, France; [5]Arhus University, Denmark; [6]Helmholtz-Zentrum & Uni Jena, Germany.*

In collaboration with the Rudenko and the Ben-Itzhak groups, we have continued our investigations of the dynamics of bound and dissociating nuclear wave packets in strong-field ionized CH_3I molecules via time-resolved Coulomb explosion imaging using an interferometric pump-probe scheme at JRML's 10-kHz PULSAR femtosecond laser system combined with a COLTRIMS ion momentum imaging setup. By analyzing the ion yields of various ionic fragments and ion-ion coincidence channels as a function of time delay between two 25-fs, 800-nm pump and probe pulses, we are able to identify vibrational motion in both neutral and cationic states. Figure 1 shows the delay and kinetic energy dependent ion yields for $CH_3^+ + I^+$ ion-ion coincidences as well as all detected I^+ ions. Both bound and dissociating nuclear wave packets can be clearly distinguished. A Fourier transform of the oscillatory features that are observed in the highlighted regions reveal frequencies corresponding to C-I stretching vibrations in both the neutral and two cationic states.

In order to expand the range of our pump-probe experiments beyond processes induced by strong-field ionization, we have recently build a third harmonic generation setup and a UV prism compressor for the PULSAR laser system and have performed first experiments studying the UV-induced photodissociation of various halomethanes. These in-house experiments complement our investigations of photodissociation and charge transfer processes in halomethanes using time-resolved photoelectron and ion imaging, which we performed at the FLASH free-electron laser within a large international collaboration that was led by my group. In addition to delay-dependent effects in the ion yields and kinetic energies similar to those shown in Figure 1, we also observe time-dependent energy shifts in the photoelectron and Auger electron spectra, which are currently under analysis.

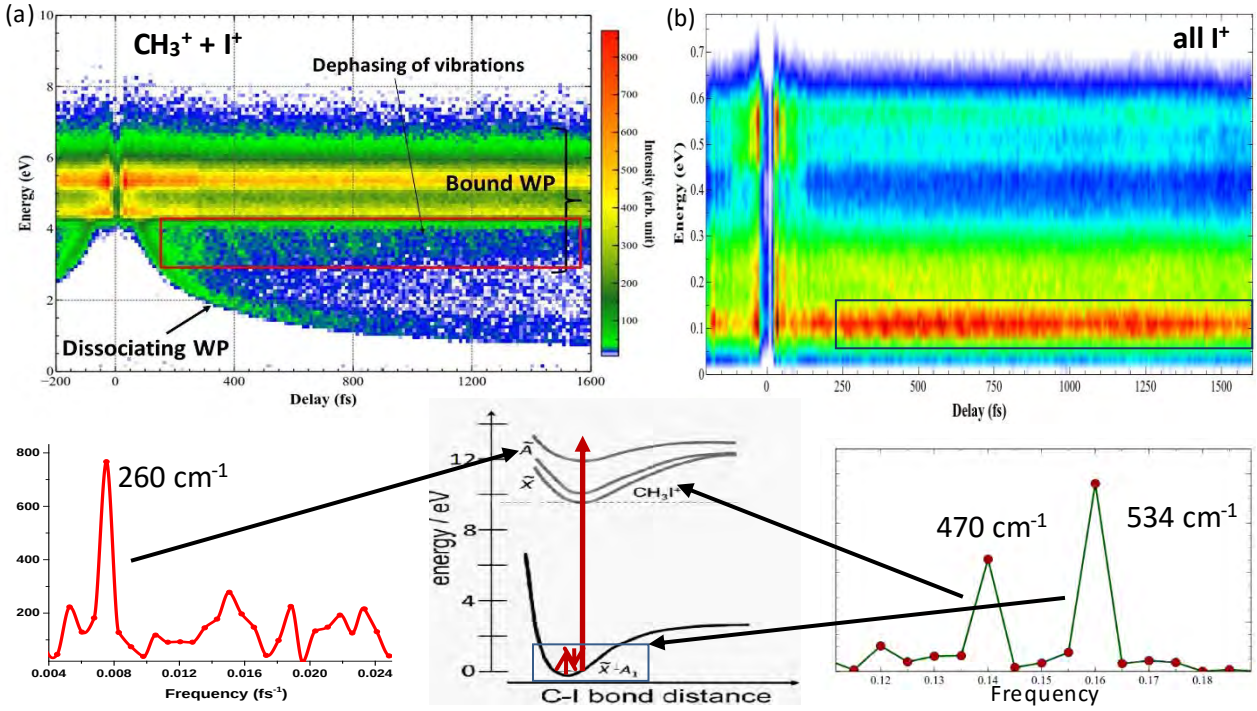

Figure 1: *Delay and kinetic energy dependent yields of the (a) $CH_3^+ + I^+$ coincidence channel and (b) all detected I^+ ion. Fourier transformation of the oscillations in the ion yield within the regions highlighted by the squares reveal three different frequencies corresponding to vibrational motion in different neutral and cationic states, as shown in the panels in the bottom row. The intensity was 1.5 x 10^{14} W/cm^2 for both, pump and probe pulses.*

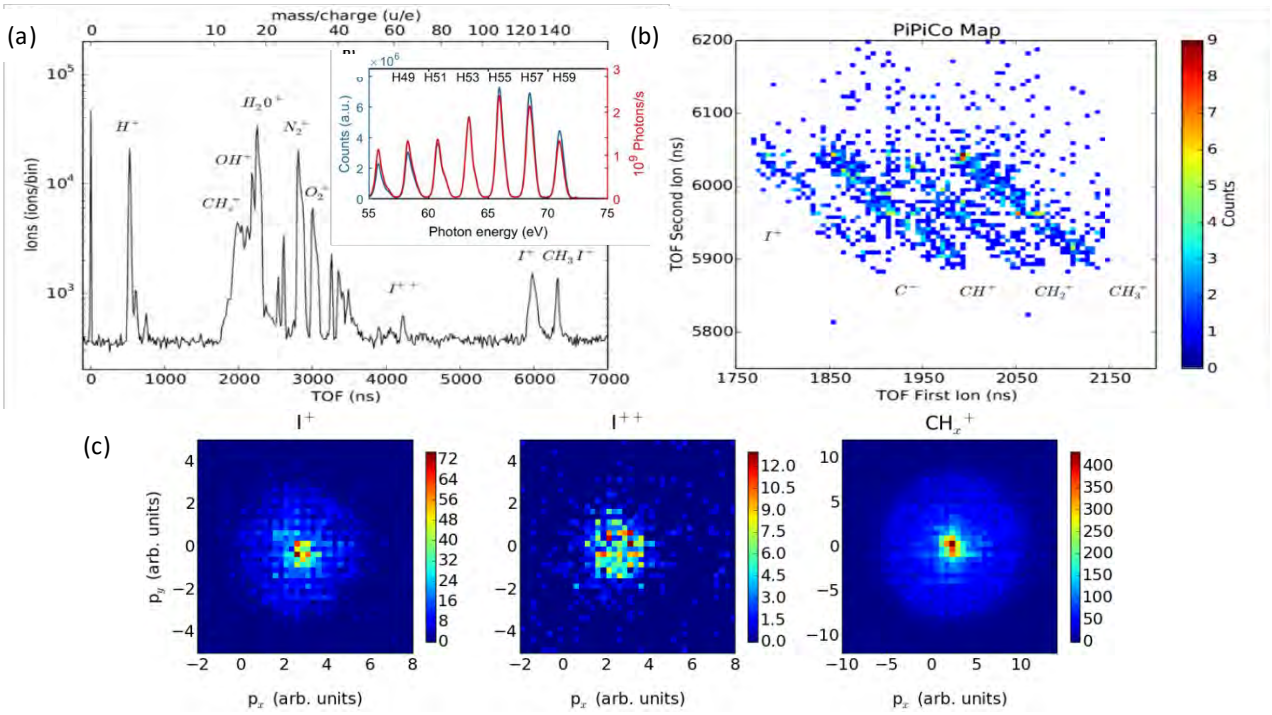

Figure 2: *(a) Ion time-of-flight spectrum of CH_3I recorded at 68.6 eV photon energy with the Jena HHG source. The inset shows the harmonic spectrum in the range of H47 to H59. (b) Ion-ion coincidence spectrum of CH_3I in the region containing the coincidences between CH_x^+ (x = 0, ..., 3) and I^+ fragments. Only those events were considered where two ionic fragments were detected in coincidence with a photo- or Auger electron. (c) Two-dimensional ion momentum distributions for I^+, CH_x^+, and CH_3I^+ fragments. The figures are taken from Ref. [1].*

Another experimental capability that we are currently developing in our lab at JRML are pump-probe experiments using our high harmonic generation XUV source XUUS in combination with NIR or UV pulses from PULSAR. As a first test, we have recently performed first RABBITT-type measurements and are now setting up an electron-ion coincidence apparatus to be used for these pump-probe experiments. In order to do some first experiments while still developing this system, we partnered with the group of Jan Rothhardt and Jens Limpert in Jena, Germany, and brought one of our electron-ion coincidence machines to their lab in order to combine it with their high-repetition rate XUV source. Using the 57th harmonic at 68.6 eV photon energy, which provided a photon flux of more than 10^{11} photons/s at a 50-100 kHz repetition rate, we were able to record photoelectron-ion coincidence data for the I(4d) inner-shell ionization of CH_3I in a pump-probe arrangement [1]. Figure 2 shows the ion time-of-flight spectrum, an ion-ion coincidence plot, and the momentum distributions of three exemplary fragment ions recorded in this experiment, demonstrating, for the first time, the capability to perform electron-ion-ion coincidence experiments after inner-shell ionization with an HHG source.

(ii) Photoionization and fragmentation dynamics of structural isomers, *U. Ablikim, B. Kaderiya, S. Augustin, A. Rudenko, V. Kumarappan, D. Rolles, C. Bomme[1], E. Savelyev[1], T. Osipov[2], R. Obaid[3], H. Xiong[3], N. Berrah[3]; [1]DESY, Hamburg, Germany; [2]LCLS, SLAC National Laboratory; [3]University of Connecticut.*

We have studied the photoionization and fragmentation dynamics of structural isomers of various halogenated hydrocarbons after inner-shell ionization by conducting photoelectron-photoion coincidence experiments with synchrotron radiation at the ALS. We demonstrate that it is possible to determine the geometric structure and to thus distinguish different geometric isomers from the momentum correlations between the ionic fragments that are detected in coincidence, as shown in for the example of *cis* and *trans* 1,2-dibromoethene in Figure 3. This allows determining isomer-resolved photoelectron spectra and ion kinetic energies as well as the isomer ratio of isomerically mixed samples, thus providing a promising experimental avenue to study isomerization reactions in time-resolved Coulomb explosion imaging experiments.

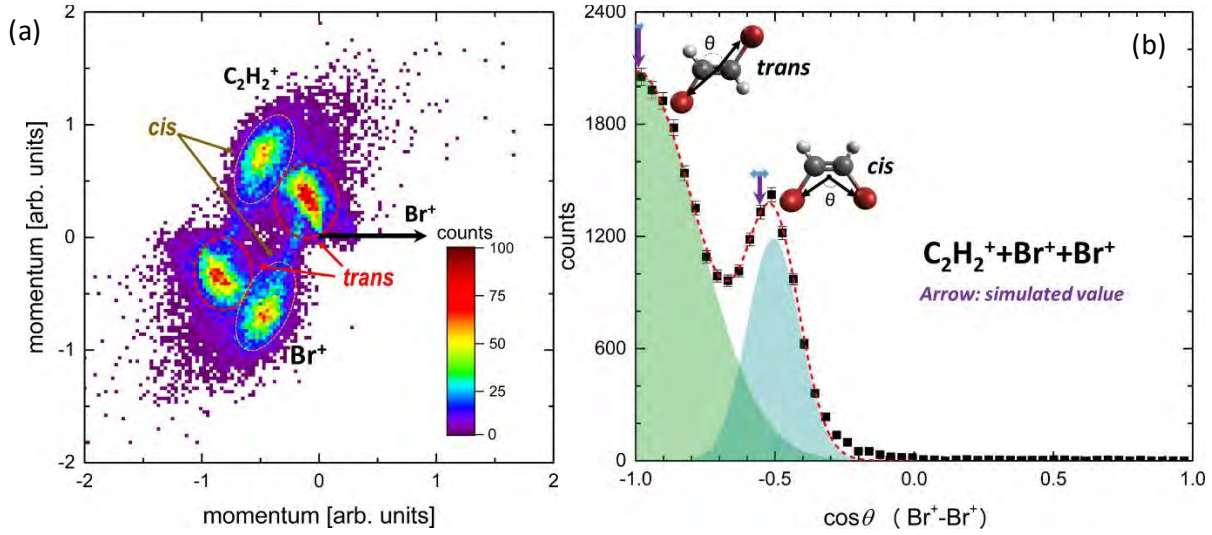

Figure 3: *(a) Newton diagram for $C_2H_2^+$-Br^+-Br^+ triple coincidences recorded after Br(3d) photoionization of 1,2-dibromoethene ($C_2H_2Br_2$) at 140 eV photon energy. The contributions corresponding to the cis and trans structures are indicated. (b) Angle between the momentum vectors of the two Br^+ ions for the $C_2H_2^+$-Br^+-Br^+ triple coincidence channel. A fit of two Gaussians (shaded areas) to the experimental data (squares) allows determining the ratio of the cis and trans isomers. The figures are taken from U. Ablikim et al., submitted (2016).*

Future Plans:
We will continue to use the pump-probe and coincidence techniques that we have developed over recent years in order to investigate photochemical reactions in gas-phase molecules while, in parallel, working on improving the existing methods and on developing new schemes for imaging molecular dynamics with femtosecond and sub-femtosecond resolution. In the immediate future, the focus will lie on exploiting the new capabilities for short-pulse UV-generation and XUV pump-probe experiments to study dissociation and isomerization reactions in halomethanes and haloethanes. We will also continue our FLASH, LCLS, and ALS experiments and have approved beamtime scheduled at all three facilities in the coming year. These experiments also aim at investigating ultrafast reaction dynamics but focus on utilizing the complementary capabilities of the X-rays provided by these facilities as compared to the ultrafast laser sources available at JRML.

Publications from DOE sponsored research since joining the program in 2015:

1. J. Rothhardt, ..., D. Rolles, *High-repetition-rate and high-photon-flux 70 eV high-harmonic source for coincidence ion imaging of gas-phase molecules*, Optics Express **24**, 18133-18147 (2016).
2. A. Picon, …, A. Rudenko, …, D. Rolles, …, S. H. Southworth, *Hetero-site-specific ultrafast intramolecular dynamics*, Nat. Commun. **7**, 11652 (2016).
3. T. Gorkhover, …, D. Rolles, A. Rudenko, T. Möller, C. Bostedt, *Femtosecond and nanometer visualization of structural dynamics in superheated nanoparticles*, Nature Photon. **10**, 93-97 (2016).
4. R. Boll, …, D. Rolles, A. Rudenko, *Charge transfer in dissociating iodomethane and fluoromethane molecules ionized by intense femtosecond X-ray pulses*, Struct. Dyn. **3**, 043207 (2016).
5. C. S. Lehmann, …, A. Rudenko, …, D. Rolles, …, S. H. Southworth, *Ultrafast x-ray-induced nuclear dynamics in diatomic molecules using femtosecond x-ray-pump – x-ray-probe spectroscopy*, Phys. Rev. A **94**, 013426 (2016).
6. C. F. Jones, …, D. Rolles, A. Rudenko, …, C. Bostedt, O. Gessner, A.F. Vilesov, *Coupled motion of Xe clusters and quantum vortices in He nanodroplets*, Phys. Rev. B **93**, 180510(R) (2016).
7. C. E. Liekhus-Schmaltz, …, D. Rolles, A. Rudenko, …, P.H. Bucksbaum, V.S. Petrovic, *Ultrafast Isomerization Initiated by X-Ray Core Ionization,* Nature Commun. **6**, 8199 (2015).
8. R.M.P. Tanyag, …, D. Rolles, …, A. Rudenko, …, C. Bostedt, O. Gessner, A.F. Vilesov, *X-ray coherent diffractive imaging by immersion in nanodroplets*, Struct. Dyn. **2**, 051102 (2015).
9. T. Kierspel…, D. Rolles, A. Rudenko, …, J. Küpper, *Strongly aligned gas-phase molecules at Free-Electron Lasers*, J. Phys. B: At. Mol. Opt. Phys. **48**, 204002 (2015).
10. A. Rudenko and D. Rolles, *Time-resolved studies with FELs*, J. Electron Spectrosc. Relat. Phenom. **204**, 228-236 (2015).
11. K. Schnorr, … A. Rudenko, …, D. Rolles, …, R. Moshammer, *Time-Resolved Study of ICD in Ne Dimers Using FEL Radiation*, J. Electron Spectrosc. Relat. Phenom. **204**, 245-256 (2015).
12. T. Ekeberg, …, D. Rolles, A. Rudenko, …, J. Hajdu, *Three-dimensional reconstruction of the giant mimivirus particle with an X-ray free-electron laser,* Phys. Rev. Lett. **114**, 098102 (2015).

Imaging light-induced dynamics of small quantum systems: From infrared to hard X-ray domain

Artem Rudenko

J. R. Macdonald Laboratory, Department of Physics, Kansas State University, Manhattan, KS 66506

rudenko@phys.ksu.edu

Program scope: The main goals of this research are (i) to understand basic physics of (non-linear) light-matter interactions in a broad span of wavelengths, from terahertz and infrared (IR) to XUV and X-ray domains, and (ii) to apply the knowledge gained for real-time imaging of ultrafast photo-induced reactions. These goals are being pursued using both, lab-based laser and high-harmonic sources, and external free-electron laser (FEL) facilities. The program aims at studying light-induced phenomena in systems of increasing complexity, from isolated atoms to small and mid-size molecules, recently extending to nanoscale particles.

Recent progress:

1. X-ray interactions with matter: extreme multiphoton ionization and charge transfer dynamics
(in collaboration with D. Rolles and Argonne National Lab group)

The development of high-intensity, short-pulsed XUV and X-ray radiation sources promises revolutionary new imaging techniques in diverse scientific fields, approaching angstrom spatial and femtosecond (or even sub-femtosecond) temporal resolution [1-5,16,17]. The basic prerequisite for designing these experiments is understanding the response of individual atoms, and tracing electronic and nuclear dynamics in the vicinity of the atom that absorbed X-ray photon(s) [2,5]. In extended systems this sheds light on basic mechanisms of local radiation damage, and is also vital for novel phase retrieval methods at high intensities. Addressing these issues, we have recently performed a series of IR-pump – X-ray probe [6,7] and XUV pump –XUV-probe [8,13] experiments aimed at studying the mechanisms of this charge rearrangement, in particular, electron transfer. Main developments within the last year focused on extending similar single pulse experiments into hard X-ray domain and ultra-high intensities, and on employing novel pump-probe schemes, including UV-pump – X-ray probe [18] and X-ray pump – X-ray probe schemes [12,19,20]. While our results obtained with UV pump pulses [18], which triggers a well-defined dissociation pathway, confirmed the conclusions of earlier experiments with 800 nm pump [6], the development of the two-colour X-ray pump-probe arrangement [19,20] allowed exploiting site-specific interactions by both, the pump and the probe steps.

Since XFEL imaging experiments mentioned above ideally require angstrom wavelengths and extreme intensities (> 10^{20} W/cm^2) to reach atomic resolution, there is a strong need to extend basic experiments on individual atom / small molecule response into this parameter regime. Recently we have accomplished first steps in this direction by studying ionization of rare gas atoms and small polyatomic molecules by ultra-intense X-ray radiation at 5-8 keV photon energy range. The experiments were performed using the nanofocus of the coherent imaging beamline (CXI) at LCLS. Focusing few mJ, 40 fs hard X-ray LCLS pulses to a spot size less than 250 nm in diameter, we were able to reach the intensities exceeding 10^{20} W/cm^2, unprecedented for this photon energy range. Under these conditions we were able to strip all electrons from argon atoms, all but two 1s electrons from krypton, and reached the record 48+ charge state for xenon ionization at 8.3 keV. Even though the highest charge states is reached at the highest photon energy (8.3 keV), the wavelength dependence of the spectra shows significant overall enhancement in the production of charge states from Xe^{30+} to Xe^{40+} at the intermediate photon energies (~ 6.5 keV). Comparing the data with the simulation based on the XATOM model of R. Santra's group, we conclude that the simple sequential ionization picture needs to be modified to include resonant excitations to explain the obtained results, although the resonant effects are not as extreme as in the soft X-ray regime [2,5]. Following the approach we developed earlier for the XUV and the soft-X-ray domains, we compared the ionization of isolated xenon atoms and iodine atoms embedded into molecular systems, and obtained first experimental results on ultrafast charge rearrangement in small and medium-size molecules. In contrast to our results in the soft X-ray regime [2,5], the presence of molecular partners does not significantly reduce the highest charge state observed for high-Z elements in small systems. As illustrated in Fig. 1, we observed I^{47+} ions from iodomethane (CH_3I) at 8.3 keV compared to Xe^{48+}. The most likely reason for this is an efficient charge rearrangement filling the created vacancies on the iodine site with the electrons from the neighbouring atoms along with a very large photon density allowing for further ionization of partially neutralized iodine. To verify this, we collaborated on similar experiments on Xe / CH_3I at the Japanese XFEL facility SACLA, which were also performed at hard X-ray photon energies, but at much lower intensities [11,22,23]. There, the outcome was rather similar to earlier results in the soft-X-ray domain, confirming that this is the high photon densities on target which results in higher ionization of molecules. Even for larger systems like iodobenzene (C_6H_5I), the maximum charge state observed is ~ I^{45+},

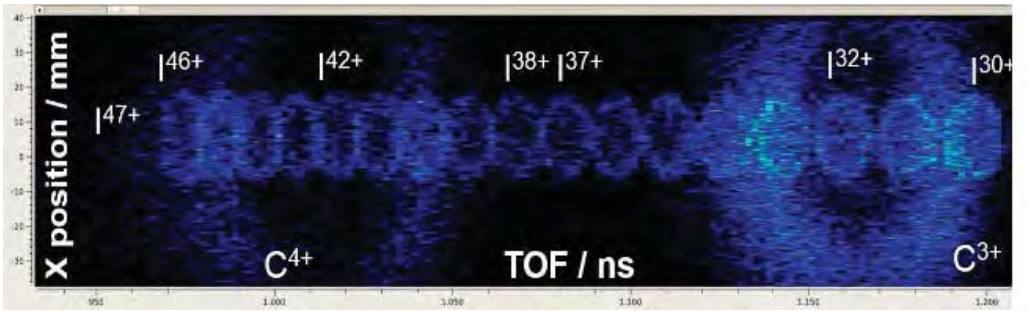

Figure 1. *Ion TOF plotted as a function of the position on the detector for CH_3I fragmentation by ultraintense LCLS pulses at 8.3 keV. This spectrum essentially represents the scaled momentum distribution of each fragment projected onto the corresponding plane. Only the region of short TOFs (high charge states) is included.*

indicating that the charge transfer from the neighbouring atoms can very efficiently fuel further ionization ifenough electrons are present. The highest charge state of carbon, which does not directly absorb X-ray photons is C^{4+} for both, CH_3I and C_6H_5I molecules, which is in good agreement with the prediction of our charge transfer model used in [6,8]. The results of this experiments are summarized in a manuscript "*Femtosecond response of small polyatomic molecules to ultra-intense hard X-rays*" to be submitted to *Nature* in September 2016.

2. Imaging of strong-field-induced molecular wave packets in small polyatomic molecules
(in collaboration with V. Kumarappan, D. Rolles and I. Ben-Itzhak)

This part of the program aims at visualizing, understanding and controlling fundamental photo-induced nuclear dynamics in small molecules. These studies rely on coincident momentum imaging of ionic fragments combined with channel-selective Fourier spectroscopy, and employ both, IR-IR and UV-IR pump-probe schemes. A detailed understanding of the nuclear wave packet motion gained in such experiments is also an essential prerequisite of the time-resolved studies employing X-ray probes described above.

As an illustrative example of the strong-field-induced molecular wave packet, we have studied the dynamics of rotational, vibrational and electronic motion triggered by intense 800 nm pulse in CO_2 molecule [24]. CO_2 represents one of the simplest polyatomic molecules with a well-known structure and a comprehensive set of spectroscopic data for both, neutral and ionic states, and has been recently employed as a target for many ultrafast and strong-field experiments. Combining the data obtained with two different pump-probe setups and employing channel-selective Fourier spectroscopy, we (i) demonstrate that a broadband, 8 fs pump pulse may result in an efficient vibrational excitation in the ground state of a neutral polyatomic molecule; (ii) visualize the dynamics in

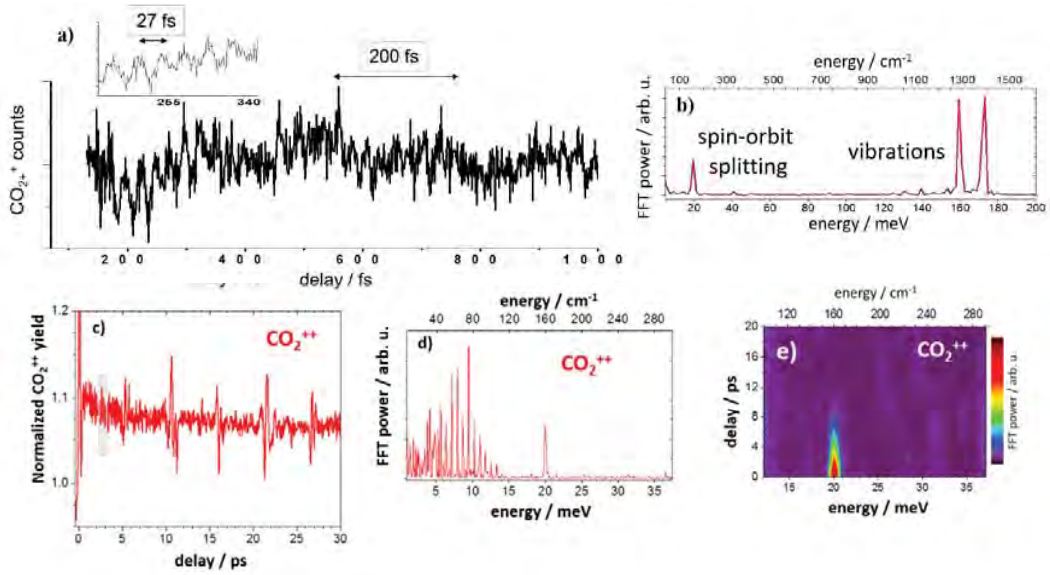

Figure 2. a) *Yields of different fragmentation pathways measured as a function of pump-probe delay between two 8 fs pulses. Intensities are 1.5x 10^{14} and 3.5x10^{14} W/cm^2 for the pump and the probe pulses, respectively.* ***b)*** *The power spectra obtained from the Fourier transforms of the ion yields shown in Fig. 2a.* ***c)*** *The measured CO_2^{++} ion yield as a function of pump-probe delay between two 35 fs pulses.* ***d)*** *The power spectra obtained from the Fourier transform of the ion yield shown in a).* ***e)*** *A sliding window Fourier transform of the delay-dependent CO2++ signal shown in c).*

the ground ionic state, including features reflecting both, vibrational and electronic coherence; and (iii) show how the electronic component of this wave packet decays within 10 ps due to coupling to rotational motion. This is illustrated in Fig. 2. The delay-dependent yield of the CO_2^{++} ion (Fig. 2a) manifests a pronounced oscillatory structure with two distinctly different time scales (~ 25-27 fs and ~ 200 fs), reflecting the vibrational and electronic components of the wave packet, respectively. The Fourier transform of these yields (shown in Fig. 2b) allows one to identify the particular states constituting the molecular wave packet. While the low-frequency component at 20 meV and the left of the two vibrational lines correspond to the spin-orbit splitting and the symmetric stretch mode in the ground state of the CO_2^+ ion, respectively, the highest-frequency line at 172 meV does not match any of the frequencies in the low-lying electronic states of the CO_2^+. This feature, which was not observed in a recent experiment of TU Vienna group (J. Chem. Phys. 144, 024306, 2016), reflects the symmetric stretching vibration in the ground state of the neutral molecule. A broad spectrum of our 8 fs pulses enables the excitation of this mode by far-off resonant two-photon Raman scattering, which was not possible for rather narrow-band 25 fs pulses used by the Vienna group.

In order to analyse the influence of rotational excitation on the electronic wave packet produced in the ground ionic state of the CO_2^+ ion, we carried out a similar measurement in a much larger delay window using 35 fs pulses. In Fig 2c the measured yield of the doubly charged CO_2^{++} in a 30 ps delay range shows a pronounced peaks and dips structure at the positions of the fractional revivals of the CO_2 rotational wave packet. Whereas the vibrational motion is not resolved here, a Fourier transform of the delay-dependent CO_2^{++} signal shown in Fig. 2d manifests a signature of the electronic wave packet motion at 20 meV. Besides this peak, a manifold of lines below 15 meV can be seen in the spectra, reflecting a broad distribution of rotational levels excited by the pump pulse. Finally, the sliding-window Fourier transform of the CO_2^{++} yield shown in Fig. 2e reveals the decay of the electronic wave packet within ~ 5 ps due to the coupling to rotational motion.

3. Light-driven dynamics in gas-phase nanoparticles
(in collaboration with C. Bostedt /Argonne, Matthias Kling / LMU Munich and Th. Fennel / TU Rostock)

Nanoscale particles bridge the gap between atomic/molecular and bulk matter and, thus, offer unique opportunities for systematic studies of light-matter interactions for systems of increasing size and complexity. We have recently built an aerosol source combined with high-energy velocity-map imaging spectrometer for gas-phase studies of isolated metal and dielectric nanoparticles. Exploiting single-short VMI images, we have developed experimental technique enabling photoelectron spectroscopy from such nanoparticles without focal volume intensity averaging [21]. Following our earlier time-resolved experiments on rare gas clusters, which employed soft X-ray scattering to map laser-induced dynamics [17], in October 2015 we have performed an IR pump – X-ray probe experiments on nearly monodisperse SiO_2 and gold nanoparticles at LCLS using our newly developed nanoparticle source. The preliminary results of this experiment are consistent with the outcome of earlier studies [17] but offer much better quantitative understanding of the laser-driven dynamics in nanoparticles.

Future plans

We plan to continue the research activities in all three areas outlined above, and increase the internal cross-links between them. In particular, the HHG setup capable of ionizing iodine 4d shell has been built up at JRML, and will be used for the pump-probe experiments on charge transfer following the 4d absorption, which can be performed at high rep. rates and with much better time resolution compared to the FEL-based experiments. In molecular wave packet diagnostics, we will focus on three-body coincident measurements, which will yield direct access to the evolving molecular geometry. We have recently extended vibrational wave packet imaging and channel-selective Fourier spectroscopy studies to halomethanes (e.g., CH_2I_2), where large-scale bending vibrations play an important role. The knowledge gained in these experiments will be applied to interpret the results of our recent FALSH experiment on halomethanes (Feb. 2016) aimed to study the correlation between the nuclear motion and electron transfer. Finally, based on the outcome of our lab-based and LCLS nanoparticle measurements described in the previous section, we also proposed a follow-up experiment on laser-driven metal nanoparticles at FLASH, which was granted machine time for February 2017.

Publications from the DOE-funded research within the last three years:

[1] *"Femtosecond photoelectron diffraction on laser-aligned molecules: Towards time-resolved imaging of molecular structure"*, R. Boll, D. Anielski, C. Bostedt, J. D. Bozek, L. Christensen, R. Coffee, S. De, P. Decleva, S. W. Epp, B. Erk, L. Foucar, F. Krasniqi, J. Küpper, A. Rouzee, B. Rudek, A. Rudenko, S. Schorb, H. Stapelfeldt, M. Stener, S. Stern, S. Techert, S. Trippel, M.J.J. Vrakking,J. Ullrich and D. Rolles, *Phys. Rev. A* 8, 061402(R) (2013).

[2] "*Strong-field interactions at EUV and X-ray wavelengths*", A. Rudenko, Chapter 15 in "Attosecond and Free-Electron Laser Physics", T. Schultz and M.J.J. Vrakking, Editors, Wiley (2014).

[3] "*X-Ray diffraction from isolated and strongly aligned gas-phase molecules with a free-electron laser"*, J. Küpper, S. Stern, L. Holmegaard, F. Filsinger, A. Rouzee, D. Rolles, A. Rudenko, P. Johnsson, A. V. Martin, M. Adolph, A. Aquila, S. Bajt, A. Barty, C. Bostedt, J. D. Bozek, R. Coffee, N. Coppola, T. Delmas, S. Epp, B. Erk, L. Foucar, Tais Gorkhover, L. Gumprecht, A. Hartmann, R. Hartmann, G. Hauser, P. Holl, N. Kimmel, K.-U. Kuhnel, J. Maurer, M. Messerschmidt, R. Moshammer, C. Reich, B. Rudek, R. Santra, I. Schlichting, C. Schmidt, S. Schorb, J. Schulz, H. Soltau, L. Strueder, T. Jan, M. J. J. Vrakking, G. Weidenspointner, T. A. White, C. Wunderer, G. Meijer, J. Ullrich, H. Stapelfeldt and H. N. Chapman, *Phys. Rev. Lett*. 112, 083002 (2014).

[4] *"Towards atomic resolution diffractive imaging of isolated molecules with X-ray free-electron lasers"*, S. Stern, L. Holmegaard, F. Filsinger, A. Rouzee, A. Rudenko, P. Johnsson, A. V. Martin, A. Barty, C. Bostedt, J. Bozek, R. Coffee, S. Epp, B. Erk, L. Foucar, R. Hartmann, N. Kimmel, K-U. Kühnel, J. Maurer, M. Messerschmidt, B. Rudek, D. Starodub, J. Thøgersen, G. Weidenspointner, T. A. White, H. Stapelfeldt, D. Rolles, H. N. Chapman and J. Küpper, *Faraday Discussions*, 171, 393 (2014).

[5] *"Probing ultrafast molecular dynamics with free-electron lasers"*, L. Fang, T. Osipov, B.F. Murphy, A. Rudenko, D. Rolles, V.S. Petrovic, C. Bostedt, J.D. Bozek, P.H. Bucksbaum, N. Berrah, *J. Phys. B: At. Mol. Opt. Phys*., 47, 124006 (2014).

[6] *"Imaging charge transfer in iodomethane upon x-ray photoabsorption"*, B. Erk, R. Boll, S. Trippel, D. Anielski, L. Foucar, B. Rudek, SW. Epp, R. Coffee, S. Carron, S. Schorb, K.R. Ferguson, M. Swiggers, J.D. Bozek, M. Simon, T. Marchenko, J. Küpper, I. Schlichting, J. Ullrich, C. Bostedt, D. Rolles, A. Rudenko, *Science* 345, 288 (2014).

[7] *"Multiple ionization and fragmentation dynamics of molecular iodine studied in IR-XUV pump-probe experiments"*, K. Schnorr, A. Senftleben, G. Schmid, A. Rudenko, M. Kurka, K.Meyer, L. Foucar, M. Kübel, M.F. Kling, Y.H. Jiang, S. Düsterer, R. Treusch, C. D. Schröter, J. Ullrich, T. Pfeifer, R. Moshammer, *Faraday Discussions* 171, 41 (2014).

[8] *"Electron Rearrangement Dynamics in Dissociating I_2^{n+} Molecules Accessed by Extreme Ultraviolet Pump-Probe Experiments"*, K. Schnorr, A. Senftleben, M. Kurka, A. Rudenko, G. Schmid, T. Pfeifer, K.Meyer, M.F. Kling, Y.H. Jiang, R. Treusch, S. Düsterer, B. Siemer, H. Zacharias, R. Mitzner, T. J. M. Zouros, J. Ullrich, C. D. Schröter and R. Moshammer, *Physical Review Letters*, 113, 073001 (2014).

[9] *"Femtosecond x-ray photoelectron diffraction on gas-phase dibromobenzene molecules";* D. Rolles, R. Boll, M. Adolph, A. Aquila, C. Bostedt, J.D. Bozek, H.N. Chapman, R. Coffee, N. Coppola, P. Decleva, T. Delmas, S.W. Epp, B. Erk, F. Filsinger, L. Foucar, L. Gumprecht, A. Hömke, T. Gorkhover, L. Holmegaard, P. Johnsson, C. Kaiser, F. Krasniqi, K.-U. Kuhnel, J. Maurer, M. Messerschmidt, R. Moshammer, W. Quevedo, , A. Rouzee, B. Rudek, I. Schlichting, C. Schmidt, S. Schorb, C.D. Schröter, J. Schulz, H. Stapelfeldt, M. Stener, S. Stern, S. Techert, J. Thogersen, M.J.J. Vrakking, A. Rudenko, J. Kupper, J. Ullrich, *J. Phys. B: At. Mol. Opt. Phys*., 47, 124035 (2014).

[10] *"Imaging molecular structure through femtosecond photoelectron diffraction on aligned and oriented gas-phase molecules"*, R. Boll, A. Rouzee, M. Adolf, D. Anielski, A. Aquila, S. Bari, C. Bomme, C. Bostedt, J. D. Bozek, H.N. Chapman, L. Christensen, R. Coffee, N. Coppola, S. De, P. Decleva, S. W. Epp, B. Erk, F.Filsinger, L. Foucar, T. Gorkhover, L. Gumprecht, A. Homke, L. Holmegaard, P. Johnsson, J.S. Kienitz, T. Kierspel, F. Krasniqi, K.-U. Kühnel, J. Maurer, M. Messerschmidt, R. Moshammer, N.L.M. Müller, B. Rudek, E. Savelyev, I. Schlichting, C. Schmidt, F. Scholz, S. Schorb, J. Schulz, J. Seltmann, M. Stener, S. Stern, S. Techert, J. Thøgersen S. Trippel, J. Viefhaus, M.J.J. Vrakking, H. Stapelfeldt, J. Küpper, J. Ullrich, A. Rudenko, and D. Rolles, *Faraday Discussions*, 171, 57 (2014).

[11] "*Charge transfer and nuclear dynamics following deep inner-shell multiphoton ionization of CH_3I molecules by X-ray free-electron laser pulses*", K. Motomura, E. Kukk, H. Fukuzawa, S. Wada, K. Nagaya, S. Ohmura, S. Mondal, T. Tachibana, Y. Ito, R. Koga, T. Sakai, K. Matsunami, A. Rudenko, C. Nicolas, X.-J. Liu, C. Miron, Y. Zhang, Y. Jiang, J. Chen, M. Anand, D. Kim, K. Tono, M. Yabashi, M. Yao, and K. Ueda, J. Phys. Chem. Lett. 6, 2944 (2015).

[12] "*Ultrafast Isomerization Initiated by X-Ray Core Ionization*", C. Liekhus-Schmaltz, I. Tenney, T. Osipov, A. Sanchez-Gonzalez, N. Berrah, R. Boll, C. Bomme, C. Bostedt, J. Bozek, S. Carron, R. Coffee, J. Devin, B. Erk, K. Ferguson, R. Field, L. Foucar, L. Frasinski, J. Glownia, M. Gühr, J. Krzywinski, H. Li, J. Marangos, T. Martinez, B. McFarland, S. Miyabe, B. Murphy, A. Natan, D. Rolles, A. Rudenko, M. Siano, E. Simpson, L. Spector, M. Swiggers, D.Walke, S.Wang, T.Weber, P. Bucksbaum, and V. Petrovic, Nature Commun. 6, 8199 (2015).

[13] "*Time-resolved studies with FELs*", A. Rudenko and D. Rolles, J. Electr. Spectr. Rel. Phen. 204, 228 (2015).

[14] "*Time-resolved study of ICD in Ne dimers using FEL radiation*", K. Schnorr, A. Senftleben, G. Schmid, S. Augustin, M. Kurka, A. Rudenko, L. Foucar, K. Meyer, D. Anielski, R. Boll, D. Rolles, M. Kubel, M. F. Kling, Y. Jiang, K. Ueda, T. Marchenko, M. Simon, G. Brenner, R. Treusch, V. Averbukh, J. Ullrich, T. Pfeifer, C. Schroter, and R. Moshammer, J. Electr. Spectr. Rel. Phen. 204, 245 (2015). (2015).

[15] "*Strongly aligned gas-phase molecules at Free-Electron Lasers*", T. Kierspel, J. Wiese, T. Mullins, J. Robinson, A. Aquila, A. Barty, R. Bean, R. Boll, S. Boutet, P. Bucksbaum, H.N. Chapman, L. Christensen, A. Fry, M. Hunter, J.E. Koglin, M. Liang, V. Mariani, A. Morgan, A. Natan, V. Petrovic, D. Rolles, A. Rudenko, K. Schnorr, H. Stapelfeldt, S. Stern, J. Thøgersen, C. H. Yoon, F. Wang, S. Trippel, J. Küpper, J. Phys. B: At. Mol. Opt. Phys. 48, 204002 (2015).

[16] "*X-ray coherent diffractive imaging by immersion in nanodroplets"*, R.M.P. Tanyag, C. Bernando, C.F. Jones, C. Bacellar, K.R. Ferguson, D.Anielski, R. Boll, S. Carron, J.P. Cryan, L. Englert, S.W Epp, B.Erk, L. Foucar, L.F. Gomez, R. Hartmann, D.M. Neumark, D.Rolles, B.Rudek, A.Rudenko, K.R Siefermann, J. Ullrich, F. Weise, C. Bostedt, O. Gessner, A.F. Vilesov, *Struct. Dyn.* 2, 051102 (2015).

[17] *"Femtosecond and nanometre visualization of structural dynamics in superheated nanoparticles"*, T. Gorkhover, S. Schorb, R. Coffee, M. Adolph, L. Foucar, D. Rupp, A. Aquila, J.D. Bozek, S.W. Epp, B. Erk, L.Gumprecht, L. Holmegaard, A. Hartmann, R. Hartmann, G. Hauser, P. Holl, A. Hömke, P. Johnsson, N. Kimmel, K.-U. Kühnel, M. Messerschmidt, C. Reich, A. Rouzée, B. Rudek, C. Schmidt, J. Schulz, H. Soltau, S. Stern, G. Weidenspointner, B. White, J. Küpper, L. Strüder, I. Schlichting, J.Ullrich, D. Rolles, A. Rudenko, T. Möller, C. Bostedt, *Nature Photonics* 10, 93 (2016).

[18] *"Charge transfer in dissociating iodomethane and fluoromethane molecules ionized by intense femtosecond X-ray pulses"*, R. Boll, B. Erk, R. Coffee, S. Trippel, T. Kierspel, C. Bomme, J.D. Bozek, M. Burkett, S. Carron, K.R. Ferguson, L. Foucar, J. Küpper, T. Marchenko, C. Miron, M. Patanen, T. Osipov, S. Schorb, M. Simon, M. Swiggers, S. Techert, K.Ueda, C. Bostedt, D. Rolles, A. Rudenko, *Structural Dynamics* 3, 043207 (2016).

[19] *"Hetero-site-specific X-ray pump-probe spectroscopy for femtosecond intramolecular dynamics"*, A. Picón, C.S. Lehmann, C. Bostedt, A. Rudenko, A. Marinelli, T. Osipov, D. Rolles, N. Berrah, C. Bomme, M. Bucher, G. Doumy, B. Erk, K.R. Ferguson, T. Gorkhover, P.J. Ho, E.P. Kanter, B. Krässig, J. Krzywinski, A.A. Lutman, A.M. March, D. Moonshiram, D. Ray, L. Young, S.T. Pratt, S.H. Southworth, *Nature Communications* 7, 11652 (2016).

[20] *"Ultrafast x-ray-induced nuclear dynamics in diatomic molecules using femtosecond x-ray-pump–x-ray-probe spectroscopy"*, C.S. Lehmann, A. Picón, C. Bostedt, A. Rudenko, A. Marinelli, D. Moonshiram, T. Osipov, D. Rolles, N. Berrah, C. Bomme, M. Bucher, G. Doumy, B. Erk, K.R. Ferguson, T. Gorkhover, PJ Ho, E.P. Kanter, B. Krässig, J. Krzywinski, A.A. Lutman, A.M. March, D. Ray, L. Young, S.T. Pratt, S.H. Southworth, *Phys. Rev. A* 94 013426 (2016).

[21] "*Intensity-dependent photoelectron spectroscopy of gas-phase nanoparticles without focal volume averaging"*, J. Powell, S.J. Robatjazi, A. Vajdu, V. Makhija, J. Stierle, X. Li, Y. Malakar, W.L. Pearson, C.Sorensen, M.F Kling and A. Rudenko, *CLEO: QELS* FTh4M.3 (2016).

[22] "*Ultrafast Dynamics of a Nucleobase Analogue Illuminated by a Short Intense X-ray Free Electron Laser Pulse"*, K. Nagaya, K. Motomura, E. Kukk, H. Fukuzawa, S. Wada, T. Tachibana, Y. Ito, S. Mondal, T. Sakai, K. Matsunami, R. Koga, S. Ohmura, Y. Takahashi, M. Kanno, A. Rudenko, C. Nicolas, X.-J. Liu, Y. Zhang, J. Chen, M. Anand, Y.H. Jiang, D.-E. Kim, K. Tono, M. Yabashi, H. Kono, C. Miron, M. Yao, K. Ueda, *Phys. Rev. X* 6, 021035 (2016).

[23] "*Femtosecond charge and molecular dynamics of I-containing organic molecules induced by intense X-ray free-electron laser pulses"*, K. Nagaya, K. Motomura, E. Kukk, Y. Takahashi, K. Yamazaki, S. Ohmura, H. Fukuzawa, S. Wada, S. Mondal T. Tachibana, Y. Ito, R. Koga, T. Sakai, K. Matsunami, K. Nakamura, M. Kanno, A. Rudenko, C. Nicolas, X.-J. Liu, C. Miron, Y. Zhang, Y. Jiang, J. Chen, M. Anand, D. E. Kim, K. Tono, M. Yabashi, M. Yao, H. Kono and K. Ueda, Faraday Discussions, accepted, DOI: 10.1039/c6fd00085a (2016).

[24] "*Strong-field-induced wave packet dynamics in carbon dioxide molecule"*, A. Rudenko, V. Makhija, A. Vajdi, Th. Ergler, M. Schuerholz, R. Moshammer, J. Ullrich, V. Kumapparan, *Faraday Discussions*, accepted, DOI 10.1039/c6fd00152a (2016).

Structure and Dynamics of Atoms, Ions, Molecules and Surfaces

Uwe Thumm
J.R. Macdonald Laboratory, Kansas State University, Manhattan, KS 66506, thumm@phys.ksu.edu

A. XUV double ionization (DI) of He

Project scope: To examine - with atomic resolution in time - correlation effects, photoexcitation, and photoemission mechanisms during the ionization of He atoms and diatomic molecules in intense short XUV and IR pulses.

Recent progress: We quantified sequential and nonsequential contributions in two-photon DI of He atoms by intense ultrashort XUV pulses with central photonenergies $\hbar\omega_{ctr}$ near the sequential ionization threshold [1]. If the spectrum of such pulses overlaps with both, the sequential ($\hbar\omega > 54.4$ eV) and nonsequential ($\hbar\omega < 54.4$ eV) DI regimes, the sequential and nonsequential DI mechanisms are difficult to distinguish. By tracking the DI asymmetry in joint photoelectron angular distributions, we introduced the two-electron forward-backward-emission asymmetry as a measure that allows the clear distinction of sequential and nonsequential contributions.

We continued to optimize and validate our new finite-element discrete-variable-representation code [1] for solving in full dimensionality the TDSE for two-electron atoms exposed to time-dependent external electric fields and found excellent agreement of our numerical results with published experimental and theoretical triply differential cross sections (TDCSs) for single-XUV-photon DI [2]. Focussing on specific values of the energy sharing between the two emitted electrons, we analysed joint angular distributions (Fig. 1 (a-c)) and mutual anular distributions (Fig 1 (d)) in coplanar emission geometry [1,2]. We extended our calculations to XUV pulses with $\hbar\omega_{ctr}$ between 30 and 99 eV, covering the non-sequential and sequential DI regimes, and examined DI in ultrashort XUV pulses that spectrally overlap both regimes.

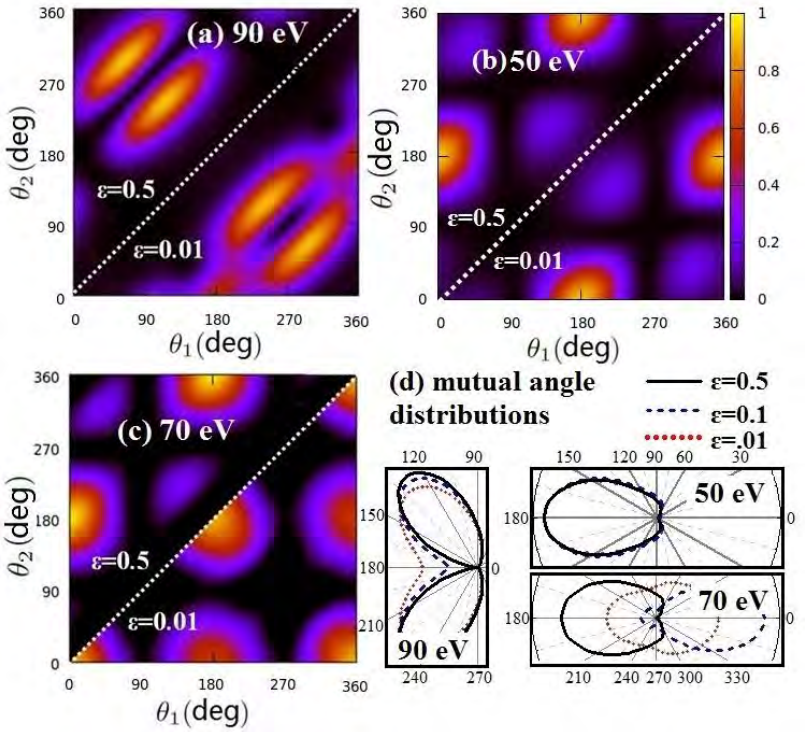

Fig. 1. Calculated joint angular distributions for single- and two-photon DI of He in (a) $\hbar\omega_{ctr}$ = 90, (b) 50, and (c) 70 eV sine-squared XUV pulses with peak intensities of 10^{14} W/cm^2 and total pulse lengths of 1 fs (corresponding to 364 as full width at half intensity maximum).

(a) Single and (b), (c) two-photon DI joint angular distributions. Upper left panels: Equal energy sharing ($\varepsilon = 0.5$). Bottom right panels: Very unequal energy sharing ($\varepsilon = 0.01$).

(d) Corresponding mutual angular distributions for energy sharings $\varepsilon = 0.01$, 0.1, and 0.5.

We found the sequential DI contribution to have a lower pulse-length limit given by a temporal constraint while being limited at longer pulse durations by vanishing spectral overlap with the sequential DI spectral domain [3]. In order to quantitatively distinguish sequential DI from nonsequential DI contributions, we evaluated the two-electron forward-backward asymmetry parameter $A(\theta_1, \theta_2=0)$ for the special case where one electron is emitted along the linear XUV and IR pulse polarization. A is given by the normalized difference of probabilies for both

electrons being emitted into the same and into opposite hemispheres. The limiting cases of both electrons being emitted into the same and opposite hemispheres correspond to A = 1 and −1, respectively. The asymmetries for 160 as and 3 fs pulse durations are large in magnitude (A ≈ −0.99) and comparatively insensitive to changes in energy sharing (Fig. 2). In contrast, the asymmetry for 500 as pulses more strongly depends on the energy sharing. It falls in between the asymmetries for 160 as and 3 fs pulses at equal energy sharing and increases to −0.956 at extremely unequal energy sharing (ε = 0.01). This weak energy sharing dependence of $A(\theta_1;\varepsilon)$ for pulses centered in the nonsequential DI regime is in sharp contrast with asymmetry changes from ≈ 1 to ≈ −1 for XUV pulses with $\hbar\omega_{ctr}$ = 70 eV in the sequential DI regime and 1 fs total pulse duration, shown in the inset in Fig. 2.

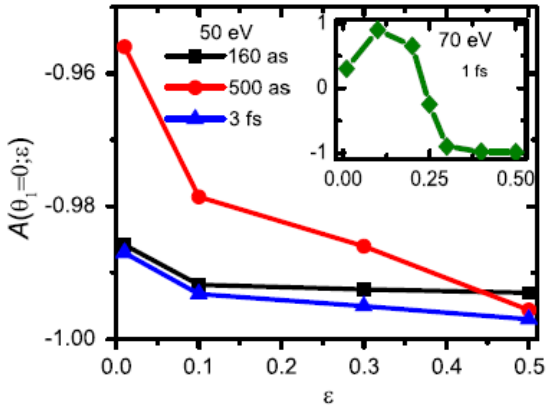

Fig. 2: Two-electron forward-backward emission asymmetries A. The inset shows asymmetries for XUV pulses with a central photon energy of 70 eV and 1 fs total pulse length, corresponding to the angular distributions in Fig. 1(c). Markers represent *ab initio* calculations and are straight-line interpolated.

Specifically, for XUV pulses with $\hbar\omega_{ctr}$ = 50 eV central photon energy and sine-squared temporal profile, we find that the sequential DI contribution is the largest at a pulse length of 650 as, due to competing temporal and spectral constraints. In addition, we validated our simple heuristic expression for the sequential DI contribution in comparison with *ab initio* calculations [3].

Future plans: (i) We plan to extend these studies to laser-assisted DI with variable delay between ultrashort XUV and IR pulses. Delay scans will allow us to resolve in time the correlated two-electron dynamics during and after sequential and non-sequential DI in ultrashort XUV pulses [3]. We intend to (ii) calculate time-resolved IR Stark shifts for He, for comparson with recent transient absorption measurements, and (iii) search for ideal laser parameters for the observation, with sub-IR-cycle resolution, of IR level shifts in delay-dependent DI. We further envision (iv) to compute laser-dressed autoionization of He and to compare our *ab initio* results with our heuristic model for the decay of laser-coupled autoionizing states [R1,R2] and (v) to extend this line of work to H_2 (in fixed-ion approximation).

B. Time-resolved photoelectron (PE) spectroscopy of flat solid surfaces

Project scope: To numerically model and understand IR-streaked (and IR side-banded) XUV PE emission and Auger decay in pump-probe experiments with atoms, molecules, and more complex targets.

Recent progress: The RABBITT technique (Reconstruction of Attosecond Beating By Interference of Two-photon Transitions) allows to probe the electronic dynamics in solids at the attosecond scale (Fig. 3) [R7]. Since the attosecond XUV pulse train (APT) spectral components have undetermined relative phases that carry over to the relative phases between RABBITT traces, Locher *et al.* [R8] have recently measured RABBITT spectra and phases from Ag(111) and Au(111) surfaces, using RABBITT spectra of gaseous argon as a reference to eliminate the unknown higher harmonics phases of the XUV pulse train.

Motivated by known striking differences in the valence electronic structure of transition metal surfaces with different crystallographic orientations [R3,R4] and by recent experiments on laser-assisted XUV photoemission from solid surfaces [R8,R9,S1], we calculated RABBITT spectra and phases (i.e., relative time delays) from the valence-bands of Ag (100), Au (100), Cu(100), and Ni(100) surfaces and from the B1- and B2 bands and surface states of Ag(111), Au(111), Cu(111), and Ni(111) [R10]. We considered different incident directions of the 827 nm, 10^{11} W/cm^2 IR pulse and XUV pulse train.

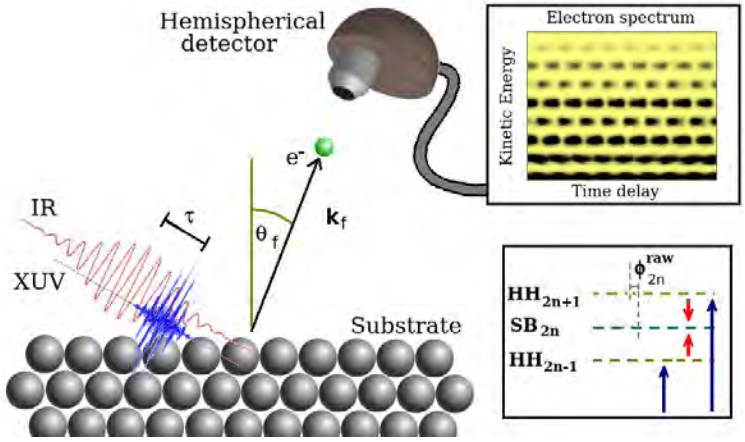

Fig. 3: Attosecond RABBITT chronoscopy of surfaces. Our comparative simulations predict distinct differences in delay-dependent PE energy distributions and photoemission time delays (phase shifts) for Cu(100) and Cu(111) surfaces. These differences can be scrutinized experimentally with existing technology in a suggested *in situ* comparative RABBITT configuration, placing the two surfaces on a sliding platform while keeping all optical components and pathlengths that affect the phases of the PE wave packets fixed.

Our RABBITT spectra from Cu(100) and Cu(111) surfaces as a function of the PE final kinetic energy and delay between the ionizing attosecond XUV pulse train and assisting IR laser pulse are shown in Fig. 4 [S2].

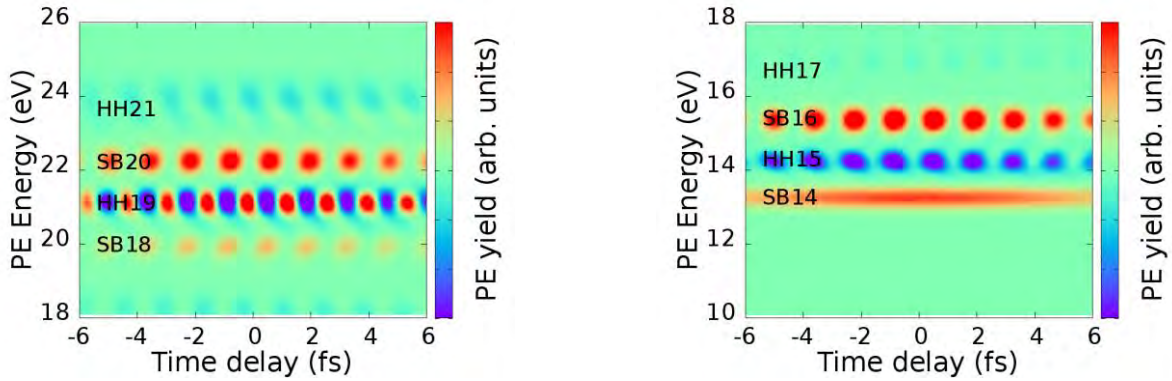

Fig. 4: RABBITT spectra of (left) Cu(100) and (right) Cu(111) conduction-band states. The yield corresponding to only XUV photon emission was substracted. The color red means increased emission, as compared with the XUV-pulse-only calculation, while blue corresponds to a yield loss due to the presence of the assisting IR pulse.

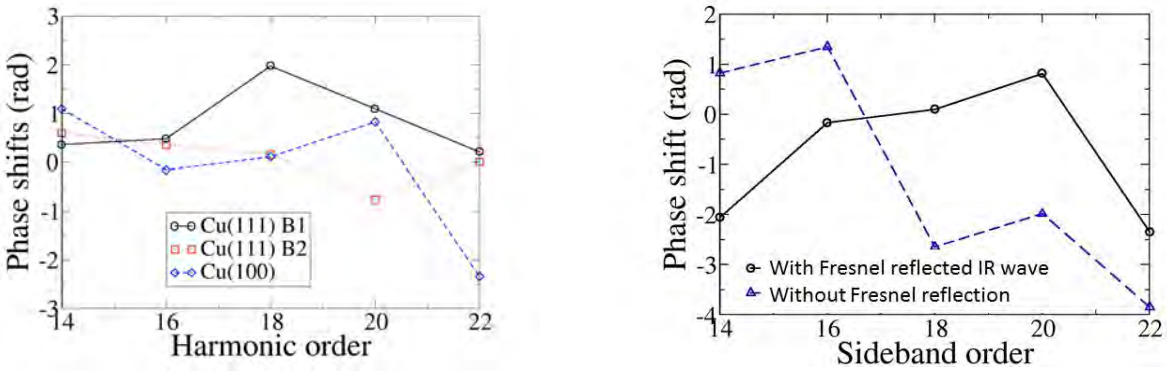

Fig. 5: Left: RABBITT phases for Cu(100) and Cu(111) bulk states minus the corresponding Cu(111) surface-state phases. Right: Cu(100) phaseshifts with respect to the Cu(111) surface-state phase, both including (solid black) and disregarding (bue dashed) the Fresnel-reflected IR field.

Since target-specific electron-transport effects are minimal for photoemision from surface states, we used surface states as references for the elimination of the unknown higher harmonic phases of the APT, in order to reveal the influence of electron transport in the bulk on the RABBITT phases (Fig. 5 (left)). Our calculations also show that the inclusion of the Fresnel-reflected incident IR pulse at the metal-vacuum interface modifes PE spectra and

photoemission time delays in a characteristic way that reveals the degree of spatial localization [R5] of the initial electronic states (Fig. 5 (right)).

Future plans: We intend to refine our modeling of (i) photoemission from solid surfaces and nanoparticles and (ii) the transport of photoreleased electrons inside complex targets. We are collaborating with experimental groups to explore the feasibility of and ideal parameters for the observation of dielectric response (plasmonic) effects during and after the XUV-pulse-triggered release of PEs from metal surfaces [R6] and nanoparticles [4,S3].

2014-2016 publications acknowledging DOE support ([1-4] addressed in this abstract)

[1] *Laser-assisted XUV few-photon double ionization of helium: joint angular distributions*, A. Liu, U. Thumm, Phys. Rev. A **89**, 063423 (2014).

[2] *Laser-assisted XUV double ionization of helium: energy-sharing dependence of joint angular distributions*, A. Liu, U. Thumm, Phys. Rev. A **91**, 043416 (2015).

[3] *A criterion for distinguishing sequential from non-sequential contributions to two-photon double ionization of helium in ultrashort XUV pulses*", A. Liu, U. Thumm, Phys. Rev. Lett. **115**, 183002 (2015).

[4] *Attosecond Physics: attosecond streaking spectroscopy of atoms and solids*, U. Thumm, Q. Liao, E. M. Bothschafter, F. Süßmann, M. F. Kling, R. Kienberger, Handbook of Photonics, Vol. **1**, Chap. XIII (Wiley, 2015).

[5] *Complementary imaging of the nuclear dynamics in laser-excited diatomic molecular ions in the time and frequency domains*, M. Magrakvelidze, A. Kramer, K. Bartschat, U. Thumm, J. Phys. B **47**, 124003 (2014).

[6] *Attosecond time-resolved photoelectron dispersion and photoemission time delays*, Q. Liao, U. Thumm, Phys. Rev. Lett. **112**, 023602 (2014).

[7] *Attosecond science – What will it take to observe processes in real time?* S. R. Leone, C. W. McCurdy, J. Burgdörfer, L. Cederbaum, Z. Chang, N. Dudovich, J. Feist, C. Greene, M. Ivanov, R. Kienberger, U. Keller, M. Kling, Z.-H. Loh, T. Pfeifer, A. Pfeiffer, R. Santra, K. Schafer, A. Stolow, U. Thumm, M. Vrakking, Nature Photonics **8**,162 (2014).

[8] *Initial-state, mean-free-path, and skin-depth dependence of attosecond time-resolved IR-streaked XUV photoemission from single-crystal magnesium,* Q. Liao, U. Thumm, Phys. Rev. A **89**, 033849 (2014).

[9] *Probing O^{2+} potential-energy curves with an XUV – IR pump – probe experiment*, P. Cörlin, A. Fischer, M. Schönwald, A. Sperl, T. Mizuno, U. Thumm, T. Pfeifer, R. Moshammer, Phys. Rev. A **91**, 043415 (2015).

[10] *Attosecond time-resolved streaked photoemission from Mg-covered W(110) surfaces*, Q. Liao, U. Thumm, Phys. Phys. Rev. A **92**, 031401(R) (2015).

Submitted manuscripts acknowledging DOE support

[S1] *Influence of the material band structure on attosecond many-electron-interactions in transition metals,* C. Chen, Z. Tao, A. Carr, P. Matyba, T. Szilvási, S. Emmerich, M. Piecuch, M. Keller, D. Zusin, S. Eich, M. Rollinger, W. You, S. Mathias, U. Thumm, M. Mavrikakis, M. Aeschlimann, P. M. Oppeneer, H. Kapteyn, M. Murnane, Science.

[S2] *Time-resolved photoemission from Cu(100) and Cu(111) surfaces*, M. Ambrosio, U. Thumm, Phys. Rev. B.

[S3] *Attosecond plasmonic streaking from gold nanospheres,* J. Li, U. Thumm, Phys. Rev. Lett.

References ([R1-R6] acknowledge our previous DOE support; [R7-R10] not DOE related)

[R1] *Attosecond time-resolved autoionization of argon,* H. Wang, M. Chini, S. Chen, C.-H. Zhang, F. He, Y. Cheng, Y. Wu, U. Thumm, Z. Chang, Phys. Rev. Lett. **105**, 143002 (2010).

[R2] *Attosecond probing of instantaneous AC Stark shifts in helium atoms,* F. He, C. Ruiz, A. Becker, U. Thumm, J. Phys. B **44**, 211001 (fast track comm., 2011).

[R3] *Resonant neutralization of hydrogen anions near Cu surfaces: Effects of the surface symmetry and ion trajectory,* H. S. Chakraborty, T. Niederhausen, U. Thumm, Phys. Rev. A **70**, 052903 (2004).

[R4] *Band-gap-confinement and image-state-recapture effects in the survival of anions scattered from metal surfaces,* A. Schmitz, J. Shaw, H. S. Chakraborty, U. Thumm, Phys. Rev. A **81**, 042901 (2010).

[R5] *Effects of wave-function localization on the time delay in photoemission from surfaces*, C.-H. Zhang, U. Thumm, Phys. Rev. A **84**, 065403 (2011).

[R6] *Probing dielectric response effects with attosecond time-resolved streaked photoelectron spectroscopy of metal surfaces*, C.-H. Zhang, U. Thumm, Phys. Rev. A **84**, 063403 (2011).

[R7] F. Calegari *et al*., J. Phys. B **49** 062001 (2016). [R8] R. Locher *et al.,* Optica **2**, 405 (2015). [R9] Z. Tao, *et al.,* Science. **353**, 62 (2016). [R10] F. Roth, *et al.,* J. Electron Spectrosc. Relat. Phenom. **208**, 2 (2016).

Strong-Field Time-Dependent Spectroscopy

Carlos A. Trallero
J. R. Macdonald Laboratory, Kansas State University, Manhattan, KS 66506
trallero@phys.ksu.edu

Scope

The main scope of my research is to measure time dependent molecular structure with ultrafast time resolution. As a complement of this goal I'm developing novel ultrafast optical sources.

1 Spectroscopy with higher-order harmonic generation

Higher-order harmonic generation (HHG) is a coherent, time dependent, and all-optical tool for learning about the molecular structure and dynamics. More precisely, it provides complete information about the photorecombination dipole in the XUV regime. The completeness in the measurement arises from the coherent relationship between the measured light and the electronic states. Therefore, through HHG we can extract the magnitude and the phase of the complex photoionization dipole as a molecular ensemble evolves after excitation.

1.1 Higher order harmonic generation interferometry with orbital angular momentum beams

Interferometry in the XUV through the generation of harmonics has been demonstrated in several groups. The technique involves the generation of two foci from which harmonics are generated and interfere in the far field as they propagate. The manipulation of laser beams with orbital angular momentum is a natural candidate for such interferometric studies providing multiple-wavefront-control and propagation in a natural basis set. In the experiment, shown in Figure 1, the laser is split into two arms that will serve as a weak

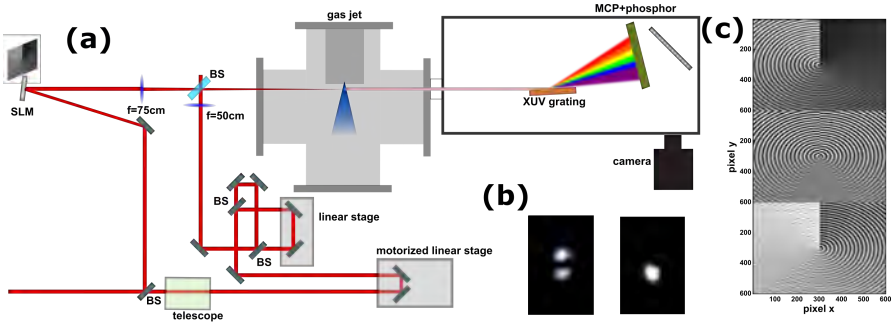

Figure 1: Experimental setup (left), SLM phase mask with $l = 1$ (top),

pump and an intense probe. The pump arm is further split into two beams to "kick" the molecule twice. In our case, the two pump beams are delayed by 4 ps, the half revival rotational period of N_2 and generate a prompt rotational wavepacket in N_2. The probe generates the higher order harmonics as a function of delay respect to the pump. A Spatial Light Modulator (SLM), based on liquid crystal on silicone technology from Hamamatsu spatially shapes the phase of the probe and a f=75 cm lens focuses both arms into a supersonic gas jet. The generated harmonics are frequency resolved with a flat-field grating, detected on an Z-stack micro channel plate, and recorded in a low-noise CMOS camera.

Laguerre-Gaussian spatial modes have the benefit of enhancing the harmonic yield due to advantageous macroscopic phase matching. By using an SLM we can, not only achieve such beams, but we can programmatically switch from a single sources to two sources by applying the right phase pattern.

The applied phase pattern to the SLM for the generation of the two foci is a combination of different orbital angular momenta (OAM), and is shown in Figure 1 b). In addition, corrections for the wavefront distortion of the SLM are applied. By Applying a phase pattern containing OAM $l = 1$ and $l = -1$ (top and lower figures in Fig. 1 b), we get a Laguerre-Gaussian profile that form a two foci pattern in the far field with a high diffraction efficiency in the SLM. By applying combinations of $l = 0$ and $l = 1$, we are able to switch to an individual focus which mimics one of the spots in the two source focus. The probe pulse is then overlapped in space with one of the two foci and delayed in time respect to the pump arm.

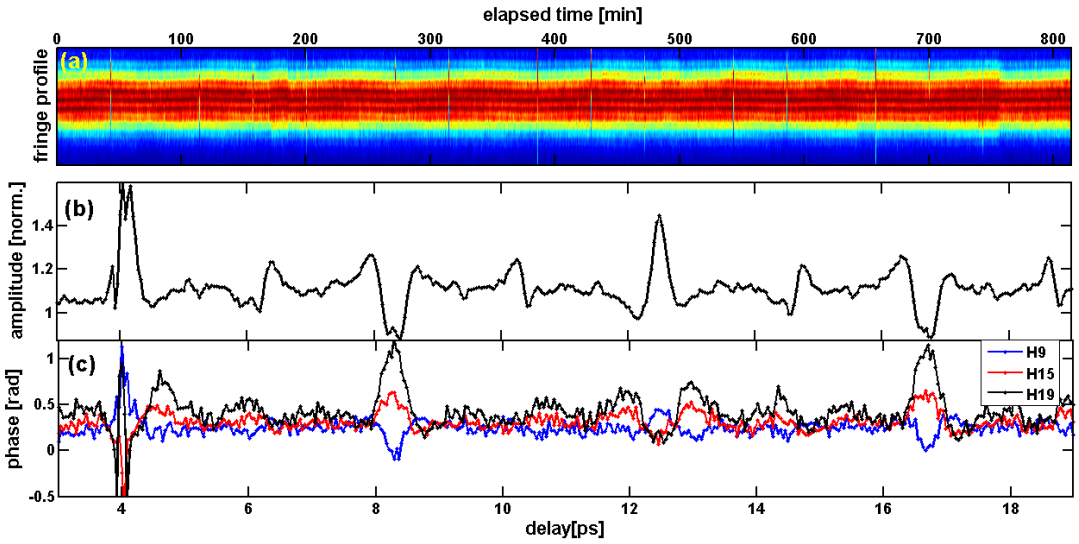

Figure 2: (a) Measured fringe outline of harmonic 13 over 13 hours. (b) Measured phase and amplitude of harmonic 19 in molecular nitrogen

The superposition of two opposing OAM creates a wavefront that does not rotate as it propagates. As a result the harmonics generated are created with OAM=0 and propagate forward producing an interference pattern in the far field as shown in Fig. 2 a). To extract the amplitude for each harmonic, we programmatically switch between one source and two sources. The revival structure of N_2, measured through the amplitude of harmonic 19 is shown in Fig. 2 b). Changes in the interference pattern of each harmonic gives us access to the phase as a function of molecular alignment. The phase for harmonics 9, 15 and 19 is shown in Fig. 2 c).

1.2 Concluding remarks

We have demonstrated how superposed Gauss-Laguerre laser modes can be used for the generation of harmonics. The superposition of OAM phases prevents the wavefront from rotating as light propagates through the focus. For superposed OAM of +1(-1) we generate two foci which can be used for interferometric studies of the harmonics. This represents a very stable method to do interferometric studies in HHG with the goal of extracting the full photoionization dipole from molecular systems. We have applied this method to N_2 and C_2H_4.

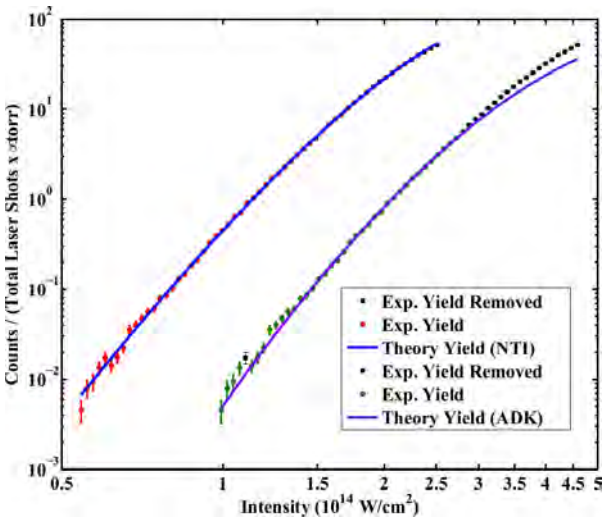

Figure 3: The experimental ionization yields as a function of intensity are fit to cycle-averaged, volume averaged, theoretical ionization yield curves generated using NTI and ADK theory. The corresponding calibration constants are $\alpha = 4.5 \times 10^{12} W/cm^2 J$ with 8 points removed and $\alpha = 8.25 \times 10^{12} W/cm^2 J$ with 20 points removed, respectively.

1.3 Future work

We will continue our HHG-based spectroscopy in different ways. We want to extend our multi-mode, interferometric pump-probe studies with time delays ranging from ps to below the atomic time unit of 25 attoseconds. At the attosecond time scale we will achieve this by controlling the delay of two different wavefronts in a spatial light modulator. Our approach has the advantage that it is jitter free because both foci will follow the same beam path and only depart from each other near the focus where the light is in vacuum. In addition we want to explore whereas HHG spectroscopy is possible with gated pulses that generate isolated attosecond pulses. Gated fields for the generation of attosecond pulses present a distinctive difficulty in that they have a time-dependent ellipticity. However, the recollision process occurs over a small window of time where the light is mostly linear.

2 Strong field ionization of molecular isomers *with A-. T. Le*

We have completed the experiments on the comparison of strong field ionization of molecular isomers. The comparison is done by measuring the ratio in the ionization yield between two pairs of isomers, cis- and trans-1,2-dichloroethylene and cis- and trans-2-butene. In the past some of the issues we faced was the lack of a precise intensity calibration. To improve in this aspect we changed a few aspects in the experiment. First we monitored and recorded the shot-to-shot energy fluctuation of the laser pulses and used these recorded energy values to tag the intensity for each ionization event. Secondly, we implemented a new method for the fitting of ionization models to a reference data. Our implementation is a variant of a weighted-exponential least-trimmed sum resistant regression method. We use Ar as the atomic specie for intensity calibration. The results of the fitting of Ar^+ to the Yudin-Invanov (NTI) model and the Ammosov-Delone-Krainov (ADK) model are shown in Fig. 3. The difference between the two models is very visible.

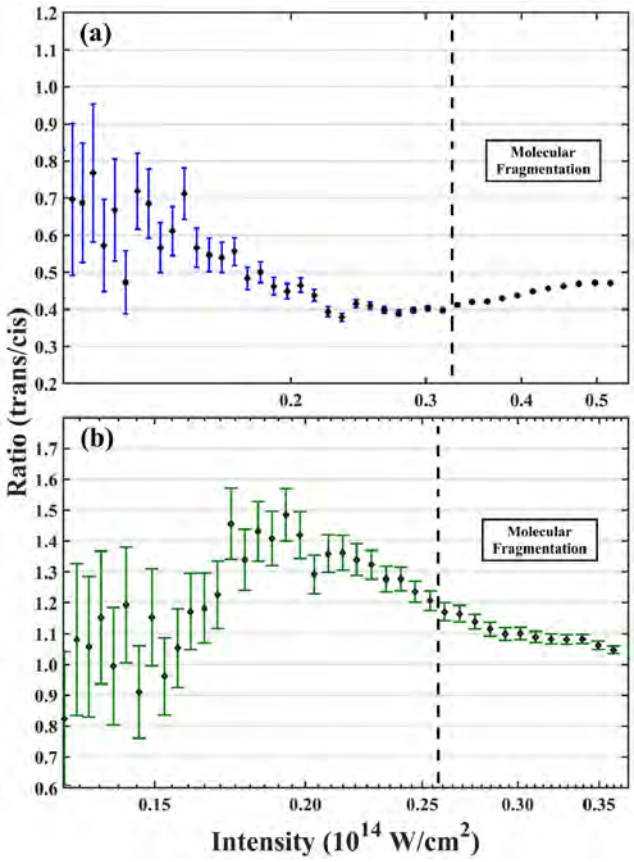

Figure 4: Ratio of the yield of the parent ion of (a) 2-butene and (b) 1,2-DCE (35-35 isotope) as a function of intensity (semi-log).

With this precise intensity calibration we proceeded to measure the ratio of the ionization yield as a function of intensity, as shown in Fig. 4. From a strong field-ionization perspective, because of the similar ionization potentials between the pairs, we would expect very similar yields (yield ratio $\approx$ 1). Especially in this case where the molecules where randomly oriented. Therefore it is surprising that our findings indicate that one isomer dominates its stereo isomer counterpart by a factor on the order of 1.5 - 2. Furthermore, we show that there is no single dominating configuration, cis versus trans. Such lack of dominant configuration suggests that molecular polarity is not a major contributor to the rate at which a molecule ionizes under strong-fields. To further establish this lack of sensitivity to molecular polarity for strong field ionization a bigger sample has to be studied.

2.1 Future work

We will expand the study to different classes of isomers such as chiral molecules and other conformal isomers. Additionally we will compare how the ionization yields will change as a function of wavelength from the near-IR (800 nm) to the mid-IR (2400 nm). For chiral molecules we will explore the influence in the yields with ellipticity. Finally, we will look at the influence of the carrier-envelope-phase in the ionization yields.

3 Technical developments

3.1 Development of an intense long-wavelength-infrared source

Using our high-energy optical parametric amplifier (HE-OPA) we were able to generate intense, tunable, few-cycle pulses in the long-wavelength-infrared (LWIR) regime. We measured the pulse durations using a home-built cross frequency-resolved-optical-gating (X-FROG) device that performs frequency sum between the fundamental 800 nm and the LWIR source. Through this method we found that the LWIR pulses change in duration between 55 fs and 80 fs corresponding to 3 to 5 cycles depending on the wavelength. We also demonstrated that we can tune the center wavelength from 5500 nm to 8500 nm without any dramatic loss in pulse energy. As a matter of fact, we were to record multiple ionization in Xe, Kr, Ar, Ne, and He at all the

wavelengths that we generated, thus demonstrating that we indeed have an ultrafast intense source capable of strong field ionization in the deep tunneling regime.

While it is still unclear how multi-ionization is achieved, we theorize that it occurs through electron-driven recollisions. Because the wavelength is so long, the ponderomotive energy is extremely large and thus can impart enough energy to the re colliding electron to multiple ionize the core. Compared with the 800 nm case, an 8000 nm pulse can produce the same ponderomotive energy with 1/100 of the peak intensity.

3.2 Material modification for micromachining operations

We use superposed Bessel beams, which are generated by a combination of a spatial light modulator (SLM) and an axicon to micro-machine borosilicate glass and scribe grooves in thin Mo with superposed Bessel beams. This "SLM + axicon" allows for the generation of complex patters overcoming many of the limitations that are found with zero-order Bessel beams.

In this study, these masks generate superpositions of Laguerre-Gaussian beams focused by an axicon to generate superpositions of Bessel beams with opposite angular momentum. By changing the order of the superposed beams we are able to control the pattern formation for the micromachining.

We also performed studies on pattern scribing. We compared narrow groove scribing on a Mo thin film with a zero-order Bessel beam and a second order Bessel beams. The results suggest that, if the 1+(-1) superposed beam is used collateral damage can be reduced. To arrive to this conclusion we measured the scribed patterns with AFM images. We observe a clean groove without any damage tracks when using a 1+(-1) Bessel mode.

Therefore, our studies demonstrate arbitrary, complex-pattern micromachining of solid materials with femtosecond lasers by using a combination of an Axicon and an SLM. In addition, we demonstrated that a superposed Bessel modes can be ideal to scribe metals where a very clean surface is desired.

DOE Supported Publications

- "Internal modification of intrinsic and doped silicon using infrared nanosecond laser", Xiaoming Yu, Xinya Wang, Margaux Chanal, Carlos A. Trallero-Herrero, David Grojo, and Shuting Lei, ***Applied Physics A***, (to appear), (2016)
- "An Atomic Photoionization Experiment by Harmonic Generation Spectroscopy", M. V. Frolov, T. S. Sarantseva, N. L. Manakov, K. D. Fulfer, B. D. Wilson, J. Troß, X. Ren, E. D. Poliakoff, A. A. Silaev, N. V. Vvedenskii, A. F. Starace and C. A. Trallero-Herrero, ***Physical Review A: Rapid Communications***, **93**, 031403(R), (2016)
- "Materials processing with superposed Bessel beams", Xiaoming Yu, Carlos A. Trallero-Herrero and Shuting Lei, ***Applied Surface Science***, **360**, 833, (2015)
- "A 260 MW light source at 7 μm center wavelength as a path to strong field science in the far infrared", Derrek J. Wilson, Adam M. Summers and Carlos A. Trallero-Herrero", ***Frontiers in Optics***, FTh4A, (2015)
- "Long term carrier-envelope-phase stabilization of a terawatt-class Ti:Sapphire laser", Adam M. Summers, Benjamin Langdon, Jon Garlick, Xiaoming Ren, Derrek Wilson, Stefan Zigo, Matthias Kling, Shuting Lei, Christopher Elles, Eric Wells, Erwin Poliakoff, Kevin Carnes, Vinod Kumarappan, Itzik Ben-Itzhak and Carlos Trallero-Herrero, ***Frontiers in Optics***, FTu3F.2, (2015)
- "A carrier-envelope-phase stabilized terawatt class laser at 1 kHz with a wavelength tunable option", Benjamin Langdon, Jonathan Garlick, Xiaoming Ren, Derrek J. Wilson, Adam M. Summers, Stefan Zigo, Matthias F. Kling, Shuting Lei, Christopher G. Elles, Eric Wells, Erwin D. Poliakoff, Kevin D. Carnes, Vinod Kumarappan, Itzik Ben-Itzhak and Carlos A. Trallero-Herrero, ***Optics Express***, **23** 4563 (2015)
- Summers, A., Ramm, A., Kling, M. F., Flanders, B. N., and Trallero-Herrero, C. A., Optical damage threshold of single-crystaline gold nanowires with ultrafast pulses. Optics Express, **22**, 4235 (2014).
- Wilson, D., Ren, X., Trallero-Herrero, C., Simultaneous broadening of the depleted pump and signal from an optical parametric amplifier. CLEO: 2014, STh4E.5, (2014).
- Ren, X., Makhija, V., Le, A.-T., Tro, J., Mondal, S., Jin, C., Trallero-Herrero, C., Measuring the angle-dependent photoionization cross section of nitrogen using high-harmonic generation. Physical Review A, **88**, 043421, (2013).

Atomic, Molecular and Optical Sciences at the Lawrence Berkeley National Laboratory

C. William McCurdy (PI), Co-Investigators: Ali Belkacem, Oliver Gessner, Martin Head-Gordon, Stephen R. Leone, Daniel M. Neumark, Thomas N. Rescigno, Daniel S. Slaughter, Thorsten Weber

Chemical Sciences, Lawrence Berkeley National Laboratory, Berkeley, CA 94720

CWMcCurdy@lbl.gov, ABelkacem@lbl.gov, OGessner@lbl.gov, MHead-Gordon@lbl.gov, SRLeone@lbl.gov, DMNeumark@lbl.gov, TNRescigno@lbl.gov, DSSlaughter@lbl.gov TWeber@lbl.gov

Objective and Scope: The AMOS program at LBNL seeks to answer fundamental questions in atomic, molecular and chemical sciences that are central to the mission of the Department of Energy's Office of Science. The essential strategy is to apply a broad span of existing and currently emerging tools such as synchrotron radiation, lasers, laboratory-based extreme ultraviolet sources, and low-energy electron beams together with state-of-the-art experimental techniques including momentum imaging, coincidence techniques, electron and x-ray absorption spectroscopy, scattering, and transient absorption, in combination with the development of advanced theoretical methodologies, to studies across a broad range of time scales and systems. This approach provides deep insight into the chemistry and physics of the fundamental interactions that drive key chemical processes in simple molecules, complex molecular systems and molecules in complex environments. The current emphasis of the program is in three major areas with important connections and overlap: inner-shell photo-ionization and multiple-ionization and dissociation dynamics of small molecules; time-resolved studies of charge dynamics involving molecules in the gas phase, in the condensed phase and at interfaces using a combination of attosecond to picosecond x-rays and laser pulses; and low-energy electron impact and dissociative electron attachment of molecules. The theory component of the program focuses on the development of new methods for solving from first-principles complex multi-atom and multi-electron processes that play a key role in these systems. The theory and experimental parts of the program are closely coupled. They are designed to work together to tackle problems of scale that are otherwise inaccessible without a strong and continuous collaboration and interaction.

The program at LBNL, recently reorganized to combine the former activities of the AMO base program and those of the former Ultrafast X-ray Sciences Laboratory into a single, integrated, AMOS program, consists of three subtasks:

1. **Photon and electron driven processes in atoms and small molecules.**
2. **Photon and electron driven processes in complex molecular systems and molecules in complex environments.**
3. **First-principles theory of dynamics and electronic structure.**

The co-investigators participate in multiple subtasks, collaborating and using common techniques in an effort in which experiment and theory are tightly integrated.

Subtask 1: Photon driven processes in atoms and small molecules

Thrust 1*: *Photon driven processes in atoms and small molecules.
A. Belkacem, O. Gessner, C.W. McCurdy, D. M. Neumark, S. R. Leone, T. N. Rescigno, D. S. Slaughter, and Th. Weber.

Ultrafast molecular dynamics studied by femtosecond inner-shell transient absorption spectroscopy *(O. Gessner, S.R. Leone, D.M. Neumark)*

Atomic site-specific inner-shell transitions are employed to monitor ultrafast light-induced dynamics in organic molecules from the viewpoint of well-defined reporter atoms. Using femtosecond extreme ultraviolet (XUV) transient absorption spectroscopy, both neutral and ionic transient molecular and atomic species are observed simultaneously, providing a comprehensive picture of the coupled electronic and nuclear dynamics.

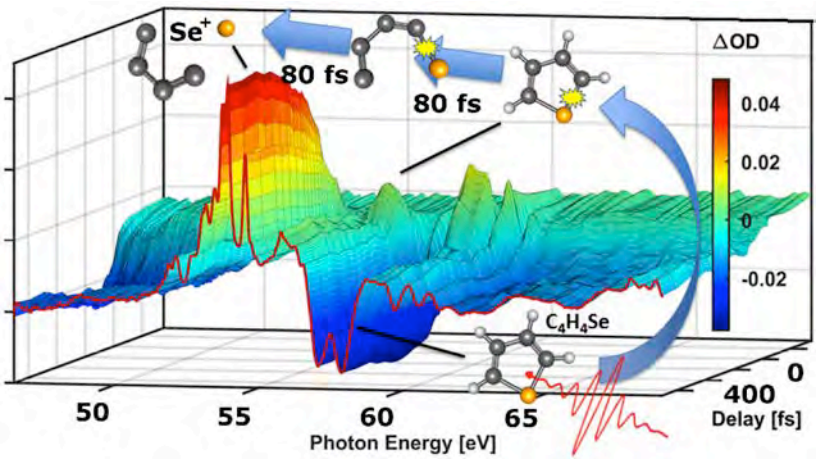

Figure 1: Ring-opening and dissociation dynamics in strong-field ionized selenophene monitored by femtosecond time-resolved inner-shell transient absorption spectroscopy. Negative (blue) features mark the depletion of parent molecules. Positive features correspond to transient molecular configurations (green) and emerging atomic fragments (yellow/red). A two-step ring-opening and dissociation mechanism is revealed whereby each step proceeds on a timescale comparable to a single vibrational period of the C-Se bonds.

Strong-field ionization induced ring-opening dynamics in the heterocyclic aromatic molecule selenophene (SeC_4H_4) are studied in a concerted experimental-theoretical effort (Fig. 1). High-resolution transient absorption spectra in the range of Se 3d to valence excitations are complemented by first-principles time-dependent density functional theory (TDDFT) simulations in order to detect and assign a variety of transient species.

The study reveals a two-step ring-opening/dissociation mechanism, whereby an initially prepared, excited cyclic cation decays within τ_1 = 80±30 fs into a transient molecular species, which then gives rise to the emergence of bare Se^+ fragments and ring-open $SeC_4H_4^+$ cations within an additional τ_2 = 80±30 fs. A comparison to simulated spectra suggests that σ* excited cation states play a central role in the observed ring-opening dynamics. Remarkably, the two steps of the reaction each proceed on the timescale of a single vibrational period of the C-Se asymmetric stretch mode, indicating

very efficient coupling between electronic and nuclear degrees of freedom, most likely with the involvement of conical intersections.

Strong-field ionization of the haloalkane 1,2-dibromoethane (DBE, $C_2H_4Br_2$) leads to the elimination of atomic fragments Br^{n+} in a variety of charge states (n=0,1,2), each emerging with a specific time scale (320 fs, 70 fs, 30 fs, respectively). Interestingly, while the relative yields of the fragments vary dramatically with the intensity of the ionizing infrared (IR) laser pulse, the appearance times remain constant. This suggests that each fragment species is associated with one or a few dominant dissociation pathways that are independent of the IR field strength inducing the dissociation. In particular, the simultaneously monitored decay time scales of IR-prepared DBE^{m+} ions (70 fs and 30 fs for m=1,2, respectively) strongly indicate a predominant production of Br^+ ions from dissociative ionization of DBE^+ rather than Coulomb explosion of DBE^{2+}. The study demonstrates how ultrafast time-resolved inner-shell spectroscopy may be used to disentangle multiple, competing reaction pathways induced by exposing molecules to intense laser fields.

Future activities will focus on extending the usable probe photon energy range of the studies to the sulfur L-edge (~160 eV). This will grant access to a significantly larger range of chemically relevant compounds and dynamics, such as photoinduced ring-opening in thiophene molecules. The extended probe photon range will be complemented by an improved sensitivity of the experiment that will enable studies with single photon excitations in the ultraviolet regime. These are of particular interest for identifying dynamics that proceed on separate, well-defined potential energy surfaces.

Attosecond dynamics *(S.R. Leone, D.M. Neumark)*

The attosecond dynamics subgroup employs attosecond extreme ultraviolet (XUV) pulses to study the electronic dynamics of gas-phase atomic and molecular systems with exceptional time and energy resolution. Conventional attosecond transient absorption spectroscopy (ATAS) is powerful, but involves complex spectra with overlapping spectral effects from numerous near infrared (NIR)-induced processes. In visible and infrared spectroscopies, the resonant nonlinear optical response of a target is commonly isolated by four wave mixing (FWM) techniques to provide background-free signals. The attosecond dynamics task has therefore extended ultrafast nonlinear spectroscopy (FWM) to the XUV regime, an important advance in both technology and scientific capability. In these experiments, attosecond XUV pulses produced by high harmonic generation (HHG) are used in combination with a time-delayed NIR pulse and, if desired, a second time-coincident NIR pulse to investigate time dependent changes in the coherent four-wave mixing emission spectrum of a target atom or molecule. The results are phase matched and, in a non-collinear geometry, precise details of the states and background free signals are obtained.

ATAS studies in argon exemplify the rich yet complex time-dependent dynamics measured by this technique. The impulsive ac Stark phase shift results in broadening and shifting of absorption lines when the NIR pulse overlaps the XUV pulse in time while horizontal sidebands emerge at longer delays between the XUV and NIR pulses due to the perturbed free induction decay of adjacent resonance states. In addition, ladder- and vee- or lambda-type population transfer processes through one-photon accessible states

manifest as fast and slow oscillations, respectively. In argon, fast oscillations with a period of 1.3 fs around 15 eV are attributable to population transfer between the spin-obit split 4s states (~11.8 eV) and the 4d/6s states (~15 eV) through the 4p manifold normally inaccessible by direct one photon transitions. These 4p states also facilitate vee-type population transfer from the 4d/6s states to a series of states approaching the ionization limits at approximately 15.75 eV, resulting in slow oscillations with a period of 5-10 fs (Cao, et al., New J. Phys. **18**, 013041 (2016)). Similar processes are present in molecules such as nitrogen, where vibronic coherences in Rydberg and valence states can be observed (Warrick, et al., J. Phys. Chem. A. **120**, 19 (2016)). From these results a measure of the anharmonicity of the b' valence state around 14 eV is obtained. Rigorous analysis of the mechanisms leading to these complicated and overlapping spectral effects often requires theoretical modeling, limiting the ability to distinguish and quantify the different pathways in ATAS.

Recent work focused on developing a FWM scheme in the XUV to detect NIR-driven population processes to measure couplings, reconstruct wavepackets, and determine the lifetimes of decaying states. A spectrally shaped XUV pulse train was used to detect much weaker 3-photon processes below the detection limit of traditional ATAS. The quadratic increase of the intensity of generated emission peaks as a function of NIR intensity provided verification that the observed features originate from FWM (Cao, et al., Phys. Rev. A. **94**, 021802 (2016)). To differentiate distinct processes in atoms and molecules in energy regions where spectral shaping is not straightforward, a non-collinear geometry was implemented in which the NIR and XUV beams intersect at a small angle (18 mrad), providing spatial rather than energetic isolation of the four-wave mixing signal by taking advantage of the phase matching conditions inherent in a FWM process. A camera image of the transmitted XUV spectrum after the arrival of the NIR pulse in argon gas exhibits features on axis with the harmonics (along the blue arrow in Fig.2(a)) due to the interference between the initial XUV pulse and the nonlinear response generated by coupling pathways in which the final state remains the same (i.e. Stark shifting) as well as approximately 85

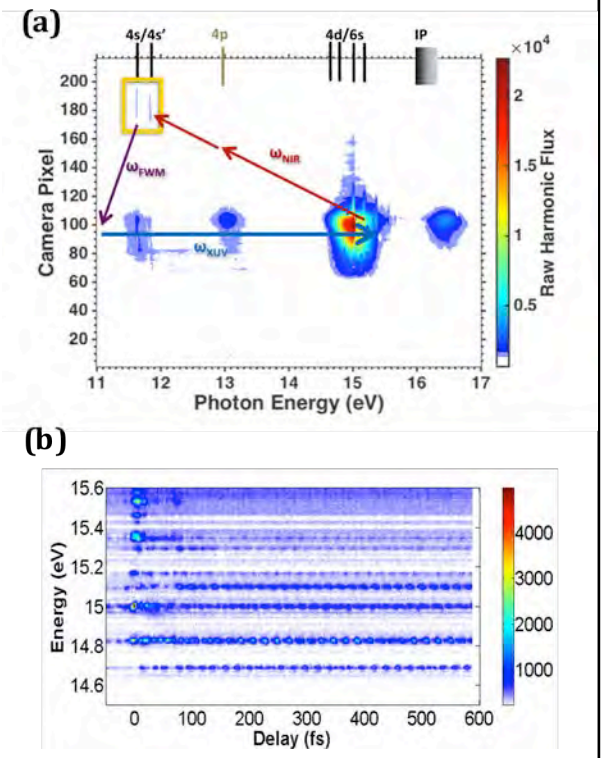

Figure 2: Four-wave mixing measurement of argon. (a) Camera image of XUV spectrum after perturbation by a non-collinear NIR pulse. The phase matching diagram for the off-axis generated signal (yellow box) is superimposed on the figure. (b) The delay dependent absorption spectrum of an off-axis signal produced by allowing the NIR pulse used for HHG to propagate with the XUV pulse. Quantum beating from a wave packet of 1-photon dipole forbidden states is observed in the manifold of states around 15 eV.

pixels above the harmonics at the 2p-4s/4s' transition energies (yellow box in Fig. 2(a)) attributable to ladder-type population transfer. The off-axis features can be selected and examined as a function of delay between the XUV and NIR pulses.

While in conventional ATAS the 1-photon dipole forbidden states participating in population transfer processes can only be determined by theoretical modeling, FWM allows for direct experimental identification of the intermediary states. When collinear and time-coincident XUV and NIR pulses arrive, they excite the long-lived 4p/4p' manifold of 2-photon allowed states around 13.3 eV in argon. These states are then coupled to the manifold of accessible states around 15 eV by the non-collinear NIR pulse. The spatially isolated quantum beating that results (Fig. 2(b)) allows for the detection of this two-photon electronic coherence. Fourier analysis reveals three distinct frequencies at 0.21 eV, 0.31 eV, and 0.39 eV, matching several of the quantum beats between the 1-photon dipole forbidden states involved in this coherence, i.e. the 4p states located at 13.095 eV, 13.17 eV, 13.27 eV and 13.48 eV.

Future work will extend the application of the attosecond FWM detection scheme to more complex systems. The background-free nature and excellent time resolution of the technique promises to simplify the measurement of autoionizing and core-excited state lifetimes, which are typically in the range of a few to 10s of femtoseconds. As a proposed initial experiment, the delay-dependent intensities of off-axis features originating from population transfer between the $4d^{-1}$ core-excited states of xenon can be utilized to determine the lifetimes of Auger-decaying states without complications from broadening mechanisms and spectral congestion that plague the extraction of lifetimes from the linewidths of static absorption spectra or the limited spectral resolution and competing processes that impede lifetime determination in ATAS experiments. Furthermore, preliminary data in nitrogen indicates that this technique can provide detailed spectroscopic information about dipole forbidden states in the XUV that are difficult to access experimentally. These experiments and the planned addition of a second independently controlled NIR arm to the experimental apparatus will constitute a significant step toward multidimensional table-top XUV spectroscopy.

Mapping and Controlling Ultrafast Dynamics of Highly Excited H_2 Molecules by Attosecond VUV Radiation *(A. Belkacem and Th. Weber)*

In this work, we used time-resolved multicolor-multiphoton attosecond radiation in combination with COLTRIMS 3D momentum imaging (published in F.P. Sturm et al., Rev. Sci. Inst., 2016) to map and control the dynamics of neutrally excited H_2* molecules. We showed how the detection of the 3D ion momenta, in combination with polarization control over laser driven VUV radiation, can be used to unravel multiple ionization and dissociation channels produced by a combination of VUV and IR pulses. In the pump probe experiment we focused a high-power infrared pulsed laser (808 nm, 25 mJ, 45 fs, 50 Hz) with a curved mirror (f = 6 m) into an argon filled 10 cm long gas cell to create a high-flux, coherent VUV photon beam (10^9 phot/shot) via High Harmonic Generation (HHG). The generated broad spectrum of harmonics is manipulated by varying the HHG gas cell pressure, an additional gas filter cell, and a B_4C coated focusing mirror to yield attosecond pulse trains with an envelope of 15 - 20 fs. A custom, in-vacuum split-mirror interferometer creates VUV – VUV/IR pulse pairs for pump-

probe studies with a relative delay range up to several picoseconds and 170 attoseconds resolution. In the experimental end-station, the incoming beam misses the supersonic H_2 gas jet and is back-focused into the jet by a spherical mirror at the exit of the COLTRIMS spectrometer.

The attosecond vacuum ultraviolet (VUV) and femtosecond infrared (IR) pump-probe scheme was used to map the dynamics and non-equilibrium dissociation channels of excited neutral H_2 molecules (published in F.P. Sturm et al., PRA 2016). A nuclear wave packet is created in the $B\ ^1\Sigma_u^+$ state of the neutral H_2 molecule by absorption of the 9th harmonic of the driving infrared laser field. Due to the large stretching amplitude of the molecule excited in the $B\ ^1\Sigma_u^+$ electronic state, the effective H_2^+ ionization potential changes significantly as the nuclear wave packet vibrates in the bound, highly electronically and vibrationally excited *B* potential energy curve. We probed such dynamics by ionizing the excited neutral molecule using time-delayed IR/VUV radiation. We identified the nonequilibrium dissociation channels by utilizing 3D momentum imaging of the ion fragments (see Fig. 3). We found that different dissociation channels

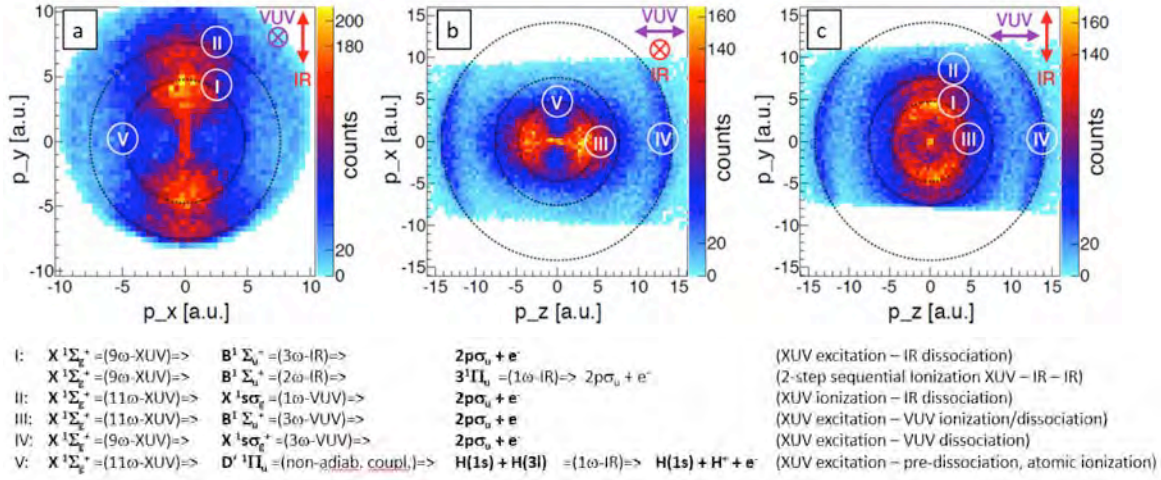

Figure 3: Momentum spheres in all three spatial directions (a-c) caused by the VUV-IR and VUV-VUV transitions. The yields are corrected for the momentum dependent detection phase space. The identified non-equilibrium channels are labeled with roman numerals and listed below.

can be controlled, to some extent, by changing the IR laser intensity, and by choosing the wavelength of the probe laser light. Our results illustrate that non-equilibrium processes are complex in nature, even in rather simple molecules such as an excited neutral H_2* molecule, and require the development of non-trivial theoretical models for a quantitative interpretation of the data. These benchmark experiments can be used to test new theoretical models and are essential for developing the concepts necessary for the interpretation of experiments involving the ionization and dissociation mechanisms of more complex molecules.

Bond-rearrangement and ionization mechanisms in the photo-double-ionization of simple hydrocarbon molecules near and above threshold *(A. Belkacem, and Th. Weber)*

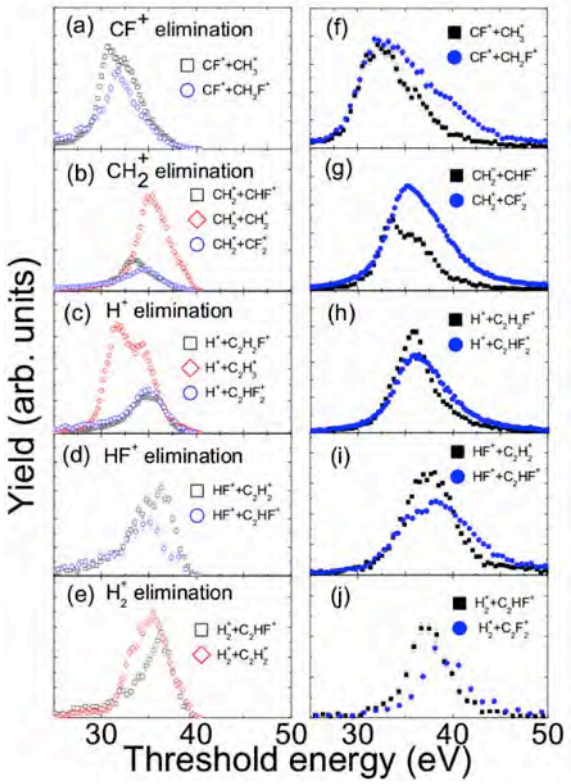

Figure 4: Threshold energies for the different two-ionic breakup channels in the PDI of C_2H_3F using 40.5 (a-e, black open squares) and 55.5 eV (f-j, black solid squares) photon energy. For comparison we have included the data of the PDI of C_2H_4 (b, c, and e, red open circles) and 1,1-$C_2H_2F_2$ (a-d, blue open diamonds for 40 eV and f-j, blue solid diamonds for 60 eV photon energy).

We have investigated and compared bond-rearrangement driven by photo-double-ionization (PDI) near and above the double ionization threshold in a sequence of carbon-carbon double bonded hydrocarbon molecules: ethylene (C_2H_4), fluoroethylene (C_2H_3F), and 1,1-difluoroethylene ($C_2H_2F_2$) (published in B. Gaire et al., PRA, 2016 and PRA, 2014). We employed the kinematically complete cold target recoil ion momentum spectroscopy (COLTRIMS) method to resolve all photo-double-ionization events leading to two-ionic fragments. We observed changes in the branching ratios of different dissociative ionization channels depending on the presence of none, one, or two fluorine atoms. The role of the fluorine atom in the bond-rearrangement channels is intriguing as evidenced by the re-ordering of the threshold energies of the PDI in the fluorinated molecules (see Fig. 4).

These effects offer a compelling argument that the electro-negativity of the fluorine (or the polarity of the molecule) strongly influences the potential energy surfaces of the molecules and drives bond-rearrangement during the dissociation process. The energy sharing and the relative angle between the 3D-momentum vectors of the two electrons enable us to distinguish between knock-out and other ionization mechanisms of the PDI processes. For fluoroethylene (C_2H_3F) molecules near and above the threshold the energy sharing between the expelled electrons is uniform and structureless for a photon energy close to the double ionization threshold (e.g. 40 eV). Here the PDI process is dominated by the knock-out mechanism. For the higher photon energy (55.5 eV) this mechanisms dies out. At this and higher photon energies higher-lying electronic states are accessible and they change the branching ratios of the molecular fragmentation channels via indirect PDI. The branching ratios change differently among the dissociative ionization channels of these molecules due to the presence of none, one, or two fluorine atoms. The fluorine atom(s) polarizes the molecules and strongly influences the dissociation dynamics and

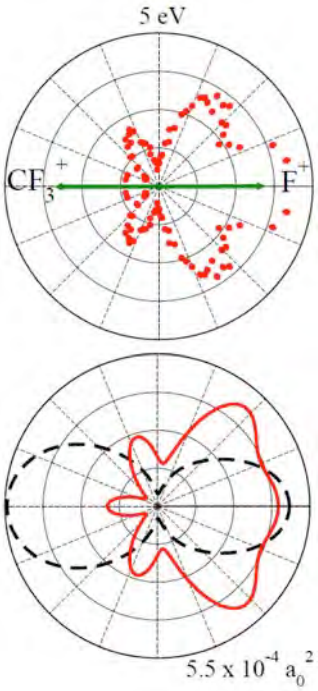

Figure 5: Experimental (relative) and theoretical (absolute) RFPADs for the light polarization (green double arrow) parallel to the C-F recoil axis. The ejected electron energy is 5 eV. The upper RFPAD shows the experimental results. In the lower angular distribution the dashed line represents delocalized and the solid line localized fluorine 1s holes in the ab initio calculations. The label indicates the theoretical absolute RFPAD value at the outer ring of the polar coordinates.

bond-rearrangement as evidenced by the drastic changes in the threshold energies of comparable two-ionic fragmentation channels. To gain more insight into the dissociation pathways the potential energy surfaces of the cation and dication states of these molecules are highly desired and need to be calculated. Our findings may stimulate time resolved measurements to investigate these fundamental bond-rearrangement processes on their natural (ultrafast) timescales of particle migration using pump-probe schemes.

Core-hole localization in CF_4 through body-frame photoelectron angular distribution

(C.W. McCurdy, T.N. Rescigno, R. Lucheese, A. Belkacem, and Th. Weber)

Through the combination of COLTRIMS experiments and *ab initio* theory we have found that under particular experimental conditions the observation of low energy photoelectrons in coincidence with F^+ ions ionized near the fluorine K-edge in CF_4 unambiguously exhibit a dramatic signature of core hole localization in the recoil frame photoelectron angular distribution (RFPAD) of the molecule (submitted as C.W. McCurdy et al, Phys. Rev. Lett. 2016). The observed process occurs in steps: X-ray photoionization within a few eV of the fluorine K-edge is followed by a fast electron transfer to the fluorine ion leaving a CF_3^+ and F* behind. Subsequently, an atomic like Auger decay of the excited fluorine atom F* occurs, while the dissociation of the molecular ion takes place.

The RFPAD measured for the $CF_3^+ + F^+$ breakup by detecting the photoelectron in coincidence with the F^+ atom is not expected to be symmetric, but the comparison between the experimentally observed RFPAD and *ab initio* calculations with the hole localized on the fluorine atom, while the molecule still has tetrahedral symmetry, show, that the fluorine atom that dissociates as F^+ after Auger decay must have been the one with the 1s vacancy. Calculations of the photoelectron angular dependence arising from the creation of a delocalized vacancy in the symmetric molecular orbitals involving fluorine 1s orbitals bear no resemblance to the observed RFPADs, while the localized hole results reproduce them faithfully, providing definitive evidence that the fluorine ion detected was the one initially having the core vacancy (see Fig 5).

The pronounced difference we see in the RFPADs for the F K-shell photoionization in CF_4 using localized or delocalized orbitals is fundamentally a chemical effect. Even if the Auger decay occurs while the molecule has moved only a few tenths of an Angstrom from its initial geometry, the 1s vacancy that is initially created can localize on one of the F atoms. That atom can achieve a closed-shell (neon-like) valence configuration by withdrawing an electron from the CF_3 fragment, which then produces a steeply repulsive interaction between CF_3^+ and F*.

Time-resolved molecular dynamics investigated by UV pump - VUV probe photoelectron and photoion imaging spectroscopy *(A. Belkacem)*

Using a bright high harmonic generation (HHG) source obtained from a 25 mJ, 25 fs, 1 kHz infrared laser, ultrafast dynamics in small molecular systems is studied via UV pump, VUV probe experiments. From the high harmonic beam, two arms are separated spectrally and temporally and used to electronically excite gas phase targets and ionize the system as it undergoes a photochemical reaction.

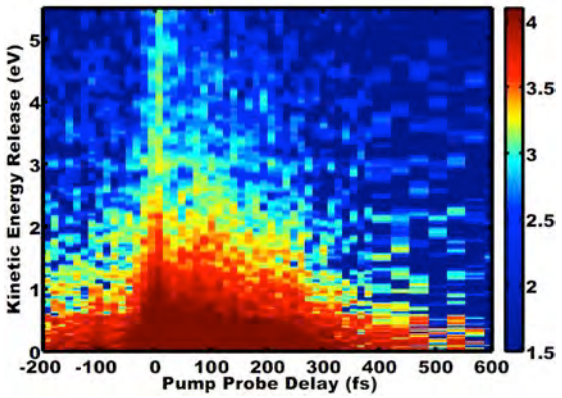

Figure 6: Total Kinetic Energy Release of CO^+ as a function of pump-probe time delay

The dissociation dynamics of the $^1\Delta_u$ and $^1\mathbf{\Pi}_g$ states of carbon dioxide upon two-photon UV excitation were studied by ionizing the system with the 7th (11.1 eV) and 9th (14.3 eV) harmonics and measuring the kinetic energy release (KER) of the resultant ion fragments (Fig. 6). By looking at the decay of the ion yield at different regions of KER, ultrafast dynamics involving a direct dissociation along the $^1\mathbf{\Pi}_g$ excited manifold and a slower dissociation channel involving the mixing of the states was observed.

Following our work in ethylene where the transient population of a low-lying Rydberg state was observed quickly following valence excitation, time-resolved photoelectron spectroscopy (TRPES) was utilized to study the dissociation of methanol upon excitation at 157 nm to the 2 ^{1}A" state (Fig. 7). Using nanosecond light sources, many dissociation channels have previously been identified, all of which ended on the 1 ^{1}A" electronic state. With ultrafast TRPES, we are able to track the excited state wave-

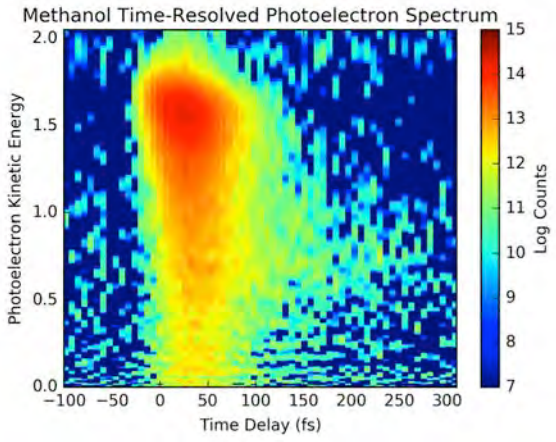

Figure 7: TRPES for methanol as a function of delay between pump and probe.

packet as it moves along the potential energy surface of the initially excited state and transitions non-adiabatically to the dissociating state with few femtosecond sensitivity. Besides these non-adiabatic dynamics, repeating the experiment with deuterated samples and comparing the photoelectron spectra with time-dependent ion yields revealed that motion of the hydroxyl side rather than the methyl side of the molecule played a key role in a hydrogen loss dissociation channel on the methyl side of the ion.

In VUV/XUV pump-probe experiments, it is usually the case that both pump and probe can ionize the target on their own, causing unwanted background. We have explored one approach to minimizing this background with a velocity map imaging (VMI) spectrometer. By tilting the beams with respect to the spectrometer, ions generated at different positions along the beam propagation direction will have different time of flight to reach the detector. Pulsing this detector then allows for a spatial gating of the measured signal, and for a reduction of the background signal arising from regions other than the overlap volume of the two beams. This technique can significantly benefit photo-ion pump-probe experiments using velocity map imaging when VUV, XUV or X-rays are involved as pump, probe or both.

Currently, we are developing the technique of Polarization Spectroscopy as a sensitive probe of ultrafast dynamics in small gas phase molecular systems. The anisotropy created in a molecule during the excitation step is used to modify the polarization state of a second pulse. By measuring this change in polarization of the second pulse as a function of time delay, the ultrafast time evolution of the excited molecule can be mapped out.

Thrust 2: *Electron driven processes in atoms and small molecules.*

A. Belkacem, C. W. McCurdy, T. N. Rescigno, D. S. Slaughter, and Th. Weber.

Detailed investigation of the dynamics of dissociative electron attachment to ammonia *(D.S. Slaughter, A. Belkacem, C.W. McCurdy and T.N. Rescigno)*

Low-energy electron collisions with small molecules are often characterized by the formation of transient negative ions. The cross sections for formation of these anions can be large and often lead to dissociation into a reactive

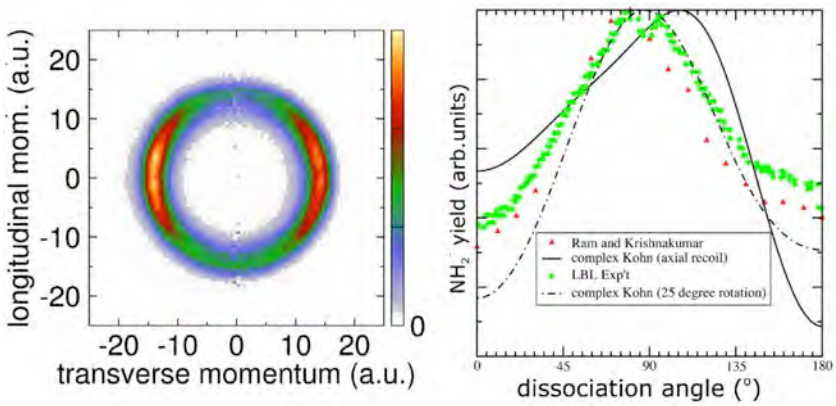

Figure 8: Measured H^- momentum distribution (left panel) from the 5.5 eV resonance following electron attachment to ammonia. The electron direction is upwards. H^- angular distribution (right panel) compared with experimental data from the literature and the axial recoil prediction with a 25^o rotation towards planar NH_3^- geometry.

negative ion and neutral species. The dynamics associated with these dissociative processes can be rich and complex, involving conical intersections between different electronic states, competition between autodetachment and one or more dissociation channels. With Cynthia Trevisan (California Maritime Academy) and Ann Orel (University of California, Davis), we recently investigated the dissociative electron attachment dynamics in ammonia.

The $NH_2^-(^1A_1)$ + $H(^2S)$ and $NH_2(^2B_1)$ + $H^-(^1S)$ dissociation channels have similar thermodynamic thresholds, the NH_2^- + H asymptote lying only ~0.02 eV below the NH_2 + H^- asymptote. Both channels are nondegenerate, so they cannot be correlated to the same anion state, yet both product channels are produced from the same 5.5 eV resonance band. Anion momentum imaging experiments were performed with a dissociative electron attachment reaction microscope to determine the final state fragment momenta for the fragments produced in these reactions (Fig. 8). Fixed-nuclei electron scattering

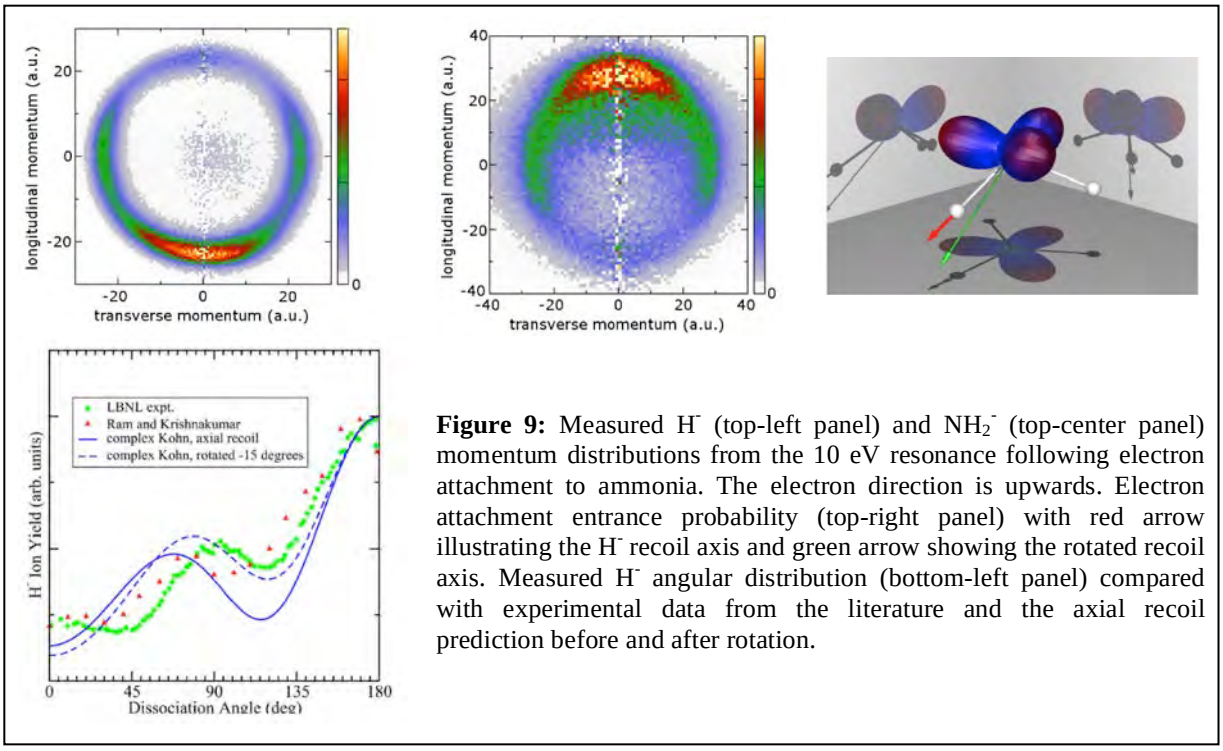

Figure 9: Measured H^- (top-left panel) and NH_2^- (top-center panel) momentum distributions from the 10 eV resonance following electron attachment to ammonia. The electron direction is upwards. Electron attachment entrance probability (top-right panel) with red arrow illustrating the H^- recoil axis and green arrow showing the rotated recoil axis. Measured H^- angular distribution (bottom-left panel) compared with experimental data from the literature and the axial recoil prediction before and after rotation.

calculations were performed to determine the electron attachment entrance amplitude allowing us to make a connection between the laboratory frame and the molecular frame.

We found agreement between our calculated and measured anion fragment angular distributions only when we included a 25° opening of the H_2N-H bond angle during the dissociation, consistent with electronic structure calculations described in subtask 3 that showed the equilibrium geometry of this resonance state is planar.

We determined that the dissociation leading to NH_2^- was due to electron exchange at large NH_2-H^- internuclear distances to the NH_2^- + H virtual state. This was confirmed by a simplified two-state time-dependent calculation of the single H-NH_2 coordinate that produced a 40% population transfer to the virtual state, in good agreement with our experiments.

For higher electron energies near 10 eV, a second electron attachment resonance produces H^- and excited $NH_2(^2A_1)$, with 15° recoil axis rotation consistent with umbrella

closing motion (Fig. 9). Surprisingly, NH_2^- is also produced by this resonance with a kinetic energy release of 5.8 eV. This channel could be coupled to the 10 eV resonance by the broad 10 eV shape resonance that does not otherwise participate in dissociative electron attachment.

Future efforts in this thrust will be directed towards extending the capabilities of anion momentum imaging to address the challenges in studying more complex electron-driven processes. Neutral fragment detection by photon and/or electron impact ionization will enable identification and spectroscopy of neutral fragments from many-body dissociation channels. Detailed investigations of the fundamental electron-driven chemical processes in model systems will be performed in order to improve our understanding of more complex electron-molecule systems.

Subtask 2: Photon and electron driven processes in complex molecular systems and molecules in complex environments.

Thrust 1: Photon driven processes in complex molecular systems and molecules in complex environments.

A. Belkacem, O. Gessner, M. Head-Gordon, S. R. Leone and D. M. Neumark

Analysis and Control of Intermolecular Coulombic Decay in small hetero-nuclear hydrogen bonded Clusters *(Th. Weber)*

The goal of this project was to go from observation of Interatomic and molecular Coulomb Decay (ICD) in single dimers to observation of ICD in a water environment as well as to the control of this decay process. Controllability through environmental changes can make this inter-molecular decay even more significant for life sustaining applications. ICD strongly depends on the energy levels in the cluster and on the internuclear distance of the atoms participating in the decay and hence on the concentration of the cluster target. The composition and structure of the cluster have a direct influence on relatively general quantities, such as the fragmentation rates, the energy spectrum of the emitted ICD electrons and the kinetic energy release of the ionic fragments.

In our work the double ionization and subsequent fragmentation of small hydrogen bonded systems has been investigated using the COLTRIMS method as an analysis tool. In the experiment a supersonic gas jet of the molecules NH_3, H_2O and clusters of these two molecules was crossed with a beam of photons from the Advanced Light Source (beamline 10.0.1) with an energy of 36 eV. The energetics of the thereby induced reactions were measured by calculating the 3D momenta of the detected particles. In the data analysis several different molecular fragmentations were identified and analyzed as follows.

The fragmentation into ions with masses of 18 au each was assigned to the breakup of water dimers into $H_2O^+ + H_2O^+$. Both, the measured KER at 4.2 eV and the range of the electron energies from 0 eV to 8 eV are in accordance with previous measurements by Jahnke et al. (Nature Physics **6**, (2010), 139–142). Although ICD is assumed to be the mechanism mainly responsible for the decay, it could not be distinctly identified in the data. Due to a manifold of states involved in the decay process the electron energy appeared washed out making it challenging to extract valuable information.

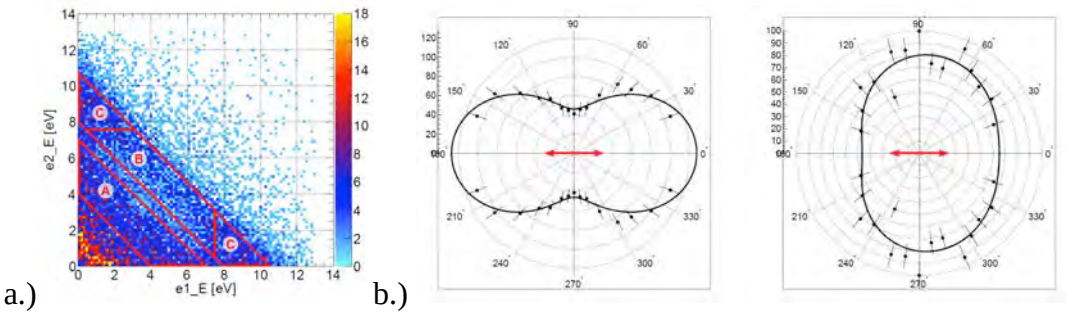

Figure 10: (a) Energy of electron 2 plotted against the energy of electron 1 of the 17/17 breakup. Electrons in region A and B presumably stem from direct double ionization, whereas region C contains electrons stemming from ICD. (b) angular distributions of the high energy electrons form region C is dipole shaped (mid), which is typical for photoelectrons, while the angular distribution of the low energy electrons (right) from region C is rather isotropic.

The breakup of ionic fragments with masses 17 au and 18 au was assigned to the ions NH_3^+ and H_2O^+. The comparison of the measured KER at 4.3 eV with the theoretical KER calculated by Stoychev et al. (Angew. Chem. Int. Ed. **50**, (2011), 1306 –1309) revealed that the cluster fragmenting into NH_3^+ and H_2O^+ is the hydrogen bonded $NH_3…H_2O$ cluster system with ammonia as the proton-donor. The KER of the cluster $H_2O…NH_3$ with ammonia as proton-acceptor is expected to be 0.5 eV higher than the measured KER. Hence, $H_2O…NH_3$ could be excluded as a candidate for the 17/18 breakup. According to the calculations some of the double ionization potentials in $NH_3…H_2O$ lie below the inner-valence single ionization potential of the N and O atom thereby allowing the system to undergo ICD. Although the energy range of the detected electrons in general corresponded to the calculated ionization potentials, no noticeable substructure indicating a specific decay mechanism was identified. In addition to a manifold of electronic transitions, the system features many other internal degrees of freedom so that the absorbed energy can be partly stored in rovibrational excitations, thereby blurring the energetics of the decay process. Many electron pairs consisting of one electron with high and one with low energy were found. Since this energy sharing is typical for electron pairs created in ICD, it is assumed to be the mechanism mainly responsible for the decay of $NH_3…H_2O$ clusters.

The third channel, that was identified, was assigned to the breakup of ammonia dimers into NH_3^+ and NH_3^+ with masses of 17 a.u. each. The kinetic energy release was measured at 4.0 eV which corresponds to an initial distance between the nitrogen atoms of 3.6 Å. This distance is not in accordance with theoretical calculations suggesting a distance ranging from 3.2 to 3.4 Å in the optimal geometry of the dimer. According to ab initio calculations by Kryzhevoi and Cederbaum the ammonia dimer has several double ionization potentials lying below the inner-valence single ionization potential of the N atom. Hence, the system is energetically allowed to undergo ICD. The examination of the electron energies revealed indications of double ionization and ICD as decay mechanisms. For ICD events the energy of the high energy electron was measured in a range of 7 to 10 eV, which is in accordance with the theoretically expected energies of the photoelectron at 8.4 and 9.2 eV. The high energy electron was distinctively identified as the photoelectron based on its characteristic angular emission distribution, which is dipole shaped and parallel to the polarization direction of the photons. The second

electron was measured with an energy below 3 eV which is in line with the expected energies of 2.1 eV and 2.9 eV for the ICD process. This is further supported by its angular distribution which does not show a preferred emission direction in the laboratory system (Fig. 10).

Finally, the molecular composition of the gas jet was examined. For this purpose, the yield of the singly ionized monomers was analyzed as a function of the event counter. Two types of measurement series with different ammonia water ratios were identified. The comparison of the 17/17 and 17/18 breakup yield for the two different types of measurement series revealed, that the 17/18 breakup occurred more often when the concentration of water in the jet was higher. The ICD yield in the 17/17 breakups is significantly higher when the concentration of water in the jet is low. Solely based on these numbers this would mean that the probability for ICD of $NH_3…NH_3$ clusters increased due to the altered molecular composition of the jet. This can be interpreted in accordance with the predictions of the Cederbaum group stating that the presence of proton donors from H_2O molecules, translating to a higher pH value, suppresses ICD. However, more reliable experimental conclusions on the dependency of ICD probabilities of the molecular composition of the gas jet could not be drawn because a direct measurement of the pH value was not possible in the current experimental setup.

Direct imaging of dynamic host-dopant interactions and strong-field induced dynamics in superfluid nanodroplets *(O. Gessner, S. R. Leone, D. M. Neumark)*

The study of dynamics in isolated nanosystems provides a crucial test for our understanding of physical phenomena that emerge from the interaction and collective response of a few up to ~10^{10} atoms. Our research in this area concentrates on coupled

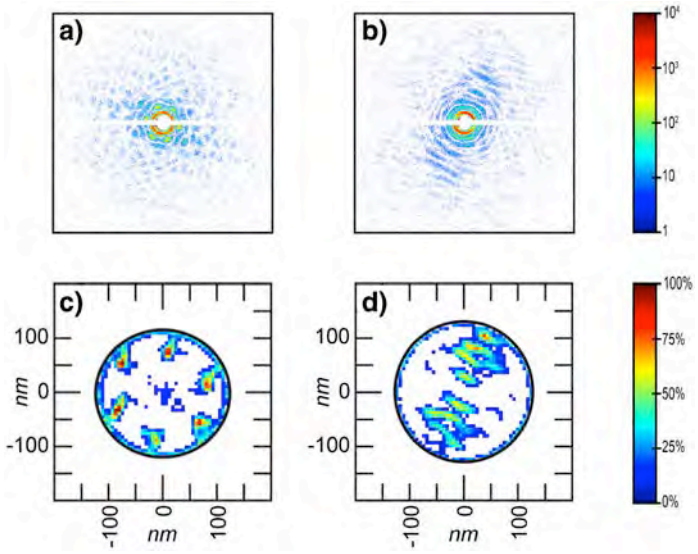

Figure 11: Monitoring the coupled motion of helium nanodroplet hosts and Xe cluster dopants. Single-shot X-ray diffraction patterns (a,b) are translated into real-space density distributions (c,d) using a novel phase retrieval algorithm. In c) and d), large black and blue circles mark the boundaries of the droplets, while the interior structures represent the distribution of embedded Xe atoms. Highly concentrated, symmetric dopant cluster distributions are observed that correspond to Xe atoms trapped inside arrangements of quantum vortices. In c) the line of sight is parallel to the vortex axes while in d) the vortices are tilted with respect to the viewing direction.

electronic-nuclear dynamics and quantum hydrodynamic phenomena in helium nanodroplets as well as their response to very intense X-ray and infrared (IR) light fields. Employing single-shot X-ray scattering and coherent diffractive imaging (CDI) techniques at the Linac Coherent Light Source (LCLS), femtosecond snapshots of single pure and doped nanodroplets are recorded, providing direct access to unique transient configurations that are inherently challenging to access by traditional spectroscopy and imaging techniques.

Among noble gas clusters, helium nanodroplets stand out as the only liquid aggregate. In fact, a previous LCLS based study within this project provided the first unequivocal evidence for the bulk superfluid nature of rotating, ~2 μm sized droplets. This result was achieved through the detection of Bragg peaks as a result of X-ray scattering off regular, Xe-doped quantum vortex lattices. Recently, a novel image reconstruction algorithm has been developed that employs the host droplet as a well-defined support and reference scatterer, facilitating a fast and reliable translation of the recorded X-ray diffraction patterns into real-space maps of the dopant density distribution (Fig. 11). The technique enables a significantly more detailed study of the coupled rotational motion and impurity distribution in doped helium nanodroplets down to the single vortex limit in ~200 nm sized droplets. The results provide direct evidence for Xe density distributions that are concentrated in a few, elongated streaks near the droplet surface. This finding is in striking contrast to the traditionally accepted picture that van der Waals interactions will force noble gas dopants to aggregate in a single cluster near the center of the helium droplet hosts. Instead, hydrodynamic forces due to the interaction of the dopants with the vortex flow field of the rotating superfluid by far dominate the spatial distribution of the dopant atoms, trapping them in the vicinity of the vortex cores. Moreover, the radial positions of the doped vortex cores themselves are significantly different from theoretical predictions for pure droplets owing to energy and angular momentum conservation in the coupled rotational motion of both host and dopants.

In a complementary series of experiments, the coupled dynamics of electrons and ions in highly ionized helium nanodroplets are studied by ultrafast X-ray scattering. A very intense ($\geq 10^{15}$ W/cm^2) IR pump pulse induces substantial ionization and, potentially, nanoplasma formation in a droplet, ultimately leading to its disintegration by Coulomb and hydrodynamic forces. Different stages of the interaction are probed by recording single-shot X-ray diffraction patterns at a variety of IR pump - X-ray probe delays. Preliminary results indicate that the experiments give access to both electronic and structural dynamics and, in particular, to anisotropic interactions that provide exceptionally sensitive tests of theoretical models for intense light-matter interactions.

A major focus of future studies will be to access coupled ultrafast *electronic* dynamics of host droplets and dopant atoms/clusters in both the weak and strong field regime. Femtosecond vacuum ultraviolet (VUV) spectroscopy will be used to monitor the exchange of charge and energy between electronically excited hosts and dopants on a molecular level of detail. Femtosecond X-ray diffraction of doped systems will give insight into possible mechanisms to control intense light-matter interactions by a suitable choice of impurities.

Thrust 2: Electron driven processes in complex molecular systems and molecules in complex environments.

A. Belkacem, C. W. McCurdy, T. N. Rescigno, D. S. Slaughter, and Th. Weber.

Dynamics of dissociative electron attachment to molecules of technological significance and hydrogen-bonded clusters. *(D.S. Slaughter, A. Belkacem, C. W. McCurdy and T. N. Rescigno)*

Low energy electrons drive important fundamental chemical processes in molecules such as dissociation, isomerization via resonant electronic states. Electron - molecule resonances are embedded in the autodetachment continuum until they electronically stabilize by the internal degrees of freedom of the transient anion. These fundamental processes have relevance in emerging technologies such as extreme ultraviolet

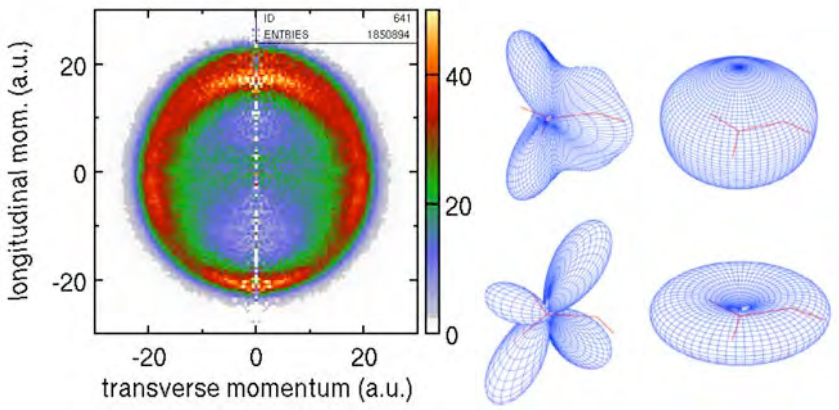

Figure 12: H- fragment momentum image (left) following dissociative electron attachment to partially-deuterated formic acid DCOOH at 7.2 eV. The electron direction is upwards. Electron attachment entrance probabilities (left column) relative to the molecular frame (stick model) and the averaged entrance probability with respect to the H^--recoil axis (right column) for electron attachment to the 2A' (7.5 eV, top row) and 2A'' (9 eV, bottom row) resonances in formic acid.

lithography, where electron-driven processes are now understood to activate photoacid generators in the chemical amplification of photoresists.

With Prof. Cynthia Trevisan (California State University, Maritime), we are investigating the dissociative electron attachment dynamics in formic acid in two Feshbach resonances that proceed to dissociation between 6 eV and 10 eV electron attachment energy. *Ab initio* electronic structure and electron scattering calculations allow us to establish the electron attachment probability in the molecular frame yield axial recoil angular distributions. We employ a modified dissociative electron attachment reaction microscope to measure each of the anion fragments from these processes in parallel to get a detailed understanding of the two transient anion dynamics from the final states of each fragment.

Formic acid is of particular fundamental interest because low energy (<10 eV) electron attachment forms a dynamically rich electron – molecule system with all of the - bonds participating: we have confirmed that the C-H, O-H, and both C-O bonds can

break in dissociative electron attachment at these energies. Preliminary experimental and theoretical results for the hydroxyl H- channel are shown in Fig. 12.

We aim to begin to address the vast knowledge gap in electron-driven chemical dynamics that currently exists between an isolated molecular system and the condensed phase systems commonly found in technological applications and in nature. This work will be extended to investigate solvation effects on the dissociative electron attachment dynamics of molecules when they are incorporated in clusters with water or other solvents First experimental efforts are currently underway to study dissociative electron attachment to hydrogen-bonded formic acid dimers.

Subtask 3: First-principles theory of dynamics and electronic structure.

D. J. Haxton, M. Head-Gordon, C. W. McCurdy, T. N. Rescigno

Continuum Electron Dynamics: "Almost" symmetric charge exchange in dissociative attachment to ammonia *(C. W. McCurdy, T. N. Rescigno)*

Our theoretical calculations on continuum electron dynamics include both (1) Electron-molecule scattering and electron-ion scattering calculations using the Complex Kohn Variational method

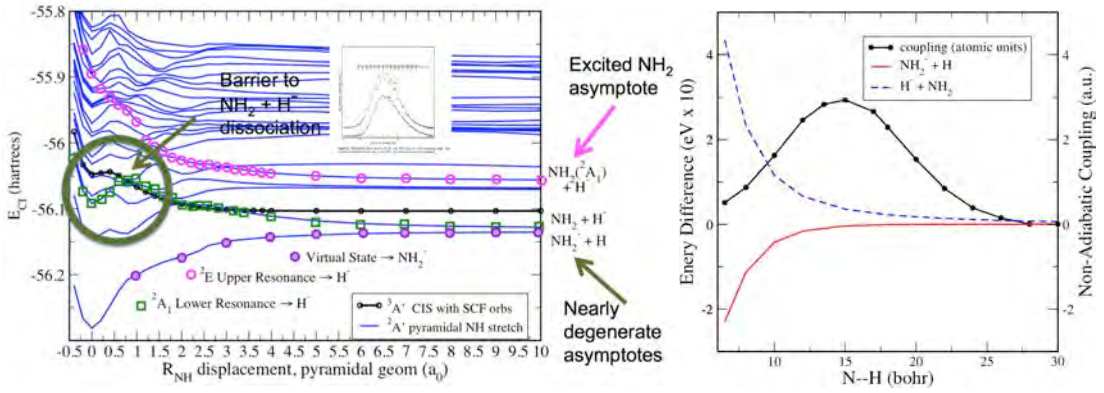

Figure 13: Multireference CI calculations on the ammonia anion (left) showing the two resonances and one virtual state that feature in DEA to ammonia (left). The nearly degenerate asymptotes and the nonadiabatic coupling between those states (right) provide the mechanism whereby attachment to one resonance state produces two different sets of products.

developed by the LBNL group, and (2) Extensive correlated electronic structure calculations on the neutral and anionic states of molecules. In the case of dissociative attachment, the Complex Kohn calculations provide the "entrance amplitude" which is the amplitude for attachment of an electron to the neutral molecule as a function of incident angle in the body frame. Some of those results for NH_3 are described in Subtask 1. Additionally, in dissociative attachment of electrons to ammonia the LBNL AMO theory group provided interpretation of the experimental results to unravel the mechanism where by the resonance at 5.5 eV can produce *both* $NH_2 + H^-$ and $NH_2^- +$ H in a ratio of about 6:4. A single electronic state cannot correspond to both of these final product arrangements because they differ only by where the extra electron is, and must therefore be different electronic states. Fig. 13 shows electronic structure calculations (an example of the "stabilization method") on the ammonia anion in which the two metastable resonance states of NH_3^- appear amid a maze of discretized continuum states. These calculations revealed that the

lower resonance state only correlates to $NH_2 + H^-$ with the additional electron on the dissociating H atom. We discovered a lower bound anion state correlating to NH_2^- + H that becomes what is known in scattering theory as a "virtual state," disappearing into the complex plane as it merges with the ground state potential curve of the neutral molecule. The discovery we made (with A. E. Orel and C. S. Trevisan collaborating) was that these two nearly degenerate asymptotes allow an unexpected "almost symmetric'' charge exchange to occur at large distances (~ 15 a_0) producing the second arrangement of products. Calculation of nonadiabatic couplings together with simplified one-dimensional wave packet calculations gave a branching ratio consistent with the 6:4 ratio observed in the LBNL experiments.

Continuum electron dynamics: The dynamics of observing core-hole localization *(C. W. McCurdy, T. N. Rescigno)*

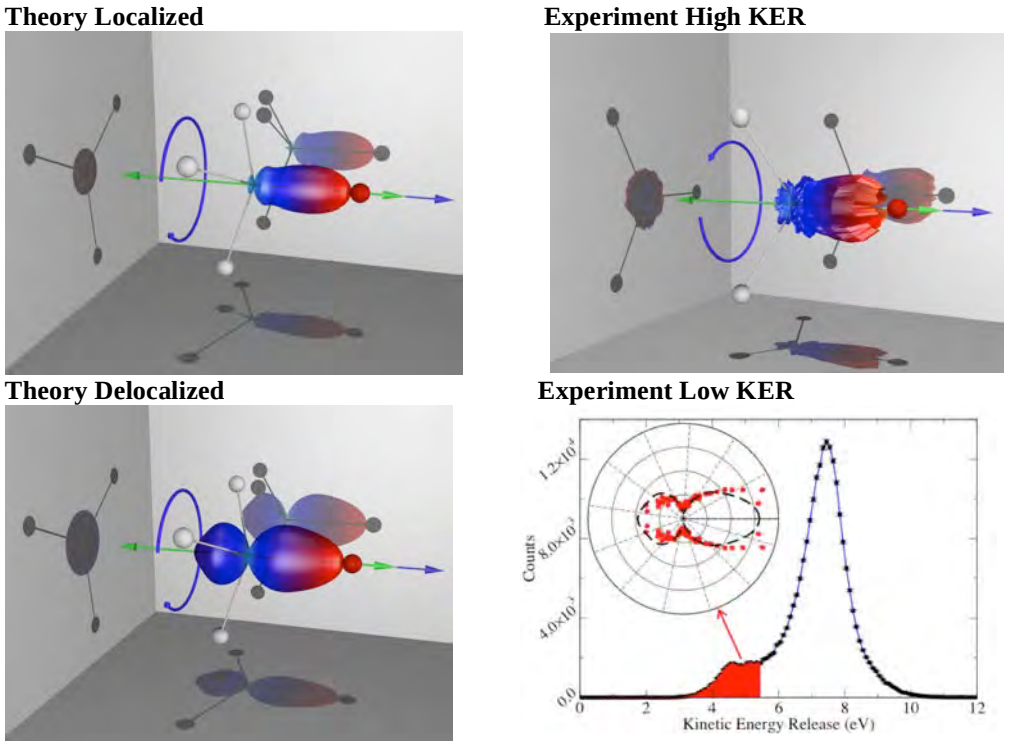

Figure 14: MFPADs for ionization at the fluorine K-edge**.** Top row left: Theory for ionization to create a core hole localized on the fluorine that is detected as F^+, Top right: experimental observation at high kinetic energy release (KER) matches it. Bottom row left: Theoretical MFPAD for delocalized fluorine 1s holes matches the distribution seen for low KER at Bottom right. The same ionization event appears to produce localized or delocalized holes depending on the dissociation channels used to detect it!

In core hole ionization of CF_4 ionization at the fluorine K-edge removes an electron from one (or all) of the four symmetry equivalent fluorines. As described in Subtask 1, the theory group performed Complex Kohn electron-ion scattering calculations to construct the photoionization amplitudes and thus the Molecular Frame Photoelectron Angular Distributions (MFPADs) for that case have the potential to reveal signatures of the symmetry breaking. The experimental results at high KER closely match only the theoretical calculation with the hole localized on the F+ atom detected after Auger decay. However low detecting F+ atoms with low KER selects different dissociating dication states that preferentially select combinations of the F 1s holes that

show a result consistent with having created delocalized F 1s ionization. A theory of this measurement-dependent phenomenon was given by the LBNL theory group in an article submitted to Physical Review Letters.

Continuum Electron Dynamics: Dissociative attachment to formic acid *(T. N. Rescigno and C. W. McCurdy)*

Our immediate future plan for our work on dissociative attachment on this system is to complete electronic structure calculations of the potential curves for dissociation in each of the two resonances described in Subtask 1 above, to illuminate the mechanisms of dissociation. We have performed Complex Kohn electron scattering calculations on electron scattering from formic acid to compute the electron scattering cross sections, and from the T-matrices in those first calculations we constructed the entrance amplitudes shown in Subtask 1 in very preliminary comparisons with experimental data from the LBNL group that is in the early stages of analysis.

Continuum Electron Dynamics: Dissociative attachment to uracil *(T. N. Rescigno)*

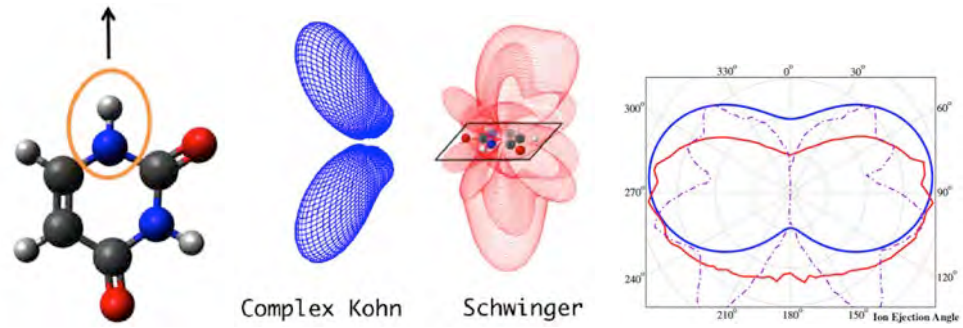

Figure 15: H^- production from DEA to uracil via the 6 eV Feshbach resonance. Left: uracil model with indicated N-H bond break; center: comparison of complex Kohn and Schwinger electron entrance probabilities; right: angular distributions – complex Kohn (blue), Schwinger (dashed-dot), experiment (red).

We have undertaken, in collaboration with Samantha Fonseca and Nicolas Douguet (Drake University), a new theoretical study of dissociative electron attachment to uracil, an RNA nucleobase that contains many of the functional groups common to the DNA bases. Experimental results on the 6 eV Feshbach resonance obtained in our Laboratory were reported in the 2015 research summary and compared with theoretical Schwinger variational results from the Caltech group. In our study, we used the complex Kohn method to carry out fixed-nuclei electron-uracil calculations with fairly elaborate trial wave functions. The total cross section shows a Feshbach resonance of ^{2}A'' symmetry at ~6.5 eV with a width of 32 meV. This doubly excited state is formed by promoting an electron from the highest occupied (a") orbital and placing two electrons in an unoccupied Rydberg (a') orbital. An analysis of the multi-channel S-matrix was then carried out to obtain a complete set of partial widths from which the entrance amplitudes and electron attachment probabilities could be calculated. There is ample experimental evidence that the ^{2}A'' resonance leads to H^- ejection from the N1 site. Figure 2 compares our calculated electron entrance probabilities with the Schwinger results. The angular distributions, computed by averaging the entrance probabilities about the H^- - $C_4H_3N_2O_2$ recoil axis under the assumption of axial recoil, are also compared in Fig. 15.

We aim to begin to address the vast knowledge gap in electron-driven chemical dynamics that currently exists between an isolated molecular system and the condensed phase systems commonly found in technological applications and in nature. This work will be extended to

investigate solvation effects on the dissociative electron attachment dynamics of molecules when they are incorporated in clusters with water or other solvents First experimental efforts are currently underway to study dissociative electron attachment to hydrogen-bonded formic acid dimers.

Future Plans for a New Grid-based Complex Kohn Computational Method *(C. W. McCurdy, T. N. Rescigno in collaboration with Prof. R. Lucchese)*

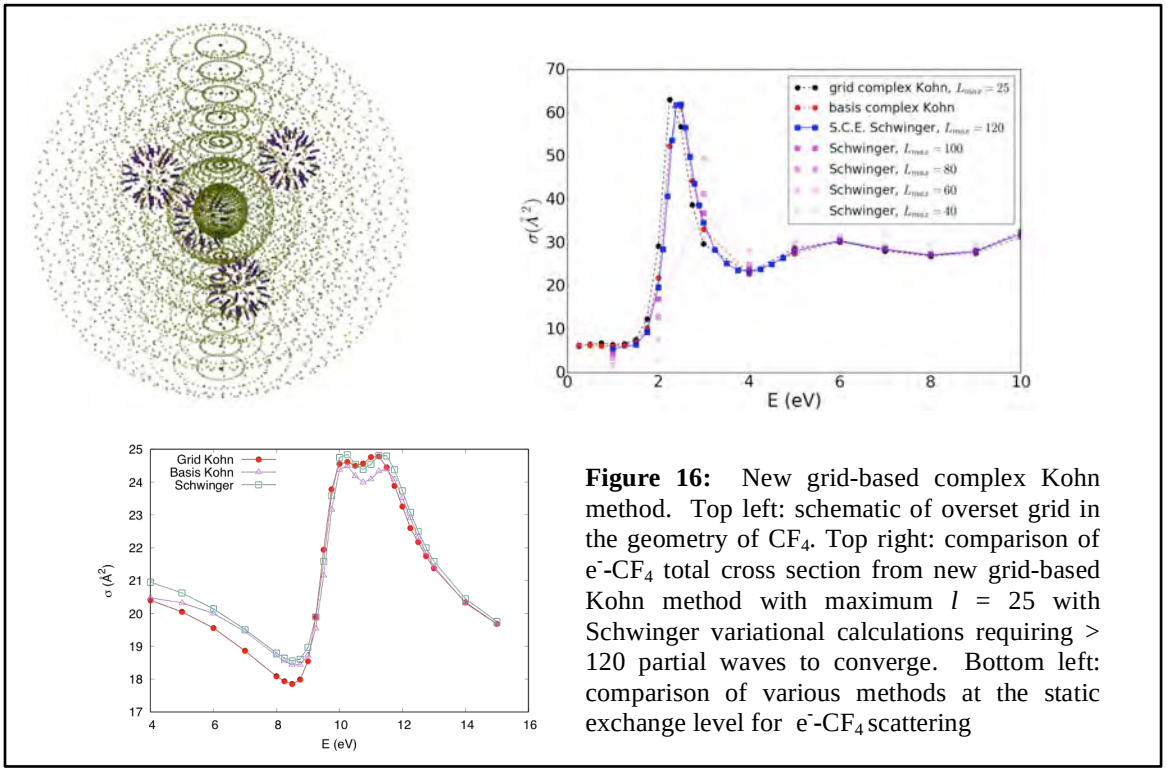

Figure 16: New grid-based complex Kohn method. Top left: schematic of overset grid in the geometry of CF_4. Top right: comparison of e^--CF_4 total cross section from new grid-based Kohn method with maximum l = 25 with Schwinger variational calculations requiring > 120 partial waves to converge. Bottom left: comparison of various methods at the static exchange level for e^--CF_4 scattering

Our principal future goal for the theory for continuum electron dynamics is to bring to bear on all of these problems a new computational implementation of the complex Kohn variational method that describes the scattered electron in each electronic channel using only numerical grid representations. The current complex Kohn capability, developed over decades by the LBNL PIs, uses Gaussian basis functions to describe the scattered electron in the interaction region leading to several limitations of method, particularly for intermediate energy scattering (> 50 eV) or ionization. The new method, which will be developed in close collaboration with Prof. R. Lucchese at Texas A&M University (also funded by the DOE AMOS program), will use overlapping grids in a method called “overset grids” in the applied mathematics literature that is shown schematically in Fig. 16 together with some preliminary results. A notable feature illustrated in Fig. 16 is that overset grids avoid the limitations of single center expansions, used in the implementation of the Schwinger variational method by Prof. Lucchese, and provide a much more compact and efficient representation of the scattering wave function.

The long-range objective is to replace our current methods with new complex Kohn computer codes for the study of electron-molecule collisions and molecular photoionization. The planned theoretical and computational developments will lead to a

modern, easy-to-use, and general electron-molecule collision code, parallelized with OpenMPI that will be made available to other users and will support experiments planned at LBNL in dissociative electron attachment, X-ray photoionization, and high harmonic generation.

Molecular Double Ionization: Future Plans for Double photoionization of H_2O, NO and O_2^+, *(T. N. Rescigno, C. W. McCurdy)*

In collaboration with Prof. Frank Yip of California State University, Maritime we are continuing our work to develop a robust, hybrid numerical method that combines Gaussian molecular orbital technology with grid-based, exterior complex scaling, finite-element DVR methodology to overcome the computational obstacles involved in treating photo-double and electron-impact ionization studies to complex molecular targets.

This year we began a new project to describe the body-frame angular distribution of one-photon double ionization of water. A new experiment at the ALS by Alan Landers of Auburn University and the LBNL COLTRIMS collaboration led by Thorsten Weber has shown that when H_2O is double ionized by removing two electrons from any combination of its highest three occupied molecular orbitals, it dissociates to produce two protons, $H_2O + h\nu \rightarrow H_2O^{2+} + 2e^- \rightarrow O + H^+ + H^+ + 2e^-$. The two protons and the two electrons can be detected in coincidence with COLTRIMS thereby producing the first ever measurement of polyatomic molecular double photoionization in the body frame! We are currently performing extensive electronic structure calculations to compute the potential surfaces for the nine states of H_2O^{++} that are involved, and will use exterior scaling and grid methods, together with the ideas for freezing all but two electrons developed in our collaboration with Prof. Yip, to attack the electron dynamics of double ionization and calculate triply differential cross sections in the body frame.

Molecular Excited States and Applications to Multielectronic Excitations. *(M. Head-Gordon)*

Multi-electron excited states are an area where standard electronic structure methods perform poorly and there is a need for new approaches. They are important in ultra-fast electron dynamics, the probing of valence electron dynamics by core excitations, and also the often poorly characterized low-lying excited states of systems that exhibit strong electron correlations. Under this program, we pioneered a new and very promising class of methods that combine the well-known active space approach (as in the Complete Active Space methods) for describing strongly correlated methods, and the spin-flip method. We have applied the resulting method to the very topical problem of singlet fission (the generation of two triplet excitations from absorption of a single photon) in solid pentacene, using a pentacene dimer model embedded in a molecular mechanics model of the extended crystal. This research identified a new singlet fission mechanism based on surface hopping between bright one-electron and dark two-electron excited states.

Our recent focus has been development of a new tool for multi-electron excited states that we first considered several years ago: non-orthogonal configuration interaction (NOCI) for excited states. Our very recent work on this problem has yielded a very

general implementation of NOCI that for the first time can treat either real or complex or general orbitals as required for spin-frustrated systems, and other molecules that exhibit strong correlations. The important advantage of NOCI is that applications to multielectron excited states in very large molecules are possible. The main limitations are that it is not obvious other than by physical understanding of the states desired how many and which configurations should be included. To illustrate that the advantage is real, and that the limitations are not critical, we have treated excited states of long polyenes, including beta carotene itself, with very promising results.

We have completed a particularly important extension of the general NOCI method, which is to combine it with our spin-flip complete active space (SF-CAS) approach, to define the SF-NOCI method. The point of the combination is that a high spin single reference defines an active space whose orbitals can be localized and then frozen. Each configuration of the resulting SF-CAS can then have its doubly occupied core relaxed independently to define the SF-NOCI method. The power of the SF-NOCI approach comes from several factors. First, whilst relaxing the core only may sound limited (and, in a variational sense it is), those relaxations allow ionic configurations to be lowered in energy relative to the covalent configurations which are energetically favored by the (covalent) orbitals of the high spin single reference configuration. The great improvement of SF-NOCI relative to SF-CAS is shown in Fig. 17 for the ionic-covalent interaction that yields the LiF molecule. Second, the individual core relaxations are well-conditioned because the active orbitals are frozen, and therefore the omnipresent NOCI threat of variational collapse is rendered null and void. This is probably the first really usable NOCI method, and is a feasible way to generate qualitatively correct wavefunctions for multielectron excited states as well as ground states.

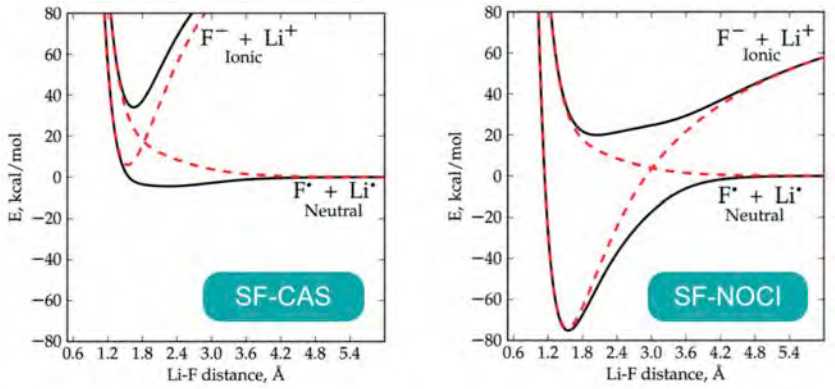

Figure 17. The potential curves obtained via SF-CAS and SF-NOCI for the LiF molecule in the identical (2,2) active space defined by the high spin triplet reference, using the cc-pVTZ basis. SF-CAS yields virtually no binding, which SF-NOCI yields 75 kcal/mol of binding, in good agreement with the experimental value of 82 kcal/mol.

Electronic Structure Methods for Excited States of Clusters *(M. Head-Gordon)*

To permit electronic structure calculations of the excited state bands associated with large homogeneous clusters (e.g. the n=2 or n=3 bands of clusters of helium atoms), we have formulated a configuration interaction with singles (CIS) excited state method that retains a number of amplitudes that scales only linearly with the size of the cluster. Physically, this model corresponds to superposing excitations that are localized on

individual monomers, and discarding charge-transfer (CT) excitations. This was rigorously accomplished using absolutely localized molecular orbitals (ALMOs) that are non-orthogonal between different molecules. In contrast to NOCI above, ALMO-CIS uses the same orbitals for all configurations to enable the Hamiltonian to be explicitly constructed and directly diagonalized to yield the large numbers of states necessary to describe absorption and dynamics in large clusters.

A production version of the implementation has been completed and applied to clusters as large as 485 atoms, to yield 4850 excited states, which is about 10 times larger than we could previously simulate. This is possible because the method scales as the cube of the number of atoms in the cluster, whilst still giving a representation of a cluster band of states whose number increases linearly with the cluster size. Neglect of CT was numerically demonstrated to yield errors relative to full CIS that gradually increase from the red edge of the n=2 band to the blue edge. While the ALMO-CIS results are qualitatively reasonable, it is desirable to remove this error, and for molecular clusters (where CT is more important than for rare gas clusters), this is probably essential.

Therefore, we have just completed a new theory to correct the ALMO-CIS model for neglected CT excitations, which we term ALMO-CIS+CT. To retain the scaling advantages of ALMO-CIS, ALMO-CIS+CT uses a distance criterion to define a neighbor list for each monomer of the cluster, and using the same tensor theory, CT configurations are included to the neighbors. For a large cluster this yields the same scaling. We have had to overcome substantial technical challenges in order to achieve an efficient implementation, but this is now completed and a manuscript is in preparation. Numerical tests show that the ALMO-CIS+CT model differs negligibly from full CIS for He_{25} clusters where direct comparison is possible. The computational challenge in efficient implementation comes from increasing the overall Hilbert space dimension by over a factor of 6 relative to ALMO-CIS, which would lead to a factor of 6^3 increase in computational effort for diagonalization. Improved algorithms, which include a special adaptive diagonalizer, cause the overall computational cost for computing entire bands of states to increase by only a factor of 4 relative to ALMO-CIS.

Simulations of Helium Clusters in Excited States *(M. Head-Gordon)*

The newly developed ALMO-CIS+CT method has been applied to model the size-dependence of helium cluster spectra, up to systems of 300 helium atoms. To correctly simulate the clusters, path integrals were applied to the nuclear motion, at a temperature of 3K (above the superfluid transition), and spherical boundary conditions were employed to establish a droplet-vapor equilibrium. The results, some of which are shown in Fig. 18, illustrate several interesting features. First, the size-dependence of the width of the 2p band (21.2 to 22.0 eV) emerges nicely from

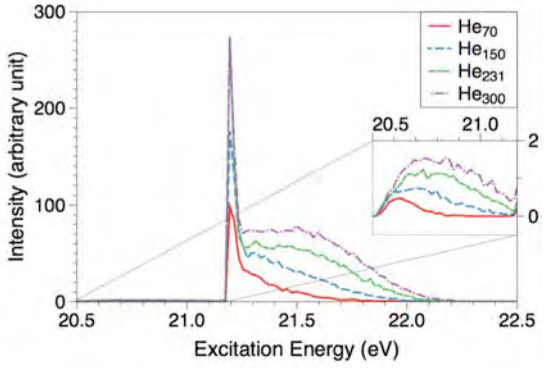

Figure 18. *Ab initio* calculations of the size-dependence of helium cluster excitation spectra, calculated using the newly developed ALMO-CIS+CT treatment of the electrons, together with path-integral treatment of nuclear motion.

the simulations, in qualitative agreement with experiments. Second, signatures of the droplet versus dense gas can be established by removing the attractive part of the potential, and comparing the spectra simulated using different cutoff radii (giving different gas densities in the gas case, and different fractions of gas versus droplet atoms in the droplet-vapor equilibrium case). The dense gas simulation shows narrower bandwidth, and that bandwidth depends strongly on the gas density, while the droplet spectrum is as shown in the figure.

To complement recent experimental studies of helium cluster dynamics in excited states, we have also conducted *ab initio* trajectory studies exploring the dynamics of photoinduced dissociation. Using small He_7 clusters for computational tractability, we have investigated their fate by ab initio molecular dynamics after excitation into the n = 2 manifold. On the 1 ps timescale of the simulation a large majority (90%) of the trajectories exhibit full dissociation to 6 ground state atoms and 1 excited atom, with kinetic energy release commensurate with the blue shift discussed above. A small fraction (3%) of the trajectories yield bound excited dimers, as $(He_2)^*$ is bound and acts as a $(He_2)^+$ core and an outer Rydberg electron. An even smaller fraction (< 0.5%) of trajectories result in trimers. In addition, the dissociation timescale, the kinetic energy release, and the range of products all bear interesting and suggestive similarities to the experimental results for n = 3,4 excitations in clusters 4 orders of magnitude larger.

HHG Simulations in Atoms and Molecules. *(M. Head-Gordon)*

There has been a large gap between the methods of bound state quantum chemistry, and numerical approaches used to simulate high harmonic generation spectra. We have begun to bridge this gap with the first calculations of molecular HHG spectra using bound state quantum chemistry methods, beginning first with the H atom. Most recently, we have applied and expand the knowledge developed in the case of the H atom to describe high-harmonic generation (HHG) for the H_2 molecule (Fig. 19) by using time-dependent configuration interaction with single excitations (TD-CIS). We explored the influence of the heuristic lifetime model on the HHG spectra. The incorporation of finite lifetimes suppresses the noisy back-ground signal which is due to the non-physical 'trapping' of high energy (continuum) states within the localized basis set. Therefore, the heuristic lifetimes allow for much clearer identification of the different harmonics and it is found to be necessary for an adequate description of the HHG process. Direct comparison of the heuristic lifetime model with the application of a CAP could provide more precise information about the role of ionization in HHG of many-electron systems. We also examined the influence of

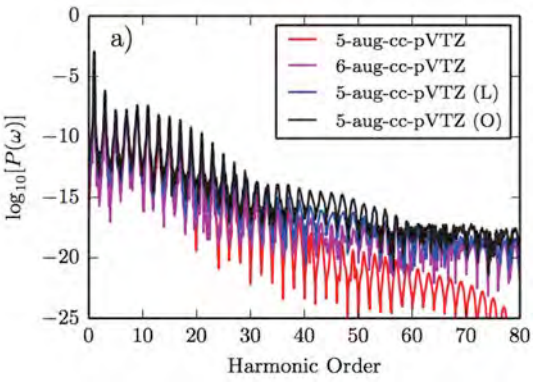

Figure 19. TD-CIS calculations of the HHG spectrum of the H_2 molecule, as a function of addition of diffuse functions. Convergence up to the 30th harmonic is relatively rapid.

the angular momentum of the basis on the computed HHG spectra. The n-aug-cc-pVTZ series of basis sets (n = d,t,q,5) are found to give a good balance of convergence and cost. In contrast, the addition of diffuse functions affects the HHG spectrum significantly. This behavior can be explained by the volume of space that is accessible to the electron at different levels of augmentation. The connection between maximum spatial extent in a Gaussian basis set and the generation of harmonics can be explained though a physical picture as in the semi-classical three-step model. This correlation makes Gaussian basis set more comparable to the traditional approaches of propagation on a grid. Finally, to improve further our Gaussian basis set, we added to our calculations ghost atoms (basis functions at additional centers) in different geometric configurations around the molecule. We analyzed linear and octahedral configurations and we observed that a better description of the states above the IP improves the description of HHG for the H_2 molecule.

Publications of the LBNL AMOS program (2014-2016)

1. Ming-Fu Lin, Daniel M. Neumark, Oliver Gessner, and Stephen R. Leone, “Ionization and Dissociation Dynamics of Vinyl Bromide Probed by Femtosecond Extreme Ultraviolet Transient Absorption Spectroscopy”, J. Chem. Phys. **140**, 064311 (2014).
2. H. Mashiko, M. J. Bell, A. R. Beck, D. M. Neumark, and S. R. Leone, “Frequency tunable attosecond apparatus,” Springer Series in Chem. Phys. **106**, 49 (2014).
3. B. Bernhardt, A. R. Beck, X. Li, E. R. Warrick, M. J. Bell, D. J. Haxton, C. W. McCurdy, D. M. Neumark, and S. R. Leone, “High-spectral-resolution attosecond absorption spectroscopy of autoionization in xenon,” Phys. Rev. A **89**, 023408 (2014).
4. A.R. Beck, B. Bernhardt, E.R. Warrick, M. Wu, S. Chen, M. Gaarde, K. Schafer, D.M. Neumark, and S.R. Leone, "Attosecond transient absorption probing of electronic superpositions of bound states in neon: detection of quantum beats," New J. Phys. **16**, 113016 (2014).
5. A. R. Beck, D. M. Neumark, and S. R. Leone, "Probing ultrafast dynamics with attosecond transient absorption," Chem. Phys. Lett. **624**, 119 (2015).
6. X. Li, B. Bernhardt, A. R. Beck, E. Warrick, A. Pfeiffer, M. J. Bell, D. Haxton, C. McCurdy, D. M. Neumark, and S. R. Leone, "Investigation of coupling mechanisms in attosecond transient absorption of autoionizing states: comparison of theory and experiment in xenon," J. Phys. B: At. Mol. Opt. Phys. **48**, 125601 (2015).
7. Adam S. Chatterley, Florian Lackner, Daniel M. Neumark, Stephen R. Leone, and Oliver Gessner, “Tracking dissociation dynamics of strong-field ionized 1,2-dibromoethane with femtosecond XUV transient absorption spectroscopy”, Phys. Chem. Chem. Phys. **18**, 14644 (2016).
8. Florian Lackner, Adam S. Chatterley, Chaitanya D. Pemmaraju, Kristina D. Closser, David Prendergast, Daniel M. Neumark, Stephen R. Leone, and Oliver Gessner, “Direct observation of ring-opening dynamics in strong-field ionized selenophene using femtosecond inner-shell absorption spectroscopy”, J. Chem. Phys., *submitted* (2016).
9. W. Cao, E. Warrick, D. M. Neumark, and S. R. Leone, "Attosecond transient absorption of argon atoms in the vacuum ultraviolet region: line energy shifts versus coherent population transfer," New J. Phys. **18**, 013041 (2016).
10. E. Warrick, W. Cao, D. M. Neumark, and S. R. Leone, "Attosecond transient absorption of a superposition of Rydberg and Valence electronic states of molecular nitrogen," J. Phys. Chem. A. **120**, 19 (2016).
11. K. Ramasesha, S. R. Leone, D. M. Neumark, "Real-Time Probing of Electron Dynamics Using Attosecond Time-Resolved Spectroscopy," *Annu. Rev. Phys. Chem.* **67**, 41-63 (2016).
12. L. J. Borja, M. Zürch, C. D. Pemmaraju, M. Schultze, K. Ramasesha, A. Gandman, J. S. Prell, D. Prendergast, D. M. Neumark, and S. R. Leone, "Extreme ultraviolet transient absorption of solids from femtosecond to attosecond timescales," J. Opt. Soc. Am. B **33**, 000C57 (2016).
13. Z. Chang, P. B. Corkum, and S. R. Leone, "Attosecond optics and technology: progress todate and future prospects," J. Opt. Soc.Am. B, **33**, 1081 (2016).
14. W. Cao, E. R. Warrick, A. Fidler, S. R. Leone, and D. M. Neumark, "Resonant four wave mixing of attosecond extreme ultraviolet pulses with near infrared pulses in neon: detection of electronic coherences," Phys. Rev. A. **94**, 021802 (2016).
15. B. Gaire, D. J. Haxton, P. Braun, S. Y. Lee, I. Bocharova, F. P. Sturm, N. Gehrken, M. Honig, M. Pitzer, D. Metz, H-K. Kim, T. Jahnke, H. Gassert, S. Zeller, J. Voigtsberger, W. Cao, M. Zohrabi, J. Williams, A. Gatton, D. Reedy, C. Nook, Th. Mueller, A. Landers, C. L. Cocke, I. Ben-Itzhak, R. Doerner, A. Belkacem, and Th. Weber, “Photo double ionization of ethylene and acetylene near threshold”, Phys. Rev. A, **89**, 013403 (2014), featured in “Editors’ Suggestion”

16. B. Gaire, I. Bocharova, F.P. Sturm, N. Gehrken, J. Rist, H. Sann, M. Kunitski, J. Williams, M.S. Schoeffler, T. Jahnke, B. Berry, M. Zohrabi, M. Keiling, A. Moradmand, A.L. Landers, A. Belkacem, R. Doerner, I. Ben-Itzhak, R. Doerner, and Th. Weber, "Hydrogen and fluorine migration in photo double ionization of 1,1-difluoroethylene ($C_2H_2F_2$) near and above threshold", Phys. Rev. A, **89**, 043423 (2014)

17. M. S. Schöffler, T. Jahnke, M. Waitz, F. Trinter, U. Lenz, C. Stuck, M. Jones, M. S. Pindzola, A. Belkacem, C. L. Cocke, A. Landers, J. Colgan, A. Kheifets, I. Bray, H. Schmidt-Böcking, R. Dörner and Th. Weber, "Single photon double ionization of Helium at 800 eV – observation of the Quasi Free Mechanism", Journal of Physics: Conference Series, **488**, 022007 (2014)

18. B. Gaire, I. Bocharova, F.P. Sturm, N. Gehrken, J. Rist, H. Sann, M. Kunitski, J. Williams, M.S. Schoeffler, T. Jahnke, B. Berry, M. Zohrabi, M. Keiling, A. Moradmand, A.L. Landers, A. Belkacem,, I. Ben-Itzhak, R. Doerner, and Th. Weber, "Auger decay and subsequent fragmentation pathways of ethylene following K-shell ionization", Phys. Rev. A, **92**, 013408 (2015)

19. C.E. Liekhus-Schmaltz, I. Tenney, T. Osipov, A. Sanchez-Gonzalez, N. Berrah, R. Boll, C. Bomme, C. Bostedt, J.D. Bozek, S. Carron, R. Coffee, J. Devin, B. Erk, K.R. Ferguson, R.W. Field, L. Foucar, L.J. Frasinski, J.M. Glownia, M. Guehr, A. Kamalov, J. Krzywinski, H. Li, J.P. Marangos, T.J. Martinez, B.K. McFarland, S. Miyabe, B. Murphy, A. Natan, D. Rolles, A. Rudenko, M. Siano, E.R. Simpson, L. Spector, M. Swiggers, D. Walke, S. Wang, Th. Weber, P.H. Bucksbaum, V, S. Petrovic, "Ultrafast Isomerization Initiated by X-Ray Core Ionization", Nature Communications, 6:8199, June 2015, DOI: 10.1038/ncomms9199

20. M. Waitz, D. Aslituerk, N. Wechselberger, H.K. Gill, J. Rist, F. Wiegandt, C. Goihl, G. Kastirke, M. Weller, T. Bauer, D. Metz, F. P. Sturm, J. Voigtsberger, S. Zeller, F. Trinter, G. Schiwietz, T. Weber, J.B. Williams, M.S. Schoeffler, L. Ph. H. Schmidt, T. Jahnke, and R. Doerner, "Electron localization in dissociating H_2^+ by retroaction of a photoelectron onto its source", Phys. Rev. Lett., **116**, 043001 (2016)

21. L. Martin, C. W. Hogle, X.M. Tong, M. M. Murnane, H.C. Kapteyn, T. Jahnke, M. S. Schoeffler, R. Doerner, Th. Weber, and P. Ranitovic, "Mapping Ultrafast Dynamics of Highly Excited D_2^+ by Attosecond XUV Radiation", submitted to Nature Physics, (2015)

22. A.J. Menssen, C. S. Trevisan, M.S. Schoeffler, A. Gatton, J. Sartor, M. Zohrabi, B. Berry, B. Gaire, F. Trinter, A. Belkacem, T. Jahnke, R. Doerner, A.L. Landers, C. W. McCurdy, T. N. Rescigno, Th. Weber, J. B. Williams, "Molecular frame photoelectron angular distributions for core ionization of ethane, carbon tetrafluoride and 1,1-diuoroethylene", J. Phys. B: At. Mol. Opt. Phys., **49**, 055203 (2016)

23. F. Trinter, T. Miteva, M. Weller, S. Albrecht, A. Hartung, M. Richter, J. Williams, A. Gatton, B. Gaire, Th. Weber, J. Sartor, A, Landers, B. Berry, V. Stumpf, K. Gokhberg, R. Doerner, and T. Jahnke, "A molecular movie of Interatomic Coulombic Decay in NeKr", Journal of Physics: Conference Series, **635**, 112100 (2015)

24. D. Reedy, B. Gairey, J. Williams, M. Wellery A. Gatton, T. Bauer, K. Henrichs, P. Burzynski, J. Sartor, B. Berry, R. Doerner, Th. Weber, A.L. Landers, "Dissociation Dynamics of Doubly Ionized Water Using 57 eV Photons", Journal of Physics: Conference Series, **635**, 112141 (2015)

25. M. Fogle, A.L. Landers, A. Moradmand, J. Sartor, D. S. Slaughter, D. J. Haxton, T. N. Rescigno, C. W. McCurdy, Th. Weber, A. Belkacem, A. E. Orel, S. Matsika, "Ion-momentum imaging of dissociative-electron-attachment dynamics in CO_2, N_2O, HCCH and CF_4", Journal of Physics: Conference Series, **635**, 072028 (2015)

26. B. Gaire, A. Gatton, F. Wiegandt, J. Neff, C. Janke, S. Zeller, D. Reedy, J. Rajput, I. Ben-Itzhak, A. L. Landers, A. Belkacem, and Th. Weber, "Bond-rearrangement and ionization mechanisms in the photo-double-ionization of simple hydrocarbons (C_2H_4, C_2H_3F, and 1,1-$C_2H_2F_2$) near and above threshold", accepted for publication in Phys. Rev. A, August 2016

27. F. P. Sturm, T.W. Wright, D. Ray, I. Zalyubovskaya, N. Shivaram, D. S. Slaughter, P. Ranitovic, A. Belkacem, and Th. Weber, “Time resolved 3D momentum imaging of ultrafast dynamics by coherent VUV-XUV radiation”, Rev. Sci. Instrum., **87**, 063110 (2016)

28. M. Waitz, D. Metz, J. Lower, C. Schober, M. Keiling, M. Pitzer, K. Mertens, M. Martins, J. Viefhaus, S. Klumpp, T. Weber, H. Schmidt-Böcking, L. Ph. H. Schmidt, F. Morales, S. Miyabe, T. N. Rescigno, C.W. McCurdy, F. Martín, J.B. Williams, M. S. Schöffler, T. Jahnke, and R. Dörner, “Two-particle interference of electron pairs on a molecular level”, Phys. Rev. Lett., **117**, 083002 (2016)

29. F. P. Sturm, X. M. Tong, A. Palacios, T. W. Wright, I. Zalyubovskaya, D. Ray, N. Shivaram, F. Martin, A. Belkacem, P. Ranitovic, and Th. Weber, “Mapping and Controlling Ultrafast Dynamics of Highly Excited H_2 Molecules by Attosecond VUV Radiation”, accepted for publication in Phys. Rev. A, August 2016.

30. C. W. McCurdy, T. N. Rescigno, C. Trevisan, R.R. Lucchese, B. Gaire, A. Menssen, M. S. Schoeffler, A. Gatton, J. Neff, P. Stammer, J. Rist, S. Eckart, B. Berry, T. Severt, J. Sartor, A. Moradmand, A. Landers, J. Williams, I. Ben-Itzak, R. Doerner, A. Belkacem, , and Th. Weber, “Unambiguous observation of F atom core-hole localization in CF_4 through body-frame photoelectron angular distribution”, submitted to Phys. Rev. Lett., July 2016.

31. J. Rist, T. Miteva, B. Gaire, H. Sann, F. Trinter, M. Keiling, N. Gehrken, A. Moradmand, B. Berry, M. Zohrabi, M. Kunitski, I. Ben-Itzhak, A. Belkacem, T. Weber, A. L. Landers, M. Schoeffler, J. B. Williams, P. Koloren, K. Gokhberg, T. Jahnke, and R. Doerner, „A comprehensive study of Interatomic Coulombic Decay in argon dimers: Extracting R-dependent absolute decay rates from the experiment”, submitted to Chem. Phys., July 2016.

32. J. Neff., “Investigation of Intermolecular Coulombic Decay in small hydrogen bonded systems”, Master’s Thesis, University of Frankfurt/Germany, July 10, 2016.

33. Douguet, N., Slaughter, D. S., Adaniya, H., Belkacem, A., Orel, A. E., Rescigno, T. N., “Signatures of bond formation and bond scission dynamics in dissociative electron attachment to methane.” Phys Chem Chem Phys 17, 25621 (2015).

34. Kosugi, S., Iizawa, M., Kawarai, Y., Kuriyama, Y., David Kilcoyne, A.L., Koike, F., Kuze, N., Slaughter, D. S., Azuma, Y., “PCI effects and the gradual formation of Rydberg series due to photoelectron recapture, in the Auger satellite lines upon Xe $4d^{-1}_{5/2}$ photoionization.” J. Phys. B At. Mol. Opt. Phys. 48, 115003. (2015).

35. Wright, T.W., Champenois, E. G., Cryan, J.P., Shivaram, N., Yang, C-S., Belkacem, A., "Ultrafast Dynamics of the Lowest Lying Neutral States in Carbon Dioxide" submitted to Phys. Rev. A 2016.

36. Champenois, E. G., Shivaram, N. H., Wright, T.W.,Yang, C-S., Belkacem, A., Cryan, J. P., "Involvement of a low-lying Rydberg state in the ultrafast relaxation dynamics of ethylene", J. Chem. Phys., 144, 014303 (2016).

37. Shivaram, N., Champenois, E. G., Cryan, J. P., Wright, T. W., Wingard, T., Belkacem, A., "Focal overlap gating in velocity map imaging to achieve high signal-to-noise ration in photo-ion pump-probe experiments", submitted to App. Phys. Lett. 2016.

38. Larsen, K. A., Cryan, J.P., Shivaram, N., Champenois, E. G., Wright, T. W., Ray, D., Kostko, O., Ahmed, M., Belkacem, A., Slaughter, D. S., “VUV and XUV reflectance of optically coated mirrors for selection of high harmonics.” Opt. Express 24, 18209. (2016).

39. Rescigno, T. N., Trevisan, C. S., Orel, A. E., Slaughter, D. S., Adaniya, H., Belkacem, A., Weyland, M., Dorn, A., McCurdy, C. W., “Dynamics of dissociative electron attachment to ammonia”. Phys. Rev. A 93, 52704. (2016).

40. Slaughter, D. S., Belkacem, A., McCurdy, C. W., Rescigno, T. N., Haxton, D. J., “Ion-momentum imaging of dissociative attachment of electrons to molecules” submitted to J. Phys. B August 2016.

41. Kristina D. Closser, Oliver Gessner, and Martin Head-Gordon, “Simulations of the dissociation of small helium clusters with ab initio molecular dynamics in electronically excited states”, J. Chem. Phys. **140**, 134306 (2014).

42. Luis F. Gomez, Ken R. Ferguson, James P. Cryan, Camila Bacellar, Rico Mayro P. Tanyag, Curtis Jones, Sebastian Schorb, Denis Anielski, Ali Belkacem, Charles Bernando, Rebecca Boll, John Bozek, Sebastian Carron, Gang Chen, Tjark Delmas, Lars Englert, Sascha W. Epp, Benjamin Erk, Lutz Foucar, Robert Hartmann, Alexander Hexemer, Martin Huth, Justin Kwok, Stephen R. Leone, Jonathan H.S. Ma, Filipe R. N. C. Maia, Erik Malmerberg, Stefano Marchesini, Daniel M. Neumark, Billy Poon, James Prell, Daniel Rolles, Benedikt Rudek, Artem Rudenko, Martin Seifrid, Katrin R. Siefermann, Felix P. Sturm, Michele Swiggers, Joachim Ullrich, Fabian Weise, Petrus Zwart, Christoph Bostedt, Oliver Gessner, Andrey F. Vilesov, "Shapes and Vorticities of Superfluid Helium Nanodroplets", Science **345**, 906 (2014).

43. K.R. Siefermann, C.D. Pemmaraju, S. Neppl, A. Shavorskiy, A.A. Cordones, J. Vura-Weis, D.S. Slaughter, F.P. Sturm, F. Weise, H. Bluhm, M.L. Strader, H. Cho, M.-F. Lin, C. Bacellar, C. Khurmi, J. Guo, G. Coslovich, J.S. Robinson, R.A. Kaindl, R.W. Schoenlein, A. Belkacem, D.M. Neumark, S.R. Leone, D. Nordlund, H. Ogasawara, O. Krupin, J.J. Turner, W.F. Schlotter, M.R. Holmes, M. Messerschmidt, M.P. Minitti, S. Gul, J.Z. Zhang, N. Huse, D. Prendergast, and O. Gessner, "Atomic-Scale Perspective of Ultrafast Charge Transfer at a Dye–Semiconductor Interface," J. Phys. Chem. Lett., **5**, 2753 (2014).

44. Michael P. Ziemkiewicz, Camila Bacellar, Katrin Siefermann, Stephen R. Leone, Daniel M. Neumark, and Oliver Gessner, "Femtosecond time-resolved XUV + UV photoelectron imaging of pure helium nanodroplets," J. Chem. Phys. **141**, 174306 (2014).

45. A. Shavorskiy, S. Neppl, D. Slaughter, J. Cryan, K. Siefermann, F. Weise, M.-F. Lin, C. Bacellar, M. Ziemkiewicz, I. Zegkinoglou, M. Fraund, C. Khurmi, M. Hertlein, T. Wright, N. Huse, R. Schoenlein, T. Tyliszczak, G. Coslovich, J. Robinson, R. Kaindl, B. Rude, A. Oelsner, S. Maehl, H. Bluhm, and O. Gessner, "Sub-Nanosecond Time-Resolved Ambient-Pressure X-ray Photoelectron Spectroscopy Setup for Pulsed and Constant Wave X-ray Light Sources," Rev. Sci. Inst. **85**, 093102 (2014).

46. Stefan Neppl, Andrey Shavorskiy, Ioannis Zegkinoglou, Matthew Fraund, Daniel S. Slaughter, Tyler Troy, Michael P. Ziemkiewicz, Musahid Ahmed, Sheraz Gul, Bruce Rude, Jin Z. Zhang, Anton S. Tremsin, Per-Anders Glans, Yi-Sheng Liu, Cheng Hao Wu, Jinghua Guo, Miquel Salmeron, Hendrik Bluhm, and Oliver Gessner, "Capturing interfacial photo-electrochemical dynamics with picosecond time-resolved X-ray photoelectron spectroscopy," Faraday Discuss. **171**, 219 (2014).

47. Michael P. Ziemkiewicz, Daniel M. Neumark, and Oliver Gessner, "Ultrafast electronic dynamics in helium nanodroplets", Int. Rev. Phys. Chem. **34**, 239 (2015).

48. S. Neppl, Y.-S. Liu, C.-H. Wu, A. Shavorskiy, I. Zegkinoglou, T. Troy, D. S. Slaughter, M. Ahmed, A. S. Tremsin, J.-H. Guo, P.-A. Glans, M. Salmeron, H. Bluhm, and O. Gessner, "Toward Ultrafast In Situ X-Ray Studies of Interfacial Photoelectrochemistry," in Ultrafast Phenomena XIX, Kaoru Yamanouchi, Steven Cundiff, Regina de Vivie-Riedle, Makoto Kuwata-Gonokami, Louis DiMauro, Eds., Springer (2015).

49. K. Hong, H. Cho, R.W. Schoenlein, T.-K. Kim, and N. Huse, "Element-Specific Characterization of Transient Electronic Structure of Solvated Fe(II) Complexes with Time-Resolved Soft X-ray Absorption Spectroscopy," Acc. Chem. Res. **48**, 2957 (2015).

50. Rico Mayro P. Tanyag, Charles Bernando, Curtis F. Jones, Camila Bacellar, Ken R. Ferguson, Denis Anielski, Rebecca Boll, Sebastian Carron, James P. Cryan, Lars Englert, Sascha W. Epp, Benjamin Erk, Lutz Foucar, Luis F. Gomez, Robert Hartmann, Daniel M. Neumark, Daniel Rolles, Benedikt Rudek, Artem Rudenko, Katrin R. Siefermann, Joachim Ullrich, Fabian Weise, Christoph Bostedt, Oliver Gessner, and Andrey F. Vilesov, "X-ray coherent diffractive imaging by immersion in nanodroplets", Struct. Dyn. **2**, 051102 (2015).

51. B.E. van Kuiken, H.Cho, K. Hong, M. Khalil, R.W. Schoenlein, T.K. Kim, and N. Huse, "Time-Resolved X-ray Spectroscopy in the Water Window: Elucidating Transient Valence Charge Distributions in Aqueous Fe(II) Complexes," J. Phys. Chem. Lett. **7**, 465 (2016).

52. Curtis F. Jones, Charles Bernando, Rico Mayro P. Tanyag, Camila Bacellar, Ken R. Ferguson, Luis F. Gomez, Denis Anielski, Ali Belkacem, Rebecca Boll, John Bozek, Sebastian Carron, James Cryan, Lars Englert, Sascha W. Epp, Benjamin Erk, Lutz Foucar, Robert Hartmann, Daniel Neumark, Daniel

Rolles, Artem Rudenko, Katrin R. Siefermann, Fabian Weise, Benedikt Rudek, Felix P. Sturm, Joachim Ullrich, Christoph Bostedt, Oliver Gessner, and Andrey F. Vilesov, "Coupled motion of Xe clusters and quantum vortices in He nanodroplets", Phys. Rev. B **93**, 180510(R) (2016).

53. Stefan Neppl, Johannes Mahl, Anton S. Tremsin, Bruce Rude, Ruimin Qiao, Wanli Yang, Jinghua Guo, and Oliver Gessner, "Towards efficient time-resolved X-ray absorption studies of electron dynamics at photocatalytic interfaces", Faraday Discuss., (Submitted) 2016.
54. Y. Kawarai, Th. Weber, Y. Azuma, C. Winstead, V. McKoy, A. Belkacem, and D.S. Slaughter, "Dynamics of the Dissociation Uracil Anion Following Resonant Electron Attachment", Phys. Chem. Lett., **5**, 3854 – 3858 (2014) .
55. Chih-Yuan Lin, C. W. McCurdy and T. N. Rescigno, "Complex Kohn Approach to Molecular Ionization by High-Energy Electrons: Application to H_2O", Phys. Rev. A **89**, 012703 (2014).
56. J. Jose, R. R. Lucchese and T. N. Rescigno, "Interchannel coupling effects in the valence photoionization of SF_6", J. Chem. Phys. **140**, 204305 (2014).
57. S. M. Poullain, C. Elkharrat, W. B. Li, K. Veyrinas, J. C. Houver, C. Cornaggia, T. N. Rescigno, R. K. Lucchese and D. Dowek, "Recoil frame photoemission in multiphoton ionization of small polyatomic molecules: photodynamics of NO2 probed by 400 nm fs pulses", J. Phys. B **47**, 124024 (2014).
58. Chih-Yuan Lin, C. W. McCurdy and T. N. Rescigno , "Theoretical study of (e/2e) from outer- and inner-valence orbitals of CH4: A complex Kohn treatment" Phys. Rev. A **89**, 052718 (2014).
59. M. Fogle, D. J. Haxton, A. L. Landers, A. E. Orel and T. N. Rescigno, "Ion-momentum imaging of dissociative electron attachment dynamics in acetylene", Phys. Rev. A 90, 042712 (2014).
60. D. J. Haxton and C. W. McCurdy, "Ultrafast population transfer to excited valence levels of a molecule driven by x-ray pulses," Phys. Rev. A **90**, 053426 (2014).
61. X. Li, C. W. McCurdy, and D. J. Haxton, "Population transfer between valence states via autoionizing states using two-color ultrafast π pulses in XUV and the limitations of adiabatic passage" Phys. Rev. A **89**, 031404(R) (2014).
62. F. L. Yip, C. W. McCurdy and T. N. Rescigno, "Hybrid Gaussian-discrete variable representation for one- and two-active electron continuum calculations in molecules", Phys. Rev. A **90**, 063421 (2014).
63. S. Fonseca dos Santos, N. Douguet, A. E. Orel and T. N. Rescigno, "Ligand effects in carbon K-shell photoionization of small linear molecules", Phys. Rev. A **91**, 023408 (2015).
64. K. Varela, L. R. Hargreaves, K. Ralphs, M. A. Khakoo, C. Winstead, V. McKoy, T. N. Rescigno and A. E. Orel, "Excitation of the 4 Lowest Electronic Transitions in Methanol by Low-Energy Electrons", J. Phys. B **48**, 115208 (2015).
65. T. N. Rescigno, C. S. Trevisan and C. W. McCurdy, "Tracking hole localization in K -shell and core-valence-excited acetylene photoionization via body-frame photoelectron angular distributions", Phys. Rev. A **91**, 023429 (2015).
66. F. L. Yip , A. Palacios, F. Martín, T. N. Rescigno and C. W.McCurdy, "Two-photon double ionization of atomic beryllium with ultrashort laser pulses", Phys. Rev. A **92** 53404 (2015).
67. Jeremiah R. Jones, Francois-Henry Rouet, Keith V. Lawler, Eugene Vecharynski, Khaled Z. Ibrahim, Samuel Williams, Brant Abeln, Chao Yang, William McCurdy, Daniel J. Haxton, Xiaoye S. Li and Thomas N. Rescigno, "An efficient basis set representation for calculating electrons in molecules," Molecular Physics **114** 2014 (2016).
68. D. J. Haxton, K. V. Lawler, and C. W. McCurdy, "Qualitative failure of a multiconfiguration method in prolate spheroidal coordinates in calculating dissociative photoionization of H_2^+," Phys.Rev. A **91**, 062502 (2015).
69. D. J. Haxton and C. W. McCurdy, "Two methods for restricted configuration spaces within the multiconfiguration time-dependent Hartree-Fock method," Phys. Rev. A **91**, 012509 (2015).

70. X. Li, D. J. Haxton, M. Gaarde, K. J. Schafer, C. W. McCurdy, “Direct extraction of intense-field induced polarization in the continuum on the attosecond time scale from transient absorption,” Phys. Rev. A **93** 023401 (2016).

71. E.J. Sundstrom and M. Head-Gordon, “Non-Orthogonal Configuration Interaction for the Calculation of Multi-electron Excited States”, J. Chem. Phys. **140**, 114103 (2014).

72. K. D. Closser, O. Gessner, and M. Head-Gordon, “Ab initio molecular dynamics simulations of the photodissociation of small helium clusters”, J. Chem. Phys. **140**, 134306 (2014).

73. D. Zuev, T.-C. Jagau, K.B. Bravaya, E. Epifanovsky, Y. Shao, E. Sundstrom, M. Head-Gordon and A.I. Krylov, “Complex absorbing potentials within EOM-CC family of methods: Theory, implementation, and benchmarks”, J. Chem. Phys. **141**, 024102 (2014).

74. N.J. Mayhall, P.R. Horn, E.J. Sundstrom, and M. Head-Gordon, “Spin-flip non-orthogonal configuration interaction: A variational and almost black-box method for describing strongly correlated electrons”, PCCP **16,** 22694-22705 (2014).

75. Y. Shao, Z. Gan, E. Epifanovsky, A.T.B. Gilbert, M. Wormit, J. Kussmann, A.W. Lange, A. Behn, J. Deng, X. Feng, D. Ghosh, M. Goldey, P.R. Horn, L.D. Jacobson, I. Kaliman, R.Z. Khaliullin, T. Kus, A. Landau, J. Liu, E.I. Proynov, Y.M. Rhee, R.M. Richard, M.A. Rohrdanz, R.P. Steele, E.J. Sundstrom, H.L. Woodcock, P.M. Zimmerman, D. Zuev, B. Albrecht, E. Alguire, B. Austin, G.J.O. Beran, Y.A. Bernard, E. Berquist, K. Brandhorst, K.B. Bravaya, S.T. Brown, D. Casanova, C.-M. Chang, Y. Chen, S.H. Chien, K.D. Closser, D.L. Crittenden, M. Diedenhofen, R.A. DiStasio Jr., H. Do, A.D. Dutoi, R.G. Edgar, S. Fatehi, L. Fusti-Molnar, A. Ghysels, A. Golubeva-Zadorozhnaya, J. Gomes, M.W.D. Hanson-Heine, P.H.P. Harbach, A.W. Hauser, E.G. Hohenstein, Z.C. Holden, T.-C. Jagau, H. Ji, B. Kaduk, K. Khistyaev, J. Kim, J. Kim, R.A. King, P. Klunzinger, D. Kosenkov, T. Kowalczyk, C.M. Krauter, K.U. Lao, A. Laurent, K.V. Lawler, S.V. Levchenko, C.Y. Lin, F. Liu, E. Livshits, R.C. Lochan, A. Luenser, P. Manohar, S.F. Manzer, S.-P. Mao, N. Mardirossian, A.V. Marenich, S.A. Maurer, N.J. Mayhall, E. Neuscamman, C.M. Oana, R. Olivares-Amaya, D.P. O’Neill, J.A. Parkhill, T.M. Perrine, R. Peverati, A. Prociuk, D.R. Rehn, E. Rosta, N.J. Russ, S.M. Sharada, S. Sharma, D.W. Small, A. Sodt, T. Stein, D.Stück, Y.-C. Su, A.J.W. Thom, T. Tsuchimochi, V. Vanovschi, L. Vogt, O. Vydrov, T. Wang, M.A. Watson, J. Wenzel, A. White, C.F. Williams, J. Yang, S. Yeganeh, S.R. Yost, Z.-Q. You, I. Y. Zhang, X. Zhang, Y. Zhao, B.R. Brooks, G.K.L. Chan, D.M. Chipman, C.J. Cramer, W.A. Goddard III, M.S. Gordon, W.J. Hehre, A. Klamt, H.F. Schaefer III, M.W. Schmidt, C.D. Sherrill, D.G. Truhlar, A. Warshel, X. Xu, A. Aspuru-Guzik, R. Baer, A.T. Bell, N.A. Besley, J.-D. Chai, A. Dreuw, B.D. Dunietz, T.R. Furlani, S.R. Gwaltney, C.-P. Hsu, Y. Jung, J. Kong, D.S. Lambrecht, W.-Z. Liang, C. Ochsenfeld, V.A. Rassolov, L.V. Slipchenko, J.E. Subotnik, T. Van Voorhis, J.M. Herbert, A.I. Krylov, P.M.W. Gill and M. Head-Gordon, “Advances in molecular quantum chemistry contained in the Q-Chem 4 program package”, Mol. Phys. 113, 184–215 (2015).

76. D.W. Small, E.J. Sundstrom, and M. Head-Gordon, “A simple way to test for collinearity in spin symmetry broken wave functions: Theory and application to Generalized Hartree-Fock”, J. Chem. Phys. **142**, 094112 (2015).

77. K.D. Closser, Q. Ge, Y. Mao, Y. Shao, and M. Head-Gordon, “A local excited state method using single substitutions in the absolutely localized molecular orbital basis with application to spectra of large helium clusters”, J. Chem. Theory Comput. 11, 5791–5803 (2015).

78. A.F. White, C.J. Heide, P. Saalfrank, M. Head-Gordon, and E. Luppi, "Computation of high-harmonic generation spectra of the hydrogen molecule using time-dependent configuration-interaction", Mol. Phys. 114, 947-956 (2016).

79. S. Lehtola, M. Head-Gordon, and H. Jónsson, “Complex orbitals, multiple local minima and symmetry breaking in Perdew-Zunger self-interaction corrected density-functional theory calculations”, J. Chem. Theory Comput. 12, 3195-3207 (2016).

80. S. Lehtola, J.A. Parkhill and M. Head-Gordon, “Cost-effective description of strong correlation: efficient implementations of the perfect quadruples and perfect hextuples models”, J. Chem. Phys. (submitted).

Page is intentionally blank.

Early Career: Ultrafast X-ray Studies of Intramolecular and Interfacial Charge Migration

Oliver Gessner

Chemical Sciences Division, Lawrence Berkeley National Laboratory, Berkeley, CA 94720

OGessner@lbl.gov

Program Scope: At the heart of many emerging sunlight-to-fuel and molecular photovoltaic concepts are interfacial processes that require an optimized, concerted flow of charge and energy on a molecular level. This program is focused at developing and applying time-domain X-ray spectroscopy techniques that enable an atomic-scale understanding of the fundamental mechanisms underlying interfacial electronic and chemical dynamics. In particular, ultrafast dynamics at interfaces between molecules, molecular domains, and semiconductors are studied by time-resolved X-ray photoelectron spectroscopy (TRXPS) and time-resolved X-ray absorption spectroscopy (TRXAS) techniques, which are deployed at the Linac Coherent Light Source (LCLS) and the Advanced Light Source (ALS).

Recent Progress and Future Plans: A major thrust of the program is the development of ultrafast X-ray techniques that may be deployed at X-ray free electron lasers and synchrotron radiation sources in order to study interfacial charge transfer phenomena

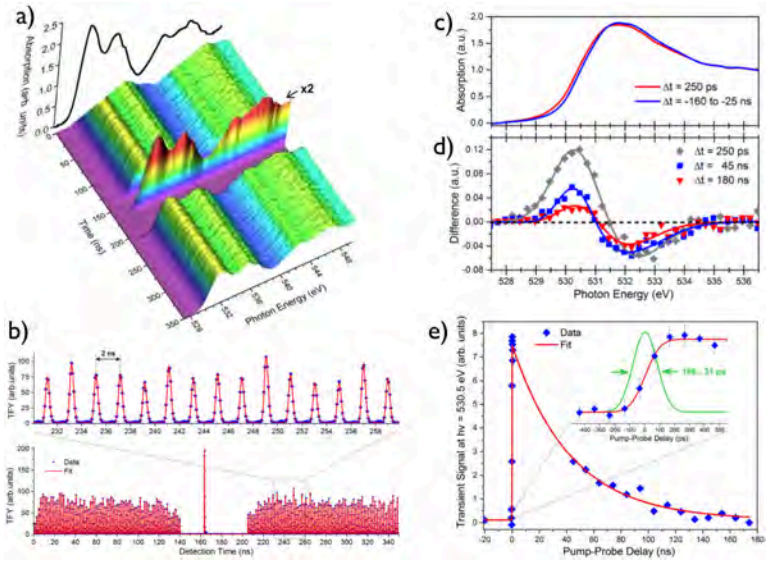

Fig. 1: A novel time-stamping technique enables simultaneous picosecond time-resolved X-ray absorption spectroscopy (TRXAS) studies across hundreds of nanosecond temporal ranges employing the multi-bunch pulse structure of the ALS. a) Oxygen K-edge TRXAS spectra of a nanoporous film of TiO_2. b) TRXAS signals at 532 eV photon energy. c) TRXAS spectra of a Cu_2O powder sample recorded at the oxygen K-edge before (blue) and after (red) excitation with 355 nm laser pulses. d) Differential TRXAS spectra for a variety of pump-probe delays as indicated. Positive values correspond to laser-induced enhanced absorption, negative values to reduced X-ray absorption. e) Temporal evolution of the differential TRXAS peak at ~530 eV. The inset shows a magnified view of the rising edge.

from the unique perspective of inner-shell transitions and with the exquisite sensitivity of time-domain methods for short-lived intermediates. In particular, methods are being developed with the vision in mind to extend them to “real-world” systems that are directly related to emerging sunlight-to-fuel and sunlight-to-electricity concepts based on hybrid materials and designs. During the most recent grant period, previously developed time-resolved X-ray photoelectron spectroscopy (TRXPS) techniques have been complemented by a time-resolved X-ray absorption spectroscopy (TRXAS) setup that has been successfully taken into operation at BL 8.0.1 of the Advanced Light Source (ALS).

Picosecond and femtosecond TRXAS techniques have been successfully applied in the past to study, in particular, excited state and charge-transfer characteristics of molecules and nanocrystalline semiconductor samples in solution. Extending these methods to non-replenishing condensed phase systems and, ultimately, operating photochemical devices holds great promise to capture transient electronic and chemical configurations that may be crucial for the overall function of a material or device but that are too short-lived to be tracked by steady-state spectroscopy techniques. The new TRXAS setup operates in total X-ray fluorescence yield (TFY) mode, i.e., in a photon-in/photon-out configuration rather than in transmission geometry in order to be compatible with a wide variety of materials as well as existing in-situ/operando soft X-ray spectroscopy techniques. A time-stamping method enables TRXAS experiments during all operating modes of the ALS. In particular, during multi-bunch mode the method takes advantage of the high X-ray pulse repetition rate (500 MHz) of the synchrotron in order to simultaneously record picosecond time-resolved TRXAS spectra across hundreds of nanosecond time ranges (Figures 1a,b).

Figures 1c-e illustrate oxygen K-edge TRXAS results for a pellet made of compressed Cu_2O powder. The sample is excited using 10 ps long 355 nm laser pulses at fluences of ~6-10 mJ/cm^2. Figure 1d shows the differential TRXAS response for a variety of pump-probe delays as indicated. Positive values of the differential absorption spectra correspond to laser-induced enhanced absorption, negative values to reduced X-ray absorption. Figure 1e shows the temporal evolution of the positive peak near ~530 eV photon energy. In particular, the response illustrated in Figure 1d may be described by an edge shift of ~2 eV to lower energies, which is comparable to the optical band gap of cuprous oxide (2.2 eV). In addition to this fast (~43 ns, Figure 1e) decaying feature, a much longer (>8 µs) lived response is detected that also corresponds to a redshift of the absorption edge but by only ~1 eV (not shown). The magnitude of this slow response reproduces the result of a previous TRXAS study by Gaffney and co-workers (Phys. Rev. B **80**, 125210 (2009)), who studied a 50 nm thin film of Cu_2O in transmission geometry. At this point, both electronic and structural dynamics in the semiconductor sample have to be considered as potential contributors to the observed TRXAS features. A conclusive physical interpretation will require more experimental and, in particular, theoretical efforts, both of which are underway. The results presented here demonstrate the capability of the new setup to record picosecond TRXAS spectra of bulk semiconductor samples without the need for high X-ray transmission or sophisticated sample preparation techniques.

In the future, the new TRXAS setup will be employed to study electronic dynamics in semiconductor materials and interfacial systems relevant for photocatalytic and photovoltaic applications. In particular, studies on pure and dye-sensitized films of

transition metal semiconductors will complement the TRXPS studies performed within this program at the ALS and the Linac Coherent Light Source (LCLS). The program will aim to extend both TRXPS and TRXAS based studies to application-relevant sample conditions and, ultimately, to operating photochemical devices.

Publications 2014-2016

1. K. R. Siefermann, C. D. Pemmaraju, S. Neppl, A. Shavorskiy, A. A. Cordones, J. Vura-Weis, D. S. Slaughter, F. P. Sturm, F. Weise, H. Bluhm, M. L. Strader, H. Cho, M.-F. Lin, C. Bacellar, C. Khurmi, J. Guo, G. Coslovich, J. S. Robinson, R. A. Kaindl, R. W. Schoenlein, A. Belkacem, D. M. Neumark, S. R. Leone, D. Nordlund, H. Ogasawara, O. Krupin, J. J. Turner, W. F. Schlotter, M. R. Holmes, M. Messerschmidt, M. P. Minitti, S. Gul, J. Z. Zhang, N. Huse, D. Prendergast, and O. Gessner, "Atomic Scale Perspective of Ultrafast Charge Transfer at a Dye-Semiconductor Interface", J. Phys. Chem. Lett. **5**, 2753 (2014).
2. Andrey Shavorskiy, Stefan Neppl, Daniel S. Slaughter, James P. Cryan, Katrin R. Siefermann, Fabian Weise, Ming-Fu Lin, Camila Bacellar, Michael P. Ziemkiewicz, Ioannis Zegkinoglou, Matthew W. Fraund, Champak Khurmi, Marcus P. Hertlein, Travis W. Wright, Nils Huse, Robert W. Schoenlein, Tolek Tyliszczak, Giacomo Coslovich, Joseph Robinson, Robert A. Kaindl, Bruce S. Rude, Andreas Ölsner, Sven Mähl, Hendrik Bluhm, and Oliver Gessner, "Sub-Nanosecond Time-Resolved Ambient-Pressure X-ray Photoelectron Spectroscopy Setup for Pulsed and Constant Wave X-ray Light Sources", Rev. Sci. Instrum. **85**, 093102 (2014).
3. Stefan Neppl, Andrey Shavorskiy, Ioannis Zegkinoglou, Matthew Fraund, Daniel S. Slaughter, Tyler Troy, Michael P. Ziemkiewicz, Musahid Ahmed, Sheraz Gul, Bruce Rude, Jin Z. Zhang, Anton S. Tremsin, Per-Anders Glans, Yi-Sheng Liu, Cheng Hao Wu, Jinghua Guo, Miquel Salmeron, Hendrik Bluhm, and Oliver Gessner, "Capturing interfacial photo-electrochemical dynamics with picosecond time-resolved X-ray photoelectron spectroscopy", Faraday Discuss. **171**, 219 (2014).
4. S. Neppl, Y.-S. Liu, C.-H. Wu, A. Shavorskiy, I. Zegkinoglou, T. Troy, D. S. Slaughter, M. Ahmed, A. S. Tremsin, J.-H. Guo, P.-A. Glans, M. Salmeron, H. Bluhm, and O. Gessner, "Toward Ultrafast In Situ X-Ray Studies of Interfacial Photoelectrochemistry", in Ultrafast Phenomena XIX, Kaoru Yamanouchi, Steven Cundiff, Regina de Vivie-Riedle, Makoto Kuwata-Gonokami, Louis DiMauro, Eds., Springer (2015).
5. Tiberiu Arion, Stefan Neppl, Friedrich Roth, Andrey Shavorskiy, Hendrik Bluhm, Zahid Hussain, Oliver Gessner, and Wolfgang Eberhardt, "Site-specific probing of charge transfer dynamics in organic photovoltaics", Appl. Phys. Lett. **106**, 121602 (2015).
6. Stefan Neppl and Oliver Gessner, "Time-resolved X-ray Photoelectron Spectroscopy Techniques for the Study of Interfacial Charge Dynamics", J. Electron Spectrosc. Relat. Phenom. **200**, 64 (2015).
7. Oliver Gessner and Markus Gühr, "Monitoring Ultrafast Chemical Dynamics by Time-Domain X-Ray Photo- and Auger-Electron Spectroscopy", Acc. Chem. Res. **49**, 138 (2016).
8. Stefan Neppl, Johannes Mahl, Anton S. Tremsin, Bruce Rude, Ruimin Qiao, Wanli Yang, Jinghua Guo, and Oliver Gessner, "Towards efficient time-resolved X-ray absorption studies of electron dynamics at photocatalytic interfaces", Faraday Discuss., 2016, DOI: 10.1039/C6FD00125D.

Page is intentionally blank.

Engineered Electronic and Magnetic Interactions in Nanocrystal Quantum Dots

Victor I. Klimov
Chemistry Division, C-PCS, MS-J567, Los Alamos National Laboratory
Los Alamos, New Mexico 87545, klimov@lanl.gov, http://quantumdot.lanl.gov

1. Program Scope

Chemically synthesized semiconductor nanocrystals, known also as nanocrystal quantum dots (QDs), have been extensively studied as both a test bed for exploring the physics of strong quantum confinement as well as a highly flexible materials platform for the realization of a new generation of solution-processed optical, electronic and optoelectronic devices. Due to readily size-tunable emission, colloidal QDs are especially attractive for applications in light-emitting diode (LED) displays, solid-state lighting, lasing, and single-photon sources. It is universally recognized that the realization of these and other prospective applications of QDs requires a detailed understanding of carrier-carrier interactions in these structures, as they have a strong effect on both recombination dynamics of charge carriers and spectral properties of emitted light. A unifying theme of this project is fundamental physics of electronic and magnetic interactions involving strongly confined carriers/spins with focus on control of these interactions via size/shape manipulation, doping/heterostructuring, and "interface engineering." Our goals in this project include: the development of high-efficiency QD-based LEDs free from detrimental effects of Auger recombination such as efficiency "roll-off" at high currents; realization of electrically pumped single-QD light sources; the achievement of QD lasing under continuous-wave (*cw*) excitation; and control over the magneto-optical properties of QDs doped with magnetic atoms.

2. Recent Progress

Our accomplishments during the past fiscal year include:

- The development of a new class of thick-shell, type-I "giant" QDs with a continuously graded $Cd_xZn_{1-x}Se$ shell (*cg*-QDs). In *cg*-QDs, the confinement potentials are graded for both electrons and holes, which leads to strong suppression of Auger recombination, as indicated by high (~50%) biexciton emission efficiencies.
- The first successful demonstration of the regime of population inversion in colloidal nanostructures of any type using *dc* electrical injection. This represents a critical milestone on the path to the practical realization of QD-based laser diodes, which might complement or even eventually displace existing laser diodes that are currently fabricated using expensive and inflexible epitaxial-growth techniques. The key in this work has been the use of our newly developed "Auger-decay-engineered" *cg*-QDs.
- Demonstration of the important role of the exact structure of the core/shell interface on carrier dynamics and lasing properties of QD heterostructures. This was achieved by performing a side-by-side comparison of the spectroscopic properties of so-called dot-in-bulk CdSe/CdS nanocrystals with and without a thin interlayer separating a quantum-confined CdSe core from an extra-thick (bulk-like) CdS shell.
- Proof-of-principle demonstration of the utility of dual-emitting dot-in-bulk nanocrystals in high-sensitivity ratiometric pressure sensing.
- Detailed studies of spectral and dynamical properties of single- and multi-exciton states in novel QDs based on all-inorganic perovskites ($CsPbX_3$). These studies have revealed an appreciable effect of the halide identity on radiative lifetimes and a considerable deviation of the size dependence of Auger decay rates from the "universal volume scaling" previously observed for many traditional QD systems.
- The development of Mn-doped perovskite QDs with dual-color emission. The unique feature of these novel nanomaterials is the possibility for fine-tuning the QD band gap via post-synthetic anion exchange. The resulting change in the energy of the band-edge optical transition versus the internal *d*-*d* Mn transitions has a dramatic effect on relative intensities of corresponding emission bands that is ascribed to the change in the rate of reverse energy transfer from the Mn ion to the semiconductor host.
- Detailed studies of magnetic polarons in Mn-doped CdSe QDs; i.e., the collective and spontaneous ferromagnetic alignment of the embedded Mn^{2+} atoms, mediated by the spin-spin exchange interactions with a single exciton. By using resonant magneto-photoluminescence (PL), we demonstrate the robust stability of these polarons due to quantum confinement, even for low Mn concentrations where conventional measurements techniques yield ambiguous results.

The above studies have been documented in 8 publications that appeared in high-profile journals including *Nature Nanotechnology*, *Nature Communications*, *Nano Letters*, *ACS Nano*, *J. Am. Chem. Soc*., and *Chemical Reviews*. Below, we provide a more detailed description of our research related to two important accomplishments: (*i*) the first demonstration of *population inversion via electrical pumping* of the QDs, and (*ii*) the direct observation of *magnetic polarons* in low-temperature emission from Mn-doped CdSe QDs.

2.1 *Population inversion in colloidal quantum dots by direct-current (dc) electrical pumping*

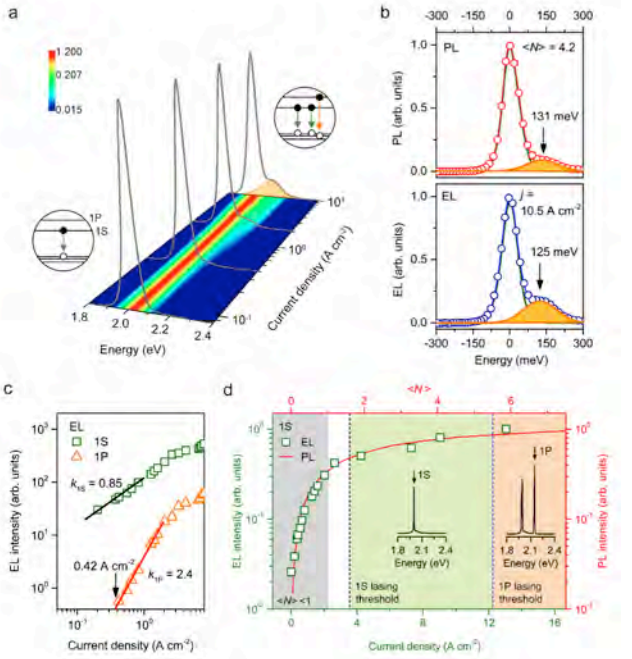

Figure 1. Double-band 1S and 1P electroluminescence (EL) from *cg*-QDs. (a) EL spectra as a function of current density (*j*). At low currents, the device shows usual single-band EL due to the band-edge 1S transition. When *j* exceeds ~0.5 A cm^{-2}, the second higher-energy band (~2.15 eV) due to 1P emission emerges in the EL spectra (orange shading). (b) Comparison of the PL (top) and EL (bottom) spectra of the *cg*-QD film shows a superposition of the 1S (green line) and the 1P (orange shading) emission bands. (c) The 1S and 1P EL intensities as a function of current density. The 1P EL band becomes clearly discernable at current densities *j* > ~0.4 A cm^{-2}. (d) The pump fluence dependence of the 1S emission intensity from optical measurements (red line) is virtually identical to the dependence on current density observed in the EL measurements (green squares) suggesting direct linear scaling between the average QD occupancy $\langle N \rangle$ and *j* ($j = b\langle N \rangle$, where b = 0.45 cm^{2}A^{-1}). Given this relationship, the maximum QD occupancy realized with electrical pumping is ~6 excitons per dot on average, which is above the thresholds for both 1S lasing ($\langle N \rangle$ = 1.6; vertical black dashed line) and 1P lasing ($\langle N \rangle$ = 5.5; vertical blue dashed line); corresponding lasing spectra obtained in optical measurements are shown by black lines.

Colloidal QDs feature near-unity emission quantum yields and widely tunable emission wavelengths controlled by their size and/or composition. Further, a wide separation between electronic levels and low degeneracies of band-edge states reduce the lasing threshold and enhance temperature stability compared to semiconductor quantum wells used in traditional laser diodes. Despite considerable progress over the past years, colloidal-QD lasing is still at the laboratory stage and an important challenge - realization of lasing with electrical injection - is still unresolved. A major complication, which hinders the progress in this field, is fast nonradiative Auger recombination of gain-active multi-carrier species. Recently, we have demonstrated that by using our newly developed continuously graded QDs (*cg*-QDs) we can considerably slow down Auger recombination to the extent that it can be outpaced by electrical injection. Incorporating these QDs into "current-focusing" device structures we have been able to realize for the first time population inversion using *dc* electrical injection. This demonstration proves the feasibility of electrically pumped QD lasers.

The realization of optical gain requires so-called "population inversion," that is, a situation wherein the occupancy of a higher energy state exceeds that of the lower energy state. As the QD band-edge levels can accommodate at least two charge carriers with opposite spins, the population inversion can be achieved only if the average number of electron-hole pairs (or excitons) per dot, $\langle N \rangle$, is greater than one. This corresponds to the situation where at least in a fraction of the QDs in the sample an exciton co-exists with other carriers. The presence of extra carriers triggers a nonradiative Auger process, whereby the exciton decays by transferring its energy not to a photon but to the third carrier. In standard (non-engineered) QDs, this process occurs on tens-to-hundreds of picoseconds, depending on QD size, which leads to very fast deactivation of optical gain.

A typical approach to overcome this complication is the use of very short laser pulses (femtosecond or picosecond duration), which allows for achieving optical gain and lasing in QD materials. Very short optical gain lifetimes create an especially serious problem in the case of electrical pumping, which is an inherently slow process as carriers in this case are introduced into the QD one-by-one. Here, we demonstrate that despite this apparent difficulty, population inversion in colloidal QDs is achievable with *dc* electrical injection (Figure 1). A key element of this work is a new class of thick-shell "giant" QDs with a continuously alloyed $Cd_xZn_{1-x}Se$ shell. In these nanostructures, the confinement potentials are graded for both electrons and holes, which leads to a considerable suppression of Auger recombination, as indicated by high (~50%) biexciton emission efficiencies.

Another novelty of this work is a special "current-focusing" device architecture which allows for obtaining high current densities (j) up to ~12 A cm^{-2}. At low driving currents, these devices show a traditional single-band emission due to the band-edge 1S transition (Figure 1a). However, as the current is increased to j > 0.5 A cm^{-2}, we observe the emergence of the second higher-energy band due to the 1P transitions (Figure 1b,c). This indicates the onset of the saturation of the 1S levels, that is, a complete population inversion of the band-edge states. Based on the quantitative analysis of EL spectra, the average QD occupancy achieved in our devices is ~6. Side-by-side lasing measurements with optical pumping indicate that in our QDs, these excitation levels allow for inverting the population of not only the 1S states, but also the higher-energy 1P states (Figure 1d). Thus, these studies indicate the feasibility of single- and even two-color lasing under *dc* electric injection.

2.2 *Observation of magnetic polarons in Mn:CdSe quantum dots via resonant photoluminescence*

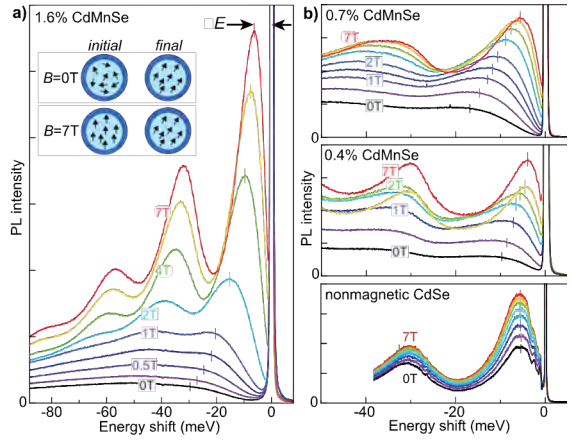

Figure 2. Observation of magnetic polarons in resonant PL of Mn:CdSe QDs. (a,b) Field-dependent resonant PL spectra from the Mn:CdSe QDs at 1.8 K. With increasing magnetic field B from 0–7T, the resonant emission sharpens dramatically and evolves into a series of discrete peaks, while the Stokes shift ΔE between the excitation laser and the first emission peak is markedly reduced. Respectively, these indicate a suppression of Mn^{2+} spin fluctuations, and a suppression of the magnetic polaron formation energy (because the Mn^{2+} are already initially aligned by B, and further alignment by the exciton is not possible). The cartoons depict the initial and final configurations of the Mn^{2+} spins (*i.e.*, when the exciton is created, and when the exciton recombines), at both zero and large B.

In semiconductor QDs, quantum confinement greatly enhances the interaction between band carriers (electrons and holes) and dopant atoms. One particularly striking manifestation of this enhancement is the increased stability of *exciton magnetic polarons (EMPs)* in magnetically-doped nanostructures. In the limit of very strong zero-dimensional confinement that is realized in colloidal QDs, a single photogenerated exciton can exert an effective magnetic exchange field B_{ex} on the embedded magnetic dopants that exceeds several Tesla.

We recently employed the very sensitive method of *resonant PL* - also known as selective excitation - to detect and directly measure the properties of EMPs in a series of Mn^{2+}- doped colloidal CdSe QDs. In these experiments, a narrow-band excitation laser, tuned to the low-energy side of the exciton absorption band, resonantly injects "cold' excitons into the QDs. Subsequently, the exciton's exchange field B_{ex} aligns the Mn^{2+} spins, forming an EMP, which in turn lowers the exciton's energy even further. When the exciton recombines, it therefore emits a lower-energy photon. Thus, the Stokes shift ΔE between the pump laser and the emitted PL directly reveals the polaron formation energy.

Despite small Mn^{2+} concentrations (0.4-1.6%), large polaron formation energies from 8-30 meV are clearly observed at low temperatures via the substantial Stokes shift between the pump laser wavelength and the resonant PL, indicating the complete alignment of all Mn^{2+} spins (see Figure 2). Temperature and magnetic field-dependent studies reveal that B_{ex} reaches *ca.* 8T in these QDs, in agreement with theoretical estimates. Further, the emission linewidths provide direct insight into the statistical fluctuations of the Mn^{2+} spins. These studies demonstrate that resonant PL provides detailed insight into collective magnetic phenomena, even in lightly-doped QDs where conventional techniques such as nonresonant PL provide ambiguous results.

3. Future work

- Evaluation of Auger-decay suppression in a new generation of type-I continuously graded QDs (*cg*-QDs) by single-dot spectroscopy. In these studies, Auger lifetimes will be inferred from direct measurements of biexciton dynamics using time-correlated single photon counting and biexciton emission efficiencies obtained from measurements of second-order intensity correlation function. The purpose of these studies will be to evaluate the distribution of Auger lifetimes across a QD ensemble and provide feedback for the parallel effort on the synthesis of "Auger-decay-engineered" QDs.
- Studies of the effect of Mn-doping on the fine structure of excitonic states, single-exciton dynamics, and

multiexciton recombination in CdSe and $CsPbX_3$ QDs. This work will take advantage of a wide range of available spectroscopic techniques including femtosecond transient absorption and PL spectroscopies, single-dot steady state and time-resolved micro-PL, single-dot photon-correlation measurements, and magneto-optical spectroscopy. A specific focus in this work will be on properties of magnetic polaron states that will be investigated at the ensemble and single-dot levels.

- Exploration of various micro-cavity designs compatible with "current-focusing" charge-injection structures used in our proof-of-principle demonstration of population inversion via *dc* electrical pumping. We will test distributed-feedback and 2D photonic gratings as well as gain-guided designs. In our initial studies we will apply optical pumping. Eventually, this work will be extended to optical-feedback structures incorporated into charge-injection architectures.

4. BES-Supported Publications (2014 - 2016)

1. W. Liu, Q. Lin, H. Li, K. Wu, I. Robel, J. M. Pietryga, and V. I. Klimov, *Mn^{2+}-doped Lead Halide Perovskite Nanocrystals with Dual-Color Emission Controlled by Halide Content*, J. Am. Chem. Soc., in press (2016)
2. M. Lorenzon, V. Pinchetti, W. K. Bae, F. Meinardi, V. I. Klimov, Sergio Brovelli, *Single-particle ratiometric pressure sensitive paints based on 'double-sensor' colloidal nanocrystals*, Nature Comm., in press (2016)
3. J. M. Pietryga, Y.-S. Park, J. Lim, A. F. Fidler, W. K. Bae, S. Brovelli, V. I. Klimov, *Spectroscopic and Device Aspects of Nanocrystal Quantum Dots*, Chem. Rev., in press (2016)
4. W. D. Rice, W. Liu, T. A. Baker, N. A. Sinitsyn, V. I. Klimov, S. A. Crooker, *Revealing giant internal magnetic fields due to spin fluctuations in magnetically doped colloidal nanocrystals*, Nature Nanotech. **11**, 137-142 (2016)
5. N. S. Makarov, S. Guo, O. Isaienko, W. Liu, I. Robel, V. I. Klimov, *Spectral and Dynamical Properties of Single Excitons, Biexcitons, and Trions in Cesium–Lead-Halide Perovskite Quantum Dots*, Nano Lett. **16**, 2349-2362 (2016)
6. V. Pinchetti, F. Meinardi, A. Camellini, G. Sirigu, S. Christodoulou, W. K. Bae, F. De Donato, L. Manna, M., Zavelani-Rossi, I. Moreels, V. I. Klimov, S. Brovelli, *Effect of Core/Shell Interface on Carrier Dynamics and Optical Gain Properties of Dual-Color Emitting CdSe/CdS Nanocrystals*, ACS Nano **10**, 6877-6887 (2016)
7. O. Isaienko and I. Robel, *Phonon-assisted nonlinear optical processes in ultrashort-pulse pumped optical parametric amplifiers*, Sci. Rep. **6**, 23031 (2016)
8. Y.-S. Park, W.-K. Bae, T. Baker, J. Lim, and V. I. Klimov, *Effect of Auger Recombination on Lasing in Heterostructured Quantum Dots with Engineered Core/Shell Interfaces***,** Nano Lett. **15**, 7319-7328 (2015)
9. Y. S. Park, S. Guo, N. S. Makarov, V. I. Klimov, *Room Temperature Single-Photon Emission from Individual Perovskite Quantum Dots*, ACS Nano **9**, 10386-10393 (2015)
10. I. Robel, A. Shabaev, D. C. Lee, R. D. Schaller, J. M. Pietryga, S. A. Crooker, Al. L. Efros, V. I. Klimov, *Temperature and Magnetic-Field Dependence of Radiative Decay in Colloidal Germanium Quantum Dot***,** Nano Lett. **15**, 2685-2692 (2015)
11. M. V. Kovalenko, L. Manna, A. Cabot, Z. Hens, D. V. Talapin, C. R. Kagan, V. I. Klimov, A. L. Rogach, P. Reiss, D. J. Milliron, P. Guyot-Sionnest, G. Konstantatos, W. J. Parak, T. Hyeon, B. A. Korgel, C. B. Murray, W. Heiss, *Prospects of Nanoscience with Nanocrystals***,** ACS Nano **9**, 1012-1057 (2015)
12. W. D. Rice, H. McDaniel, V. I. Klimov, S. A. Crooker, *Magneto-Optical Properties of $CuInS_2$ Nanocrystals***,** J. Phys. Chem. Lett. **5**, 4105-4109 (2014)
13. J. Lim, B. G. Jeong, M. Park, J. K. Kim, J. M. Pietryga, Y.-S. Park, V. I. Klimov, C. Lee, D.C. Lee, W.K. Bae, *Influence of shell thickness on the performance of light emitting devices based on $CdSe/Zn_{1-x}Cd_xS$ core/shell quantum dots*, Adv. Mater. **26**, 8034 (2014)
14. Y.-S. Park, W. K. Bae, J. M. Pietryga, V. I. Klimov, *Auger recombination of biexcitons and negative and positive trions in individual quantum dots*, ACS Nano **8**, 7288 (2014)
15. S. Brovelli, W. K. Bae, F. Meinardi, M. Lorenzon, C. Galland, V. I. Klimov, *Electrochemical control of two-color emission from colloidal dot-in-bulk nanocrystals*, Nano Lett. **5**, 3855 (2014)
16. V. I. Klimov, *Multicarrier interactions in semiconductor nanocrystals in relation to the phenomena of Auger recombination and carrier multiplication*, Annu. Rev. Condens. Matter Phys. **5**, 13.1 (2014)
17. S. Brovelli, W. K. Bae, C. Galland, U. Giovanella, F. Meinardi, V. I. Klimov, *Dual-color electroluminescence from dot-in-bulk nanocrystals*, Nano Lett. **14,** 486 (2014)

PULSE Ultrafast Chemical Science

P.H. Bucksbaum, D.A. Reis, K. Gaffney, T. Heinz, T. Martinez, T. Wolf, M. Guehr, J. Cryan, S. Ghimire, A. Cordones-Hahn, SLAC National Accelerator Laboratory, 2575 Sand Hill Rd. MS 59, Menlo Park, CA 94025. Email michelley@slac.stanford.edu

Mission: The PULSE Ultrafast Chemical Science program focuses on ultrafast chemical physics research at SLAC that is enabled by SLAC's x-ray and relativistic electron facilities, including LCLS, SSRL, Ultrafast Electron Diffraction (UED) and in the future, LCLS-II. Our research at SLAC makes optimal use of these unique tools for fundamental discoveries and new insights in ultrafast science. The two distinguishing advantages of this program are the on-site presence of the LCLS; and our connection to Stanford University. These help to keep us competitive on an international level.

Major Themes: The Ultrafast Chemical Science program has connections to many of the themes in the current BESAC Transformation Opportunities. We have particular emphasis on the transformation opportunities of "Imaging Matter across Scales", "Harnessing Coherence in Light and Matter". We also have high relevance to the Grand Challenges in the areas of "Energy and Information on the Nanoscale" and "Control at the Level of Electrons."

Imaging matter across scales: The nanoscale in space and the femtoscale in time. Microscopy at its most essential level in both space and time is paramount to the BES mission to control matter. Non-periodic nano-structures and ultrafast timescales dominate the workings of biology and chemistry. To understand and control function we therefore must first observe structure and motion on these scales.

X-ray lasers are revolutionary sources of short wavelength coherent radiation for investigations on the nanoscale, and this year we are reorganizing and reinvigorating our subtasks devoted to developing science using coherent x-ray imaging techniques at x-ray free electron lasers. Adding to previous work in serial femtosecond nanocrystal imaging on the few-Angstrom scale, we have an emerging program in coherent self-diffraction as a technique especially useful for femtosecond molecular movies.

We also image molecules using other techniques, such as particle fragment velocity maps, and electron holography. Here we are exploring fundamental energy-relevant processes such as photo-induced isomerization, dissociation, and x-ray damage, using optical and x-ray probes, and a combination of linear and nonlinear spectroscopic methods.

Much of chemistry happens at the femtosecond scale, and it is necessary to develop new methods to simultaneously achieve this level of temporal resolution with simultaneous chemical and structural sensitivity. FEL and laser-based sources of x-ray and extreme ultraviolet radiation afford the opportunity for atomic specificity combined with femtosecond resolution. To realize this opportunity, pump-probe spectroscopy at visible and infrared wavelengths must be extended to the soft and hard x-ray range, and to new sources such as FELs. Much of our efforts are devoted to developing new methods and advancing ultrafast science in this area, including impulsive stimulated Raman and other nonlinear x-ray scattering methods.

Energy and Information: The architecture of light conversion chemistry. Light from the sun is the primary source of energy on earth, and so we are exploring light conversion to electron motion and then to chemical bonds. Some molecules are particularly adept at this conversion and we would like to understand how they work. For example, how does non-adiabatic dynamics affect the process of photocatalysis within coordination complexes and similar materials.

Energy conversion is initiated by charge separation, and we know that the charge distribution of the electron and hole, as well as the presence of low-energy ligand field excited states greatly influence the lifetime of optically generated charge transfer excited states. The detailed mechanism for the excited state quenching remains unclear. New methods of linear and nonlinear spectroscopy, and especially x-ray spectroscopy involving short-pulse FELs, can help provide the answer.

An equally important problem is the protection of some chemical bonds, particularly in biology, from destruction in the presence of ultraviolet sunlight. Photoprotection is also an ultrafast process involving charge transfer, and so these new techniques such as ultrafast x-ray absorption and Auger emission can show how critical bonds are protected.

The incorporation of theory within this FWP is critical for rapid progress in light conversion chemistry, and helps us to focus our efforts in areas of greatest impact.

Harnessing coherence on the eV scale in time, space, and field strength. This is the fundamental scale that determines structure and dynamics of electrons in molecules, and motivates advances in sub-femtosecond time-resolution and Angstrom spatial resolution in theory and experiments. To achieve an adequate view of the molecular realm with at this level, we must interrogate atoms with fields comparable to Coulomb binding fields, and on time scales set by the electronic energy splittings in atoms.

One method to reach this scale is through nonlinear frequency conversion, known as high harmonic generation (HHG). We are constructing new intense sources of attosecond pulsed vacuum ultraviolet radiation based on HHG, and will use it to develop new spectroscopies that can detect the motion of electrons within molecules.

We are particularly interested in the response of atoms to fields strong enough to ionize them multiple times. It has long been known that the ionization thresholds are greatly suppressed for multiple ionization, and a number of theories about this will be tested during the next contract period. This is an example of coupled motion among multiple electrons, which goes beyond the single active electron approximation that has dominated thinking about strong field laser-atom physics. New theoretical approaches are also required for this, and we are tackling these as well.

LCLS is also capable of sub-femtosecond or few femtosecond pulses, and these have the unique property of wavelengths short enough to reach the most deeply bound electrons in first through third row atoms. We will use LCLS to image the strong-field electronic response during HHG in solids at the atomic-scale in length and time, and to explore nonlinear x-ray Compton scattering as a means to achieve simultaneous chemical and structural sensitivity. Through the use of novel methods such as low bunch charge, double-slotted spoilers, strong laser fields, and novel data sorting methods, as well as future methods such as self-seeding, we will incorporate LCLS fully as a tool for sub-femtosecond spectroscopy.

Management Structure: This Ultrafast Chemical Science research program resides within the Chemical Science Division within the SLAC Science Diractorate. The current CS Director is Tony Heinz. Chi-Chang Kao is the Acting Associate Laboratory Director for the Science Directorate.

Space allocations: Most of our research activities take place in laboratories in SLAC Building 40a. SLAC currently provides office space for our research groups, and also allocates approximately 8000 square feet to research laboratories and a computer room for this FWP. The co-location of most of our program within Building 40 and 40a is a distinct advantage, but is not entirely sufficient for the space requirements of this program, and so we also perform some of this research in PULSE Institute space within the Varian Physics Lab and the Mudd Chemistry Lab on the Stanford campus (approximately 1000 square feet, including offices and labs, in each building). Further details are in the Facilities and Resources Section 11 of this document.

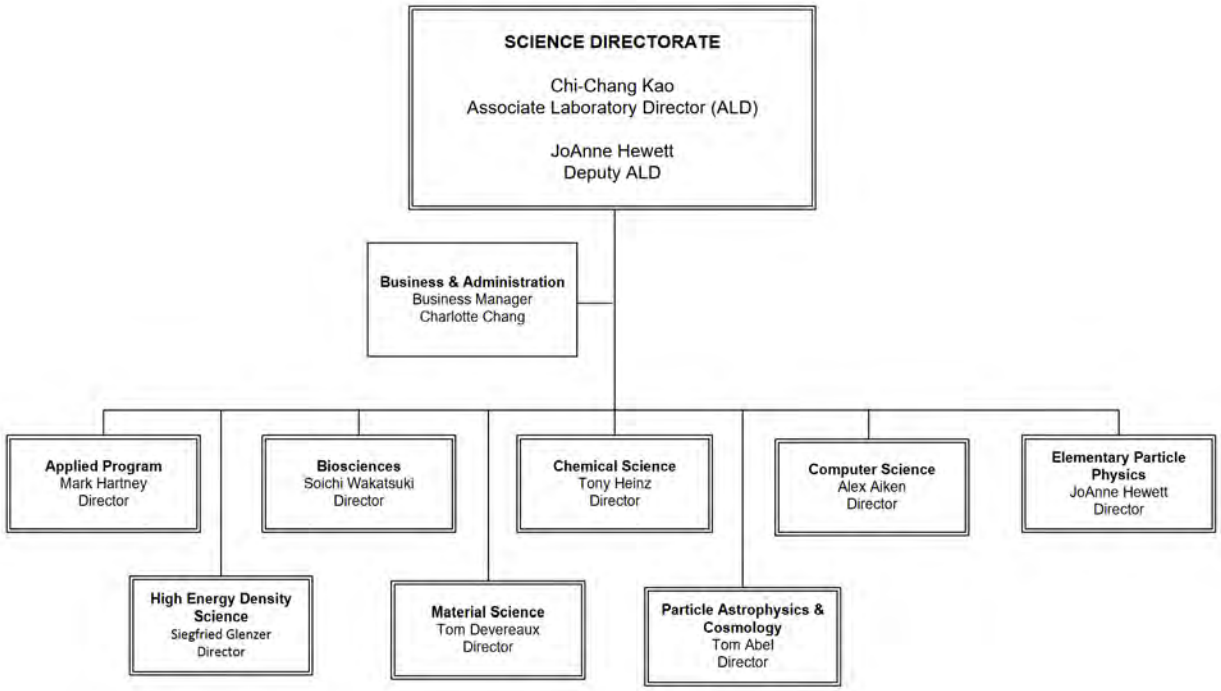

Figure 1. Partial organization chart for SLAC, showing the relation of the Ultrafast Chemical Science FWP to other units with close research ties.

Subtasks and allocations: Seven key personnel are responsible for six subtasks, which represent six different areas of expertise:

1. UTS: Ultrafast Theory and Simulation (Martinez)
2. ATO: Attoscience (Bucksbaum, Cryan)
3. SPC: Solution Phase Chemistry (Gaffney)
4. NPI: Non-periodic X-ray Imaging (Open)
5. SFA: Strong Field AMO Physics (Bucksbaum)
6. NLX: Nonlinear X-ray Science (Reis, Ghimire)
7. EDN: Electron Dynamics on the Nanoscale (Heinz)
8. EIM: Excitations in Molecules (Wolf)

There were two key changes in the past twelve month. The first was the departure of Markus Guehr to a faculty position in Potsdam, and the promotion of Thomas Wolf to fill his position as the task leader of the Excitations in Molecules subtask, which has now been incorporated into the Ultrafast Chemical Science FWP in PULSE. The second has been the reorganization of the Nonperiodic Imaging subtask. These are described in the abstracts for those subtasks.

Support operations (finance, HR, safety, purchasing, travel) are directed by the Associate Laboratory Director for Science and the Chemical Sciences Director and their staff. They provide oversight and delegate the work to appropriate offices in the SLAC Operations Directorate or to the staff of the Stanford PULSE Institute.

Connections to other units within the SLAC organizational structure: Close collaborations are maintained with the Science R&D Division within the LCLS Directorate; the Materials Science Division (SIMES) within the Science Directorate; SSRL; and the SUNCAT Center within our own Chemical Sciences Division, as shown in figure 4.1. Our location near these facilities and research organizations at SLAC greatly aids collaboration.

Other important connections: The PIs have affiliations with other Stanford University research and academic units: All members of this FWP are members of the Stanford PULSE Institute, and several are affiliated with the SIMES Institute, Bio-X, the Ginzton Laboratory, and the Departments of Chemistry, Physics, and Applied Physics.

We also have collaborative connections to other outside research labs, including DESY, the Lawrence Berkeley Laboratory, the Center for Free Electron Lasers (CFEL) in Hamburg, and BES funded groups at the University of Michigan, the Ohio State University, the University of Connecticut, Louisiana State University, and Northwestern University.

Knowledge transfer to LCLS: Transfer of knowledge to and from LCLS is extremely fluid and critical to our success. Much of our research creates benefits for LCLS by providing new research methods and research results, and in addition there are several more direct transfers of our research product to help LCLS:

- We continue to help to commission several LCLS instruments and setup space, particularly with the LCLS Single Particle Imaging Initiative, the XLEAP attosecond pulse initiative, and other initiatives that develop research protocols.
- Some of our graduate students provide user support through to LCLS users, particularly in cooperation with CXI, AMO, and the Laser Division, and they receive salary supplements for this work. This activity has been endorsed by review panels and is supported by the Associate Laboratory Directors and the SLAC Director.
- Several of our postdocs and students have transferred to permanent staff positions at LCLS.
- Several LCLS Scientists and Staff have become members of the PULSE Institute, and this provides a connection to the larger research community of Stanford.
- Some LCLS Instrument Scientists have a direct connection to the research activities of this FWP. In the previous year this included collaborations with XPP, AMO, and CXI scientists.
- PULSE has helped LCLS to institute a Graduate Fellowship program, and PULSE manages several LCLS graduate student campus appointments.
- PULSE conducts an annual Ultrafast X-ray Summer School to train students and postdocs about LCLS science opportunities.

Advisory committee. The SLAC Science Policy Committee advises SLAC and the Stanford Provost on all science activities at the laboratory. Neither the SLAC Chemical Sciences Division nor the SLAC Science Directorate has their own standing science advisory committee at present. The PULSE External Advisory Board advises us on our DOE activities. This board meets annually and reports to the PULSE Director and to the Stanford Dean of Research. The reports are also forwarded to the SLAC Director, the ALD for Science, and to the SLAC Science Policy Committee.

Educational programs and outreach activities. We have an active outreach and visitors program supported by Stanford through the PULSE Institute. Each year one or more scientists receive sabbatical travel supplements to permit them to be in residence in PULSE. This year, Jan-Michael had a partial sabbatical here. This visitors program also helps postdocs with fellowships or from other institutes to work at PULSE and collaborate with us.

PULSE continues to serve the larger ultrafast community with our annual Ultrafast X-ray Summer School. This school, which was founded by the PIs of this FWP in 2006, continues to be a main mechanism for expanding the research community interested in using x-ray free electron lasers for their research. In 2011 we began a cooperative activity with CFEL in Hamburg to rotate the school between DESY and SLAC in alternate years. The school has received continued strong supported from BES, Stanford, and from CFEL. The tenth edition of the school was held at SLAC in June 2016.

Ultrafast Theory and Simulation, Todd J. Martínez PI

SLAC National Accelerator Laboratory, 2575 Sand Hill Rd. MS 59, Menlo Park, CA 94025

Email: toddmtz@slac.stanford.edu

Program Scope: This program is focused on developing and applying new methods for describing molecular dynamics on electronically excited states, as well as the interaction of molecules with radiation fields. We continue to develop and apply the *ab initio* multiple spawning (AIMS) method that solves the electronic and nuclear Schrodinger equations simultaneously from first principles, including the treatment of cases where the Born-Oppenheimer approximation breaks down (e.g. around conical intersections where two or more electronic states are exactly degenerate). We are working to extend this methodology to incorporate the effects of novel pump and probe pulses using high energy photons, including those obtained from modern x-ray sources such as LCLS. We also focus on understanding the behavior of molecular excited states in paradigmatic phenomena such as light-induced isomerization, excited state proton transfer, and excitation energy transfer.

Recent Progress and Future Plans

Extending Ab Initio Multiple Spawning to Include Shaped Laser Pulses: We extended the AIMS method to account for *both* light field and nonadiabatic coupling-induced breakdown of the Born-Oppenheimer approximation. (Kim, Tao, Martinez and Bucksbaum 2015) This new "Floquet AIMS" method uses dressed states within the Floquet picture and models light absorption as a surface-crossing event. This allows us to investigate light-induced conical intersections as well as control induced by shaped laser pulses. As shown in Figure 1, the new method is quantitatively accurate when compared to exact solution of the time-dependent Schrodinger equation. However, it is also directly applicable to large molecules and compatible with "on the fly" calculation of the electronic structure. We intend to use this new method to model laser-induced control of molecules.

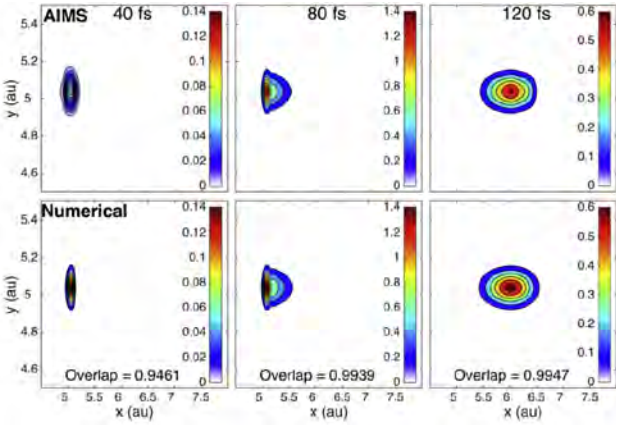

Figure 1. Comparison of exact ("Numerical") and AIMS evolution of wavepackets after photon absorption induced by a transform-limited femtosecond laser pulse. This is a two-state/two-dimensional model, where numerically exact simulations are feasible for assessing accuracy.

GPU-Based Electronic Structure For Nonadiabatic Dynamics: We used our newly developed GPU-based complete active space self-consistent field method to study excited state dynamics of the provitamin D_3 molecule. (Snyder, Curchod and Martinez 2016) This is the largest molecule studied with first principles nonadiabatic molecular dynamics using multireference wavefunctions. Before our new GPU-CAS method, time-dependent density functional theory (TDDFT) was the only tractable method for the excited state dynamics of such a large molecule (with more than 50 atoms). However, the TDDFT method is known to have serious flaws for excited state dynamics – for example, there are no conical intersections between the ground and first-excited electronic states in TDDFT. Indeed, our work showed that GPU-CAS results differed significantly from previous work using TDDFT on this molecule. For example, the excited state lifetime is clearly biexponential in our simulations (and in previous experiments),

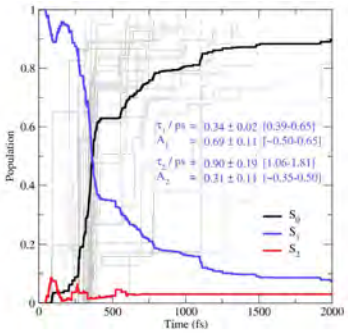

Figure 2. Electronic population dynamics of provitamin D_3 after photoexcitation. Experimental time constants and amplitudes in brackets.

while a monoexponential (and much too fast) decay was observed with TDDFT. Subsequent experiments (published after our work) were in agreement with a primary prediction from our work that there would be no correlation between reactivity and lifetime (in contradiction to the previous TDDFT study which claimed such a correlation should be observed). We have also been exploring avenues to incorporate dynamic electron correlation into multireference methods by combining CAS with DFT. (Filatov, Martinez and Kim 2016)

Towards Excited State Dynamics of Organometallic Complexes: We have extended the AIMS method to incorporate both spin-conserving and spin-changing transitions. The generalized AIMS (GAIMS) method (Curchod, Rauer, Marquetand, Gonzalez and Martinez 2016) was shown to be accurate even in cases where traditional surface hopping types of schemes break down. It also maintains the rotational invariance that is physically required (but not respected in numerous surface hopping methods that have been recently introduced). We implemented GAIMS in the context of CPU-based electronic structure codes, where spin-orbit integrals and the Breit-Pauli Hamiltonian are readily available. In preparation for the use of GAIMS in our GPU-based codes, we also developed effective core potential (ECP) integrals on GPUs. (Song, Wang, Sachse, Preiss, Presselt and Martinez 2015)

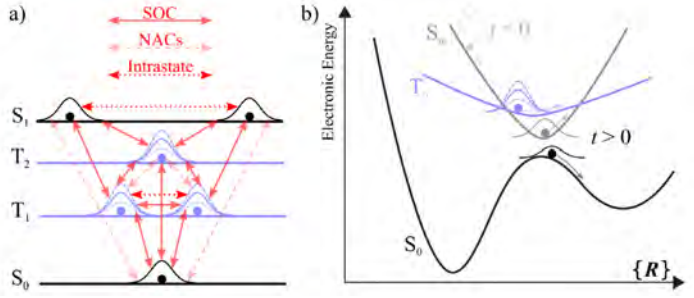

Figure 3. Left: Schematic of the different types of couplings which are present in the GAIMS method for singlet and triplet spins states. Right: Schematic of the GAIMS method for both intersystem crossing and internal conversion.

Future Plans: We have begun application of our *ab initio* exciton model to the photosynthetic LH2 complex. We are implementing AIMS dynamics within this context to describe nonadiabatic effects and explore the role of electronic coherence in this system. We are also planning to devote effort to the modeling of excited state dynamics in coordination complexes containing transition metals. This is now feasible with the GPU-accelerated methods, the effective core potentials we have implemented on GPUs, and the GAIMS method for modeling both internal conversion and intersystem crossing. It remains to implement a Breit-Pauli Hamiltonian (and the required integrals) to compute spin-orbit couplings within our GPU-accelerated framework. This will allow us to investigate excited state dynamics of paradigmatic inorganic photochemical systems such as $Fe(CO)_5$, as well as energy-relevant complexes like $Ru(bpy)_3$ and Fe-containing analogs.

Publications Supported by the AMOS Program

Kim, J., H. Tao, T. J. Martinez and P. Bucksbaum (2015). "Ab initio Multiple Spawning on Laser-Dressed States: A Study of 1,3-Cyclohexadiene Photoisomerization via Light-Induced Conical Intersections." *J. Phys. B* **48**: 164003.

Liekhus-Schmaltz, C. E., I. Yenney, T. Osipov, A. Sanchez-Gonzalez, N. Berrah, R. Boll, C. Bomme, C. Bostedt, J. D. Bozek, S. Carron, R. Coffee, J. Devin, B. Erk, K. R. Ferguson, R. W. Field, L. Foucar, L. J. Frasinski, J. M. Glownia, M. Guehr, A. Kamalov, J. Krzywinski, H. Li, J. P. Marangons, T. J. Martinez, B. K. McFarland, S. Miyabe, B. Murphy, A. Natan, D. Rolles, A. Rudenko, M. Siano, E. R. Simpson, L. S. Spector, M. Swiggers, D. Walke, S. Wang, T. Weber, P. H. Bucksbaum and V. S. Petrovic (2015). "Ultrafast Isomerization Initiated by X-ray Core Ionization." *Nature Comm.* **6**: 8199.

Song, C., L.-P. Wang, T. Sachse, J. Preiss, M. Presselt and T. J. Martinez (2015). "Efficient implementation of effective core potential integrals and gradients on graphical processing units." *J. Chem. Phys.* **143**: 014114.

Curchod, B. F. E., C. Rauer, P. Marquetand, L. Gonzalez and T. J. Martinez (2016). "Communication: GAIMS-Generalized Ab Initio Multiple Spawning for Both Internal Conversion and Intersystem Crossing Processes." *J. Chem. Phys.* **144**: 101102.

Filatov, M., T. J. Martinez and K. S. Kim (2016). "Using the GVB Ansatz to Develop Ensemble DFT Method for Describing Multiple Strongly Correlated Electron Pairs." *Phys. Chem. Chem. Phys.* **18**: 21040.
Liu, L., J. Liu and T. Martinez (2016). "Dynamical Correlation Effects on Photoisomerization: Ab Initio Multiple Spawning Dynamics with MS-CASPT2 for a Model trans-Protonated Schiff Base." *J. Phys. Chem. B* **120**: 1940-1949.
Snyder, J. W., B. F. E. Curchod and T. Martinez (2016). "GPU-Accelerated State-Averaged Complete Active Space Self-Consistent Field Interfaced with Ab Initio Multiple Spawning Unravels the Photodynamics of Provitamin D3." *J. Phys. Chem. Lett.* **7**: 2444-2449.

ATO: Attosecond Science

Philip H. Bucksbaum, James Cryan, SLAC National Accelerator Laboratory, 2575 Sand Hill Rd MS 59, Menlo Park, CA 94025. Email phb@slac.stanford.edu

Objective and Scope: Electron motion underlies and is responsible for almost all chemical reactions. These ultrafast motions may be both initiated and studied by utilizing light sources with comparable timescales. Our goal is to track the evolution of electrons on their natural time scales, to understand the earliest processes involved in chemical change.

Broad bandwidth ultrafast laser pulses at extreme ultraviolet (XUV) and x-ray wavelengths can excite localized core electrons into a superposition of valence-excited states. Subsequent ultrafast laser pulses can probe this localized excitation. For low intensity pulses, interaction of the molecular system with XUV and x-ray photons results in ionized molecular species, and so most work with coherent electronic excitation focuses on superpositions of cationic states. If the exciting pulse has sufficient bandwidth it is possible to stimulate emission of a photon and thus de-excite the molecular system to a low-lying valence excited state. This process, stimulated Raman scattering, can result in superpositions of non-degenerate states that all couple to the near-edge resonances, provided the coherent bandwidth of a single pulse exceeds the ground-to-valence-excited state energies, and the Raman transition is allowed. This coherent redistribution of population among many excited states creates a spatially localized excitation that is critical to studies of charge migration in neutral molecules.

Recent Progress:

Impulsive Electronic Raman Redistribution: Two years ago we began and collaboration with Daniel Haxton (LBNL) who has also been calculating cross-sections for impulsive stimulated Raman scattering (ISRS) using his MCTDHF approach. In this past year, we have continued this collaboration and have successfully implemented a rate-equation based model that accurately predicts the results obtained using Haxton's MCTDHF approach. A rather surprising finding from this model is that the presence of the auto-ionizing states in our target system have almost no effect on the Raman cross-section as shown in Fig. 1. We are currently drafting a manuscript that summarizes the properties of attosecond impulsive Raman scattering using broad bandwidth XUV pulses.

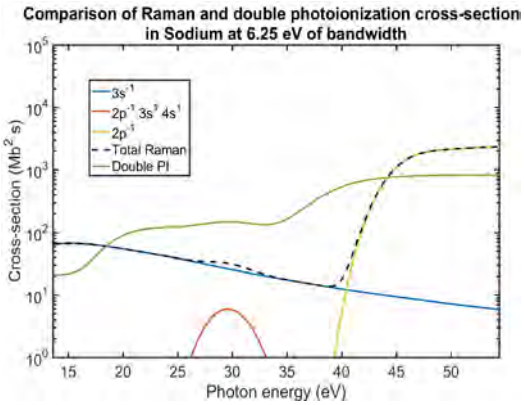

Figure 1 – Raman Cross-sections calculated using our rate equation model. The dashed curve shows the total Raman cross-section for a 6.25 eV (FWHM) laser pulse. The green curve shows the ionization losses, and the other curves show the partial Raman cross-sections.

We have also explored ISRS in the x-ray domain, and are again collaborating with Dan Haxton to finish a manuscript for a proposed experiment that will use broadband x-ray pulses to create a superposition of valence excited-states via impulsive Raman scattering near the oxygen K-edge in NO_2. We then propose a scheme to probe the valence wavepacket as a function of time using time-resolved Auger spectroscopy.

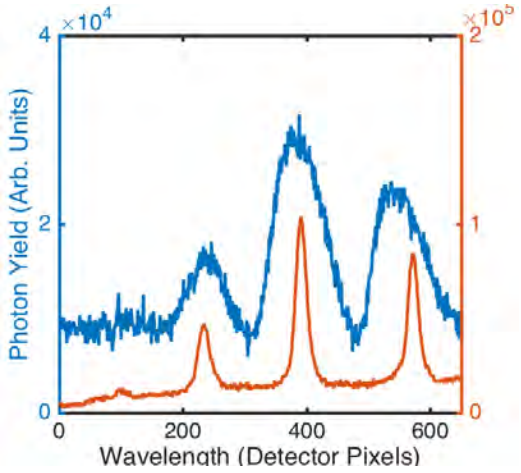

Figure 2 – Spatially integrated XUV spectrum resulting from our double gating technique. The red curve shows the measured XUV spectrum when the two non-collinear laser pulses have no time delay, which should produce collinear train of attosecond bursts. As the time-delay between the pulses is increased we see a broadening of the spectral fringes indicative of non-overlapping attosecond bursts (blue curve).

High Intensity Attosecond Bursts: In the past year we have made progress building a source capable of producing excited-state electronic wavepackets. Exploiting the process of strong-field drive high harmonic generation (HHG), which produces attosecond bursts of XUV radiation every half cycle of the driving laser field, we have recently demonstrated nearly isolated attosecond pulses. Our technique employees a crossed beam geometry that produces a spatial-temporal coupling in the laser focus and leads to an angular separation between the attosecond bursts. Using a double gating technique with two-color (ω+2ω) laser pulses we have successfully demonstrated isolation of the attosecond bursts, as shown in Fig. 2. Our current efforts focus on optimizing the angular separation between the observed bursts, and increasing the brightness of these bursts.

HHG Spectroscopy: We have other on-going projects, which use HHG as a probe of molecular dynamics. The first project focuses on the dynamics following the strong-field ionization of water molecules. The strong-field ionization event produces a superposition of the $^1A_1$ and $^1B_1$ cationic states. This wavepacket dephases due to the very fast nuclear motion of the excited A_1 state. We have previously observed this dephasing by comparing the HHG spectrum from H_2O and D_2O. Currently advances are being made in using THz pulses to create oriented molecular samples, which should provide control over the population of the $^1A_1$ and $^1B_1$ states.

Future Projects:

Charge Dynamics: We plan to use our newly developed IAP source to induce and probe electronic coherence in small molecular systems. We also plan to use our novel source to investigate the possibility of controlling the electron dynamics through precision tailoring of the attosecond pulse train since the attosecond bursts are spatially separated in this technique.

Connecting our work to LCLS and LCLS-II: The LCLS affords unique opportunities to create broadband x-ray pulses capable of driving ISRS in small molecular systems (for example NO_2). We will continue to submit proposals to use this tool to create and probe coherent superposition of electronic states.

Publications:

Publications based on research that was primarily supported by this FWP in 2014-2016.

1. Bucksbaum, Philip. 2014. “Molecular Dissociation Dynamics Driven by Strong-Field Multiple Ionization.” *Bulletin of the American Physical Society 59*.
2. James P. Cryan, Andrei Kamalov, Matthew R. Ware, Shungo Miyabe, Daniel J. Haxton, and Philip H. Bucksbaum, 2016. “Impulsive Stimulated Raman Scattering by Attosecond Pulses.” *Ultrafast Phenomena 2016*.
3. J Devin, S Wang, A Kaldun, and P Bucksbaum, 2016. “High harmonic generation from impulsively aligned SO2.” *Bulletin of the American Physical Society*.
4. Rex Garland, Song Wang, Matthias Hoffmann, and Phil Bucksbaum, 2016, “Highly-parallel photoconductive antenna array for generating intense THz pulses.” In prep.
5. Andrei Kamalov, Matthew Ware, Philip Bucksbaum, and James Cryan, 2016. “Developing a High-Flux Isolated Attosecond Pulse Source.” *Bulletin of the American Physical Society*.
6. Kamalov (2016) In Prep.
7. Chelsea Liekhus-Schmaltz, Gregory A McCracken, Andreas Kaldun, James P Cryan, and Philip H Bucksbaum 2016. “Coherent control using kinetic energy and the geometric phase of a conical intersection.” arXiv:1607.0255.
8. McFarland, B. K., J. P. Farrell, S. Miyabe, F. Tarantelli, A. Aguilar, N. Berrah, C. Bostedt, et al. 2014. “Ultrafast X-Ray Auger Probing of Photoexcited Molecular Dynamics.” *Nature Communications* 5 (June): 4235. doi:10.1038/ncomms5235.
9. S. Miyabe and P. H. Bucksbaum, “Tranisent Impulsive Electronic Raman Redistribution,” *Phys. Rev. Lett.* 114 143005 (2015)
10. Spector, Limor S, Maxim Artamonov, Shungo Miyabe, Todd Martinez, Tamar Seideman, Markus Guehr, and Philip H Bucksbaum. 2014. “Axis-Dependence of Molecular High Harmonic Emission in Three Dimensions.” *Nature Communications* 5: 3190. doi:10.1038/ncomms4190.
11. Spector, L.S., M. Artamonov, S. Miyabe, T. Martinez, T. Seideman, M. Guehr, and P.H. Bucksbaum. 2014. “Quantified Angular Contributions for High Harmonic Emission of Molecules in Three Dimensions.” arXiv:1207.2517.
12. Song Wang, Julien Devin, Matthias Hoffmann, James Cryan, Andreas Kaldun, and Philip Bucksbaum, 2016. “High-harmonic generation in aligned water molecules.” *Bulletin of the American Physical Society*.
13. Matthew R Ware, James Cryan, and Philip H Bucksbaum, 2016. “Understanding x-ray driven impulsive electronic state redistribution using a three-state model.” *Bulletin of the American Physical Society*.

SPC: Solution Phase Chemistry (Kelly Gaffney (PI), Amy Cordones-Hahn (co-PI))
Stanford PULSE Institute, SLAC National Accelerator Laboratory
2575 Sand Hill Rd, Menlo Park, CA 94025, kgaffney@slac.stanford.edu

Program Scope: Electronic excited state phenomena provide a compelling intersection of fundamental and applied research interests in inorganic chemistry. Harnessing the strong optical absorption and photocatalytic activity of compounds depends on our ability to control fundamental physical and chemical phenomena associated with the non-adiabatic dynamics of electronic excited states. The central events of excited state chemistry can all critically influence the dynamics of electronic excited states, including internal conversion and intersystem crossing events governed by non-adiabatic interactions between electronic states in close proximity to conical intersections, as well as solvation and electron transfer.

The research opportunities enabled by LCLS direct both the scientific and technical focus of the Solution Phase Chemistry (SPC) sub-task. Scientifically, this sub-task focuses on two critical aspects of electronic excited state dynamics emphasizing the fundamental understanding of phenomena relevant to solar energy applications:

- We use ultrafast time resolution measurements, simple ligand exchange reactions, and simulation to understand the molecular properties that control excited state relaxation dynamics in coordination compounds.
- We use photo-excitation to change the electronic structure and reactivity of inorganic complexes and track site specific changes in metal solvation and coordination dynamics with ultrafast time-resolved measurements and molecular simulation.

In order to harness the strong optical absorption and photocatalytic activity of coordination complexes in solar energy applications we must robustly characterize the metal center inner shell electronic and nuclear dynamics. We are achieving this goal by utilizing a wide range of ultrafast non-linear spectroscopic methods and developing two critical ultrafast x-ray methods: (1) simultaneous hard x-ray diffuse scattering (XDS) and x-ray emission spectroscopy (XES) as probes of charge, spin, and metal-ligand bonding dynamics in electronic excited states and (2) soft x-ray Resonant Inelastic X-ray Scattering (RIXS) to probe metal-ligand covalency in electronic excited states.

Recent Progress and Future Plans

Controlling MLCT excited state lifetimes in 3*d* coordination complexes (McFarland 2014; Zhang 2014; Zhang 2015; Biasin 2016; Kjær 2016; Kunnus 2016a; Kunnus 2016c): Understanding the electronic excited state relaxation dynamics of transition metal complexes requires a detailed characterization of multiple electronic excited state potential energy surfaces, their relative energies as a function of molecular geometry, and how the distinct levels couple with one another. Given the complexity of the phenomena, a coordinated effort including experiment, synthesis, theory, and simulation increases the rate of progress. Our development of femtosecond resolution x-ray spectroscopic probes of charge and spin dynamics in electronic excited states puts us in an excellent position to investigate the mechanism and rate of relaxation dynamics of charge transfer excited states in transition metal complexes. We will focus our research on two classes of systems, transition metal-based iron complexes that have potential in light harvesting applications and ruthenium-based complexes with demonstrated long excited state lifetimes for studies of charge migration in extended molecular complexes.

Cost effective solar energy applications necessitate the use of abundant materials, but the majority of inorganic artificial photosynthetic materials have been based on rare 4*d* and 5*d* transition metals. Replacing ruthenium dyes with iso-electronic iron dyes has been a long standing target for solar energy

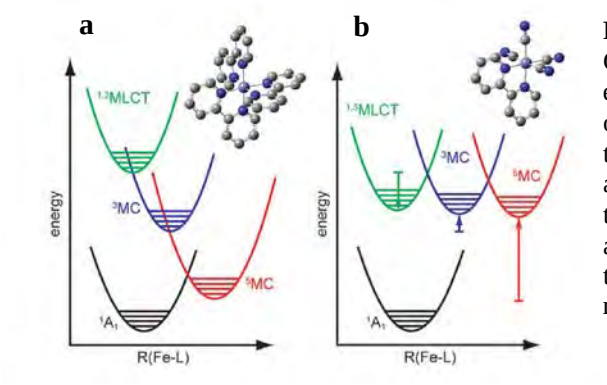

Figure 1: Schematic depiction of the influence of CN^- substitution for bpy. **a** Schematic potential energy curves consistent with the dynamics observed for $[Fe(bpy)_3]^{2+}$. **b** For $[Fe(bpy)(CN)_4]^{2-}$, the combination of MLCT excited state stabilization and metal-center excited state destabilization leads to significantly distinct dynamics. The colored arrows indicate the shift in the energy levels from **a** to **b**. Experiments confirm $[Fe(bpy)(CN)_4]^{2-}$ does not form ^{3}MC or ^{5}MC excited states.

applications, but to date the ultrafast spin crossover dynamics have inhibited the usefulness of iron dyes. A schematic of our strategy for manipulating the relaxation rate and mechanism appears in Figure 1. Suppressing spin crossover requires destabilizing high (^{5}MC) and intermediate (^{3}MC) spin metal-centered excited states relative to the optically allowed charge transfer excited states (Figure 3**b**). For metal to ligand charge transfer (MCLT) excited states, this can be achieved by using a single ligand with a low lying electron acceptor molecular orbital, and choosing the other ligands to maximize the ligand field splitting energy.

The $[Fe(bpy)_N(CN)_{6-2N}]^{2N-4}$, where bpy = 2,2'-bipyridine, series provided a straight forward means of manipulating the relative energy of the MLCT, ^{3}MC, and ^{5}MC excited states which is further enhanced by the strong solvatochromism of the mixed ligand complexes. These studies have shown that the MLCT excited state lifetime can be extended by more than two-orders of magnitude from roughly 100 fs to 20 ps. Present work is focused on changing the electron acceptor orbital by substituting the 2,2'-bipyridine ligand with other aromatic ligands. No systematic connection between the MLCT state energy and lifetime has been observed, indicating that non-equilibrium dynamics, not just thermodynamics, strongly influence the excited state relaxation mechanism.

Future studies will focus on identifying the structural properties that control the relaxation mechanism. Preliminary analysis of time resolved x-ray scattering and Fe XES spectra indicate that triplet MLCT and MC states strongly hybridize in mixed ligand iron complexes, leading to much larger metal-ligand bond length changes in MLCT states than occurs in $[Fe(2,2'\text{-bipyridine})_3]^{2+}$. Vetting this preliminary analysis and determining the influence of electronic excited state covalency on charge transfer excited state lifetime will be a central objective of future studies. Critical to this process will be the use of soft x-ray RIXS at the Fe L-edge and the N K-edge to observe time dependent changes in metal covalency. At present, these measurements prove very challenging at LCLS, but are ideally suited to the capabilities of LCLS-II.

Site-specific solvation and coordination dynamics in model photo-catalysts studied with diffuse scattering (Wernet 2015; Kunnus 2016b; van Driel 2016; Yang 2016a; Yang 2016b): The site-specific interaction of solvent and reactants with metal centers in electronically excited molecules controls photocatalytic reactions. Femtosecond resolution x-ray scattering provides a means of measuring the site-specific solvation and coordination dynamics of photocatalysts. Ultrafast x-ray diffuse scattering (XDS) directly probes the time dependent changes in the distribution of distances between all unique pairs of atoms, a property directly available from molecular dynamics simulations. This makes the comparison between experiment and simulation straight forward by avoiding the often complex conversion of simulation results to spectroscopic observables. Additionally, ultrafast x-ray diffuse

scattering accentuates significantly different dynamics than optical spectroscopies; XDS preferentially samples the dynamics associated with the most electron-rich atoms and directly probes bond distances and angles, while optical spectroscopy preferentially samples Franck-Condon active motions. Franck-Condon analysis suffers from the fact that these motions need not be chemically relevant and accurate electronic excited state potential surfaces are needed to extract structural information.

The properties of ultrafast diffuse x-ray scattering make the method an optimal approach to study the dynamics occurring locally around the photocatalytically active Ir atoms where the largest changes in intramolecular electronic and nuclear structure of $[Ir_2(dimen)_4]^{2+}$ occur, where dimen = para-diisocyanomenthane. These studies show that acetonitrile coordinates to Ir much more strongly in the electronic excited state than the electronic ground state. Extending these studies to photocatalytic reactions directs our future objectives.

Publications supported by AMOS Program (2014-2016):

Biasin, E., T. B. van Driel, K. S. Kjaer, et al. (2016). Femtosecond X-Ray Scattering Study of Ultrafast Photoinduced Structural Dynamics in Solvated $Co(terpy)_2^{2+}$. *Phys. Rev. Lett.* **117**.

Kjær, K. S., W. K. Zhang, R. Alonso-Mori, et al. (2016). Manipulating Charge Transfer Excited State Relaxation and Spin Crossover in Iron Coordination Complexes with Ligand Substitution. *Chem. Sci.* **accepted**.

Kunnus, K., I. Josefsson, I. Rajkovic, et al. (2016a). Anti-Stokes Resonant X-ray Raman Scattering for atom specific and excited state selective dynamics. *New J. Phys.* **under revision**.

Kunnus, K., I. Josefsson, I. Rajkovic, et al. (2016b). Identification of the dominant photochemical pathways and mechanistic insights to the ultrafast ligand exchange of $Fe(CO)_5$ to $Fe(CO)_4EtOH$. *Struct. Dyna.* **3**: 043204.

Kunnus, K., W. K. Zhang, M. G. Delcey, et al. (2016c). Viewing the Valence Electronic Structure of Ferric and Ferrous Hexacyanide in Solution from the Fe and Cyanide Perspectives. *J. Phys. Chem. B* **120**: 7182.

McFarland, B. K., J. P. Farrell, S. Miyabe, et al. (2014). Ultrafast X-ray Auger probing of photoexcited molecular dynamics. *Nature Comm.* **5**.

van Driel, T. B., K. S. Kjær, R. W. Hartsock, et al. (2016). Atomistic Characterization of the Active-Site Solvation Dynamics of a Model Photocatalyst. *Nature Comm.* **under revision**.

Wernet, P., K. Kunnus, I. Josefsson, et al. (2015). Orbital-specific mapping of the ligand exchange dynamics of $Fe(CO)_5$ in solution. *Nature* **520**: 78.

Yang, J., M. Guehr, T. Vecchione, et al. (2016a). Femtosecond Gas Phase Electron Diffraction with MeV Electrons. *Faraday Discuss.* **accepted**.

Yang, J., M. Guehr, T. Vecchione, et al. (2016b). Diffractive imaging of a rotational wavepacket in nitrogen molecules with femtosecond megaelectronvolt electron pulses. *Nature Comm.* **7**: 11232.

Zhang, W. K., R. Alonso-Mori, U. Bergmann, et al. (2014). Tracking Excited State Charge and Spin Dynamics in Iron Coordination Complexes *Nature* **509**: 345.

Zhang, W. K. and K. J. Gaffney (2015). Mechanistic Studies of Photoinduced Spin Crossover and Electron Transfer in Inorganic Complexes. *Acc. Chem. Res.* **48**: 1140.

NPI: Non-Periodic Imaging

PI: (Position open, Bucksbaum is acting). Scientists: C. A. Stan, R. G. Sierra, H. Demirci
Stanford PULSE Institute, SLAC National Accelerator Laboratory
2585 Sand Hill Rd., Menlo Park, CA 94025
phb@slac.stanford.edu

Mission: The mission of NPI has been to develop coherent diffractive x-ray imaging research areas within ultrafast AMO Science. This subtask has made major contributions to the methods that are now used routinely for single-particle coherent femtosecond diffraction, including several sample injector technologies and image retrieval protocols, as well as the physics of important atmospheric aerosols such as soot and salt, and the physics of liquid droplets used for injection.

NPI Reinvention: This subtask is fully engaged in large collaborations in coherent x-ray imaging for large molecules and nanocrystals, but at the same time we see a transition with many of the methods of coherent x-ray imaging now carried out within the LCLS CXI team and through the LCLS Single Particle Initiative project. In addition, Bogan, Starodub, Loh and Laksmono have departed from NPI. There is an emerging frontier of coherent hard-x-ray imaging for ultrafast AMO science in the area of high resolution femtosecond and angstrom movies of fundamental processes in small molecules. NPI and PULSE has therefore organized a new internal initiative on femtosecond angstrom molecular movies, with our initial emphasis on coherent self-referencing "Schroedinger Cat" methods, described in the SFA abstract this year. At the same time our team of bioscience researchers have formed their own subtask within the Stanford PULSE Institute but funded outside of the AMOS program, with support coming through SLAC Biosciences and the Stanford Medical School.

RECENT PROGRESS

Robust XFEL sample delivery with a concentric-flow electrokinetic injector. We developed a new type of electrokinetic injector, which uses a liquid sheath to protect the samples and stabilize the injection of challenging samples (high viscosity media, fragile protein cystals) and opens the way for chemical mixing studies. Using this injector, we determined the room temperature structure of an antibiotic-bound 30S ribosome structure with less than 1 mg of sample.

We recently demonstrated that the injector can be operated in air, and that we can deliver viscous media vital to membrane protein studies at both XFELs and synchrotrons. It also works in helium environments, developed at SLAC and SACLA for biomolecular crystallography. We conducted two collaborative experiments that acquired full data structure data on CypA and iCH proteins, as well as structural studies of the photosystem-II complex and of a mosquito larvicide.

Generation of extreme negative pressures in water at LCLS. We generated tension pulses with nanosecond rise times in water by reflecting cylindrical shock waves, produced by X-ray laser pulses from LCLS, at the internal surface of drops of water. Depending on the X-ray pulse energy, a range of cavitation phenomena occurred, including the rupture and detachment, or spallation, of thin liquid layers at the surface of the drop. We evaluated that negative pressures below −100 MPa were reached in some drops, more than in any other experiments with bulk water. We find that rapid decompression leads to a transition from a heterogeneous to a homogeneous cavitation mechanism, and generates transient negative pressures that are larger than those corresponding to heterogeneous cavitation. The time scale at which this transition occurs is given by the concentration of heterogeneous nuclei.

An accurate measurement of the nuclei concentration will provide an important clue for understanding the mechanism of cavitation in water. Such a measurement requires investigating cavitation at nanosecond time scales, and can be studied experimentally using XFEL explosions. In addition to the LCLS experiment described above, we were awarded a beamtime at SACLA to make accurate measurements of the cavitation pressure in water subjected to nanosecond decompression, and to explore the possibility of reaching homogeneous cavitation in bulk water.

Liquid explosions generated by X-ray pulses. We completed the analysis of the jet and drop explosions induced by X-ray lasers, a phenomenon that we observed and imaged for the first time. Our primary focus was characterizing and modeling the hydrodynamic flow induced by explosions at time scales comparable to the repetition rate at high-repetition-rate XFELs such as LCLS-II. We provided analytical formulas that predict the damage to two of the most important sample delivery schemes for XFELs: liquid microjets and liquid drops. This study also revealed that XFEL explosions in microjets generate shock waves, which could damage samples in future experiments even when radiation damage does not occur. We compared the XFEL explosions with the explosions induced by optical lasers, and we found that XFEL explosions are simpler, and more reproducible. These characteristics of XFEL explosions make them a promising method to generate extreme conditions in the liquid phase and study their effect of chemical and biological samples.

In a follow-up experiment at FLASH in Germany, we investigated the explosions induced by XFEL pulses on our electrospinning injector using pulses at a 1 MHz repetition rate. Although the photon and pulse energies at FLASH are much lower than at LCLS, the high absorption of soft X-rays in water enabled us to simulate a LCLS-II experiment with hard X-rays. We found that the electrospinning injector recovers very quickly after explosions, and might be usable at LCLS-II.

De novo phasing at LCLS using Se anomalous diffraction. The majority of biomolecule structures solved at X-ray FELs have been phased using external information via molecular replacement. De novo phasing at X-ray FELs has proven challenging due in part to per-pulse variations in intensity and wavelength. We solved a selenobiotinyl-streptavidin structure using phases obtained by the anomalous diffraction of selenium measured at a single wavelength (Se-SAD) at the Linac Coherent Light Source. Our results demonstrate that Se-SAD, routinely employed at synchrotrons for novel structure determination, is now possible at X-ray FELs.

Single-particle imaging. We have continued to work towards LCLS's single particle imaging initiative (SPI); our contributions include sample injection, synthesis and characterization. In this collaboration, we achieved a 6 Å resolution on 100-nm viruses. In addition, we are participating on a project that aims to study extracellular vesicles with a size range too small to be observed by standard optical imaging techniques, and too disordered and heterogeneous for standardX-ray structural techniques.

Crystal damage due to XFEL-induced shock waves. We used a two-color pump-probe setup at LCLS to investigate the effect of shock waves on protein crystals delivered with microjets. In this experiment, the two pulses were separated vertically, and the probe investigated crystals that had not been exposed to radiation from the first pulse, but had been subjected to shock waves launched in the microjet by the first pulse. We used femtosecond crystallography to probe the shocked lysozyme crystals, and found that the quality and resolution of the diffraction patterns were worse than that from unperturbed crystals. Therefore, the shock waves induced by XFEL pulses in microjets can damage protein crystals and could prevent efficient data acquisition at high repetition rate XFELs.

PUBLICATIONS WHICH NPI WAS PRIMARY AUTHOR

Dao, E. H. , *et al.* (2015). "Goniometer-based femtosecond X-ray diffraction of mutant 30S ribosomal subunit crystals.", *Struct. Dyn.* **2**, 041706.

Hunter, M., *et al.* (2016). "Selenium single-wavelength anomalous diffraction de novo phasing using an X-ray Free Electron Laser." *Nat. Commun.*, accepted.

Laksmono, H., *et al.* (2015). "Anomalous behavior of the homogeneous ice nucleation rate in "No-man's land. ", *J. Phys. Chem. Lett.* **6**, 2826.

Sierra, R. G., *et al.* (2016). "Concentric-flow electrokinetic injector enables serial crystallography of ribosome and photosystem II." *Nat. Methods* **13**, 59.

Stan, C. A., *et al.* (2016). "Negative Pressures and Spallation in Water Drops Subjected to Nanosecond Shock Waves " *J. Phys. Chem. Lett.* **7**, 2055.

Stan, C. A., *et al.* (2016). "Liquid explosions induced by X-ray laser pulses" *Nat. Phys.*, accepted. doi:10.1038/nphys3779

PUBLICATIONS IN WHICH NPI WAS A COLLABORATOR

Blaj, G., *et al.* (2016). "Detector Damage at X-Ray Free-Electron Laser Sources." *IEEE Trans. Nucl. Sci.* **63**, 1818.

Decker, F. –J. , *et al.* (2016). "Two bunches with ns-separation with LCLS." *Proceedings of the 37th International Free Electron Laser Conference*, WEP025.

Johansson, L. C., *et al.* (2013). "Structure of a photosynthetic reaction centre determined by serial femtosecond crystallography." *Nat. Commun.* **4**, 3911.

Kern, J., *et al.* (2014). "Methods development for diffraction and spectroscopy studies of metalloenzymes at X-ray free-electron lasers." *Phil. Trans. R. Soc. B* **369**, 20130590

Kern, J., *et al.* (2014). "Taking snapshots of photosynthetic water oxidation using femtosecond X-ray diffraction and spectroscopy." *Nat. Comm.* **5**, 4371.

Kupitz, C., *et al.* (2014). "Serial time-resolved crystallography of photosystem II using a femtosecond X-ray laser.", *Nature* **513**, 261.

Mitzner, R., *et al.* (2013). "L-Edge X-ray Absorption Spectroscopy of Dilute Systems Relevant to Metalloproteins Using an X-ray Free-Electron Laser.", *J. Phys. Chem. Lett.* **4**, 3641.

Munke, A., *et al.* (2016). "Coherent diffraction of single Rice Dwarf virus particles using hard X-rays at the Linac Coherent Light Source.", *Sci. Data* **3**, 160064.

Park, H. J., *et al.* (2013). "Toward unsupervised single-shot diffractive imaging of heterogeneous particles using X-ray free-electron lasers." *Opt. Express* **21**, 28729.

Schreck, S., *et al.* (2014). "Reabsorption of Soft X-Ray Emission at High X-Ray Free-Electron Laser Fluences." *Phys. Rev. Lett.* **113**, 153002.

Sellberg, J. A., *et al.* (2014). "Ultrafast X-ray probing of water structure below the homogenous ice nucleation temperature" *Nature*, **510**, 381.

Sellberg, J. A., *et al.* (2014) "X-ray Emission Spectroscopy of Bulk Liquid Water in 'No-man's Land", *J. Chem. Phys.* **142**, 044505.

SFA: Strong-field laser matter interactions

PI: Phil Bucksbaum; Research Associate: Adi Natan; Graduate Students: Matthew Ware, Lucas Zipp; LCLS collaborators: Ryan Coffee, J.M. Glownia

PULSE Ultrafast Chemical Science Program, SLAC National Accelerator Laboratory, Menlo Park, CA 94025. Email: phb@slac.stanford.edu

Program Scope: The SFA task investigates ***strong field interactions*** in small molecules and atoms. We have recently developed a self-referenced ultrafast x-ray diffraction method that allows to image atomic dynamics of molecules in strong fields de-novo with angstrom and femptosecond resolution. We imaged the breakdown of molecular frame dynamics and observed light induced conical intersections and cusp catastrophes in strong field dissociation.

Recent Progress and Future Work:

Self-referenced coherent diffraction x-ray movie of Angstrom-and femtosecond-scale atomic motion:

Time-resolved femtosecond x-ray diffraction patterns from laser-excited molecular iodine were used to create a movie of intramolecular motion with time and space resolution of 30 fs and 0.3 Å. The high spatial fidelity is due to interference between the moving excitation and the static initial charge distribution (Fig 1). This x-ray interference has not been employed to image internal motion in molecules before. The initial state is used as the local oscillator for heterodyne amplification of the excited charge distribution to retrieve real-space movies of atomic motion on Ångstrom and femtosecond scales. Coherent vibrational motion and dispersion, dissociation, and rotational dephasing are all clearly visible in the data, thereby demonstrating the stunning sensitivity of heterodyne methods.

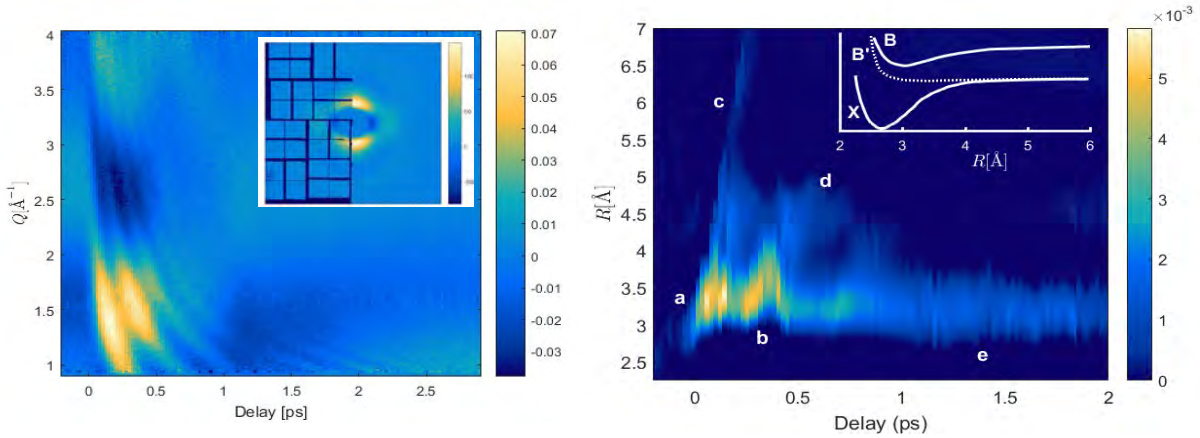

Fig 1. (Left) Scattering vs. time delay for the projection onto the mean subtracted β_2 Legendre coefficient. This term captures most of the excited state scattering signal and the holographic interference between the excited state and the reference ground state is uncovered. The principal features are long-period oscillations in Q that are due to the B state, and much shorter period oscillations in Q caused by dissociation. (Inset) the left side of the CSPAD detector showing the mean subtracted raw data at a specific delay of 150fs, and its Legendre fit on the right side. (Right) Iodine excited charge distribution vs time using the β_2 projected data, after applying the relevant steps to uncover the heterodyne signal and deconvolve it. The letters refer to specific type of molecular motion as follows: a) onset of the excited pulse, the B-state is directly over the X-state centered on 2.7 Å. b) vibrational oscillations. c) Dissociation d) wavepacket dispersion e) rotational dephasing.

Imaging the breakdown of molecular frame dynamics through rotational uncoupling: We have observed directly in the time domain the uncoupling of electron motion from the molecular frame due to rotational-electronic coupling in a molecular Rydberg system. In contrast to Born- Oppenheimer dynamics, in which the electron is firmly fixed to the molecular frame, there exists a regime of molecular dynamics known as l-uncoupling where the motion of a non-penetrating Rydberg electron decouples from the instantaneous alignment of the molecular frame. We have imaged this unusual regime in time-dependent photoelectron angular distributions of a coherently prepared electron wave packet in the 4f manifold of N_2. Angle-resolved time-domain studies of this uncoupled regime present new opportunities to study the ultrafast dynamics of electron and nuclear motion in a non-Born Oppenheimer setting.

Observation of Quantum Interferences via Light-Induced Conical Intersections in Diatomic Molecules intersection We observe energy-dependent angle-resolved diffraction patterns in protons from strong-field dissociation of the molecular hydrogen ion H+2. The interference is a characteristic of dissociation around a laser-induced conical intersection (LICI), which is a point of contact between two surfaces in the dressed two-dimensional Born-Oppenheimer potential energy landscape of a diatomic molecule in a strong laser field. The interference magnitude and angular period depend strongly on the energy difference between the initial state and the LICI, consistent with coherent diffraction around a cone-shaped potential barrier whose width and thickness depend on the relative energy of the initial state and the cone apex. These findings are supported by numerical solutions of the time-dependent Schrödinger equation for similar experimental conditions. LICIs are particularly attractive for future quantum control experiments due to their high degree of controllability using the polarization and frequency of the laser. The interaction is not limited to just a single LICI, and allows control of the timing of its appearance as well. Understanding the dynamics LICI induce in diatomic molecules will facilitate understanding and applicability to systems of increasing complexity. Implementing and understanding LICIs in bigger systems will open the way to novel spectroscopy techniques in physics and chemistry

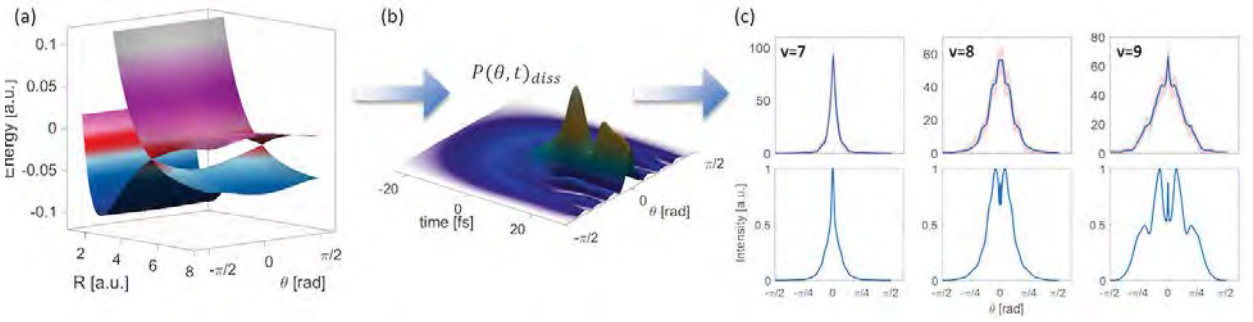

Fig 3 (a) The dressed potential energy surfaces of H_2^+ featuring LICIs. (b) The calculated instantaneous probability of dissociation $P(\theta,t)_{diss}$ from a given vibrational state (for example, v=9) during the interaction with the laser pulse reveals the interference. (c) Experimental (top) and calculated (bottom) angular distributions of H_2^+ dissociation at kinetic energy releases that correspond to specific initial vibrations states.

Observation of Cusp Catastrophes in Strong Field Dissociation: Catastrophe phenomena are ubiquitous in nature, for example, in optical caustics at the bottom of the pool, creation of rainbows and atmospheric haloes. When a system under study has a singularity that produces a catastrophe of some order, it will always follow the same universal laws described by singularity theory. As a result, there is a robust way to focus a wave-like behavior of the system into a particular part of it's phase space. Such robustness makes the realization of the catastrophes attractive for controlling systems with limited controllability. In particular, catastrophes in the dynamics of strongly driven quantum rotors were studied and played an instrumental role in field free molecular alignment. It was theoretically shown that for

intense enough ultrashort fields, a quantum rotor with even a uniform angular distribution will evolve to have a sharp cusp peak in angle space by the so called temporal focusing phenomenon. Subsequently, the wave function evolves to create a wave front fold that result with a rainbow like angular structure. We have observed cusp type catastrophe in H2+ photodissociation over broad kinetic energy releases range, arising from angular focusing of non-resonant rovibration states that couple to the strong laser field.

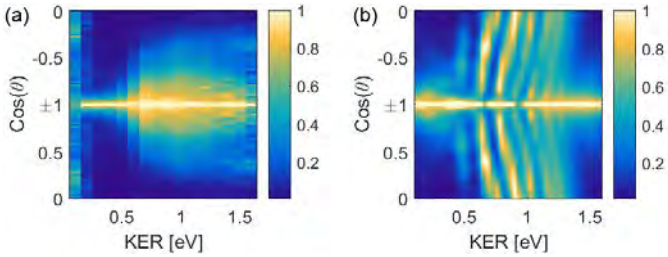

Fig. 4 (a) Measured dissociation of H2+ yield as function of kinetic energy release (KER) and *cos(θ)* by 30 fs, $4x10^{13}$ W/cm^2 pulses at 800 nm, normalized per energy bin and symmetrized. The cusp structure is observed throughout the energy range. (b) Calculated KER and *cos(θ)* for the same field strength.

References:

1. Bucksbaum, P. (2014). "Molecular dissociation dynamics driven by strong-field multiple ionization." *Bulletin of the American Physical Society* **59**.
2. Fang, L., T. Osipov, B. Murphy, A. Rudenko, D. Rolles, V. Petrovic, C. Bostedt, J. Bozek, P. Bucksbaum and N. Berrah (2014). *Journal of Physics B: Atomic, Molecular and Optical Physics* **47**(12): 124006.
3. Glownia, J. M., Natan, A. Cryan J., Hartsock R, Kozina M, Minitti MP, Nelson S, Robinson J, Sato T, van Driel T, Welch G, Weninger C, Zhi D, and Bucksbaum PH (2016) *Physical Review Letters* (accepted) arXiv preprint arXiv:1608.03039
4. McFarland, B., N. Berrah, C. Bostedt, J. Bozek, P. Bucksbaum, J. Castagna, R. Coffee, Cryan, L. Fang and J. Farrell (2014). *Journal of Physics: Conference Series* **488**: 012015.
5. Natan, A., M. R. Ware and P. H. Bucksbaum (2014). *International Conference on Ultrafast Phenomena*, Optical Society of America.
6. Natan, A., M. R. Ware and P. H. Bucksbaum (2014). *CLEO: QELS_Fundamental Science*, Optical Society of America.
7. Natan, A. L. Zipp and P. H. Bucksbaum (2015). *Frontier in Optics (*FTh4A.4*)*, Optical Society of America.
8. Natan, A., Ware, M.R., Prabhudesai, V.S., Lev, U., Bruner, B.D., Heber, O. and Bucksbaum, P.H., (2016). Observation of Quantum Interferences via Light-Induced Conical Intersections in Diatomic Molecules. *Physical review letters*, 116(14), p.143004.
9. Natan, A. L. Zipp and P. H. Bucksbaum (2016) *International Conference on Ultrafast Phenomena*, Optical Society of America.
10. Natan, A., M. R. Ware and P. H. Bucksbaum (2016). *International Conference on Ultrafast Phenomena*, Optical Society of America.
11. Zipp, L., A. Natan and P. H. Bucksbaum (2014). Optica, 1, 361-364 (2014)
12. Zipp, L., A. Natan and P. H. Bucksbaum (2014). *CLEO: QELS_Fundamental Science*, Optical Society of America.
13. Zipp, L., A. Natan and P. Bucksbaum (2014). *Bulletin of the American Physical Society* **59**.
14. Zipp, L., A. Natan and P. Bucksbaum (2015). *Bulletin of the American Physical Society* **60**.
15. Zipp, L., Natan, A. and Bucksbaum, P.H., (2016), June. Observing the Uncoupling of Electron Motion from the Molecular Frame in Photoelectron Angular Distributions. In CLEO: QELS_Fundamental Science (pp. FTh4M-2). Optical Society of America.
16. Zipp L. J., Natan, A., and Bucksbaum, P. H. (2016). "Imaging the Breakdown of Molecular Frame Dynamics through Rotational Uncoupling". arXiv preprint arXiv:1606.02663. (under review in PRL)

NLX: Nonlinear X-ray Science

David A. Reis*, Shambhu Ghimire

Stanford PULSE Institute
SLAC National Accelerator Laboratory, MS 59
2575 Sand Hill Rd.
Menlo Park, CA 94025

*dreis@slac.stanford.edu

Program Scope:

In the NLX *program, we are focused on the nonlinear optics of short-wavelength, ultrafast coherent radiation.* We seek to understand strong-field and multi-photon interactions and exploit them to probe electronic structure at the atomic-scale in space and time. We are interested in fundamental interactions, with a primary focus on coherent non-sequential processes such as wave-mixing and two-photon Compton scattering using hard x rays. In the upcoming funding period, we propose experiments on x-ray and optical wave-mixing to image the strong-field-driven attosecond electronic dynamics responsible for solid-state high-harmonic generation. We will also explore the bound-state contribution to two-photon Compton scattering. The new scattering mechanism holds promise as a nonlinear photons-in/photon-out method of achieving simultaneous chemical specificity and atomic-scale structure in low Z materials. Our program is synergistic with other strong-field investigations in PULSE and makes use of the unprecedented intensities at hard x-ray wavelengths of LCLS and SACLA free-electron lasers. The results could have a profound impact on future light sources such as the LCLS-II.

Progress Report

Non-sequential two-photon interactions at x-ray wavelengths became possible with the advent of the LCLS free-electron laser. In this program we continue to explore several fundamental nonlinear x-ray processes on the LCLS and SACLA with an emphasis on the hard x-ray regime, where it may be possible to gain simultaneous structure and spectroscopy information. Recently we have reported first measurements on x-ray and optical wave-mixing (diamond), phase-matched x-ray second harmonic generation (diamond) and anomalous nonlinear Compton scattering (beryllium) on LCLS. More recently we report two-photon K-shell absorption (zirconium) on the SACLA FEL (Ghimire et al PRA 2016). For hydrogenic ions the generalized cross-section for an n-photon process (in the applied field) is expected to scale as Z^{4n+2} in the dipole approximation at scaled frequency ωZ^{-2}, and is thus expected to scale as Z^{-6} for the two photon process (Zernik Phys Rev 1964). The figure on the right shows measured two-photon absorption cross-sections as a function of nuclear charge Z compared the Zernik Z^{-6} scaling (solid line) referencing to the calculated cross-section in H atom [Klarsfield Nuovo Cim. 1970, Karule JOSA B 1971]. The data for He is for 41.8 eV, above the single photon threshold, taken from Hasegawa et al. PRA 2005. The value for Ne^{8+} is from Doumy et al., PRL 2011 The measurement for Ge is from Tamasaku et al., Nat. Photon. 2014. While our

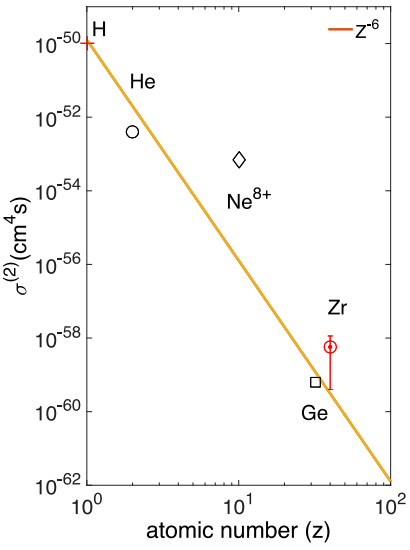

measurement for Zr is clearly above the Zernik scaling, we cannot rule it out given the large uncertainties in the x-ray intensity typical of XFEL experiments. In general, these experiments involve especially careful design to separate the signal from backgrounds, particularly in the scattering experiments were background from the undulator harmonics and parasitic scattering of the fundamental can easily overwhelm the signals. Even so, uncertainties in the pulse duration and focal spot can lead to large systematic uncertainties in the measured cross-section. In order to explore deviations from the simple hydrogenic scaling e.g. due to retardation and screening better x-ray metrology will required.

Far from resonance, the linear x-ray matter interaction can be well approximated by the scattering off a collection of free-electrons. We find that models that treat the solid as a collection of free-electrons are successful at describing both the x-ray second-harmonic generation and the (optically modulated) x-ray susceptibility in x-ray–optical sum frequency generation. However we found that in nonlinear two-photon Compton scattering, the free-electron model breaks down spectacularly. We find that the spectrum shows an anomalously large broadening and redshift as compared to both the free-electron theory and to the simultaneously measured linear scattering from the weak residual FEL second harmonic generated by the undulators. Our observations are incompatible with kinematics for the ground state electron distribution in the usual impulse approximation (IA). These anomalies are consistent with a novel nonlinear scattering mechanism involving bound-state electrons, despite an X-ray energy of approximately two orders of magnitude above the 1*s* binding energy. We have recently extended our original measurements (Fuchs et al. Nature Physics 2015) to significantly *larger* red-shift and *smaller* scattering angles. We have also been pursuing phase-matched nonlinear Compton and had preliminary beamtime on SACLA and have upcoming beamtime on LCLS.

Following our discovery of nonperturbative high harmonics in solids, there has been much recent experimental and theoretical work trying to understand the physical mechanism and how it differs from typical gas phase harmonics. Under AMOS funding, we have studied HHG in rare gas solids as compared them directly to the dilute gas. Rare gas solids are a near ideal platform for studying the differences between gas and solid harmonics: they are weakly bound by van der Waals interactions and thus at some level they best approximate a dense atomic solid. In Ndabashimiye et al., Nature 2016 we report a direct comparison of solid and gas phase Kr and Ar. We find that the harmonics in the solid extend beyond the gas-phase 3.2 U_p limit and exhibit the sudden onset of multiple plateaus. In collaboration with the theory group of Mette Gaarde and Ken Schafer this behavior can be largely reproduced in a single-electron model that couples multiple higher order bands in the solid, while the location of the plateaus suggest that correlation effects may play a role.

The next three years:

We continue to concentrate our efforts on x-ray nonlinear optics. We will investigate more thoroughly the fundamental physics of two-photon Compton scattering. Recent experimental data seem to rule out hot plasma effects and support our identification of a novel bound-state nonlinearity. A consequence of the bound-state nonlinearity is that it is possible to phase-match in a single crystal. We will compare phase-matched nonlinear Compton to x-ray second harmonic generation. We will also explore the use of two-color interactions as a simultaneous spectroscopic and structural tool, including non-degenerate two-photon Compton scattering and x-ray optical wavemixing in the presence of strong-fields**.**

References to publications of DOE sponsored research

2016

[1] S. Ghimire, M. Fuchs, J. B. Hastings, S. Herrmann, Y. Inubushi, J. Pines, S. Shwartz, M. Yabashi, and D. A. Reis. Nonsequential two-photon absorption from the k shell in solid zirconium. *Phys. Rev. A*, in press, 2016.

[2] G. Ndabashimiye, S. Ghimire, M. Wu, D. A. Browne, K. J. Schafer, M. B. Gaarde, and D. A. Reis. Solid-state harmonics beyond the atomic limit. *Nature*, 534(7608):520–523, 06 2016.

[3] Y. S. You, D. Reis, and S. Ghimire. High harmonics from solids probe angstrom scale structure. Bulletin of the American Physical Society, 2016.

2015

[1] M. Fuchs, M. Trigo, J. Chen, S. Ghimire, S. Shwartz, M. Kozina, M. Jiang, T. Henighan, C. Bray, G. Ndabashimiye, P. H. Bucksbaum, Y. Feng, S. Herrmann, G. A. Carini, J. Pines, P. Hart, C. Kenney, S. Guillet, S. Boutet, G. J. Williams, M. Messerschmidt, M. M. Seibert, S. Moeller, J. B. Hastings, and D. A. Reis. Anomalous nonlinear x-ray compton scattering. *Nature Physics*, 11(11):964–970, 11 2015.

[2] D. Reis. High harmonic generation in rare gas solids. *Bulletin of the American Physical Society*, 60, DAMOP, 2015.

[3] M. Wu, S. Ghimire, D. A. Reis, K. J. Schafer, and M. B. Gaarde. High-harmonic generation from bloch electrons in solids. *Physical Review A*, 91(4):043839, 2015.

2014

[1] S. Ghimire, G. Ndabashimiye, A. D. DiChiara, E. Sistrunk, M. I. Stockman, P. Agostini, L. F. DiMauro, and D. A. Reis. Strong-field and attosecond physics in solids. *Journal of Physics B: Atomic, Molecular and Optical Physics*, 47(20):204030, 2014.

[2] J. Goodfellow, M. Fuchs, D. Daranciang, S. Ghimire, F. Chen, H. Loos, D. A. Reis, A. S. Fisher, and A. M. Lindenberg. Below gap optical absorption in gaas driven by intense, single-cycle coherent transition radiation. *Optics Express*, 22(14):17423–17429, 2014.

[3] S. Shwartz, M. Fuchs, J. B. Hastings, Y. Inubushi, T. Ishikawa, T. Katayama, D. A. Reis, T. Sato, K. Tono, M. Yabashi, S. Yudovich, and S. E. Harris. X-ray second harmonic generation. *Physical Review Letters*, 112:163901, 2014.

[4] G. Ndabashimiye, S. Ghimire, and D. Reis. High harmonic mixing in solid argon. *Bulletin of the American Physical Society*, 59, P5.00005 DAMOP, 2014.

Electron Dynamics on the Nanoscale, Tony Heinz, PI

SLAC National Accelerator Laboratory, 2575 Sand Hill Road MS 59, Menlo Park, CA 94025

theinz@slac.stanford.edu

Program Scope

This research program, recently initiated at SLAC, seeks to obtain fundamental understanding of the dynamics of electronic excitations in nanostructures. The research addresses central issues for photoexcited electrons in atomically thin two-dimensional (2D) layers of van-der-Waals crystals and heterostructures, with particular emphasis on monolayers of transition metal dichalcogenide crystals. The investigations make use of complementary experimental techniques based on ultrafast spectroscopy to probe radiative and non-radiative relaxation pathways after photoexcitation, addressing the role of Coulomb and vibrational interactions as manifest in exciton formation, exciton-exciton and exciton-carrier interactions, intervalley scattering, and exciton radiative decay. The research also examines electron dynamics in heterostructures composed of atomically thin 2D van der Waals layers combined with other 2D layers and with 0D structures, such as quantum dots. Because of the unreactive character of 2D van der Waals layers, combinations of a wide variety of structures can be prepared by mechanical assembly, as well as by chemical deposition techniques. The research program addresses the dynamics of both charge and energy transfer processes for these heterostructures using ultrafast spectroscopy techniques.

Progress Report

During the past reporting period, we have investigated two-dimensional van-der-Waals layers such as graphene and ultrathin layers of transition metal dichalcogenide materials in the class of MX_2 (M = Mo, W and X = S, Se, Te) and the interactions with other nanoscale materials. In particular, we have examined energy transfer processes from colloidal quantum dots to different model 2D layers as a function of layer thickness. The experimental approaches have included investigation both of fluorescence quenching and direct time-resolved photoluminescence measurements. We have also investigated the dynamics of electrons in the 2D semiconductor layers by means of precise linewidth measurements and through pump-probe spectroscopy. These methods have revealed the role of different scattering processes in the relaxation dynamics in these model 2D semiconductors. Below we briefly summarize progress in these areas. A further area of study concerned identification of dark exciton states that play a key role in the photophysics of these 2D semiconductors through detailed photoluminesce and time-resolved photoluminescence measurements as a function of temperature. These investigations revealed the presence of spin-forbidden (triplet-like) states lying tens of meV below the optically active A exciton.

<u>Probing energy transfer from 0D structures to 2D layers</u>

We have prepared hybrid structures consisting of well-defined 0D semiconducting colloidal quantum dots supported on 2D layers of model van-der-Waals materials. Using these systems, we have investigated the nature of energy transfer processes from the 0D chromophore to the 2D layer through a set of measurements in which we vary the thickness of the 2D material in integral monolayer steps. Through the use of core-shell quantum dots and the presence of organic ligands, we were able to suppress charge transfer processes, thus allowing us to probe in detail relaxation of excitation in the quantum dots through energy transfer to the 2D layers. In our experiments, we examined the behavior for both the prototypical 2D material of graphene and the model 2D semiconductor layer of MoS_2. Strong fluorescence quenching is observed for both single-layer graphene and for single-layer MoS_2, as shown in Fig. 1. Given the close

proximity of the 2D layer and the strong optical absorption of the material at the emission energy of the CdSe/CdZnS core−shell quantum dots, such rapid energy transfer is not unexpected. The strong observed quenching was also reflected in measurements of time-resolved photoluminescence; in which significantly decreased emission times were recorded for the supported quantum dots compared to isolated quantum dots in solution.

We also determined the variation of the energy transfer rate with the thickness of the 2D graphene or MoS_2 layers. As shown in Fig. 1, a striking and surprising behavior was observed. For the case of graphene, we found that the quenching rate increased with increasing layer thickness (the emission time decreased). However, for the case of MoS_2, precisely the opposite trend was found: The quenching rate *decreased* with decreasing thickness. Working jointly with the Reichmann group at Columbia University, we developed a detailed model elucidating the origin of these countervailing trends. While the increased absorption of thicker layers offers more decay channels and increases the rate of energy transfer, this trend can be fully counterbalanced by the increased screening of the quantum dot electric fields in the 2D layers. Which trend is dominant depends critically on the relative real and imaginary parts of the dielectric function of the 2D layer, as well as its in-plane/out-of-plane anisotropy. Understanding these factors is crucial for the application of nanoscale materials to light harvesting applications.

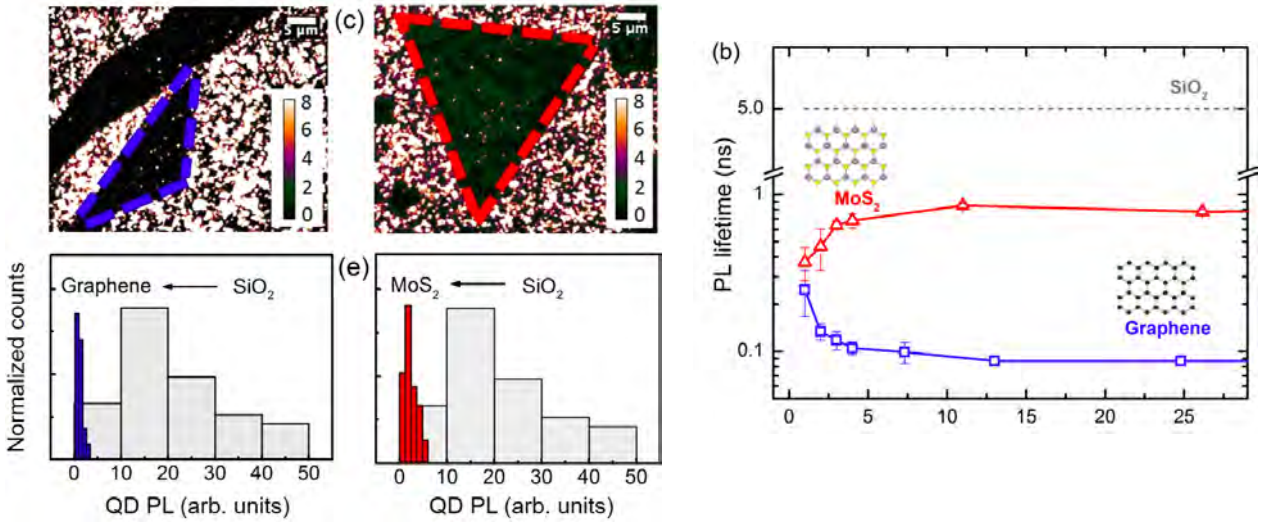

Fig. 1: Experimental results on energy transfer processes between colloidal CdSe/CdZnS core−shell quantum dots and 2D layers of the semi-metallic graphene and the semiconducting MoS_2 systems. (Left) Images and analysis of fluorescence quenching of quantum dots on the two materials relative to their emission on the underlying SiO_2 substrate. Strong quenching is seen for both systems as a result of energy transfer processes into the relevant 2D material. (Right) Measured fluorescence emission times of the two material systems as a function of the layer thickness of the 2D material. The differing behaviors reflect the competition between increased absorption channels and increased screening effects with growing layer thickness.

Exciton coherence lifetimes in 2D semiconductors

2D semiconductors in the TMDC family are direct-gap materials in the monolayer limit. They exhibit bright photoluminesce and are also characterized by unusually strong excitonic interactions. Their low-energy absorption and emission spectra are dominated by the role of excitons and excitonic transitions, as illustrated in Fig. 2 for the case of monolayer WS_2. The high oscillator strength of the excitonic transition leads to the remarkable situation of peak absorptions in a single monolayer of 10's of percent.

We have been exploring the nature of these excitonic transitions and of their decay channels. In a recent investigation, we have determined the temperature dependent linewidth of these lowest lying (A) excitonic state as a function of temperature. While the very high radiative emission rates contribute appreciably to the observed linewidth, this factor (as well as inhomogeneous broadening) is expected to be largely independent of temperature. The variation with temperature can be attributed to exciton phonon scattering processes.

In a collaborative study with the Ermin Malic and Andreas Knorr groups in Europe, we have used the measurements of the temperature dependence of the exciton linewidth to evaluation scattering channels. As indicated in Fig. 2, with increasing temperature, we see a strong activation of different exciton-phonon scattering channels. The cases of WS_2 and of $MoSe_2$ offer an interesting comparison because of the differing characteristics of the conduction bands in the two systems and the differing types of phonons that can contribute to inelastic scattering processes.

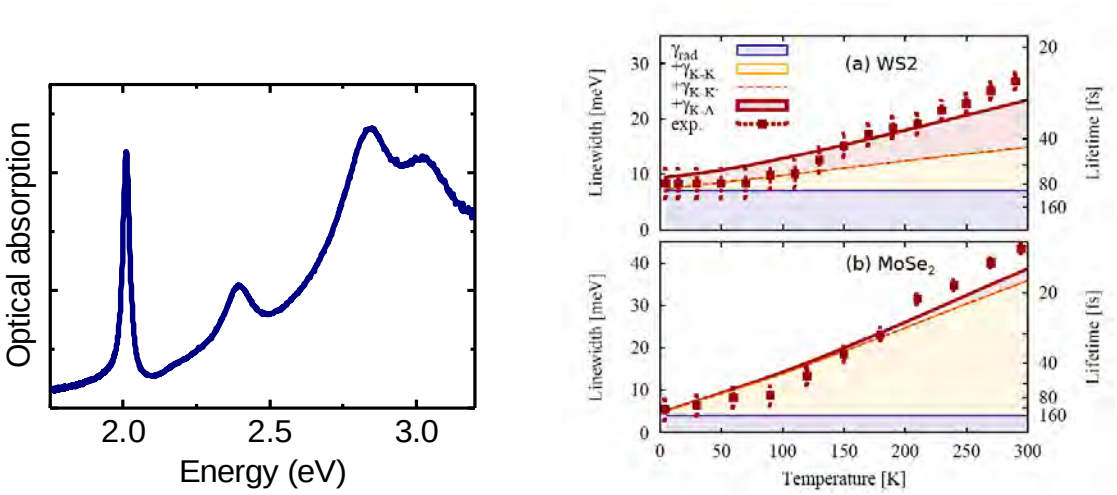

Fig. 2: Linewidth of the fundamental (A) exciton in transition metal dichalcogenide monolayers and its relation to differing contributions to the decoherence processes. (Left): Representative measured absorption spectrum of monolayer WS_2. The strong low-energy feature is the band-edge exciton. The temperature dependence of the width of this feature was investigated. (Right) Measured variation in the width of the A exciton in monolayer WS_2 and $MoSe_2$ compared to calculations of the different components of the linewidth: Radiative lifetime (temperature independent) and exciton-phonon scattering processes, as indicated. The error bars on the experimental data reflect uncertainty associated with the role of residual inhomogeneous broadening of the transitions.

Future Plans

We plan to expand our research efforts to obtain greater insight into ultrafast electron dynamics in individual layers of 2D materials and, particularly, into the interlayer dynamics that occurs in tailored structures consisting of stacks of 2D layers, in which both energy and charge transfer processes are allowed. We will take advantage of the ability to prepare structures with precisely defined spacer layers to examine the varying distance dependence of these processes.

Publications Acknowledging AMOS Support

1. Raja, A. Montoya-Castillo, J. Zultak, X. X. Zhang, Z. Ye, C. Roquelet, D. A. Chenet, A. M. van der Zande, P. Huang, S. Jockusch, J. Hone, D. R. Reichman, L. E. Brus and T. F. Heinz, "Energy transfer from quantum dots to graphene and MoS_2: absorption vs. screening," *Nano Lett.* **16**, 2328 (2016).

2. M. Selig, G. Berghuser, A. Raja, P. Nagler, C. Schuller, T. F. Heinz, T. Korn, A. Chernikov, E. Malic, and A. Knorr. "Excitonic linewidth and coherence lifetime in monolayer transition metal dichalcogenides," *Nature Commun*. (in press).

3. Interplay between carrier and phonon populations in monolayer WS_2 after pulsed excitation, C. Ruppert, A. Chernikov, H. M. Hill, A. F. Rigosi, and T. F. Heinz, submitted.

4. X.X. Zhang, Y. You, S. Y. F. Zhao, and T. F. Heinz, "Experimental Evidence for Dark Excitons in Monolayer WSe_2," *Phys. Rev. Lett.* **115**, 257403 (2015).

5. H. M. Hill, A. F. Rigosi, C. Roquelet, A. Chernikov, T. C. Berkelbach, D. R. Reichman, M. S. Hybertsen, L. E. Brus, and T. F. Heinz, "Observation of Excitonic Rydberg State in Monolayer MoS_2 and WS_2 by Photoluminescence Excitation Spectroscopy," *Nano Lett.* **15**, 2992 - 2997 (2015).

6. Y. You, X. X. Zhang, T. C. Berkelbach, M. S. Hybertsen, D. R. Reichman, and T. F. Heinz, "Observation of Biexcitons in Monolayer WSe_2," *Nature Phys*. **11**, 477-481 (2015).

7. A. F. Rigosi, H. M. Hill, Y. Li, A. Chernikov, T. F. Heinz, "Probing Interlayer Interactions in Transition Metal Dichalcogenide Heterostructures by Optical Spectroscopy: MoS_2/WS_2 and $MoSe_2/WSe_2$," *Nano Lett.* **15**, 5033–5038 (2015).

8. A. Chernikov, C. Ruppert, H.M. Hill, A.F. Rigosi, T.F. Heinz, "Population inversion and giant bandgap renormalization in atomically thin WS_2 layers," *Nature Photon*. **9**, 466-470 (2015).

9. G. Jnawali, Y. Rao, J.H. Beck, N. Petrone, I. Kymissis, J. Hone, T.F. Heinz, "Observation of Ground-and Excited-State Charge Transfer at the C_{60}/Graphene Interface," *ACS Nano* **9**, 7175-7185 (2015).

10. O. Yaffe, A. Chernikov, Z. M. Norman, Y. Zhong, A. Velauthapillai, A. van der Zande, J. S. Owen, and T. F. Heinz, "Excitons in Ultrathin Organic-Inorganic Perovskite Crystals," *Phys. Rev. B* **92** 045414 (2015).

11. A. Chernikov, A. M. van der Zande, H. M. Hill, A. F. Rigosi, A. Velauthapillai, J. Hone, and T. F. Heinz, "Electrical Tuning of Exciton Binding Energies is Monolayer WS_2," *Phys. Rev. Lett.* **115**, 126802 (2015).

EIM: Excited States in Isolated Molecules

Task lead: Thomas Wolf; Participating Scientist: Markus Guehr
SLAC National Accelerator Laboratory, 2575 Sand Hill Road, Menlo Park, CA 94025
tw2809@slac.stanford.edu

Objective and Scope: Our interest is the investigation of elementary chemical processes in isolated molecules on their natural time scale of femtoseconds and picoseconds. We are especially interested in non-Born-Oppenheimer approximation (non-BOA) dynamics, because of its importance for light harvesting, atmospheric chemistry and DNA nucleobases photoprotection. For this purpose, we use time resolved spectroscopy with extreme ultraviolet (EUV) light from laboratory-based high harmonic generation (HHG) and soft x-rays (SXR) from the Linac Coherent Light Source (LCLS). Those techniques allow a site and element specific access to non-BOA dynamics. We complement spectroscopic investigation methods with gas phase ultrafast electron diffraction (UED).

Management: Thomas Wolf took over the management of this subtask this year when Markus Guehr joined the faculty at the University of Potsdam. This subtask has joined the main PULSE Ultrafast Chemical Science FWP this year.

Recent Progress:

The nucleobases, the building blocks of the DNA, exhibit large absorption cross-sections in the ultraviolet (UV) spectral range. Despite this fact, they do not likely undergo photoinduced reactions like isomerizations or bond dissociations due to an ultrafast photoprotection mechanism efficiently transforming the absorbed photoenergy into heat. The details of this mechanism are still unclear. In the nucleobase thymine, it involves two low-lying excited states with ππ* and an nπ* electronic character. We recently investigated the photoprotection mechanism of thymine using two experimental approaches, time-resolved photoelectron spectroscopy with vacuum UV (VUV) photon energies from high harmonic generation (HHG) and time-resolved near-edge absorption fine structure spectroscopy (NEXAFS) at the oxygen edge using the linac coherent light source (LCLS).

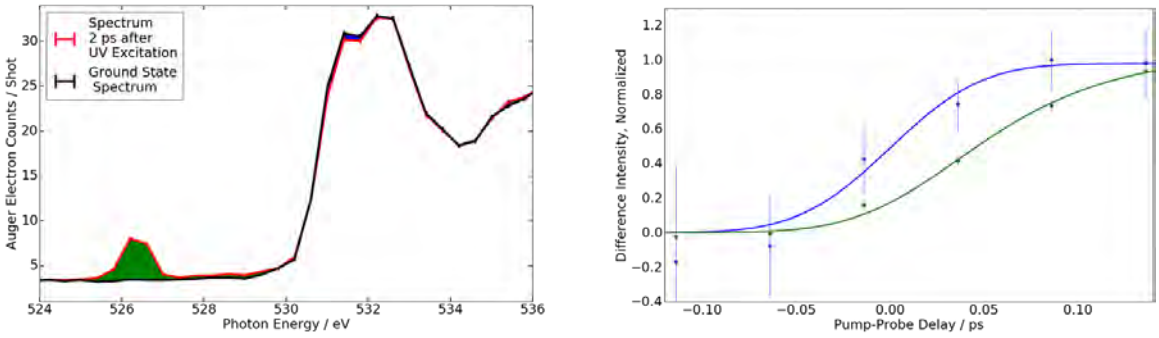

Figure 1: Oxygen edge NEXAFS spectra (left) without and 2 ps after UV excitation. Two UV-induced features can be discerned, a bleach of the ground state resonance around 531.4 eV (blue) and an additional resonance from the nπ* state (green) at 525.4 eV. Their dependence on the pump-probe delay (right) shows a delay between the onset of the bleach and the nπ* state signature, which resembles the time scale for internal conversion between the ππ* and the nπ* state.

NEXAFS probing of nucleobase photoprotection: It is well established that after

excitation in to an electronic state with ππ* character, thymine can undergoe internal conversion to an optically dark excited state with nπ* character. The time scale and therefore also the efficiency of this process is, however, under debate. It is hard to measure this time scale experimentally, since most spectroscopic methods are not selectively sensitive to the internal conversion process. In a recent LCLS experiment in July 2015, we could show that time-resolved NEXAFS spectroscopy at the oxygen edge exhibits this selective sensitivity. In NEXAFS spectroscopy, resonant transitions between core electron levels and empty valence orbitals are investigated. Since core levels of carbon, nitrogen, and oxygen are hundreds of eV apart, this spectroscopy method is site and element specific. The intensity of the resonant transition, furthermore, crucially depends on the local wavefunction overlap between the localized core and the more diffuse valence orbital. The initially UV-excited ππ* state of thymine is characterized by a single electron excitation from a strongly delocalized occupied π to an equally delocalized π* orbital. The electron hole in the π orbital in principle can give rise to a new, excited state NEXAFS transition. The wavefunction overlap is, however, poor and the transition therefore too weak to be detected. Internal conversion to the nπ* state leads to transition of the electron hole to the n orbital, which is considerably more localized at the oxygen. It leads to a strong excited state NEXAFS transition, which is clearly observable in our experimental data (see Fig. 1). High level coupled cluster simulations of NEXAFS spectra from our collaborators of the PULSE theory subtask confirm this assignment. We, furthermore, observe a delay between the onset of the UV-induced bleach of the ground state spectrum, which marks the begin of the dynamics, and the onset of the nπ* state signature, which directly resembles the time the molecule needs for internal conversion between the ππ* and the nπ* state.

Time-resolved VUV photoelectron spectroscopy: We performed an investigation of the ultrafast UV-induced dynamics of the nucleobase thymine using time-resolved photoelectron spectroscopy with VUV photoionization from high harmonic generation (HHG). Earlier investigations on thymine using UV photoionization could only observe the excited state nuclear wavepacket leaving the Franck-Condon region, since the excited state ionization potential quickly exceeded the UV photon energy. In our study with 14 eV photoionization, we do not only resolve early < 70 fs nuclear wavepacket dynamics, but are also able to follow the wavepacket down to a low-lying electronic state which is stable for at least 100 ps. We are currently collaborating with the PULSE theory subtask to determine the nature of this low-lying excited state with the help of high-level quantum chemical simulations of the experimental observables.

Direct probing of nuclear rearrangements by ultrafast electron diffraction: To gain a complete picture of ultrafast chemical processes, we complement our site specific spectroscopy with a direct access to the nuclear wavefunction by gas phase ultrafast electron diffraction (UED). With SLAC's ultrafast MeV electron source, a suitable tool with unprecedented time resolution is now at hand. In first UED experiments, we could identify the signatures of rotational revivals in impulsively aligned nitrogen and Investigate the excited state vibrational wavepacket in iodine.

Future Projects:

We plan to investigate additional nucleobases in our VUV photoelectron spectroscopy setup. We have started preliminary experiments on the RNA base uracil.

We have proven the feasibility and sensitivity of the TR-NEXAFS technique at the example of thymine. We plan to further explore its potential in future LCLS beamtimes on ring opening reactions and bond dissociations.

We started a project together with the PULSE UTS subtask to explore the sensitivity of time-resolved x-ray photoelectron spectroscopy to bond dissociation reactions. Our preliminary simulation results show a high sensitivity to the electronic structure change induced by bond dissociations. We plan to apply for LCLS beamtime for a proof of principle experiment.

We are part of the second UED gas phase run. The goal is to move now from diatomic to more complicated chemical systems. Along these lines, we will investigate the ultrafast photoinduced ring opening reaction in stilbene oxide.

Publications:

[1] B. F. Murphy, T. Osipov, Z. Jurek, L. Fang, S.-K. Son, M. Mucke, J. H. D. Eland, V. Zhaunerchyk, R. Feifel, L. Avaldi, P. Bolognesi, C. Bostedt, J. D. Bozek, J. Grilj, M. Guehr, L. J. Frasinski, J. Glownia, D. T. Ha, K. Hoffmann, E. Kukk, B. K. McFarland, C. Miron, E. Sistrunk, R. J. Squibb, K. Ueda, R. Santra, and N. Berrah, Nature Communications 5, (2014).
[2] M. Koch, T. J. A. Wolf, J. Grilj, E. Sistrunk, and M. Gühr, Journal of Electron Spectroscopy and Related Phenomena 197, 22 (2014).
[3] L. S. Spector, M. Artamonov, S. Miyabe, T. Martinez, T. Seideman, M. Guehr, and P. H. Bucksbaum, Nature Communications 5, (2014).
[4] B. K. McFarland, N. Berrah, C. Bostedt, J. Bozek, P. H. Bucksbaum, J. C. Castagna, R. N. Coffee, J. P. Cryan, L. Fang, J. P. Farrell, R. Feifel, K. J. Gaffney, J. M. Glownia, T. J. Martinez, S. Miyabe, M. Mucke, B. Murphy, A. Natan, T. Osipov, V. S. Petrovic, S. Schorb, T. Schultz, L. S. Spector, M. Swiggers, F. Tarantelli, I. Tenney, S. Wang, J. L. White, W. White, and M. Gühr, Journal of Physics: Conference Series 488, 012015 (2014).
[5] B. K. McFarland, J. P. Farrell, S. Miyabe, F. Tarantelli, A. Aguilar, N. Berrah, C. Bostedt, J. D. Bozek, P. H. Bucksbaum, J. C. Castagna, R. N. Coffee, J. P. Cryan, L. Fang, R. Feifel, K. J. Gaffney, J. M. Glownia, T. J. Martinez, M. Mucke, B. Murphy, A. Natan, T. Osipov, V. S. Petrović, S. Schorb, T. Schultz, L. S. Spector, M. Swiggers, I. Tenney, S. Wang, J. L. White, W. White, and M. Gühr, Nature Communications **5**, (2014).
[6] A. Aquila, A. Barty, C. Bostedt, S. Boutet, G. Carini, D. dePonte, P. Drell, S. Doniach, K. H. Downing, T. Earnest, H. Elmlund, V. Elser, M. Gühr, J. Hajdu, J. Hastings, S. P. Hau-Riege, Z. Huang, E. E. Lattman, F. R. N. C. Maia, S. Marchesini, A. Ourmazd, C. Pellegrini, R. Santra, I. Schlichting, C. Schroer, J. C. H. Spence, I. A. Vartanyants, S. Wakatsuki, W. I. Weis, and G. J. Williams, Structural Dynamics 2, 041701 (2015).
[7] M. Gopalakrishnan and M. Gühr, American Journal of Physics 83, 186 (2015).
[8] J. Grilj, E. Sistrunk, J. Jeong, M. Samant, A. Gray, H. Dürr, S. Parkin, and M. Gühr, Photonics 2, 392 (2015).
[9] M. Koch, T. J. A. Wolf, and M. Gühr, Physical Review A 91, (2015).
[10] T. J. A. Wolf, M .Koch, E. Sistrunk , J.Grilj, M. Guehr in: Ultrafast Phenomena XIX, p. 48 (Springer, 2015).
[11] S. P. Weathersby, G. Brown, M. Centurion, T. F. Chase, R. N. Coffee, J. Corbett, J. P. Eichner, J. Frisch, A. R. Fry, M. Guehr, N. Hartmann, C. Hast, R. Hettel, K. Jobe, E. N. Jongewaard, J. Lewandowski, R. Li, A. M Lindenberg, I. Makasyuk, J. E. May, D. McCormick, M.

N. Nguyen, A. H. M. Reid, X. Shen, K. Sokolowski-Tinten, T. Vecchione, S. L. Vetter, J. Wu, J. Yang, H. Durr, X. Wang, Rev. Sci. Instr. 86, 073702 (2015).
[12] C. Liekhus-Schmaltz, I. Tenney, T. Osipov, A. Sanchez-Gonzalez, N. Berrah, R. Boll, C. Bomme, Ch. Bostedt, J. Bozek, S. Carron, R. Coffee, J. Devin, B. Erk, K. Ferguson, R. Field, L. Foucar, L. Frasinski, J. Glownia, M. Guehr, A. Kamalov, J. Krzywinski, H. Li, J. Marangos, T. Martinez, B. McFarland, S. Miyabe, B. Murphy, A. Natan, D. Rolles, A. Rudenko, M. Siano, E. Simpson, L. Spector, M. Swiggers, D. Walke, S. Wang, Th. Weber, P. Bucksbaum, V. Petrovic, Nature Comm. 6, 8199 (2015)
[13] A. Sanchez-Gonzalez, T. R. Barillot, R. J. Squibb, P. Kolorenč, M. Agaker, V. Averbukh, M. J. Bearpark, C. Bostedt, J. D. Bozek, S. Bruce, S. Carron Montero, R. N. Coffee, B. Cooper, J. P. Cryan, M. Dong, J. H. D. Eland, L. Fang, H. Fukuzawa, M. Guehr, M. Ilchen, A. S. Johnsson, C. Liekhus-Schmaltz, A. Marinelli, T. Maxwell, K. Motomura, M. Mucke, A. Natan, T. Osipov, C. Östlin, M. Pernpointner, V. S. Petrovic, M. A. Robb, C. Sathe, E. R. Simpson, J. G. Underwood, M. Vacher, D. J. Walke, T. J. A. Wolf, V. Zhaunerchyk, J.-E. Rubensson, N. Berrah, P. H. Bucksbaum, K. Ueda, R. Feifel, L. J. Frasinski, J. P. Marangos J. Phys. A 48, 234004 (2015).
[14] N. Berrah, B. Murphy, H. Xiong, L. Fang, T. Osipov, E. Kukk, M. Guehr, R. Feifel, V.S. Petrovic, K.R. Fergusond, J.D. Bozek, C. Bostedt, L.J. Frasinski, P.H. Bucksbaum, J.C. Castagna, J. Mod. Opt., 63, 390 (2015).
[15] E. Sistrunk, J. Grilj, J. Jeong, M. G. Samant, A. X. Gray, H. A. Dürr, S. S. P. Parkin, and M. Gühr, Optics Express 23, 4340 (2015).
[16] E. Sistrunk and M. Gühr, Journal of Optics 17, 015502 (2015).
[17] E. Sistrunk, J. Grilj, J. Jeong, M. G. Samant, A. X. Gray, H. A. Dürr, S. S. P. Parkin, M. Gühr in: Ultrafast Phenomena XIX, p. 64 (Springer, 2015)
[18] T. J. A. Wolf , T. S. Kuhlman, O. Schalk, T. J. Martínez, K. B. Møller, A. Stolow, A.-N. Unterreiner in: Ultrafast Phenomena XIX, p. 184 (Springer, 2015)
[19] H. A. Ernst, T. J. A. Wolf, O. Schalk, N. González-García, A. E. Boguslavskiy, A. Stolow, M. Olzmann, A.-N. Unterreiner, J. Phys. Chem. A 119, 9225 (2015)
[20] Zhaunerchyk, V., Kamińska, M., Mucke, M., Squibb, R.J., Eland, J.H.D., Piancastelli, M.N., Frasinski, L.J., Grilj, J., Koch, M., McFarland, B.K., Sistrunk, E., Gühr, M., Coffee, R.N., Bostedt, C., Bozek, J.D., Salén, P., Meulen, P. v d, Linusson, P., Thomas, R.D., Larsson, M., Foucar, L., Ullrich, J., Motomura, K., Mondal, S., Ueda, K., Richter, R., Prince, K.C., Takahashi, O., Osipov, T., Fang, L., Murphy, B.F., Berrah, N., Feifel, R., J. Phys. A 48, 244003 (2015).
[21] M. Gühr in: Ultrafast Dynamics Driven by Intense Light Pulses, eds.: M. Kitzler S. Graefe (Springer, Heidelberg, 2016).

Early Career: Strongly-driven attosecond electron-dynamics in periodic media

Shambhu Ghimire, SLAC National Accelerator Laboratory
2575 Sand Hill Rd, Menlo Park, CA, 94025
shambhu@slac.stanford.edu

Scope of the program

Since the discovery of high-order harmonic generation (HHG) in bulk crystals, there has been growing interest in understanding and exploiting the underlying microscopic strong-field response. In this program, we are particularly interested in comparing these novel nonperturbative phenomena with the well-studied attosecond electronic response in isolated atoms. In the condensed phase, the field-driven electron is never far from the core; therefore the standard strong-field approximation (SFA), and subsequently the three-step re-collision model, becomes questionable. There are two potentially competing mechanisms for HHG in bulk media: radiation from pure intraband non-linear current and emission from interband non-linear current. The main fundamental questions we are trying to address in this program are as follows: (i) can harmonics serve as an atomic-scale probe of the generating medium similar to the gas phase molecules? (ii) What does the time-domain profile of harmonics look like, and would that information resolve the generation mechanism? And, finally (iii) what is the role of periodicity in generating harmonics.

Progress report

1. Demonstration of atomic-scale sensitivity

We demonstrate the strong sensitivity of HHG to the interatomic bonding directions in the cubic, wide-band gap crystal MgO. This is analogous to molecular alignment-dependent HHG in the gas phase. The schematics of the experimental method and a highlight of results are shown in Figure below. We rotate the crystal about its normal and measure harmonics in transmission. Using a linearly polarized field, we measure a highly- anisotropic angular distribution – despite isotropic linear and fairly isotropic perturbative optical susceptibilities of the cubic lattice. The spectra show sharp peaks along the Mg-O,{100} bonding directions (0, 90, 180 and 270 degrees). Additionally, we discover a strong ellipticity and helicity dependence of the HHG, including generation of high harmonics from a circularly polarized driving field in certain crystal orientations.

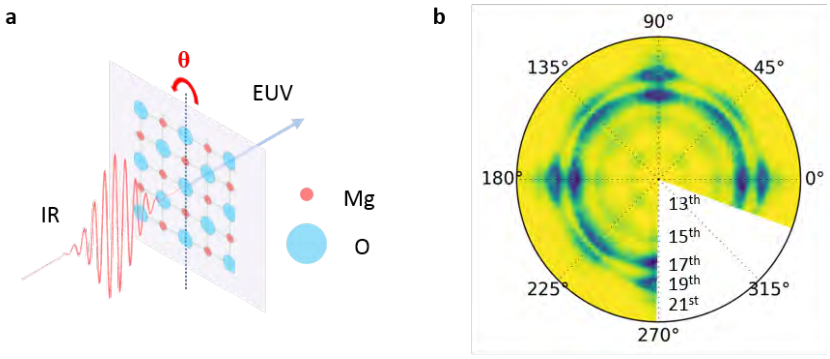

Figure 1 Orientation dependent high-harmonic generation in MgO crystal. **a** shows experimental setup, where a strong infrared laser beam with wavelength centered at 1.3 micrometer is focused onto a MgO crystal, and harmonics are collected in transmission. The crystal is rotated to various angles (θ) with respect to fixed laser polarization. **b** shows the measured spectrum high harmonics for various orientations. The maxima along θ = 0, 90, 180 and 270 ° correspond to the bonding direction in the crystal. Secondary maxima along θ = 45, 135 and 225° correspond to Mg-Mg (or O-O) directions.

In order to understand the measured anisotropy in HHG, we perform a semi-classical electron trajectory analysis including the conduction band motion of the electron. In this picture, radiation is the result of coherent collisions at atomic sites. We find that harmonic efficiency is enhanced (diminished) for semi-classical electron trajectories that connect (miss) neighboring atomic sites in the crystal. We note that in atomic HHG, strongly-elliptical polarization does not yield high harmonics because the electron does not come back to the ion for recombination. Alternatively, our trajectory analysis shows that coherent collision to neighboring sites also produces high harmonics. This explains the generation from circularly-polarized driving fields. Given that the polarization is preserved in the generation process, our results indicate the possibility of circularly-polarized high harmonics in a simple experimental setup. On the imaging aspects of HHG, similar to the molecular HHG, our results in MgO presents a new possibility of using material's own electrons for retrieving the interatomic potential and thus the valance electron density in an all-optical setting [1].

2. Time-domain investigation of HHG

The goal in this experiment is to measure the emission time of high harmonics in bulk crystals. Our collaborative work with the *Gaarde/Schafer* group from LSU shows that time-frequency profiles for inter and intra-band currents are significantly different [2]. Emission from inter-band current should exhibit atto-chirp, while the emission from intra-band current should not have intrinsic phase delay between harmonics. In the experiment, this information can be employed to resolve the generation mechanism. On the attosecond pulse metrology aspects of HHG, phase delay between harmonics must be considered, and compensated. Our preliminary results in bulk MgO crystals indicate a signature of phase delay between harmonics in the plateau. Currently, we are working on modeling the case of MgO, and comparing this finding with other optical media.

3. a) HHG from single layer (Collaboration with Heinz group and Reis group)

We investigate strong-field response in two-dimensional system and compare with the response in bulk. We observe generation of nonperturbative high-order harmonics in a single layer MoS_2 subjected to intense mid-infrared laser fields [3]. Intriguingly, monolayer efficiency is higher than the per-layer efficiency in bulk, suggesting the importance of strong many-body correlations in the two-dimensional system.

b) HHG from rare gas solids (Collaboration with Reis group, Gaarde/Schafer group)

We compare HHG in rare gas solids with their atomic cousins (Ar and Kr). We find that the role of the periodic potential is important even in a weakly-bound system such as a van der Waals solid. These novel effects manifested in the form of multiple plateaus and a high-energy cutoff beyond the atomic limit [4]. Generation of multiple plateaus in the high harmonic spectrum is understood as the contribution from higher-lying conduction bands.

Planned Research

We plan to complete the time-domain studies next year. This includes the modeling for two-color HHG experiments in MgO. Then, we will move to weakly bound system like rare gas solids

because those results can be compared directly with the gas-phase results, where the basic microscopic mechanism has been well understood. We plan to characterize polarization of high harmonics driven by circularly polarized laser fields. In order to investigate multi-site recombination for HHG, we plan a controlled experiment in mixed rare gas solids (for example Ar and Kr). We plan to compare the strong-field response in crystalline solids with other high-density non-periodic media to understand the role of both short- and long-range periodicity.

Publications from DOE sponsored research (2014-2016)

[1] Yong Sing You, David A. Reis, and Shambhu Ghimire, "Anisotropic high harmonic generation in bulk crystals", *submitted*.

[2] Menxi Wu, Shambhu Ghimire, David A. Reis, Ken J. Schafer, and Mette B. Gaarde. "*High-harmonic generation from Bloch electrons in solids*" Physical Review *A*, 91(4):043839, 2015.

[3] Hanzhe Liu, Yilei Li, Yong Sing You, Shambhu Ghimire, Tony F. Heinz, and David A. Reis, "*Observation of high harmonics from an atomically thin semiconductor*", under review, Nature Physics.

[4] Georges Ndabashimiye, Shambhu Ghimire, Mengxi Wu, Dana A. Browne, Kenneth J. Schafer, Mette B. Gaarde, David A. Reis "*Solid-state harmonics beyond the atomic limit*", in press, 534, 520, Nature 2016.

[5] Yong Sing You, David Reis, and Shambhu Ghimire, "*High harmonics from solids probe Angstrom scale structure*" CLEO 2016.

[6] Hanzhe Liu, Yilei Li, Yong Sing You, Shambhu Ghimire, Tony F. Heinz, and David A. Reis, "*Observation of High-Harmonic Generation from an Atomically Thin Semiconductor*", Ultrafast Phenomena 2016.

[7] Yong Sing You, David Reis, and Shambhu Ghimire, "*High harmonics from solids probe Angstrom scale structure*" Bulletin of American Physical Society, DAMOP 2016

[8] Hanzhe Liu, Yilei Li, Yong Sing You, Shambhu Ghimire, Tony F. Heinz, and David A. Reis, "*Observation of High-Harmonic Generation from an Atomically Thin Semiconductor*", APS March Meeting 2016.

[9] Shambhu Ghimire, Georges Ndabashimiye, Anthony D. DiChiara, Emily Sistrunk, Mark I. Stockman, Pierre. Agostini, Louis F. DiMauro, and David A. Reis. "*Strong-field and attosecond physics in solids"*, Journal of Physics B: Atomic, Molecular and Optical Physics, 47(20):204030, 2014.

[10] J. Goodfellow, M. Fuchs, D. Daranciang, S. Ghimire, F. Chen, H. Loos, D. A. Reis, A. S. Fisher, and A. M. Lindenberg. "*Below gap optical absorption in gaas driven by intense, single-cycle coherent transition radiation*", Optics Express, 22(14):17423–17429, 2014.

[11] Georges Ndabashimiye, Shambhu Ghimire, and David A. Reis. "*High harmonic mixing in solid argon"*, Bulletin of the American Physical Society, 59, P5.00005 DAMOP, 2014.

Page is intentionally blank.

University Research Summaries
(by PI)

Page is intentionally blank.

Early Career: Ultrafast Dynamics of Molecules on Surfaces Studied with Time-Resolved XUV Photoelectron Spectroscopy

Thomas K. Allison
Departments of Chemistry and Physics
Stony Brook University, Stony Brook, NY 11794-3400
email: thomas.allison@stonybrook.edu

Program Scope

The capture and storage of solar energy involves the separation and steering of electrons and holes created by the absorption of light. In dye-sensitized solar cells, electrons are injected from a photo-excited dye molecule into a semiconductor. In heterogeneous photo-catalysis, excitation of the electrons in a solid can cause reactions on the surface, storing the photon's energy in chemical bonds. In both cases, the dynamics of charge separation and subsequent reactions are complex and often involve multiple intermediate states. The objective of this work is to provide important fundamental insight into these dynamics using time-resolved photoelectron spectroscopy to track the motion of electrons, holes, and nuclei at molecule/semiconductor interfaces.

Recent Progress

Photoemission spectroscopy using synchrotron radiation is one of the most important methods for establishing relationships between structural and electronic properties at surfaces, with core and valence level shifts providing information about charge transfer, electronic screening, and the geometrical structure of molecules at surfaces. The quasi-CW nature of synchrotron radiation ($\sim$100 ps pulses at MHz repetition rates), which produces few photoelectrons per pulse, is essential for surface experiments where electrons emerge from a small volume of space at the surface, and space charge/image charge effects can blur and shift the photoelectron spectrum.

Many attempts to extend XUV photoemission spectroscopy to the ultrafast time domain using either high-order harmonic generation (HHG) from femtosecond lasers or x-ray pulses from free electron lasers have encountered limitations due to low repetition rates, limited average flux, and space charge/image charge effects. The ideal XUV light source for extending photoemission techniques to the time domain would have the flux and duty cycle characteristics of a synchrotron, but with ultrashort pulse durations. At Stony Brook, we have been working to develop this ideal instrument based on cavity-enhanced high-order harmonic generation and apply it to surface dynamics.

A schematic and photograph of the instrument are shown in figure 1. Light from a home-built, 80 W Yb:fiber frequency comb laser operating at 1035 nm is coupled to a 6 mirror enhancement cavity with an input coupler transmission of 1%, a finesse of ~ 500, and a buildup > 300. We can sustain more than 10 kW of circulating (average) power in this cavity, allowing high-order harmonics from Kr gas at the full repetition rate (87 MHz) of our Yb comb. XUV light is coupled out of the cavity using a sapphire plate at Brewster's angle and directed to a time-preserving monochromator consisting of two toroidal mirrors and a plane diffraction grating. The monochromator selects one harmonic with minimal pulse broadening.

The exit slit of the monochromator is imaged to the sample using a third grazing-incidence toroidal mirror. The sample is housed in an ultra-high vacuum (UHV) chamber with a double μ-metal shield and a full suite of surface preparation and characterization tools. The sample and spectrum of photoelectrons from the sample is measured using a hemispherical electron energy analyzer.

For exciting the surface in pump/probe experiments, we use either the second (518 nm) or third harmonic (345 nm) of our Yb:fiber laser. Splitting off 9 W of NIR light from the Yb:fiber laser, using thin BBO crystals we generate more than 2 W of second harmonic and 120 mW of 3rd harmonic. This allows us to either directly excite electrons and holes in the solid or excite the electrons initially bound to the adsorbed molecules.

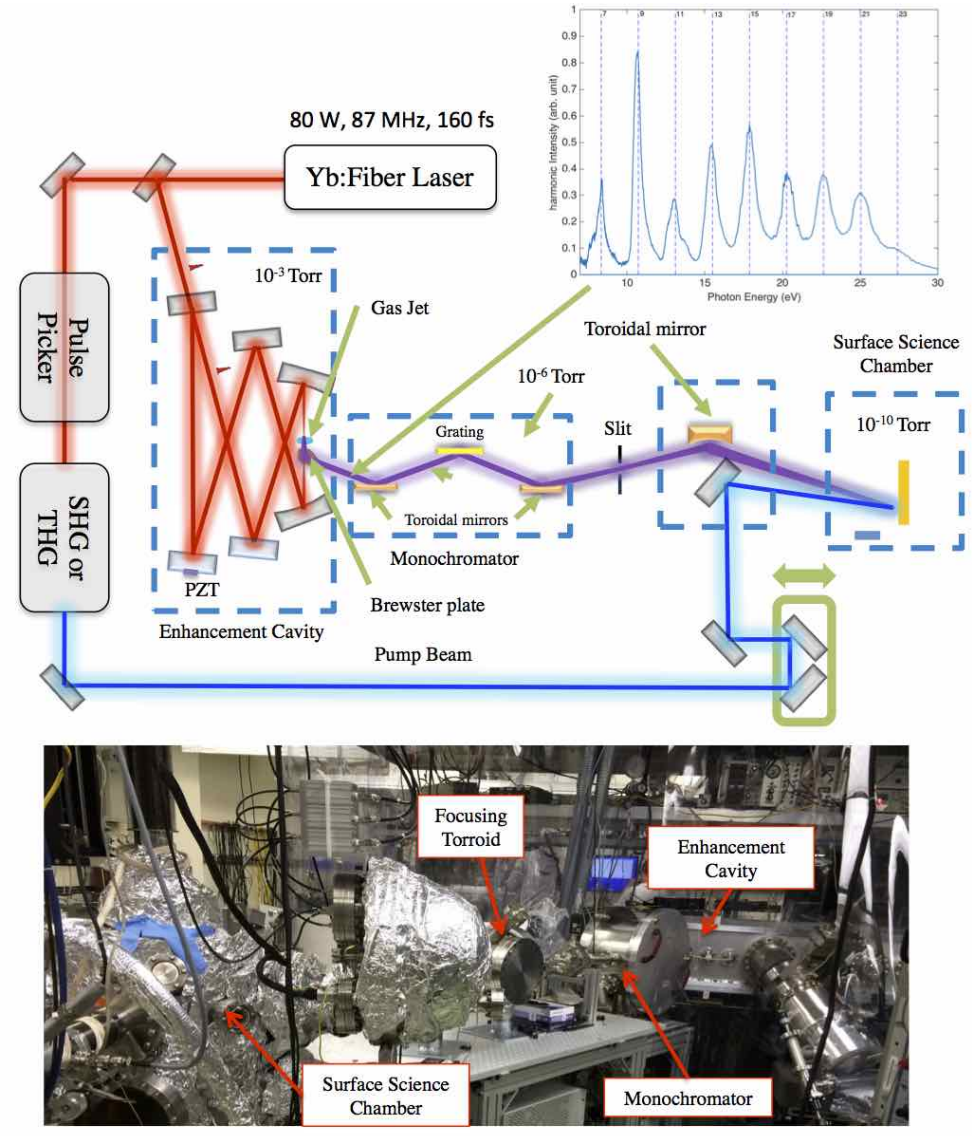

Figure 1: **The Stony Brook time-resolved UPS instrument.** High order harmonics between 10 and 40 eV photon energies are generated at the focus of a 6 mirror bow-tie cavity and coupled out of the cavity using a sapphire wafer at Brewster's angle. A single harmonic is selected with a time-preserving monochromator and focused onto the crystal sample with a torroidal mirror. Pump pulses are derived from the second (SHG) or third (THG) harmonic of the Yb:Fiber laser. A pulse-picker (optional) can be used to decimate the rep-rate if the surface requires more time than $1/f_{\text{rep}} = 12$ ns to relax. Electrons and ions emitted from the crystal surface are recorded as the pump-probe delay is varied.

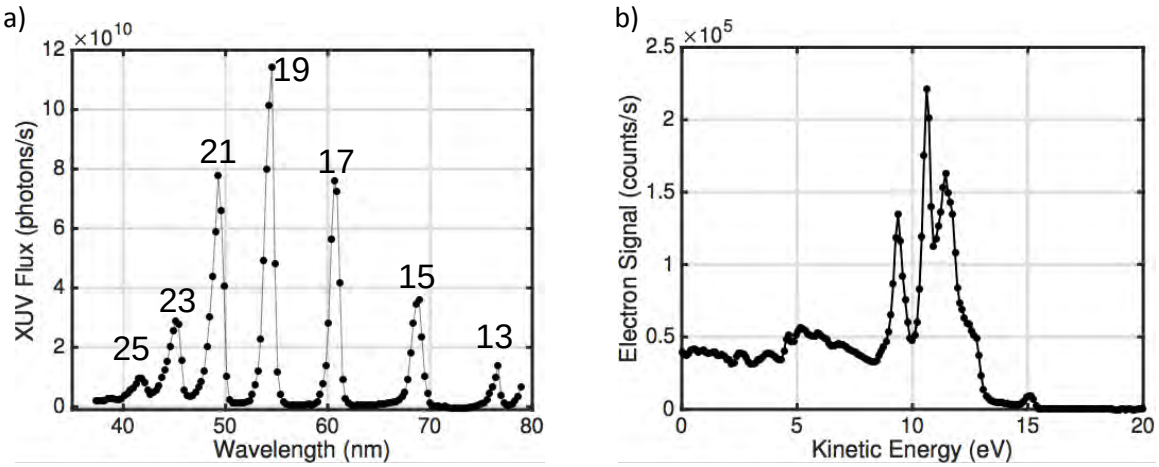

Figure 2: **XUV Results** a) Spectrum of harmonics measured by rocking the monochromator grating and recording the XUV flux after the exit slit using an XUV photodiode. The y-axis is calculated using the photodiode manufacturer's specifications, without further calibration. As most of the beamline's losses occur in the monochromator and out-coupling from the cavity, this represents the flux available for experiments. b) First static photoemission data from a gold surface with ¿ 200 kHz counts rates. The d-bands and the Fermi edge are clearly visible. At low temperatures, the sharpness of the Fermi edge is limited by the energy resolution of the analyzer ($\sim$ 90 meV), and there are no problems with space-charge effects even at such high data rates.

This past summer, we were able to get XUV light all the way down the beamline to the sample and record our first static photoemission data. Figure 2a) shows a calibrated XUV spectrum at the exit of the monochromator, obtained by recording the signal from an aluminum coated XUV photodiode (Optodiode AXUV100Al) after the slit as the grating angle is rocked. More than 10^{11} photons/second in the 19th harmonic, or about 1000 photons/pulse, can be delivered to the sample. Figure 2b) shows a photoelectron spectrum recorded from a clean gold surface with count rates in excess of 200 kHz. At low sample temperatures, the sharpness of the Fermi edge is limited by the energy resolution of the analyzer ($\sim$ 90 meV), and there are no problems with space-charge effects even at such high data rates.

In the process of obtaining this inital data, we realized that we needed to do a better job aligning the last toroidal mirror to be sure we get a small spot on the sample. For the static photoemission shown in figure 2b) the spot size is not critical, but for time-resolved experiments it will be necessary to have a small spot for both the pump and the probe at the sample. We have thus redesigned the chamber housing the last toroidal mirror to incorporate a motorized translation stage and tip/tilt of the mirror. The mirror is also electrically isolated from the chamber such that we can record the photocurrent of electrons emitted from the mirror with a picoammeter and use this for correction of any drifts in the XUV flux. This system is assembled and we are aligning it now. A photograph of the system is shown in figure 3.

Future Plans

We are setting up our first time-resolved experiment to calibrate the instrument. We will perform time-resolved photoemission experiments from a clean gold (Au) surface, first exciting the gold

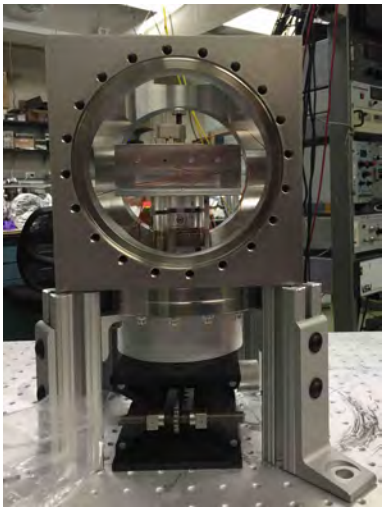

Figure 3: **New mirror tank**. A new vacuum chamber and mount for the last toroidal mirror. Light is incident on the mirror at 3 degrees grazing angle. The mirror is electrically isolated from chamber and mirror mount such that we can record the photocurrent from the mirror surface for normalization.

sample with third harmonic pulses. XUV photoemission will follow the relaxation and cooling of the initially non-thermal distribution of electrons created by the UV pump pump pulses. Measurements of these phenomena have already been done using two-photon photoemission with near-UV pulses. Comparison of our experiments with this previous work will allow us to determine the time resolution and dynamic range of our instrument. We will then proceed to studying charge transfer between adsorbed dye molecules on a TiO_2 surface, electron and hole dynamics on bare TiO_2 surfaces, and photocatalysis reactions.

References

We have only started to receive DOE funding in July of this year and have not yet produced a publication that attributes DOE support. Our fledgling laboratory has produced three independent publications related to this effort since starting at Stony Brook in 2013:

- T. K. Allison. Cavity-enhanced two-dimensional spectroscopy using higher-order modes [INVITED]. Submitted (2016). arXiv:1608.08102
- M. A. R. Reber, Y. Chen, and T. K. Allison. Cavity-enhanced ultrafast spectroscopy: ultrafast meets ultrasensitive. *Optica* **3**, 311 (2016)
- X. L. Li, M. A. R. Reber, C. Corder, Y. Chen, P. Zhao, and T. K. Allison. High-power ultrafast Yb:fiber laser frequency combs using commercially available components and basic fiber tools. Accepted at *Rev. Sci. Inst.* (2016), arXiv:1606.05234.

Attosecond dynamics in molecules driven by ultrashort laser pulses

Principal Investigator: Andreas Becker

JILA and Department of Physics, University of Colorado at Boulder,
440 UCB, Boulder, CO 80309-0440

andreas.becker@colorado.edu

Program Scope

The application of high intensity laser systems has been closely linked to research in ultrafast science and the development of ultrafast optical techniques as laser pulses have been generated with shorter and shorter pulse durations. Substantial progress in the understanding and controlling of electron dynamics in the highly nonlinear process of harmonic generation throughout the last 15 years has been the gateway to the creation of the shortest pulse durations available today. These controlled electron dynamics over a sub-cycle of the driving laser pulse enables the emission of coherent light at extreme ultraviolet and soft X-ray wavelengths on a sub-optical cycle time scale, i.e. on a sub-femtosecond time scale. With this technological advance comes the ability to shift the frontier of temporal resolution of dynamical processes to the time scale of electron dynamics, which ultimately determines the structure of matter as well as the outcome of chemical reactions. The natural time scale of electron dynamics is given by the atomic unit of time, which is 24 attoseconds (1 as = 10^{-18} s). With our projects, we seek to provide theoretical support related to the establishment of ultrafast optical techniques as a tool to uncover new insights regarding the attosecond electron dynamics in atoms and molecules.

Our research is focused on two areas in attosecond science. First, we perform theoretical studies on the application and interpretation of the ultrafast measurement techniques in molecules, in particular attosecond streaking, which enable the retrieval of temporal information of ultrafast processes. Using ab-initio numerical solutions of the time-dependent Schrodinger equation we intend to analyze if and how temporal aspects of the dynamic coupling between electrons and nuclei can be retrieved. In the second research thrust we aim to study and identify features of the laser induced nonadiabatic electron dynamics in molecules using observables such as high harmonic and photoelectron energy spectra. The response of molecules to a strong electric field is complicated beyond the atomic picture by the addition of rotational and vibrational degrees of freedom, a multi-center nuclear frame, and a more complex electronic energy level structure. In particular, strong field ionization and fragmentation from molecular targets can be significantly altered from expectations informed by quasistatic or cycle-averaged formulations of electron dynamics.

Recent Progress

Developments undertaken and accomplishments completed in the research thrusts during the last year can be summarized as follows.

A. Wigner-Smith Time Delays and Application to Attosecond Streaking

The application of the attosecond streaking technique [1] requires the analysis and interpretation of the observed time delays in the experiment [2,3]. We extended our previous analysis of the representation of the time delay as a sum of piecewise field- free time delays, weighted by the instantaneous streaking field strength relative to the streaking field strength at the instant of transition of the electron into the continuum [DOE1, DOE2]. To this end, we made

use of the cut-off Coulomb potential and single active electron potentials to calculate photoemission phase shifts in atoms, and obtained the associated field-free delays by taking the spectral derivative of the calculated phases. The result is an *analytical model* for the calculation of the streaking time-delays in hydrogenic atoms, as well as for noble gases within the single active electron approximation.

The results are in good agreement with those of ab-initio calculations of time delays, performed in our as well as other groups. The model reduces the actual calculation time from several hours (in ab-initio simulations) to a few minutes. Physically, our results indicate that in most cases, the influence of the streaking field on the short-range parts of the potential is a small effect. This provides a sound theoretical basis for the representation of the streaking delay as the sum of the Wigner-Smith delay from scattering theory and the coupling between the streaking and Coulomb fields, as it has been used by various other groups.

B. Extension of Attosecond Streaking to Two-Photon-Ionization of Molecules

Previously, we have shown that for two-photon ionization of atoms the attosecond streaking time delays consist of two contributions, namely, a time delay acquired during the absorption of the two photons from the extreme ultraviolet field and a time delay accumulated by the photoelectron after photoabsorption [DOE5]. We have now extended our studies to molecular systems, in order to - as a long term goal - analyze how temporal information about the coupling between electrons and nuclei, as well as between electrons can be retrieved using the attosecond streaking technique. In the last year we have developed a computer code to simulate the attosecond streaking of photoionization of the hydrogen molecular ion, first considering a model with nuclei at a fixed internuclear distance. Calculations for single photoionization were performed successfully and showed results similar to those previously obtained in the atomic case [DOE5]. We now consider two-photon ionization of the molecular ion model, and preliminary results indicate the importance of contributions due to resonant processes, involving more than one intermediate state.

C. Detection of Nonadiabatic Electron Dynamics with High Harmonic Spectroscopy

Our previous theoretical studies have indicated that transient electron localization [4] modifies fragmentation patters in dissociating molecules [5] and photoelectron momentum distributions [4] (for a review, see [DOE9]). Motivated by these studies we have demonstrated the capacity for transient electron localization to strongly modify and modulate the generated signal of high harmonic generation (HHG) [DOE8]. We have studied this behavior in the context of a fixed-internuclear distance model of the hydrogen molecular ion, for which the nonadiabatic behavior of interest is well-understood. Strong laser field induced transient electron localization is accompanied with instants of suppression of ionization, corresponding to localizations of the electron on the uphill side of the molecule. Through classical analysis of the emitted electron trajectories, we associated the timing of this ionization suppression to the energetic location of the HHG spectrum minimum. Consequently, the minimum can be used to trace the ongoing electron dynamics. This capacity is extended to image changing dynamics by isolating different recombination events and studying the emergence and movement of spectral minima within separated attosecond pulses.

In addition to developing our understanding for the conditions which enable transient electron localization to suppress harmonic emission at critical energy intervals, we have also explored the mechanism causing the highly-structured interference pattern at the highest plateau energies of molecules undergoing nonadiabatic electron behavior [6]. The breaking of the inversion symmetry of the electron distribution at the time of recombination during sequential

half-cycles of the laser field is seen to interrupt the conditions conventionally producing distinct odd harmonics. Expression of this modified interference structure within the total HHG spectrum relies upon the modulation of the HHG signal, which equalizes the amplitude of harmonic emission during the middle field cycles and along the rising and trailing ends of the field. In combination, these two effects result in a complex high-energy structure.

D. Single active electron models

In the regime of strong-field physics it is common to use the single-active-electron approximation to a multielectron system, in which one electron responds to the influence of the external field while the rest of the electrons are considered as frozen. While this framework did not follow from ab-initio theoretical principles, it had, in the past, achieved agreement with experimental results of ionization studies. We applied an algorithm that used density functional theory to fully compute electronic interactions of a field-free system. We then considered, developed, and tested the output of a strategy for fitting numerical pseudopotentials to a concise analytic expression which was physically grounded in structure of the exchange-correlation component of the full potential. So far, our models successfully reproduced the Cooper minimum in the HHG spectrum of argon, which is known to be highly sensitive to the electronic structure of the generating system.

Future Goals

In the next year we plan to continue our efforts in the two thrust areas. In particular, it is our goal to analyze and disentangle the different contributions to the calculated time delays for two-photon ionization of the hydrogen molecular ion: these are the time delay accumulated in the continuum and the parts arising due to the interaction with more than one intermediate state. We then plan to investigate how information about the different intermediate states can be retrieved from the time delay spectra. Once this task is completed, we will consider three- and four-photon ionization processes to investigate the prospects of an extension of the attosecond streaking technique in this direction. Finally, we plan to take the first steps towards the major goal in this research thrust: that is the application of the attosecond streaking technique to molecular photoionization including the motion of nuclei in the model, in order to analyze whether the coupling between electron and nuclear dynamics can be temporally resolved.

In the second research thrust we plan to continue our studies on the detection of nonadiabatic electron dynamics using high harmonic spectroscopy. Having established the signatures of the dynamics via a minimum in the spectrum, we plan to perform investigations regarding the potential observation of the signature in the experiment. This includes the consideration of the robustness of the feature with respect to the variation of the laser parameters, in particular those within the laser focus. Furthermore, we will analyze the macroscopic response of the high harmonic yield within a gas jet.

References

[1] J.Itatani et al., Phys. Rev. Lett. **88**, 173903 (2002).

[2] M. Schultze et al., Science **328**, 1658 (2010).

[3] A.L. Cavalieri et al., Nature **449**, 1029 (2007).

[4] N. Takemoto and A. Becker, Phys. Rev. Lett. **105**, 203004 (2010).

[5] F. He, A. Becker, and U. Thumm, Phys. Rev. Lett. **101**, 213002 (2008).

[6] M.R. Miller et al., submitted for publication

Publications of DOE sponsored research (2014-2016)

[DOE1] J. Su, H. Ni, A. Becker and A. Jaron-Becker, *Attosecond streaking time delays: Finite-range property and comparison of classical and quantum approaches,* Physical Review A **89**, 013404 (2014).

[DOE2] J. Su, H. Ni, A. Becker and A. Jaron-Becker, *Numerical simulations of attosecond streaking time delays in photoionization (invited paper),* Chinese Journal of Physics **52**, 404 (2014).

[DOE3] M.-C. Chen, C. Mancuso, C. Hernández-García, F. Dollar, B. Galloway, D. Popmintchev, P.-C. Huang, B. Walker, L. Plaja, A. A. Jaroń-Becker, A. Becker, M. M. Murnane, H. C. Kapteyn, and T. Popmintchev*, Generation of bright isolated attosecond soft X-ray pulses driven by multicycle midinfrared lasers*, Proceedings of the National Academy of Sciences of the United States of America **111**, E2361 (2014).

[DOE4] M.R. Miller, C. Hernandez-Garcia, A. Jaron-Becker, and A. Becker, *Targeting multiple rescatterings through VUV-controlled high-harmonic generation*, Physical Review A **90**, 053409 (2014).

[DOE5] J. Su, H. Ni, A. Jaroń-Becker and A. Becker, *Time delays in two-photon ionization*, Physical Review Letters **113**, 263002 (2014).

[DOE6] D.D. Hickstein, F.J. Dollar, P. Grychtol, J.L. Ellis, R. Knut, C. Hernández-García, D. Zusin, C. Gentry, J.M. Shaw, T. Fan, K.M. Dorney, A. Becker, A. Jaroń-Becker, H.C. Kapteyn, M.M. Murnane, and C.G. Durfee, *Noncollinear generation of angularly isolated circularly polarized high harmonics*, Nature Photonics **9**, 743 (2015).

[DOE7] D. Popmintchev, C. Hernández-García, F. Dollar, C. Mancuso, J.A. Pérez-Hernández, M.-C. Chen, A. Hankla, X. Gao, B. Shim, A. Gaeta, M.Tarazkar, D. Romanov, R. Levis, J.A. Gaffney, M. Foord, S.B. Libby, A. Jaron-Becker, A. Becker, L. Plaja, M.M. Murnane, H.C. Kapteyn, and T. Popmintchev, *Efficient soft X-ray high harmonic generation in multiply-ionized plasmas: the ultraviolet surprise,* Science **350**, 1225 (2015).

[DOE8] M.R. Miller, A. Jaron-Becker, and A. Becker, *High-harmonic spectroscopy of laser driven nonadiabatic electron dynamics in the hydrogen molecular ion,* Physical Review A **93**, 013406 (2016).

[DOE9] M.R. Miller, Y. Xia, A. Becker and A. Jaron-Becker, *Laser driven nonadiabatic electron dynamics in molecules,* Optica **3**, 259-269 (2016).

Probing Complexity using the LCLS and the ALS

Nora Berrah
Physics Department, University of Connecticut, Storrs, CT 06268
e-mail:nora.berrah@uconn.edu

Program Scope

The goal of our research program is to investigate *fundamental interactions between photons and molecular systems* to advance our quantitative understanding of electron correlations, charge transfer and many body phenomena. Our research investigations focus on probing, on femtosecond time-scale multi-electron interactions, and tracing nuclear motion in order to understand and ultimately control energy and charge transfer processes from electromagnetic radiation to matter. Most of our work is carried out in a strong partnership with theorists.

Our current interests include: **1)** The study of non-linear and strong field phenomena in the x-ray regime using free electron lasers (FELs), and in particular, the ultrafast linac coherent light source (LCLS) x-ray FEL facility at the SLAC National Laboratory. We have also recently used IR lasers to prepare our FELs experiments with the added benefit of comparing multi-photon ionization dynamics in the IR and x-ray regimes. **2)** Time-resolved molecular dynamics investigations using pump-probe techniques. Our experiments probe physical and chemical processes that happen on femtosecond time scales. This is achieved by measuring and examining both electronic and nuclear dynamics subsequent to the interaction of molecules and clusters with LCLS pulses of various (4-80 fs) pulse duration. **3)** The study of dynamics and correlated processes in select molecules as well as anions with vuv-soft x-rays from the Advanced Light Source (ALS) at Lawrence Berkeley Laboratory.

We present below results completed and in progress this past year and plans for the immediate future.

Recent Progress

1) A Two Mirrors X-ray Pulse Split and Delay Instrument for Femtosecond Time Resolved Investigations at the LCLS Free electron Laser Facility

We built a two-mirrors based x-ray split and delay (XRSD) system for soft x-rays to be used by any user who receives beamtime at the Linac Coherent Light Source (LCLS) free electron laser at SLAC National Laboratory. The instrument is based on an edge-polished mirror design covering an energy range of 250 eV-1800 eV and producing a delay between the two split pulses variable up to 400 femtoseconds with a sub-100 attosecond resolution. We carried out experimental measurements and simulations regarding molecular dissociation dynamics in CH_3I and CO probed by the XRSD. We observed both ion kinetic energy and branching ratio dependence on the delay times which were reliably produced by the XRSD [1]. This instrument was used successfully in LCLS approved beamtimes [11, a]

2) Time-Resolved Femtosecond Dynamics of C_{60} at High X-Ray Intensity: A Show Case Model System for Any Extended System Studied with LCLS and Future FELs

We carried out a time-resolved *benchmark* experiment in C_{60} to observe and measure *the predicted critical change in pump-probe behavior* where the ionization behavior stops being

"molecular" due to the complete C_{60} fragmentation at high LCLS fluence. This time-resolved experiment was guided by Molecular Dynamics Modeling to reveal, from a fundamental point of view, the physical and chemical processes, involved in the formation of a nanoplasmas as well as radiation damage, not previously reported. We have validated in previous *static* work [18,20] the successful use of classical mechanics to describe all moving particles in C_{60}. This approach scales well to larger systems, such as biomolecules. The recent experiment carried out in February 2016, which was successful, will test a recent predicted two-step Coulomb explosion model that stipulates ejection of high kinetic energy atomic fragment ions in 10 fs followed by slower molecular fragments up to the ps range. We used the accelerator based x-ray pump-x-ray probe technique to carry out the experiment with a variable time delay that covered 25-925 fs (not possible with the XRSD). We detected ions and electrons using a 2m long magnetic bottle spectrometer [6] attached to the LAMP instrument. We are presently analyzing the data; the ion fragments, the ejected electrons and their kinetic energy resulting from C_{60} photoionization as a function of time delay between the x-ray pump and the x-ray probe. One important impact of this experiment is that the comparison of the time-resolved models to the C_{60} experiment will allow the extension of the model to be applicable for x-ray interactions with *any extended system*, *and* with *different FEL parameters*.

1) Inner-shell Photodetachment of Anions using the ALS: The Case of Ni^-

Inner-shell photodetachment from Ni^-([Ar] $3d^9 4s^2$) leading to Ni^+, Ni^{2+}, and Ni^{3+} ion production was studied near and above the 3p excitation region (45 - 90 eV) photon energy range, using the merged ion-photon beam technique at the ALS. The absolute photodetachment cross section of Ni^- leading to Ni^+ ion production was measured. The 3p → 3d photoexcitation in Ni^- negative ion gives rise to Feschbach resonances. In the near-threshold region, Fano profiles accurately fit the Ni^- single photodetachment cross section. Simultaneous double-photo-detachment was also observed, resulting in an increased Ni^{2+} production which obeys a Wannier law. Despite the large number of possible terms resulting from the Ni^- 3d -open shell, a low-order LS coupling configuration interaction (CI) calculation qualitatively agrees well with the experimental data. A manuscript is under preparation.

References

[a] J. Stohr et al., Condensed Matter beamtime at the AMO hutch using the XRSD, (publication under preparation)

Future Plans.

The principal areas of investigation planned for the coming year are:
1) Analyze the time-resolved ionization dynamics data on C_{60} induced by 20 fs x-ray pulses generated during our February LCLS 2016 beamtime. **2)** Finish writing the manuscript regarding the multi-photon ionization of $Ho_3N@C_{80}$ with IR laser in order to compare the multi-photon ionization mechanisms of this system in two energy regimes; x-rays from the LCLS and 1.5 eV photons from an IR laser. **3)** Finish writing the paper from the LAMP LCLS instrument commissioning beamtime. **4)** Finish writing the paper from the analyzed ALS K-shell photodetachment data in C_{60}^-. **5)** Write the paper relevant to the data we analyzed in 2015-2016 regarding the K-shell photodetachment experiments of the carbon anions chain (C_2^- - C_{12}^-) at the ALS. **6)** Continue the analysis of our June 2015 and January 2016 ALS beamtimes on the single-photon ionization of $Sc_3N@C_{80}$ and $Ho_3N@C_{80}$. These ALS-baseline experiments will be

published on their own right but they also will provide us the backbone of our future LCLS proposals.

Publications from DOE Sponsored Research

1. N. Berrah, L. Fang, B. F Murphy, E. Kukk, T.Y. Osipov, R. Coffee, K. R Ferguson, H. Xiong, J-C. Castagna, V. S Petrovic, S. Carron-Montero, and J. D. Bozek , "A two mirrors x-ray pulse split and delay instrument for femtosecond time resolved investigations at the LCLS free electron laser facility" Optics Express **24** (11), 11768-11781 (2016).
2. A. Picon, C. S. Lehmann, C. Bostedt, A. Rudenko, A. Marinelli, T. Osipov, D. Rolles, N. Berrah, C. Bomme, M. Bucher, G. Doumy, B. Erk, K. R. Ferguson, T.Gorkhover, P. J. Ho, E. P. Kanter, B. Krassig, J. Krzywinski, A. A. Lutman, A.M. March, D. Moonshiram, D. Ray, L. Young, S. T. Pratt, and S. H. Southworth, "Hetero-site-specific ultrafast intramolecular dynamics", Nature Comm. **7**, 11652(2016).
3. Liu, Ji-Cai; Berrah, Nora; Cederbaum, Lorenz; Cryan, James; Glownia, James; Schafer, Kenneth; Buth, Christian "Rate equations for nitrogen molecules in ultrashort and intense x-ray pulses " J. Phys. B: Atomic, Molecular and Optical Physics **49,** 075602 (2016) doi:10.1088/0953-4075/49/7/075602.
4. Nora Berrah, "Molecular Dynamics Induced by Short and Intense X-rays Pulses from the LCLS" Physica Scripta **T169** (2016) (Article based on an invited talk at the **Nobel Symposium**, Stigtuna, Stockholm, Sweden, June 15, 2015).
5. A. Sanchez-Gonzalez, T. Barillot, R. Squibb, et al., C. Bostedt, J. Cryan, A. Natan, T. Osipov, N. Berrah, P. Bucksbaum, et al., J. Marangos, J, "Auger electron and photoabsorption spectra of glycine in the vicinity of the oxygen K-edge measured with an X-FEL", J. Phys. B: At. Mol. Opt. Phys. **48** 234004 (2015).
6. V. Zhaunerchyk, M. Kaminska, M. Mucke, R.J. Squibb, J.H.D. Eland, et al., B.K. McFarland, E. Sistrunk, M. Guhr, R.N. Coffee, C. Bostedt, J.D. Bozek, …T. Osipov, L. Fang, B.F. Murphy, N. Berrah, and R. Feifel, "Disentangling formation of multiple-core holes in aminophenol molecules exposed to bright XFEL radiation ", J. Phys. B: At. Mol. Opt. Phys. **48** 244003 (2015).
7. N. Berrah and P. H. Bucksbaum, "The Ultimate X-ray Machine" Scientific American Special Collector's edition, **54**, (2015).
8. N. Berrah, B. Murphy, H. Xiong, L. Fang, T. Osipov, E. Kukk, M. Guehr, R. Feifel, V. S. Petrovic, K. R. Ferguson, J. D. Bozek, C. Bostedt, L. J. Frasinski, P. H. Bucksbaum and J. C. Castagna , "Femtosecond x-ray induced fragmentation of fullerenes" J. of Mod. Opt., **63**, No. 4, 390–401 (2015) doi:10.1080/09500340.2015.1064175.
9. P. Bucksbaum & N. Berrah, "Brighter and faster: The promise and challenge of the x-ray free-electron laser", Physics Today, **68** (7), 26 July 2015.
10. N. Berrah and L. Fang "Chemical Analysis: Double Core-Hole Spectroscopy with Free-Electron Lasers" J. Electr. Spect. And Rel. Phenom. **204,** 284–289 (2015).
11. C. E. Liekhus-Schmaltz, I. Tenney, T. Osipov, A. Sanchez-Gonzalez, N. Berrah, R. Boll, et al., P.H. Bucksbaum, V. Petrovic et al.,"Ultrafast Isomerization Initiated by X-Ray Core Ionization" Nature Comm., **6,** 8199, doi:10.1038/ncomms9199 (2015).
12. M. Mucke, V. Zhaunerchyk, L.J. Frasinski, R.J.Squibb, M. Siano, J.H.D. Eland, P. Linusson, P. Salen, P. v.d. Meulen, R.D. Thomas, M. Larsso3, L. Foucar, J. Ullrich, K. Motomura, S. Mondal, K.Ueda, T. Osipov, L. Fang;12, B.F. Murphy, N Berrah, C. Bostedt, J.D. Bozek, S. Schorb, M.Messerschmidt, J.M. Glownia, J.P. Cryan, R.N. O. Takahashi, S. Wada, M.N. Piancastelli, R. Richter, K.C. Prince, and R. Feife, "Covariance mapping of two-photon double core hole states in C_2H_2 and C_2H_6 produced by an X-ray free electron laser" New Journal of Physics, **17,** 073002, doi:10.1088/1367-2630/17/7/073002, (2015).
13. F. Penent, M. Nakano, M. Tashiro, T. P. Grozdanov, M. Žitnik, K. Bucar, S. Carniato, P. Selles, L. Andric, P. Lablanquie, J. Palaudoux, E. Shigemasa, H. Iwayama, Y. Hikosaka, K. Soejima,

I.H. Suzuki, N. Berrah, A. Wuosmaa, T. Kaneyasu and K. Ito, "Double core hole spectroscopy with synchrotron radiation" J. Electr. Spect. and Relat. Phenom. **204,** 303–312, doi:10.1016/j.elspec.2015.06.015, (2015).

14. A. Dubrouil, M. Reduzzi, M. Devetta, C. Feng, J. Hummert, P. Finetti, O. Plekan, C. Grazioli, M. Di Fraia, V. Lyamayev, A. La Forge, R. Katzy, F. Stienkemeier, Y. Ovcharenko, M. Coreno, N. Berrah, K. Motomura, S. Monda, K. Ueda, K. C. Prince, C. Callegari, A. I Kuleff, Ph .V Demekhin and G. Sansone, "Two-photon resonant excitation of interatomic coulombic decay in neon dimers ", J. Phys. B: At. Mol. Opt. Phys. **48** 204005, doi:10.1088/0953-4075/48/20/204005, (2015).
15. L Fang, Z Jurek, T Osipov, B F Murphy, R Santra, and N Berrah, "Investigating Dynamics of Complex System Irradiated by Intense X-ray Free Electron Laser Pulses", Journal of Physics: Conference Series, **601,** 012006 (2015).
16. Ann Marks, Cathy Foley, Adriana Predoi-Cross, Nora Berrah "Girls and Physics: Four Contrasting National Situations", La Physique au Canada, **71**, No. 2 (2015).
17. Marc. Humphrey, Paul V. Pancella and Nora Berrah, "Idiots Guides for Quantum Physics", ALPHA Books publishing, ISBN 97781615643172, Jan 6, 2015.
18. B. F. Murphy, T. Osipov, Z. Jurek, L. Fang, S.-K. Son, L. Avaldi, P. Bolognesi, C. Bostedt, J. Bozek, R. Coffee, J. Eland, M. Guehr, J. Farrell, R. Feifel, L. Frasinski, J. Glownia, D.T. Ha, K. Hoffmann, E. Kukk, B. McFarland, C. Miron, M. Mucke, R. Squibb, K. Ueda, R. Santra, and N. Berrah "Bucky ball explosion by intense femtosecond x-ray pulses: a model system for complex molecules", Nature Comm, **5**, 4281, doi:10.1038/ncomms5281 (2014).
19. B. K. McFarland, J. P. Farrell, S. Miyabe, F. Tarantelli, A. Aguilar, N. Berrah, C. Bostedt, J. Bozek, P.H. Bucksbaum, J. C. Castagna, R. Coffee, J. Cryan, L. Fang, R. Feifel, K. Gaffney, J. Glownia, T. Martinez, M. Mucke, B. Murphy, A. Natan, T. Osipov, V . Petrovic, S. Schorb, Th. Schultz, L. Spector, M. Swiggers, I. Tenney, S. Wang, W. White, J. White and M. Gühr " Delayed Ultrafast X-ray Auger Probing (DUXAP) of Nucleobase Ultraviolet Photoprotection , Nature Comm, **5**, 4235, doi:10.1038/ncomms5235 (2014).
20. N. Berrah, L. Fang, T. Osipov, Z. Jurek, B. F. Murphy, and R. Santra, Faraday Discussion, " Emerging photon technologies for probing ultrafast molecular dynamics" Faraday Disc., **171** (1), 471 – 485 (2014).
21. L. Fang, D. Rolles, A. Rudenko, V. Petrovich, C. Bostedt, J. D. Bozek, P. Buckbaum and N, Berrah "Probing ultrafast electronic and molecular dynamics with free electron lasers" J. Phys. B: At. Mol. Opt. Phys. **47,** 124006 doi:10.1088/0953-4075/47/12/124006, (2014).
22. M. Mucke, V. Zhaunerchyk, R.J. Squibb, M. Kamiska, J.H.D. Eland, P. v.d.Meulen, P. Salén, P. Linusson, R.D. Thomas, M. Larsson, L.J. Frasinski, M. Siano, T. Osipov, L. Fang,B. Murphy, N. Berrah, L. Foucar, J. Ullrich, K. Motomura, S. Mondal, K. Ueda, R. Richter,K.C. Prince, M.N. Piancastelli, M. Glownia, J. Cryan, R. Coffee, C. Bostedt, J. Bozek, S. Schorb, M. Messerschmidt, O. Takahashi, S. Wada, and R. Feifel, "Mapping the decay of double core hole states of atoms and molecules", Journal of Physics: Conference Series **488**, 032021 (2014).
23. N. Berrah, L. Fang, T. Osipov, B. Murphy, C. Bostedt and J.D. Bozek, "Multiphoton Ionization and Fragmentation of Molecules with the LCLS X-Ray FEL , J. Elec. Spect and Rela. Phen, **196**, 34-37 (2014).
24. N. Berrah and P. H. Bucksbaum, "The Ultimate X-ray Machine" Scientific American, **310**, 64, January 2014.
25. B.K. McFarland, N. Berrah ,C. Bostedt, J. Bozek, P. H. Bucksbaum, J. C. Castagna, R. N. Coffee, J. P. Cryan, L. Fang, J. P. Farrell, R. Feifel, K. J. Gaffney, J. M. Glownia, T. J. Martinez, S. Miyabe,M. Mucke, B. Murphy, A. Natan, T. Osipov , V. S. Petrović, S. Schorb, Th.Schultz, L. S. Spector, M. Swiggers, F. Tarantelli, I. Tenney, S. Wang, J. L. White, W. White, and M Gühr, "Experimental strategies for optical pump – soft x-ray probe experiments at the LCLS" J. Phys.: Conf. Ser. **488**, 012015 doi:10.1088/1742-6596/488/1/012015 (2014).

Ultrafast Electron Diffraction from Aligned Molecules

PI: Martin Centurion
Department of Physics and Astronomy, University of Nebraska, Lincoln, NE 68588-0299
mcenturion2@unl.edu

Program Scope or Definition

This project aims to investigate photochemical reactions at the molecular level by observing how the molecular structure changes upon light absorption. The project relies on ultrafast electron diffraction to image photo-induced reactions in isolated molecules with atomic resolution. A sample of molecules in the gas phase is excited by a femtosecond laser pulse, and the structure is probed by a femtosecond electron pulse. The scattering pattern of the probe electrons contains information on the structure of the molecule, and under certain conditions an image of the molecule can be retrieved with atomic resolution. Using a laser pulse to pre-align the molecules before excitation increases the amount of structural information that can be retrieved from the images and makes it possible to retrieve the three-dimensional structure.

Introduction

In photo-induced molecular reactions light can be converted into chemical and kinetic energy on femtosecond time scales. Observing the motion of atoms and the resulting transient structures during these processes is essential to understand them. Diffraction methods are an ideal tool because they are directly sensitive to the spatial distribution of charge, and are thus complementary to spectroscopic methods that probe the energy landscape. We will implement ultrafast electron diffraction (UED) with femtosecond temporal resolution to observe structural dynamics.

A gas-phase diffraction experiment comprises four major parts: i) An electron gun that delivers short pulses on a target, ii) a laser that triggers both the electron gun and the photochemical reaction, iii) a sample delivery system that creates a gas jet target in a vacuum environment, and iv) a detection system. Two different systems will be used in this project. The first is the MeV electron gun at the ASTA test facility at SLAC National Lab. This RF photoelectron gun produces femtosecond electron pulses in an energy range between 2 MeV and 5 MeV, with a repetition rate of 120 Hz. We have designed and constructed an experimental chamber for gas phase diffraction experiments, in collaboration with the group of Xijie Wang at SLAC. The main advantage of using MeV electrons is that they are relativistic, which minimizes the velocity mismatch between laser and electrons and also the pulse spreading due to Coulomb forces. The velocity mismatch has been a major limitation in the temporal resolution of UED experiments with sub-relativistic pulses.

Experiments will also be performed in the PI's lab at UNL using a photoelectron gun that combines a DC accelerator with an RF compression cavity. Electrons are accelerated to energies of up to 100 keV and then compressed at the target position by a small RF cavity, at a repetition rate of 5 kHz. This setup will include an optical system to deliver laser pulses with a tilted intensity front on the sample. The tilted pulses will serve to compensate the velocity mismatch of laser and electrons through the sample to reach femtosecond resolution. The setup at SLAC is expect to reach better temporal resolution due to the use of relativistic electron pulses, while the setup at UNL is expected to reach a better spatial resolution due to the higher average beam current that will allow for capturing the scattering at larger angles.

Recent Progress

We have performed, at SLAC, the first ultrafast electron diffraction experiments from isolated molecules. A chamber for gas phase experiments was designed and constructed, in collaboration with Markus Guehr from Potsdam University. The setup uses a pulsed valve to deliver a gas jet at 120 Hz, synchronized to the electron gun. A heated bubbler is used to deliver molecules with a low vapor pressure into the experiment. The sample is heated, and helium gas flows through the sample to carry the molecules into the jet. The bubbler was used to make a gas jet of helium and iodine, although it did not work as expected. The sample density was lower than expected, but still sufficient for experiments. We are currently working on improving this part of the experiment. We used a collinear setup (shown in Figure 1) where the laser and electron beams were almost parallel, to take advantage of the fact that the velocity of the electrons is close to the speed of light and minimize temporal blurring due to geometrical factors. The laser is introduced using a mirror that has a hole in the center to transmit the electron beam. Similarly, a second holey mirror is used to extract the laser beam and transmit the diffraction pattern. At an energy of 3.7 MeV, the deBroglie wavelength of the electrons is λ = 0.30 pm and the speed is 0.993c. The gas jet is perpendicular to the laser and electron beams. The diffraction patterns were captured using a phosphor screen that has a hole in the center to avoid saturation due to the unscattered electron beam, and is imaged on an EMCCD.

Two experiments were performed to demonstrate the capabilities of the new setup. In the first experiment, we have impulsively aligned nitrogen molecules with a femtosecond laser pulse (wavelength of 800 nm), and captured the dynamics of the rotational wavepacket using UED. The main idea was to use the fast dynamics as a way to measure the overall temporal resolution of the setup. Figure 2 shows the rotational dynamics captured with diffraction. When the molecules are aligned by the laser, the diffraction pattern becomes anisotropic. The changes in the pattern are used to map the anisotropy vs time, which for low degrees of alignment is approximately proportional to the $< \cos^2 \theta >$ value, where θ is the angle between the molecular axis and the alignment axis (along the laser polarization) and the value is averaged over all molecules. We have observed the prompt alignment and mulmultiple revivals. It is worth noting that at the revivals, the angular distribution changes between prolate and oblate in about 300 fs. In order to extract the resolution, we fitted the data to a simulated alignment curve, using the convolution due to the limited temporal resolution as a free parameter in the fit. The best fit was for a resolution of 100 fs RMS, or 230 fs FWHM. This temporal resolution is a factor of 4 better than what was previously achieved in UED from isolated molecules. The previous record was 850 fs, achieved in the PI's

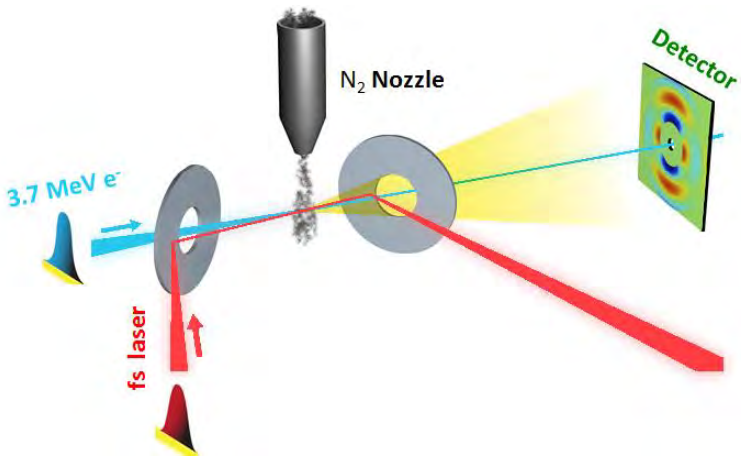

Figure 1. Experimental setup. The laser and electron pulses are approximately collinear at the sample. Two mirrors with a hole in the center direct the laser in and out of the setup.

lab in 2012. We believe the resolution is currently limited by the electron pulse duration and by timing jitter between the laser and electron pulses. The effect of velocity mismatch is negligible at these energies.

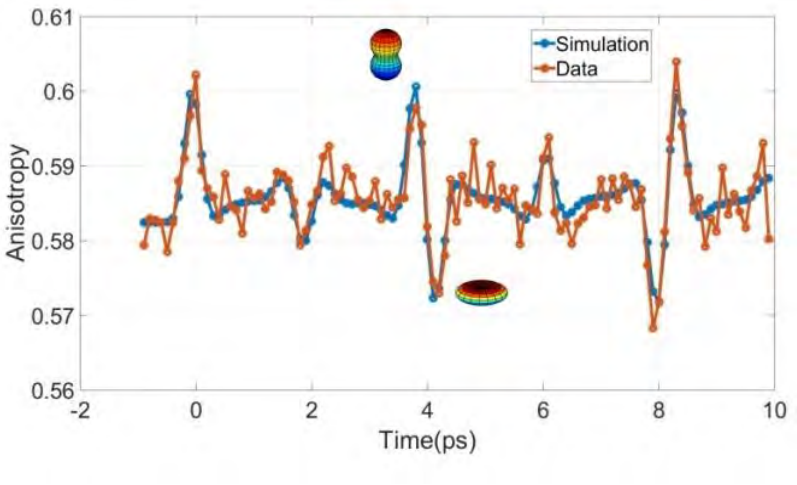

Figure 2. Rotational dynamics of Nitrogen measured with MeV UED, showing a temporal resolution of 100 fs RMS (230 fs FWHM).

This temporal resolution opens the door to capture coherent nuclear motion in isolated molecules with electron diffraction for the first time. In order to demonstrate this capability, we recorded diffraction patterns of a vibrational wavepacket in Iodine. The bound nuclear wavepacket is created by exciting the molecules with a laser pulse with a wavelength of 530 nm. According to simulations, the wavepacket then oscillates between the ground state bond length of 2.7 Å and a maximum bond length of 3.9 Å, with a period of approximately 400 fs. Figure 3a shows the experimentally measured bond length as a function of time. The bond length was extracted from the diffraction patterns. Figure 3b shows the nuclear wavepacket extracted from the experimental diffraction patterns (blue lines) along with the simulated wavepackets (red and green lines). The figure shows that both the motion and shape of the wavepacket can be measured. In this experiment, the measured broadening of the moving wavepacket was mostly due to the motion itself, limited by the temporal resolution. With a temporal resolution improvement of a factor of two or three, the intrinsic broadening of the wavepacket will be measurable. However, the bond length can be determined very accurately because it relies only on finding the most probable distance between the atoms, as shown in Figure 3a the error is less than 0.1 Å.

The setup at UNL is currently being finalized and tested. We have separately tested the components and are currently combining them. We a constructed and tested a gas delivery system that includes the possibility of heating molecules with low vapor pressure and introducing them in vacuum using helium as a carrier gas. We also have implemented an optical system that can deliver tilted laser pulses to match the longitudinal components of the velocities of electron and laser pulses as they traverse the sample. More recently, we have characterized the temporal resolution of our electron gun that uses RF compression. The resolution was measured using a home-made streak camera that has a resolution on the order of 100 fs. We have consistently measured a temporal resolution around 400 fs for our setup, two times better than in our previous experiments. In addition, with RF compression we can increase the beam current by two orders of magnitude while still achieving improved temporal resolution. We are currently at the stage

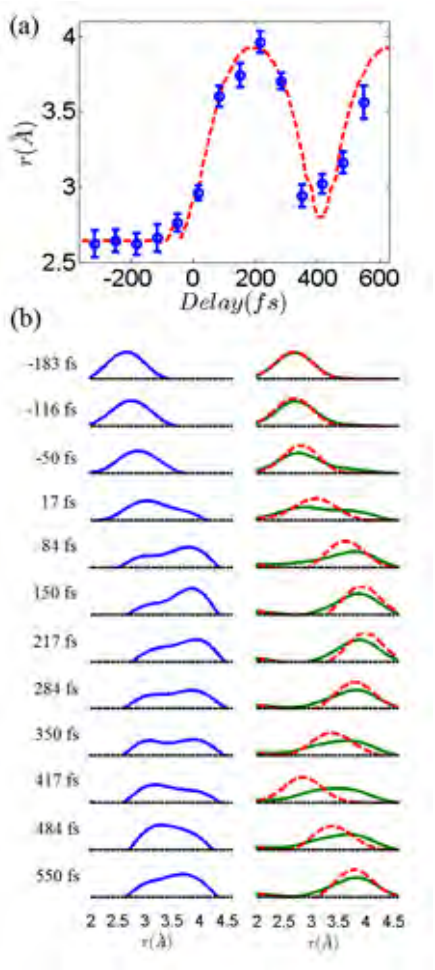

Figure 3. Nuclear wavepacket motion in Iodine. a) Measured interatomic distance vs time (the red line is the simulation). b) Measured nuclear wavepackets (left panel) and simulated (right panels). The simulations include the same spatial resolution as in the experiment. The green curves include also the effect of

of putting all the pieces together, gas delivery, tilted laser pulses and compressed pulses, and installing a new detection system.

Future plans

We will start time-resolved experiment with the setup at UNL. This setup has a very high beam current and will be optimal to work with molecules with low vapor pressure. We will continue with time resolved experiment at SLAC. Over the next year we expect to investigate dissociation and isomerization reactions.

BES-Supported Publications over the last 3 years

J. Yang, V. Makhija, V. Kumarappan, M. Centurion, "Reconstruction of three-dimensional molecular structure from diffraction of laser-aligned molecules" *Struct. Dyn*. **1**, 044101 (2014).

2. S. P. Weathersby, G. Brown, M. Centurion, T. F. Chase, R. Coffee, J. Corbett, J. P. Eichner, J. C. Frisch, A. R. Fry, M. Gühr, N. Hartmann, C. Hast, R. Hettel, R. K. Jobe, E. N. Jongewaard, J. R. Lewandowski, R. K. Li, A. M. Lindenberg, I. Makasyuk, J. E. May, D. McCormick, M. N. Nguyen, A. H. Reid, X. Shen, K. Sokolowski-Tinten, T. Vecchione, S. L. Vetter, J. Wu, J. Yang, H. A. Dürr, and X. J. Wang, "Mega-electron-volt ultrafast electron diffraction at SLAC National Accelerator Laboratory", *Rev. Sci. Inst*. **86**, 073702 (2015).

3. J. Yang, M. Centurion, "Gas phase electron diffraction from laser-aligned molecules" *Struct. Chem*. **26** 1513–20 (2015)

4. J. Yang, J. Beck, C. J. Uiterwaal, M. Centurion, "Imaging of alignment and structural changes of carbon disulfide molecules using ultrafast electron diffraction" *Nature Commun*. **6**, 8172 (2015).

5. M. Centurion, "Ultrafast imaging of isolated molecules with electron diffraction (Topical Review)", *J. Phys. B*. **49**, 062002 (2016).

6. J. Yang, M. Guehr, T. Vecchione, M. S. Robinson, R. Li, N. Hartmann, X. Shen, R. Coffee, J. Corbett, A. Fry, Ke. Gaffney, T. Gorkhover, C. Hast, K. Jobe, I. Makasyuk, A. Reid, J. Robinson, S. Vetter, F. Wang, S. Weathersby, C. Yoneda, M. Centurion, X. Wang, "Diffractive imaging of a rotational wavepacket in nitrogen molecules with femtosecond megaelectronvolt electron pulses" *Nature Commun*. **7**, 11232 (2016).

7. J. Yang, M. Guehr, X. Shen, R. Li, T. Vecchione, R. Coffee, J. Corbett, A. Fry, N. Hartmann, C. Hast, K. Hegazy, K. Jobe, I. Makasyuk, J. Robinson, M. S. Robinson, S. Vetter, S. Weathersby, C. Yoneda, X. Wang, M. Centurion, "Diffractive Imaging of Coherent Nuclear Motion in Isolated Molecules" *Phys. Rev. Lett*. (accepted).

8. J. Yang, M. Guehr, T. Vecchione, M. S. Robinson, R. Li, N. Hartmann, X. Shen, R. Coffee, J. Corbett, A. Fry, Ke. Gaffney, T. Gorkhover, C. Hast, K. Jobe, I. Makasyuk, A. Reid, J. Robinson, S. Vetter, F. Wang, S. Weathersby, C. Yoneda, X. Wang, M. Centurion, "Femtosecond gas phase electron diffraction with MeV electrons" *Faraday Discuss*. (accepted).

Atomic and Molecular Physics in Strong Fields

Shih-I Chu
Department of Chemistry, University of Kansas
Lawrence, Kansas 66045
E-mail: sichu@ku.edu

Program Scope

In this research program, we address the fundamental physics of the interaction of atoms and molecules with intense ultrashort laser fields. The main objectives are to develop new theoretical formalisms and accurate computational methods for *ab initio* nonperturbative investigations of multiphoton quantum dynamics and very high-order nonlinear optical processes of one-, two-, and many-electron quantum systems in intense laser fields, taking into account detailed electronic structure information and many-body electron-correlated effects. Particular attention will be paid to the exploration of the effects of electron correlation on high-harmonic generation (HHG) and multiphoton ionization (MPI) processes, multi-electron response and underlying mechanisms responsible for the strong-field ionization of atoms, and diatomic, and small polyatomic molecules, new time-frequency transform, dynamical origin of near- and below- threshold harmonic generation of atomic and molecular systems in mid-IR laser fields, coherent control of HHG processes for the development of shorter and stronger attosecond laser pulses, etc.

Recent Progress

1. Coherent Phase-Matched VUV Generation by Field-controlled Bound States and Dynamical Origin of Near- and Below-Threshold Harmonic Generation of Atoms in an Intense Mid-IR Laser Field

HHG has been the enabling technology for ultrafast science in the VUV and soft-X-ray spectral regions. Recently, ultrafast sources of below-threshold harmonics, with photon energies below the target ionization potential, have been demonstrated. Such harmonics are critical to the extension of time-resolved photoemission spectroscopy to megahertz repetition rates and to the development of high-average-power VUV sources, because they can be generated with relatively low driving laser intensities ($\sim 1 \times 10^{13}$ W/cm^2). Ultrafast VUV sources of low-order harmonics are also critical tools for studying wave packet dynamics in bound states of atoms and molecules. However, compared to the high-order above-threshold harmonics, which have been extensively studied, little attention has been devoted to the development and characterization of below-threshold harmonic sources. Recently in collaboration with the experimental group led by Dr. Z. Chang in UCF, we extend our *self-interaction-free* time-dependent density functional theory (TDDFT) [1,2] and generalized Floquet formalism [3] and demonstrate a new regime of phase-matched below-threshold harmonics generation, for which the generation and phase matching is enabled only near Stark-shifted resonance structures of the atomic target [4]. The coherent VUV line emission exhibits sub-100 meV linewidth, low divergence and quadratic growth with increasing target density, and can be controlled by the sub-cycle field of a few-cycle driving laser with intensity of only 10^{13} W/cm^2. This work opens the door to the future development of compact, high flux and ultrafast VUV light sources without the need for cavity or nanoplasmonic enhancement. This work has been recently published in Nature Photonics [4].

More recently we have presented an *ab initio* investigation of the below-threshold harmonics (BTHs) of helium atoms in few-cycle IR laser fields by accurately solving the time-dependent Schrödinger equation and Maxwell's equation simultaneously [5]. We find that the enhancement of the BTH can occur only near the resonance structure of He, for which this mechanism is in agreement with the recent experimental study [4]. Moreover, we introduce a new time-frequency method, the *synchrosqueezed transform* (SST) [6], for the accurate analysis of the time-frequency HHG spectrum below the threshold [5].

Most recently, we further perform an *ab initio* quantum study of the near- and below-threshold harmonic generation of cesium (Cs) atoms in an intense 3,600-nm mid-infrared laser field [7]. Combining with the SST transform of the quantum time-frequency spectrum and an extended semiclassical analysis, the roles of multiphoton and multiple rescattering trajectories on the near- and below-threshold harmonic generation processes are clarified. We find that the multiphoton-dominated trajectories only involve the electrons scattered off the higher part of the combined atom-field potential followed by the absorption of many photons in near- and below-threshold regime. Furthermore, only the near-resonant below-threshold harmonic is exclusive to exhibit phase locked features. Our results uncover the dynamical origin of near- and below- threshold harmonics as well as the role of multi-rescattering trajectories to the resonance-enhanced BTH [5,7] for the first time.

2. Enhancement of VUV and EUV Generation by Field-controlled Resonance Structures of Diatomic Molecules

Below- and near-threshold harmonic generation provides a potential approach to achieve a high conversion efficiency of vacuum-ultraviolet and extreme-ultraviolet sources for the advancement of spectroscopy [4]. Most of the current studies in this field are focused on atomic systems. Here, we perform an *ab initio* time-dependent density functional theory study for the nonperturbative treatment of below- and near-threshold harmonic generation of CO and N_2 diatomic molecules subject to short near-infrared laser pulses and aligned parallel to the laser field polarization [8]. We find that with the use of different driving laser pulse shapes, we can control and enhance harmonic generation through the excited-state resonance structures. Depending on the pulse shape, the enhancement can reach five to seven orders of magnitude as compared to the reference sine-squared laser pulse of the same duration.

3. Sub-optical-cycle Transient HHG Dynamics and Ultrafast Spectroscopy in the Attosecond Time Domain

The recent development of attosecond metrology has enabled the real-time experimental observation of ultrafast electron dynamics and transient sub-cycle spectroscopy in atomic and molecular systems. While they are some recent experimental and theoretical studies of subcycle transient absorption, there has been no study of the subcycle transient behavior of the harmonic emission. We have recently initiated such a direction by extending the *self-interaction-free* TDDFT [1,2] and the time-dependent generalized pseudospectral (TDGPS) method [1,9] for the first *ab initio* study of the subcycle HHG dynamics of He atoms [1]. We have explored the dynamical behavior of the subcycle HHG for transitions from the excited states to the ground state and found oscillation structures with respect to the time delay between the single extreme ultraviolet (XUV) attosecond pulse (SAP) and near-infrared (NIR) fields. The oscillatory pattern in the photon emission spectra has a period of ~1.3 fs which is half of the NIR laser optical cycle, similar to that recently measured in the experiments on transient absorption of He [10]. We present the photon emission spectra from 1s2p, 1s3p, 1s4p, 1s5p, and 1s6p excited states as functions of the time delay. We explore the subcycle a. c. Stark shift phenomenon in NIR fields and its influence on the photon emission process. Our analysis reveals several novel features of the subcycle HHG dynamics and we identify the mechanisms responsible for the observed peak splitting in the photon emission spectra.

More recently, we have further extended the *subcycle* HHG study to the Ar atoms [11]. We present and analyze the harmonic emission spectra from $3snp_0$, $3p_0ns$, $3p_1nd_1$, $3p_1np_1$, $3p_0nd_0$, $3p_0np_0$, and $3p_0ns$ excited states and the $3p_04p_0-$ virtual state as functions of the time delay. In addition, we explore the subcycle a.c. Stark shift phenomenon in NIR fields and its influence on the harmonic emission process. Our analysis reveals several novel features of the subcycle HHG dynamics and spectra as well as temporal energy level shift.

4. High Precision Study of HHG of H_2^+ in Intense Elliptically and Circularly Polarized Laser Fields

We present an *ab initio* 3D precision calculation and analysis of HHG of H_2^+ subject to intense elliptically polarized laser pulses by means of the TDGPS method in two-center prolate spheroidal coordinates [12]. The calculations are performed for the ground and first excited electronic states of H_2^+ at the equilibrium internuclear

separation R = 2 a.u. as well as for the stretched molecule at R = 7 a.u. The spectral and temporal structures of the HHG signal are explored by means of the wavelet time-frequency analysis. Several novel aspects of ellipticity-dependent dynamical behaviors are uncovered. We found that the production of above-threshold harmonics for nonzero ellipticity is generally reduced, as compared with linearly polarized fields. However, below-threshold harmonics still appear quite strong except when the polarization plane is perpendicular to the molecular axis. Weak even harmonics are detected in the HHG spectra of stretched molecules. This effect can be explained by the broken inversion symmetry due to dynamic localization of the electron density near one of the nuclei. Multiphoton resonance and two-center interference effects are analyzed for the exploration of the quantum origin of the predicted HHG spectral and dynamical behavior [12].

We have also performed an *ab initio study* of the generation of below-threshold *even harmonics* by a stretched H_2^+ molecular ion in intense linearly and circularly polarized laser fields [13]. Even harmonics are detected in the harmonic spectra of stretched molecules, mostly with the internuclear separations of 5 to 9 a.u. Consecutive dynamic localization of the electron density near each of the nuclei is responsible for the broken inversion symmetry, which in turn leads to emission of low-order even harmonics. An intuitive picture of the process is provided by the analysis of the time evolution of the electron density and time-frequency spectra of the dipole acceleration. A clear theoretical explanation of the phenomenon is given within the Floquet formalism. Most recently, we have further explored the *anomalous dependence* of near-threshold harmonics in the H_2^+upon the ellipticity of the driving near-infrared laser field [14]. For these harmonics, the maximum radiation energy corresponds to a non-zero ellipticity of the driving field. Our analysis reveals that the origin of the phenomenon lies in the near-resonant excitation of π-symmetry molecular orbitals. The excited states responsible for the anomalous ellipticity dependence of different near threshold harmonics are identified. The effect is confirmed at the equilibrium internuclear separation R = 2 a.u. as well as for stretched molecules at R = 3 a.u.

5. Coherent Control of the Electron Quantum Paths for the Optimal Generation of Single Ultrashort Attosecond Laser Pulse

We recently report a new mechanism and experimentally realizable approach for the coherent control of the generation of an isolated and ultrashort attosecond (*as*) laser pulse from atoms by means of the optimization of the two-color [15] and three-color [16] laser fields with proper time delays. Optimizing the laser pulse shape allows the control of the electron quantum paths and enables high-harmonic generation from the long- and short-trajectory electrons to be enhanced and split near the cutoff region. Then we further investigated the effect of macroscopic propagation on t he supercontinuum harmonic spectra and the subsequent attosecond-pulse generation [17]. The effects of macroscopic propagation are investigated in near and far field by solving Maxwell's equation. Further we propose an efficient method for the generation of ultrabroadband supercontinuum spectra and isolated ultrashort attosecond laser pulses from He atoms with two-color mid-infrared laser fields [18]. We found that the optimizing two-color mid-IR laser pulse allows the HHG cutoff to be significantly extended, leading to the production of an ultrabroadband supercontinuum. As a result, an isolated 18-attosecond pulse can be generated directly by the superposition of the supercontinuum harmonics.

More recently, we present an efficient high-order-harmonic *optimal control scheme* for the generation of the ultrabroad supercontinuum spectrum and an isolated ultrashort attosecond pulse in gases with a two-color mid-IR laser field [19]. The optimal control scheme is implemented using a derivative-free unconstrained optimization algorithm called NEWUOA (NEW Unconstrained Optimization Algorithm). It is shown that optimally shaped laser waveforms can greatly enhance and extend the HHG plateau and efficiently generate an isolated ultrashort attosecond pulse. Further we present a numerical study for optimization of ultrabroad supercontinuum spectrum by controlling the waveforms of laser fields, with the ultimate goal to generate isolated ultrashort attosecond pulses. Specifically, we extend the NEWUOA for maximization of the supercontinnum power spectrum near HHG cutoff. It is found that optimally shaped *inhomogeneous* two-color mid-infrared laser

fields can greatly enhance and extend the high-order harmonic generation plateau. And the superposition of resulting hydrogen HHG supercontinuum effectively gives rise to a robust isolated 5-as pulse [20].

6. We have completed several invited review articles on the recent development of *self-interaction-free* time dependent density functional theory (TDDFT) for the nonperturbative treatment of atomic and molecular multiphoton processes in intense ultrashort laser fields in the past 2 years [21, 22].

Future Research Plans

In addition to continuing the ongoing researches discussed above, we plan to initiate the following several new project directions: (a) Extension of the exploration of the coherent control and giant enhancement of MPI and HHG driven by intense frequency-comb laser fields [23, 24] to rare gas atoms. (b) Extension of the TDGPS method in momentum space [25, 26] to the study of HHG/ATI processes in intense free electron x-ray laser fields. (c) Development of Bohmian mechanics approach [27, 28] for the exploration of the electron quantum dynamics associated with HHG/MPI processes. (d) Development of nonperturbative methods for the accurate treatment of transient absorption and subcycle HHG dynamics in NIR+ XUV attosecond pulses. (e) Development of the new time-frequency method, the *synchrosqueezing transform* (SST) [6,7], for the exploration of the novel quantum dynamics for below- and near- threshold harmonics of diatomic molecules.

References Cited (* Publications supported by the DOE program in the period of 2013-2016).

*[1] J. Heslar, D. A. Telnov, and S. I. Chu, Phys. Rev. A **89**, 052517 (2014).
[2] S. I. Chu, J. Chem. Phys. **123**, 062207 (2005).
[3] S. I. Chu and D. A. Telnov, Phys. Rep. **390**, 1-131 (2004).
*[4] M. Chini, X. Wang, Y. Cheng, H. Wang, Y. Wu, E. Cunningham, P.-C. Li, J. Heslar, D.A. Telnov, S.I. Chu, and Z. Chang, Nature Photonics **8**, 437 (2014).
*[5] P. C. Li, Y. L. Sheu, C. Laughlin, and S. I. Chu, Phys. Rev. A **90**, 041401(R) (2014).
*[6] Y.L. Sheu, L.Y. Hsu, H.T. Wu, P. C. Li, and S.I. Chu, AIP Advances **4**, 117138 (2014)
*[7] P.-C. Li, Y.L. Sheu, C. Laughlin, and S.I. Chu, Nature Comm. **6**, 7178 (2015).
*[8] J. Heslar, D.A. Telnov, and S.I. Chu, Phys. Rev. A **93**, 063401 (2016).
[9] X. M. Tong and S. I. Chu, Chem. Phys. **217**, 119–130 (1997).
*[10] M. Chini, X. Wang, Y. Cheng, Y. Wu, D. Zhao, D. A. Telnov, S. I. Chu, and Z. Chang, (Nature) Sci. Rep. **3**, 1105 (2013).
*[11] J. Heslar, D.A. Telnov, and S.I. Chu, Phys. Rev. A **91**, 023420 (2015).
*[12] K.N. Avanaki, D.A. Telnov, and S. I. Chu, Phys. Rev. A **90**, 033425 (2014).
*[13] K.N. Avanaki, D.A. Telnov, H.Z. Jooya, and S.I. Chu, Phys. Rev. A **92**, 063811 (2015).
*[14] K.N. Avanaki, D.A. Telnov, and S.I. Chu, J. Phys. B **49**, 114002 (2016).
[15] I. L. Liu, P.-C. Li, and S.I. Chu, Phys. Rev. A **84**, 033414 (2011).
[16] P. C. Li, I. L. Liu, and S.I. Chu, Opt. Express **19**, 23857 (2011).
[17] P. C. Li and S.I. Chu, Phys. Rev. A **86**, 013411 (2012).
*[18] P. C. Li, C. Laughlin, and S. I. Chu, Phys. Rev. A**89**, 023431 (2014).
*[19] Y. Chou, P.-C. Li, T.S. Ho, and S.I. Chu, Phys. Rev. A **91**, 063408 (2015).
*[20] Y. Chou, P.-C. Li, T.S. Ho, and S.I. Chu, Phys. Rev. A **92**, 023423 (2015).
*[21] J. Heslar, D. A. Telnov, and S. I. Chu, in *Concepts and Methods in Modern Theoretical Chemistry: Statistical Mechanics,* Volume 2, edited by S.K. Ghosh and P.K. Chattaraj (Taylor & Francis Inc., Bosa Roca, USA, 2013), pp. 37-55.
*[22] J. Heslar, D.A. Telnov, and S. I. Chu, Chinese J. Phys. **52**, 578 (2014).
*[23] D. Zhao, F. l. Li, and S.I. Chu, Phys. Rev. A **87**, 043407 (2013).
*[24] D. Zhao, F. l. Li, and S. I. Chu, J. Phys. B: At. Mol. Opt. Phys. **46**, 145403 (2013).
[25] Z. Y. Zhou and S. I. Chu, Phys. Rev. A **83**, 013405 (2011).
*[26] Z. Y. Zhou and S. I. Chu, Phys. Rev. A **87**, 023407 (2013).
*[27] H.Z. Jooya, D.A. Telnov, P. C. Li, and S. I. Chu, Phys. Rev. A **91**, 063412 (2015).
*[28] H.Z. Jooya, P.-C. Li, S.-L. Liao, and S.I. Chu, Phys. Lett. A **380**, 316 (2016).

Optical Two-Dimensional Spectroscopy of Disordered Semiconductor Quantum Wells and Quantum Dots

Steven T. Cundiff
Department of Physics, University of Michigan, Ann Arbor, MI 48109
cundiff@umich.edu

September 13, 2016

Program Scope: The goal of this program has been to implement optical 2-dimensional coherent spectroscopy and apply it to electronic excitations, including excitons, in semiconductors. Specifically of interest are epitaxially grown quantum wells that exhibit disorder due to well width fluctuations and quantum dots. In both cases, 2-D spectroscopy provides information regarding coupling among excitonic localization sites.

Progress: In the last year, a significant fraction of our progress has been on quantum wells, rather than quantum dots, which have been more our focus in recent years. The two main results are 1) providing an understanding of the polarization dependence of the homogeneous linewidth in quantum wells based on using an anharmonic boson model, and 2) using multidimensional spectroscopy to observe spectral diffusion due to exciton migration amongst within localized states due to disorder.

Many-body interactions (MBIs) between electrons and holes, which form bound states known as excitons, are critical to understanding the optical response of semiconductor quantum wells (QWs). Microscopic models have been developed to understand these MBIs. They write the light-matter interaction in terms of fermionic operators for electrons and holes, as in the case of semiconductor Bloch equations. Alternatively, the Hamiltonian can be written in terms of bosonic operators for excitons. While microscopic models are critical for the theoretical understanding of exciton physics, they are computationally intensive to implement. Consequently, a few-level model of excitons is often used to interpret experimental results and gain physical understanding of MBIs. One approach treats an exciton as a two-level system, which ignores their bosonic nature. A complimentary treatment of MBIs in excitons is inspired by their bosonic nature at low excitation densities. Our results shows that the latter approach explains some previous experimental results.

One enduring puzzle from early four-wave mixing (FWM) experiments on quantum wells is the dependence of signal decay rate on the polarization of the excitation pulses. In the 1990s, it was observed that the FWM signal decays faster for cross-linearly polarized pulses than for co-circularly or co-linearly polarized pulses. A satisfactory explanation of this observation is lacking although the contribution of disorder-mediated coupling, excitation-induced dephasing (EID) and unbound two-exciton states to the FWM signal have been proposed as explanations. Specifically, these models cannot reproduce the correct FWM signal phase, as observed in two-dimensional coherent spectroscopy (2DCS) and attributed to excitation-induced shift (EIS). The inadequacies of previous models can be partially attributed to the limitations of one-dimensional FWM experiments with respect to unraveling MBIs. We use 2DCS, which is a powerful technique to study coherent dynamics in semiconductors due to its ability to separate signals from different quantum pathways, to address this limitation.

We show that the polarization dependent decay rate and phase are direct consequences of the bosonic nature of excitons. Although these observations have been *separately* discussed previously, a self-consistent and physical explanation for both the observations has not been presented. Important physical insight into exciton-exciton interactions is gained by modeling excitons as interacting bosons to interpret experimental observations. We find that the interference between multiple pathways that contribute to the FWM signal

result in different decay rates of the FWM signal and excitonic coherences. This finding is used to show that the linewidth for cross-linearly-polarized excitation pulses can be *predicted* from the co-circularly-polarized results using this model.

The result for the co-circular polarization scheme is simpler to interpret because the biexciton state does not contribute to the signal. An absolute value 2D spectrum for the co-circular polarization scheme is shown in Fig. 1(a), which has a single peak labeled P1. For a system dominated by inhomogeneous broadening, the diagonal and cross-diagonal widths of the peak indicate the inhomogeneous and homogeneous linewidths, respectively. Figure 1(c) shows the real part of the spectrum; the signal phase is obtained through a complimentary pump-probe experiment. The peak in Fig. 1(c) has a dispersive lineshape, which has been previously attributed to EIS.

We calculate the FWM signal by analytically solving the density matrix perturbatively up to third order in the excitation field for delta-function pulses in time. The parameters are quantified using a nonlinear fitting procedure. We simulate 2D spectra and then take slices through the peak in the real part and absolute value spectra of both the experiment and simulation. The simulated slices are then fit to the experimental ones to obtain the parameter values. The simulated absolute value and real part spectra, using the best-fit parameter values, are shown in Figs. 1(b) and 1(d), respectively. We obtain an excellent match between the measured and simulated spectra. Based on the fits, we conclude that EIS is a more dominant effect compared to EID. The measured dephasing rate is nearly a factor of two different than that obtained by fitting the diagonal and cross-diagonal slices of absolute value spectrum to lineshapes obtained by considering exciton as a two-level system.

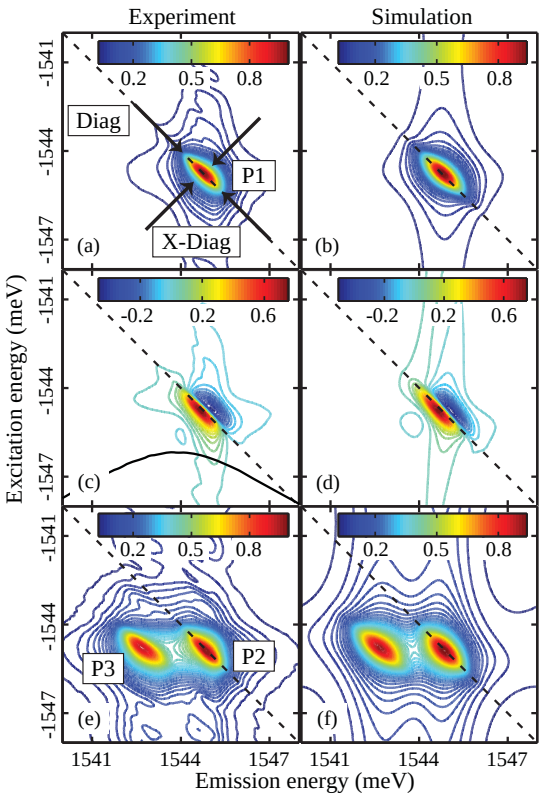

Figure 1: Measured 2D spectra for (a) co-circular (absolute value), (c) co-circular (real part) and (e) cross-linear (absolute value) polarization scheme. The corresponding simulated spectra using best-fit parameter values are shown in (b), (d) and (f), respectively. Equal excitation and emission energy magnitudes are indicated by the dashed line in the spectra. The diagonal (Diag) and cross-diagonal (X-Diag) directions are indicated by arrows in (a). The different peaks are labeled P1, P2 and P3. The excitation spectrum is shown as the solid line in (c).

Figure 1(e) shows the measured absolute value 2D spectrum for cross-linear polarization. We see two distinct peaks, P2 and P3. P2 has the same origin as P1. P3 arises from pathways that involve the biexciton.

An important observation is that peaks P1 and P2 in Figs. 1(a) and 1(e), respectively, have different cross-diagonal widths. While the peak-width along the cross-diagonal for co-circular and co-linear polarization are identical, it is greater for cross-linear polarization. We emphasize that all the parameters that affect the linewidth of peak P2 were fixed during the fitting procedure for the cross-linear polarization scheme; the larger width naturally comes out of the bosonic theory.

The QW exciton resonance can be inhomogeneously broadened due to spatial variations in the well-width and/or alloy concentrations. Phonon-assisted spatial migration can change the exciton energy resulting in spectral diffusion, which can be treated as temporal fluctuations in the exciton resonance energy. In the strong redistribution approximation, there is an equal probability of an increase or decrease in the exciton energy. Thus these energy fluctuations can be considered random and, consequently, can be quantified through the frequency-frequency correlation function (FFCF). It has previously been observed that the strong

redistribution approximation is not valid for sample temperatures below 10 K; the FFCF formalism cannot be used to quantify spectral diffusion in that regime. Here, we will discuss results from experiments performed at higher sample temperatures for which the strong redistribution approximation is valid.

We show that the FFCF can be measured using 2DCS through a non-linear fitting procedure. We demonstrate our method by quantifying the FFCF for heavy hole (HH) excitons in GaAs QWs. Unlike previous methods of calculating the FFCF, this method does not make any assumptions about its decay dynamics. Our measurements demonstrate that the Gauss-Markov approximation, which has been assumed in previous results, is only valid for higher temperatures.

The experiment is performed by measuring the phase and spectrally-resolved FWM signal field as a function of delay τ. A numerical Fourier transform along this delay yields a 2D spectrum. The coherence created by the first two excitation pulses creates a population grating, which exists during delay T. Thus, spectral diffusion is monitored by measuring a series of 2D spectra for different values of wait time, T, from 0.2 to 50 ps. The minimum wait time of 0.2 ps is selected to ensure the correct time-ordering between the excitation pulses.

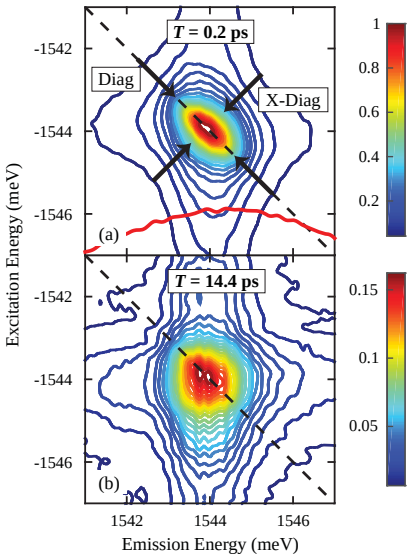

Figure 2: Measured 2D spectra of HH excitons in GaAs QWs for (a) $T = 0.2$ ps and (b) $T = 14.4$ ps with a sample temperature of 30 K. Equal magnitudes of excitation and emission energies are indicated by the dashed diagonal line. The solid red line in (a) denotes the excitation laser spectrum. The diagonal (Diag) and cross-diagonal (X-Diag) directions are indicated by arrows in (a). Note the change in the peak shape in (b) due to spectral diffusion.

Figure 2 shows the effect of spectral diffusion on the measured peak shape in 2DCS by comparing 2D spectra for different wait times for a sample temperature of 30 K. The 2D spectrum in Fig. 2(a) was taken at $T = 0.2$ ps, for which the effect of spectral diffusion is negligible. It shows a single peak that is elongated along the dashed diagonal line due to inhomogeneous broadening of the HH exciton resonance. The 2D spectrum for $T = 14.4$ ps is shown in Fig. 2(b). In addition to a decay in the total signal strength, the peak in this figure is almost equally broadened along the diagonal and cross-diagonal directions. The altered peak shape is due to a change in exciton energy resulting from spectral diffusion during the wait time. The uniform broadening of the 2D peak on either side of the diagonal line indicates that the strong redistribution approximation is valid at this temperature. We use this change in the peak shape in 2D spectra to measure the FFCF and quantify spectral diffusion of excitons.

These measurements allowed us to quantify spectral diffusion of excitons in GaAs QWs by directly measuring the FFCF using 2DCS. We implemented a numerical fitting procedure to make these measurements. To the best of our knowledge, this is the first direct measurement of the FFCF for excitons in semiconductor QWs without making any assumptions about the its time-decay profile. Our results show that the Gauss-Markov approximation is not valid for low sample temperatures contrary to previous studies. Comparisons with other commonly used observables from 2DCS highlights the advantage of using this technique. This procedure can be used to measure the FFCF in any system where it is possible to simulate the 2D spectrum without significant computational cost. It can especially be useful to accurately extract relevant parameters in systems where overlapping peaks in congested spectra make it difficult to separate out the dynamics of individual resonances. In addition to measuring the FFCF more accurately in other systems, similar numerical fitting procedure can be applied more generally to situations where an analytical form of lineshapes do not exist for slices through the 2D spectrum.

Future plans: During the next grant cycle we propose to focus on exploiting the ability of 2DCS to make size resolved measurements on an ensemble sample to study size dependent effects in both self-organized

epitaxially grown quantum dots and colloidal quantum dots. Previously, size dependent phenomena could only be explored by single dot studies, which are challenging to perform. In addition, the process of isolating a single dot may modify the results, either through sample preparation or by choosing to work on an outlier because it is easier to isolate. Furthermore, determining trends, such as size dependence, is challenging because it requires a series of difficult measurement, thus the data sets are often small.

In general, quantum dots show strong inhomogeneous broadening due to size dispersion because the size variation leads to variation in the quantization energy of the electronic states. The inhomogeneous broadening means that linear measurements on ensembles, such as absorption or luminescence, do not measure the properties of individual dots, but rather the properties of the ensemble. For example the width of the linear spectra are completely determined by the size fluctuations, not the linewidth of the individual dots. Furthermore, the individual dots may have multiple transitions, for example exciton and biexciton or fine-structure splitting, that is completely obscured by the inhomogeneity.

Traditional nonlinear spectroscopies, such as photon echoes, can observe the homogeneous linewidth even in the presence of inhomogeneous broadening. In addition, they can give evidence of multiple transitions as beating. However, photon echo measurements give an ensemble average value for the dephasing rate and for any energetic splitting. An ensemble average is problematic if the homogeneous width or an energetic splitting varies within the inhomogeneous distribution. In this case non-exponential decays are observed as well as possibly a beat frequency that varies with delay. While a photon echo signal with a non-exponential decay would indicate that the homogeneous linewidth is not constant, it does not give any information on how it is varying with transition energy, for example it does not even indicate if it is increasing or decreasing with dot size. Indeed this exact issue has been the subject of controversy for the photon echo measurements on CdSe/ZnS colloidal dots.

Two-dimensional coherent spectroscopy overcomes this limitation by correlating absorption and emission frequencies so that an inhomogeneous distribution is spread out along the diagonal. It is then possible to measure the homogeneous width, which is the cross diagonal width, as a function of energy. We have demonstrated this in natural quantum dots. In GaAs quantum wells, we have also observed that the biexciton binding energy varies with emission energy within the inhomogeneous distribution. In this case the inhomogeneity is due to disorder in the quantum well, so it loosely corresponds to the size of a quantum dot. But the important point is the demonstration that 2D spectroscopy can indeed measure a variation in a splitting energy within an inhomogeneous distribution.

We specifically plan to study both epitaxially grown self-organized InAs quantum dots and three types of colloidal quantum dots, CdTe/ZnS dots, PbSe/CdSe dots and Ge dots.

Publication during the the last 3 years from this project:

1. G. Nardin, G. Moody, R. Singh, T.M. Autry, H. Li, F. Morier-Genoud and S.T. Cundiff, "Coherent Excitonic Coupling in an Asymmetric Double InGaAs Quantum Well", Phys. Rev. Lett. **112**, 046402 (2014).
2. G. Moody, I.A. Akimov, H. Li, R. Singh, D.R. Yakovlev G. Karczewski, M. Wiater, T. Wojtowicz, M. Bayer and S.T. Cundiff, "Coherent Coupling of Excitons and Trions in a Photoexcited CdTe/CdMgTe Quantum Well", Phys. Rev. Lett. **112**, 097401 (2014).
3. G. Nardin, T.M. Autry, G. Moody, R. Singh, H. Li and S.T. Cundiff, "Multi-Dimensional Coherent Optical Spectroscopy of Semiconductor Nanostructures: Collinear and Non-collinear Approaches," J. Appl. Phys. **117**, 112804 (2015).
4. R. Singh, G.M. Moody, H. Li, M. Siemens and S.T. Cundiff, "Quantifying Spectral Diffusion by Direct Measurement of the Correlation Function for Excitons in Semiconductor Quantum Wells," J. Opt. Soc. Am. B **33**, C137 (2016).
5. R. Singh, T. Suzuki, T. M. Autry, G. Moody, M. E. Siemens, and S. T. Cundiff, "Polarization Dependent Exciton Linewidth in Semiconductor Quantum Wells a Consequence of Bosonic Nature of Excitons," Phys. Rev. B **94**, 081304(R) (2016).
6. T. Suzuki, R. Singh, M. Bayer, A. Ludwig, A. D. Wieck, and S. T. Cundiff, "Coherent Control of the Exciton/Biexciton System in an InAs Self Assembled Quantum Dot Ensemble," to appear in Phys. Rev. Lett. (2016).

SISGR: Understanding and Controlling Strong-Field Laser Interactions with Polyatomic Molecules

DOE Grant No. DE-SC0002325

Marcos Dantus, dantus@msu.edu
Department of Chemistry and Department of Physics and Astronomy, Michigan State University, East Lansing MI 48824

1. Program Scope

When intense laser fields interact with polyatomic molecules, the energy deposited leads to fragmentation, ionization, and electromagnetic emission. The objective of this project is to determine to what extent these processes can be controlled by modifying the phase and amplitude characteristics of the laser field according to the timescales for electronic, vibrational, and rotational energy transfer. Controlling these processes will lead to order-of-magnitude changes in the outcome from laser-matter interactions, which may be both of fundamental and technical interest. The proposed work is unique because it seeks to combine knowledge from the field of atomic, molecular-optical physics with knowledge from the fields of analytical and organic ion chemistry. This multidisciplinary approach is required to understand to what extent the shape of the field affects the outcome of the laser-molecule interaction and to which extent the products depend on ion stability. The information resulting from the systematic studies will be used to construct a theoretical model that tracks the energy flow in polyatomic molecules following interaction with an ultrafast pulse.

2. Recent Progress

Our interest in electronic and vibrational coherence and the development of laser pulse shaping approaches led us to some 'model' experiments in (a) polyatomic molecules in strong fields (b) electronic coherence in condensed phase, and (c) a new concept in femtosecond laser pulse compression.

(a) Polyatomic molecules in strong (10^{14}-10^{15} W/cm^2) fields:

1. M. Nairat, J. Lantis, V. V. Lozovoy, and M. Dantus, "Order of Magnitude Dissociative Ionization Enhancement Observed for Pulses with High Order Dispersion", J. Phys. Chem. A (Submitted August 2016)

While the interaction of atoms in strong fields is well understood, the same cannot be said about polyatomic molecules. We consider how dissociative ionization of molecules depends on the quality of the femtosecond laser pulses, in particular the presence of third- and fourth-order dispersion (TOD and FOD). We find that high-order dispersion (HOD) unexpectedly results in order-of-magnitude enhanced ion yields, along with factor of three greater kinetic energy release compared to transform-limited (TL) pulses with equal peak intensities. The magnitude of these effects is not caused by increased pulse duration. We evaluate the role of pulse pedestals produced by HOD and other pulse shaping approaches, for a number of molecules, and discuss our findings in terms of processes such as pre-alignment, pre-ionization, and bond softening. We conclude, based on the quasi-symmetric temporal dependence of the observed enhancements, that cascade ionization is likely responsible for the large accumulation of charge prior to the ejection of energetic fragments along the laser polarization axis.

The pedestals arising from HOD seem to be negligible in the autocorrelations shown in Fig. 1. FOD causes a time-symmetric pedestal, while TOD causes a leading (negative) or following (positive) pedestal. The intensity of these pedestals is about 1-2 orders of magnitude smaller than the main pulse and extends for about 200 fs. In strong field laser experiments, where the peak intensity can exceed 1×10^{15} W/cm^2, these pedestals cannot be ignored. Here we investigate the role of these pedestals on the strong laser field ionization and fragmentation of polyatomic molecules.

Results are depicted in logarithmic Spider plots in Fig. 2 for toluene. Based on this plotting scheme, where ion yields are normalized to yields obtained from TL pulses at the given intensity, the mass spectrum using TL pulses is represented as a unity circle. This allows one to determine the relative associated changes in the ion yields when using HOD pulses. Each of the Spider plots represents the changes in the relative yield at certain peak intensity.

We have found similar effects caused by pulses with HOD for smaller molecules such as acetylene, methanol, and acetone. These studies will help understand the transition from atoms and diatomic molecules to processes that are observed in clusters such as cascade ionization. We have started a collaboration with the group of Kalman Varga (Vanderbilt) who is carrying out time dependent DFT calculations using our shaped fields to explore the source of the enhancements observed.

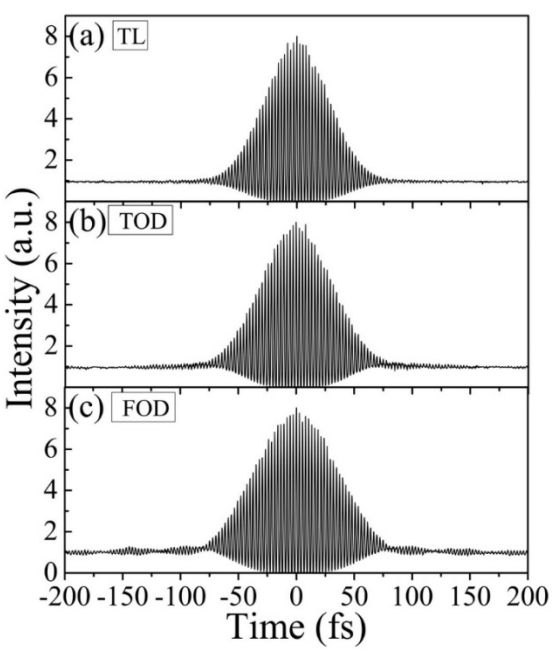

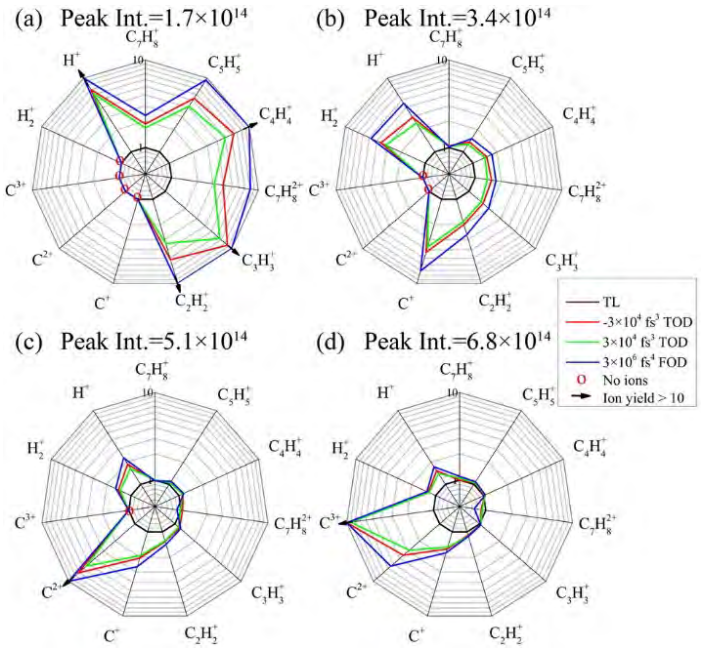

FIG. 1 (left). Interferometric AC for (a) TL, (b) -3 × 10^4 fs^3 TOD, and (c) 3 × 10^6 fs^4 FOD pulses.
FIG. 2 (right). Spider plots on a logarithmic scale for the observed toluene fragment ions using FOD (blue), negative (red), and positive (green) TOD pulses compared to TL (b lack) pulses at (a) 1 .7, (b) 3 .4, (c) 5.1, and (d) 6.8 × 10^{14} W/cm^2 peak intensity.

(b) Electronic coherence in condensed phase:

2. A. Konar, V.V. Lozovoy, and M. Dantus, "Stimulated Emission Enhancement Using Shaped Pulses," J. Phys. Chem. A 120, 2002-2008 (2016).

Controlling stimulated emission is of importance because it depletes excited state population. We performed resonant nonlinear optical spectroscopy measurements using femtosecond pulses shaped by π- or π/2-step phase functions and carried out calculations based on density matrix representation to elucidate the experimental results. In addition, we compared enhancements obtained when using other pulse shaping functions (chirp, third-order dispersion, and a time-delayed probe). The light transmitted through the high optical density solution was dominated by an intense stimulated emission feature that was 14 times greater for shaped pulses than for transform limited pulses. Coherent enhancement depending on the frequency, temporal, and phase characteristics of the shaped pulse is responsible for the experimental observations

The purpose of this study is to determine the optimum characteristics of a femtosecond pulse for enhancing stimulated emission and concomitantly excited state depletion, beyond what can be achieved through properly timed pump-probe pulses or chirped pulses. Here we refer to the third-order polarization resulting from the interaction with a single phase-shaped pulse, and not to the stimulated emission often associated with laser amplification where a pump laser creates population inversion and a seed pulse with very different characteristics is amplified through stimulated emission. We chose phase-step functions because the corresponding time-domain ultrafast pulses are compact and have a temporally long out-of-phase component. Using ±π/2-step phase-functions we explore if phase is of importance beyond the presence of a sharp step. Finally, we compare results from a number of measurements including linear chirp, cubic phase, and pump-probe type excitation.

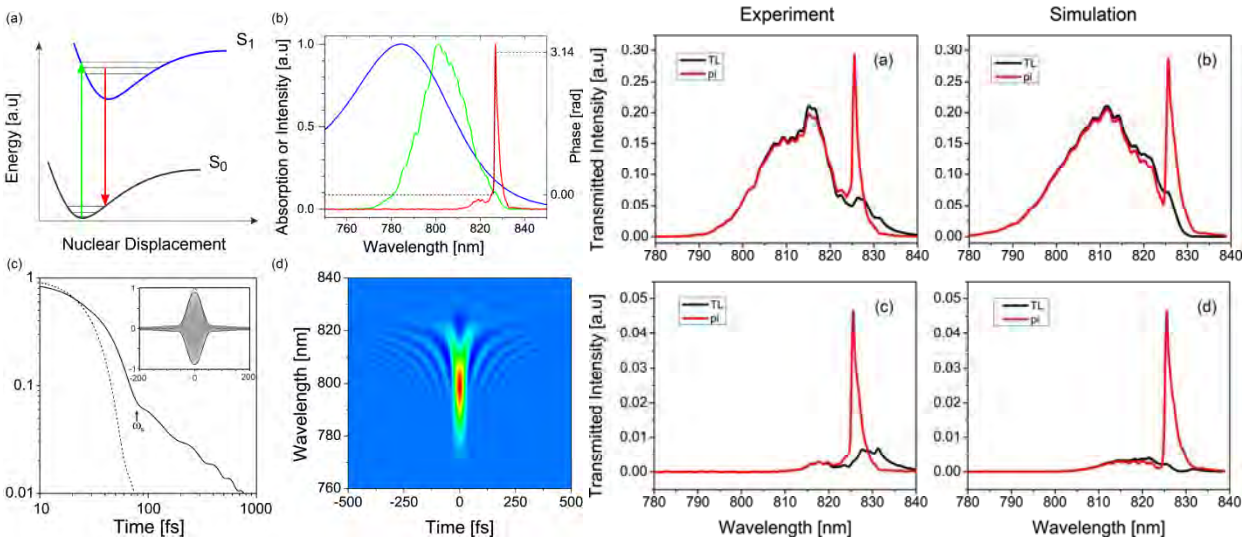

FIG. 3 (left). (a) Jablonski diagram showing the excitation pulse (green) and stimulated emission (red) between the ground and excited states. (b) Normalized absorption spectrum for indocyanine green in methanol (blue), laser excitation spectrum (green) and unfiltered stimulated emission spectrum (red) due to a π phase-step (dashed black) on the excitation spectrum. (c) Double logarithmic plot of the electric field amplitude of a TL pulse (dashed) and a pulse having a π phase step at 826.5 nm on the excitation spectrum (black). Inset shows the real part of the electric field (gray) and electric field amplitude (black) for the phase-modulated pulse along with the electric field amplitude of the TL pulse (dashed). (d) Corresponding Wigner representation of the phase-step shaped pulse.

FIG. 4 (right). Transmitted signals showing a sharp stimulated emission near 827nm. Results are shown for TL (black) and shaped pulses having π-phase step at 825.6 nm (red). Experimental results are shown in panels (a) and (c) for samples having an OD~0.7 and 2.5 respectively. Corresponding numerical simulations are shown in panels (b) and (d).

(c) Re-thinking femtosecond pulse compression:

V. V. Lozovoy, M. Nairat, and M. Dantus, "Binary phase compression of stretched pulses," J. Opt. Soc. Am. B. (Submitted September 2016).

Stretching and compression of ultrafast laser pulses is essential for energy scale up. It is instructive to analyze how different spectral components add together to produce the stretched pulse. We note that there are spectral regions where the phase difference between spectral components equals π. These components are out of phase, or in other words, they have opposite signs because $e^{i\pi} = -1$. For large chirp values, there are many close spectral components of approximately equal amplitude with opposite signs that destructively interfere, therefore, the peak intensity decreases and the pulse is stretched. To compress such a stretched pulse, we propose to modify the spectral phase of the components that are out of phase. To accomplish this we find the frequencies that are out of phase. The frequencies we are looking for have a phase equal to nπ, with n an odd number. For those frequencies, we add π phase value to make them constructively interfere. When n is even we do not change the phase. We plot such a compression binary phase in figure 5a (red line). The 'staircase'-looking line crosses the spectral phase at frequencies where the phase equals to nπ. The dotted red line corresponds to a different presentation of the same (red solid) phase because phase is a cyclic function with period a 2π, and any odd nπ can be replaced with π, any even nπ with 0. Appling this phase compresses the pulse in time domain, as shown in figure 5b. The red line corresponds to the binary phase compressed pulse (chirped and binary phase compressed). When normalized to unit intensity, the TL pulse (black dash line) in figure 5c is very close to the profile of the stretched and binary phase compressed pulse. For this example, the pulse was stretched by only a factor of 10, when plotted in logarithmic scale, figure 5d, the chirped pulse (black line) has 10 times smaller peak intensity than the TL pulse (dash line). The amplitude of the binary phase compressed pulse (red line) is about 0.5 from the maximum, the compressed pulse duration at FWHM is very close to the TL pulse. Because we use pure phase modulation in this example, approximately half of the energy is not lost but spread over very long times. This energy looks like noise beyond the chirped pulse duration in the log-log plot shown in figure 1d. We find cross-phase modulation (XPW) cleans the pulse making it possible to deliver TL pulses with contrast ratios greater than 10 orders of magnitude. This new concept of binary phase stretching and compression, if implemented in a multi-layer optic, would eliminate the need for traditional pulse stretchers and compressors and facilitate the design of high-energy femtosecond laser sources.

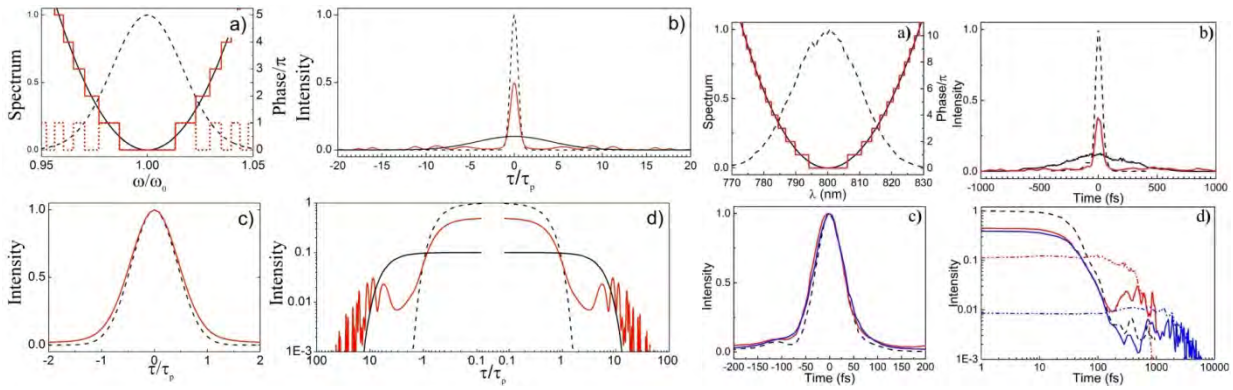

FIG. 5 (left). Principle of binary phase compression. a) (x axis – is relative to carrier frequency) dash – spectrum, black – parabolic phase dispersion to stretch the pulse, red solid and dotted – phase to compensate back to TL duration. b) (x-axis is ratio of time to the duration of the pulse) on y axis are intensity of TL (dash), chirped (black) and red (compressed) pulses. c) Intensities of TL (dash) and compressed (red) pulses normalized on max. d) Plots of the same intensities as on b) but log-log scales to show how energy of laser pulse stretched to the long times.

FIG. 6 (right). Experimental results (a) Spectrum and phases used to stretch the pulse 10 times using a chirp value of 10,000 fs^2 (black) and binary (red) phase added to compress it back to have FWHM as for TL pulse. (b) Cross-correlation functions of TL pulse (dash) 10 times stretched (black) and binary compressed pulse (red) (c) Cross-correlation functions of TL pulse (dash) binary compressed pulse that is originally 10 times stretched (red) and 100 times stretched (blue) normalized on maximum and at short times. (d) long time behavior of TL (black dash), chirped at 10 (red dash) and 100 (blue dash) times, and binary compressed pulses that were originally chirped at 10 times (red) and 100 times (blue) in log-log scales for positive delay times.

3. Future Plans

The proposed research addresses Grand Challenge questions related to quantum control of electrons in matter, and in particular coherent control of excited electronic states, optimal control, and control pushed to higher energy, broader bandwidth and shorter times. We plan to complete our work on electronic coherence observed in dicyclopendadiene, and we have started to get data from our PEPICO instrument. Both of these challenging projects will be completed possible thanks to two outstanding postdocs that joined the research group this August (one funded by DOE the other by our university). Finally, we want to explore the process leading to formation of H_3^+ from methanol and other small molecules. We hope to determine the timescale for this unusual reaction in which multiple bonds are broken and formed. These projects will require pulse-shaping, exploration of molecular isomers and isotopic substitutions, knowledge of electron-impact mass spectrometry, thermochemistry, and ab initio calculations.

4. BES-Supported Publications 9/15/13 to 9/13/16 (one year under NCE) at least three more will be submitted in 2016.

1. A. Konar, V.V. Lozovoy, and M. Dantus, "Solvent Environment Revealed by Positively Chirped Pulses," J. Phys. Chem. Lett. 5, 924–928 (2014)

2. A. Konar, Y. Shu, V.V. Lozovoy, J.E. Jackson, B.G. Levine, and M. Dantus, "Polyatomic Molecules under Intense Femtosecond Laser Irradiation," J. Phys. Chem. A 118, 11433-11450 (2014)

3. A. Konar, V.V. Lozovoy, and M. Dantus, "Electronic dephasing of molecules in solution measured by nonlinear spectral interferometry," J. Spectrosc. Dyn. 4, 26 (2014). The journal was renamed and the paper reassigned to ScienceJet 4 (2015)

4. R. Mittal, R. Glenn, I. Saytashev, V. V. Lozovoy and M. Dantus, "Femtosecond Nanoplasmonic Dephasing of Individual Silver Nanoparticles and Small Clusters," J. Phys. Chem. Lett. 6, 1638–1644 (2015)

5. A. Konar, V.V. Lozovoy, and M. Dantus, "Stimulated Emission Enhancement Using Shaped Pulses," J. Phys. Chem. A 120, 2002-2008 (2016).

PROGRAM TITLE: ATTOSECOND, IMAGING AND ULTRA-FAST X-RAY SCIENCE

PI: Louis F. DiMauro
Co-PI: Pierre Agostini
Co-PI: Terry A. Miller
Department of Physics
The Ohio State University
Columbus, OH 43210
dimauro@mps.ohio-state.edu
agostini@mps.ohio-state.edu
tamiller@chemistry.ohio-state.edu

1.1 PROJECT DESCRIPTION

This grant aims at exploring the realm of ultrafast dynamics using different complementary tools. In one thrust, fundamental aspects of generation and measurement of high harmonic and attosecond pulses are explored and used to access fundamental atomic and molecular processes. A second thrust provides a naturally linked to our attosecond effort via the same underlying strong field physics, laboratory infrastructure and technical approach. The strong field driven "self-imaging" method uses elastic scattering of field-driven electron wave packets as an alternative route for spatial-temporal imaging in the gas phase. In 2012, the OSU and KSU groups demonstrated the viability of this approach for achieving femtosecond timing and picometer spatial resolution. A third scope is the implementation of an AMO science program using the ultra-fast, intense x-rays available at LCLS XFEL. The objective is the study of fundamental atomic processes involving multiple inner-shell ionization, x-ray nonlinear optics and the development of new methods for time-resolved x-ray physics. Our overall objective is advancing these methods as robust tools for imaging and probing electron dynamics thus producing the complete molecular movie.

Progress over the past year includes (1) measurement of the atomic phase near threshold, (2) a precise measure of the complex recombination dipole in the molecular frame, (3) implementation of two source interferometric high harmonic spectroscopy, (4) measurement of x-ray shaping at the LCLS, (5) studies of complex molecules using FABLES imaging and (6) initiated dynamical strong-field imaging studies on pumped fullerenes at OSU and LCLS.

1.2 PROGRESS IN FY16: THE ATTOSECOND PROGRAM

The technical approach of the Ohio State University (OSU) group is the use of long wavelength ($\lambda >$ 1 μm) driving lasers for harmonic and attosecond generation, and imaging. Through support of this program, the long wavelength approach has been successful and adopted by many groups world-wide. Our program over the last several years has turned towards using these long wavelength generated harmonics for measurements, ultimately of dynamics. We are interested in addressing two basic questions related to attosecond physics. First, can high harmonic and attosecond spectroscopy extract atomic/molecular structure and second, what is really being measured.

Near threshold & resonant photoionization with attosecond pulses. These investigations have a two-fold purpose. First, they are designed to increase our understanding of light-matter interactions in the XUV. Second, they provide stringent tests on the "real world" limits of an attosecond measurement. One example is the metrological itself, RABBITT and streaking are standard methods for characterizing attosecond trains and isolated pulses, respectively. These methods rely on photoionizing an atom in the presence of a phase-locked, intense reference field, typical the fundamental field itself. In their implementation, it is assumed that the reference field dominates and the effect of the atomic potential on the energy transfer is negligible. However, this approximation should breakdown near-threshold for low energy photoelectrons. In an previous experiment conducted by Robert Jones (UVa), a two order of

magnitude enhancement in the maximum energy transfer was observed when barium atoms were photoionized in a microwave field. Can this low energy behavior be observed with attosecond spectroscopy thus providing guidance to theory in this problematic regime?

In collaboration with Prof. Jones (Virginia), we have conducted a series of RABBITT measurements on argon, neon and helium close to threshold. The "simpleman" semi-classical model would predict that the dressing-field induced sideband amplitude will decrease towards zero as the photon energy approaches threshold. We have studied this behavior by measuring the RABBITT amplitude and phase as a function of energy near threshold. However, there are several technical difficulties associated with this measurement. One major systematic error we encountered in our earlier Wigner delay study was the characterization of the electron spectrometer's transmission function near zero energy. We have now established improved operating conditions in our magnetic bottle electron spectrometer that permits reliable measurements down to ~1 eV. As adopted in our Wigner study, we use pairwise atomic comparison to minimize systematic errors. Most importantly, the measurement is performed using a HHG frequency comb from a mid-infrared driver (1.2-2.2 μm), thus enhancing our sampling frequency.

Our measurements display a clear non-zero amplitude near threshold at variance with the classical interpretation. Instead the study shows that specific, time-resolved information about the effective binding potential through which a photoelectron travels is directly accessible through attosecond streaking or augmented RABBITT experiments. Using the RABBITT approach, we have measured the average and gradient of the effective potential experienced by near threshold photoelectrons in He and Ne during the first 1.4 fs after their birth. In principle, finer details of the long-range part of the potential may be accessible by comparing the changes in these observables as a function of electron energy. Thus, the approach could enable measurements of potential changes due to atomic or molecular ionization, or ultrafast structural rearrangement in molecules. A paper is in preparation for publication.

Harmonic spectroscopy: a precise measure of the complex recombination dipole in the molecular frame. In 2004 the NRC group proposed that high-order harmonics generation (HHG) could be used to reconstruct the Highest Occupied Molecular Orbital (HOMO) of nitrogen using a tomographic procedure [1]. In that paper, the titanium-sapphire driven HHG intensity from aligned nitrogen was monitored by changing the *alignment angle* in the molecular frame. On the contrary, the HHG phase was not measured but derived from the plane-wave approximation dipole moment. In 2010, Saclay group of Pascal Salieres reported HHG group delay measurements for ten different *alignment angles* using the RABBITT method at 0.8 μm [2]. Later, it was shown that these results strongly depend on the driving laser intensity because of the contribution of both HOMO and HOMO-1. At 0.8 μm, ionization is not very deep into the tunneling regime and other multiphoton effects including Raman stimulated vibrational levels population contribute. Furthermore, the comb density is low and not so many points are sampled. All of these factors make it very difficult to predict the phase of the attosecond emission.

In our N_2 experiment, the HHG process is driven by 1.3 and 2 μm pulses while 0.8 μm pulses are used to implement a 4-kick transient stacker enabling a high degree of molecular alignment. We measure the HHG intensity and group delay as a function of alignment angle using the RABBITT method. We take advantage of the long driving wavelength to investigate the HOMO recombination dipole moment with high spectral density over a 50 eV bandwidth. Our results are compared with simulations based on angle-averaged 3 and 8 channels photo-ionization scattering-wave dipole moments performed in collaboration with Robert Lucchese (TAMU). They show good qualitative agreement for all angular distributions. Our group delay precision measurement reveals the existence of previously unseen angle-resolved sharp spectral features and opens the road to high precision time resolved attosecond dynamic studies in the molecular frame using High Harmonic Spectroscopy. A manuscript has been submitted to Phys. Rev. Lett.

1.3 Progress in FY16: The Molecular Imaging Program

Ultrafast imaging of hydrocarbons and the "construction" of a single-molecule electron wave packet grating. Perhaps unsurprisingly, for the first ultrafast molecular imaging application we focus our attention to the complexity-rich world of organic chemistry, beginning with linear alkanes. Previous theoretical work performed by Prof. C.D. Lin (KSU) revealed that in mid-infrared fields, deep in the tunneling regime, the ionization rate of linear alkanes, e.g. n-butane, strongly peaks along the carbon chain. Therefore, even randomly aligned gases will provide a "signature" similarly to an oriented molecule and thus a good candidate for ultrafast electron diffraction. However, a second important phenomenon, not present for diatomics, exists for linear alkanes: upon recollision, during the "imaging" phase the broadband returning electron wave packet (EWP) diffracts from a periodic arrangement of carbon atoms, resulting in an enhanced interference signal. Similar to the optical diffraction grating, this one-molecule electron grating effect could become an extremely valuable ultrafast imaging asset, as it will not only enhance the molecular image, but also pave the way towards "spectroscopic" studies of the broadband returning EWP itself.

We have recorded ultrafast images of methane, ethane, propane and butane using 3 μm, 80 fs pulses, which establishes the ability of FABLES for imaging complex organic compounds. These studies revealed that as the alkane chain length increases, FABLES is able to measure all C-C bond lengths (C-H are not visible) with < 10 pm resolution, a performance comparable to our previous N_2 work performed.

We have also begun a separate study on the wavelength dependence of fragmentation and ionization tuned around the C-H stretch of linear alkanes. These experiments revealed enhanced fragmentation pathways and increases in overall ionization rates, indicating the efficient energy transfer from the laser directly into molecular degrees of freedom. Although these ultrafast processes are the very ones we want to image, investigation are needed to understand these effects before direct imaging in a pump-probe scheme is implemented.

Ultrafast molecular imaging of fullerenes. Fullerenes such as C_{60} are an extremely interesting class of candidates for ultrafast molecular imaging. On one hand, despite their large sizes they possess a high degree of symmetry and are often referred to as "superatoms", greatly simplifying the diffraction pattern and analysis. On the other hand, the large number of atoms present in the molecule provides a test of the limits of our theoretical tools based on the independent atom model.

In FY16 we continued our study of ultrafast imaging of C_{60}, with the objective of conducting pump-probe experiments. In particular, we are interested in "seeing" upon visible/UV excitation the (i) various breathing modes of the cage and (ii) dissociation. Progress has been made in three areas. (1) We improved our static imaging capabilities for C_{60} and recorded images at several mid-infrared wavelengths, providing tests of the FABLES method and theoretical models. (2) We began an international collaboration with Prof. Jens Biegert (University of Barcelona, Spain) and Prof. Matthias Kling (Ludwig Maximilian University of Munich, Germany) to perform pump-probe experiments in C_{60} using the 150 kHz mid-infrared laser facility in Barcelona. An initial campaign aimed at seeing the breathing mode of $C_{60}$was conducted in May 2016 and a second run is scheduled in FY17. Finally, our group participated in an LCLS run in July 2016 as part of a multi-institutional international effort aimed at X-ray diffractive imaging of the C_{60} breathing mode pumped by 0.8 μm pulse. The LCLS experiment concluded successfully and the results are currently being analyzed.

1.4 Future Plans

e-2e simulator: Direct double ionization is a paradigm for understanding many-body effects. As part of near term plans, we will use a tunneling simulator to time-resolved double ionization of helium atoms. In the experiment, attosecond pulses will photoionize helium above the one-electron threshold (>24 eV) in the presence of an intense dressing field. The linearly polarized dressing field will quiver the electron in a manner similar to the second step (field-driven EWP) in the rescattering model. In this scenario the

attosecond photoionization replaces tunnel ionization in a strong low-frequency field while the dressing field acts as the driver of the EWP. Subsequent interaction of the EWP with the helium core will promote, among others, the (*e,2e*) process. The requirement is that $3U_p \geq 54$ eV (He^+ ionization potential) and that the dressing field alone does not ionize helium. Simple estimates show that this is only possible with mid-infrared dressing fields. If successful, the tunnel simulator will allow exquisite control over the (*e,2e*) process. We have evaluated the technical feasibility and are currently assembling the apparatus. Initial measurements will start at end of 2016 in collaboration with Robert Jones (UVa) and Ken Schafer (LSU).

Imaging: The goal for FY17 is the application of LIED/FABLES to study ultrafast molecular dynamics using pump-probe geometries. (1) Work will continue on hydrocarbons. Our recent 3 μm static images of butane were captured in ~15 minutes with good S/N which makes a pump-probe measurement feasible. The initial study aims at time-resolving the dissociation of the carbon chains following VIS/UV excitation; (2) extend the hydrocarbon studies to image aromatic compounds (benzene and its derivative); (3) continue the molecular grating effect studies on linear hydrocarbons; (4) continue the work on fullerenes, including a second campaign in Barcelona for visualizing the breathing mode of C_{60}.

LCLS: We had LCLS time in March 2015. We have explored the chemical sensitivity of Auger decay by observing Carbon 1s Auger electrons originating from CO, a simple diatomic molecule as well as from CF_4, a more complicated yet symmetric system. The experiment uses the self-referencing Streaking method proposed by our collaboration (DESY, OSU, Dublin). The data is still under analysis. A second beam time was awarded in July 2016. In this run, x-ray diffraction was used to dynamically image C_{60}. The results are under analysis.

1.5 References Cited

[1] J. Itatani *et al.*, Nature **432**, 867-871 (2004).

[2] S. Haessler et al. Nat Phys **6**, 200-206 (2010).

1.6 Publication Resulting from this Grant from 2014-2016

1. "*Attosecond Pulse Shaping around a Cooper Minimum*", S.B. Schoun, R. Chirla, J. Wheeler, C. Roedig, P. Agostini, L.F. DiMauro, K.J. Schafer, and M.B. Gaarde, Phys. Rev. Lett. **112**, 153001 (2014).
2. "*Atomic delay in helium, neon, argon and krypton*", C. Palatchi, J. Dahlstrom, A. S. Kheifets, I. A. Ivanov, D. M. Canaday, P. Agostini and L. F. DiMauro, J. Phys. B **47**, 245003 (2014).
3. *"Measuring the temporal structure of few-femtosecond free-electron laser X-ray pulses directly in the time domain",* W. Helml *et al.*, Nat. Photonics **8**, 950 (2014).
4. "*Strong-field interactions at long wavelengths*", M. Kremer, C. I. Blaga, A. D. DiChiara, S. B. Schoun, P. Agostini, and L. F. DiMauro, in Attosecond and XUV Physics: Ultrafast Dynamics and Spectroscopy eds. T. Schultz and M. Vrakking (Wiley-VCH Verlay, Weinheim, 2014), Chapter 11.
5. *"Diffraction using laser-driven broadband electron wave packets"*, Junliang Xu, C. I. Blaga, Kaikai Zhang, Yu Hang Lai, C. D. Lin, T. A. Miller, P. Agostini and L. F. DiMauro, Nat. Comm. **5**, 4635 (2014).
6. *"Strong-field and attosecond physics in solids"*, S. Ghimire *et al.*, J. Phys. B **47**, 204030 (2014).
7. *"Time-resolved molecular imaging"*, Junliang Xu, C. I. Blaga, P. Agostini and L. F. DiMauro, J. Phys. B **49**, 112001 (2016).
8. *"Synthesis and characterization of attosecond light vortices in the extreme ultraviolet",* R. Géneaux *et al.,* Nat. Comm. DOI: 10.1038 (2016).
9. *"X-ray pulse shaping at free-electron lasers"*, M. C. Hoffmann *et al.*, Nat. Photonics, submitted.

Extended Numerical Detector Theory and Tunneling Exit Momentum

J. H. Eberly
Department of Physics and Astronomy
University of Rochester, Rochester, NY 14627
eberly@pas.rochester.edu

Introduction

We are interested to understand how very intense laser pulses excite electrons in atoms, with intensities in the range $I \geq 0.1$ PW/cm^2. This is the trigger for high-field physics effects of recent and current interest, from multi-electron ejection to high-harmonic generation to the emergent area of atto-science. The combination of phase-coherent character and short-time nature of laser pulses creates substantial challenges to theoretical study in this domain. We have listed the challenges and discussed the successes in an invited review [1]. The intensities are high enough to mandate development of non-perturbative approaches and this has led to several partially conflicting and partially overlapping theoretical approaches. I am reporting here early results in a study of electron momenta closely following ionization. This builds on the successes reported previously [2, 3] obtained by application of the so-called SENE method that is described below.

As experimental versatility increases, the need to understand new features emerges. Unexpected consequences of Coulomb effects in tunnel ionization have captured attention. What is prominently missing is agreement about the nature of electron behavior in the near neighborhood of the semi-mythical SFA "tunnel exit", as these quotes from the past 2-4 years make evident [4, 5, 6, 7, 8, 9]:

"It has therefore typically been assumed that the Coulomb correction along the minor axis of polarization is negligible." {Landsman-etal-13}

"... the tunneling time and intial transverse momentum have dominant roles on Coulomb asymmetry." {Li-etal-13}

"The initial longitudinal momentum distribution at the exit of the tunnel is conceptually more difficult to obtain." {Pfeiffer-etal-12}

"... we study the longitudinal momentum spread of the electronic wave packet at the tunnel exit point, a quantity that has raised substantial interest and controversy." {Pfeiffer-etal-12}

"We find a surprisingly sensitive dependence of Coulomb focusing on the initial transverse momentum distribution, i.e., the momentum at the moment of birth of the photoelectron." ... and "... the momentum distribution transverse to the polarization plane has been shown to provide a window into the the interaction of the photoelectron with its parent ion potential." {Shafir-etal-13}

"We confirm that Coulomb effects depend on the recollision parameters, which in turn depend sensitively on the the initial conditions of the tunneled wave packet." {Shafir-etal-13}

"... there is no clear way of calculating the longitudinal momentum spread at the exit point from tunneling models." {Hofmann-etal-13}

"Much effort has been concentrated on exploring the inital longitudinal momentum spread, but it is still controversial." {Sun-etal-14}

This is an issue that has been waiting to be recognized. The origin of the difficulty, or controversy or whatever term is best, was well anticipated in an overview a decade earlier by Ivanov, Spanner and Smirnova. As they said:

... "Identifying the wavepacket dependence on v_x is much harder. The crucial difficulty stems from the fact that the laser field accelerates the electron while it tunnels out. The velocity distribution along the field is changed continuously during tunneling. ... Uncertainty in the moment of tunneling, which is responsible for the uncertainty in the initial velocity, also means that it is virtually impossible to separate the initial velocity distribution from the distortions caused by the electric field during this temporal uncertainty." {Ivanov-etal-05}

Research Summary and in Progress

We have introduced the numerical SENE approach (SENE = TDSE + TDNE) to theoretical analysis of high-field ionization events. SENE results build on our earlier DOE-BES supported studies of momentum distributions arising from high-field ionization under elliptical polarization [2, 3, 11, 12, 13, 14, 15, 16]. The new method combines short-range solutions of the time-dependent Schrödinger equation (TDSE) with long-range solutions of time-dependent Newton equations (TDNE).

The key feature of the approach is our extension and application of the Feuerstein-Thumm idea [17] to make early "virtual" detection of the wave function by a purely numerical recording of its quantum phase. From this quantum record a distribution of electron momenta is easily extracted from the gradient of the wave function's phase at each point on the detector ring, as shown in the left panel of Fig. 1. Those momenta are used to initiate Newtonian evolution into the far field, where

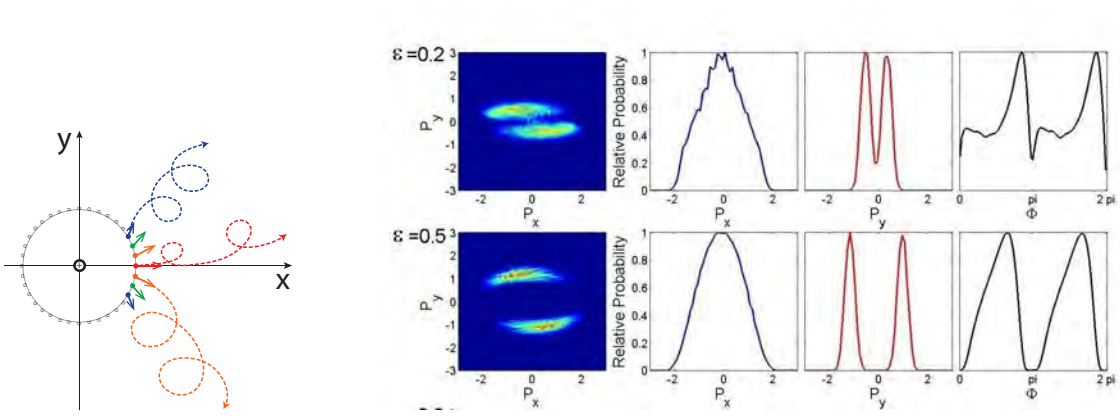

Figure 1: (left) Ionized electron momenta are sketched departing from the numerical detector ring. (right) Their TDNE evolution gives far-field electron momentum distributions consistent with data reported by Pfeiffer, et al. [6].

quantum propagation is numerically impractical. In the right panel we note the asymmetry of the SENE result for $\varepsilon = 0.2$. This is consistent with the similar asymmetry in the experimental record on helium (see Fig. 2b of Pfeiffer, et al. [6]). The numerical detector SENE method has obvious attractive features, but substantial development of it is still ongoing.

To date we have used the SENE method to investigate the discrepant initial longitudinal momentum distributions used to interpret the laboratory results for helium and krypton reported by the Zurich [6] and Beijing [9] groups, respectively. Our approach is to make a wave function calculation for an ionizing electron with the detector ring set near the mythical 'exit point' of SFA tunneling theory. Then SENE momentum analysis will provide what has been missing, namely direct information about the actual longitudinal momentum and its average and variance in that vicinity. The quoted comments in the Introduction show that this is a source of current controversy, and a missing link in systematic comparison of tunneling theory with current experiments.

At the peak intensity of the laser pulse the tunneling radius is about 6 a.u. for He (Zurich) and about 8.0 a.u. for Kr (Beijing). The field strength decreases with ellipticity, so we set the detector rings at 10 a.u. The initial results are shown in Fig. 2 for a pulse model using two carrier envelope phases. The longitudinal momentum standard deviation for Kr is smaller than for He. Our standard deviations of Kr (green dashed line) range from 0.2 to 0.3 a.u., close to the Beijing prediction [9] given by the *ad hoc* backward processing method. In a large range of ellipticity values ($\varepsilon \in [0.3, 0.8]$), our simulation results for helium show good agreement with their backward processing TIPIS method in [6].

The experimental *ad hoc* backward processing method uses the observed far-field momentum distributions to impute what must have been the case initially, near to the tunnel exit. Our *ab initio* momentum variances agree quantitatively with both groups' results, basically because both correspond to similar far-field behaviors. The important difference is obvious - the SENE approach has a predictive aspect not available from backward processing.

The laser peak intensity drops from He to Kr (0.8 PW/cm^2 to 0.12 PW/cm^2), so a smaller average $|P_x|$ value and a smaller $\bar{\sigma}_x$ are predictable results with the SENE method.The SENE approach shows that an outgoing wave packet will be accelerated and stretched in the direction of the laser field. The source of potential conflict of results from different atoms comes from the adiabatic assumption. In an adiabatic tunneling model, the electron cannot gain energy during the tunneling process. Under this assumption, the initial longitudinal momentum distribution is at least not sensitive to the laser intensity change. This assumption is correct for transverse momenta, but may reach misleading conclusions for longitudinal momentum distributions. For example, effects of the temporal oscillations shown in Fig 2 will be missed.

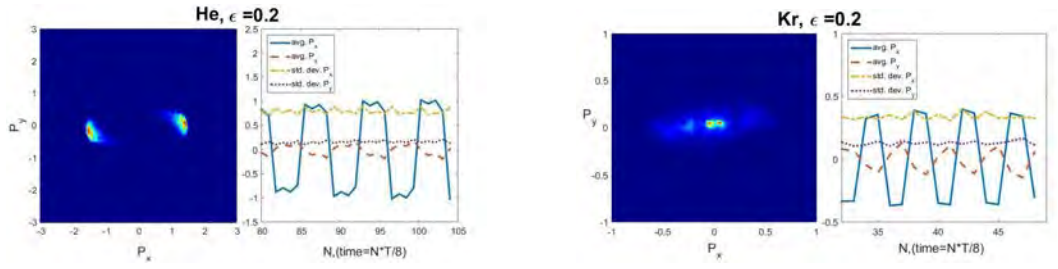

Figure 2: (left) Ionized electron momenta are sketched departing from the numerical detector ring. (right) Their TDNE evolution gives far-field electron momentum distributions consistent with data reported by Pfeiffer, et al. [6].

Publications supported in the two most recent grant periods are marked with * in the listing.**

References

[1] ***W. Becker, X.J. Liu, P.J. Ho and J.H. Eberly, "Theories of Photo-Electron Correlation in Laser-Driven Multiple Atomic Ionization," *Rev. Mod. Phys.* **84**, 1011 (2012). [ISI Highly Cited Paper]

[2] ***X. Wang, J. Tian and J.H. Eberly, "Extended Virtual Detector Theory for Strong-Field Atomic Ionization," *Phys. Rev. Lett.* **110**, 243001 (2013).

[3] ***Justin Tian, Xu Wang and J.H. Eberly, "Extended Breakdown of the Simpleman Approximation," Chin. Opt. Lett. **11**, 010001 (2013).

[4] A.S. Landsman, C. Hoffman, A.N. Pfeiffer, C. Cirelli, and U. Keller, *Phys. Rev. Lett.* **111**, 263001 (2013).

[5] M. Li, Y. Q. Liu, H. Liu, Q. C. Ning, L. B. Fu, J. Liu, Y. K. Deng, C. Y. Wu, L. Y. Peng, and Q. H. Gong, *Phys. Rev. Lett.* **111**, 023006 (2013).

[6] A.N. Pfeiffer, C. Cirelli, A.S. Landsman, M. Smolarski, D. Dimitrovski, L.B. Madsen and U. Keller, *Phys. Rev. Lett.* **109**, 083002 (2012).

[7] D. Shafir, H. Soifer, C. Vozzi, A. S. Johnson, A. Hartung, Z. Dube, D. M. Villeneuve, P. B. Corkum, N. Dudovich, and A. Staudte, *Phys. Rev. Lett.* **111**, 023005 (2013).

[8] C. Hofmann, A. S. Landsman, C. Cirelli, A. N. Pfeiffer, and U. Keller, *J. Phys. B* **46**, 125601 (2013).

[9] X. F. Sun, M. Li, J. Z. Yu, Y. K. Deng, Q. H. Gong, and Y. Q. Liu, *Phys. Rev. A* **89**, 045402 (2014).

[10] M. Y. Ivanov, M. Spanner, and O. Smirnova, *J. Mod. Opt*. **52**, 165 (2005).

[11] *** Xu Wang, Justin Tian and J.H. Eberly, "Angular correlation in strong-field double ionization under circular polarization," *Phys. Rev. Lett.* **110**, (7) 073001 (2013).

[12] ***X. Wang and J.H. Eberly, "Nonadiabatic Theory of Strong-Field Atomic Effects under Elliptical Polarization", *J. Chem. Phys.* **137**, 22A542 (2012).

[13] ***Xu Wang and J.H. Eberly, "Classical theory of high-field atomic ionization using elliptical polarization," *Phys. Rev. A* **86**, 013421 (2012).

[14] Xu Wang and J.H. Eberly, "Elliptical Polarization and Probability of Double Ionization," *Phys. Rev. Lett.* **105**, 083001 (2010).

[15] Xu Wang and J.H. Eberly, "Elliptical Trajectories in Nonsequential Double Ionization," *New J. Phys.* **12**, 093047 (2010).

[16] Xu Wang and J.H. Eberly, "Effects of Elliptical Polarization on Strong-Field Short-Pulse Double Ionization," *Phys. Rev. Lett.* **103**, 103007 (2009).

[17] B. Feuerstein and U. Thumm, in *J. Phys. B* **36**, 707 (2003).

Image Reconstruction Algorithms

Office of Basic Energy Sciences
Division of Chemical Sciences, Geosciences, and Biosciences
Program in Atomic, Molecular, and Optical Sciences

Veit Elser, Department of Physics
PSB 426, Cornell University
Ithaca, NY 14853
(607) 255-2340
ve10@cornell.edu
uuuuuu.lassp.cornell.edu

Program Scope

The many-orders-of-magnitude gains in X-ray brightness achieved by free-electron laser sources such as the LCLS are driving a fundamental review of the data analysis methods in X-ray science. It is not just a question of doing the old things faster and with greater precision, but doing things that previously would have been considered impossible. Our group is working closely with experimental groups at LCLS and elsewhere to develop data analysis tools that exploit the full range of opportunities made possible by the new light sources. We also provide imaging expertise to the groups of Sol Gruner (Cornell, Physics), David Mueller (Cornell, Applied Physics), and Uli Wiesner (Cornell, Materials Science).

Recent Highlights

Sparse data crystallography

This project aims to make protein crystallography feasible for crystals that are so small that in synchrotron data there are no discernible Bragg peaks, so that even establishing the crystal orientation is a challenge. We have adapted the EMC algorithm, originally developed for single-particle imaging and XFEL data, to handle low signal crystal datasets at synchrotrons. Data is collected by the Gruner group, currently in proof-of-principle experiments with known structures such as lysozyme. In the past year we added a second axis for generating rotations of the crystal. The algorithm successfully determined crystal orientations just by imposing consistency of the sparse data frames. About 90% of the detected photons were background (between Bragg peaks). We plan to submit this work for publication by September of this year [9]. Further information about this project is given in Figures 1 and 2.

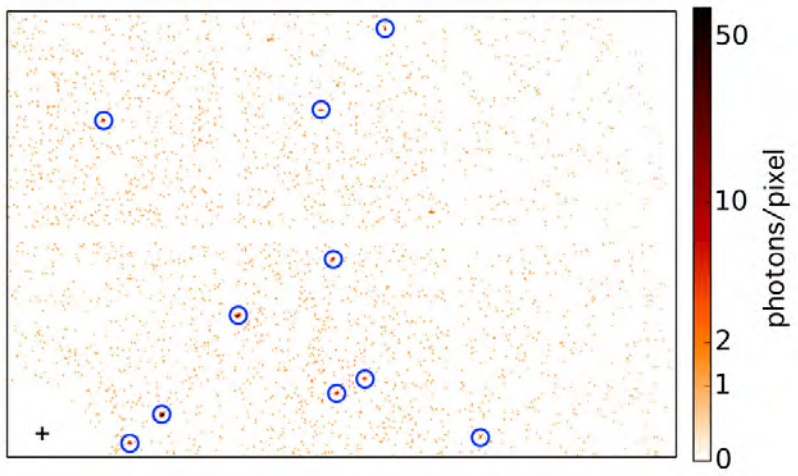

Figure 1: Typical sparse frame of lysozyme data. The incident (unscattered) beam position is marked by the + ; the upper right corner corresponds to 2Å resolution. About 90% of the photons are background, and very few sets (circled) cluster and resemble Bragg peaks.

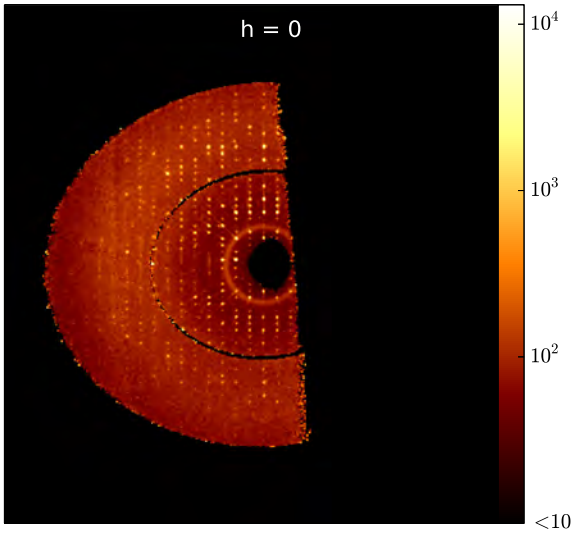

Figure 2: The slice of the lysozyme intensity in the $h = 0$ plane, reconstructed from data such as shown in Figure 1.

Electron ptychography

Over the past several years we have been working with the group of David Mueller to improve and automate tomographic (3D) reconstructions of solid state materials. Motivated by the acquisition of a high dynamic range, fast read-out detector, we recently implemented a ptychographic imaging system. Ptychography is an enhanced mode of scanning-probe transmission microscopy, where contrast is recorded not just by the total number of electrons scattered into the detector for each scan position, but by the 2D diffraction patterns that are produced. High spatial frequency information is captured in these images and can be accurately interpreted because consistency among the diffraction patterns allows for the precise reconstruction of the electron focus, the "probe function". Figures 3 and 4 show reconstruction results for a freely supported WS_2 film that are being readied for publication.

Future Plans

In addition to supporting the single-particle imaging effort at LCLS, we plan to extend the sparse data crystallography project with microcrystals delivered by lipid gels. For the ptychography project, we have simulated how changes in the angular momentum of the electron wavefunction can be used to infer magnetic properties. We hope to apply this principle to $PbTiO_3$ and $SrTiO_3$ superlattices. Most recently we initiated tomographic reconstructions of silica coated micelles for the Wiesner group.

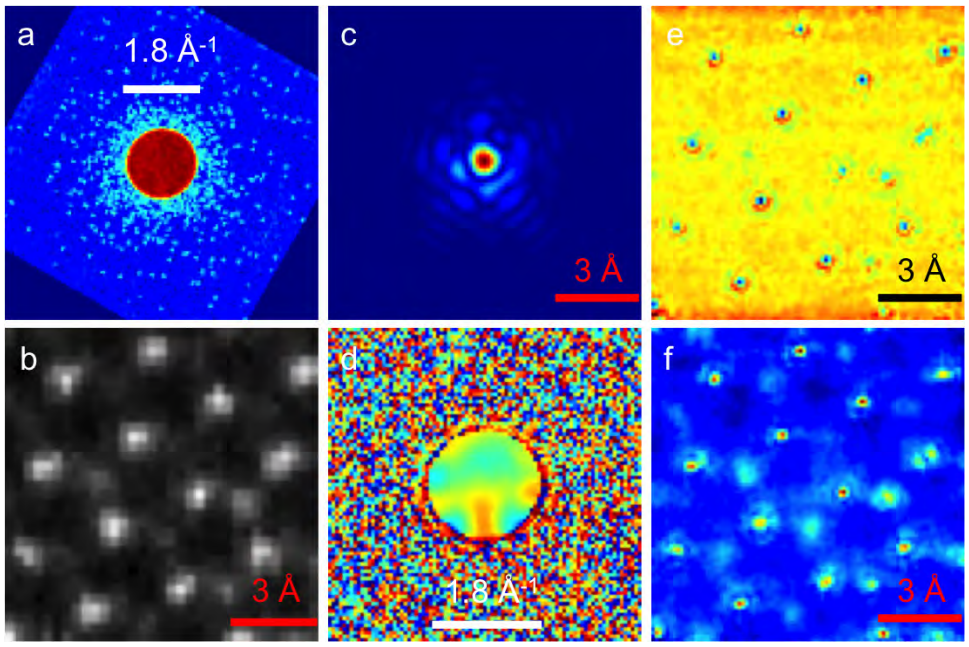

Figure 3: Electron ptychography of a WS_2 film. (a) Typical diffraction pattern. (c) & (d) Reconstructed magnitude and phase of probe. (e) & (f) Magnitude and phase of reconstructed transmission function. Reconstruction (f) shows much better contrast between light and heavy atoms than conventional dark field imaging in panel (b).

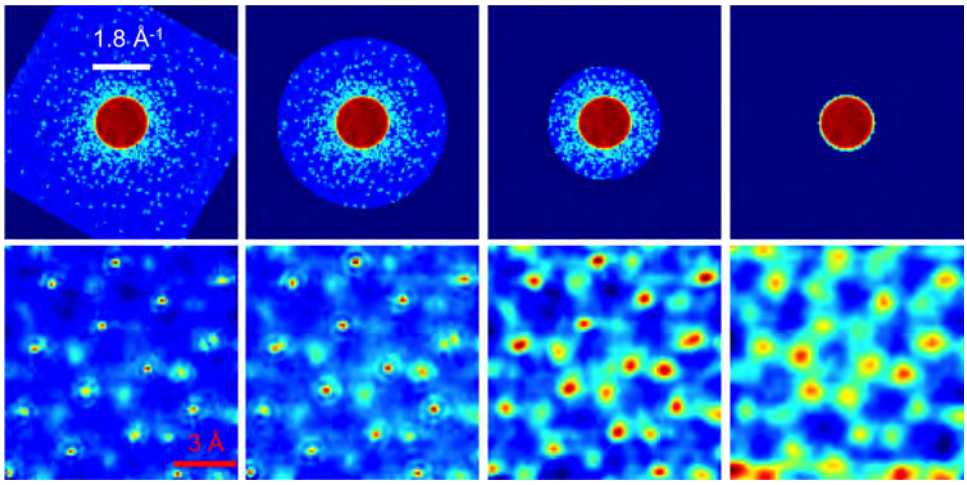

Figure 4: Effect of detector cutoff (top panels, boundary of light-blue regions) on the resolution of ptychographic reconstructions of a WS_2 film (lower panels).

BES-Supported Publications (2014-2016)

[1] K. Ayyer, H.T. Philipp, M.W. Tate, V. Elser & S.M. Gruner, *Real-space x-ray tomographic reconstruction of randomly oriented objects with sparse data frames*, Opt. Express **22**, 2403-2413 (2014).

[2] R. Hovden *et al.*, *Breaking the Crowther limit: Combining depth-sectioning and tilt tomography for high-resolution, wide-field 3D reconstructions*, Ultramicroscopy **140**, 26-31 (2014).

[3] K. Ayyer, H.T. Philipp, M.W. Tate, J.L. Wierman, V. Elser & S.M. Gruner, *Determination of crystallographic intensities from sparse data*, IUCrJ **2**, 29-34 (2015).

[4] A. Aquila *et al.*, *The linac coherent light source single particle imaging road map*, Structural Dynamics **2**, 041701 (2015).

[5] J.L. Wierman, T.-Y. Lan, M.W. Tate, H.T. Philipp, V. Elser & S.M. Gruner, *Protein crystal structure from non-oriented, single-axis sparse x-ray data*, IUCrJ **3**, 43-50 (2016).

[6] A. Munke *et al.*, *Coherent diffraction of single Rice Dwarf virus particles using hard x-rays at the Linac Coherent Light Source*, Scientific Data **3**, (2016).

[7] B.D.A. Levin *et al.*, *Nanomaterial datasets to advance tomography in scanning transmission electron microscopy*, Scientific Data **3**, (2016).

[8] K. Ayyer, T.-Y. Lan, V. Elser & N.D. Loh, *Dragonfly: an implementation of the expand-maximize-compress algorithm for single particle imaging*, J. App. Cryst. **49**, 1320-1335 (2016).

[9] T.-Y. Lan, J.L. Wierman, M.W. Tate, H.T. Philipp, S.M. Gruner & V. Elser, *Solving protein crystal structure from diffraction images with few photons*, to be submitted.

Quantum Correlated Multi-Fragment Reaction Imaging

Department of Energy 2015-2016

James M Feagin
Department of Physics
California State University–Fullerton
Fullerton CA 92834
jfeagin@fullerton.edu

Innovations in few-body science at molecular and nano levels are a critical component of ongoing efforts to establish sustainable environmental and energy resources. The varied research paths taken will require the development of basic science on broad fronts with increasing flexibility to crossover technologies. We thus continue work to extract understanding and quantum control of few-body microscopic systems based on our long-time experience with more conventional studies of correlated electrons and ions.

Given the enormous advances over the past 20 years to our understanding of quantum correlations with photon interferometry, AMO collision science generally is ready to move beyond the one-particle, single-port momentum detection that has dominated collision physics since Rutherford. Nevertheless, our familiar theoretical tools for collision theory need to be upgraded to incorporate these more generalized measurement formalisms and ultimately to give incentive for a new generation of experiments.

Our interest in these topics remains motivated by the recent surge in and success of experiments involving few-body atomic and molecular fragmentation and the detection of all the fragments. In this ending year of this support, we will work to complete two parallel efforts with (i) emphasis on reaction imaging while (ii) pursuing longtime work on quantum correlated collective excitations.

Quantum Imaging

In a recent paper,[1] we have shown how the fully time-independent scattering theory leads to the definition of a classical time outside the microscopic dimensions of the interaction zone and how quantum position variables can be used to define classical momenta. Then time-dependent quantum propagation applies in this far zone. In the case of free motion, this quantum propagation leads to the *imaging theorem* (IT),[3] an aspect we analyzed in detail in another recent paper[2] restricting to field-free detection to equate the asymptotic spatial wavefunction to the quantum scattering amplitude. In a third recent paper,[3] we have generalized the IT to uniform electric and magnetic field extraction and COLTRIMS detection.

It has become widely accepted that the reason we observe a classical world, although the motion of particles is governed by a quantum description, can be attributed to the phenomenon of decoherence. This is the change in the wave function of a quantum system due to interaction with a quantum environment, variously taken to be the ambient surroundings, a measuring apparatus, or a combination of both. One change necessary to achieve a classical status is shown to be the transition from an entangled and delocalized state to an incoherent superposition of probabilities, rather than a coherent superposition of amplitudes. To represent a spatially localized classical particle, the wave function must become extremely narrow so that the probability to detect the particle becomes correspondingly localized. Even though a particle may travel macroscopic distances before detection, it is necessary that the localization due to decohering

---

[1] J. S. Briggs and J. M. Feagin, Phys. Rev. A **90**, 052712 (2014).
[2] J. S. Briggs and J. M. Feagin, J. Phys. B: At. Mol. Opt. Phys. **46**, 025202 (2013).
[3] J. M. Feagin and J. S. Briggs, J. Phys. B: At. Mol. Opt. Phys. **47**, 115202 (2014).

interaction overcomes the natural spreading of the wave function. It is assumed that spatial localization of a wave function is a prerequisite for classical behavior, and this is achieved by environmental decoherence.

The deterministic propagation of the quantum system under the sole influence of its own Hamiltonian is generally considered not to lead to classical behavior. We have been able to demonstrate generally that features of the quantum transition to classical motion appear autonomously from such propagation, including that due to applied external fields and mutual particle interactions. In particular, we have shown in a recent paper[4] that the locus of points of equal quantum probability defines a classical trajectory. Hence classical motion will be inferred at all distances at which particle detection is made in practical experiments. Thus we have demonstrated that aspects of the quantum to classical transition do indeed arise from the undisturbed Schrödinger propagation of the system wave function without coupling to a quantum environment. After propagation to distances which are still on the nanoscale, we show that classical motion is encoded in the wave function itself in that *each and every point* of the wave function at different times are connected by a classical relation between coordinates and momenta. This is a far more powerful statement than Ehrenfest's theorem involving only averages.

The essential ingredient of our proof is simply to unify two well-known aspects of quantum dynamics whose connection previously has not been fully appreciated. The first is that classical motion arises simply as a result of deterministic Schrödinger propagation in that, for large asymptotic times and distances, the quantum propagator can be approximated by its semiclassical form. This form is decided purely by classical mechanics through the classical action function; the techniques are well developed and basic to the whole field of semiclassics and quantum chaos. The second aspect is the IT.

We have combined these two aspects in that we use the results of semiclassical quantum theory to generalize the IT to (nonrelativistic) motion under the influence of arbitrary external laboratory fields and particle interactions. Our generalized IT shows that the spatial wave function of any quantum system of particles propagating over macroscopic distances and times becomes proportional to the initial momentum wave function, *where the position and momentum coordinates are related by classical mechanics.* Most importantly, this implies that the probability to measure a particle at a given position at a certain time is identically equal to the probability that it started with a given momentum at an earlier time and has moved according to a classical trajectory. If an experiment is designed to define a final position *and* momentum the trajectory is unique. If only position is measured then more than one trajectory can contribute to the wave function and give rise to interference, as is well documented with neutron and atom interferometry and beautifully demonstrated recently with a single cold helium atom.[5] Hence, a detection, whether showing interference or not, will infer classical behavior of the quantum system *without any environmental interaction whatsoever,* which would lead to decoherence. In short, an observer would conclude that the motion is classical despite it being governed by the Schrödinger equation. There is no change in the wave function apart from that due to external forces deciding the particles' quantum motion.

The IT and Decoherence

Using known results of semi-classical quantum mechanics we have generalised the IT to describe arbitrary motion of particles emanating from a microscopic reaction zone to a detector at macroscopic distance away. Although the motion is according to the Schrödinger equation, the space variables of the asymptotic wavefunction vary in time according to classical trajectories. Most importantly, the asymptotic behaviour is reached at times and distances which are on a microscopic scale. This result justifies the standard practice of experimentalists to use classical

---

[4] J. S. Briggs and J. M. Feagin, New J. Physics **18**, 033028 (2016).
[5] A. G. Manning, R. I. Khakimov, R. G. Dall, and A. G. Truscott, Nature Physics **11**, 539 (2015).

mechanics to propagate measured position and momentum values back to the reaction zone. It also justifies the interpretation of many aspects of ionisation processes in strong laser fields, e.g. the generation of high harmonics, in terms of classical electron trajectories. However, since the IT provides a wavefunction, at the same time it allows quantum interference patterns to be explained in terms of interfering contributions of classical trajectories. In this way the generalised IT gives a concrete mathematical explanation of the apparent dichotomy of well-defined classical trajectories being associated with a quantum wavefunction.

We have shown that the diagonal elements of the quantum density matrix, in the case where a measurement specifies both vector position and momentum, have a *purely classical form* describing a distribution of classical trajectories. If less than complete information is measured then more than one trajectory may contribute. If the time or spatial resolution is sufficient, then the diagonal elements can show interference structure.

The off-diagonal elements of the quantum density matrix generally contain oscillatory terms which average to zero unless a high-resolution measurement is carried out. Such an elimination of off-diagonal matrix elements is considered the hallmark of decoherence due to interactions *external* to the quantum system and the signature of the transition from quantum to classical. However, the IT is a result of unitary Schrödinger propagation devoid of external influence. Of course, any interaction with the environment will provide the additional changes in the quantum system ascribed to the decoherence phenomenon.

The emergence of classical trajectories from quantum waves of course bears great similarity to the far-field emergence of ray optics from wave optics. Also in that case the inference of ray trajectories or observation of optical interference depends upon the resolution of detection. In particular, the IT relation of the asymptotic space wavefunction to the initial momentum wavefunction is mathematically similar to the Fraunhofer diffraction limit of Fresnel diffraction. Interestingly, the origin of the classical characteristics of the IT are to be found in the wave nature of quantum physics itself. It is the cancelling out of differing oscillatory terms arising from action phase functions which leads mathematically to the stationary-phase approximation which isolates individual classical trajectories. In short, any quantum system propagating from a microscopic region to a macroscopic observation point will exhibit the classical characteristics described here; the quantum world autonomously becomes classical.

Publications

Autonomous Quantum to Classical Transitions and the Generalized Imaging Theorem, J. S. Briggs and J. M. Feagin, New J. Physics **18**, 033028 (2016).

Scattering Theory, Multi-Particle Detection and Time, J. S. Briggs and J. M. Feagin, Phys. Rev. A **90**, 052712 (2014).

Reaction Imaging in Uniform Electric and Magnetic Fields, J. M. Feagin and J. S. Briggs, J. Phys. B: At. Mol. Opt. Phys. **47**, 115202 (2014).

Momentum and Spatial Imaging of Multi-Fragment Dissociation Reactions, J. S. Briggs and J. M. Feagin, J. Phys. B: At. Mol. Opt. Phys. **46**, 025202 (2013).

Loss of Wavepacket Coherence in Stationary Scattering Experiments, J. M. Feagin and L. Hargreaves, Phys. Rev. A **88**, 032705 (2013).

Vortex Kinematics of a Continuum Electron Pair, J. M. Feagin, J. Phys. B: At. Mol. Opt. Phys. **44**, 011001 (2011).

Electron-Pair Excitations and the Molecular Coulomb Continuum, J. M. Feagin, J. Colgan, A. Huetz, and T. J. Reddish, Phys. Rev. Lett. **103**, 033002 (2009).

Page is intentionally blank.

NONLINEAR X-RAY OPTICS

Matthias Fuchs[1] (PI)**, David Reis**[2] (Co-PI)

[1]*Department of Physics and Astronomy, University of Nebraska - Lincoln, Lincoln, NE 68588, USA*
[2]*Stanford PULSE Institute, SLAC National Accelerator Laboratory, Menlo Park, CA 94025, USA*

Project Scope

The scope of the project is the investigation of fundamental nonlinear X-ray - matter interactions. We are interested in studying the mechanism of coherent *non*-sequential multi-photon nonlinearities at X-ray wavelengths including novel effects and methods to increase their efficiency. In particular, we will investigate the physics of a recently observed unexpected result in two-photon Compton scattering, where the energy of the nonlinearly generated photon is significantly lower than expected.
This is a new project with a start date of 8/1/16.

Future Plans

Novel X-ray free-electron lasers (XFELs) are capable of producing radiation with unprecedented properties. Specifically, their ultrashort coherent X-ray pulses can generate extreme peak intensities where ordinary rules of light-matter interaction may no longer apply and nonlinear processes start to become important. XFELs have made it possible to observe some of the most important coherent *non*-sequential nonlinearities, including X-ray - optical sum frequency generation (SFG), X-ray second harmonic generation (XSHG)[1], two-photon absorption (TPA)[2] and nonlinear two-photon Compton scattering (2PCS)[3]. In particular, the 2PCS experiment has led to unexpected results, namely the observation of a substantial anomalous red shift in the energy of photons generated by nonlinear two-photon X-ray Compton scattering in beryllium. The energy shift is in addition to the predicted nonlinear Compton shift and was neither expected from extrapolations from linear X-ray interactions nor from nonlinear effects at optical wavelengths. Our results suggest a novel nonlinear scattering mechanism that can only be observed at high fields at X-ray wavelengths, where the photon energy is a significant fraction of the electron rest mass (and thus a significant momentum transfer to the electron occurs during the scattering) and where the interaction is not dominated by the quiver motion of the electron in the field (ponderomotive potential) as is usually the case at longer (optical) wavelengths.
The goal of this research project is the investigation of fundamental nonlinear X-ray - matter interactions. As these processes are typically weak, part of this research is the exploration of more efficient nonlinear X-ray processes by studying novel mechanisms including solid-state effects, the assistance of optical radiation and novel phase-matching techniques. These experiments require extremely large X-ray field strengths, such as produced by XFELs. Nonlinear X-ray effects can lead to important applications in many research fields. For example, it could lead to instantaneous plasma diagnostics for materials in extreme conditions, as a method for combining atomic-scale structural sensitivity with chemical specificity, or as a probe of electron dynamics in solids on the attosecond (1 as = 10^{-18} s) time- and Ångstrom (10^{-10} m) length scales. In addition, a detailed understanding of nonlinear X-ray matter interactions is crucial for understanding and extending the limits of structural determination at high intensity such as in serial femto-crystallography. The results could have a profound impact on future light sources such as the LCLS-II.
We will investigate the detailed mechanism of the generation of a single higher-energetic photons through the concerted nonlinear Compton scattering of two identical hard X-ray photons in a solid. Our recent results suggest a previously unobserved scattering process in which the bound state of the interacting electron plays an important role, despite the fact that the photon energy is significantly above any atomic resonances. If our proposed mechanism can be confirmed, there is the possibility to significantly increase

the yield through phase matching. In this mechanism, the phase-matching condition can be fulfilled over a broad angular and energy range, where the energy of the emitted photon for a given angle depends on the crystal orientation. We will explore the details of phase-matching in nonlinear Compton scattering and potential applications for this novel mechanism, namely atomic-scale structural determination with simultaneous chemical specificity. Furthermore, we will investigate novel nonlinearities based on collective solid-state effects that have the potential for significantly higher efficiencies. First, using X-ray – optical sum frequency generation, we will investigate the microscopic details of nonperturbative generation of higher-order harmonic emission of a strong near infrared laser beam. Second, we will investigate this collective solid-state nonlinearity as a source of higher-order X-ray effects, such as third-harmonic generation, self-phase modulation and self-focusing. Third, we will explore this nonlinearity for the generation of second X-ray harmonic with a significantly increased efficiency by using an optical beam as assistance.
If one can find a robust X-ray nonlinearity to exploit, the potential applications are numerous spanning from atomic physics, chemistry, materials science, to plasma physics and other disciplines.

BES-Supported Publications

[1] Shwartz, S., Fuchs, M., Hastings, J. B *et. al.* X-Ray Second Harmonic Generation. *Phys. Rev. Lett.* **112**, 163901 (2014).

[2] Ghimire, S., Fuchs, M., Hastings, J., *et al.* Nonsequential Two-photon Absorption from the K-shell in Solid Zirconium. *Phys.Rev. A, accepted*

[3] Fuchs, M., Trigo, M., Chen, J. *et. al.* Anomalous nonlinear X-ray Compton scattering. *Nat Phys* **11**, 964-970 (2015).

Studies of Autoionizing States Relevant to Dielectronic Recombination

T.F. Gallagher
Department of Physics
University of Virginia
P.O. Box 400714
Charlottesville, VA 22904-4714
tfg@virginia.edu

At its outset this research program was focused on using laser spectroscopy to explore the properties of doubly excited autoionizing states of atoms, with the goal of providing a better understanding of the inverse process, dielectronic recombination (DR). DR is the recombination of an ion and an electron via an intermediate autoionizing state,[1,2] and it is precisely the inverse of the isolated core excitation (ICE) laser technique we have employed. [3,4] DR's is important in that it provides an efficient recombination mechanism for ions and electrons in astrophysical and laboratory plasmas.[5-7] The most important pathway for DR is through the autoionizing Rydberg states converging to the lowest lying excited states of the parent ion. Because Rydberg states are involved, DR rates are profoundly influenced by other charged particle collision processes and any small electric and magnetic fields in the plasma.[2,8-10] Consequently, a major thrust of this program has been understanding how autoionization rates, and thus DR rates, are affected by collisions and external fields. We began to use a microwave field to mimic electron collisions, but the experiments are, in essence, laser photoionization of atoms in the presence of a strong microwave field. An atom in the presence of both a strong microwave field and a visible laser field is quite analogous to an atom in an intense infrared (IR) field and the field of an attosecond pulse train (APT) of xuv pulses, a problem under investigation by many research groups.[11-15] A second similarity between Rydberg atom-microwave and ground state-intense laser experiments is that in both cases not only ionization but the production of atoms in very highly excited states is observed. [16,18] Although our initial interest was the doubly excited Rydberg states, bound Rydberg states are also of interest. From the energy intervals between the bound high angular momentum states of an alkaline earth atom one can determine the polarizability of its ionic core.[19-21] The polarizability determines the blackbody frequency shift of a trapped ion, and it is the most important frequency shift in an optical clock. [22]

During the past year we have worked on two projects. The first is an experiment in which we excite Li atoms in the presence of a strong microwave field using an amplitude modulated laser field, with the modulation phase locked to the microwave field. This experiment is motivated by analogous experiments done with combined xuv APT and IR fields[11-13] and our experiments in which we excited atoms in a microwave field phase locked to a mode locked laser producing ps pulses[23,24] A significant difference is that in our experiment there was only one ps laser pulse during the microwave pulse, while there were many xuv pulses in the APT during the IR pulse. In both experiments the sign and the amount of energy transfer to the electron produced by the xuv or ps laser pulse was dependent on the phase of the low frequency field at which the laser excitation occurred.[11,13, 23, 24] According to the theoretical analysis accompanying the IR/APT experiment, a single xuv pulse would produce a small phase dependent signal, less than

1% of the total signal. The large magnitude of the observed phase dependent ionization signal, ~30%, is due to the coherent effect of the multiple pulses in the APT.[11] However, an experiment with a single attosecond pulse was not done. In our experiments with a single ps pulse we observed a very small phase dependence, ~0.1%, consistent with the theory.[11] In the present experiment we have introduced the phase coherence by replacing the single ps laser pulse by the multiple pulses of an amplitude modulated laser beam. We produce an 819 nm beam amplitude modulated at 28 GHz by combining the beams from two 819 nm diode lasers with frequencies 28 GHz apart. The 28 GHz beat note between the two 819 nm lasers is detected by a fast photodiode and phase locked to the second harmonic of the 14 GHz microwave oscillator which provides the microwave field in a Fabry-Perot microwave cavity in which the atoms are excited by the laser.

When the laser is tuned above the limit we have observed as large as a 10% modulation in the number of atoms which are recombined into bound states as we vary the phase of the microwave field at which laser excitation occurs. When the laser is tuned below the limit, we observe up to a 10% variation in the number of atoms which are ionized as the phase is varied. In both cases this variation represents a one hundredfold increase in the modulation over that observed with single ps laser pulse excitation, confirming the importance of coherence suggested by the original theoretical work.[11] Further evidence for the importance of quantum mechanical coherence is that we observe the onset of the recombination at a lower field than expected on the basis of a classical model. In contrast to the IR/APT experiments, we are able to see energy transfer to both higher and lower energies.

The experiments described above have all been done in zero static field. When a static field parallel to the microwave field is present we observe a phase dependent signal using an optical field amplitude modulated at the microwave frequency, not its second harmonic. Specifically, we have used a microwave frequency of 16 GHz. With no static field, or a static field perpendicular to the microwave field, we observe no signal, as expected. If the laser is tuned below the zero field ionization limit, as the static field is raised from zero the signal grows from zero to a maximum, then decreases, changing sign at approximately the static field which depresses the classical ionization limit to the energy of the laser tuning.

A significant experimental challenge is keeping the stray electric fields under control, and the higher the microwave frequency the less stringent this requirement becomes. For this reason we have begun to implement a new method of generating the amplitude modulated optical beam. It is based on frequency modulating the laser beam using the same microwave source which generates the microwave field the atoms see. This approach eliminates the need for phase locking and the high frequency photodiode, allowing the use of microwave frequencies up to 40 GHz. We plan to use the two sidebands displaced from the optical carrier by ± the microwave frequency to generate the amplitude modulated beam. Operating the experiment at a microwave frequency of 40 GHz enormously reduces the deleterious effects of small stray electric fields, so we can expect to obtain cleaner results showing more subtle features. As a first experiment we plan to use the frequency modulated optical beam to excite atomic states which are frequency modulated by the microwave field. To our knowledge, this problem, which can be expected to arise when the excitation involves two harmonically related frequencies, has not been investigated.

We have begun experiments with Yb for two reasons. Yb^+ is a clock candidate, [25] and the cold Rydberg states of Yb are candidates for trapping using ICE.[26] For a Yb^+ clock blackbody radiation makes the Yb^+ polarizability critical. As part of a program to determine the polarizability of Yb^+, we have made microwave resonance measurements of the intervals of Yb 6snℓ Rydberg states. Specifically, we have observed the 6sns-6s(n+1)s, 6snd-6s(n+1)d, 6sns-6s(n-1)d, and 6snd-6s(n-3)g two photon transitions. Where they overlap our measurements agree with previous measurements.[28] We plan to use the quantum defects of the 6snd, 6sng, and 6snh states to extract the Yb^+ polarizability. Unfortunately, the 6snd series is perturbed, albeit weakly, by a doubly excited state lying between the 6s26 d and 6s27d states. To characterize the 6snd series we have made a quantum defect theory analysis of the 6snd energies as determined from the 6snd-6s(n+1)d and 6sns-6s(n-2)d intervals and forced autoionization spectra. We take advantage of the fact that the 6sns series is not perturbed in this energy range. As a consistency check we have made lifetime measurements of the 6snd states, which are consistent with our analysis based on the microwave intervals and forced autoionization spectra. Once we have prepared a report of the work on the perturbed 6snd series we shall measure the 6snd-6snh intervals and carry out the core polarization analysis. We then plan to conduct ICE of the Yb 6snℓ states.

References

1. A. Burgess, Astrophys. J. **139**, 776 (1964).
2. A. Burgess and H. P. Summers, Astrophysical Journal **157**, 1007 (1969).
3. W. E. Cooke, T. F. Gallagher, S. A. Edelstein, and R. M. Hill, Phys. Rev. Lett. **40**, 178 (1978).
4. N. H. Tran, P. Pillet, R. Kachru, and T. F. Gallagher, Phys. Rev. Lett. **29**, 2640 (1984).
5. A.L. Merts, R.D. Cowan, and N.H. Magee, Jr., Los Alamos Report No. LA-62200-MS (1976).
6. S. B. Kraemer, G. J. Ferland, and J. R. Gabel, Astrophys. J. **604** 556 (2004).
7. N. R. Badnell, M. G. O'Mullane, H. P. Summers, Z. Altun, M. A. Bautista, J. Colgan, T. W. Gorczyca, D. M. Mitnik, M. S. Pindzola, and O. Zatsarinny, Astronomy and Astrophysics, **406**, 1151 (2003).
8. V. L. Jacobs, J. L. Davis, and P. C. Kepple, Phys. Rev. Lett. **37**, 1390 (1976).
9. F. Robicheaux and M. S. Pindzola, Phys. Rev. Lett. **79**, 2237 (1997).
10. E. S. Shuman, Y. Wang, and T. F. Gallagher, Phys. Rev. A **76**, 031401 (2007).
11. P. Johnsson, R. Lopez-Martens, S. Kazamias, J. Mauritsson, C. Valentin, T. Remetter, K. Varju, M. B. Gaarde, Y. Mairesse, H. Wabnitz, P. Salieres, Ph. Balcou, K. J. Shafer, and A. L'Huillier, Phys. Rev. Lett. **95**, 013001 (2005).
12. P. Ranitovic, X. M. Tong, B. Gramkow, S. De, B. DePaola, K. P. Singh,. W. Cao, M. Magrakelidze, D. Ray, I. Bocharova, H. Mashiko, A. Sandhu, E. Gagnon, M. M. Murnane, H. C. Kapteyn, I. Litvinyuk, and C. L. Cocke, New J. Phys. **12**, 013008 (2010).
13. P. Johnsson, J. Mauritsson, T. Remetter, A. L'Huillier, and K. J. Schafer, Phys. Rev. Lett. **99**, 233001 (2007).
14. X. M. Tong, P. Ranitovic, C. L. Cocke, and N. Toshima, Phys. Rev. A **81**, 021404 (2010).
15. P. Riviere, O. Uhden, U. Saalmann, and J. M. Rost, New J. Phys. **11**, 053011 (2009).
16. T. Nubbemeyer, K. Gorling, A. Saenz, U. Eichmann, and W. Sandner, Phys. Rev. Lett. **101**, 233001 (2008).

17. U. Eichmann, A Saenz, S. Eilzer, T. Nubbemeyer, and W. Sandner, Phys. Rev. Lett. **110**, 203002 (2013).
18. A. Arakelyan and T. F. Gallagher, Phys. Rev. A **89**, 053412 (2014).
19. J. E. Mayer and M. G. Mayer, Phys. Rev. **43**, 605 (1933).
20. J. H. Van Vleck and N. G. Whitelaw, Phys. Rev. **44**, 551 (1933).
21. S. R. Lundeen, in *Advances in Atomic , Molecular, and Optical Physics*, edited by P. Berman and C. Lin (Elsevier Academic Press, San Diego, 2005).
22. C. W. Chou, D. B. hume, J. C. J. Koelmeij, D. J. Wineland, and T. Rosenband, Phys. Rev. Lett. **104**, 070802 (2010).
23. K. R. Overstreet, R. R. Jones, and T. F. Gallagher, Phys. Rev. Lett. **106**, 033002 (2011).
24 K. R. Overstreet, R. R. Jones, and T. F. Gallagher, Phys. Rev. A **85**, 055401 (2012).
25. T. Schneider, E. Peik, and C. Tamm, Phys. Rev. Lett. **94**, 230801 (2005).
26. P. Pillet (private communication).
27. H. Maeda, Y. Matsuo, M. Takami, and A. Suzuki, Phys. Rev. A **45**, 1732 (1992).
28. P. Camus, A. Debarre, and C. Morillon, J. Phys. B **13**, 1089 (1980).

Publications 2013-2016

1. E. G. Kim, J. Nunkaew, and T. F. Gallagher, "Detection of Ba 6sng→6snh, 6sni, and 6snk microwave transitions using selective excitation to autoionizing states," Phys. Rev. A **89**, 062503 (2014).
2. J. Nunkaew and T. F. Gallagher, "Microwave spectroscopy of the Ca 4snf→4s(n+1)d, 4sng, 4snh, 4sni, and 4snk transitions," Phys. Rev. A **91**, 042503 (2015).
3. V. Carrat, E. Magnuson, and T. F. Gallagher, "Coherence, ionization, and recombination in a microwave field," , Phys. Rev. A **92**, 063414 (2015).
4. A. Arakelyan and T. F. Gallagher, "Resonant production of high lying states in the microwave ionization of Na," Phys. Rev. A **93**, 013411 (2016).

Experiments in Ultracold Molecules

Phillip L. Gould
Department of Physics U-3046
University of Connecticut
2152 Hillside Road
Storrs, CT 06269-3046
<phillip.gould@uconn.edu>

Program Scope:

The area of ultracold atoms and molecules continues to see tremendous progress. These advances have not only proved beneficial to atomic, molecular and optical (AMO) physics, but they have also impacted a variety of other fields, including condensed-matter physics, plasma physics, fundamental symmetries, chemistry, and quantum information. Molecules have a much richer level structure than atoms, and as a result, are more difficult to cool and manipulate. However, these additional degrees of freedom, which include electronic state, vibration, rotation, electron spin, and nuclear spin, do have their benefits. They span a wide range of energy scales, from the optical to the rf, allowing interactions with a variety of other systems. Furthermore, heteronuclear molecules can exhibit permanent electric dipole moments, whose long-range and anisotropic potentials lead to novel and useful interactions. There are two general techniques for producing cold and ultracold molecules. "Direct" methods, such as buffer gas cooling, electrostatic slowing, and laser cooling, reduce the translational motion of already existing molecules. In contrast, "indirect" methods, such as photoassociation and magnetoassociation, assemble the molecules from already ultracold atoms. Once produced, samples of ultracold molecules can be confined and compressed in various optical, magnetic, and electrostatic traps. The numerous applications of ultracold molecules include: ultracold chemistry and collisions; quantum degenerate molecular gases; quantum computation; simulations of condensed-matter systems; novel quantum phases of dipolar gases; and tests of fundamental symmetries and fundamental constants. In the present grant period, the main thrust of our experimental program has been to coherently produce and manipulate ultracold molecules using pulses of frequency-chirped light on the nanosecond time scale.

Our experiments employ laser diodes to cool and confine Rb atoms in a magneto-optical trap (MOT). Rubidium is the atom of choice for several reasons: 1) its D_2 line (780 nm) and D_1 line (795 nm) are well matched to available diode lasers; 2) it has two naturally occuring isotopes, ^{85}Rb and ^{87}Rb; 3) ^{87}Rb is the most popular atom for BEC studies; and 4) we and others have extensively studied the photoassociative formation of Rb_2 and its state-selective ionization detection. In our experiments, we load a phase-stable MOT with cold atoms from a low-velocity intense source (LVIS). The ultracold molecules are formed by illuminating the ultracold atoms with a sequence of pulses of frequency-chirped light. These pulses are as short as 15 ns FWHM and the chirp rates as fast as 2 GHz in 38 ns. The ground-state Rb_2 molecules thus formed are detected by resonance-enhanced multiphoton ionization (REMPI) with a tunable pulsed dye laser.

Time-of-flight (TOF) mass spectrometry is used to distinguish the resulting molecular ions from background atomic ions.

Recent Progress:

We have made significant progress in several areas: quantum simulations of chirped photoassociation on various time scales and with shaped frequency chirps; enhanced formation of ground-state molecules using short pulses and fast shaped chirps; and production of intensity pulses and frequency chirps on faster time scales using intensity and phase modulators in conjunction with with a double-pass tapered amplifier.

In order to understand the dependence on chirp parameters, we continue to collaborate with Shimshon Kallush at ORT Braude and Ronnie Kosloff at Hebrew University (both in Israel), on quantum simulations of the molecule formation process. We include the bound vibrational levels in both the ground-state ($a^3\Sigma_u^+$) and excited-state (0_g^- and 1_g) molecular potentials, as well as the ground-state continuum. For a positive chirp, the pulse first populates various excited states, and these can in turn populate high vibrational levels of the ground state, either by spontaneous (incoherent) or stimulated (coherent) emission. A negative chirp is less efficient because the stimulated emission transition, connecting the excited state to the ground state, becomes resonant first, before the excited state has been populated. By following the temporal evolution of the various state populations, we learn how to optimize the formation rate. The optimum chirp shape begins with a slow chirp, followed by a fast chirp, and ending with a slow chirp. The simulations tell us why this optimum chirp does so well. The slow portions of the chirp occur near the photoassociation and stimulated emission resonances, making these transitions more adiabatic, and therefore more efficient. The fast central portion of the chirp minimizes the time spent in the excited state, thereby minimizing the effects of spontaneous emission.

In the simulations, we have also explored other ways, besides the shape of the chirp, to improve the molecular formation rate. Using higher intensities will certainly help, since the formation rate for this two-photon process is quadratic in intensity. Also using a different vibrational level in the excited state, which has better Franck-Condon overlap with the ground state, is predicted to give at least two orders of magnitude improvement. Finally, using two frequencies, which are synchronously chirped, will allow us to access more deeply bound levels in the ground state.

In the experiment, we use photoassociation with pulses of frequency-chirped light to form ultracold molecules in high vibrational levels of the $a^3\Sigma_u^+$ triplet ground state. The chirp is centered on a 0_g^- photoassociation resonance located 7.8 GHz below the $5S_{1/2}$ + $5P_{3/2}$ asymptote. Molecules ending up in the $a^3\Sigma_u^+$ state are detected by REMPI with a pulsed dye laser at ~600 nm. We use an electo-optical modulator in a fiber loop to produce rapid chirps (2 GHz in 38 ns) and short pulses (15 ns FWHM), and to incorporate shaping into the frequency chirps. The most efficient chirp shape is the one predicted by the simulations, where the beginning and ending portions have a small slope, and the central portion has a large slope.

We have developed the technology to produce even faster chirped pulses and to be able to shape them arbitrarily. We drive fiber-based electro-optic phase and intensity modulators with a 4 GHz arbitrary waveform generator (AWG). Using this setup, we can

produce intensity pulses as short as 0.15 ns and chirps as fast as 5 GHz in 2.5 ns. By incorporating a tapered amplifier in a delayed double-pass geometry, we are able to boost peak powers to several hundred mW.

Future Plans:

This project is not being renewed.

Recent Publications:

"Population Inversion in Hyperfine States of Rb with a Single Nanosecond Chirped Pulse in the Framework of a Four-Level Atom," G. Liu, V. Zakharov, T. Collins, P. Gould, and S.A. Malinovskaya, Phys. Rev. A **89**, 041803(R) (2014).

"Enhancement of Ultracold Molecule Formation by Local Control in the Nanosecond Regime," J.L Carini, S. Kallush, R. Kosloff, and P.L. Gould, New J. Phys. **17**, 025008 (2015).

"Enhancement of Ultracold Molecule Formation Using Shaped Nanosecond Frequency Chirps," J.L Carini, S. Kallush, R. Kosloff, and P.L. Gould, Phys. Rev. Lett. **115**, 173003 (2015).

"Efficient Formation of Ultracold Molecules with Chirped Nanosecond Pulses," J.L Carini, S. Kallush, R. Kosloff, and P.L. Gould, J. Phys. Chem. A **120**, 3032 (2016).

"Nanosecond Pulse Shaping at 780 nm with Fiber-Based Electro-Optical Modulators and a Double-Pass Tapered Amplifier," C.E. Rogers III and P.L. Gould, Opt. Express **24**, 2596 (2016).

Page is intentionally blank.

Physics of Correlated Systems

Chris H. Greene
Department of Physics & Astronomy, Purdue University, West Lafayette, IN 47907-2036
chgreene@purdue.edu

Program Scope

Across virtually all subfields of physics and physical chemistry, major theoretical challenges continue to be posed by systems involving particle interactions that go beyond the simplest mean-field-type behavior, which this project views as correlated systems. In many cases of interest, especially when the states of interest are electronically bound, the correlations between electrons in an atom or small- to modest-sized molecule can be described using the always-improving techniques of quantum chemistry. These often begin from traditional methods such as the Hartree-Fock approach, but build on that simplest idea using multi-configuration superpositions or more sophisticated schemes such as equation-of-motion or coupled-cluster methodologies. The focus of this project is on the development of theoretical techniques capable of describing many different aspects of such correlations, not only between atomic or molecular electrons, but in some cases between electronic and nuclear motion in a molecule which can drive chemical processes. In the absence of such correlations, no chemical reactivity can ever occur. Another class of problems where this project develops non-perturbative theoretical techniques to improve the existing state-of-the-art is in describing the coupling between incompatible motions in the presence of one or more external fields and the internal fields of an electron in an atom or molecule. Our efforts are not aimed only at abstract theoretical development, however, as it is important for us to seek out and encourage experimental tests and realizations of the phenomena being addressed.

The publications listed below [1-18] have been supported primarily by this project.

Recent Progress and Immediate Plans

(i) Few-body collisions from low energy up to chemically interesting temperatures

If one starts from a fairly dilute gas of simple alkali atoms such as rubidium, one normally imagines that it would not be a promising environment for studying chemically reactive processes. In fact, spectroscopic studies of Rydberg states in such an atomic gas have been explored extensively, with a tremendous number of studies since the 1970s. In addition to typical phenomena that are frequently investigated in such a gas, such as atomic energy level shifts and broadening, some evidence has accrued over the years suggesting that occasionally molecular ions such as Rb_2^+ are also formed. The detailed mechanism by which this reactive process occurs had, not been identified, however, until it was tracked down this year in a collaboration with the experimental group of Tilman Pfau in Stuttgart.[3] Specifically, the mechanism that forms these molecular ions turns out, surprisingly, to be triggered by the low energy $^3P^o$ electron-Rb scattering resonance that was shown in 2002 (independently by our group and by the Fabrikant group in Nebraska) to produce "butterfly molecule" potential curves that can accelerate a ground state atom inward towards the nucleus of a Rydberg atom. Such an implosion can drive the diatomic molecule into the autoionization region of the Born-Oppenheimer potential curves, and the resulting autoionization produces the molecular ions that are observed experimentally. Implementation of this theoretical mechanism explains much of

the experimental observations by the Stuttgart group, although it appears to fail at very high principal quantum numbers n>100, for reasons that are still not fully understood and will receive further investigation in the coming year.

During the past year the P.I. has worked with postdoctoral associate Jesus Perez-Rios to build on our 2015 progress in developing a classical Newtonian description of three-body recombination reactions between an ion and two neutral atoms, which can create molecular ions at a high rate. [2,4] Even though most of the focus of our group over the years has concentrated on developing quantum mechanical theoretical ideas and methods, this ion-atom-atom recombination reaction turns out to be reasonably well described classically, even down to temperatures in the millikelvin regime. Our theoretical work based on this classical picture has derived a new threshold law that applies in the intermediate temperature range, i.e. low energy but still high enough to have multiple partial waves contributing. For instance, in the case of the recombination process $Ba^+ + Rb + Rb \rightarrow (BaRb)^+ + Rb$ this classical threshold behavior has been shown to be valid for energies from 0.2 mK up to at least around 1K and probably higher. Experiments performed by the Ulm group of Johannes Denschlag have now confirmed aspects of these theoretical predictions, [2,4] although it is challenging because hybrid ion-neutral traps almost always have a complicated ionic micromotion that needs to be accounted for.

(ii) Atomic and molecular electron dynamics in internal and external fields

A highly useful element of the theorists' toolkit in theoretical atomic and molecular physics in recent decades has been the technique called local frame transformation theory. The past year has seen a breakthrough in this project, driven by postdoctoral associate Panagiotis Giannakeas and in collaboration with Francis Robicheaux, which has developed a reformulation of the frame transformation that removes its largest errors and improves its accuracy by one or more orders of magnitude. An important generalization of the theory to handle nonperturbative external field effects on Rydberg atoms and molecules was developed in the early 1980s, initially by Fano and Harmin, with subsequent extensions by other researchers. The resulting Stark theory of Rydberg states of atoms and molecules was a particularly powerful combination of quantum defect ideas and local coordinate transformations that is now called local frame transformation theory (LFT).

Despite its remarkable successes for a number of atoms and molecules, the LFT has been subjected to increasingly careful and quantitative scrutiny over the years, and a few examples from careful experiment and theory have suggested that it has inaccuracies which limit its usefulness in some regimes of energy and electric field strength. One example is the Stark effect for lithium Rydberg states, studied carefully in 1996 by Bergeman, Metcalf, and coworkers, which found errors in the LFT calculated resonance energies ranging from 50 to a few thousand parts per million. The previous year of funding has resulted in our development of significant improvements to the atomic Stark effect theory and tests of the improved theory have been highly promising, as judged by comparison with both experiment and with large computations that are more exact (but more expensive). The resulting theory [1] is a significant improvement over the original Fano-Harmin quantum treatment, which can be applied now with confidence to a wider class of physical systems and regimes. A subsequent goal is to apply the theory to other problems such as strong-field ionization of an atom or molecule by a powerful short pulse laser.

(iii) Implosive interatomic Coulombic decay processes

Most ICD processes produce a double positively-charged system is formed during the decay, which subsequently undergoes a Coulomb explosion. We have been focusing on a different class where the products formed in the decay experience an attractive interaction. The differences and similarities with the more typical type of explosive ICD process are challenging to calculate, but we have identified the major problems to solve and we expect to be able to complete a first example study of such a system within the coming year.

(iv) Fano resonances and short-pulse phase control

Since a paper co-authored by the P.I. was published in 2013 in *Science*, the result of a project with the Heidelberg group of Thomas Pfeifer and other collaborators, interest has grown in finding the broader implications of that technique for manipulating the absorption and transmission and dispersion properties of a gas. We have initiated some explorations in the direction of trying to find other scenarios in collision physics where Fano lineshapes or even more complicated multichannel lineshapes can be modified through ultrafast phase control. This project will receive significant attention and effort during the next year of funding, which should also advance some of the goals articulated in paper [13] below.

Papers published since 2014 that were supported primarily by this grant.

[1] *Generalized local-frame-transformation theory for excited species in external fields*, P. Giannakeas, Chris H. Greene, and F. Robicheaux, Phys. Rev. A **94**, 013419-1 to -9 (2015).

[2] *Energy Scaling of cold atom-atom-ion three-Body recombination,* A. Kruekow, A.Mohammadi, A. Haerter, J. H. Denschlag, J Pérez-Ríos, and C H Greene, Phys. Rev. Lett. **116**, 193201-1 to -5 (2016).

[3] *Ultracold chemical reactions of a single Rydberg atom in a dense gas*, M. Schlagmueller, T. C. Liebisch, F. Engel, K. S. Kleinbach, F. Boettcher, U. Hermann, K. M. Westphal, A. Gaj, R. Loew, S. Hofferberth, T. Pfau, J Pérez-Ríos, and C H Greene, Phys. Rev. X **6**, 031020-1 to -14 (2016).

[4] *Communication: Classical threshold law for ion-neutral-neutral three-body Recombination,* J Pérez-Ríos and C H Greene, J. Chem. Phys. **143**, 041105-1 to -3 (2015).

[5] *Photoionization microscopy in terms of local-frame-transformation theory*, P. Giannakeas, F. Robicheaux, and Chris H. Greene, Phys. Rev. A **91**, 043424-1 to -14 (2015).

[6] *Comment on "Test of the Stark-effect theory using photoionization microscopy"*, P. Giannakeas, F. Robicheaux, and Chris H. Greene, Phys. Rev. A **91**, 067401-1 to -4 (2015).

[7] *Schwinger-variational-principle theory of collisions in the presence of multiple potentials*, F. Robicheaux, P. Giannakeas, and Chris H. Greene, Phys. Rev. A **92**, 022711-1 to -21 (2015).

[8] *Hyperspherical asymptotics of a system of four charged particles*, K. M. Daily, Few Body Systems, online publication 2015, pp 1-14, DOI 10.1007/s00601-015-0979-7.

[9] *Scattering properties of the $2e^{-}2e^{+}$ polyelectronic system*, K. M. Daily, J. von Stecher, and C. H. Greene, Phys. Rev. A **91**, 012512-1 to -7 (2015).

[10] *Two-photon total annihilation of molecular positronium*, J Pérez-Ríos, S. T. Love, and C. H. Greene, Europhys. Lett. **109**, 63002-1 to -4 (2015).

[11] *Adiabatic hyperspherical analysis of realistic nuclear potentials*, K. M. Daily, A. Kievsky, and C. H. Greene, Few Body Systems 56, 753-759 (2015), DOI 10.1007/s00601-015-1012-x.

[12] *Comparison of classical and quantal calculations of helium three-body recombination,* J Pérez-Ríos, S Ragole, J Wang, and C H Greene, J. Chem. Phys. **140**, 044307-1 to -12 (2014).

[13] *What will it take to observe processes in 'real time'?,* S R Leone, C W McCurdy, J Burgdörfer, L S Cederbaum, Z Chang, N Dudovich, J Feist, C H Greene, M Ivanov, R Kienberger, U Keller, M F Kling, Z-H Loh, T Pfeifer, A N Pfeiffer, R Santra, K Schafer, A Stolow, U Thumm and M J J Vrakking, Nature Photonics **8**, 162-166 (2014).

[14] *Analyzing Feshbach resonances: A ^{6}Li-^{133}Cs case study*, R. Pires, M. Repp, J. Ulmanis, E. D. Kuhnle, and M. Weidemueller, T. G. Tiecke, C H Greene, B P Ruzic, J L Bohn, and E Tiemann Phys. Rev. A 90, 012710-1 to -14 (2014).

[15] *Two-photon total annihilation of molecular positronium*, J Pérez-Ríos, S. T. Love, and C. H. Greene, Europhys. Lett. **109**, 63002-1 to -4 (2015).

[16] *Effective single photon decay mode of positronium via electroweak interactions*, J Pérez-Ríos and S. T. Love, J. Phys. B **48**, 244009-1 to -5 (2015).

[17] *Formation of ultracold (LiRb)-^{7}Li-^{85}Rb molecules in the lowest triplet electronic state by photoassociation and their detection by ionization spectroscopy*, A. Altaf, S. Dutta, J. Lorenz, J Pérez-Ríos, Y. P. Chen, and D. S. Elliott, J. Chem. Phys. **142**, 114310-1 to -9 (2015).

[18] *Rotational relaxation in molecular hydrogen and deuterium: Theory versus acoustic experiments*, S. Montero and J Pérez-Ríos, J. Chem. Phys. **141**, 114301-1 to -13 (2014).

Using Strong Optical Fields to Manipulate and Probe Coherent Molecular Dynamics

Robert R. Jones, Physics Department, University of Virginia
382 McCormick Road, P.O. Box 400714, Charlottesville, VA 22904-4714
bjones@virginia.edu

I. Program Scope

This project focuses on the exploration and control of dynamics in atoms, small molecules, and nano-structures driven by strong laser fields. Our goal is to exploit strong-field processes to implement novel ultrafast techniques for manipulating and probing coherent electronic and nuclear motion within atoms, molecules, and on surfaces. Ultimately, through the application of these methods, we hope to obtain a more complete picture of correlated multi-particle dynamics in molecules and other complex systems.

II. Recent Progress and Results

This project has been on a no-cost extension with only a small amount of residual funding since the end of November 2015. Accordingly, progress has been substantially slowed. During the current funding year we have continued previous work, including: (i) investigation of THz-induced, electron field-emission from nano-structured metals and the accompanying large energy transfer to the ejected electrons in the locally enhanced THz field; and (ii) our collaboration with the DiMauro/Agostini group at OSU, employing an augmented RABITT method to obtain time-resolved information about the effective binding potential experienced by low-energy photo-electrons as they leave their parent ion. In addition, we have begun collaborating with Christoph Hauri and Mostafa Shalaby at the Paul Scherrer Institute, using their extremely intense THz source to explore transient THz-induced alignment and orientation of gases at room temperature and atmospheric pressure.

i) THz-Induced Electron Field Emission from Nano- and Micro-Structured Metal Wires

Due to the wavelength scaling of the pondermotive potential, electrons that are free to move over large distances can attain energies exceeding 100 eV directly from intense single-cycle THz pulses with peak fields approaching 0.5 MV/cm [1,2,c]. Therefore, such pulses might be useful for high-energy streaking of photo-electrons from condensed matter targets, providing a time-resolved probe of electron emission without causing permanent sample damage. In addition, electron emission from a scanning probe tip, induced by non-damaging ultrashort THz pulses, might enable time-resolved electron microscopy. Indeed, THz pulses were recently employed to gate the tunnel current in a STM [3] as well as optical field emission from metal nano-tips [4]. Some applications might also benefit from direct field emission induced by THz pulses alone. Unfortunately, the < 1 MV/cm field strengths available from typical laser-based THz sources are two to three orders of magnitude too small to induce tunneling ionization from bulk metals [5]. However, we and others [6,7] have recently observed THz-induced field-emission from nano- and micro-structured metals by exploiting the substantial field enhancements near the surface of these structures.

We find that we can generate high-energy electrons (> 5 keV) by focusing intense THz pulses with peak field strengths of ~ 400 kV/cm on unbiased nano- and micro-tipped tungsten wires.

These energies exceed, by more than an order of magnitude, those previously produced via field-emission in THz [6], infrared [7] or optical fields [8] alone. Interestingly, despite the significant reduction in the enhanced field expected for blunter tips, the maximum energy transfer we observe for a given THz field differs by only a factor of 2 for wires with tip radii varying by nearly a factor of 50. A manuscript describing our results has been submitted to Nature Communications. In addition, graduate student Sha Li, who led the THz photoemission work, successfully defended her Ph.D. dissertation.

(ii) Probing Atomic Potentials with Near Threshold Attosecond Photoelectrons
In collaboration with the DiMauro/Agostini group at OSU, attosecond pulse trains have been used to photoionize noble gas atoms near threshold in the presence of a moderately intense, infrared dressing laser. As in the standard RABITT technique, which is typically used to reconstruct the field in attosecond pulse trains [9], we monitor the phase of interference modulations in photoelectron sidebands as a function of the delay between the dressing laser and the attosecond pulse train. These sidebands are produced via energy transfer between the dressing field and the photoelectrons produced directly by the XUV harmonic radiation. We add an additional dimension to the measurement by considering the information that can be extracted from the sideband amplitudes, in addition to the phase of the interference modulations. By comparing the amplitudes and phases of the low-energy sidebands for different atoms we can extract time-resolved information regarding the average depth and gradient of the binding potentials experienced by the photoelectrons during the first 1 fs or so following their birth.

During the past year, improved data was obtained at a longer dressing wavelength (1.8 microns), allowing us to reduce the uncertainties in the information that we are able to obtain regarding the effective binding potentials in He and Ne. In principal, a variant of these measurements might provide time-resolved information on changes in an atomic/molecular potential due to an external stimulus. A manuscript describing this work is in preparation.

(iii) Transient Field-Free THz-Induced Molecular Alignment and Orientation
Christoph Hauri's group at PSI has developed a source of very intense few-cycle THz pulses with peak fields approaching 100 MV/cm and central frequencies near 3 THz [10]. This is an extremely interesting strong-field, long-wavelength source. Together, we have been exploring several applications of these pulses to THz-based alignment and orientation [11] of gas-phase molecules at room temperature and at atmospheric pressure. To date, the UVa group has been providing computational support and technical guidance for experiments performed at PSI.

III. Future Plans
Pending grant renewal, we plan to continue our exploration of strong field dynamics in atoms, molecules, and nanostructures. First, we will further characterize the THz-induced field emission from nano-tips (e.g. angular and temporal distributions) as a potential source of short electron bursts for initiating and probing molecular dynamics. In addition, we intend on exploiting the enhanced THz field in the vicinity of micro-tipped wires to manipulate laser-driven tunneling ionization and electron recollisions, and perhaps improve THz-based field-free molecular orientation. Second, we plan to test the improved apparatus at UVa for enabling THz-induced field-free molecular orientation at kHz repetition rates, and will continue our collaboration with the PSI group exploring strong field physics in gas phase molecules in the extreme low-

frequency limit. Third, we will work to improve our experimental capabilities to revisit a problem that we have been studying for several years, namely the coupled dynamics of electrons and nuclei during asymmetric strong-field multi-electron dissociative ionization. Two recent experiments [12,d] have offered conflicting views as to the importance of multi-electron processes during enhanced ionization. We plan to reduce the duration of the laser pulses available from our hollow-core-fiber compressor to < 7 fs to perform 2-color pump probe experiments in an attempt to resolve that conflict.

IV. DOE Sponsored Publications from the Last 3 Years

[a] Sha Li, "Field Ionization and Field Emission with Intense Single-Cycle THz Pulses," Ph.D. Dissertation, Univ. of Virginia (2016).

[b] K. Egodapitiya, Sha Li, and R.R. Jones, "THz Induced Field-Free Orientation of Rotationally Excited Molecules," Physical Review Letters **112**, 103002 (2014).

[c] Sha Li and R.R. Jones, "Ionization of Excited Atoms by Intense Single-Cycle THz Pulses," Physical Review Letters **112**, 143006 (2014).

[d] X. Gong, M. Kunitski, K.J. Betsch, Q. Song, L. Ph. H. Schmidt, T. Jahnke, Nora G. Kling, O. Herrwerth, B. Bergues, A. Senftleben, J. Ullrich, R. Moshammer, G.G. Paulus, I. Ben-Itzhak, M. Lezius, M.F. Kling, H. Zeng, R.R. Jones, and J. Wu, "Multielectron Effects in Strong-field Dissociative Ionization of Molecules," Physical Review A **89**, 043429 (2014).

[e] M. Kubel, Nora G. Kling, K. J. Betsch, N. Camus, A. Kaldun, U. Kleineberg, I. Ben-Itzhak, R.R. Jones, G.G. Paulus, T. Pfeifer, J. Ullrich, R. Moshammer, M.F. Kling, and B. Bergues, "Non-Sequential Double-Ionization of N2 in a Near Single-Cycle Laser Pulse," Physical Review A **88**, 023418 (2013).

V. References

[1] Janos Hebling, Ka-Lo Yeh, Matthias C. Hoffman, Balazs Bartal, and Keith A. Nelson, "Generation of High-Power Terahertz Pulses by Tilted-Pulse-Front Excitation and Their Application Possibilities," J. Opt. Soc. Am. B **25**, B6 (2008).

[2] H. Hirori, A. Doi, F. Blanchard, and K. Tanaka, "Single-cycle Terahertz Pulses with Amplitudes Exceeding 1MV/cm Generated by Optical Rectification in LiNbO3," Appl. Phys. Lett. **98**, 091106 (2011).

[3] Tyler L. Cocker *et al.*, "An ultrafast terahertz scanning tunnelling microscope," Nat. Photonics **7**, 620 (2013).

[4] L.Wimmer, G. Herink, D. R. Solli, S. V. Yalunin, K. E. Echternkamp and C. Ropers, "Terahertz control of nanotip photoemission," Nat. Physics **10**, 432 (2014).

[5] R. H. Fowler, L. Nordheim, “Electron Emission in Intense Electric Fields,” Proc. Roy. Soc. A **119**, 173 (1928).

[6] G. Herink, L. Wimmer and C. Ropers, “Field emission at terahertz frequencies: AC-tunneling and ultrafast carrier dynamics,” New J. Phys. **16**, 123005 (2014).

[7] Krysztof Iwaszczuk, Maksim Zalkovskij, Andrew C. Strikwerda, and Peter U. Jepsen, “Nitrogen plasma formation through terahertz-induced ultrafast electron field emission,” Optica **2**, 116 (2015).

[8] G. Herink, D. R. Solli, M. Gulde, and C. Ropers, “Field-driven photoemission from nanostructures quenches the quiver motion,” Nature **483**, 190 (2012).

[9] P.M. Paul, E.S. Thoma, P. Breger, G. Mullot, F. Auge, Ph. Balcou, H.G. Muller, and P. Agostini, “Observation of a Train of Attosecond Pulses from High Harmonic Generation,” Science **292**, 1689 (2001).

[10] Mostafa Shalaby and Christoph P. Hauri, “Demonstration of a lo-frequency three-dimensional terahertz bullet with extreme brightness,” Nat. Commun. **6**, 5976 (2015).

[11] Sharly Fleischer, Yan Zhou, Robert W. Field, and Keith A. Nelson, “Molecular Orientation and Alignment by Intense Single-Cycle THz Pulses,” Phys. Rev. Lett. **107**, 163603 (2011).

[12] V. Tagliamonti, H. Chen, and G. N. Gibson, “Multielectron Effects in Charge Asymmetric Molecules Induced by Asymmetric Laser Fields,” Phys. Rev. Lett. **110**, 073002 (2013).

Quantum Dynamics Probed by Coherent Soft X-Rays

Henry C. Kapteyn and Margaret M. Murnane
JILA and Department of Physics, University of Colorado at Boulder
Phone: (303) 492-8198; FAX: (303) 492-5235; E-mail: kapteyn@jila.colorado.edu

The goal of this work is to develop novel short wavelength probes of molecules and to understand the response of atoms, molecules and nanosystems to strong laser fields. We made exciting advances in several areas since 2014.[1-11] Recent highlights include –

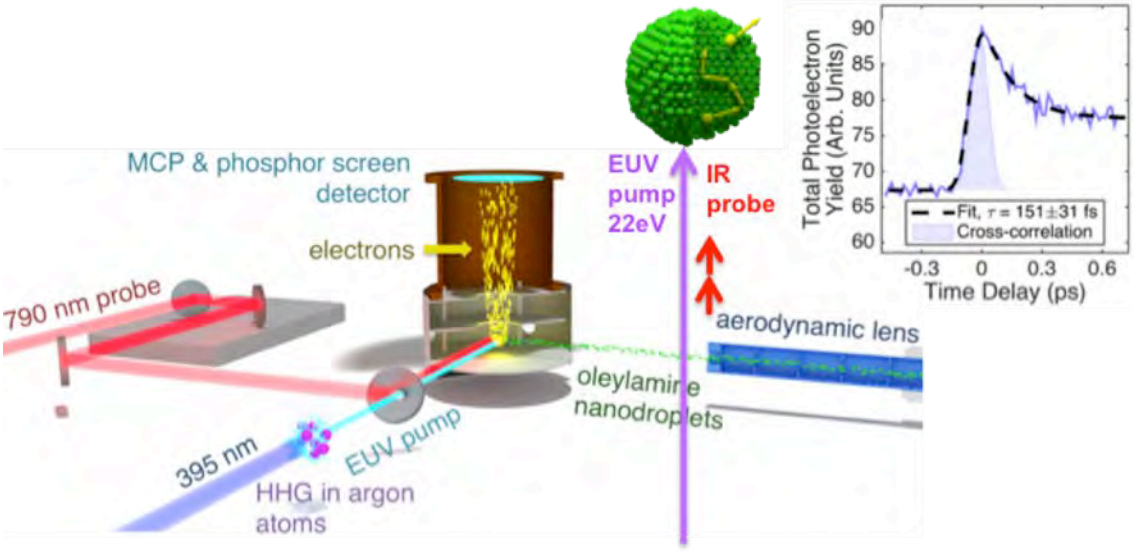

Figure 1: Time-resolved photoemission measurements of isolated nanoparticles using EUV light. The absorption of high harmonic photons creates excited-state solvated electrons in oleylamine nanodroplets. The initial 151±31fs decay (inset) probed using a time-delayed IR laser probe is consistent with the time taken for excited-solvated electrons to decay to the ground 1s state in ammonia.

Dynamics of Isolated Nanoparticles and Nanodroplets using Ultrafast EUV Beams [1, 7]: In this work, we present the first experimental study of the properties and dynamics of fully isolated nanoparticles of varying composition using ultrashort pulses of EUV light. This breakthrough is accomplished through the combination of high-harmonic generation (HHG) to produce ultrashort pulses of EUV light, a velocity-map-imaging (VMI) photoelectron spectrometer to provide high electron-collection efficiency, and an aerodynamic lens for introducing collimated beams of nanoparticles into vacuum. We present two demonstrations of how this technique can provide new insights into nanosystems. First, we demonstrate that EUV photoelectron yields can provide a surface-specific probe of nanoparticle properties. Specifically, we measure the static EUV photoelectron yield from ~100 nm diameter nanoparticles with a wide variety of compositions—ranging from organic materials to ionic crystals—and find that the photoelectron yield changes by more than an order of magnitude depending on the composition of the nanoparticles. We attribute this difference in photoelectron yield to varying electron MFPs and interfacial scattering (electron effective mass) in different nanoparticle systems. Second, we conduct time-resolved photoemission measurements of isolated nanoparticles using EUV light, finding that the absorption of EUV high harmonic (HHG) photons can create excited-state solvated electrons in oleylamine nanodroplets. The

initial 151±31 fs decay is consistent with the time taken for excited-solvated electrons to be created and decay to the ground 1s state in ammonia.

In other work recently published in JACS, we explored the influence of the solvent through a comparison of quantum dot charge transfer processes occurring in both liquid phase and in vacuum. By comparing solution phase transient absorption spectroscopy and gas-phase photo-electron spectroscopy, we show that hexane, a common nonpolar solvent for quantum dots, has negligible influence on charge transfer dynamics. Our experimental results, supported by insights from theory, indicate that the reorganization energy of nonpolar solvents plays a minimal role in the energy landscape of charge transfer in quantum dot devices. Thus, this study demonstrates that measurements conducted in nonpolar solvents can indeed provide insight into nanodevice performance in a wide variety of environments. This is important in order to predict and understand the performance of nanodevices in different environments.

Probing nanoscale transport and mechanical properties [6, 9]: We are developing a series of techniques to probe the nanoscale mechanical and transport properties of materials, uncovering new rgimes of nanoscale heat flow, and new information about the properties of materials. This work is already generating much interest across a broad range of energy and nano science, because it can inform smart designs of heat dissipation in nanostructures such as integrated circuits, thermoelectric devices, heat therapies mediated via nanoparticles, and nanoenhanced solar cells used in clean energy technologies.

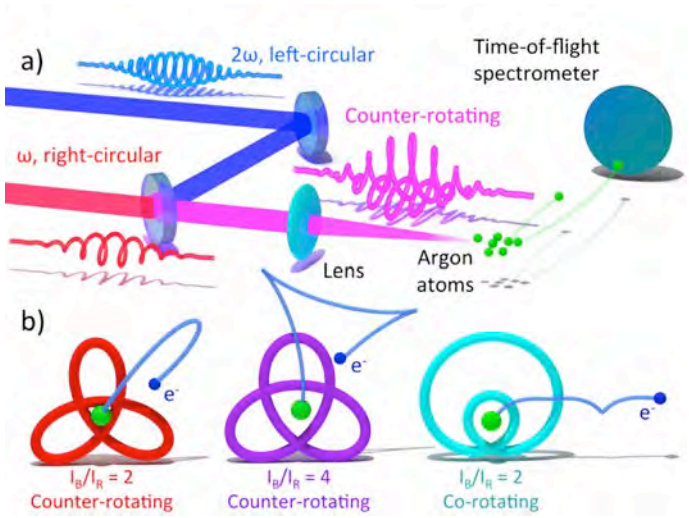

Figure 2: (a) **Setup for studying nonsequential double ionization in two-color (ω, 2ω) circularly polarized fields.** (b) Electric fields for two-color counter-rotating fields for blue/red laser intensity ratios of 2 (red) and 4 (purple), and for a co-rotating field at a ratio of 2 (cyan). Counter-rotating fields can efficiently drive electrons (blue sphere) back to the parent ion (green sphere) in 2D trajectories, whereas it is much harder for an electron to return to the parent ion in co-rotating fields.

Controlling nonsequential double ionization in two-color circularly polarized femtosecond laser fields [2, 3, 8]: In recent work (see Fig. 2), we made the first experimental observation of nonsequential double ionization (NSDI) in two-color circularly polarized laser fields, providing new insights into electron dynamics in such fields. We find that we can control NSDI by changing the intensity ratio and helicity of the two driving laser fields, where counter-rotating fields significantly enhance NSDI while co-rotating fields suppress it. Moreover, we can enhance NSDI in counter-rotating fields further by changing the intensity ratio of the two laser fields to maximize high-energy electron–ion rescattering. To qualitatively describe our experimental results, we employ classical ensemble (CE) simulations, which capture two-electron dynamics. Additionally, we consider single-electron dynamics within the tunneling approximation via classical trajectory Monte Carlo (CTMC) simulations since they provide intuitive explanations of the underlying

mechanisms of NSDI in two-color circularly polarized fields. These calculations confirm that the returning electron energy spectrum can be varied significantly by changing the relative intensity ratio between the two laser fields, where NSDI is maximized for a ratio of the intensity of the second harmonic ("Blue") beam to the intensity of the fundamental ("Red") beam of ≈ 3. Finally, the returning electron energy spectrum in two-color counter-rotating fields exhibits a narrower bandwidth than that of a linearly polarized field at the fundamental frequency, and also exhibits a tunable cutoff energy. Thus, HHG driven by two-color counter-rotating fields can generate a unique quasi-monochromatic light source with tunable photon energy.

Generating circularly polarized high harmonics [5]: In past work published in 2015 in Nature Photonics, we generated isolated beams of circularly polarized high harmonics (HHG) using noncolinear counter-rotating driving lasers. This allowed us to control the direction and polarization of HHG beams using visible lasers. This new scheme has many advantages - including separating the HHG beams from the laser beam without using filters or optics, the production of both left and right circularly polarized HHG at each wavelength, and the ability to separate different HHG orders without using a spectrometer. This approach is also the only way to generate isolated attosecond bursts of circularly polarized HHG, and enables precision differential measurements of ultrafast XMCD simultaneously at each HHG order. More recently, we investigated the angular dependence of phase-matching conditions for HHG in a noncollinear geometry. We extended the phase matching cutoff of noncollinear circularly polarized HHG by almost a factor of two compared with previous work, reaching photon energies of 90 eV. Finally, we experimentally observed phase matching of noncollinear HHG above the critical ionization level that usually limits single-color HHG, which may provide a straightforward route for generating even higher energy photons. This work was done at JILA in collaboration with Charles Durfee from the Colorado School of Mines.

Future work: First, we are using ultra-broad bandwidth, ultrafast HHG soft X-rays to capture NEXAFS over hundreds of electron volt energies simultaneously. To implement dynamic NEXAFS, gas, solid and liquid-phase samples will be excited using mid-IR – UV light, and then probed using soft X-ray HHG supercontinua. Second, we will capture orbital dynamics in molecules and nanosystems using photoelectron spectroscopy. Finally we will produce and characterize circularly and linearly polarized pulses in the EUV and soft x-ray regions.

Publications from DOE AMOS support since 2014

1. J. Ellis, D. Hickstein, W. Xiong, F. Dollar, B. Palm, K. Keister, K. Dorney, C. Ding, T. Fan, M. Wilker, K. Schnitzenbaumer, G. Dukovic, J. Jimenez, H. Kapteyn, M. Murnane, "Materials Properties and Solvated Electron Dynamics of Isolated Nanoparticles and Nanodroplets Probed with Ultrafast EUV Beams", J. Phys. Chem. Lett. **7** (4), 609-615 (2016).
2. C. Mancuso, K. Dorney, D. Hickstein, J. Chaloupka, J. Ellis, F. Dollar, R. Knut, P. Grychtol, D. Zusin, C. Gentry, M. Gopalakrishnan, H. Kapteyn, M. Murnane, "Controlling nonsequential double ionization in two-color circularly polarized femtosecond fields", in press, Physical Review Letters (2016).
3. C.A. Mancuso, D.D. Hickstein, K.M. Dorney, J.L. Ellis, E. Hasovic, R. Knut, P. Grychtol, C. Gentry, M. Gopalakrishnan, D. Zusin, F.J. Dollar, X.M. Tong, D.B. Milosevic, W. Becker, H.C. Kapteyn, M.M. Murnane, "Controlling electron-ion rescattering in two-color circularly polarized femtosecond laser fields", Physical Review A **93** (5), 053406 (2016). *Also selected as an Editor's Suggestion.*
4. C. Hern´andez-Garcıa, C.G. Durfee, D. Hickstein, T. Popmintchev, A. Meier, M. M. Murnane, H. C. Kapteyn, I. J. Sola, A. Jaron-Becker, A. Becker, "Schemes for generation of isolated attosecond pulses of pure circular polarization", Physical Review A **93**, 043855 (2016). *Also selected as an Editor's Suggestion.*

5. D. Hickstein, F. Dollar, P. Grychtol, J. Ellis, R. Knut, C. Hernández-García, C. Gentry, D. Zusin, J. Shaw, T. Fan, K. Dorney, A. Becker, A. Jaroń-Becker, H. Kapteyn, M. Murnane, C. Durfee, "Angularly separated beams of circularly polarized high harmonics," Nature Photonics **9**, 743–750 (2015).
6. K.M. Hoogeboom-Pot, J.N. Hernandez-Charpak, T. Frazer, E.H. Anderson, W. Chao, R. Falcone, X. Gu, R. Yang, M.M. Murnane, H.C. Kapteyn, D. Nardi, "A new regime of nanoscale thermal transport: collective diffusion increases dissipation efficiency", *PNAS* **112**, 4846–4851 (2015).
7. Jennifer L. Ellis, Kyle J. Schnitzenbaumer, Daniel Hickstein, Molly B. Beernink, Brett B. Palm, Jose L. Jimenez, Gordana Dukovic, Henry C. Kapteyn, Margaret M. Murnane, Wei Xiong, "Revealing solvent effects on charge transfer between quantum dots and surface adsorbates", JACS **137** (11), 3759–3762 (2015).
8. C. Mancuso, D. Hickstein, P. Grychtol, R. Knut, O. Kfir, X. Tong, F. Dollar, D. Zusin, M. Gopalakrishnan, C. Gentry, E. Turgut, J. Ellis, M. Chen, A. Fleischer, O. Cohen, H. Kapteyn, M. Murnane, "Observation of photoelectron distributions resulting from strong field ionization from two-color circularly polarized laser fields using tomographic methods", Physical Review A **91**, 031402(R) (2015).
9. D. Nardi, M. Travagliati, M. Murnane, H. Kapteyn, G. Ferrini, C. Giannetti, F. Banfi, "Impulsively Excited Surface Phononic Crystals: a Route towards Novel Sensing Schemes", IEEE Sensors Journal **15**, 5142 (2015).
10. M. Chen, C. Hernández-García, C. Mancuso, F. Dollar, B. Galloway, D. Popmintchev, P.. Huang, B. Walker, L. Plaja, A. Jaron-Becker, A. Becker, T. Popmintchev, M. Murnane, H. Kapteyn, "Generation of Bright Isolated Attosecond Soft X-Ray Pulses Driven by Multi-Cycle Mid-IR Lasers", *PNAS* **111**, E2361- (2014).
11. C. Ding, W. Xiong, T. Fan, D. Hickstein, T. Popmintchev, X. Zhang, M. Walls, M. Murnane, H. Kapteyn, "High flux coherent supercontinuum soft X-ray source driven by a single-stage 10mJ, kHz, Ti:sapphire laser amplifier," Optics Express **22**(5), 6194-6202 (2014).

Student and Faculty Awards since 2014

2016 Best paper award, International Conference on Ultrafast Phenomena (Jennifer Ellis)

2016 NSF Graduate Fellowship (Quynh Nguyen)

2016 Honorary Degree of Doctor of Science, Uppsala University (Margaret Murnane)

2015 NRC Postdoctoral Fellowship, Dan Hickstein

2015 Kathy Hoogeboom-Pot, 'Karel Urbanek Best Student Paper' at SPIE Lithography Conference

2015 Kathy Hoogeboom-Pot, Selected as a DARPA Rising Star for Nanoscale Heat Transport

2015 Elected to Member, American Philosophical Society (Margaret Murnane)

2015 Honorary Degree of Doctor of Science, National University of Ireland (Margaret Murnane)

2015 Honorary Degree of Doctor of Science, University College Dublin (Margaret Murnane)

2015 Honorary Degree of Doctor of Science, Trinity College Dublin (Margaret Murnane)

2014 CU Boulder Inventor of the Year (shared between Henry Kapteyn and Margaret Murnane)

Exploiting Non-equilibrium Charge Dynamics in Polyatomic Molecules to Steer Chemical Reactions

Wen Li, Wayne State University (wli@chem.wayne.edu)
Raphael Levine, University of California-Los Angeles (rafi@chem.ucla.edu)
Henry C. Kapteyn, University of Colorado at Boulder (Henry. Kaptyen@colorado.edu)
H. Bernhard Schlegel, Wayne State University (hbs@chem.wayne.edu)
Françoise Remacle, University of Liège, Belgium (FRemacle@ulg.ac.be)
Margaret M. Murnane, University of Colorado at Boulder (Margaret.murnane@colorado.edu)

Program Scope

The project has two aims: (1) Creating and probing photoinduced charge migration dynamics of pure electronic origin on the attosecond to few femtoseconds time scales and studying the role of non-equilibrium charge distributions in inducing selectivity of chemical reactions in polyatomic molecules. (2) Achieving mode-selective chemistry in polyatomic molecules using intense ultrashort mid-infrared pulses. In the second funding period, our research teams have made significant progress in both theoretical and experimental effort in probing attosecond charge dynamics and controlling chemical reactions. We are detailing the progress of each research team in the following:

Wayne State University

Recent Progress

1. Attosecond pump-probe of electron correlation dynamics in benzene

Previously, the Li group developed a novel 3D coincidence imaging system capable of highly efficient electron-electron coincidence detection. In the past year, a breakthrough was achieved by combing this new technique with attosecond angular streaking principle to develop a general attosecond pump-probe method. By achieving the shortest dead-time of two electron detection, the pump-probe delay was pushed down to tens of attoseconds while also capable of a range up to more than one femtosecond. We have applied this new technique to study the time-resolved double ionization of a large molecule, benzene (C_6H_6), in a close-to-circular laser field (ellipticity ~0.81)[1]. The main result is shown in figure 1a, in which the double ionization yield is plotted against the relative ejection angle of the two electrons in the plane of polarization. Only the electrons in coincidence with non-dissociative benzene dications are studied. Because of the observed precipitous decay of the double ionization yield, the contribution from the longer time delay will be small and thus it is reasonable to implement the conversion of the angle to the time. This conversion is further supported by two more observations. Figure 2b shows the ratio between back-to-back events and side-by-side events along the direction perpendicular to the plane of polarization for three different angle range (0º-40º, 40º-140º, 140º-180º) in the plane of polarization, which correspond to a time range of 0-300 as, 300-1030 as, 1030-1330 as, respectively. It is well established that when electrons are ejected simultaneously (0-300 as in this case), Coulomb repulsion in the final states will force electron ejection in the opposite directions and thus back-to-back events are favored over side-by-side events. As the time separation (distance) increases, the Coulomb repulsion becomes weaker and the electrons

relative ejection direction loses preference. This is exactly what we see in the data. This also demonstrates that it is crucial to obtain 3D momentum of both emitted electrons.

A sequential calculation, performed by the Schlegel group, assumed no electron correlation between the first and second electron has failed to reproduce the trend of the time-resolved transient and this suggests that a different mechanism is at play in the ionization dynamics at the short time scale (< 500 as). The Schlegel group then implemented a classical ensemble calculation to elucidate the nonsequential nature of the electron dynamics. It shows the majority of the ionization events take place with delays of less than 500 as. This is a clear sign of the recollision mechanism and is further verified by a close inspection of trajectories leading to double ionization. The agreement between the experiment and theory unequivocally shows that recollision plays an important role in double ionization driven by circularly polarized light. This is the first direct measurement of such dynamics.

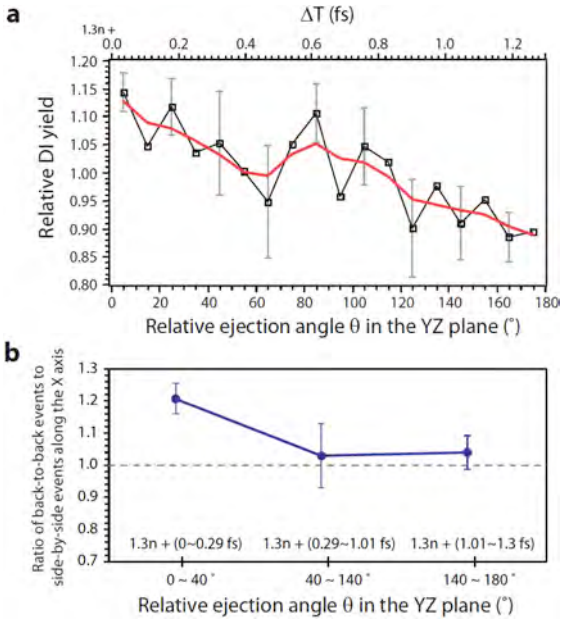

Figure 1. (a) time- and angle- dependent double ionization yield; (b) time- and angle- dependent ratio between back-to-back and side-by-side electron pairs in the perpendicular direction.

2. Molecular frame subcyle electron dynamics in methyl iodide

The Li group also obtained exciting results in probing molecular frame charge dynamics in methyl iodide. Exploiting the full coincidence capability of the apparatus, the momentum of methyl and iodine ions can be used to reconstruct the molecular orientation during ionization with axial recoil approximation. A two-dimensional double ionization yield map was generated (Fig. 2). Three interesting features were observed: 1) electrons prefer coming out of the iodine end; 2) Sequential double ionization dominates the overall double ionization yield; 3) The asymmetry between 0-180 and 180-360 in the channel involving one electron released from the iodine end could be a signature of subcyle nonadiabatic charge dynamics. The Schlegel group and the Levine and Remacle groups are currently working to extract time-resolved dynamics.

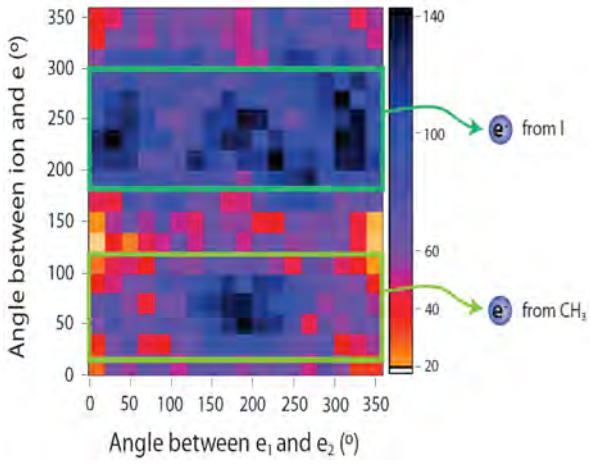

Figure 2. 2D map of double ionization yield of methyl iodide. The angle between e_1 and e_2 indicates the relative time between two ionization events while the angle between the ion recoil momentum and electron shows the ejection site of the electron.

Over the past year, the Schlegel group, in collaboration with the Li group have used ab initio molecular dynamics (AIMD) to study the behavior of oriented molecules in intense laser fields and have used time-dependent configuration interaction (TDCI) to examine the angular dependence of strong field ionization.

3. Modeling Angular dependent strong field ionization in large molecules

We have extended our previous studies on the angle-dependence of strong field ionization to a set of molecules containing triple bonds, Fig. 3.[2] At low field strengths, the angular dependence can be understood in terms of ionization from the highest occupied orbitals. At higher laser intensities, ionization also occurs from lower lying orbitals. The ionization yield for directions parallel to the molecular axis increases more rapidly than perpendicular to the axis as the conjugation length is increased. NH_2 substitution substantially increases the ionization yield along the molecular axis but has only a small effect for perpendicular directions.

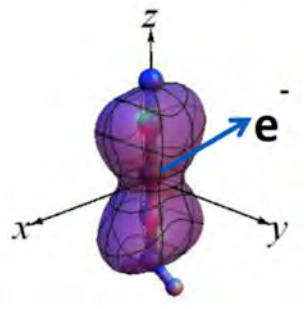

Figure 3. TDCI simulations angle depend ionization of $H_2NC{\equiv}C\text{-}C{\equiv}N$ for a 800 nm 7 cycle cosine squared pulse with E_{max}=0.04 a.u. (5.62×10^{13} W/cm^2).

4. Mode-selective chemistry driven by circularly polarized light

We have examined the effect of circularly polarized light on the fragmentation of $ClCHO^+$.[3] TDCI simulations of angle-dependent strong field ionization of ClCHO indicate the ionization rate in the molecular plane is nearly twice as large as perpendicular to the plane (Fig. 4), suggesting a degree of planar alignment of $ClCHO^+$ might be obtainable experimentally. AIMD classical trajectory calculations show that circularly polarized light yields larger branching ratios for higher energy fragmentation channels than linearly polarized light with the same maximum field strength. This suggests that circularly polarized mid-IR pulses cannot only achieve control on reactions but also provides an experimentally accessible implementation.

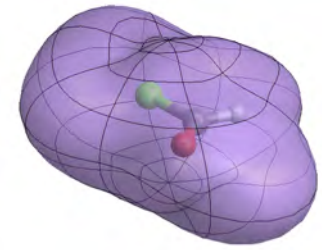

Figure 4. Angular dependence of the total yield for ionization of ClCHO as a function of the polarization direction.

Polarization	Branching ratio for $ClCHO^+$		
	Cl + HCO^+	H + $ClCO^+$	HCl^+ + CO
Left circular	30%	47%	23%
Right circular	29%	52%	19%
Linear (0 - 360° averaged)	57%	22%	21%

5. Circular hydrogen migration induced mid-IR by circularly polarized light

The hydrogens in protonated acetylene are very mobile and can easily migrate around the C_2 core by moving between classical and non-classical structures of the cation. The effect of circularly polarized light on the migration of hydrogens in oriented $C_2H_3^+$ has been simulated by AIMD classical trajectory calculations using linearly and circularly polarized 700 fs, 7 μm

cosine squared pulses[4]. For circularly polarized light, this results in an appreciable amount of average angular displacement of the three hydrogens relative to the C_2 core, but only an insignificant amount for linearly polarized light. Over the course of the simulation with circularly polarized light, this corresponds to a propeller-like motion of the three hydrogens around the C_2 core of protonated acetylene (Fig. 5).

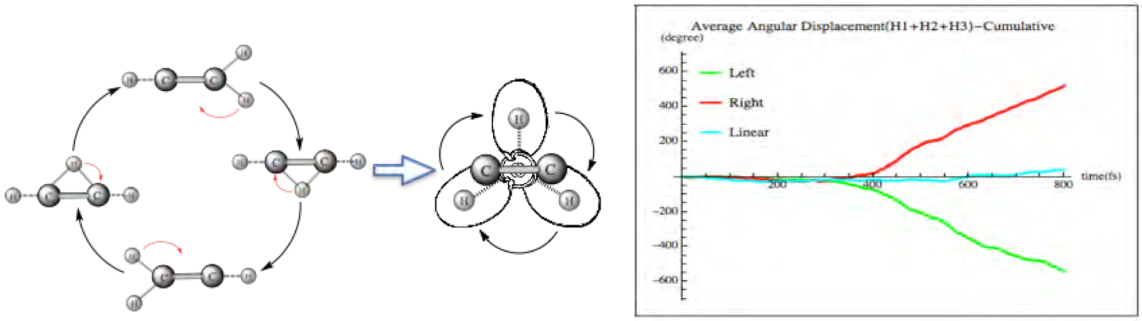

Figure 5. Non-classical (bridged, 0. kcal/mol) and classical (Y shaped, 4. kcal/mol) structure of $C_2H_3^+$ (left panel), showing the propeller-like motion of the hydrogens around the C_2 core (middle panel). Cumulative average angular displacement over time (right panel).

Future plans

Further development and applications of the new attosecond pump-probe technique will be the focus of the next funding period. Recently, we started working with the UCLA-ULg groups on probing the charge dynamics in PENNA. We will continue our effort on PENNA and other large molecules such as ABCU. We will also work with the JILA group to study the wavelength dependent fragmentation pattern and energy deposition in polyatomics.

In our theoretical effort, the TDCI simulations will be extended to probe the direction of the electron ejected during ionization. For the molecular dynamics studies in strong fields, we will analyze the time dependence of energy deposited into various vibrational modes and the effect of multiple pulses with different wavelength on dissociation branching ratios.

References (WSU)

1. Winney, A., Lee, S. K., Lin, Y. F., Liao, Q., Adhikari, P., Schlegel, H. B., Li, W., Attosecond Pump-Probe Spectroscopy of Electron Correlation Dynamics in the Double Ionization of Benzene, International Conferences on Ultrafast Phenomena, Santa Fe, New Mexico (accepted)
2. Liao, Q., Li, W., Schlegel, H. B., Angle-Dependent Strong Field Ionization of Triple Bonded Systems Calculated by Time-Dependent Configuration Interaction, with an Absorbing Potential. Can. J. Chem. (accepted) (10.1139/cjc-2016-0185).
3. Shi, X., Thapa, B., Li, W., Schlegel, H. B., Controlling Chemical Reactions by Short, Intense Mid-Infrared Laser Pulses: Comparison of Linear and Circularly Polarized Light in Simulations of ClCHO(+) Fragmentation. J. Phys. Chem. A **120**, 1120 (2016) (10.1021/acs.jpca.5b12327).
4. Shi, X., Li, W., Schlegel, H. B., Computational Simulations of a "Molecular Propeller": Hydrogen Circular Migration in Protonated Acetylene Induced by Circularly Polarized Light. J. Chem. Phys. **145**, 084309 (2016)

JILA/University of Colorado

Recent Progress

For the second funding period, we report time-resolved photoelectron-photoion coincidence (PEPICO) experiments using 8.0 eV pump photons, where we investigate a molecule relevant to atmospheric chemistry (acetone), and another molecule relevant to astronomical chemistry (methyl azide). In acetone we find that the excited state prepared by 8 eV photons, which was previously assigned as $(n_y \rightarrow 3d)$, is actually a strongly mixed state consisting of $(n_y \rightarrow 3p)$ and $(\pi \rightarrow \pi^*)$ which decays with a time constant of 340 fs. Here, a reliable assignment of this state required a comparison of single-photon ionization with several pump-probe scheme that could access both n^{-1} and π^{-1} cation states. For methyl azide, we find that the excited state prepared by 8 eV photons exhibits strong mixing between electronically different Rydberg series that are converging to different ion states: $(HOMO \rightarrow 3p)$ and $(HOMO - 1 \rightarrow 3s)$. This mixed Rydberg state undergoes very rapid (~20 fs) wavepacket motion before undergoing a surprisingly quick (~25 fs) internal conversion that may indeed proceed through a conical funnel.

1. VUV Excitation and Dynamics of Acetone

Ionization of acetone using either 7ω (11.2 eV) or via a 5ω pump, ω/2ω/3ω probe scheme produces two ions: an acetone ion (58 amu) and an acetyl ion (43 amu) formed by the loss of a methyl radical. As shown in Fig. 1, different channels can have the same total energy of 11.2 eV: the 7ω single-photon-ionization channel, the 5ω pump ω+ ω probe channel, or the 5ω pump 2ω probe channel. The resultant electron energy can then distinguish the resonant pump-probe pathways from simultaneous absorption of multiple photons near time zero. We find that the resonant pathways all have a decay time of 340 *fs* for all 3 pump-probe schema, for both acetone and acetyl ions. This finding suggests that dissociation of acetone occurs after the probe pulse.

By analyzing the electrons coincident with the acetone ions, we see a clear difference of 0.7 eV in electron energy between the single-photon ionization and pump-probe ionization channels. This electron energy is not consistent with a previous assignment of the intermediate state as $(n_y \rightarrow 3d)$ for our pump-probe ionization channels[1]. There are three likely candidates for the intermediate state, as shown in Fig. 1: $(n_y \rightarrow 3p)$, $(n_y \rightarrow 3d_{yz})$, and $(\pi \rightarrow \pi^*)$[2]. The HOMO, n_y, is a nonbonding orbital, and thus the Rydberg states have short Franck-Condon progressions. The band origin for $(n_y \rightarrow 3d_{yz})$ is 7.7 eV, so no more than 0.3 eV could be transferred to vibrations from this excitation scheme. The band origin for $(n_y \rightarrow 3p)$ is 7.4 eV, which would allow 0.6 eV to transfer to vibrations. However, this would require a very long Franck-Condon progression, which indicates substantial mixed character for the state. In order to test $(\pi \rightarrow \pi^*)$, we used a 4.8 eV probe, which gives a total pump-probe energy of 12.8 eV, enough to reach the second cation state π^{-1}. If the pump were exclusively accessing $(\pi \rightarrow \pi^*)$, we would expect a 4.8 eV probe to show a prominent peak in the PEPICO spectrum at higher electron binding energy. However, we do not see any substantial difference in binding energy after switching probe energies from 2ω to 3ω. This indicates that the intermediate state must have an allowed transition directly to the ground cation state; that is, there must be significant HOMO-excited character. We believe our 8 eV pump excites a mixed-character state of $(n_y \rightarrow 3p_y)$ and $(\pi \rightarrow \pi^*)$, which would have a long Franck-Condon progression as well as allowed transitions to

both cation states. Such mixing is symmetry-allowed as both states have A_1 symmetry, and has been suggested previously[3]. Here we present the first experimental evidence that state mixing dominates VUV absorption at energies as high as 8 eV.

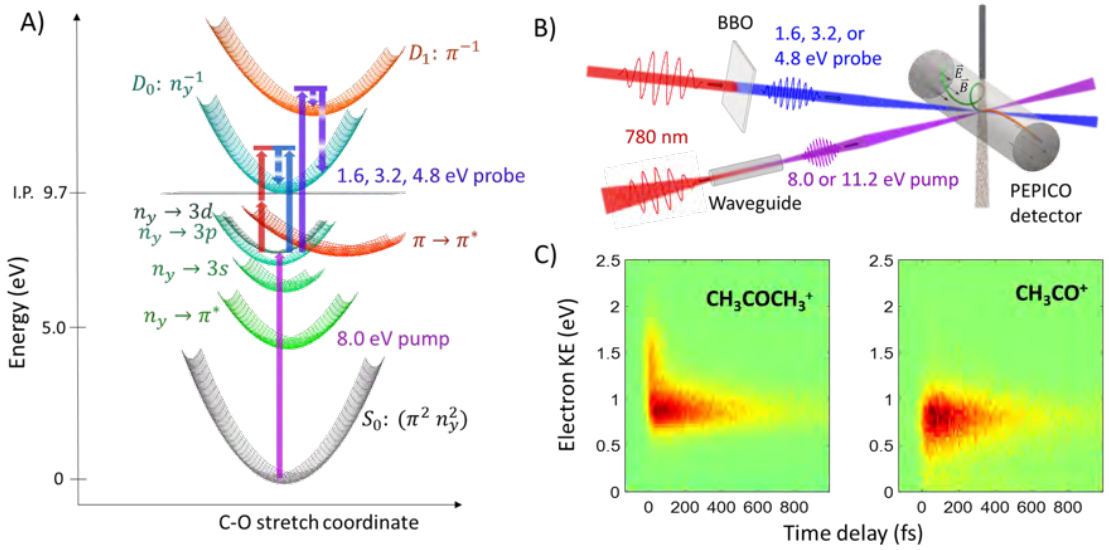

Figure 1. a) An energy level diagram illustrating highly excited states of acetone and the two lowest cation states, with arrows indicating various pump-probe pathways investigated. b) An illustration of pulse upconversion techniques and PEPICO detection. c) Photoelectron energy vs. time plots in coincidence with acetone molecular ion (left) and the acetyl fragment ion (right).

2. VUV Excitation and Dynamics of Methyl Azide

Both single-photon (7ω) and pump-probe (5ω pump, ω/2ω/3ω probe) ionization of methyl azide produce two ions, with the parent ion at mass 57 amu and a fragment with mass 28 amu. This is an $HCNH^+$ ion, probably through the loss of N_2, leaving behind a CH_3N^+ ion, which goes on to lose an H atom during rearrangement[4]. In the pump-probe data of Fig. 2, the parent ion signal only exists near time zero, while the $HCNH^+$ fragment signal grows on a timescale of 20 fs, before decaying with a 25 fs time constant. We were unable to fit the data with a null assumption of unrelated signal pathways, but we did achieve good fits using a model where the parent signal decays as the fragment signal grows (which then decays to a state outside our detection bandwidth). Photoelectron spectra taken in coincidence with the fragment show that this signal arises from both of the lowest two cation states of methyl azide, with both electron energies displaying identical dynamics. A comparison with single-photon ionization photoelectrons and ion kinetic energy release measurements confirm that both electronic states are contributing, and that they exhibit identical dynamics.

The PEPICO data from methyl azide indicate the presence of an electronic intermediate excited state that has a mixture of the $HOMO$ electron and the $(HOMO - 1)$ electron. We performed a*b initio* calculations, CCSD/d-aug-cc-pVTZ, which reveal two electronic states nearby, at 7.9 eV and at 7.4 eV, which are mixtures of $(HOMO \rightarrow 3p)$ and $(HOMO - 1 \rightarrow 3s)$. The near-degeneracy of these two states arises due to the difference in the first two ionization potentials of methyl azide (vertical energies are 9.95 eV and 11.4 eV), and expected quantum defects of $\delta \approx 1.1$ for an s-wave and $\delta \approx 0.5$ for a p-wave[5]. The very fast shift (20 fs) from the parent to the fragment ion is due to wavepacket motion along the CNN bond angle, which

reduces wavefunction overlap with low vibrational states of the ground cation state. Ionization to high vibrational states places the molecule above the appearance energy for the mass 28 $HCNH^+$ fragment. The *ab initio* calculations indicate that the geometry change should not move the wavepacket outside our detection window, indicating that our final decay constant must stem from internal conversion to a lower electronic state. This ultrafast population transfer may proceed through a conical funnel.

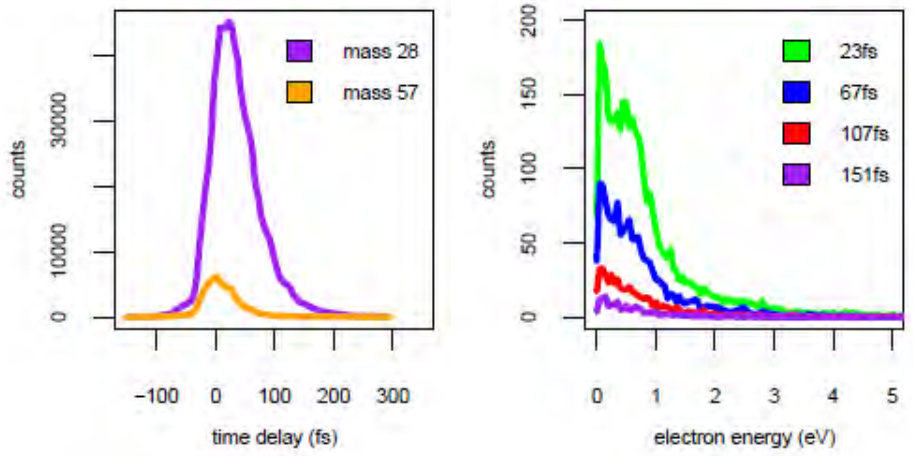

Figure 2. Transient ion yields and photoelectron spectra of methyl azide for an 8 eV pump, and a 2x1.6 eV probe.

Future Plans

We report that unique 20fs - 100fs, 2μm - 6μm lasers are now ready and will be used to test the Wayne State prediction that long wavelength driving lasers enables mode-selective molecular fragmentation. We will also implement a 3D velocity mapping imaging setup developed by the Li group to study electron dynamics driven by two color circularly polarized light.

References (JILA)

1. Farmarnara, P., Stert, V., and Radloff, W., Ultrafast photodissociation dynamics of acetone excited by femtosecond 155 nm laser pulses, Chem. Phys. Lett. **320**, 697-702 (2000).
2. Nobre, M., Fernandes, A., Ferreira da Silva, F. *et al.,* The VUV electronic spectroscopy of acetone studied by synchrotron radiation, Phys. Chem. Chem. Phys. **10**, 550-560 (2008).
3. Merchán, M., Roos, B., McDiarmid, R., and Xing, X., A combined theoretical and experimental determination of the electronic spectrum of acetone, J. Chem. Phys. **104**, 1791 (1996).
4. Travers, M. J., Cowles, D. C., Clifford, E. P. *et al.*, Photoelectron spectroscopy of the CH_3N^- ion, J. Chem. Phys. **111**, 5349 (1999)
5. Schőnnenbeck, G. *et al.*, VUV photolysis of hydrazoic acid: absorption and fluorescence excitation spectra, J. Chem. Phys. **109**, 2210 (1998)

University of California-Los Angeles and University of Liege

Recent progress

During the second period, the UCLA-ULg group has pursued theoretical studies of steering chemical reactivity by a strong, short optical pulse. In collaboration with the experiment of the Li group, we have simulated the electronic dynamics of double ionization in the modular PENNA ($C_{10}H_{15}N$) molecule and the fragmentation of its cation upon excitation with an intense IR fs pulse. We also demonstrated control for two diatomic molecules: the homonuclear N_2 and the heteronuclear LiH. The UCLA-ULg and the Schlegel group jointly work on integrating methodologies for computing photoionization and strong field ionization widths. A detailed report of our recent work is available at the address http://www.tcp.ulg.ac.be/projects.php

1. Spectroscopic probing charge migration induced by ultrafast photoexcitation in N_2

The homonuclear N_2 molecule has no dipole when it is in a stationary state. Charge migration induced by an attosecond excitation can result in a time dependent dipole moment. Using the pulse parameters of the Li group to excite the N_2 molecule while retaining a full description of the nuclear motion we computed the resulting dipole moment of the molecule. Charge migration is faster than the nuclear motion so that there is a dipole only when the excited state is in the Franck Condon region of the ground state. Monitoring the dipole by inducing it to emit using a probe pulse can therefore serve as a sensitive test of charge migration. We have previously shown that the electronic dynamics in N_2 is strongly influenced by coupling of the diabatic valence and Rydberg states. Diabatic coupling to the Rydberg states brings population into the valence states and distorts the regularity of the large amplitude beating of the wave packet on the valence state in and out the FC region. These results have been published in the Journal of Physical Chemistry A.[1] We are currently computing the frequency spectrum that corresponds to probing the time changing dipole moment. The UC Berkeley group has measured this spectrum and they provided us with the parameters of their pump and probe pulses. The pump used is rather broad in energy and also accesses ionizing states. To compare with these results we therefore need the transition dipoles to these states and we are currently computing them.

We are also reporting on the probing of charge migration in N_2 by Raman spectroscopy. This takes advantage of the large amplitude motion of the nuclear wavepacket on the diabatic potential of the valence state as noted above. Following its initiation, the nuclear wavepacket moves away from the Franck Condon region as determined by the ground state. When the wavepacket reaches higher internuclear distances it has transition dipoles to emit to high lying vibrational states on the ground electronic state. The wavepacket on the valence state reaches the outer turning point and is reflected and goes back to the Franck Condon region. It goes out again and so on. But the valence state potential is rather anharmonic so different vibrational energies have rather different vibrational frequencies and very quickly the nuclear wavepacket on the valence state bifurcates into many components. Figure 1 shows the absolute values of the amplitudes for emission from the nuclear wavepacket on the valence state to different vibrational states *n* of the ground electronic states as a function of time. The pump peak is at 12 fs. There are two columns for the two valence states of Σ and of Π symmetry. As indicated the results are shown both without and with diabatic coupling to the Rydberg states. In the first period of the wavepacket motion it is seen how the motion on the valence state can emit to high *n* states. Then in the second round on the upper potential the nuclear wavepacket is seen to begin to bifurcate. The Rydberg states are about as tightly bound as the ground electronic state and so do not emit to higher *n* states. Therefore the Raman spectrum probes the valence state charge migration.

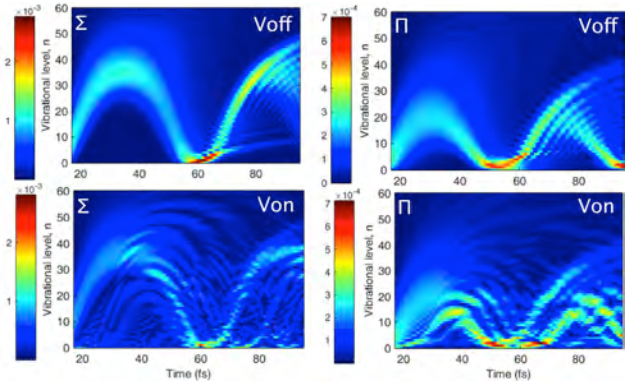

Figure 1. Emission probabilities, $\left|\left\langle b'(t)\middle|n\right\rangle\right|$ (left column), and $\left|\left\langle b(t)\middle|n\right\rangle\right|$ (right column), for the Σ and Π valence state respectively, computed with the diabatic coupling Voff (top) and Von (bottom). The carrier frequency of the ultrashort pulse is 13.61 eV and its width 1eV.

2. Control of fragmentation yields in the excited electronic states of LiH using a carrier envelope phase shift of a strong one cycle IR pulse

We studied computationally how ultrashort polarized strong one cycle IR pulses can be used for steering coherent nuclear dynamics in LiH and controlling fragmentation yields[2,3] . LiH possesses low lying Σ and Π states that can be selectively accessed by controlling the polarization of the pump pulse along the bond or perpendicularly to it. In addition, when using a one cycle pulse, controlling the carrier envelope phase (CEP) enables selecting the states that will be coherently excited according to their polarity. Polarization and CEP control of the pump pulse leads to controlling the dissociation yields.

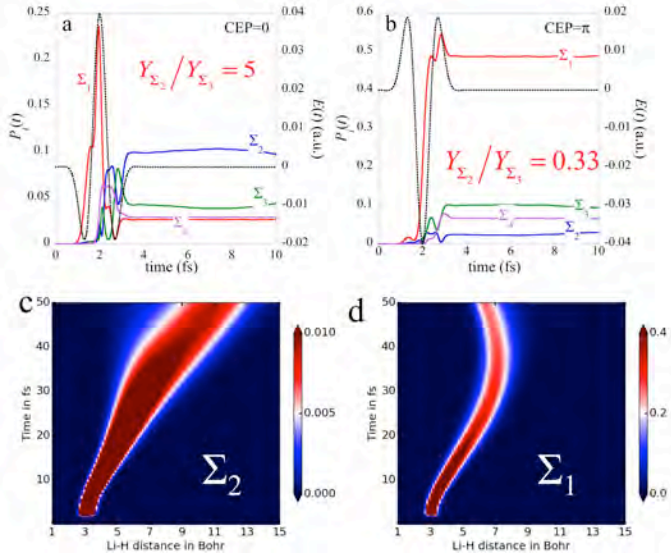

Figure 2. Control of the fragmentation of LiH by the CEP. Shown is the yield ratio $Y_{\Sigma_2}/Y_{\Sigma_3}$ using the CEP controlled one cycle 800nm pulse (σ = 0.68 fs, electric field strength=0.04 a.u. polarized along the molecular axis). Panels (a) and (b) show the computed populations in the Σ manifold below the IP for two pulses differing by the value of the CEP. The electric field time profile is shown in dots. Panels (c) and (d) show the wave packet dynamics for the CEP=π pulse for Σ_2 that dissociates and Σ_1 that does not.

In particular, our quantum dynamics simulations show that the ratio of the fragmentation yields of the Σ_2 and Σ_3 states can be changed by a factor of 10 when the CEP of a one cycle IR pulse polarized along the bond is switched from 0 to π, see Fig. 2. This control can be rationalized on the basis of the polarities of the Σ states. A simple qualitative summary is that successive excited states of Σ symmetry have opposite polarities. The GS is ionic in the sense of $Li^{\delta+}H^{\delta-}$. The first excited Σ_1 state has the charge transferred to the other end, $Li^{\delta-}H^{\delta+}$. The next excited, Σ_2 state is polar like the GS etc. In addition, Σ_1, Σ_2 and Σ_3 dissociates to different Rydberg states of the Li atom, Li(2p),Li(3s) and Li(3p) respectively, which allows measuring the fragmentation yields of the different excited states.

In addition to probing the dynamics by following the fragmentation, we also report on probing the coherent vibronic wave packet using transient absorption spectra that results from

the interaction of the molecular transition dipole with the electric fields of the pump and the probe pulses[2,3].

3. **Probing the correlation in the double ionization in the modular PENNA molecule**

In the first project period the Li group reported a new experimental set-up able to measure the momentum electron correlation in double ionization. Results were presented for the nonsequential double ionization in benzene. In close collaboration with the Li group, we investigated theoretically if this new experimental set-up could be used to probe charge migration in the cation of the modular PENNA molecule, $C_{10}H_{15}N$, a modular molecule where a phenyl is linking to a dimethyl amine by an ethylene bridge, see inset fig. 3a. We computed the electronic and photoionization dynamics of the PENNA molecule induced by a pulse similar to the ones used in the Li group, a 8.5 fs 800 nm IR pulse with a field strength of 2 10^{12}W/cm^2. The photoionization to the cation leads to a complex coherent superposition of electronic states of the cation that involves states with a hole localized on the phenyl and states with a hole localized on the amine end. During the pulse and after it is over, the electronic coherences drive the charge migration with different periods that correspond to the transition frequencies between the states of the cations localized in the two end moieties. There is mainly a 5.9 fs period that corresponds to the transition frequency between the GS (hole on amine) and the two nearly degenerate lowest excited states that have a hole on the amine and a faster period of a 1.35 fs period that corresponds to the beating between the GS and the 6 and 7th excited states. These beatings are reflected in the time dependence of the molecular dipole shown in fig. 3a.

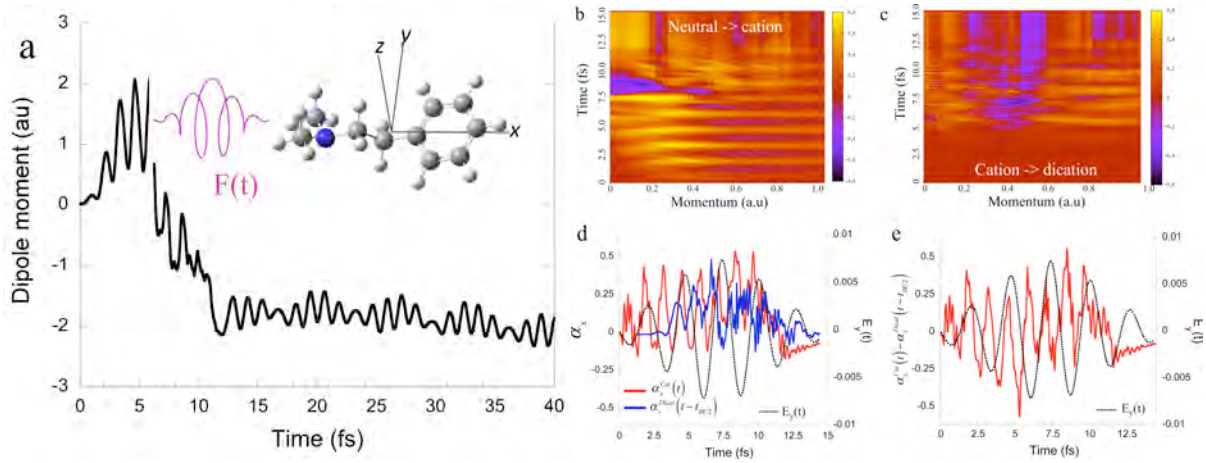

Figure 3. Left (a) The time dependence of the molecular dipole of PENNA. Fast (1.35 fs) and slower (5.9 fs) beatings correspond to the transition frequencies between states of the cation localized on different moieties. The PENNA molecule in the molecular frame shown in the inset is excited by an IR pulse circularly polarized in the plane perpendicular to the axis of charge migration. Right : Heatmaps of the anisotropy ionization parameter, α_x, along the charge migration direction computed as a function of the momentum of the ionized electron and as a function of time for the photoionization of the neutral to the cation (b) and for the photoionization of the cation to the dication (c). Bottom : Cuts of the anisotropy ionization parameter at the electron kinetic energy of 4.8 eV for the cation and the dication (d) and the difference between the two (e). The curve of the dication is shifted by $t_{IR}/2$ to highlight the correlation between the two ionization processes.

By analyzing the angular distribution of the second electron ionized to the dication after a half period of the electric field of the IR laser, it is possible to probe the charge migration in the states of the cation. Preliminary results are shown in Fig.3 (right). Figs. 3b and 3c show

heatmaps of the anisotropy ionization parameter along *x*, $\alpha_x = \left(Y_{+x}(t) - Y_{-x}(t)\right) / \left(Y_{+x}(t) + Y_{-x}(t)\right)$, plotted as a function of the momentum of the electron ionized and as a function of time during the pulse for the ionization of the neutral to the cation (a) and that of the cation to the dication (b). Fig. 3 bottom right show the anisotropy parameter value for a kinetic energy of the photoelectron of 4.8 eV, the difference between the two curves is shown in fig. 3e. When the difference goes through a maximum or a minimum, it means that the two electrons are photoionized in opposite directions. Work is in progress to simulate the momentum correlation between the two electrons, which could be directly compared with the experimental measurements of the Li group.

In collaboration with the Li group who studied the fragmentation patterns of the PENNA cation, we also investigated the femtosecond nuclear dynamics in the cation states of the PENNA that follows the photoionization of the neutral. The energetics of the stable conformers, conical intersections (CI) and transition states have been characterized at the SA-CASSCF level for the 3 lowest electronic states (D0, D1 and D2). Ab initio on the fly molecular dynamics simulations was performed on the six lowest states simultaneously with the semi-classical SHARC code [sharc-md.org (2014)], that implements non-adiabatic molecular dynamics simulations using Tully's surface hopping. The relaxation to the D_0 state is found to occur on a fats time scale of 60 fs which is followed by fragmentation through a late transition state. See the report on the web for more details. Work in progress aims at implementing a semiclassical approach[4] that goes beyond Ehrenfest dynamics and surface hopping to exploit the effect of electronic coherences on the nuclear dynamics.

Future plans

Following the work of Leone and Neumark at UCBerkeley we are extending the study of charge migration in N_2 to higher excitation energies where ionization is also possible.

Towards possible experiments of the Li group we are computing both the absorption and the Raman spectrum of attosecond pumped N_2.

Following scientific discussions during the 1st year meeting in Gaithersburg, collaboration has started with the group of Nora Berrah (UCONN) on the photoionization of the doped fullerene. Thus far we have demonstrated that steering the electron density and thereby achieving chemical control is possible in diatomic molecules. We have also simulated spectroscopic experimental responses (photoelectron, transient Raman and absorption spectra) that allow following in time electronic and nuclei motion. Next we have started to investigate nuclear dynamics in larger polyatomic molecules, i.e. on PENNA as reported above and on the cage molecule ABCO ($C_7H_{14}N$), not reported here. During the third year emphasis will be put on continuing the simulation of electronic and nuclear time dependent responses and demonstrating control in larger polyatomic molecules, in collaboration with the Li group.

Additional work in progress is reported on the web, loc. cit.

References (UCLA-ULg)

1. Ajay, J., Šmydke, J., Rermacle, F., Levine, R. D., Probing in Space and Time the Nuclear Motion Driven by Nonequilibrium Electronic Dynamics in Ultrafast Pumped N_2. J. Phy. Chem. A, **120,** 3335 (2016)
2. Nikodem, A., R.D. Levine, and F. Remacle, Quantum Nuclear Dynamics Pumped and Probed by Ultrafast Polarization Controlled Steering of a Coherent Electronic State in LiH. J. Phys. Chem. A, **120**, 3343 (2016)
3. Nikodem, A., R.D. Levine, and F. Remacle, Controlling coherent quantum nuclear dynamics in LiH by ultrashort IR attopulses, in Progress in Ultrafast Laser Science XIII, K. Yamanouchi, W. Hill, and F. Paulus, Editors. 2016, Springer: New York.
4. M. Ben-Nun and R. D. Levine, Chem. Phys. **201**,163(1995)

Publications supported by DOE grant (2015-2106) with institutions contribution

1. Sun, S. T., Mignolet, B., Fan, L., Li, W., Levine, R. D., and Remacle, F., Ultrafast photodissociative nuclear driven charge transfer of the PENNA cation: an experimental and computational study, (in preparation) (UCLA-ULg-WSU)
2. Fan, L., Mignolet, B., Levine, R. D., Remacle, F., and Li, W., Angular streaking charge dynamics in PENNA, (in preparation) (WSU-UCLA-ULg)
3. Ajay, J., Šmydke, J., Remacle, F., Levine, R. D., Probing in Space and Time the Nuclear Motion Driven by Nonequilibrium Electronic Dynamics in Ultrafast Pumped N_2. J. Phy. Chem. A, **120,** 3335 (2016) DOI: 10.1021/acs.jpca.6b00165. (UCLA-ULg)
4. Nikodem, A., R.D. Levine, and F. Remacle, Quantum Nuclear Dynamics Pumped and Probed by Ultrafast Polarization Controlled Steering of a Coherent Electronic State in LiH. J. Phys. Chem. A, **120**, 3343 (2016) DOI: 10.1021/acs.jpca.6b00140. (UCLA-ULg)
5. Šmydke, J., Ajay, J., Levine, R. D., Electronic and Nuclear Dynamics for a Non-Equilibrium Electronic State: the Ultrafast Pumping of N_2. Intl. J. Quant. Chem., 2016: (accepted) (UCLA-ULg)
6. Nikodem, A., R.D. Levine, and F. Remacle, Controlling coherent quantum nuclear dynamics in LiH by ultrashort IR attopulses, in Progress in Ultrafast Laser Science XIII, K. Yamanouchi, W. Hill, and F. Paulus, Editors. 2016, Springer: New York. (UCLA-ULg)
7. Mignolet, B. and F. Remacle, Time-efficient computation of the electronic structure of the C_{60} super-atom molecular orbital (SAMO) states in TDDFT. AIP conference proceedings, 2016: accepted. (UCLA-ULg)
8. Shi, X., Thapa, B., Li, W., Schlegel, H. B., Controlling Chemical Reactions by Short, Intense Mid-Infrared Laser Pulses: Comparison of Linear and Circularly Polarized Light in Simulations of ClCHO(+) Fragmentation. J. Phys. Chem. A **120**, 1120 (2016) DOI:10.1021/acs.jpca.5b12327 (WSU)
9. Liao, Q., Li, W., Schlegel, H. B., Angle-Dependent Strong Field Ionization of Triple Bonded Systems Calculated by Time-Dependent Configuration Interaction, with an Absorbing Potential. Can. J. Chem. (accepted) DOI: 10.1139/cjc-2016-0185 (WSU)
10. Shi, X., Li, W., Schlegel, H. B., Computational Simulations of a "Molecular Propeller": Hydrogen Circular Migration in Protonated Acetylene Induced by Circularly Polarized Light. J. Chem. Phys. **145**, 084309, (2016) DOI: 10.1063/1.4961644 (WSU)
11. Peters, W., Couch, D., Fortenberry, R. C., Kapteyn, H. C., Murnane, M. M., Electronic Dynamics in Highly Excited States of Acetone and Methyl Azide Studied with Ultrafast PEPICO Spectroscopy, International Conferences on Ultrafast Phenomena, Santa Fe, New Mexico (accepted) (JILA)
12. Winney, A., Lee, S. K., Lin, Y. F., Liao, Q., Adhikari, P., Schlegel, H. B., Li, W., Attosecond Pump-Probe Spectroscopy of Electron Correlation Dynamics in the Double Ionization of Benzene, International Conferences on Ultrafast Phenomena, Santa Fe, New Mexico (accepted) (WSU)

Probing Electron-Molecule Scattering with HHG: Theory and Experiment

Robert R. Lucchese, Department of Chemistry, Texas A&M University, College Station, TX, 77843, lucchese@mail.chem.tamu.edu

Carlos Trallero-Herrero, J. R. Macdonald Laboratory, Kansas State University, KA 66506, trallero@phys.ksu.edu

Program Scope

Understanding electron-molecular scattering dynamics is the overall theme of our program. The main focus is the study electron-molecule collisions that occur in high-field processes such as high harmonic generation (HHG) and recollision spectroscopy. In the last year Erwin Poliakoff has withdrawn from this project and for the coming year Carlos Trallero-Herrero will be the experimental co-PI. We will continue to collaborate closely with the theory group at Kansas State (A. T. Le and C. D. Lin) as well as with the Atomic, Molecular, and Optical (AMO) theory group at Lawrence Berkeley National Laboratory (LBNL) (C. W. McCurdy). All of these research efforts benefit the Department of Energy because the results elucidate electron dynamics that will be indispensable for probing complex and disordered systems of interest to DOE such as clusters, catalysts, reactive intermediates, transient species, and related species.

Recent Progress

Atomic HHG

With respect to high harmonic spectra, we have worked on both atomic and molecular targets. In particular, we have worked with Tony Starace at the University of Nebraska and his collaborators in order to develop methods for extracting photoionization data quantitatively from HHG spectra via ellipticity measurements. More specifically, we have shown [11] that it is possible to extract photoionization asymmetry parameters via measurements of the ellipticity dependence of HHG spectra of Ar.

Molecular Aspects of HHG

We have studied HHG in relatively complex molecules, in particular we have completed a study of HHG in SF_6. Experimentally we have considered a wide variation of both the intensity of the exciting laser and the position of its focus relative to the gas jet. The main qualitatively feature seen in the measured HHG yield is a narrow peak centered at 23 eV (H15) and a broad peak centered at 32 eV (H21). These two features were observed under almost all of the conditions considered.

Theoretically we have applied the quantitative rescattering (QRS) theory to isolated molecules and considered the excitation of the electrons from the three most weakly bound orbitals, i.e. the highest occupied molecule orbital (HOMO), the HOMO-1, and the HOMO-2. These three orbitals have ionization potentials that are all within 1.5 eV of each other. For the recombination step in the three-step model, which is the basis of the QRS, we have considered results from relatively simple single-channel static-exchange type calculations and from coupled-channel calculations that include dynamic electron correlation effects. The two features seen in the experiments were also seen in the QRS results. In the calculations, these features were due to

shape resonances in excitation from the different orbitals. In the single-channel static-exchange calculations, the resonance at 23 eV was only seen in the HHG from the HOMO-1 and HOMO-2 orbitals, whereas in the coupled-channel results the resonance appears in the HOMO channel with some reduction in the other two channels. In the comparison with experimental data, obtained with different macroscopic propagation conditions, we found that the relative intensity of these two peaks in the QRS calculations was in the best agreement the experiments where the laser focal point was a few mm in front of the gas jet.

Grid Based Electron-Molecule Scattering Calculations

Another component of our research program is the development of a next-generation electron-molecule scattering code. This work is being done in collaboration with the AMO theory group at LBNL, led by Bill McCurdy. This code is based on the complex Kohn approach with a numerical grid-based representation of the scattering wave functions. We employ an overset grid representation where there is one encompassing spherical grid and centered on each nucleus in a molecule there is an additional local grid which has spherical symmetry around that center. Over the last year, significant progress has been made in the implementation of the overset grids at the level of a static-exchange calculation. The code has been written, however additional debugging and evaluation of details of the implementation are still in progress. Very promising results have been obtained for electron scattering from CF_4.

Coherence in Molecular Photoionization

Another project that is a close collaboration with the AMO theory group at LBNL, is the study of the theory of coherence in ionization of molecules with very short pulses. When a short laser pulse is used to ionize a molecule, and the pulse has a bandwidth that is broad enough to ionize two different ion states with the ejected photoelectron having the same asymptotic kinetic energy from each state, then there can be a coherence in the population of the two ionic states. The coherence comes from photoelectrons emitted from the two ion states that have the same asymptotic momentum, both in magnitude and direction. Thus the coherence will require a non-zero overlap in the molecular frame angle-dependent transition amplitudes. With only an ionization step, the population coherence in the ions, for a system that is not oriented in space, results from an average over all orientations of the molecules with respect to the exciting field and an integration of the product of the emission amplitudes over all photoelectron ejection directions. This can only lead to non-zero coherence when the two ion states have the same symmetry. However, if there is a subsequent probe that takes the system to a common final state, then even with orientation averaging and integration over all photoelectron emission directions, the coherence can be observed more generally. We have developed explicit formulas for computing these coherences that involve the same photoionization amplitudes that are found in expressions for molecular frame photoelectron angular distributions.

Other Photoionization Studies

Photoionization of Linear Alkynes. In our study of the photoionization of a sequence of alkyne molecules [9], we have found a case where channel coupling is very important. In an alkyne molecule there is a C-C triple bond that contains two π bonds. When the molecule has enough symmetry so that these two orbitals are degenerate then a single-channel photoionization calculation done with the full symmetry of the molecule can correctly include the coupling between the two ionization channels using symmetry. When the molecule has lower symmetry

the two π orbitals have similar energies, but are not degenerate. In such a case it is important to include the two strongly interacting ionization channels in a photoionization calculation, especially to obtain the correct position of shape resonance features.

RFPADS in Non-Linear Molecules Including Molecular Rotation. In a study of the recoil-frame photoelectron angular distributions (RFPADs) of the C $(1s)^{-1}$ photoionization of CH_4 we derived an expression to include the effects of rotation between the time of the photoionization and the subsequent fragmentation of the molecule [10]. We found that computed RFPADs where rotation was included during a 0.5 ps delay between ionization and fragmentation lead to good agreement with the experimental RFPADs for low fragment kinetic energy release (KER). Additionally, the high KER measured RFPADs could be explained using no time delay, suggesting that the different fragment KERs corresponded to different fragmentation pathways with different lifetimes.

Orientation and Alignment of Molecular Ions Produced in Photoionization. In photoionization leading to an excited state of a molecular ion, the polarization of the subsequent fluorescence can yield information about the orientation and alignment of the intermediate ion state. We have derived expressions for this process based on rotation specific photoionization cross sections and then determined the dependence of the fluorescence intensity on the polarization parameters (Stokes parameters) of both incident and emitted light. For the photoionization of N_2 leading to N_2^+ $B\,^2\Sigma_u^+$ state, a comparison of computed fluorescence intensity as a function of its polarization parameters with the experimental results obtained by J. E. Furst and coworkers, shows that the final residual molecular photoion, N_2^+ $X\,^2\Sigma_g^+$, is oriented and this is generally opposite to the direction reached in the simple excitation of the neutral nitrogen molecule by the absorption of circularly-polarized light. This clearly shows that the ejected electron in the ionization process carries away most of the free angular momentum in the collision.

Experimental Developments

Since the experimental half of the grant was transferred to Kansas State University, we purchased a spatial light modulator (SLM) that works in the 1000 nm to 1600 nm range. With this SLM we will be able to generate interference patterns of the driving pulse for interferometric studies with HHG. In particular, we can generate two foci from which harmonics can be generated and then interfere in the far field. However, for the types of molecules we are interested in studying, most of which have low ionization potentials, wavelengths longer than 800 nm are desired. For longer wavelengths the ponderomotive energy is larger and thus, the amount of observed harmonics increases with the wavelength squared. While some extension of the cutoff harmonics can be achieved by increasing the intensity, this approach is severely limited by the complete ionization of the molecule at higher intensities. In addition to extending the spectral range of the observed harmonics, using longer wavelengths also has the benefit of increasing the resolution of the measurement since the spacing between harmonics is twice the frequency of the fundamental. The SLM is currently being tested with a low power optical parametric amplifier (OPA).

Future Plans

Theoretically, we will explore the effects of resonances and electron correlation on the ellipticity of the light generated in the HHG process from aligned molecules. The next phase of the overset-grid iterative complex-Kohn project will be to include correlation effects first with

simple channel coupling, and subsequently including target correlation and polarization through optical potentials.

Experimentally, we will generate harmonics from two optical sources for interferometric studies with HHG with long wavelengths. We are particularly interested in studying the generation of harmonics from molecules that have similar chemical composition such molecular isomers. Because the SLM doesn't introduce any polarization, we have full control of the polarization state of the pulses after the SLM that will be relevant for studying molecules with chiral symmetry for example.

Publications in 2014-2016 Acknowledging Support from DOE

1. J. Jose, R. R. Lucchese, and T. N. Rescigno, Interchannel coupling effects in the valence photoionization of SF_6, *J. Chem. Phys.* **139**, 204305:1-10 (2014).
2. S. Marggi Poullain, C. Elkharrat, W. B. Li, K. Veyrinas, J.C. Houver, C. Cornaggia, T. N. Rescigno, R. R. Lucchese and D. Dowek, Recoil frame photoemission in multiphoton ionization of small polyatomic molecules: Photodynamics of NO_2 probed by 400 nm femtosecond pulses, *J. Phys. B* **47**, 124024:1-18 (2014).
3. M. Okunishi, R. R. Lucchese, T. Morishita, and K. Ueda, Rescattering photoelectron spectroscopy of small molecules, *J. Electron Spectrosc. Relat. Phenom.* **195**, 313-319 (2014).
4. Jesús A. López-Domínguez, Robert R. Lucchese, K. D. Fulfer, David Hardy, E. D. Poliakoff, and A. A. Aguilar, Vibrationally specific photoionization cross sections of acrolein leading to the $\tilde{X}\,^2A'$ ionic state, *J. Chem. Phys.* **141**, 094301:1-7 (2014).
5. U. Jacovella, D. M. P. Holland, S. Boyé-Péronne, D. Joyeux, L. E. Archer, N. de Oliveira, L. Nahon, R. R. Lucchese, Hong Xu, and S. T. Pratt, High-resolution photoabsorption spectrum of jet-cooled propyne, *J. Chem. Phys.* **141,** 114303:1-14 (2014).
6. J. Jose and R. R. Lucchese, Vibrational effects in the shape resonant photoionization leading to the $A\,^2T_{1u}$ state of SF_6^+, *Chem. Phys.* **447**, 64-70 (2015).
7. U. Jacovella, D. M. P. Holland, S. Boyé-Péronne, B. Gans, N. de Oliveira, D. Joyeux, L. E. Archer, R. R. Lucchese, H. Xu, and S. T. Pratt, High-resolution vacuum-ultraviolet photoabsorption spectra of 1-butyne and 2-butyne, *J. Chem. Phys.* **143**, 034304:1-14 (2015).
8. K. D. Fulfer, D. Hardy, A. A. Aguilar, and E. D. Poliakoff, High resolution photoelectron spectroscopy of the pyrimidine-type nucleobases, *J. Chem. Phys.* **142**, 224310:1-9 (2015).
9. Ugo Jacovella, David Holland, Séverine Boyé-Péronne, Bérenger Gans, Nelson de Oliveira, Kenji Ito, Denis Joyeux, Lucy Archer, Robert Lucchese, Hong Xu, Stephen Pratt, A Near-threshold Shape Resonance in the Valence-shell Photoabsorption of Linear Alkynes, *J. Phys. Chem. A* **119**, 12339-48 (2015).
10. Jesús A. López-Domínguez and Robert R. Lucchese, Effects of molecular rotation after ionization and prior to fragmentation on observed recoil-frame photoelectron angular distributions in the dissociative photoionization of non-linear molecules, *Phys. Rev. A* **93**, 033421:1-11 (2016).
11. M. V. Frolov, T. S. Sarantseva, N. L. Manakov, K. D. Fulfer, B. P. Wilson, J. Troß, X. Ren, E. D. Poliakoff, A. A. Silaev, N. V. Vvedenskii, A. F. Starace, and C. A. Trallero-Herrero, "Atomic photoionization experiment by harmonic-generation spectroscopy," *Phys. Rev. A* **93,** 031403(R):1-5 (2016).

Complexity and Correlated Motion of Electrons in Free and Confined Atomic Systems

Steven T. Manson, Principal Investigator
Department of Physics and Astronomy, Georgia State University, Atlanta, Georgia 30303
(smanson@gsu.edu)

Program Scope

The goals of this research program are: to further our understanding of the the interaction of radiation with matter; to provide theoretical support to, and collaboration with, various experimental programs that employ latest generation light sources, particularly ALS, APS and LCLS; and to study the properties (especially photoionization) of confined atoms and ions. Specifically, calculations are performed using and upgrading state-of-the-art theoretical methodologies to help understand the essential physics of the experimental results; to suggest future experimental investigations; and seek out new phenomenology, especially in the realm of confined systems. The primary areas of programmatic focus are: nondipole and relativistic effects in photoionization; photoabsorption of inner and outer shells of atoms and atomic ions (positive and negative); dynamical properties of atoms endrohedrally confined in buckyballs, primarily C_{60}; studies of Wigner time delay on the attosecond scale in photoionization of free and confined atomic systems. Flexibility is maintained to respond to opportunities as they arise.

Highlights of Recent Progress

The study of confined atoms is a rapidly growing field. Theoretical investigations of various atoms endohedrally confined in C_{60} [1,2] abound, but experimental studies are sparse [3-5]. Our theoretical program, at various levels of approximation, is aimed at mapping out the properties of such systems, especially photoionization, to guide experiment and uncover new phenomena. Among our major results, we have found that a huge transfer of oscillator strength from the C_{60} shell, in the neighborhood of the giant plasmon resonance, to the encapsulated atom for both $Ar@C_{60}$ [6] and $Mg@C_{60}$ [7]. And confinement resonances [8], oscillations in the photoionization cross section of an endohedral atom due to interferences of the photoelectron wave function for direct emission with those scattered from the surrounding carbon shell, were predicted in a broad range of cases; and their existence has been confirmed experimentally [4,5]. Further, in the photoionization of endohedral atoms within nested fullerenes, as a result of the multi-walled confinement, the confinement resonances become considerably more complicated [9]. In addition, spin-orbit induced confinement resonances in photoionization have been found owing to interchannel coupling between inner-shell spin-orbit split channels in endohedral atoms [10]. Confinement resonances also found to induce rather significant resonances in the attosecond time delay of photoelectron emission [11], which suggests that time-domain spectroscopy might be efficacious in studying endohedral systems and clusters. We have also explored the interatomic Coulomb decay (ICD) phenomenon in confined atoms and found, owing to hibridization between atomic and shell orbitals, that ICD occurs both ways, from atom to shell and

shell to atom, and the rates (widths) are often much larger than the ordinary Auger rates [12-14].

A number of aspects of attosecond time delay in the photoionization process were explored. Time delay of photoemission from valence subshells of noble-gas atoms were theoretically scrutinized within the framework of the dipole relativistic random phase approximation [15] with a focus on the variation of time delay in the vicinity of the Cooper minima where the corresponding dipole matrix element changes its sign while passing through a node. It was found that the presence of the Cooper minimum in one photoionization channel has a strong effect on time delay in other channels owing to interchannel coupling, and that relativistic effects strongly affect time delay significantly in regions of Cooper minima. A study of Wigner time delay in Mn photoionization in the region of the $3p \rightarrow 3d$ giant resonance showed the dramatic effect of the resonance on the time delay of photoemission from the $3d$ and $4s$ valence subshells of the Mn atom [16]. Similar features are expected to emerge in photoionization time delays of other transition-metal and rare-earth atoms with half-filled subshells that possess giant autoionization resonances as well. It was shown that photoionization time delay in the autoionizing resonance region is explicitly associated with the resonance lifetime, which can, thus, be directly measured in attosecond time-delay experiments. We also conducted a systematic study of the dipole phase and the Wigner time delay in inner-shell photoionization of noble gas atoms from Ne to Xe [17] using both the relativistic and the nonrelativistic versions of the random-phase approximation and found that the time delay, as a function of photoelectron energy, follows more or less a universal shape. And the angular distribution of Wigner time delay was investigated and it was found that strong angular anisotropy of the time delay in photoemission occurs near Cooper minima while the spin-orbit splitting affects the time delay near threshold [18].

Future Plans

Our future plans are to continue on the paths set out above. In the area of confined atoms, expand on our studies of interatomic Coulomb decay (ICD) of resonances. We will also work on ways to enhance the time-dependent local-density approximation to make it more accurate in our calculations of confined atoms. In addition, we shall work towards upgrading our theory to include relativistic interactions to be able to deal with heavy endohedrals with quantitative accuracy. We will also continue investigations into the attosecond time delay in photoionization that has been found in various experiments, and we will work to further our understanding of how confinement might affect this time delay. In addition, the search for cases where nondipole effects are likely to be significant, as a guide for experiment, and quadrupole Cooper minima, will continue. And we shall respond to new experimental results as they come up.

Publications over the Past 3 Years Citing DOE Support

- "Pronounced Effects of Interchannel Coupling In High-Energy Photoionization," W. Drube, T.M. Grehk, S. Thiess, G. B. Pradhan, H. R. Varma, P. C. Deshmukh and S. T. Manson, J. Phys. B **46**, 245006-1-6 (2013).
- "Positron differential studies: Comparison to photoionization," A. C. F. Santos, R. D. DuBois and S. T. Manson, AIP Conference Proceedings **1525**, 441-443 (2013).
- "Innershell Photoionization of Atomic Chlorine," W. C. Stolte, Z. Felfli, R. Guillemin, G. Ohrwall, S.–W. Yu, J. A. Young, D. W. Lindle, T. W. Gorczyca, N. C. Deb, S. T. Manson, A. Hibbert, and A. Z. Msezane, Phys. Rev. A **88**, 053425-1-11 (2013).

● "Photoionization of the 5s subshell of Ba in the region of the second Cooper minimum: cross sections and angular distributions," A. Ganesan, S. Deshmukh, G. B. Pradhan, V. Radojevic, S. T. Manson and P. C. Deshmukh, J. Phys. B **46**, 185002-1-5 (2013).
● "Probing confinement resonances by photoionizing Xe inside a C_{60}^{+} molecular cage," R. A. Phaneuf, A. L. D. Kilcoyne, N. B. Aryal, K. K. Baral, D. A. Esteves-Macaluso, C. M. Thomas, J. Hellhund, R. Lomsadze, T. W. Gorczyca, C. P. Ballance, S. T. Manson, M. F. Hasoglu, S. Schippers, and A. Müller, Phys. Rev. A **88**, 053402-1-7 (2013).
● "A Comprehensive X-ray Absorption Model for Atomic Oxygen," T. W. Gorczyca, M. A. Bautista, M. F. Hasoglu, J. Garcia, E. Gatuzz, J. S. Kaastra, T. R. Kallman, S. T. Manson, C. Mendoza, A. J. J. Raassen, C. P. de Vries and O. Zatsarinny, Astrophys. J. **779**, 78-1-11 (2013).
● "Photoionization study of Xe 5*s*: Ionization Cross Sections and Photoelectron Angular Distributions," G. Aarthi, J. Jose, S. Deshmukh, V. Radojević, P. C. Deshmukh and S. T. Manson, J. Phys. B **47**, 025004-1-5 (2014).
● "Valence Photoionization of Noble Gas Atoms Confined in the Fullerene C_{60}," M. H. Javani**,** H. S. Chakraborty, and S. T. Manson, Phys. Rev. A **89**, 053402-1-12 (2014).
● "Resonant Auger-intersite-Coulombic hybridized decay in the photoionization of endohedral fullerenes" by M. H. Javani, J. B. Wise, R. De, M. E. Madjet, H. S. Chakraborty, and S. T. Manson, Phys. Rev. A **89**, 063420-1-4 (2014).
● "Attosecond time delay in the photoionization of endohedral atoms A@C_{60}: A new probe of confinement resonances," P. C. Deshmukh, A. Mandal, S. Saha, A. S. Kheifets, V. K. Dolmatov and S T Manson, Phys. Rev. A **89**, 053424-1-4 (2014).
● "Photoionization of Ca 4s in a spherical attractive well potential: dipole, quadrupole and relativistic effects," A. Kumar, G. B. Pradhan, H. R. Varma, P. C. Deshmukh and S. T. Manson, J. Phys. B **47**, 185003-1-8 (2014).
● "Photoionization of bonding and antibonding-type atom-fullerene hybrid states in Cd@C_{60} vs Zn@C_{60}," M. H. Javani, R. De, M. E. Madjet, S. T. Manson and H. S. Chakraborty, J. Phys. B **47,** 175102-1-7 (2014).
● "Empirical Formulae for Direct Double Ionization by Bare Ions: Z= -1 to +92," A. C. F. Santos, R. D. DuBois and S. T. Manson, Phys. Rev. A **90**, 052721-1-10 (2014).
● "Relativistic effects in photoionization time delay near the Cooper minimum of noble gas atoms," S. Saha, A, Mandal, J. Jose, H. R. Varma, P. C. Deshmukh, A. S. Kheifets, V. K. Dolmatov and S. T. Manson, Phys. Rev. A **90**, 053406-1-7 (2014).
● "Fano shape analysis of autoionization resonances in neon isoelectronic sequence using relativistic multichannel quantum defect theory," M. Nrisimhamurty, G. Aravind, P. C. Deshmukh and S. T. Manson, Phys. Rev A **91**, 013404-1-12 (2015).
● "Attosecond time delay in the photoionization of Mn in the 3p → 3d giant resonance region," V. K. Dolmatov, A. S. Kheifets, P. C. Deshmukh and S. T. Manson, Phys. Rev. A **91**, 053415-1-7 (2015).
● "Model potentials for a C_{60} shell." A. S. Baltenkov, S. T. Manson and A. Z, Msezane, *Proceedings of Dynamic Systems and Applications* **7**, 275-281 (2016).
● "Photoabsorption studies of some closed-shell ions in the La isonuclear sequence," S. Kalyadan, H. R. Varma, P. C. Deshmukh, J. T. Costello, P. Hayden and S. T. Manson, Phys. Rev. A **91**, 053422-1-8 (2015).
● "Photoionization of Endohedral Atoms: Molecular and Interchannel Coupling Effects" A. Ponzi, P. Decleva and S. T. Manson, Phys. Rev. A **92**, 023405-1-7 (2015).
● "Jellium Model Potentials for the C_{60} Molecule and the Photoionization of Endohedral Atoms, A@C_{60}," A. S. Baltenkov, S. T. Manson S. T. and A. Z. Msezane, J. Phys. B **48**, 185103-1-8 (2015).
● "Wigner time delay studies of the photoionization of atomic zinc and cadmium," S. Saha, A. Mandal, P. C. Deshmukh, A. Kheifets, V. K. Dolmatov and S. T. Manson, J. Phys. Conf. Ser. **635**, 092061 (2015).
● "Time delay in photoionization of half-filled shell atoms," V. K. Dolmatov, A. S. Kheifets, S. T. Manson and P. C. Deshmukh, J. Phys. Conf. Ser. **635**, 092004 (2015).
● "Wigner time delay in quadrupole photoionization channels in atomic Hg," A. Mandal, S. Saha, T. Banerjee, P. C. Deshmukh, A. Kheifets, V. K. Dolmatov and S. T. Manson J. Phys. Conf. Ser. **635**, 092097 (2015).
● "Effect of coulomb confinement resonances on time delay in Ne@C_{60}^{-5}," A. Kumar, H. R. Varma, P. C. Deshmukh, S. T. Manson, V. K. Dolmatov and A. S. Kheifets, J. Phys. Conf. Ser. **635**, 092042 (2015).
● "Multiple Cooper minima in ground state E2 photoionization of high Z atoms," T. Banerjee, A. Mandal, P. C. Deshmukh and S. T. Manson, J. Phys. Conf. Ser. **635**, 092128 (2015).
● "Possible Evidence of 3rd and 4th order Contributions to Double Ionization of Helium by Protons and Antiprotons," A. C. F. Santos, R. D. DuBois, and S. T. Manson, J. Phys. Conf. Ser. **635**, 022017 (2015).
● "Auger-intercoulombic hybridized decay resonances in Kr@C_{60}," M. Magrakvelidze, R. De, S. T. Manson and H. S. Chakraborty, J. Phys. Conf. Ser. **635**, 112023 (2015).
● "Confinement Effects On Spin-Orbit Activated Interchannel Coupling," D. A. Keating, P. C. Deshmukh and S. T Manson, J. Phys. Conf. Ser. **635**, 092009 (2015).

● "Shape of Model Potentials for a C_{60} Shell," S. T. Manson, A. S. Baltenkov, and A. Z. Msezane, J. Phys. Conf. Ser. **635**, 112005 (2015).
● "K-shell Photoionization of Atomic Cl," Z. Felfli, S. T. Manson and A. Z. Msezane, J. Phys. Conf. Ser. **635**, 092132 (2015).
● "Photoionization of the 2p subshell in the Ar isonuclear sequence," Aarthi Ganesan, Sudha Deshmukh, Jobin Jose, Gagan B. Pradhan, Vojislav Radojevic, Pranawa C. Deshmukh and Steven T. Manson, J. Phys. Conf. Ser. **635**, 092054 (2015).
● "Inner-shell autoionization resonances along Mg isoelectronic sequence," K. Sindhu, H. R. Varma, P. C. Deshmukh and S. T. Manson, J. Phys. Conf. Ser. **635**, 092055 (2015).
● "Dipole phase and photoelectron group delay in inner shell photoionization," A. S. Kheifets, S. Saha, P. C. Deshmukh, D. A. Keating, and S. T. Manson, Phys. Rev. A **92**, 063422-1-9 (2015).
● "Coherence of Auger and inter-Coulombic decay processes in the photoionization of $Ar@C_{60}$ versus $Kr@C_{60}$," M. Magrakvelidze, Ruma D., M. H. Javani, M. E. Madjet, S. T. Manson, and H. S. Chakraborty, Eur. Phys. J. D **70**, 96-1-7 (2016).
● "Correlation Study of Endohedrally Confined Alkali Earth Atoms (A@C 60)," M. F. Hasoğlu, H.-L. Zhou, and S. T. Manson, Phys. Rev. A **93**, 022512-1-5 (2016).
● "First prediction of inter-Coulombic decay of C_{60} inner vacancies through the continuum of confined atoms," R. De, M. Magrakvelidze, M. E. Madjet, S. T. Manson and H. S. Chakraborty, J. Phys. B **49**, 11LT01-1-5 (2016).
● "Relativistic calculations of angular dependent photoemission time delay," A. Kheifets, A. Mandal, P. C. Deshmukh, V. K. Dolmatov, D. A. Keating and S. T. Manson, Phys. Rev. A **94**, 013423-1-7 (2016).
● "Wigner photoemission time delays from endohedral anions," A. Kumar, H. R. Varma, P. C. Deshmukh, S. T. Manson, V. K. Dolmatov and A. S. Kheifets, Phys. Rev. A (in press).
● "Spin-Orbit Activated Confinement Resonances," D. A. Keating, P. C. Deshmukh and S. T. Manson, Phys Rev. A (submitted).

References

[1] V. K. Dolmatov, A. S. Baltenkov, J.-P. Connerade and S. T. Manson, Radiation Phys. Chem. **70**, 417 (2004) and references therein.
[2] V. K. Dolmatov, Advances in Quantum Chemistry, **58**, 13 (2009) and references therein.
[3] A. Müller *et al*, Phys. Rev. Lett. **101**, 133001 (2008).
[4] A. L. D. Kilcoyne, A. Aguilar, A. Müller, S. Schippers, C. Cisneros, G. Alna'Washi, N. B. Aryal, K. K. Baral, D. A. Esteves, C. M. Thomas, and R. A. Phaneuf, Phys. Rev. Lett. **105**, 213001 (2010).
[5] R. A. Phaneuf, A. L. D. Kilcoyne, N. B. Aryal, K. K. Baral, D. A. Esteves-Macaluso, C. M. Thomas, J. Hellhund, R. Lomsadze, T. W. Gorczyca, C. P. Ballance, S. T. Manson, M. F. Hasoglu, S. Schippers, and A. Müller, Phys. Rev. A **88**, 053402-1-7 (2013).
[6] M. E. Madjet, H. S. Chakraborty and S. T. Manson, Phys. Rev. Letters **99**, 243003 (2007).
[7] M. E. Madjet, H. S. Chakraborty, J. M. Rost and S. T. Manson, Phys. Rev. A **78**, 013201 (2008).
[8] V. K. Dolmatov and S. T. Manson, J. Phys. B **41**, 165001 (2008).
[9] V. K. Dolmatov and S. T. Manson, J. Phys. Rev. A **78**, 013415 (2008).
[10] D. A. Keating, P. C. Deshmukh and S. T. Manson, Phys Rev. A (submitted).
[11] P. C. Deshmukh, A. Mandal, S. Saha, A. S. Kheifets, V. K. Dolmatov and S T Manson, Phys. Rev. A **89**, 053424 (2014).
[11] H. S. Chakraborty, M. E. Madjet, T. Renger, J.-M. Rost and S. T. Manson, Phys. Rev. A **79**, 061201(R) (2009).
[12] M. H. Javani, J. B. Wise, R. De, M. E. Madjet, H. S. Chakraborty, and S. T. Manson, Phys. Rev. A **89**, 063420 (2014).
[13] M. Magrakvelidze, Ruma D., M. H. Javani, M. E. Madjet, S. T. Manson, and H. S. Chakraborty, Eur. Phys. J. D **70**, 96 (2016).
[14] R. De, M. Magrakvelidze, M. E. Madjet, S. T. Manson and H. S. Chakraborty, J. Phys. B **49**, 11LT01-1-5 (2016).
[15] S. Saha, A. Mandal, J. Jose, H. R. Varma, P. C. Deshmukh, A. S. Kheifets, V. K. Dolmatov and S. T. Manson, Phys. Rev. A **90**, 053406 (2014).
[16] V. K. Dolmatov, A. S. Kheifets, P. C. Deshmukh and S. T. Manson, Phys. Rev. A **91**, 053415 (2015).
[17] A. S. Kheifets, S. Saha, P. C. Deshmukh, D. A. Keating, and S. T. Manson, Phys. Rev. A **92**, 063422 (2015).
[18] A. Kheifets, A. Mandal, P. C. Deshmukh, V. K. Dolmatov, D. A. Keating and S. T. Manson, Phys. Rev. A **94**, 013423 (2016).

ABSTRACT

ELECTRON-DRIVEN PROCESSES IN POLYATOMIC MOLECULES

Investigator: Vincent McKoy

A. A. Noyes Laboratory of Chemical Physics
California Institute of Technology
Pasadena, California 91125

email: mckoy@caltech.edu

PROJECT DESCRIPTION

The focus of this project is the development and application of accurate, scalable methods for computational studies of low-energy electron–molecule collisions, with emphasis on larger polyatomics relevant to electron-driven chemistry in biological and materials-processing systems. Because the required calculations are highly numerically intensive, efficient use of large-scale parallel computers is essential, and the computer codes developed for the project are designed to run both on tightly-coupled parallel supercomputers and on workstation clusters.

HIGHLIGHTS

In the past year we wrapped up a series of electron-impact excitation studies and made significant progress in developing more efficient techniques for accurate electron collision calculations on large molecules. Highlights include:

- Completed and published a joint experimental-theoretical study of electron-impact excitation of ethanol
- Published initial results using local orbitals to treat polarization in elastic electron-molecule scattering
- Published results of a joint experimental-theoretical study of elastic electron scattering by pyrimidine

ACCOMPLISHMENTS

We have continued to investigate the use of local orbitals in the treatment of polarization effects, which are essential to accurate descriptions of low-energy electron-molecule collisions. A pilot study on the ethene dimer was completed and published [1] and we are following up that work with calculations on the uracil-adenine base pair that is found in ribonucleic acid (RNA) and on smaller model systems (small-molecule dimers) that can also be treated accurately by conventional techniques. The results of the pilot study demonstrated that the local-orbital approach produces physically reasonable results, but aspects of the convergence behavior need further clarification—in particular, why the method seemed to work better than expected.

During the year we also completed and published a study of electron-impact excitation to low-lying electronic states of ethanol (ethyl alcohol) [2]. This work completed a series of studies on related molecules carried out in collaboration with the experimental groups of Profs. Murtadha Khakoo and Leigh Hargreaves at California State University, Fullerton, with earlier papers addressing water [3] and methanol [4].

In the context of the same longstanding collaboration with the experimental program at California State University, Fullerton, we published results from a study of chloroethane, C_2H_5Cl [5], and initiated studies on electron scattering by propene (propylene), C_3H_6. Because some literature data already exists for propene, our principal interest here is detailed comparison with experimental results at the lowest collision energies, where accurate treatment of resonances and target polarization are critical. This work is nearing completion and will be published in the coming year.

In collaboration with the experimental group of Michael Allan (University of Fribourg, Switzerland) and with theories using a different computational approach, we also published a paper [6] extending our earlier work [7] on elastic electron scattering from the pyrimidine molecule, which is the prototype for the "pyrimidine" nucleobases found in RNA and DNA. Aside from demonstrating highly satisfactory agreement

between our calculations and the Allan group's measurements, this work suggested that single-point, fixed-nuclei calculations of electron-molecule cross sections may best be compared with vibrationally summed, rather than vibrationally elastic, measurements.

PLANS FOR COMING YEAR

In the coming year we plan to wrap up and publish all ongoing work, including studies of the uracil-adenine base pair and of propene. Additional studies applying local orbitals to electron collisions with large targets will be undertaken as time permits.

REFERENCES

[1] C. L. Winstead and V. McKoy, Eur. Phys. J. D **70**, 117 (2016).
[2] L. R. Hargreaves, M. A. Khakoo, C. Winstead, V. McKoy, J. Phys. B **49**, 185201 (2016).
[3] K. Ralphs, G. Serna, L. R. Hargreaves, M. A. Khakoo, C. Winstead, and V. McKoy, J. Phys. B **46**, 125201 (2013).
[4] K. Varela, L. R. Hargreaves, K. Ralphs, M. A. Khakoo, C. Winstead, V. McKoy, T. N. Rescigno, and A. E. Orel, J. Phys. B **48**, 115208 (2015).
[5] A. Sakaamini, C. Navarro, J. Cross, L. R. Hargreaves, M. A. Khakoo, Kamil Fedus, C. Winstead, and V. McKoy, J. Phys. B **48**, 205202 (2015)
[6] K. Regeta, M. Allan, C. Winstead, V. McKoy, Z. Mašín, and J. D. Gorfinkiel, J. Chem. Phys. **144**, 024301 (2016).
[7] P. Palihawadana, J. Sullivan, M. Brunger, C. Winstead, V. McKoy, G. Garcia, F. Blanco, and S. Buckman, Phys. Rev. A **84**, 062702 (2011).

PROJECT PUBLICATIONS AND PRESENTATIONS, 2014–2016

1. "Low-Energy Elastic Electron Scattering by Acetaldehyde," A. Gauf, C. Navarro, G. Balch, L. R. Hargreaves, M. A. Khakoo, C. Winstead, and V. McKoy, Phys. Rev. A **89**, 022708 (2014).

2. "Low-Energy Elastic Electron Scattering from Isobutanol and Related Alkyl Amines," K. Fedus, C. Navarro, L. R. Hargreaves, M. A. Khakoo, F. M. Silva, M. H. F. Bettega, C. Winstead, and V. McKoy, Phys. Rev. A **90**, 032708 (2014).

3. "Excitation of the 4 Lowest Electronic Transitions in Methanol by Low-Energy Electrons," K. Varela, L. R. Hargreaves, K. Ralphs, M. A. Khakoo, C. Winstead, V. McKoy, T. N. Rescigno, and A. E. Orel, J. Phys. B **48**, 115208 (2015).

4. "Low-energy elastic electron scattering from chloromethane, CH_3Cl," C. Navarro, A. Sakaamini, J. Cross, L. R. Hargreaves, M. A. Khakoo, Kamil Fedus, C. Winstead, and V. McKoy, J. Phys. B **48**, 195202 (2015).

5. "Low-energy elastic electron scattering from chloroethane, C_2H_5Cl," A. Sakaamini, C. Navarro, J. Cross, L. R. Hargreaves, M. A. Khakoo, Kamil Fedus, C. Winstead, and V. McKoy, J. Phys. B **48**, 205202 (2015).

6. "Resonance Effects in Elastic Cross Sections for Electron Scattering on Pyrimidine: Experiment and Theory," K. Regeta, M. Allan, C. Winstead, V. McKoy, Z. Mašín, and J. D. Gorfinkiel, J. Chem. Phys. **144**, 024301 (2016).

7. "Excitation of the Lowest Electronic Transitions in Ethanol by Low-Energy Electrons," L. R. Hargreaves, M. A. Khakoo, C. Winstead, and V. McKoy, J. Phys. B **49**, 185201 (2016).

8. "Local Orbitals in Electron Scattering Calculations," C. L. Winstead and V. McKoy, Eur. Phys. J. D **70**, 117 (2016).

ELECTRON/PHOTON INTERACTIONS WITH ATOMS/IONS

Alfred Z. Msezane (email: amsezane@cau.edu)

Clark Atlanta University, Department of Physics and CTSPS**,** Atlanta, Georgia 30314

PROGRAM SCOPE

The project's primary objective is to gain a fundamental understanding of the near-threshold electron attachment mechanism in atoms as well as identify and delineate resonances. We have now linked directly low-energy electron scattering resonances with chemical reaction dynamics. This has allowed us to probe sensitively low-energy electron attachment in complex atoms, resulting in short- and long-lived negative ion formation. The complex angular momentum (CAM) methodology, wherein is fully embedded the crucial electron-electron correlations and the core polarization interaction, is used for the investigations. Regge trajectories allow us to probe electron attachment at the fundamental level near threshold, thereby uncovering new manifestations, including the mechanism of nanocatalysis.

We have also investigated the electronic structure of the doubly-charged C_{60}^{-} negative ion as well as electronic confinement in cylindrical potential well. R-matrix computation of the demanding inner-shell photoionization of atomic Cl continues.

PROGRESS – Accomplishments in 2015-16

A.1 Electron elastic scattering by lanthanide atoms Nd, Eu, Tb and Tm

In exploring electron elastic scattering from atomic Au in the electron impact energy range $0.01 \leq E \leq 5.0$ eV, searching for negative ion formation in Au, the CAM calculated electron elastic scattering total cross section (TCS) for Au was benchmarked through the measured electron affinity (EA) value of 2.309 eV [1]. This value corresponded to the energy of the dramatically sharp resonance appearing at the second Ramsauer-Townsend (R-T) minimum of the TCS for Au [2]. A similar procedure was adopted for the electron scattering from Pt and In, where the energies of the sharp resonances in their TCSs matched the measured EAs of Pt [3] and In [4]. Here we have benchmarked the CAM calculated TCS for Eu through the measured EAs [5, 6], corresponding to the energies of the very sharp resonances appearing at 0.116eV and 1.053eV, respectively. Also, the energies of the sharp resonances in the CAM calculated TCSs for Nd, Tb and Tm agreed excellently with the experimental EAs [7, 8]; thus the TCSs were benchmarked.

It must be emphasized here that the benchmarked TCSs were calculated independently of the measurements; the extracted energy positions of the resonances were then compared with the measured EAs. The energy of the very sharp resonance at the second R-T minimum of the CAM calculated TCS for At agreed very well with the existing theoretical EAs ~ 2.5 eV [9, 10]. The agreement between the CAM calculated energy positions of the resonances in the TCSs and the measured or calculated EAs of simple and complex atoms is no surprise. The reason is that Regge poles, singularities of the S-matrix, rigorously define resonances. Therefore, the Regge-pole (also known as the CAM) method is appropriate for the present investigations of the binding energies (BEs), including the EAs of the lanthanide atoms. We should stress that the Regge-pole method requires no *a priori* knowledge of experimental or other theoretical data as input for the TCSs calculations.

The CAM calculated energy positions of the dramatically sharp resonances, particularly those appearing at the second Ramsauer-Townsend (R-T) minima of the TCSs, for many simple and complex atoms have been identified with the measured or calculated EAs. These resonances span a wide range of the electron impact energies, from near zero to about 3.5 eV. So, the CAM method can be used comfortably to investigate low-energy electron scattering through the TCS calculation searching for electron attachment manifesting as

long-lived resonances. For the Nd, Eu, Tb and Tm atoms we found new resonances at the electron energies of 1.88 eV, 2.64 eV, 3.05 eV and 3.36 eV, respectively at their second R-T minima.

Indeed, the appearance of the bound states of the negative ions, created during the collisions at the R-T minima of the TCSs, provides an excellent environment and mechanism for breaking up molecular bonds in new molecules creation from atoms as well as in catalysis through negative ions.

A.2 Novel mechanism for creating long-lived metastable atomic negative ions

A novel mechanism is proposed for creating long-lived metastable atomic negative ions and demonstrated in the lanthanide atoms Tb and Dy. It exploits the orbital collapse of the 5d orbital in Gd(Z=64) into the 4f orbital of Tb(Z=65). The importance of the d orbital collapse phenomenon enhancing the influence of the core-polarization has been demonstrated in the isoelectronic sequence of the singly ionized Yb [11]. In the region of collapse the properties of the 5d and 4f orbitals are quite sensitive to the changes in the effective potential. Consequently the collapse phenomenon impacts the core-polarization interaction in the relevant atom, Tb. As a result, a new excited state is induced in the Tb atom. Its TCS resembles that of the ground state TCS with a dramatically sharp resonance appearing in its second R-T minimum at the energy of 1.20eV, corresponding to a Tb^- metastable negative ion formation. The ground state resonance energy is at 3.05 eV, also appearing at the second R-T minimum of the ground state TCS.

The complete 5d orbital collapse occurring in Gd does not lead necessarily to maximum polarization in Tb, which occurs in the Dy atom. Consequently, the proposed novel mechanism of creating long-lived metastable negative ions should be observable in both Z=65 and Z=66 atoms through the appearance of dramatically sharp resonances in the newly generated TCSs. We expect the mechanism to be realizable in the isoelectronic sequences of these atoms as well.

A.3 Resonances in low-energy electron scattering from complex open subshell atoms

The CAM method is used to investigate low-energy electron elastic scattering from the representative complex open d-subshell atoms: Nb, Rh, W, Hf, Os and Th, open p-subshell atom Sn and the open f-subshell atoms Eu and At through the calculation of their elastic TCSs in the electron impact energy range $0.01 \leq E \leq 7.0$ eV. We search for dramatically sharp resonances in the TCSs manifesting long- and short-lived negative ion formation during the collisions, and extract the energy positions of the R-T minima and shape resonances (SRs) as well. The objective is toward gaining a fundamental understanding of electron interactions with and attachment in these open subshell atoms. The common and striking features of these TCSs, resembling those of atomic Au and Pt are the appearance of a dramatically sharp resonance at large electron impact energy ~ 2.5 eV in the second R-T minimum of the ground state TCS and a broad deep R-T minimum in the first excited state TCS for the open d- and f-subshell atoms.

The TCSs for the experimentally studied extensively Sn atom resemble those of Au and Pt as well; therefore they are also used as benchmarks. The listed atoms through their negative ions promise to be useful *inter alia* in nanocatalysis including in methane partial oxidation to methanol without CO_2 emission. The results for these atoms spanning a wide range of Z values and electronic structure complexities demonstrate that the CAM method is very efficient in calculating accurate resonance positions as well as EAs, requiring only a few poles and *no a priori* knowledge of the experimental or other theoretical data; this is its power. Henceforth electron attachment in many complex atoms, particularly the lanthanide and actinide atoms will be probed efficiently and reliably.

A.4 Electronic Quantum Confinement in Cylindrical Potential Well

The effects of quantum confinement on the momentum distribution of electrons confined within a cylindrical potential well have been analyzed. The motivation is to understand specific features of the momentum distribution of electrons when the electron behavior is completely controlled by the parameters of a non-isotropic potential cavity. It is shown that studying the solutions of the wave equation for an

electron confined in a cylindrical potential well offers the possibility to analyze the confinement behavior of an electron executing one- or two-dimensional motion in the remaining three-dimensional space within the framework of the same mathematical model of the potential well. Some low-lying electronic states with different symmetries have been considered and the corresponding wave functions have been calculated; the behavior of their nodes and their peak positions with respect to the parameters of the cylindrical well has been analyzed.

Additionally, the momentum distributions of electrons in these states have been calculated. The limiting cases of the ratio of the cylinder length L and its radius R_0 have been considered; when the cylinder length L significantly exceeds its radius R_0 and when the cylinder radius is much greater than its length. The cylindrical quantum confinement effects on the momentum distribution of electrons in these potential wells have been analyzed. The possible application of the results obtained here for the description of the general features in the behavior of electrons in nanowires with metallic type of conductivity (or nanotubes) and ultrathin epitaxial films (or graphene sheets) are discussed. Possible experiments are suggested where the quantum confinement can be manifested.

A.5 Doubly-charged Negative Ion of C_{60} Molecule

Within the Dirac- and Lorentz-bubble potential models an electronic structure of the doubly-charged negative ion C_{60}^{2-} has been studied by a variational method. It is shown that even in the first approximation of this method when a trial wave function of the two electrons is represented as a product of one-electron functions the total energy of the system is negative, a manifestation of the existence of a stable state of the doubly-charged negative ion in these models. The second electron affinity of C_{60} according to estimation is about $\varepsilon_2 \approx 1$ eV. The photodetachment cross sections $\sigma(\omega)$ of this ion have been calculated as well. Near threshold $\sigma(\omega)$ is found to exhibit peculiar and interesting behavior. The first cross section accompanied by the transformation of the doubly-charged negative ion into a singly-charged one is exponentially small near the process threshold. The second cross section corresponds to the photodetachment of a singly-charged ion; it increases at the threshold as a power function of the kinetic energy of the photoelectron. These cross sections are of the same order as the photodetachment cross sections of atomic ions with the same electron affinity.

A.6. Innershell Photoionization of Atomic Chlorine

Relative partial cross sections have been measured following photoexcitation of atomic chlorine near the Cl 2p and Cl 1s ionization thresholds. In addition, Breit-Pauli R-matrix calculations have been carried out in the region of the 2p thresholds, and the results are compared with experiment [12]. Owing to angular-momentum considerations, it was found that the resonances associated with the higher $2p^{-1}$ thresholds should be significantly wider than the lower ones, and this is borne out both in the experimental and the theoretical results. It is shown that a large number of resonance series contribute to the cross section, which make it difficult to untangle, and suggestions for further work to better understand the spectra are presented.

CONTINUING Investigations

The finding under A.3 that the common and characteristic features of the TCSs for the open d- and f-subshell atoms are the appearance of a dramatically sharp resonance at large electron impact energy ~ 2.5 eV in the second R-T minimum of the ground state TCS and a broad deep R-T minimum in the first excited state TCS, has motivated us to continue to investigate low-energy electron scattering from the lanthanide atoms in the electron impact energy range $0.11 \leq E \leq 5.0$ eV. We search for both electron attachment manifesting as resonances in the TCSs and long-lived metastable negative ions due to orbital collapse as described under section **A.2.** The sophisticated potential used in the CAM method is being adapted for use in electron elastic scattering from C_{60} and other fullerenes. And investigations of inner-shell photoionization of atomic Cl will be completed.

References

[1] H. Hotop and W. C. Lineberger, J. Phys. Chem. Ref. Data 14, 731(1985)
[2] A.Z. Msezane, Z. Felfli and D. Sokolovski, J. Phys. **B 41**, 105201 (2008)
[3] R.C. Bilodeau, M. Scheer, H.K. Haugen and R.L. Brooks, Phys. Rev. A **61,** 012505 (1995)
[4] C.W. Walter, N.D. Gibson, Y.G. Li, and D.J. Matyas, Phys. Rev. A **82**, 032507 (2010)
[5] S. -B. Cheng and A.W. Castleman, Jr., Sci. Rep. **5**, 12414 (2015)
[6] V. T. Davis and J. S. Thompson, J. Phys. B **37**, 1961 (2004).
[7] V. T. Davis, J. S. Thompson, and A. Covington, NIMB **241**, 118 (2005)
[8] V. T. Davis and J. S. Thompson, Phys. Rev. A **65**, 010501 (R) (2001).
[9] R.J. Zollweg, J. Chem. Phys. **50**, 4251 (1969)
[10] J. Li, Z. Zhao, M. Andersson, X. Zhang, and C. Chen, J. Phys. B **45,** 165004 (2012)
[11] J. Migdalek and W. Siegel, Phys. Rev. A **61**, 062502 (2000)
[12] W. C. Stolte, Z. Felfli, R. Guillemin, G. Ohrwall, S.–W. Yu, J. A. Young, D. W. Lindle, T. W. Gorczyca, N. C. Deb, S. T. Manson, A. Hibbert, and A. Z. Msezane, Phys. Rev. A **88**, 053425 (2013).

Publications acknowledging DOE Grant 2015-2016

[1] "Electronic Quantum Confinement in Cylindrical Potential Well", A. S. Baltenkov and A. Z. Msezane, Euro Phys. J. D **70**, 81 (2016).
[2] "Photoabsorption spectra of Xe atoms encapsulated inside fullerenes", Zhifan Chen and Alfred Z Msezane, Eur. Phys. J. D **69**, 88 (2015) http://dx.doi.org/10.1140/epjd/e2015-50608-8
[3] "Heavy fermion spin liquid in herbertsmithite", V.R. Shaginyan, M.Ya. Amusia, A.Z. Msezane, K.G. Popov, V.A. Stephanovich, Phys. Lett. A **379**, 2092-2096 (2015) doi:10.1016/j.physleta.2015.05.036
[4] "Jellium Model Potentials for the C60 Molecule and the Photoionization of Endohedral Atoms, A@C60", Baltenkov, Arkadiy; Manson, Steven; Msezane, Alfred, J. Phys. B **48,** 185103 (2015)
[5] "Doubly-charged Negative Ion of C60 Molecule", A. S. Baltenkov and A. Z. Msezane, Proceedings of Dynamic Systems and Applications **7**, 239–245 (2016)
[6] "Model Potentials for a C60 Shell", S. T. Manson, A. S. Baltenkov and A. Z. Msezane, Proceedings of Dynamic Systems and Applications 7, 275–281(2016).
[7] "Tunable catalysis of water to peroxide with Anionic, Cationic and Neutral Atomic Au, Ag, Pd, Rh and Os", K. Suggs, F. Kirros, A. Tesfamichael, Z. Felfli and A. Z. Msezane, Nanosci. Technol. **2(2),** At Press (2016)
[8] "Scaling behavior of the thermopower of the archetypal heavy-fermion metal YbRh2Si2", V. R. Shaginyan, A. Z. Msezane, G. S. Japaridze, K. G. Popov and V. A. Khodel, Front. Phys**. 11**(2), 117101 (2016).
[9] "Off center effect on the photoabsorption spectrum of the Xe@C60 endohedral fullerene", Zhifan Chen, A. Z. Msezane, J. Phys: Conference Series, **488**, 022001 (2015)
[10] "Shape of Model Potentials for a C60 Shell", Manson S. T., Baltenkov A. S., and Msezane A. Z., Journal of Physics: Conference Series **635,** 112005 (2015).
[11] "K-shell Photoionization of Atomic Cl", Felfli Z., Manson S. T. and Msezane A. Z., Journal of Physics: Conference Series **635,** 092132 (2015).
[12] "Charge modification of metal atoms: Catalysis of Water to Peroxide", K. Suggs, F. Kiros, A. Tesfamichael, Z. Felfli and A. Z. Msezane, Journal of Physics: Conference Series **635** (2015) 052018
[13] "Topological grounds for challenging behavior of the heavy-fermion metal *beta*-YbAlB4 under the application of magnetic field and pressure", V. R. Shaginyan, A. Z. Msezane, K. G. Popov, J. W. Clark, V. A. Khodel, and M. V. Zverev, Phys. Rev. B **93**, 205126 (2016)
[14] "Strongly correlated Fermi systems as a new state of matter", V. R. Shaginyan, A. Z. Msezane, G. S. Japaridze, K. G. Popov, and V. A. Khodel, Front. Phys. **12(1),** 127101 (2017).

Theory and Simulation of Nonlinear X-ray Spectroscopy of Molecules

Shaul Mukamel
University of California, Irvine, CA 92697
smukamel@uci.edu
Progress Report September 2016
DOE DE-FG02-04ER15571

Program Scope

Nonlinear X-ray spectroscopy experiments which use sequences of coherent broadband X-ray pulses are made possible by new ultrafast X-ray free electron laser (XFEL) and high harmonic generation (HHG) sources. These techniques provide unique windows into the motions of electrons and nuclei in molecules and materials and offer novel probes for electron and energy transfer in molecular complexes. This program is aimed at the design of X-ray pulse sequences for probing core and valence electronic excitations, and the development of effective simulation protocols for describing multiple-core excited state energetics and dynamics. Applications are made to time-resolved photoelectron spectroscopy, detecting strongly coupled electron-nuclear dynamics in molecules through electronic coherence observed in multidimensional broadband stimulated X-ray Raman signals, and investigating multiple core excitations in molecules by X-ray double-quantum coherence signals.

Recent Progress

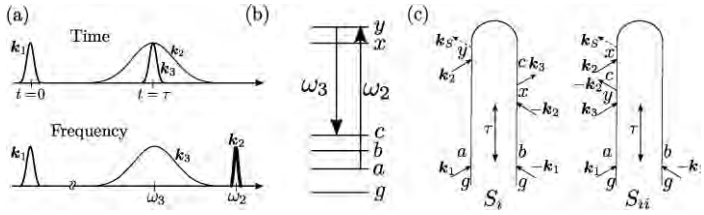

Fig. 1: (a) Pulse sequence for the hybrid (narrow pump/broad probe) stimulated Raman experiment. (b) Level scheme g is the ground-state of the neutral molecule, a, b and c are valence-states of the cation with a core hole, and x and y are two-core-hole states. (c) The two contributing loop diagrams.

Hybrid stimulated X-ray Raman spectroscopy (HSXRS) is an extension of femtosecond optical stimulated Raman spectroscopy to the X-ray regime. This technique combines a narrowband pump and a broadband probe pulse, to induce an X-ray Raman process and create a valence excited state wavepacket (Fig. 1) that can be probed with high temporal and spectral resolutions. One possibility to realize this technique is by using a 200 fs XFEL pulse as the narrowband pump and a HHG pulse as the broadband attosecond probe.

The technique was applied to monitor conical intersections CoIn in the ring opening of furan. [1] Attosecond X-ray pulses are short enough to capture snapshots of molecules undergoing nonadiabatic electron and nuclear dynamics at CoIns. We showed that HSXRS can probe the nonadiabatic dynamics and detect the ultrafast (4.5 fs) passage through a CoIn. This is demonstrated by a multiconfiguration self-consistent-field study of the dynamics and spectroscopy of the furan ring-opening reaction. Trajectories generated by surface hopping simulations were used to predict signals at reactant and product structures as well as representative snapshots along the conical intersection seam (Fig. 2). The signals were shown to be particularly sensitive to the changes in nonadiabatically coupled electronic structure and geometry.

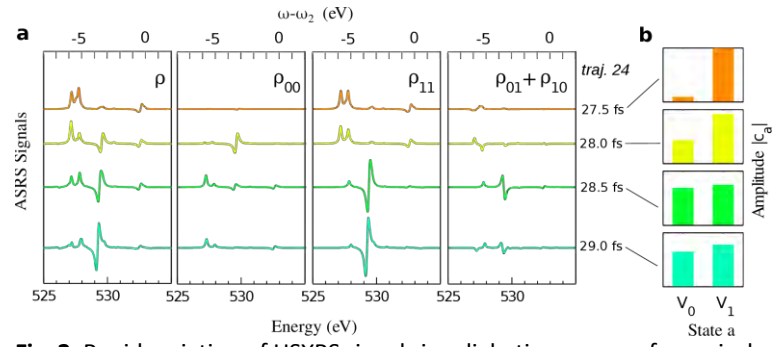

Fig. 2: Rapid variation of HSXRS signals in adiabatic passage of a conical intersection. (a) Simulated O1s HSXRS signals of furan at different times. From left to right, total signals and contributions from ρ_{00} and ρ_{11} populations, and $\rho_{01}+\rho_{10}$ coherence (0 and 1 refer to states V_0 and V_1). (b) Absolute amplitudes of the two constituting states [2].

Nonadiabatic dynamics may be alternatively probed through electronic coherence in time-resolved photoelectron spectroscopy [2,3] with short ionization pulses. We derived a hierarchy of Fermi golden rules (FGRs) that incorporate strongly coupled electronic/nuclear dynamics in time-resolved photoelectron spectroscopy (TRPES) signals at different levels of theory. Expansion in the joint electronic and nuclear eigenbasis yields the numerically most challenging exact FGR (eFGR). The quasistatic Fermi Golden Rule (qsFGR) neglects nuclear motion during the photoionization process but takes into account electronic coherences initially present in the pumped matter as well as those generated internally by coupling between electronic surfaces. The standard semi-classical Fermi Golden Rule (scFGR) neglects the electronic coherences and the nuclear kinetic energy during the ionizing pulse altogether, resulting in the classical Condon approximation. The electronic coherence contributions depend on the phase-profile of the ionizing field, allowing coherent control of TRPES signals.

The photoelectron spectra for model systems were simulated using these three levels of theory. These show temporal oscillations originating from the electronic or vibrational coherences generated as the nuclear wave packet traverses a conical intersection. These oscillations, which are missed when electronic coherence is neglected, directly reveal the time-evolving splitting between electronic states of the neutral molecule in the curve-crossing regime (see Fig. 3). Streaking was shown to greatly enhance the temporal resolution [4].

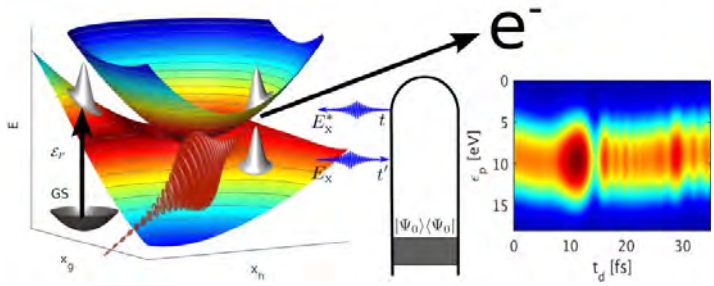

Fig. 3: Time resolved photoelectron spectroscopy. The molecule is excited by an actinic pump-pulse. The nuclear wave packet evolves on the exited state surface (left). When it reaches the conical intersection the wave packet splits up, evolving on both surfaces. The created electronic coherence can be probed with attosecond XUV pulses, and shows up as a beating pattern in the time resolved photoelectron spectrum [6] (right).

A streaking scheme has been originally developed in order to characterize attosecond X-ray pulses: photoelectron spectra in an atomic gas are recorded in the presence of both an ionizing X-ray pulse and a low frequency (typically near IR or visible) streaking pulse. By varying the delay between the X-ray and the streaking pulse and detecting the photoelectrons, one can determine the duration and the phase of the X-ray pulse through a frog protocol. In our work [4], we set a different goal and showed how streaking may be used to investigate the matter when the ultrashort pulse is known. This technique allows to monitor in real time the evolution of a non-stationary superposition state created by a preparation pulse (see Fig. 4). We had demonstrated that streaking of photoelectrons can monitor nonadiabatic dynamics in the vicinity of CoIns and avoided crossings.

Future Plans

We plan to develop a simulation protocol for nonlinear X-ray spectroscopy signals based real-time time-dependent density functional theory (RT-TDDFT). The rotating wave approximation (RWA) will be applied to overcome the short time step requirement in real-time propagation calculation stemming from the high frequency core excited states. Nonlinear X-ray spectroscopy signals generated at specific phase matching directions will be evaluated by the phase-cycling technique. This technique will allow for an efficient *ab initio* calculation of non-linear X-ray signals. These applications will be implemented into a development version of the NWChem package. Hybrid stimulated X-ray Raman spectroscopy (HSXRS. Signals will be simulated for the amino acids tryptophan and glycine. Selected valence electrons will be removed suddenly and RT-TDDFT simulations will reveal the evolution of the hole. The other X-ray four-wave mixing processes will be simulated as well.

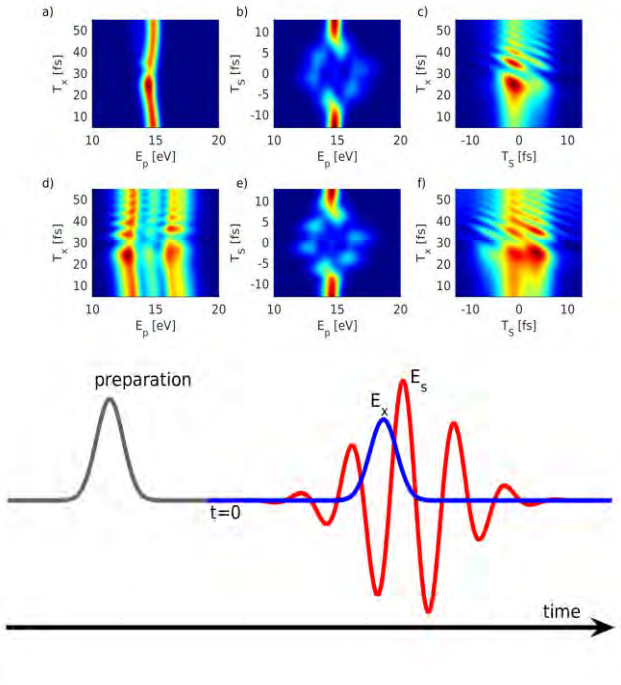

Fig. 4: Bottom: pulse configuration for the streaked TRPES. An initial pulse (grey) prepares the molecule in a nonstationary state followed, after a delay, by an ionizing pulse (blue) that has a temporal overlap with the streaking field (red). Top: Streaking spectra for various delays between the ionizing beam and the streaking field. T_x is the delay between the preparation and the ionization, Ts is the delay between the ionizing pulse and the streaking pulse, E_p is the detected photoelectron energy [4].

Considerable effort has been made to search for efficient photosensitizers based on earth-abundant metal complexes such as the Fe-complex, $[Fe^{II}(bpy)_3]^{2+}$. X-ray spontaneous emission and transient optical absorption experiments show conflicting results on its spin crossover (SCO) dynamics, regarding to whether the ^{3}MLCT state decays to the ^{5}T directly, or via an intermediate ^{3}T state. Nonlinear stimulated X-ray spectroscopy techniques can probe the coupling between excitations residing at different sites, thus they are more sensitive to the local electronic structure changes and can provide better windows for probing transient states compared to conventional linear techniques such as X-ray absorption spectroscopy (XAS) and spontaneous X-ray emission spectroscopy (XES). Two types of nonlinear X-ray spectroscopy techniques will be applied to unravel the SCO dynamics: (i) Stimulated Valence-to-Core X-ray emission spectroscopy (S-VtC-XES). Unlike the spontaneous Kβ XES technique used in previous studies, VtC-XES is sensitive to the ligands, so it offers a promising window into the ^{1,3}MLCT states. We can control the observation window by the stimulating pulse parameters (frequency and bandwidth). In addition, we shall tune the X-ray pulse frequency to stimulate the emission process after core ionization, which enhances the chemical sensibility of VtC-XES. (ii) Hybrid band Stimulated X-ray Raman Spectroscopy (HSXRS). Expressions for the proposed signals will be derived and simulated. The electronic structure information of all the transient species involved in the SCO dynamics will be obtained from DFT/TDDFT calculations performed with the NWChem package, and then used to simulate the S-VtC-XES and HSXRS signals. The same simulation protocol will also be used to study the electron transfer and excited state dynamics in other photosensitizer systems such as Cu (I) complexes.

Publications Resulting from the Project

1. *" Monitoring conical intersections in the ring opening of furan by Attosecond Stimulated X-ray Raman Spectroscopy",Weijie Hua , Sven Oesterling , Jason Biggs , Yu Zhang , Hideo Ando , Regina De Vivie-Riedle , Benjamin Fingerhut. Structural Dynamics. 3, 023601 (2016)*

2. *"Probing Electronic and Vibrational Dynamics in Molecules by Time-Resolved Photoelectron, Auger-Electron, and X-ray Photon Scattering Spectroscopy", K. Bennett, M. Kowalewski, and S. Mukamel.* Faraday Discussions*, 2014, DOI: 10.1039/C4FD00178H*
3. *"Nonadiabatic Dynamics may be Probed through Electronic Coherence in Time-Resolved Photoelectron Spectroscopy", Kochise Bennett, Markus Kowalewski, and Shaul Mukamel. J. Chem. Theory Comput., 12, 740 (2015)*
4. *"Monitoring nonadiabatic electron-nuclear dynamics in molecules by attosecond streaking of photoelectrons", Markus Kowalewski, Kochise Bennett, Jeremy Rouxel, and Shaul Mukamel. Phys. Rev. Lett. 117, 043201 (2016)*
5. *"Catching Conical Intersections in the Act; Monitoring Transient Electronic Coherences by Attosecond Stimulated X-ray Raman Signals", Konstantin Dorfman, Kochise Bennett, Markus Kowalewski, and Shaul Mukamel. Phys. Rev. Lett. 115, 193003 (2015).*
6. *"Stimulated Raman Signals of Conical Intersections; ab Initio Surface Hopping Simulation Protocol, Markus Kowalewski and Shaul Mukamel. J. Chem. Phys. 143, 044117 (2015)*
7. *"On the Resolution Limit of Femtosecond Stimulated Raman Spectroscopy: Modeling fifth-order signals with overlapping pulses ", G. Fumero, G. Batignani, K. E. Dorfman, S. Mukamel, and T. Scopigno. ChemPhysChem. doi:10.1002/cphc.201500548 (2015)*
8. *"Time-and-frequency gated photon coincidence counting; a novel multidimensional spectroscopy tool", Konstantin E. Dorfman and Shaul Mukamel. Phys. Scr.. 91, 083004 (2016)*
9. *"Multidimensional Resonant Nonlinear Spectroscopy with Coherent Broadband X-ray Pulses", Kochise Bennett, Yu Zhang, Markus Kowalewski, Weijie Hua, and Shaul Mukamel. 2016 Phys. Scr. 91 083004 doi:10.1088/0031-8949/91/8/083004*
10. *"Non-local real space analysis of chiral optical signals with nanoshaped fields", Jérémy Rouxel, Vladimir Y. Chernyak, and Shaul Mukamel. Chemical Science (Submitted, 2016)*
11. *"Study of double core hole excitations in molecules by X-ray double-quantum coherence signals: a multi-configurational simulation", Weijie Hua, Kochise Bennett, Zu Zhang ,Yi Luo, and Shaul Mukamel. Chemical Science, 2016, DOI: 10.1039/C6SC01571A*

Revealing Nanoscale Energy Flow Using Ultrafast THz to X-ray Beams

Keith A. Nelson
Department of Chemistry, Massachusetts Institute of Technology
Cambridge, MA 02139
Email: kanelson@mit.edu

Margaret M. Murnane
JILA, University of Colorado and National Institutes of Technology
Boulder, CO 80309
E-mail: murnane@jila.colorado.edu

Program Scope

We are developing novel spectroscopic methods and making use of them to study energy flow and material properties on nanometer length scales and ultrafast time scales. Access to short length scales is provided through the use of light beams with short wavelengths (EUV through hard x-ray spectral ranges) and/or fabricated structural elements with nanometer dimensions. Recent advances in tabletop high harmonic generation of extreme ultraviolet (EUV) pulses are exploited to measure thermal transport and acoustic vibrations using time-resolved diffraction from photoexcited periodic nanostructures, revealing new physics that arises at length scales of tens to hundreds of nm. A key further step is to employ coherent diffractive imaging to make possible detailed visualization of thermoelastic responses from a single heated nanostructure or an irregular nanostructural pattern. Finally, we will use light at optical and terahertz frequencies to excite and monitor ultrahigh-frequency acoustic waves at ultraflat interfaces and multilayer structures, extending our recent measurements of the highest-frequency coherent acoustic waves observed to date. Our measurements of acoustic properties will allow direct calculation of thermal conductivities which will be compared with our measurements of thermal transport and with first-principles calculations. Terahertz-frequency acoustic measurements will also be used to reveal complex relaxation dynamics in glass-forming liquids and partially disordered solids. Acoustic measurements will also be used to investigate the confinement effect in ultrathin liquid layers and to characterize mechanical properties of ultrathin solid layers. The methods we develop have broad fundamental applications and may also enable new practical metrology for use in nanoelectronics, just as earlier methods we developed have found commercial applications in microelectronics metrology.

Complementary to work at both JILA and MIT is our use of free-electron laser (FEL) facilities at the Stanford Linear Accelerator (SLAC) and ELETTRA in Trieste to measure nanoscale thermoelastic responses. The tabletop EUV sources and the ELETTRA FEL soft x-ray pulses will be used to generate as well as measure nanoscale thermoelastic responses without the need for patterned nanostructures, with the short length scale coming from optical interference patterns formed by crossing pairs of beams in transient grating experiments. We hope to demonstrate similar experiments at the LCLS to access the shortest length scales with hard x-rays.

Recent Progress

Probing thermal and elastic properties of nanoscale materials

A broad range of materials science and nanotechnology relies on the fabrication of ultrathin films that can now be deposited with single-atom layer precision. However, how the elastic properties change with film thickness, doping or structural changes in the deep nanoscale regime <100nm is not yet understood, since full characterization techniques only work for dimensions >100nm. Fortunately, laser-like beams at very short wavelengths can now be routinely generated using the process of high harmonic (HHG) upconversion of femtosecond laser pulses. These new quantum light sources are providing powerful new tools for probing and understanding nanoscale material properties. The short wavelengths of EUV beams are sensitive to picometer-scale displacements of the surface, while the femtosecond duration of HHG pulses is fast enough to capture thermal and acoustic dynamics in few-nm scale structures. Recent work using coherent HHG beams has uncovered new nanoscale materials properties, including how thermal transport changes

dramatically at dimensions on the order of the phonon mean free path, and how the mechanical properties of sub-5nm films dramatically change from bulk, even when the density does not.[1-4]

In recent work we used the exquisite sensitivity and stability of short wavelength coherent EUV high harmonic beams to characterize the full elastic tensor of low-*k* dielectric films of 11nm to 50nm thickness for the first time.[1] We simultaneously extracted the Young's modulus and Poisson's ratio in a single measurement to characterize the elastic properties of isotropic, low-*k* a-SiC:H dielectric films with varying degrees of hardness, with Young's modulus from 5GPa to 197GPa and average bond coordination from 2.1 to 3.2. Our extracted Young's modulus values are in excellent agreement with measurements using alternate techniques on the same materials. However, contrary to past assumptions, the Poisson's ratio of such films is not constant, but rather increases significantly from 0.25 to 0.45 for films with Young's modulus in the range of 5 - 30GPa. These films have an average bond coordination below a critical value <2.5, showing for the first time that the bond coordination can significantly change the Poisson's ratio in these materials. This increase in Poisson's ratio can be explained intuitively as a decrease in compressibility of the film with increasing bond breaking, due to hydrogenation used in the fabrication process.

The successful extraction of the full elastic tensor of an 11nm ultrathin film, in combination with uncovering a previously unknown trend in the Poisson's ratio, demonstrates that EUV HHG-based nanometrology can probe a wide range of novel complex materials to extract new information that could not be accessed using existing traditional approaches.

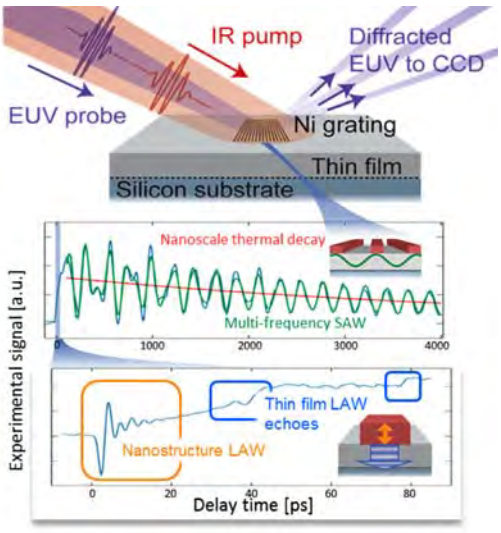

Fig. 1. Probing nanoscale thermal and mechanical properties using HHG. (top) Experimental setup. (lower) Multiple physical phenomena are visible in the change in diffraction signal (bottom). First, on picosecond time scales, the resonant vertical breathing mode of the nanowires is visible (yellow), as well as the echoes from longitudinal acoustic waves launched into the film which reflect from the film-substrate interface (blue). On nanosecond time scales, the SAWs dynamics (green) are superimposed on the thermal decay of the Ni nanowires as the energy dissipates into the film and substrate (red).

Optical Measurements of acoustic waves in glass forming liquids

Complementary to the study of mechanical properties of thin solid films described above, we have begun study of the effect of confinement on the mechanical properties of a glass forming liquid octamehylcyclotetrasiloxane (OMCTS) using optical generation and detection of acoustic waves in the tens of GHz range. It has been shown that simple liquid molecules can go through an abrupt transition showing orders of magnitude increase in shear modulus as the separation between two confining surfaces decreases down to a few layers apart. We are uniquely positioned to study the frequency-dependence of this dramatic mechanical change, using the methods we have demonstrated for optical generation of both compressional and shear acoustic waves in the MHz-GHz frequency range and the use of the methods for study of glass-forming liquids [5] including their nonlinear acoustic responses.[6] We have begun a study of this nearly spherical molecule including its temperature dependence in order to measure changes in its elastic tensor. The liquid is confined between a curved lens and a flat substrate, with variable liquid thickness down to a minimum which we are in the process of determining quantitatively and which is on the order of one or two molecular layers.

Thermal transport and coherent phonons investigated by EUV transient grating spectroscopy

Up to now, EUV measurements of thermal transport and coherent phonons used optical excitation of fabricated periodic nanostructures to initiate the responses, as described in the previous section. New

prospects will be open by using EUV (and eventually X-rays) to excite high-wavevector thermal transport and coherent phonons without the need for fabricated structures. We have made the first experimental observations of coherent acoustic and optic phonons as well as thermal transport dynamics initiated by EUV excitation (wavelength of 12.7 nm, 97 eV photon energy). The experiments were conducted at the DiProI beamline at the FERMI free electron laser (FEL) in the Elettra Synchrotron Facility in Trieste, Italy, dedicated to EUV transient grating (XTG) measurements. The work was a collaboration among the MIT, JILA, and Trieste research groups. In XTG, two pump EUV pulses are crossed within a sample, whereby interference and absorption lead to a spatially periodic profile whose time dynamics are measured via diffraction of a probe pulse [7]. In these initial measurements, an optical probe pulse (399 nm wavelength) was available, and the TG period was 272 nm; an EUV probe pulse scheduled for installation later this year will allow far shorter TG periods. XTG signal decays revealing thermal transport were measured in silicon and in $Si_{0.94}Ge_{0.06}$ alloy, as shown in Fig. 2. The decays indicated effective thermal conductivities κ_{eff} of ~15% and ~50% of their bulk values in Si and $Si_{0.94}Ge_{0.06}$ respectively, indicating highly non-diffusive regime thermal transport on the TG peak-to-null length scale of 136 nm.

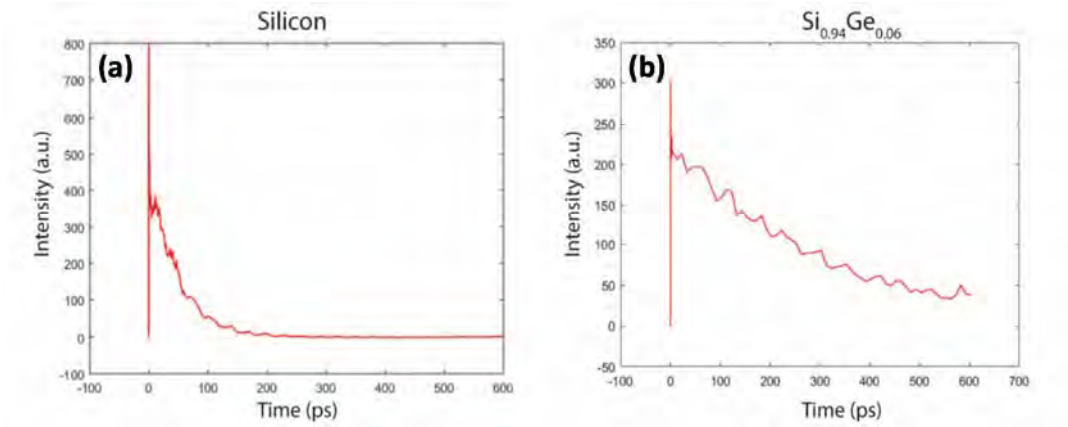

Fig. 2. XTG thermal decay signal for (a) Si and (b) $Si_{0.94}Ge_{0.06}$ alloy. The decay times are much longer than predicted by the conventional heat equation, indicating that thermal transport is in the highly nondiffusive regime.

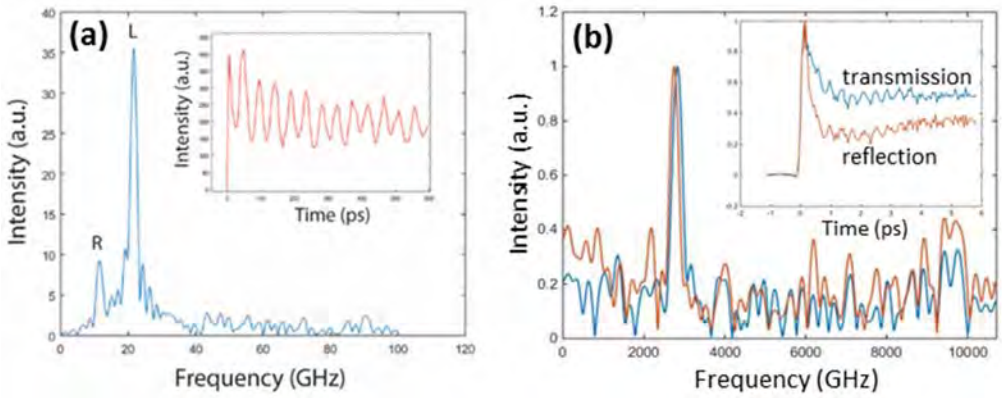

Fig. 3. (a) XTG spectrum of BK7 glass showing Rayleigh and longitudinal acoustic modes. (b) XTG spectrum of $Bi_4Ge_3O_{12}$ (BGO) showing a coherent optic phonon mode at 2.8 THz, observed by diffraction in both transmission and reflection modes. The insets show the time-domain signals from which the spectra were determined.

XTG is also a promising technique for study of high-wavevector coherent phonons. We have observed EUV-generated longitudinal acoustic waves and Rayleigh surface waves in several samples including diamond, silicon carbide, silicon, BK7 glass, and bismuth germinate $Bi_4Ge_3O_{12}$ (BGO). Figure 3a shows acoustic phonon oscillations in BK7 glass, where the Rayleigh and longitudinal acoustic modes are clearly observable. We also observed EUV TG excitation of the optic phonon mode at 2.8 THz in BGO. The time-

domain data and the corresponding Fourier spectrum for BGO are shown in Fig. 3b. This is the first observation of coherent optic phonons with EUV light.

Future Plans

Work is continuing at JILA on EUV measurements of thermoelastic responses of thin layers using 1D and 2D nanoscale structures to access novel regimes of thermal transport. HHG pulses now have intensities sufficient to try tabletop EUV transient grating measurements as well. Seeking fundamental understanding, the JILA group is completing the development of the first comprehensive models of nanoscale heat flow in 1D and 2D systems. This has posed major challenges that currently are met using phenomenological models or extremely complex first-principles calculations whose results remain incompletely tested.

Complementary study of extremely thin liquid layers is continuing at MIT. We are also testing the use of self-assembled monolayers to improve the thermal transport and high-wavevector phonon propagation between solids and liquids. In tabletop optical TG measurements of thermoelastic responses, we are extending our wavelengths into the near-UV (~ 266 nm wavelengths) and using "solid immersion" prism couplers (to shorten the wavelength by a factor of the prism refractive index) to reduce the TG period down to almost 100 nm. Together the MIT and JILA groups are measuring responses from microns to nanometers and are developing tabletop TG method that will cover the entire range.

We will continue complementary work in another collaborative beamtime scheduled at FERMI-Elettra at the EIS-TIMER beamline which is scheduled to come online in early 2017 and which will have a transient grating set-up incorporating both EUV excitation and EUV probing. This will allow us to generate transient gratings with periods down to single digit nanometers. We plan to extend the methodology for EUV experiments on liquids, using ultrathin SiN membranes or graphene to contain liquid samples in a vacuum environment. We are also applying for beamtime at the LCLS to attempt preliminary TG measurements using hard x-rays. This will open the door to wide-ranging x-ray four-wave mixing measurements. Finally, pending approval of a collaborative beamtime proposal with Stanford Professor David Reis, we will use hard x-rays at the LCLS to probe high-wavevector coherent phonons, as well as squeezed thermal phonons, in some of the same materials that we are studying in TG experiments.

References (all from DOE AMOS Support)

1. Jorge N. Hernandez-Charpak et al., "Full characterization of the mechanical properties of 11-50nm ultrathin films: influence of bond coordination on the Poisson's ratio," in prep. (2016).
2. K.M. Hoogeboom-Pot, J.N. Hernandez-Charpak, T. Frazer, E.H. Anderson, W. Chao, R. Falcone, X. Gu, R. Yang, M.M. Murnane, H.C. Kapteyn, D. Nardi, "A new regime of nanoscale thermal transport: collective diffusion increases dissipation efficiency", *PNAS* **112**, 4846 (2015).
3. D. Nardi, M. Travagliati, M. Murnane, H. Kapteyn, G. Ferrini, C. Giannetti, F. Banfi, "Impulsively Excited Surface Phononic Crystals: a Route towards Novel Sensing Schemes", IEEE Sensors Journal **15**, 5142 (2015).
4. K. Hoogeboom-Pot, J. Hernandez-Charpak, T. Frazer, X. Gu, E. Turgut, E. Anderson, W. Chao, J. Shaw, R. Yang, M. Murnane, H. Kapteyn, M. Nardi, "Mechanical and thermal properties of nanomaterials at sub-50nm dimensions characterized using coherent EUV beams", *SPIE Advanced Lithography* **9424**, 942417-1 (2015).
5. T. Hecksher, D. H. Torchinsky, C. Klieber, J. A. Johnson, J. C. Dyre, and K. A. Nelson, "Direct Test of Supercooled Liquid Scaling Relations," submitted.
6. C. Klieber, V.E. Gusev, T. Pezeril, and K.A. Nelson, "Nonlinear acoustics at GHz frequencies in a viscoelastic fragile glass former," *Phys. Rev. Lett*. **114**, 065701 1-5 (2015).
7. F. Bencivenga et al. "Four-wave-mixing experiments with seeded free electron lasers," Faraday Discussions, accepted for publication.

ñLow-Energy Electron Interactions with Complex Molecules and Biological Targetsò

Thomas M. Orlando
School of Chemistry and Biochemistry and School of Physics,
Georgia Institute of Technology, Atlanta, GA 30332-0400
Thomas.Orlando@chemistry.gatech.edu, Phone: (404) 894-4012, FAX: (404) 894-7452

Project Scope: The primary objectives of this program are to investigate the fundamental physics and chemistry involved in low-energy (1-250 eV) electron and soft x-ray interactions with complex targets. There is a particular emphasis on understanding correlated electron interactions and energy exchange in the deep valence and shallow core regions of the collision targets. The energy loss channels associated with these types of excitations involve ionization/hole exchange and negative ion resonances. Thus, the energy decay pathways are extremely sensitive to many body interactions and changes in local potentials. Our investigations should help determine the roles of hole exchange via inter-atomic and inter-molecular Coulomb decay (ICD), electron transfer mediated decay (ETMD) and energy exchange via localized shape and Feshbach resonances in the non-thermal damage of weakly interacting heterogeneous interfaces. We also seek to understand the primary mechanisms of secondary electron induced damage of complex bio-molecules such as DNA and RNA.

Recent Progress: We have carried out work on two main tasks during the past year. The first task focused on inter-atomic coulomb decay (ICD) and electron transfer mediated decay (ETMD) at weakly interacting interfaces. The second task probed the role of secondary electrons and substrate interactions in x-ray induced DNA and RNA nucleotide damage.

Task 1. Investigating intermolecular Coulomb decay (ICD) and electron transfer mediated decay (ETMD) at weakly interacting interfaces.

We have carried out preliminary studies of intermolecular Coulomb decay (ICD) and electron transfer mediated decay (ETMD) at weakly interacting interfaces. Specifically, we have begun probing ICD and ETMD in mixed rare gas (50%Ar: 50%Xe) samples condensed at 25K on graphite surfaces. Though the deposition of Ar and Xe was sequential using separate dosing beams, background dosing and interlayer diffusion leads to the formation of a mixed overlayer. Discreet layers are not easily produced and the target is likely a complicated collection of clusters of an ill-defined composition and identity. The low-energy electron-induced threshold for the formation and desorption of cluster ions and mixed dimer ions seems to primarily correlate with the ionization of the Ar 3s level. This excitation can decay by either ICD and/or ETMD. Since the relative forces in the 2-hole-final states produced by ICD and ETMD will likely lead to different kinetic energies of the desorbing products, velocity (kinetic energy) resolved measurements are underway. Deconvolution of these distributions should allow us to determine the relative contributions of ICD and ETMD in this simple rare gas mixture.

Task 2. X-ray induced damage of DNA and RNA nucleotides.

Our collaboration at Argonne National Laboratory has focused on examining secondary electron transmission and induced damage of DNA using tunable x-rays.[1,2] Presently, we are examining the cross sections and rates of low-energy electron damage of

DNA and RNA nucleotides. Specifically, we have examined the damage of 5ô-deoxyadenosine monophosphate (5ô-dAMP) and 5ô-adenosine monophosphate (5ô-rAMP). Thin film samples of 5ô-dAMP and 5ô-rAMP were prepared on gold plated silicon wafers by drop casting dilute 1:1 water:MeOH solutions and slow drying in an unheated vacuum desiccator. In these experiments, the impinging x-ray beam is not only the initiator for ejecting electrons that interact with the molecules, but is also the method by which the chemical environment is probed. A 950 eV synchrotron x-ray beam was used to take snapshot spectra of the samples (the C 1s and O 1s transitions) over the course of approximately 2 hours. For the C 1s peaks, the only detectable change over time occurs within the two lowest binding energy (BE) components. For the O 1s peaks, the largest middle BE peak also decays in time. These stark changes after 2 hours of irradiation are clear indicators that the nucleotides are undergoing a chemical change. The C 1s and O 1s decay constants for both dAMP and rAMP are very similar. This indicates that there is no discernable difference in dAMP and rAMP nucleotide survival when using x-rays as both the probe and source of slow electrons.

The time dependent photoemission from C, O and P core levels are being compared directly to damage studies using slow electron irradiation of dAMP and rAMP adsorbed on pristine and graphene covered nano-structured Au surfaces followed by Raman micro-spectroscopy.[3] The overall focus of this project is to observe and determine the sites of low energy electron induced bond breaking within the nucleotides and to correlate these observations with the identity of the sugar and the potential coupling to the underlying Au substrate. This information will be generally valuable to ongoing studies in the fields of radiation-induced DNA damage and cancer radiotherapies.

Future Plans.

Once we complete the rare gas studies, we are particularly interested in extending our initial ICD studies to water clusters adsorbed on weakly coupled molecular solids such as ethane (C_2H_6), acetylene (C_2H_2), and formaldehyde (HCHO). This series span the regime of essentially no coupling (C_2H_6), to weak π-interactions (C_2H_2), and hydrogen bonding (HCHO). HCHO can also be considered a building block for more complicated biomolecules and has hydrogen bonding interactions expected in biochemical systems. These interactions can also lead to proton transfer processes.

Continuing work on decay experiments and near-edge x-ray absorption fine structure spectroscopy (NEXAFS) will be carried out in the next beam-time run. We will also continue low energy electron induced damage studies of nucleotides using the graphene platform and Raman micro-spectroscopy. In this case, the nucleotides we plan to study include but are not limited to deoxycytidine monophosphate (dCMP) and cytidine monophosphate (rCMP).

References:

1. R. A. Rosenberg, J. M. Symonds, V. Kalyanaraman, T.Z. Markus, T. M. Orlando and R. Naaman, ñThe relationship between interfacial bonding and radiation damage in adsorbed DNAò, *Phys. Chem. Chem. Phys.* 2014, Advance Article DOI: 10.1039/C4CP01649A (2014).

2. R. A. Rosenberg, J. M. Symonds, V. Kalyanaraman, T. Z. Markus, T. M. Orlando, R. Naaman, E. a. Medina, F. A. Lopez and V. Muijca, ñKinetic Energy Dependence of Spin Filtering of Electrons Transmitted through Organized Layers of DNAò, *J. Phys. Chem. C.* **117,** 22307-22313, (2013).

3. A. N. Sidorov and T. M. Orlando, ñMonolayer graphene platform for the study of DNA damage by low-energy electron irradiationò, *J. Phys. Chem. Lett*., 2013, 4 (14), 2328ï 2333 (2013).

Recent publications acknowledging support from this program

1. A. N. Sidorov and T. M. Orlando, Correction to ñMonolayer Graphene Platform for the Study of DNA Damage by Low-Energy Electronsò *J. Phys. Chem. Lett.* 7, 2168, (2016).

2. E. Alizadeh, T. M. Orlando and L. Sanche, ñBiomolecular damage induced by ionizing radiation; The direct and indirect effects of low-energy electrons on DNAò, *Ann. Rev. of Phys. Chem*. 66, 379-98 (2015).

3. R. A. Rosenberg, J. M. Symonds, V. Kalyanaraman, T.Z. Markus, T. M. Orlando and R. Naaman, ñThe relationship between interfacial bonding and radiation damage in adsorbed DNAò, *Phys. Chem. Chem. Phys.* 2014, Advance Article DOI: 10.1039/C4CP01649A (2014).

Presentations acknowledging support from this program

1. T. M. Orlando, ñLow energy (<5 eV) electron interactions with DNA and RNA nucleotidesò, XIX International symposium on electron-molecule collisions and swarmsò, July 17-20, Lisbon, Portugal 2015.

2. T. M. Orlando, ñVery low energy electron-induced damage of DNAò, Dept. of Physics, Auburn University, March 21, 2015.

3. T. M. Orlando, ñVery low energy electron-induced damage of DNAò, Dept. of Physics, University of Georgia, March 21, 2014.

Page is intentionally blank.

SISGR - Structure from Fleeting Illumination of Faint Spinning Objects in Flight

A. Ourmazd
Dept. of Physics, University of Wisconsin Milwaukee
3135 N. Maryland Ave, Milwaukee, WI 53211
ourmazd@uwm.edu

Program Scope

The advent of the X-ray Free Electron Laser (XFEL) has made it possible to interrogate molecules and their assemblies "in flight" with intense short pulses of radiation, and record "snapshots" before they are destroyed. We are developing a new generation of powerful algorithms to recover structure and dynamics from such ultra-low-signal random sightings. Combining concepts from machine learning, differential geometry, general relativity, graph theory, and diffraction physics, these techniques promise to revolutionize our understanding of ultrafast dynamics in molecular systems, and key processes in biological machines, such as viral infection, and water-splitting in photosystem II.

Recent Progress

Dynamics from noisy data recorded with extreme timing uncertainty
With R. Fung, A.M. Hanna, O. Vendrell, S. Ramakrishna, T. Seideman, R. Santra
Imperfect knowledge of the time-points at which "snapshots" of a system were recorded often degrades our ability to recover dynamical information, and can even scramble the sequence of events. In XFELs, for example, the uncertainty – the so-called timing jitter – between the arrival of an optical trigger ("pump") pulse and a probing X-ray pulse can exceed the X-ray pulse-length by up to two orders of magnitude (*1*), thus marring the otherwise exquisite time-resolution capabilities of this powerful class of instruments. The widespread notion that little information is available on timescales significantly shorter than the timing uncertainty has spawned a variety of elaborate hardware schemes to reduce timing uncertainty [see, e.g., (*2-4*)]. These schemes are expensive, tend to be specific to one experimental approach, and cannot be employed when the record was created under ill-defined or uncontrolled conditions, as, for example, in geological events. We have developed and validated a data-analytical approach (*5*), loosely named "*Super-resolution Dynamics*", which can recover histories and dynamics from a dense collection of noisy snapshots spanning a sufficiently large multiple of the timing uncertainty. The power of the algorithm is demonstrated by extracting the underlying dynamics on the few-femtosecond timescale from noisy experimental XFEL data recorded with 300 fs timing uncertainty (*5*) [see Figs. 1 and 2]. The approach can potentially be applied whenever dynamical or historical information is tainted by timing uncertainty.

The fundamental premise of our approach is simple. A series of snapshots concatenated (appended) to each other in the order of their inaccurate timestamps will contain some time-evolutionary information ("a weak arrow of time"), provided the concatenation window spans a period comparable with, or longer than the timing uncertainty associated with each individual snapshot. This realization leads one to consider a series of *c*-fold

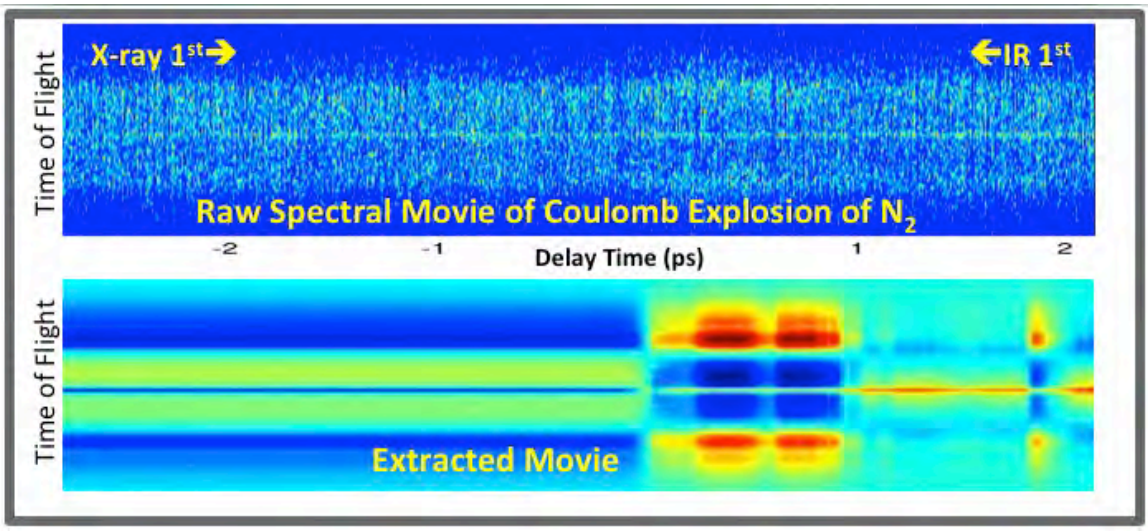

Fig. 1. Raw vs. extracted spectral movies. Top: Raw Time-of-Flight spectral movie of the Coulomb explosion of N_2 recorded with an uncertainty of 300fs FWHM (*1*). **Bottom:** Movie extracted data-analytically as described in (*5*)

concatenated snapshots, formed by moving a window *c* frames wide over the raw dataset ordered according to the inaccurate timestamps. The dynamical history can then be extracted from the series of concatenated snapshots by powerful techniques developed to extract signal from noise, such as Singular Value Decomposition (SVD) (*6*) or appropriate, its nonlinear analogue Nonlinear Laplacian Spectral Analysis (NLSA) (*7*), as appropriate to the problem at hand. Such data-analytical techniques yield a series of statistically significant modes, each consisting of a characteristic pattern (topogram, or "topo") and its time evolution (chronogram, or "chrono"). A topo can, for example, be a characteristic image, or spectrum, with the corresponding chrono showing its change with time. Fig. 1 shows raw spectral movie of the Coulomb explosion of N_2, together with the time evolution of the first mode extracted from the data.

The observation in the X-ray-first regime of vibrational wave packets with frequency components as high as 15fs constitutes a salient feature of our data-analytical results. Fig. 2 shows the wavepacket oscillations in the time domain, and compares the observed frequency components with the known the frequency components of the N_2 system. The close agreement is noteworthy.

In conclusion, we have demonstrated a purely data-analytical approach capable of extracting the evolution and dynamics of complex systems from noisy snapshots on timescales far beyond the uncertainty with which the data were recorded. We expect our approach to have a broad impact in many areas of science and technology. Examples include geology and climate science, where timing of events can be uncertain; chemistry and biology, where reaction initiation can be non-uniform across a sample; and signal processing, where noise and timing jitter are prevalent.

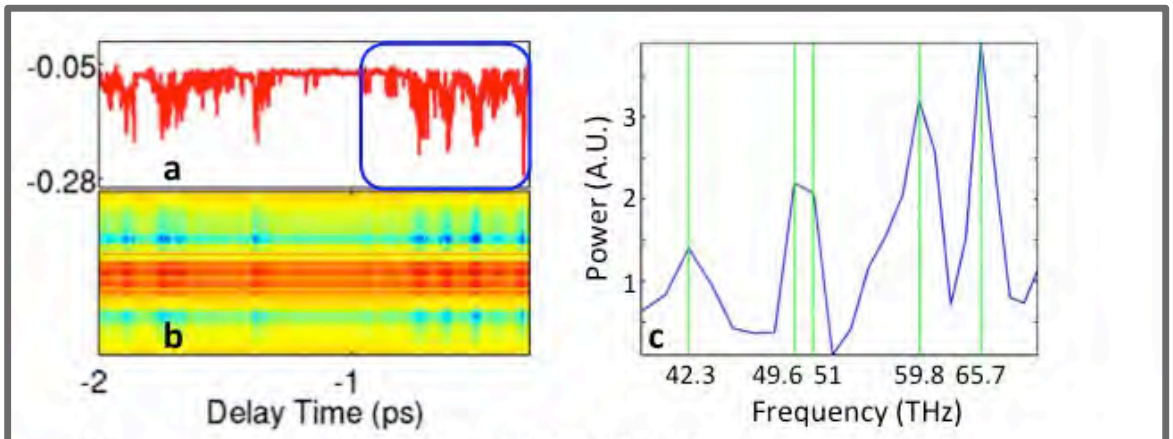

d **Vibrational Periods (fs)**

Measured	Theory	State	Remarks
15.2	15.1	$X^2\Sigma_g^+$	Previously observed in time domain
16.7	16.7	$X^1\Sigma_g^+$	
19.6	17.7	$A^2\Pi_u$	Overlap between peaks degrades accuracy
20.2	22.4	$a^3\Pi_u$	
23.6	23.7	$A^1\Pi_u$	

Fig. 2. Vibrational wave packets in X-ray first region. a. Mode-4 chrono in the X-ray-first region, showing the time evolution of a wave packet and its revival. **b.** Reconstructed Time-of-Flight spectral movie in the X-ray-first region. (Rainbow color scale. Lowest signal: dark blue; highest: red.) **c.** Fourier spectrum of the chrono in the 690-fs-long boxed region, showing the frequency and period of each component. **d.** Comparison of observed periods with known vibrational modes of N_2 (*5*).

References

1. J. M. Glownia *et al.*, *Optics Express* **18**, 17620 (2010).
2. C. Gahl *et al.*, *Nature Photonics* **2**, 165 (2008).
3. F. Lohl *et al.*, *Physical Review Letters* **104**, 144801 (2010).
4. M. Harmand *et al.*, *Nature Photonics* **7**, 215 (2013).
5. R. Fung *et al.*, *Nature* **532**, 471 (2016).
6. N. Aubry, R. Guyonnet, R. Lima, *J Stat Phys* **64**, 683 (1991).
7. D. Giannakis, A. J. Majda, *Proc Natl Acad Sci U S A* **109**, 2222 (2012).

Future Plans

We plan to extend the range of applicability of the “super-resolution dynamics” algorithm outlined above to other important applications, especially ultrafast structural dynamics. This is expected to make a particular impact on time-resolved serial femtosecond crystallography, where the dynamical information recorded at each time point represents

only a small fraction (~1%) of the information needed to map the three-dimensional diffraction volume at that time point.

Publications supported in whole or in part by this grant over last three years

1. Coherent diffraction of single Rice Dwarf virus particles using hard X-rays at the Linac Coherent Light Source, A. Munke et al., **Scientific Data** (accepted).
2. Dynamics from Noisy Data with Extreme Timing Uncertainty, R. Fung, A.M. Hanna, O. Vendrell, S. Ramakrishna, T. Seideman, R. Santra, and A. Ourmazd, **Nature 532**, 471 (2016).
3. Single-particle Structure Determination by X-ray Free Electron Lasers: Possibilities and Challenges (Invited Perspective), A. Hosseinizadeh, A. Dashti, P. Schwander, R. Fung, and A. Ourmazd, **Structural Dynamics 2**, 041601 (2015).
4. The Linac Coherent Light Source Single-particle Imaging Roadmap, A. Aquila et al., **Structural Dynamics 2**, 041701 (2015).
5. Trajectories of the Ribosome as a Brownian Nanomachine, A. Dashti, P. Schwander, R. Langlois, R. Fung, W. Li, A. Hosseinizadeh, H.Y. Liao, J. Pallesen, G. Sharma, V.A. Stupina, A. E. Simon, J. Dinman, J. Frank, and A. Ourmazd, **PNAS 111**, 17492 (2014).
6. High Resolution Structure of Viruses from Random Snapshots, A. Hosseinizadeh, P. Schwander, A. Dashti, R. Fung, R.M. D'Souza, and A. Ourmazd, **Philosophical Transactions of the Royal Society B**, 20130326 (2014).
7. Conformations of Macromolecules and their Complexes from Heterogeneous Datasets, P. Schwander, R. Fung, and A. Ourmazd, **Philosophical Transactions of the Royal Society B**, 20130567 (2014).

Control of Molecular Dynamics: Algorithms for Design and Implementation

Herschel Rabitz and Tak-San Ho

Princeton University, Frick Laboratory, Princeton, NJ 08540

hrabitz@princeton.edu, tsho@princeton.edu

A. Program Scope:

This research considers the conceptual and algorithmic developments addressing control over molecular dynamics phenomena. The research is theoretical and computational in nature, but its ultimate significance lies in the associated implications and applications in the laboratory. The goal of the research is to develop a good understanding of the principles of quantum control processes as well as to provide new algorithms to extend the laboratory control capabilities.

B. Research Progress:

In the past year, a broad variety of research topics were pursued in the general area of controlling quantum dynamics phenomena. A summary of these activities is provided below.

[1] Measuring the distance from saddle points and driving to locate them over quantum control landscapes: In this study we developed methods for seeking critical saddle submanifolds, corresponding to suboptimal saddle objective values, over two types of quantum control landscapes: the observable landscape and the unitary transformation landscape. The numerical examples demonstrated that the algorithms can successfully address the targeted saddle submanifolds with arbitrarily high accuracy. The concepts and methodology provided here are general and can be applied in further studies of the landscape saddle points by simulation. The tools developed here can aid in understanding landscape saddles, including how far a current field is from a saddle and how to approach or avoid the saddles. The latter prospect opens up consideration of new or modified algorithms accelerating the search for optimal fields.

[2] Quantum control and pathway manipulation in rubidium: This work theoretically explored various strategies for manipulating pathway amplitudes in rubidium in the context of a laser field interacting with a multilevel system similar to atomic rubidium for both narrow-band and broadband ultrafast fields. For narrow-band field control, the analysis was carried out in the time domain with the laser field including only four narrow-band envelope subpulses centered at the resonant frequencies. For broadband field control, the dynamics were treated in the frequency domain with the laser field including both resonant and continuous nonresonant frequency components. Various control strategies based on manipulating the phase of selected spectral components were tested. The quantum control of pathways investigated in this work provides valuable insights on how to incorporate known information about the structure of quantum systems for the effective reduction of quantum control complexity.

[3] Efficient method to generate time evolution of the Wigner function for open quantum

systems: In this study, we presented an efficient fast-Fourier method for evolving the Wigner function that has a complexity of O (N log N) where N is the size of the array storing the Wigner function. The efficiency, stability, and simplicity of this method allows us to simulate open-system dynamics previously thought to be prohibitively expensive. As a demonstration we simulated the dynamics of both one-particle and two-particle systems under various environmental interactions. For a single particle we also compared the resulting evolution with that of the classical Fokker–Planck and Koopman–von Neumann equations and showed that the environmental interactions induce the quantum-to-classical transition as expected. In the case of two interacting particles we showed that an environment interacting with one of the particles leads to the loss of coherence of the other.

[4] Coherent revival of tunneling: In this study, we introduced a tunneling effect by a driving field, referred to as coherent revival of tunneling (CRT), corresponding to complete tunneling (transmission coefficient = 1) that is revived from the circumstance of total reflection (transmission coefficient ≈ 0) through application of an appropriate perpendicular high-frequency ac field. To illustrate CRT, we simulated electron transport through fish-bone-like quantum-dot arrays by using single-particle Green's functions along with Floquet theory, and we explored the corresponding current-field amplitude characteristics as well as current-polarization characteristics. In regard to the two characteristics, we showed that CRT exhibits entirely different features than coherent destruction of tunneling and photon-assisted tunneling. We also discussed two practical conditions for experimental realization of CRT.

[5] The role of dissociation channels of excited electronic states in quantum optimal control of ozone isomerization: A three-state dynamical model: In the calculations we used a three-state, one-dimensional dynamical model constructed from the lowest five potential energy curves obtained with high-level ab initio calculations. Besides the laser field-dipole couplings between all three states, this model also includes the diabatic coupling between the two excited states at an avoided crossing leading to competing dissociation channels that can further hinder the isomerization process. The present three-state optimal control simulations examined two possible control pathways previously considered in a two-state model, and reveal that only one of the pathways is viable. This work represents a step towards an ultimate model for the open/cyclic ozone transformation capable of giving adequate guidance about the necessary experimental control field resources as well as an estimate of the rovibronic spectral character of cyclic ozone as a basis for an appropriate probe of its formation.

[6] On choosing the form of the objective functional for optimal control of molecules: This work more broadly considered the freedom in the choice of objective functions to yield trap-free landscapes for optimal control of molecules upon satisfaction of certain basic assumptions. The latter freedom can be exploited to possibly accelerate the search for an optimal control, but we also showed that the choice of functional needs to be made carefully to avoid inducing artificial landscape traps.

[7] Wigner–Lindblad Equations for Quantum Friction: In this study, we constructed a quantum counterpart of classical friction, a velocity-dependent force acting against the direction of motion. In particular, a translationary invariant Lindblad equation was derived satisfying the appropriate dynamical relations for the coordinate and momentum (i.e., the Ehrenfest equations). Numerical simulations establish that the model approximately equilibrates. These findings significantly advanced a long search for a universally valid Lindblad model of quantum friction and open opportunities for exploring novel dissipation phenomena.

[8] Frequency domain quantum optimal control under multiple constraints: This work

presented a theoretical method that can be utilized to optimize the control fields subject to multiple constraints while guaranteeing monotonic convergence towards desired physical objectives. This optimization method has been formulated in the frequency domain in line with the current ultrafast pulse shaping technique, providing the possibility for performing quantum optimal control simulations and experiments in a unified fashion.

[9] Identifying a cooperative control mechanism between an applied field and the environment of open quantum systems: This work expanded the scope of the Hamiltonian-encoding and observable-decoding (HE-OD) technique for understanding the control mechanisms has remained a challenge, especially the role played by the interaction between the field and the environment. The results of open-system HE-OD analysis presented here provided quantitative mechanistic insights into the roles played by a Markovian environment. Two model open quantum systems were considered for illustration.

[10] Monotonic convergent quantum optimal control method with exact equality constraints on the optimized control fields: This work presented a monotonic convergent quantum optimal control method that can be utilized to optimize the control field while exactly enforcing multiple equality constraints for steering quantum systems from an initial state towards desired quantum states. For illustration, special consideration was given to finding optimal control fields with (i) exact zero area and (ii) exact zero area along with constant pulse fluence.

[11] Efficient computations of quantum canonical Gibbs state in phase space: In this study we solved a long standing problem for computing the Gibbs state Wigner function with nearly machine accuracy by solving the Bloch equation directly in the phase space. Furthermore, the algorithms were provided yielding high quality Wigner distributions for pure stationary states as well as for Thomas-Fermi and Bose-Einstein distributions. The developed numerical methods furnish a long-sought efficient computation framework for nonequilibrium quantum simulations directly in the Wigner representation.

C. Future Plans:

The research in the coming year will include the following:

(1) We are continuing to build on our current study, in collaboration with Dr. Yuzuru Kurosaki in Japan, to form a more elaborate assessment of the prospects of performing ozone isomerization by executing OCT calculations to include rotation under the sudden approximation in order to reveal more the general nature of the field necessary for a learning control experiment.

(2) We plan to extend the monotonically convergent constrained optimal control framework to general quantum control optimal problems subject to an arbitrary number of equality constraints in both the time and frequency domains, either separately or simultaneously. This extension aims at potential applications in quantum physics including multi-objective optimal control problems.

(3) We plan to broaden the study of quantum control landscape structure to classical molecular control landscape structure by steering the phase space coordinates of classical systems to given target landscape values and examining underlying metric defined as the ratio of the gradient-based optimization path length of the control field evolution to the Euclidean distance between a given initial control field and the resultant optimal control field, which lies at the top of the landscape.

(4) We plan to explore two opposing optimal control scenarios of orientation/entanglement involving couplings between coupled molecular rotors. Preliminary studies have been performed for two identical rotors coupled via a distance-dependent dipole-dipole interaction.

(5) We plan to develop computational efficient and robust time-dependent Hartree-based approaches for optimal control problems of multi-dimensional inter/intra-molecular dynamics. Some preliminary results have been obtained showing the potential applications in diverse areas involving molecular complexes, for example, photo-dissociation and photo-excitations of van der Waals molecules.

D. Publications acknowledging DOE support (2014–2016):

[1] G. Riviello, C. Brif, R. Long, R.-B. Wu, K. Moore Tibbitts, T.-S. Ho, and H. Rabitz, Phys. Rev. A, **90**, 013404, (2014).
[2] Y. Paskover, D. Xie, F. Laforge, and H. Rabitz, J. Opt. Soc. Am. B, **31**, 1165, (2014).
[3] X. Xing, R. Rey-de-Castro, and H. Rabitz, New Journal of Physics 16, 125004 (2014).
[4] A. Donovan and H. Rabitz, Math. Chem. 53, 718–736 (2015).
[5] A. Nanduri, O. M. Shir, A. Donovan, T.-S. Ho, and H. Rabitz, Phys. Chem. Chem. Phys., 17, 334 (2015).
[6] K. M. Tibbetts and H. Rabitz, Phys. Chem. Chem. Phys., 17, 3164 (2015).
[7] C. Joe-Wong, T.-S. Ho, H. Rabitz, and R. Wu, J. Chem. Phys. 142, 154115 (2015).
[8] C.-C. Shu, M. Edwalds, A. Shabani, T.-S. Ho, and H. Rabitz, Phys. Chem. Chem. Phys., 17, 18621 (2015).
[9] G. Riviello, K. M. Tibbetts, C. Brif, R. Long, R. Wu, T.-S. Ho, and H. Rabitz, Phys. Rev. A 91, 043401 (2015).
[10] Q. Sun, I. Pelczer, G. Riviello, R. Wu, and H. Rabitz, Phys. Rev. A 91, 043412 (2015).
[11] Q. Sun, G. Riviello, R.-B. Wu, and H. Rabitz, J. Phys. A: Math. Theor. **48**, 465305 (2015).
[12] F. Gao, Y. Wang, R. Rey-de-Castro, H. Rabitz, and F. Shuang, Phys. Rev. A **92**, 033423 (2015).
[13] R. Cabrera, D. I. Bondar, K. Jacobs, and H. Rabitz, Phys. Rev. A **92**, 042122 (2015).
[14] L.-Y. Hsu and H. Rabitz, Phys. Rev. B **92**, 035410 (2015).
[15] Y. Kurosaki, T.-S. Ho, and H. Rabitz, Chem. Phys. **469-470**, 115 (2016).
[16] C. Joe-Wong, T.-S. Ho, and H. Rabitz, J. Math. Chem. **54**, 1 (2016).
[17] D. I. Bondar, R. Cabrera, A. Campos, S. Mukamel, and H. Rabitz, J. Phys. Chem. Lett. **7**, 1632 (2016).
[18] C.-C. Shu, T.-S. Ho, X. Xing, H. Rabitz, Phys. Rev. A **93**, 033417 (2016).
[19] F. Gao, R. Rey-de-Castro, Y. Wang, H. Rabitz, and F. Shuang, Phys. Rev. A **93**, 053407 (2016).
[20] C.-C. Shu, T.-S. Ho, H. Rabitz, Phys. Rev. A **93**, 053418 (2016).
[21] D. I. Bondar, A. Campos, R. Cabrera, and H. Rabitz, Phys. Rev. A **93**, 063304 (2016).

"Atoms and Ions Interacting with Particles and Fields"

F. Robicheaux
Purdue University, Department of Physics, 525 Northwestern Ave, West Lafayette IN 47907
(robichf@purdue.edu)

Program Scope

This theory project focuses on the time evolution of systems subjected to either coherent or incoherent interactions represented by fields and particles, respectively. This study is divided into three categories: (1) coherent evolution of highly excited quantum states, (2) incoherent evolution of highly excited quantum states, and (3) the interplay between ultra-cold plasmas and Rydberg atoms. Some of the techniques we developed have been used to study collision processes in ions, atoms and molecules. In particular, we have used these techniques to study the correlation between two (or more) continuum electrons and electron impact ionization of small molecules.

Recent Progress 2015-2016

Short Pulse Photodetachment: We published three papers relevant to short pulse ionization of negative ions.[17,19,20] R.R. Jones recently published results in PRL where a single-cycle electric-field ionized highly excited atoms. Inspired by these experiments, the postdoc Baochun Yang performed systematic studies of single cycle ionization of atoms, from highly excited states down to the ground state.[11,12] In the past year, we investigated how a single cycle pulse can modify the photodetachment process in negative ions.[17,19] The basic idea is that a laser pulse initiates a photodetachment giving a free electron at low energy. A single cycle pulse with a similar duration to the laser pulse can strongly modify the outgoing electron's energy distribution and direction of ejection. In Ref. [17], we presented theory and calculations of a real-time-domain interferometry for the photodetachment dynamics. The photoelectron can follow two or more classical trajectories to arrive at a detector simultaneously allowing the electron waves to interfere. Both the in-phase and antiphase oscillations can be observed from negative hydrogen and fluorine ions depending on the pulse strength and observation angle. A temporal-caustic bifurcation is observed when the detection angle is not in line with the pulse polarization. In Ref. [19], we extended the standard closed-orbit theory for photodetachment of negative ions in a time-dependent electric field. The photodetachment in the presence of a strong single-cycle pulse was studied using exact quantum simulations and semiclassical analysis. Three types of closed classical orbits were identified for the photoelectron motion and their connections with the oscillatory photodetachment rate were established quantitatively by generalizing the standard closed-orbit theory to a time-dependent form. By comparing the negative hydrogen and fluorine ions, both the in-phase and antiphase oscillations can be observed. In Ref. [20], the postdoc Hua-Chieh Shao pursued a different type of photodetachment where the short, high-frequency laser pulse has a duration comparable to or shorter to an estimate of the response time given by the inverse of the binding energy. We investigated the dependence of the photoelectron spectra on the duration, chirp, and intensity of the pulses concentrating on the low-energy distributions in the spectra that result from the Raman transitions of the broadband pulses. Contrary to the one- and two-photon ionization, the low-energy distribution maintains an almost constant width as the laser bandwidth is expanded by chirping the pulse. In addition, we studied the transitions of the detachment dynamics from the perturbative to the strong-field regime.

Quasistable states in a strong IR field: The stabilization of atoms in strong, oscillating fields has been an important issue for ~20 years. In 2013, we were involved in an experimental and theoretical study with T.F. Gallagher's group of how atoms can have resonance states in extremely strong microwave fields[5] In Ref. [15] (an Editor's Choice for July 2015), the graduate student Changchun Zhong performed calculations for the analogous system but for excitation in a strong IR field. In Ref. [18], we extended these studies to investigate the coherence of these quasistable states. Instead of a single frequency, the UV pulse train contains two frequency components which leads to coherent excitation of two quasistable states. When the two components have frequencies separated by two IR photons, the population of surviving electrons is modulated by up to ten percent by changing the relative phase of the two UV lasers. When electrons are excited to right above or below the threshold, the survival probabilities have inverted phase delay dependence. When the two frequencies are one IR photon apart, the angular symmetry of the quasistable electrons is broken, and the asymmetry is also controlled by the phase delay between the UV lasers. The asymmetrical distribution can be observed while the IR is on and smoothly evolves to a nonzero asymmetry that only weakly depends on the duration of the IR field.

Two electron physics: In Ref. [21], we reviewed the application of the time-dependent close-coupling method to the study of ion-impact ionization of atoms and molecules. The basic theory and practical aspects of the implementation were covered in detail. Ionization cross sections were presented for bare ion, antiproton, and neutron collisions with light atoms and molecules.

Fundamental investigations in scattering theory: With the postdoc Panos Giannakeas and with Chris Greene, we have embarked on a series of studies in fundamental scattering theory. The basic problem in scattering theory is to calculate the amplitude for a system to start in channel i and scatter into channel j. As a paradigm, we investigated the case where the scattering center has a small range but has a different symmetry from the channel functions.[13,14,16] Using these studies as a springboard, we revisited the Fano-Harmin theory of the Stark effect. In Ref. [23], a rigorous theoretical framework was developed for a generalized local-frame-transformation theory (GLFT). The GLFT is applicable to many systems that have only been approximately treated using the local-frame-transformation theory. A first test application to the photoionization spectra of Rydberg atoms in external electric fields demonstrates dramatic improvement over the first version of the local-frame-transformation theory developed by Fano and Harmin. This revised GLFT theory yields nontrivial corrections because it now includes the full on-shell Hilbert space without adopting the truncations in the original theory. Comparisons of the semianalytical GLFT Stark spectra with ab initio numerical simulations yield errors in the range of a few tens of MHz, an improvement over the Fano-Harmin theory by factors of ~100 or more. The success of this treatment suggests that other systems treated by the local-frame-transformation can be put on a rigorous footing.

Imaging of quantum state inside atom: We were involved in several joint experimental and computational projects to image a part of the wave function inside an atom (for example, see Ref. [7]). Reference [22] contains the general description of our findings over the past few years. Photoionization of an atom in the presence of a uniform electric field proves the unique opportunity to expand and visualize the wave function at a macroscopic scale. In a number of seminal publications, it was shown that this goal could be achieved by projecting slow (meV) photoionizaed electrons onto a position-sensitive detector. The uncovering of resonant signatures was achieved recently in our previous paper on lithium atoms. In Ref. [22], we provide more details and investigate situations with emphasis on the various manifestations of resonant

character. Lithium was chosen as an illustrative example between the two limiting cases of hydrogen, where resonance effects are more easily identified, and heavy atoms like xenon, where resonant effects were not observed.

Finally, this program has several projects that are strongly numerical but only require knowledge of classical mechanics. This combination is ideal for starting undergraduates on publication quality research. Since 2004, twenty-nine undergraduates have participated in research projects in my group. Most of these students have completed projects published in peer reviewed journals. Two undergraduates, Michael Wall in 2006 and Patrick Donnan in 2012, were one of the 5 undergraduates invited to give a talk on their research at the undergraduate session of the DAMOP meeting. Four publications during the past three years [1,2,6,10] had an undergraduate supported by DOE as first author or coauthor.

Future Plans

Single cycle: We will study the analog of a single cycle pulse by calculating the effect from the ponderomotive potential from a traveling wave laser pulse on a Rydberg atom. If a traveling laser pulse with high frequency interacts with a Rydberg atom, the electron experiences an effective potential proportional to the intensity. Since the duration of the laser pulse times the speed of light is larger than the atom, the electron experiences an effective force proportional to the time derivative of the envelope. This is formally equivalent to having a single cycle electric field interact with the electron. The interesting aspects will be the controllability of the intensity and duration of the pulse.

Basic scattering theory: We will further apply the developments in Refs. [16,23] to perform precision studies of Stark states. Previously, the local-frame-transformation theory gives qualitative agreement with measurements but allows an intuitive method for including the effects from strong fields. We will extend our recent developments to perform calculations for actual atoms including the strong fields, spin-orbit interactions, etc. A successful implementation will confirm that the GLFT can be used both as an intuitive method and as a spectroscopically accurate technique.

Two electron physics: The graduate student Xiao Wang will lead the study of time dependent two electron systems. We will focus on the cases where two electrons are launched successively into Rydberg wave packets as in the joint experiment/calculation with R.R. Jones in 2013. The first studies will probe where the classical and quantum correspondence breaks down. If we can make rapid progress, we will also investigate whether stable wave packet states can be formed by this technique and, if they can, we will study their generic properties.

DOE Supported Publications (9/2013-8/2014)

[1] G.W. Gordon and F. Robicheaux, J. Phys. B 46, 235003 (2013).
[2] P.L. Price, L.D. Noordam, H.B. van Linden van den Heuvell, and F. Robicheaux, Phys. Rev. A **89**, 033414 (2014).
[3] M.S. Pindzola, Sh.A. Abdel-Naby, F. Robicheaux, and J. Colgan, J. Phys. B **47**, 085002 (2014).
[4] F. Robicheaux, Phys. Rev. A **89**, 062701 (2014).
[5] A. Arakelyan, T. Topcu, F. Robicheaux, and T.F. Gallagher, Phys. Rev. A **90**, 013413 (2014).
[6] F. Robicheaux, M.M. Goforth, and M.A. Phillips, Phys. Rev. A **90**, 022712 (2014).

[7] A.S. Stodolna, F. Lepine, T. Bergeman, F. Robicheaux, A. Gijsbertsen, J.H. Jungmann, C. Bordas, and M.J.J. Vrakking, Phys. Rev. Lett. **113**, 103002 (2014).

DOE Supported Publications (9/2014-8/2015)

[8] M.S. Pindzola, T.G. Lee, Sh.A. Abdel-Naby, F. Robicheaux, J. Colgan, and M.F. Ciappina, J. Phys. B **47**, 195202 (2014).
[9] Q. Wang, S. Sheinerman, and F. Robicheaux, J. Phys. B **47**, 215003 (2014).
[10] F. Robicheaux, B.J. Bender, and M.A. Phillips, J. Phys B **47**, 245701 (2014).
[11] B.C. Yang and F. Robicheaux, Phys. Rev. A **90**, 063413 (2014).
[12] B.C. Yang and F. Robicheaux, Phys. Rev. A **91**, 043407 (2015).
[13] P. Giannakeas, F. Robicheaux, and C.H. Greene, Phys. Rev. A **91**, 043424 (2015).
[14] P. Giannakeas, F. Robicheaux, and C.H. Greene, Phys. Rev. A **91**, 067401 (2015).
[15] C. Zhong and F. Robicheaux, Phys. Rev. A **92**, 013406 (2015).
[16] F. Robicheaux, P. Giannakeas, and C.H. Greene, Phys. Rev. A **92**, 022711 (2015).

DOE Supported Publications (9/2015-8/2016)

[17] B.C. Yang and F. Robicheaux, Phys. Rev. A **92**, 063410 (2015).
[18] C. Zhong and F. Robicheaux, Phys. Rev. A **93**, 033410 (2016).
[19] B.C. Yang and F. Robicheaux, Phys. Rev. A **93**, 053413 (2016).
[20] H.-C. Shao and F. Robicheaux, Phys. Rev. A **93**, 053414 (2016).
[21] M.S. Pindzola, J. Colgan, F. Robicheaux, T.G. Lee, M.F. Ciappina, M. Foster, J.A. Ludlow, and Sh.A. Abdel-Naby, Adv. At. Mol. Opt. Phys. **65**, 291 (2016).
[22] S. Cohen, M. M. Harb, A. Ollagnier, F. Robicheaux, M. J. J. Vrakking, T. Barillot, F. Lepine, and C. Bordas, Phys. Rev. A **94**, 013414 (2016).
[23] P. Giannakeas, Chris H. Greene, and F. Robicheaux, Phys. Rev. A **94**, 013419 (2016).

Generation of Bright Soft X-ray Laser Beams

Jorge J. Rocca
Department of Electrical and Computer Engineering and Department of Physics
Colorado State University, Fort Collins, CO 80523-1373,
jorge.rocca@colostate.edu

Program description

The great interest in the use of high intensity coherent soft x-ray and x-ray light motivates the development of compact sources of intense coherent soft x-ray light that can be readily accessible. The project goals are to explore amplification of atomic transitions in plasma regimes leading to compact soft x-ray lasers emitting high energy pulses of femtosecond pulsewidth, and to investigate approaches that achieving high average powers by increasing the conversion efficiency and the repetition rate. This research builds on recent progress in the generation of bright soft x-ray laser beams on a table-top. We have recently made use of a diode-pumped laser driver to demonstrated soft x-ray laser operation at 100 Hz repetition rate, producing a record 0.1 mW average power at 13.9 nm from a table-top laser. The project studies the amplification of soft x-ray radiation in high plasma density regimes in which collisions broaden the laser transitions to create a gain medium with the increased bandwidth necessary to amplify femtosecond soft x-ray laser pulses. The ultrafast high energy pump laser that we are developing to enable this research will also allow us to explore lasing at wavelengths below 8 nm in transitions of Ni-like lanthanide ions. The combination of an increased efficiency with a further increase in repetition rate can be expected to yield soft x-ray laser beams with an unprecedented average power on a table-top high photon flux demanding applications. Newest results include a first demonstration of an 18.9 nm soft x-ray laser operation at 400 Hz repetition rate, the highest reported today for a soft x-ray laser.

High repetition rate soft x-ray lasers: first demonstration of 400 Hz operation

The best approach to increase the average power of table-top soft x-ray lasers consists in simultaneously increasing the repetition rate and improving the conversion efficiency of pump laser light into soft x-ray laser light. During the past year of research we succeeded in advancing the first by making a first demonstration of soft x-ray laser operation at a record repetition rate of 400 Hz at a wavelength of 18.9 nm in a transition of nickel-like molybdenum.

Lasing at 400 Hz repetition rate was achieved in the $4d^1S_0$ --> $4p^1P_1$ transition of Ni-like Mo (Mo^{14+}) in a laser-created plasma. The setup used is similar to that shown in Fig. 1, in which the pump laser impinges at grazing incidence into a polished molybdenum target to form a long narrow line focus (in this experiment ~30 μm x 4 mm FWHM). The soft x-ray laser amplifier plasma was created and heated with temporally-shaped laser pulses of ~1 J. These pulses consist of a nanosecond duration pedestal followed by a short pulse of 6 ps FWHM. The nanosecond pedestal or pre-pulse contains about 40 percent of the total laser pump energy. The short pulse, which contains the majority of the laser energy, is about 1000 times more intense. The nanosecond long ramp has the purpose of forming a plasma column ionized to the Ni-like Mo ionization stage. This plasma is allowed to expand to reduce sharp electron density gradients that could refract the amplified soft x-ray laser beam out of the gain region. The pre-pulse is followed by the intense short pulse that rapidly heats the plasma creating a large population of fast electrons. These fast electrons collide with Ni-like ground state ions to create a transient population inversion and a sufficiently large gain for the ASE to reach gain saturation in a single pass through the plasma column. The pump pulse impinges onto the target at a grazing incidence angle of 29 degrees to make use of beam refraction in the plasma to efficiently deposit its energy into a region of reduced density gradients and optimum density for amplification.

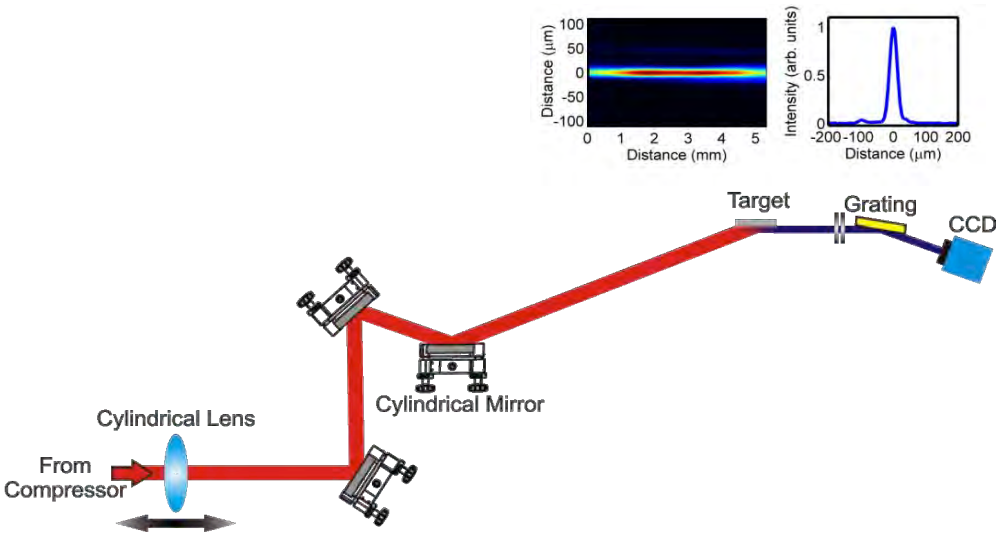

Fig. 1. Schematic of the experimental set up for the 400 Hz repetition rate soft x-ray laser experiments. For short runs (i.e. < 10,000 uninterrupted shots) the target consisted of a Mo slab displaced a few micrometers between shots. For uninterrupted laser operation during longer periods of time a rotating circular target is used. The inset shows an image of the line focus that creates the plasma. The focus line is about 30μm wide.

The pump pulses were generated with a high energy diode-pumped laser. This pump laser is currently capable to operate at up to 500 Hz repetition rate. At the time this first soft x-ray laser experiment was conducted it was operating at 400 Hz repetition rate. The laser consists of a Yb:KYW oscillator mode locked with a saturable absorber mirror, followed by a chain of amplifiers and a vacuum pulse compressor. An schematic of the laser is shown in Fig.2. The first amplifier is a room temperature diode- pumped Yb:YAG regenerative amplifier. The output of this regenerative amplifier is further amplified by two cryogenically cooled Yb:YAG amplifiers which operate at near liquid nitrogen

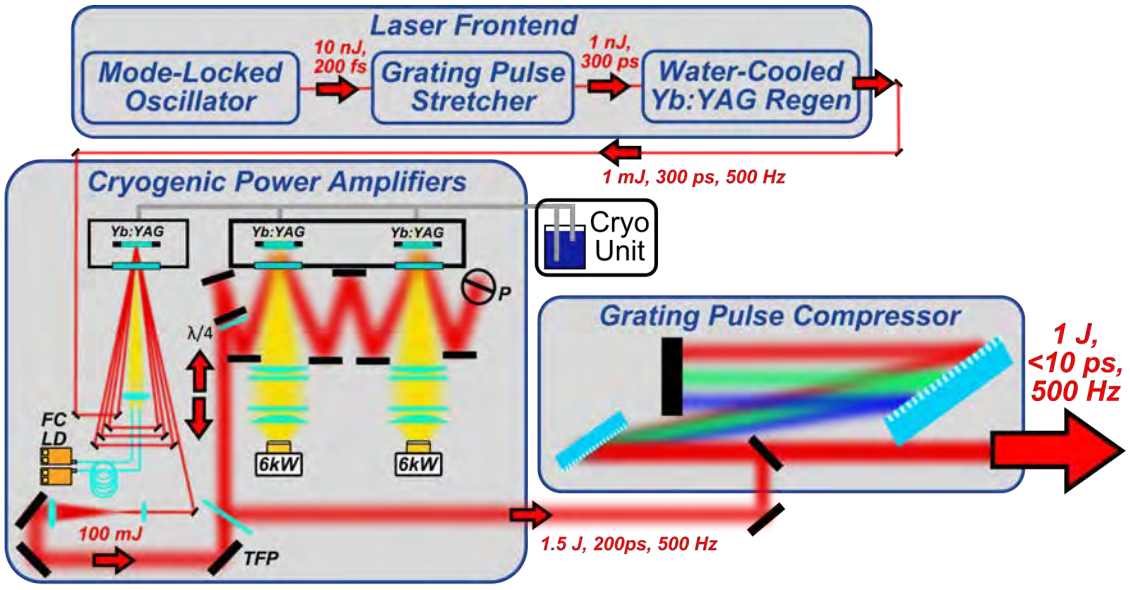

Fig. 2. Schematic diagram of the chirped-pulse-amplification Yb:YAG pump laser used in the high repetition rate soft x-ray laser experiments. The laser front end consists of a mode-locked Yb-KYW oscillator, a grating stretcher and a room temperature Yb:YAG regenerative amplifier. The ~ 1 mJ pulses from this front end are amplified in two cryogenically cooled amplifiers. The compressed pulses have 1 J energy and pulsewidth as short as 5 ps.

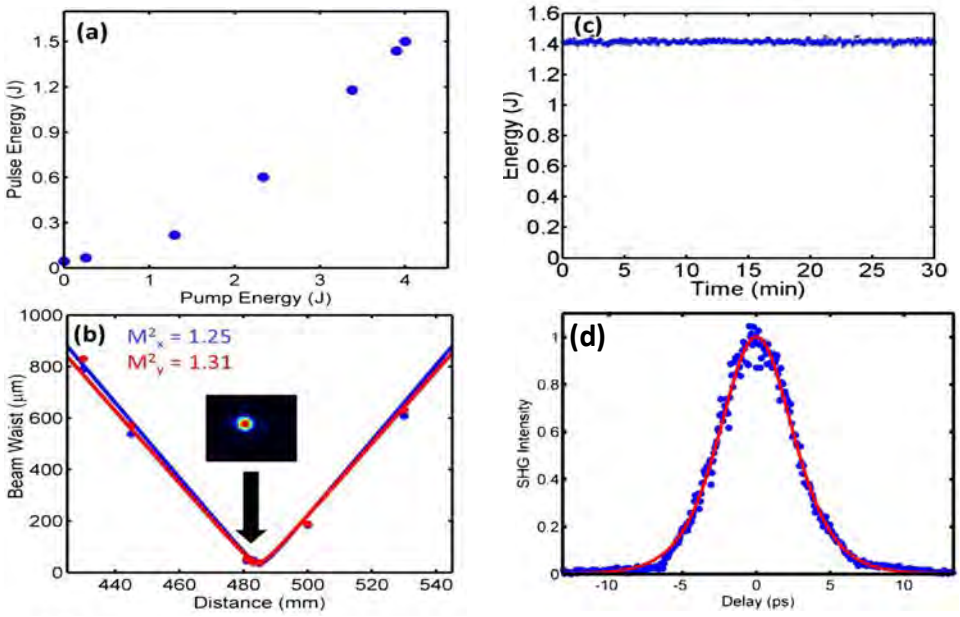

Fig. 3. a) Measured pulse energy of the pump laser as a function of diode laser pump power at 500 Hz repetition rate; b) M^2 measurement for 1.4 J pulses. c) Measured pulse energy for 30 minutes of continuous operation. The mean energy is 1.41 J with a standard deviation of 0.75 %. d) Second harmonic autocorrelation after pulse compression. The solid line is a $sech^2$ fit with a pulse duration of 3.8 ps FWHM.

temperature. The last power amplifier in the chain contains two Yb:YAG laser crystals mounted in the same cryogenically cooled embodiment. The pulses exiting this amplifier have an energy of up to 1.5 J (Fig.3a), and excellent shot-to-shot stability (Fig. 3b). As shown in Fig. 3c the laser displays good beam quality with values of M^2~ 1.3, which is necessary to create a high quality line focus for soft x-ray laser operation. The amplified pulses have a bandwidth of 0.36 nm FWHM, which support compression to sub-5ps pulses (Fig. 3d). The pulses are compressed to about 5 ps (6 ps in the soft x-ray laser experiment discussed herein) in a vacuum grating compressor using dielectric gratings.

The soft x-ray laser output was diagnosed acquiring on-axis spectra of the plasma emission. Spectra in the region surrounding 18.9 nm were obtained using a grazing incidence flat-field diffraction grating and a back-thinned CCD detector array. Thin Al filters were used to reject visible/ultraviolet plasma spontaneous emission and scattered pump laser light. Fig. 4(a) shows a single shot spectra recorded during laser operation at 400 Hz repetition rate. Strong, highly monochromatic lasing is observed in the at λ = 18.9 nm line of Ni-like Mo. The linewidth is un-resolved by the spectrometer, but it is known from previous measurements we conducted in similar Ni-like Mo laser–created plasma to be about $\Delta\lambda/\lambda \sim 3 \times 10^{-5}$. Operation at 400 Hz repetition rate was monitored using a

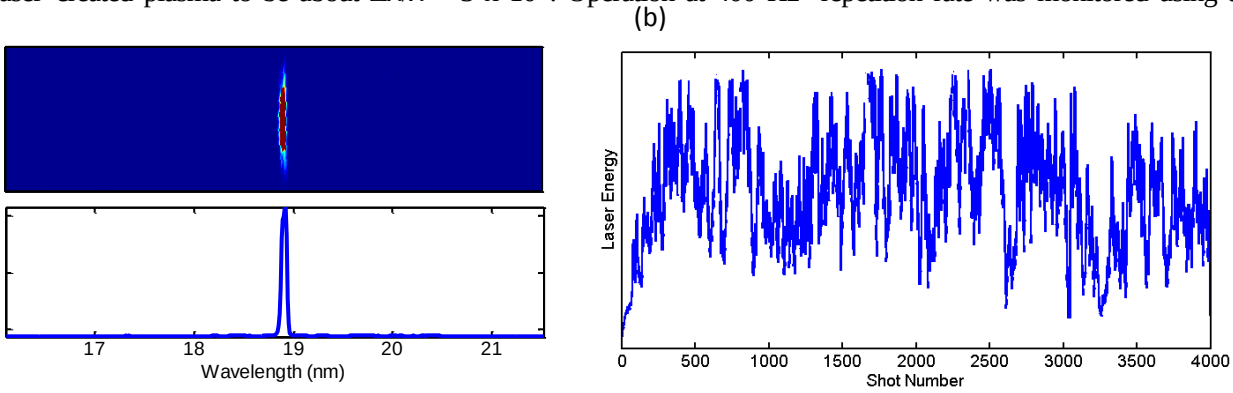

Fig. 4. (a) Single shot end-on spectra of the Ni-like Molybdenum soft x-ray laser amplifier operating at 400 Hz repetition rate. The single line observed is the $4d^1S_0$ --> $4p^1P_1$ λ=18.9 nm laser transition in Ni-like molybdenum. (b) Series of 4000 consecutive laser shots at 400 Hz repetition rate.

regtangular silicon photodiode placed vertically to resembe the slit of an spectrometer. A recording of 4000 consecutuve shots at 400 Hz repetition rate is shown in Fig. 4(b). This is the highest repetition rate reported for a table-top soft x-ray laser. These results were recently published in Optics Letters [2].

We also collaborated with scientists of the University of York (UK) to investigate the interaction of intense EUV/soft x-ray laser pulses with materials [3]. The interaction of an 46.9 nm laser beam with a parylene foil was studied in experiments at CSU and the results were compared to hydrodynamic simulations. A single EUV laser pulse of nanosecond duration focused to an intensity of 3×10^{10} Wcm^{-2} was used to perforate micrometer thick targets and to diagnose the interaction by a transmission measurement. A combination of 2-dimensional radiation-hydrodynamic and diffraction calculations was used to model the ablation, leading to good agreement with experiment. This theoretical approach allows predictive modeling of the interaction with matter of intense EUV beams over a broad range of parameters.

Future Plans

We plan to continue our efforts in using atomic transitions in highly ionized ions to develop compact plasma-based soft x-ray lasers at shorter wavelength, with shorter pulse duration, and increased average power. Specifically, during the next year of the project we plan to study amplification in lanthanide ions at sub-8 nm wavelengths, and to investigate plasma gain media with increased bandwidth to allow the amplification of bright soft x-ray pulses of femtosecond duration. Efforts of increasing the average power of table-top soft x-ray lasers will include a further increase of the repetition rate beyond the 400 Hz we recently demonstrated using new pump laser technology.

Publications resulting from DOE-AMOS supported work (2014-2016)

1. Y. Wang, S. Wang, E. Oliva, L. Lu, M. Berrill, L. Ying, J. Nejdl, B.M. Luther, C. Proux, T.T.T. Le, J. Dunn, D. Ros, P. Zeitoun, J.J. Rocca, “Gain dynamics in a soft X-ray laser amplifier perturbed by a strong injected X-ray field,” Nature Photonics **8**, 381 (2014).
2. .C. Baumgarten, M. Pedicone, H. Bravo, H.C. Wang, L. Yin, C.S. Menoni, J.J. Rocca, B.A. Reagan, “1 J, 0.5 kHz repetition rate picosecond laser”, Optics Letters **41**, 3339 (2016).
3. V. Aslanyan, I. Kuznetsov, H. Bravo, M. R. Woolston, A. K. Rossall, C. S. Menoni, J. J. Rocca, and G. J. Tallents, “Ablation and transmission of thin solid targets irradiated by intense extreme ultraviolet laser radiation”, Applied Physics Letters Photonics, **1,** 066101 (2016).
4. B. A. Reagan; C. M. Baumgarten; M. A. Pedicone; H. Bravo; L. Yin; M. Woolston; H. Wang; C. S. Menoni; J. J. Rocca, “Development of a kilowatt-class, joule-level ultrafast laser for driving compact high average power coherent EUV/soft x-ray sources”, Proc. SPIE 9740, Frontiers in Ultrafast Optics: Biomedical, Scientific, and Industrial Applications XVI (March 9, 2016); doi:10.1117/12.2212790.
5. C. M. Baumgarten, B. A. Reagan, M. Pedicone, H. Bravo, L. Yin, H. Wang, M. Woolston, B. Carr, C. Menoni, and J. Rocca, "Demonstration of a Compact 500 Hz Repetition Rate Joule-Level Chirped Pulse Amplification Laser," in *Conference on Lasers and Electro-Optics*, OSA Technical Digest (2016) (OSA, 2016), paper STu3M.3.
6. B.A. Reagan, C. Baumgarten, K.A. Wernsing, M. Berrill, M. Woolston, L. Urbanski, W. Li, M.C. Marconi, C.S. Menoni, and J.J. Rocca, “Advances in High Average Power, 100 Hz Repetition Rate Table-top Soft X-ray Lasers), (Invited), Springer Procc. in Physics, Vol. 169, X-Ray Lasers 2014, pp. 11-19 (2016) ISBN 978-3-319-19521-6.
7. B. A. Reagan, C. Baumgarten, K. Wernsing, H. Bravo, M. Woolston, A. Curtis, F. J. Furch, B. Luther, D. Patel, C. Menoni, and J. J. Rocca, "1 Joule, 100 Hz Repetition Rate, Picosecond CPA Laser for Driving High Average Power Soft X-Ray Lasers," in *CLEO: 2014*, OSA Technical Digest (online) (OSA, 2014), paper SM1F.4.
8. L. Li, Y. Wang, S. Wang, E. Oliva, L. Yin, T. T. T. Le, S. Daboussi, D. Ros, G. Maynard, S. Sebban, B. Hu, J. J. Rocca, and Ph. Zeitoun, “Wave Front Study of Fully Coherent Soft X-Ray Laser Using Hartmann Sensor”, Springer Proceedings in Physics, Vol. 169, X-Ray Lasers 2014, pages 323-330 (2016).
9. J. J. Rocca, "Table-top Soft X-Ray Lasers," in *Conference on Lasers and Electro-Optics*, OSA Technical Digest (OSA, 2016), Invited AM1K.1.

Spatial Frequency X-ray Heterodyne Imaging and Ultrafast Nanochemistry

Christoph G. Rose-Petruck
Department of Chemistry, Box H, Brown University, Providence, RI 02912
phone: (401) 863-1533, fax: (401) 863-2594, Christoph_Rose-Petruck@brown.edu

Program Scope

The goal of this research program is the study of chemical processes at nanometer length scales and ultrafast to slow time scales. We study the structure of nanometer-sized materials using Spatial Frequency Heterodyne Imaging (SFHI), an x-ray imaging modality developed during the past DOE funding cycle. Ultrafast dynamics of molecules in their solvation environment are studied with ultrafast x-ray absorption fine structure (UXAFS) spectroscopy using an endstation that we developed in collaboration with Bernhard Adams at 7ID-C of the Advanced Photon Source, Argonne National Laboratory. This abstract focuses primarily on the results of the UXAFS research.

Recent Progress

We carried out UXAFS measurements in combination with QM/MM calculations and showed the generation of 2^{nd} harmonic phonons in aqueous solutions at room temperature. The measurements were conducted by launching 13.5-GHz longitudinal phonons through impulsive Brillouin backscattering in millimolar, aqueous $KMnO_4$ solutions. The solutes served as probe molecules around which water's phonon dynamics was measured by UXAFS. Second-harmonic phonons at 27 GHz were detected and their 40 ps decay times measured. While slow relaxation times in glass forming liquids are known, our results apply to warm water implying that water can be substantially more rigid than commonly assumed.

50-mM $KMnO_4$ aqueous solution at 30°C were prepared with distilled water. The solvated MnO_4^- anions served as probes for measuring the response of surrounding water molecules after impulse excitation of phonons in the solution. No chemical reaction was observed. Transmission changes of the solution were measured around the MnO_4^- 1s → 3d pre-edge absorption line (6542.8 eV) with ~150ps X-ray pulses at 7ID-C of the Advanced Photon Source, Argonne National Laboratory. This formally forbidden dipole transition has non-vanishing oscillator strength because the tetrahedral symmetry of the complex permits mixing with p-orbitals. The transmitted X-rays were detected by a streak camera systems with 2-ps temporal resolution described elsewhere. Any distortion of the complex's symmetry results in a change of the X-ray absorbance at this spectral position. We used the permanganate's X-ray absorption sensitivity to deformations as a surrogate marker for the motions of the complex. Since permanganate forms univalent ions and is used in millimolar concentration, it is unlikely that the HB structure of water is strongly disturbed beyond the first solvation shell,. Nevertheless, since permanganate is hydrogen bonded to the surrounding water molecules, the complex's motions are strongly coupled to the surrounding water. Pre-edge absorption of X-rays promotes an inner-shell electron into the solute's LUMO, which overlaps with orbitals of the molecules in the solvation shell. Therefore, the X-ray absorbance of the permanganate pre-edge peak probes the dynamics of the surrounding water. By carrying out XAS measurements in the time domain, signals that decay quickly can be more easily detected than in frequency domain measurements where they would be broadened and hard to find.

We created monochromatic phonons by impulsive stimulated Brillouin scattering of 266-nm, 50-fs laser pulses. The intensity of the laser light on the sample was about 10^{13} W/cm², which lead to substantial electrostriction. Brillouin scattering is most intense in the backward and forward directions. Within the pulse length of the laser beam the backward scattered light will interfere with the incoming light, creating an interference grating in the backward scattering direction with a period $a_{grating} = a_{laser}/2n$. Here n is the index of refraction of the solution. As a consequence, phonons are emitted predominantly with an acoustic wavelength $\lambda_{ac} = \lambda_{grating}$. Assuming a refractive index n=1.23 at 270 nm, interference period of the laser light $\lambda_{grating}$ = 109 nm. This refractive index is lower than that of pure water at 270 nm. However, the absorbance of permanganate solution has a distinct minimum near 270 nm, which causes some anomalous dispersion, thereby lowering n. The sound speed of water is 1480 m/s and, thus, λ_{ac} = 109 nm corresponds to a phonon frequency of 13.5 GHz. The phonons' effect on the molecular structure of the permanganate ion becomes apparent only after several picoseconds, when the laser pulse has long since decayed.

Fig. 1 shows the measured transmittance change $\Delta T(t)$ with data points every 1.3 ps. The data points are the average of transmittances measured at 6542.8 eV, the pre-edge peak maximum, as well as 0.7 eV above and 0.8 eV below this peak. $\Delta T(t)$ is fitted as the sum of three functions: one double-exponential (pulse) function (plotted in grey color) and two dampened sinusoidal functions plotted in green and blue. The sum of the fitted functions was plotted as a black line. At zero delay-time, the transmittance changes at a nearly instrument-limited exponential rise

with a time constant τ_{rise} of 4 ps followed by an exponential decay with a time constant τ_{rise} of 19 ps. A 13.5-GHz wave (green) is produced 11ps after excitation. A quarter period later, at 30 ps, a wave with twice the frequency is measured (blue). We identified these waves as the fundamental and second harmonic (SH) acoustic phonons. The initial pulse is caused by the intense laser radiation, which likely induces strong electrostriction, sample heating and solute-specific reactions such as charge transfers to solvent and ligand dissociations. The decay time constant is consistent with thermal relaxation but details cannot be extracted from these data, nor are these events the focus of this study. Instead, we focus on the evolution of the phonons after laser excitation. The frequency of 13.5 GHz obtained from the fit shown in Fig. 1 is uncertain by about ±0.5 GHz. The second oscillation used to fit the data presented in Fig. 1 has a frequency of 27 GHz, which matches that of a 2nd harmonic acoustic wave. The decay time of the fundamental waves is long. The fit indicates a time constant of at least 300 ps. As long as a coupling between two waves exist and the fundamental wave amplitude is constant, the SH wave should be produced with constant amplitude. We observe, however, that the SH wave decays with a time constant of 39 ps, which implies non-thermal molecular relaxation processes must exist that either reduce the pressure amplitude in the solvation shell or that other changes of the solvation shell structure exist that prevent the generation SH waves.

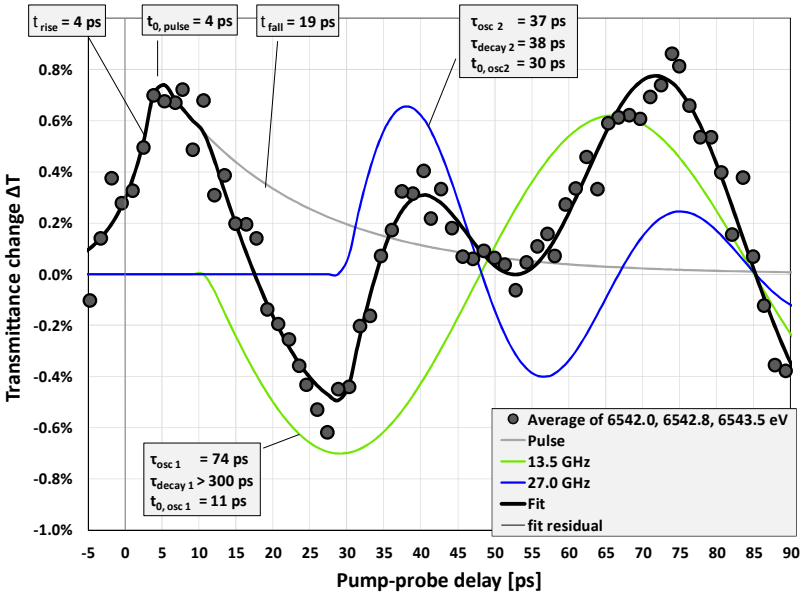

Fig. 1. Changes of the X-ray transmittance at the manganese pre-edge absorption line vs. time after laser excitation. A fit to the data points is shown in black.

To extract more information on the molecular level, theoretical studies were conducted using a combination of QM/MM Molecular Dynamics (QM/MM MD) and X-ray Absorption Spectra (XAS) simulations, see Fig. 2. We started with the equilibrated structure of single gas molecules obtained from structure optimization in Gaussian and MnO_4^--water cluster from MD simulation. Then we varied the complex bond angle, bond length, and solvation shell radius, calculated the XAS of these modified structures and then compared the XAS peak positions and amplitudes with respect to the original structure. We found that Mn-O bond length changes as well as reductions of the solvation shell radius modify both, position and amplitude. Upon expansion, however, the peak amplitude change saturates while the position still varies proportionally to the solvation shell radius. Among all the simulations we did, the only motion that does not shift the peak position is O-Mn-O bond angle changing.

Additionally to the UXAFS spectrum shown in Fig. 1 we measured UXAFS spectra at several other X-ray energies. We then constructed a mathematical model that describes all UXAFS spectra simultaneously. In combination with our simulations, we determined that the oscillations at 13.5GHz is caused by solvation shell radius oscillations and the in-phase oscillation of Mn-O bond length, a motion that corresponds to longitudinal acoustic phonons. The blue curve in Fig. 1 oscillate with 27 GHz and is 90° phase shifted to the fundamental wave as expected for a 2nd harmonic wave. Importantly, the X-ray line peak position barely oscillates at this frequency. Our simulations show that the only dynamics that changes line amplitude without changing line position is associated with permanganate symmetry deformations but not radial motions. Since the complex is hydrogen-bonded to the surrounding water, complex deformation is most likely caused by transversal water motions which in turn suggest that the SH wave is a transversal acoustic wave. Therefore, we observe a longitudinal-transverse phonon coupling from the fundamental to the 2nd harmonic phonons. This longitudinal-transverse coupling is in agreement with the proposed existence of tens to hundreds of nanometers dipole correlation lengths of aqueous solutions measured by hyper-Rayleigh light scattering experiments.

Combining the amplitude of the X-ray absorption line position oscillation with our simulations, we estimate that the solvation shell radius oscillates with an amplitude of no less than 0.8 Å. Using the compressibility of water, we estimate that this diameter change corresponds to a pressure oscillation of about 1 GPa. Such high pressure will

certainly cause the stress-strain tensor to be non-linear, which is the reason for the 2nd harmonic generation in the first place. The decay of the SH wave could be caused by the amplitude reduction of the pressure oscillation. This, however, would be visible in the simultaneous reduction of the fundamental amplitude in the UXAFS data (green curve in Fig. 1), which is not the case. Alternatively, the SH amplitude may be reduced by structural changes of the solvation shells without a reduction of pressure.

An alternative explanation is related to the existence of ice-like domains in liquid water. In principle two sounds speed exist in water, the hydrodynamics speed of 1480 m/s and the viscoelastic speed at about 3000 m/s (Fast Sound). UV-Brillouin scattering studies reported in the literature measured Fast Sound in neat water even at wave numbers below 0.1 nm^{-1} at 300 K. Thus, under our conditions acoustic waves propagating with about 3 km/s can exist. This speed is very close to the sound speed in ice and is therefore associated with the fleeting existence of ice-like domains in liquid water. These domains react to mechanical stimuli with an ice-like stiffness but they only exist until the water molecules rearrange, forming new hydrogen-bonded domains. Such rearrangements should occur on the few-picoseconds timescale, driven, for instance, by thermal motions. We hypothesize that the SH wave propagates at the Fast Sound Seed. Since Fast Sound requires the existence of ice-like domains, the measured 39-ps decay of the SH wave is the lower limit of the lifetime of ice-like domains in water at ambient temperature. Since we observe very small wave-vector phonons with wavelengths of about 109 nm, the ice like domains must be of similar size. Thus, our data support recent simulation results that indicate the water is much more ice-like than previously assumed. This last interpretation is supported by our UXAFS measurements of the dynamics of aqueous ferrohexacyanide solution. There we observed the direct generation of 27.9-GHz phonons under identical laser excitation conditions. Brillouin backscattering with such a frequency shift requires a sound speed of 3060 m/s. Thus, for this solution with much higher ionic strength than the permanganate solutions, ice like structure must exist. A 160 ps decay time of the oscillation was measured, much longer than the one in the permanganate solution. This seems reasonable considering the stronger influence of the ferrohexacyanide on its solvation shells, which inhibits molecular reorientations of the water molecules.

Our Spatial Frequency Heterodyne Imaging (SFHI) research was refocused

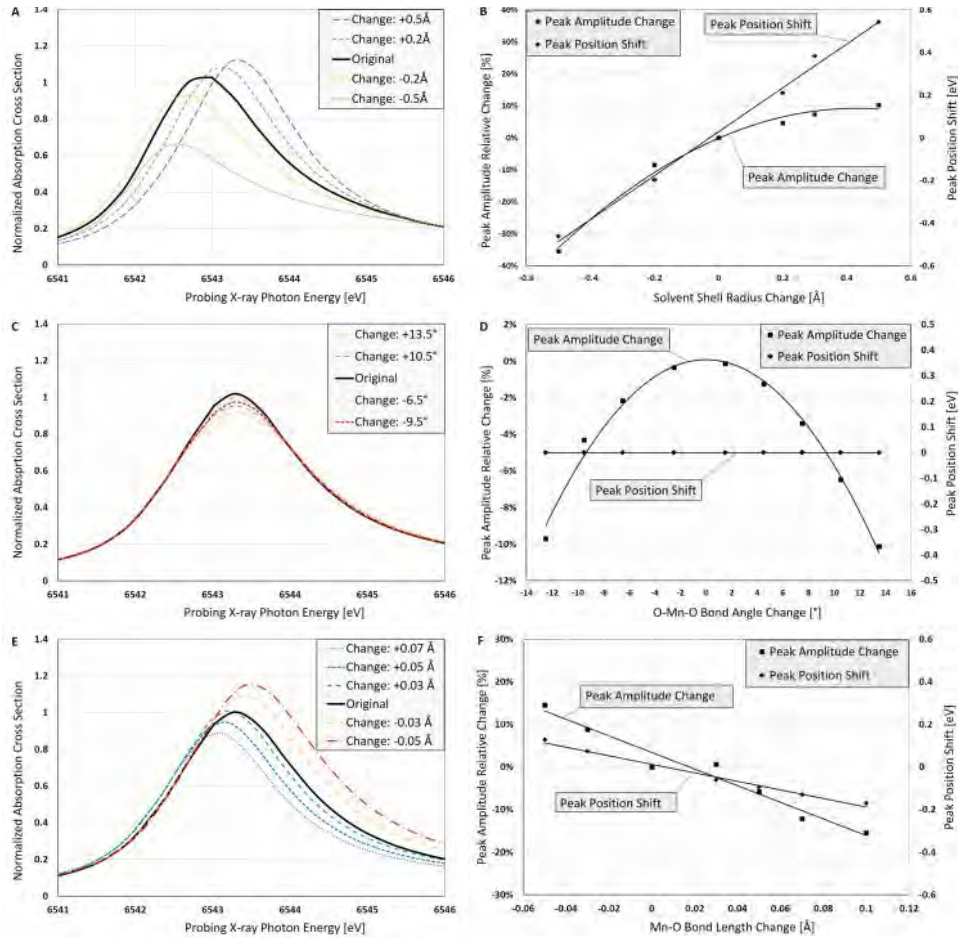

Fig. 2. (**A**)**.** Effect of solvation shell radius change on the XAS; (**B**). Summary of the characteristic features shown in (**A**); the peak position can be fitter to a line E = 1.0307 r + 0.0281 and the peak amplitude can be fitted to a parabola A = -0.5032 r^2 + 0.4339 r -0.0016. (**C**). The XAS for various O-Mn-O bond angle changes are shown; (**D**). Summary of the characteristic features shown in (d); the peak amplitude can be fitted to a parabola A = -0.0006 θ^2 + 0.000005 θ +0.0008; (**E**). Effect of solute bond length change on the XAS; (**F**). Summary of the characteristic features shown in (**E**); the peak position can be fitter to a line E = -2.0049 r + 0.013 and the peak amplitude can be fitted to another line A = -1.9513r + 0.0341

on energy and nanoparticle-related topics. A thesis was completed on the SFHI measurements of carbon nanotubes during water loading and unloading. In collaboration with the Brown School of Engineering we recently began *in situ* SFHI of lithium ion batteries with silicon nanoparticle (NP) electrodes during charge cycling. SFHI can image the changes of the electrode NPs, e.g. their agglomeration and fracturing, with very high sensitivity. This information has been inaccessible so far. We expect that the data will have impact on the design of Li-ion batteries with improved life. These results will be reported at a later time.

Future Plans

The goal of future UXAFS experiments is the study of the ionic strength on the stiffness of water surrounding ionic solutes. Furthermore, the coupling of longitudinal and transversal modes will be clarified. To these ends measurements will be carried out at various ionic strength and temperatures. Potassium permanganate will remain the choice for the probe molecules because it allows the X-ray spectroscopic distinction between longitudinal and transversal modes. Increasing the ionic strength should enable the direct Brillouin excitation of 27GHz waves, which require the existence of fast sound and therefore ice-structures. As discussed above this effect has been observed for ferrohexacyanide but demonstrating it for permanganate would clearly identify the SH waves we observed as the surrogate marker for ice-like water. Experiments in D_2O will be carried out. The hydrogen bond (HB) in D_2O is somewhat stronger and shorter than in H_2O. While the HB-stretching mode in D_2O is weaker than in H_2O, the bending mode is stronger. Since collective reorientations of water molecules limit the life-time of ice-like structure, we speculate that the SH decay times in D_2O would be longer than in H_2O.

The recent research was carried out at 7ID-C of the Advanced Photon Source. In the future we will use a laser-driven plasma X-ray source at Brown University. The concept of this liquid-metal target source was originally developed with support from this BES program. The temporal resolution will be 100 fs at an X-ray flux.

Our work on SFHI of Li-ion batteries will continue in order to understand the aging process of Si-nanoparticle-coated electrodes. The goal is to develop electrodes with increased lifetime.

BES-Supported Publications (2014 – 2016)

1. "Mesoscopic, long-lived, ice-like structures in aqueous solution measured by ultrafast X-ray spectroscopy," Y. Jiao, B. Adams, A. O. Dohn, H. Jonsson and C. Rose-Petruck, Phys. Rev. Lett. submitted (2016).
2. "Picosecond-resolved x-ray absorption spectroscopy at low signal contrast using a hard x-ray streak camera," B. Adams, Y. Jiao and C. Rose-Petruck, Journal of Synchrotron Radiation 22 (4), 1022 (2015).
3. "X-ray focusing scheme with continuously variable lens," B. Adams and C. Rose-Petruck, Journal of Synchrotron Radiation 22, 16 (2015).
4. "Spatial Frequency Heterodyne Imaging of Aqueous Phase Transitions inside Multi-walled Carbon Nanotubes," F. Schunk, D. Rand and C. Rose-Petruck, PCCP 17, 31237 (2015).
5. "Spatial frequency heterodyne imaging in the soft x-ray water window," P. Bruza, D. Panek, M. Vrbová, V. Fidler and C. Rose-Petruck, Applied Physics Letters 104, 254101 (2014).
6. "X-Ray Spatial Frequency Heterodyne Imaging of Protein-Based Nanobubble Contrast Agents," D. Rand, M. Uchida, T. Douglas and C. Rose-Petruck, Optics Express 22 (19), 23290 (2014).
7. "X-Ray Spatial Frequency Heterodyne Imaging with Protein-Based Nanobubble Contrast Agents," C. Rose-Petruck, T. Douglas, D. Rand and M. Uchida, Pat. Appl. Publ. 2014 US Patent Appl. Number: 61/981,945, (2014)

Synergistic publications and patents co-supported by BES

8. "Methods, compositions and kits for imaging cells and tissues using nanoparticles and spatial frequency heterodyne imaging," C. Rose-Petruck, J. R. Wands, Z. Derdak, D. Rand and V. Ortiz, Pat. US 9,316,645 (2016)
9. "X-ray Scatter Imaging of Hepatocellular Carcinoma in a Mouse Model Using Nanoparticle Contrast Agents," D. Rand, Z. Derdak, J. R. Wands and C. Rose-Petruck, Scientific Reports 5, 15673 (2015).
10. "A Highly Sensitive X-ray Imaging Modality for Hepatocellular Carcinoma Detection," D. Rand, E. G. Walsh, Z. Derdak, J. R. Wands and C. Rose-Petruck, Physics in Medicine and Biology 60, 769 (2014).

BES-supported and co-supported Ph.D. theses

1. “Ultrafast X-ray Spectroscopy of solvation shell dynamics in aqueous solution,” Y. Jiao, Brown University, Defense Dec. 2016
2. “Harmonic Imaging of Nano-confined Aqueous Phase Transitions and the Electrochemical Reduction of Carbon Dioxide Using a Nano-structured Electrolyte,” F. Schunk, Brown University 2016
3. "Pulse Plasma Soft X-ray Source in Biomedical Research," P. Bruza, Czech Technical University, 2014.
4. "X-Ray Spatial Frequency Heterodyne Imaging of Hepatocellular Carcinoma Using Nanoparticle Contrast Agents," D. Rand, Brown University, 2014.

Transient Absorption and Reshaping of Ultrafast Radiation

DE-FG02-13ER16403

Kenneth J. Schafer (schafer@phys.lsu.edu)
Mette B. Gaarde (gaarde@physics.lsu.edu)

Department of Physics and Astronomy, Louisiana State University
Baton Rouge, LA 70803

September 2016

Program Scope

Our program is centered around the theoretical study of transient absorption of ultrafast extreme ultraviolet (EUV) radiation by atoms and materials interacting with a precisely synchronized near-to-mid infrared (IR) laser pulse. Transient absorption spectroscopy can in principle provide high spectral resolution and high (attosecond) time resolution simultaneously, by spectrally resolving the light transmitted through a sample as a function of delay between the dressing laser pulse and the broadband attosecond EUV probe. As in all transient absorption calculations/measurements, one of the main challenges we confront is the extraction of time-dependent dynamics from delay-dependent information. In addition, we must also account for the reshaping of the broadband XUV light in the macroscopic medium. We study attosecond transient absorption (ATA) using a versatile theoretical treatment that takes account of both the strong laser-atom interaction at the atomic level via the time-dependent Schrodinger equation (TDSE), as well as propagation of the emitted radiation in the non-linear medium via the Maxwell wave equation (MWE), often in the single-active electron (SAE) approximation [1]. We have also extended our TDSE/MWE treatment in atoms to fully-active two electron calculations in helium, in both full and reduced dimensions. Consistent with our goals in the original proposal, we have built a program that emphasizes both fundamental theoretical research and a close connection with experimental groups doing attosecond physics.

Recent Progress

We have completed a number of research projects in collaboration with experimental groups carrying out attosecond transient absorption (ATA) measurements. Several have now appeared as journal articles, see [R1-R6]. We have also recently published an *Invited Topical Review* in *Journal of Physics B* [R7] that summarizes and places in context many of the theoretical results on attosecond transient absorption that we have obtained in the course of our work over the past three years. We concentrate on one of these projects in this abstract.

As part of our work on the fundamental properties of ATA, we have an ongoing collaboration with the experimental group of Prof. A. Sandhu at the University of Arizona in which we explore the interplay between microscopic and macroscopic effects that influence the shape of the absorption spectrum (the line shape) around a resonant state in strong-field ATA. In particular, we have studied the influence of resonant pulse propagation (RPP) on the absorption line shape. RPP describes a very general *macroscopic* phenomenon in which a short pulse propagating through a medium with long-lived resonances will undergo strong temporal reshaping. It was first discussed in the 1970s [2] and detailed analysis of the effects of RPP is available for the propagation of visible and near-infrared (IR) femtosecond and picosecond pulses [3, 4]. The temporal reshaping caused by RPP is illustrated in Fig. 1(a) for an XUV pulse with a duration $\tau_{\rm xuv} = 5$ fs propagating through an (IR field free) 16 Torr helium gas in which it is resonant with a transition with a decay time $\gamma = 60$ fs. The figure illustrates how the short pulse initially builds up a long tail that subsequently develops into a series of sub-pulses. Each sub-pulse is longer in duration and weaker than the previous sub-pulse, and in each sub-pulse the electric field changes its phase by π relative to the previous sub-pulse (not shown).

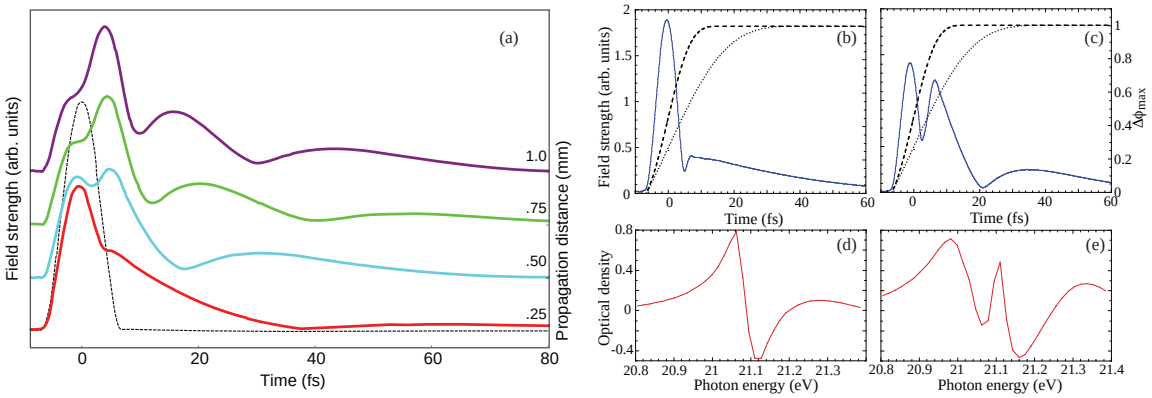

Figure 1: Illustration of resonant pulse propagation of a 5 fs XUV pulse through a helium gas in which the XUV light excites a resonance with a 60 fs decay time. (a) shows the XUV electric field strength at different propagation distances up to 1 mm, with the initial pulse shown as the dotted line. The XUV pulse quickly develops a long tail consisting of a series of sub-pulses which shorten with propagation. The He gas pressure of 16 Torr, and no IR pulse is present. (b-e) RPP effects in an 8 Torr IR-laser-dressed He gas. (b,c) XUV time profiles at two different propagation distances $z = 0.25$ mm (b) and $z = 1$ mm (c). Also shown are approximate time-dependences of the phase shift imposed by two different IR pulses of duration 13 fs (thin dashed lines) and 33 fs (thin dotted line). The macroscopic optical densities are shown for the $z = 0.25$ mm (d) and $z = 1$ mm (e) cases. Adapted from [R6].

The RPP effect is driven by the large spectral phase which can be accumulated due to dispersion (each accumulated phase of π in the spectral domain leads to a sign change of the electric field in the time domain) and leads to reduced absorption compared to Beer-Lambert's law [2]. RPP does not dramatically alter the absorption profile of the XUV light unless an IR pulse is used to field-dress the helium gas.

The *microscopic* effect of the IR-laser-dressing on the absorption line shape around a resonance has been investigated by a number of groups [5–7] and is well understood at a conceptual level: the presence of the external IR field modifies the time-dependent dipole moment which has been initiated by the XUV field, predominantly by the addition of a time-dependent phase due to the AC Stark shift of the excited state. In the spectral domain, this leads to a redistribution of energy between the light field and the atom and generally gives rise to transient absorption profiles that include both positive and negative values, corresponding to absorption (loss) or emission (gain) at different frequencies. In the simplest possible case in which one starts with a purely Lorentzian absorption line shape around a bound state resonance and then adds an instantaneous phase shift due to a short IR pulse, the resulting absorption line shape can be varied smoothly between a Lorentzian, a dispersive (Fano-like), and a window resonance line shape depending on the magnitude of the *laser induced phase* (LIP) shift. This was discussed extensively in [6] and other papers. An example of a dispersive absorption line shape around the $1s2p$ resonance in helium is shown in Fig. 1(d).

Our theory-experiment collaboration with Sandhu's group focuses on how the interplay between the microscopic LIP and the macroscopic RPP, both in the temporal domain, manifests itself in the spectral absorption profiles. We have found, both in experimental and theoretical results, that RPP alters the absorption line shape in multiple ways: (i) for short propagation distances, the first sub-pulse in the RPP-reshaped XUV pulse acts like a new effective lifetime for the XUV-excited dipole moment which leads to broadening of the LIP-controlled line shape. This is illustrated in the comparison between the width of the dispersive line shapes shown in Fig. 1(d) and (e). (ii) When the XUV pulse propagates sufficiently far that a second sub-pulse appears in the XUV time profile, a new narrow feature appears on line center in the absorption profile (shown in Fig. 1(e)). This is because the second sub-pulse is phase-shifted by π relative to to the first sub-pulse and therefore generally will give rise to absorption (as opposed to the emission on line center caused by the LIP). Additional narrow features would appear in the absorption spectrum, nested around line center, for longer propagation distances as additional sub-pulses would appear in the XUV temporal profile. (iii) Finally, at very long propagation lengths, the microscopic and macroscopic effects

become intertwined and can no longer be separated in a simple manner. We have published two papers on this topic: a PRL which focused on the discovery of the RPP effect in transient absorption [R4], and a longer study focusing on how the RPP-LIP interplay manifests itself in both the time and frequency domain, and how it is influenced by the choice of IR and gas parameters [R6].

Future directions

As one of several research directions detailed in our recent renewal proposal, we will continue to explore the effects of RPP in ultrafast transient absorption, building on the work described above. We are interested in RPP effects both at the fundamental and the applied level. At the fundamental level, we observe that RPP is sensitive to the dressing of the resonant transition with an IR laser. In our calculations we have observed a number of differences between the with-IR and without-IR time profiles:

(i) *Effects of the laser-induced phase (LIP).* In [R6] we discussed that the timing of the first and second sub-pulses in the propagating XUV field changes by several fs in the presence of the IR pulse, and that a longer IR pulse leads to larger changes. While there is a closed form expression for the electric field envelope of the propagating field in RPP in the limit of very long lifetime in the absence of a dressing IR field [3], it is not realistic to obtain a closed-form expression for the pulse envelope in the presence of an actual IR pulse with a finite duration. Nevertheless, it would be worthwhile to seek a closed-form expression in the limit that the IR pulse is a delta function and acts merely to induce an instantaneous phase shift on the XUV time-dependent dipole moment. We propose to more quantitatively investigate the influence of the LIP on the XUV temporal reshaping. This would be a complement to the works in [R4, R6] which predominantly concentrate on the influence of the RPP-LIP interplay on the absorption spectrum.

(ii) *Effects of nearby XUV-excited states.* When the IR and the XUV pulses overlap, so-called light-induced states (LIS) will appear in the absorption spectrum [8,9]. In the simplest possible understanding of this effect, each LIS can be associated with a phase-sensitive Raman-like two-photon process which involves the absorption of an XUV photon and then either absorption or emission of an IR photon, so that the atom may end up with population in a dark (non-dipole allowed in absence of the IR) state. In helium, there are several LISs that are close in energy to the $1s2p$ energy, associated with population transfer to the $1s2s$, $1s3s$, and $1s3s$ states. This means that if one is considering the propagation of a few-fs XUV pulse, which would excite both the $2p$ state itself and the three neighboring LISs, the time-dependent dipole moment is initially very complex because it consists of the long-lived $2p$ dipole radiation, and the radiation from the three LISs which lasts for the duration of the IR pulse. This effect can be seen at short time scales in the propagating XUV pulse, for instance comparing the beginning of the first sub-pulse, around 2 fs, in the 0.5 mm case in Fig. 1(a) and the 1 mm case in Fig. 1(c). In the with-IR case in (c), there is a deep minimum between the main pulse and the first sub-pulse which is absent in the no-IR case in (a). The depth (and sub-cycle timing) of this minimum also depends on the sub-cycle value of the delay between the IR and the XUV pulses; in the figure we show a value which has been averaged over one half laser-cycle. This first minimum is thus created in the interference between the radiation oscillating at the four slightly different frequencies. While it would be reasonable to assume that the short lifetime of the light-induced states would mean that they would not influence the long tail of the propagating XUV pulse, we do not actually know that this is true and we propose to investigate in more detail both the short-term and the long-term effects of the presence of the IR pulse on the RPP temporal reshaping.

Publications resulting from DOE/AMOS support, previous three years

R1 A. R. Beck, B. Bernhardt, E. R. Warrick, M. Wu, S. Chen, M. B. Gaarde, K. J. Schafer, D. M. Neumark, and S. R. Leone, *Attosecond transient absorption probing of electronic superpositions of bound states in neon: detecting quantum beats by laser coupling of individual states*, **New J. Phys.** 16, 113016 (2014).

R2 J. Herrmann, M. Lucchini, S. Chen, M. Wu, A. Ludwig, L. Kasmi, K. J. Schafer, L. Gallmann, M. B. Gaarde, U. Keller, *Multiphoton transitions for delay-zero calibration in attosecond spectroscopy*, **New J. Phys.** 17, 013007 (2015).

R3 M. Reduzzi, J. Hummert, A. Dubrouil, F. Calegari, M. Nisoli, F. Frassetto, L. Poletto, S. Chen, M. Wu,

M. B. Gaarde, K. J. Schafer, G. Sansone, *Polarization-control of absorption of virtual dressed-states in helium*, **Phys. Rev. A** 92, 033408 (2015).

R4 C.-T. Liao, A. Sandhu, S. Camp, K. J. Schafer, and M. B. Gaarde, *Beyond the single-atom response in absorption line shapes: Probing a dense, laser-dressed helium gas with attosecond pulse trains*, **Phys. Rev. Lett.** 114, 143002 (2015).

R5 X. Li, D. J. Haxton, M. B. Gaarde, K. J. Schafer, and C. W. McCurdy, *Direct extraction of intense-field-induced polarization in the continuum on the attosecond time scale from transient absorption*, **Phys. Rev. A** 93, 023401 (2016).

R6 C.-T. Liao, A. Sandhu, S. Camp, K. J. Schafer, and M. B. Gaarde, *Attosecond Transient Absorption in Dense Gases: Exploring the Interplay between Resonant Pulse Propagation and Laser-Induced Line Shape Control*, **Phys. Rev. A** 93, 033405 (2016).

R7 M. Wu, S. Chen, S. Camp, K. J. Schafer, and M. B. Gaarde, *Invited Topical Review: Theory of strong-field attosecond transient absorption*, **J. Phys. B** 49, 062003 (2016).

R8 X. Guan, M. Wu, M. B. Gaarde, and K. J. Schafer, *Correlated attosecond transient absorption in helium atoms above the first ionization threshold*, to be submitted to Phys. Rev. A (2016).

References

[1] Mette B. Gaarde, Christian Buth, Jennifer L. Tate, and Kenneth J. Schafer. Transient absorption and reshaping of ultrafast XUV light by laser-dressed helium. *Phys. Rev. A*, 83(1):013419, January 2011.

[2] MD Crisp. Propagation of small-area pulses of coherent light through a resonant medium. *Phys. Rev. A*, 1(6):1604–1611, 1970.

[3] Mohamed Bouchene. Phase control of dispersion effects for an ultrashort pulse train propagating in a resonant medium. *Phys. Rev. A*, 66:065801, Dec 2002.

[4] J. Delagnes and M. Bouchene. Gain-dispersion coupling induced by transient light shifts in an atomic medium. *Phys. Rev. A*, 76:023422, Aug 2007.

[5] H Wang, M. Chini, S. Chen, C.-H. Zhang, F. He, Y. Cheng, Y. Wu, U. Thumm, and Z. Chang. Attosecond time-resolved autoionization of argon. *Phys. Rev. Lett.*, 105:143002, 2010.

[6] Christian Ott, A. Kaldun, P. Raith, K. Meyer, M. Laux, J. Evers, C. H. Keitel, C. H. Greene, and T. Pfeifer. Lorentz Meets Fano in Spectral Line Shapes: A Universal Phase and Its Laser Control. *Science*, 340(6133):716–720, 2013.

[7] Shaohao Chen, Mengxi Wu, Mette B. Gaarde, and Kenneth J. Schafer. Laser-imposed phase in resonant absorption of an isolated attosecond pulse. *Phys. Rev. A*, 88(3):033409, September 2013.

[8] Shaohao Chen, M. Justine Bell, Annelise R. Beck, Hiroki Mashiko, Mengxi Wu, Adrian N. Pfeiffer, Mette B. Gaarde, Daniel M. Neumark, Stephen R. Leone, and Kenneth J. Schafer. Light-induced states in attosecond transient absorption spectra of laser-dressed helium. *Phys. Rev. A*, 86(6):063408, December 2012.

[9] Michael Chini, Xiaowei Wang, Yan Cheng, Yi Wu, Di Zhao, Dmitry a Telnov, Shih-I Chu, and Zenghu Chang. Sub-cycle Oscillations in Virtual States Brought to Light. *Sci. Rep.*, 3:1105, January 2013.

Time Resolved High Harmonic Spectroscopy: A Coherently Enhanced Probe of Charge Migration

Science Using Ultrafast Probes: DE-SC0012462

Kenneth Schafer[1], Mette Gaarde[1], Kenneth Lopata[2],
Louis DiMauro[3], Pierre Agostini[3], Robert Jones[4]
1) Department of Physics and Astronomy, Louisiana State University, Baton Rouge, LA
2) Department of Chemistry, Louisiana State University, Baton Rouge, LA
3) Department of Physics, The Ohio State University, Columbus, OH
4) Department of Physics, University of Virginia, Charlottesville, VA

Program Scope

Understanding the quantum transport of electrons and holes, and the correlations between them, provides an avenue toward improving the efficiency of chemical processes including energy conversion and catalysis. The relevant electron dynamics evolve on exceedingly fast time scales down to the natural time scale of the electron, the attosecond. For this reason, attosecond science has increasingly focused on the possibilities for measuring and controlling correlated electron motion in complex many body systems such as polyatomic molecules as one of the key applications of this new science.

There are two broad motivations for extending the measurement of electron/hole dynamics in chemical systems to the attosecond time scale. The first is the study of electron correlation itself. Though electrons interact on an attosecond time scale, currently measurements are made over much longer time scales, meaning that two and many-electron interactions are averaged over. Attosecond studies open a new perspective on these interactions beyond the mean-field picture and without time-averaging. The second motivation is the study of the earliest phase of charge transfer reactions. These reactions are among the simplest processes in chemistry yet the efficiency with which electrons move around in a molecule is one of the primary regulation mechanisms in biology. As an important example of correlated electron dynamics in many-body systems we will study ultrafast charge migration in complex chemical environments. Charge migration refers to the rapid movement (femtosecond or faster) of positively charged holes in a molecule following localized excitation or ionization.

Attosecond charge migration in molecular systems is thought to be driven by a complex interplay between many-electron correlation effects and dephasing/relaxation due to weak coupling with nuclear motion. Understanding the mechanisms of this migration, and developing experimental tools for observing this process, are crucial to advancing ultrafast science. The objective of the ATTO-CM team is to advance ultrafast science in the US both on small-scale and large-scale facilities using a concerted effort of both theorists and experimentalist solving these problems side by side. Our emphasis is to evaluate high harmonic spectroscopy as a sensitive probe for studying charge migration dynamics in chemical systems by developing a symbiotic relationship between theory and experiment. The initial experimental campaigns will be laboratory based but with the probes maturation will translate onto a large-scale facility, like LCLS, a natural progression for the science.

Louisiana State University Node

Recollision Physics

One of the main goals of the theoretical node of the project is the development of a framework to model, analyze and predict high-harmonic generation (HHG) spectra in complex molecules experiencing charge migration. For this purpose, we combine the molecular recollision picture (see Fig. 1) with a quantum chemistry description of matter in terms of molecular orbitals. Besides matching the framework used by the theoretical chemistry node, this provides an intuitive picture of the processes in terms of seemingly independent particles. One should, however, keep in mind that even in the recollision picture charge

migration is fundamentally a multi-electron/multi-orbital effect. With exactly one electron removed from the molecule, we find it more convenient to follow the dynamics of the hole. We then decompose the hole dynamics in the basis of molecular orbitals, broadly referred to as "channels".

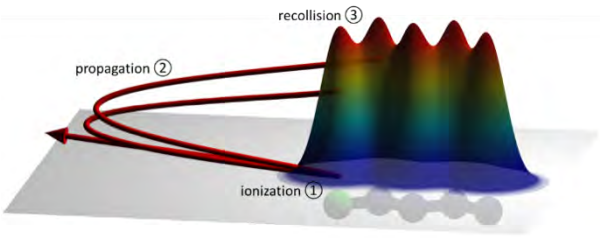

Figure 1: Recollision picture for a molecular target: ① ionization of an electron from one molecular site; ② propagation in the field; ③ recollision with its parent ion.

A fundamental challenge of high harmonic spectroscopy is that the dynamics – both the recollision and the hole motion – lives in the temporal domain while experimental measurement and HHG spectra live in the frequency domain. We therefore need to build a bridge between the two domains.

Building the Bridge [Mauger 2016]

We begin by bridging the temporal and frequency domains for a single active electron (SAE) system. We developed a semiclassical model and showed how the three steps of the recollision picture (see Fig. 1) can be factorized in the temporal domain and then how this factorization can be mapped into the frequency domain. This analysis, published in [Mauger 2016] confirmed the importance of having accurate ionization rates and scattering cross sections as inputs to model HHG spectra. We also use this SAE-static-hole model as a benchmark to compare to and identify the effects of hole dynamics.

We then expand the previous model to account for charge migration effects. With the molecular recollision picture and in the basis of molecular orbitals, we decompose the hole dynamics and its contribution to HHG into ionization/recollision channels. Each individual channel is relatively similar to the SAE case and they are added coherently to obtain the full HHG signal. This model also shows that, in addition to the channel-resolved ionization rates and scattering cross-sections, we need the ionic dipole matrix elements to model the hole dynamics. All these elements are/will be computed with the quantum chemistry models and density functional theory (DFT) developed by the theoretical chemistry node.

A crucial point we keep in mind in our investigations is that we do not observe "directly" the charge migration, but rather its imprint on the HHG spectra, through the time-frequency map. In our joint effort, the theoretical node will pursue clear and unique signatures of charge migration and the conditions in which they can be observed, compatible with experimental conditions available at the experimental nodes. We also keep in mind that HHG is fundamentally a macroscopic response and that our semiclassical model must eventually be expanded to account for effects such as phase matching. In the future we will include these effects into our model and investigate how they can be harnessed to select and/or enhance relevant signal and signatures of charge migration.

Application: The N_2 Molecule

Our choice of N_2 as a first theoretical study candidate is motivated by the large body of literature to benchmark our results against, including evidence of multi-electrons effects in N_2 as shown in [Mairesse 2010]. In addition, [Mairesse 2010] showed that charge migration in N_2 is mostly explained by a two orbital description, making it the lowest dimensional configuration to study hole dynamics. N_2 is also simple enough to consider direct numerical simulations – from pure time-dependent Hartree-Fock to time-dependent density functional theory (TDDFT), with different hybrid functionals, as used by the theoretical chemistry node – as additional sources of benchmarks for our semiclassical model and identification of the sources and signatures of hole dynamics in HHG spectra. We also see the N_2 molecular model as a means to assess the role and importance of each component in the hole dynamics and the associated HHG spectra.

We model the hole dynamics in a basis of molecular orbitals. This simplified two-active-orbital model for N_2 offers a clear illustration of the connection between our semiclassical time-frequency map and the hole dynamics (see Fig. 2). In the mapping, each harmonic order is associated with a given ionization and recollision time (left panel). Scanning through the harmonic spectrum amounts to scanning through varying ionization-to-recollision delays and therefore "following" the hole dynamics, as illustrated on the right panels.

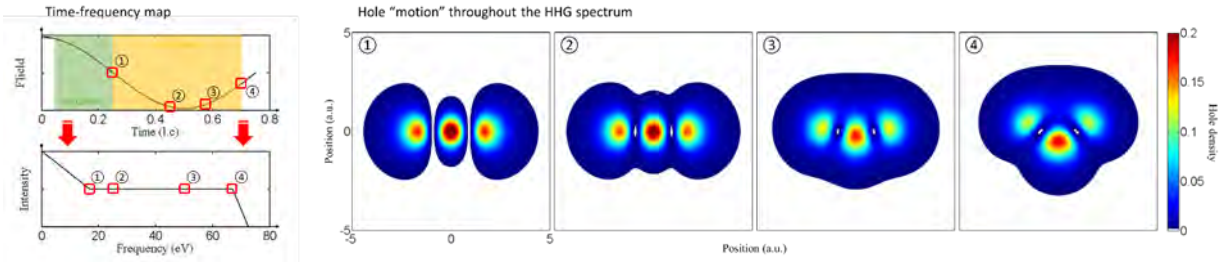

Figure 2: Left panel: Time-frequency map as provided by the semiclassical model of HHG. Right panels: Hole density for a two-dimensional two-active-orbital model of N_2 assuming ionization from the HOMO orbital with a 1.3 μm, 10^{14} W·cm^2 laser aligned at 45° with the molecular axis. In all panels, numbers indicate matching recollision time, harmonic order and hole density.

The next steps for improving and extending the semiclassical modeling is to benchmark the matrix elements used to simulate the hole dynamics against TDDFT computations. The channel resolved scattering cross-sections – including the scattering phase information – used to account for the recollision component of HHG spectra are computed using high performance scattering programs developed by Prof. R. Lucchese (BNL). We are collaborating with him to ensure that scattering cross-sections are accurately computed and benchmark our results against previously published results, when available.

Progress: Angle-Dependent Ionization

We have developed and validated TDDFT tools for capturing the angle and intensity-dependent ionization rates of molecules. These channel resolved rates will be used to model the initialization of the hole upon ionization by the laser. Our approach, which uses atom-centered basis sets and optimally tuned range-separated hybrid functionals, offers a range of advantages over traditional TDDFT including: reduced self-interaction errors, the correct asymptotic Coulomb form, and the ability to capture core-level dynamics (see [Sissay 2016]).

One important advantage of using this class of DFT functionals is that in addition to quantitative ionization rates (Fig. 3), this method also gives a robust description of the angle-dependence (i.e., rate as a function of molecular orientation). Our results demonstrate significantly improved agreement with experiment as compared with alternative approaches. Figure 4 shows the relative angle-dependent rates for N_2. LC-PBE* (tuned TDDFT) agrees well with experiment, whereas time-dependent Hartree-Fock, MO-ADK, and MO-SFA all deviate significantly. Essentially, this is a consequence of the static description of the molecular orbitals in MO-ADK, the neglect of ion/electron interactions in MO-SFA, and the incorrect orbital ordering of Hartree-Fock.

In addition, our method requires no input from experiment. The DFT functional is tuned self-consistently, and no a priori selection of molecular orbitals is required, as contributions from all MO channels are automatically included. This becomes especially advantageous for larger molecules where the role of each orbital might not be simple to predict. Systems with closely spaced MOs, for example, allow for ionization from multiple channels which can potentially yield rich ionization-triggered dynamics.

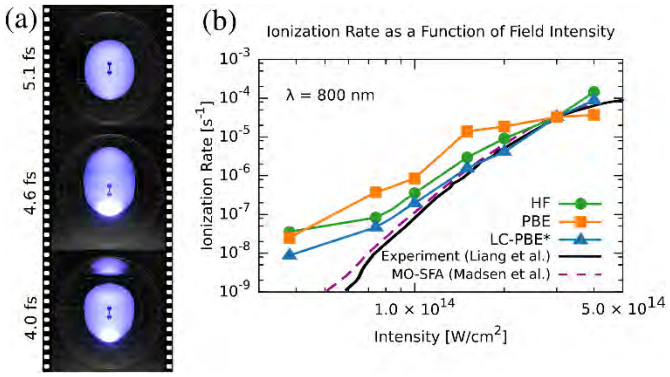

Figure 3: (a) Snapshots of the electron density (blue) during strong-field ionization by 800 nm laser, intensity 2×10^{14} W/cm^2 light. The gray mesh represents the start of a complex absorbing potential. (b) Intensity-dependent angle-averaged ionization rates for N_2. All calculations scaled to agree at 2×10^{14} W/cm^2. Tuned range-separated TDDFT (LC-PBE*, blue curve) yields good agreement with experiment and MO-SFA calculations. Deviations at lower intensity are due to basis set limitations.

Future Plans: Angle-Dependent Ionization

The long-term goal of the ongoing UVa/LSU effort is to align, measure, and

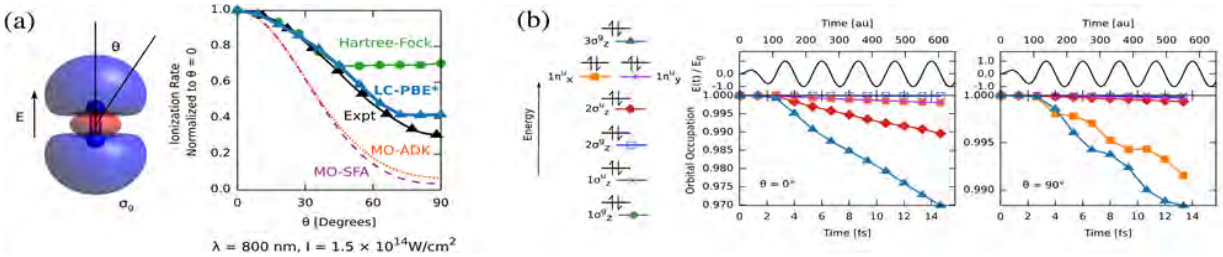

Figure 4: (a) Angle-dependent ionization rates for N_2 normalized to the parallel (on-axis, θ=0) value. Our tuned range-separated TDDFT approach (LC-PBE*, blue curve) agrees well with experiment, whereas Hartree-Fock (green) is unphysically insensitive to angle due to incorrect molecular orbital ordering. MO-ADK and MO-SFA significantly overestimate the ionization anisotropy likely due to the use of static orbitals and neglect of ion/electron interactions, respectively.

model angle-dependent ionization from molecules predicted to exhibit ionization-triggered electron/hole migration. As a first step in this direction, our recently developed experimental setup (Jones, UVa) and theoretical tools (LSU, Lopata) are currently being validated using the carbonyl sulfide (OCS) molecule. This linear molecule facilitates alignment via rotational pumping, but discrepancies between theory and experiment have been reported. MO-ADK and TDDFT have been shown to qualitatively fail to predict the angle-dependence, whereas saturation-corrected weak field asymptotic theory (WFAT) reproduces the observed trends. The role of electronic excitations and orbital shifting, especially for higher intensities, remains an open question. We will use these side by side theoretical/experimental comparisons of strong-field ionization as an independent benchmark of the first step for our semiclassical model of HHG with charge migration. Indeed, understanding the role of these processes during the ionization step is vital for future studies of electron/hole dynamics [Hansen 2012, Penka Fowe, 2011, Johansen 2016].

After this validation stage, we will move on to fluoroiodomethanes (e.g, CHF_2I) which are easy to handle experimentally and yet are predicted to exhibit non-trivial ionization dynamics. For example, these compounds have a spatially localized orbital on the iodine that can be ionized with a strong, off resonant, field. Finally, in conjunction with simulations of ionization-triggered charge migration (LSU, Lopata), this will lead to studies collaborative studies charge migration in molecules such as benzene derivatives that are para-functionalized with electron donating and withdrawing groups.

Future Plans: TDDFT for Charge Migration Dynamics

In parallel with the ionization studies, we are currently developing TDDFT tools for capturing electron/hole migration (which we abbreviate to "CM") following ionization. This is crucial for both validation of the theory against previous calculations, and for screening potential molecules to determine those capable of supporting charge migration.

One key challenge facing CM simulations is the choice of the initial wavefunction. This problem is similar to the case of vertical excitations, where a prohibitively long continuous wave simulation would be required to fully populate an excited state to 100% probability. Compounding this, slight inconsistencies in the theory for the ground versus excited state can lead to spurious detuning during resonant excitation [Fuks 2015]. Thus a typical "cheat" is to instead prepare the system at t=0 in some desired excited state. However, without knowledge of the correct wavefunction this yields a highly non-physical state and the results are highly sensitive to the initial condition [Eshuis 2009]. Analogous issues occur for ionization-triggered dynamics where "sudden" removal of an electron from a molecular orbital can be a drastic oversimplification. Instead the initial ionic wavefunction should be built from hole contributions from various orbitals, with the correct complex phase between them. In the absence of this proper description of the initial state, CM simulations are likely to be qualitatively wrong.

To this end, we have made progress towards constructing meaningful initial states using the results of our ongoing strong-field ionization simulations. Using the same theory for ionization and dynamics eliminates potential spurious responses due to inconsistencies in the electronic structure. As an initial step in this direction, we extract the relative contribution of each molecular orbital (MO) to the ionization. Figure 4 (b), for example, shows the ionization rates from each MO of N_2. For 800 nm on-axis (θ=0) polarized light, the ionization is dominated by the HOMO ($3\sigma^g z$) and the HOMO-3 ($2\sigma^u z$). A valid initial

wavefunction should therefore be dominated by hole density in these two orbitals. As a future improvement, we are also working on extrapolating the time-dependent density matrix from the TDDFT ionization simulations to t→∞, which will yield not only the orbital contributions but also the phases, albeit approximately.

In conjunction, we are also developing approaches for interpretation of electron/hole dynamics simulations. Developing simple metrics for interpreting and visualizing charge migration is crucial for "screening" potential molecules of interest and for validating TDDFT against other theories. Due to the delocalized nature of charge in molecules, quantities such as the electron density, dipole moments, and charges on the atoms are not illustrative. Instead we have developed a time-dependent electron localization function (TDELF) [Becke 1990, Burnus 2005] adapted for Gaussian basis sets. In essence, the TDELF is a dimensionless quantity that describes how electrons are localized for a specified spin. A value of 1 represents completely localized electrons, 0.5 represents localization equivalent to a homogeneous electron gas, and 0 corresponds to no electron density. The time-dependent electron localization function is defined as:

$$\eta(r) = \frac{1}{1 + (D_\sigma / D_\sigma^0)^2}$$

where $D_\sigma(r)$

$$D_\sigma(r) = \tau_\sigma(r) - \frac{1}{4}\frac{|\nabla\rho_\sigma(r)|^2}{\rho_\sigma(r)} - \frac{|j_\sigma(r)|^2}{\rho_\sigma(r)}$$

$D_\sigma(r) = (3/5)(6\pi)^{2/3}\rho_\sigma^{5/3}(r)$ is the homogeneous electron gas kinetic density function, $\tau_\sigma(r) = \sum_{i\in occ}|\nabla\psi_i|^2$ is the kinetic density function, and $j_\sigma(r) = (i/2)\sum_{i\in occ}(\psi_i^*\nabla\psi_i - \psi_i\nabla\psi_i^*)$ is the current density for the σ spin. This localization function does not describe where electrons are, but rather their concentration and thus offers a chemical interpretation of the charge migration, including motion of lone pair electrons and weakening/strengthening of bonds.

Figure 5 shows an example for dimethylaminobenzonitrile (DMABN), which is a well-studied charge transfer compound [Rappoport 2004]. Here, the molecule has undergone "sudden" ionization from the HOMO-3, such that a hole is initially localized on the cyano (-CN) group and the dynamics propagated using TDDFT with the LC-PBE* tuned range-separated functional. The resulting time-dependent electron density $\rho_H(r,t) \equiv \rho_{neutral}(r) - \rho_{ion}(r)$ (a) shows little variation. The hole density (b) and TDELF (c), on the other hand, show clear electron/hole dynamics. At t=0 there is a hole localized on the cyano group, which is reflected in the TDELF as an increase in localization above and below the plane of the molecule (contraction of electrons around nuclei due to hole). At t = 0.56 fs electrons are extracted from the benzene ring to fill the hole, with additional charge accumulating around the nitrogen of the dimethylamine (-N(CH_3)$_2$) group drawn from the methyl groups. The TDELF shows reduced localization due to the electron/electron repulsion. At 0.85 fs the excess charge has moved into the benzene ring, and eventually accumulates around the cyano group at 1.86 fs, with a delocalized hole around the benzene and amine groups. This corresponds to reduced localization around the cyano and increased localization around the amine.

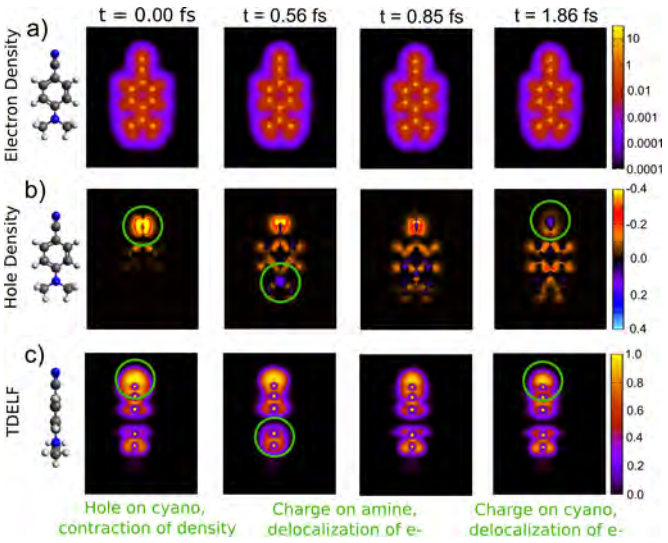

Figure 5: Snapshots of the electron density (a), hole density (b), and time-dependent electron localization function (TDELF) (c) for the dimethylaminobenzonitrile (DMABN) molecule. The dynamics were triggered by suddenly ionizing an electron from a molecular orbital localized on the cyano group. Charge migration from the amine to fill the hole takes ~ 1.5 fs.

Overall the ionization-triggered charge migration in this system takes about 1.5 fs, which is qualitatively consistent with previous theoretical predictions in similar molecular systems. It is important to note that due to the non-physical initial condition, in addition to charge migration, a wide range of excited ionic states are present in the system. Interpretation in cases like this is complicated by the multiple frequencies of dynamics. In addition to an improved description of the initial state, we are also developing techniques based on orbital decomposition of the density matrix [Bruner 2016] or frequency analysis of the hole density and TDELF to selectively visualize the charge migration.

LSU Node Publications

[Abanador 2016] P.M. Abanador et al., "Semiclassical modeling of high-order harmonic generation driven by an elliptically polarized laser field: the role of recolliding periodic orbits", submitted to J. Phys B (2016)

[Mauger 2016] F. Mauger et al., "Semiclassical-wave-function perspective on high-harmonic generation" Phys. Rev. A 93, 043815 (2016)

[Sissay 2016] A. Sissay et al., "Angle-dependent strong-field molecular ionization rates with tuned range-separated time-dependent density functional theory", J. Chem. Phys. 145, 094105 (2016)

University of Virginia Node

Recent Progress and Results

The effort at Virginia has been distributed over a number of tasks to address problems relevant to both the principal project goal of exploring femto- and attosecond electron dynamics in molecules and to deepening the collaborative interactions between participants at the different nodes. First, working with collaborators at LSU, we are utilizing transient molecular alignment to measure angular dependent molecular ionization rates as a critical test of the computational methods employed to model the ionization-step of HHG (see ionization section above). Second, with members of the OSU node, we have developed an augmented RABITT method that utilizes low-energy, attosecond photoelectron wavepackets as a time-resolved probe of the effective electronic binding potential sampled by an electron as it leaves its parent ion. Third, we are exploring the use of nano- and micro-structured metals to enhance the magnitude of the THz fields that can be applied to a molecular ensemble, thereby improving the degree of transient (head versus tail) molecular orientation available to high-harmonic spectroscopy measurements. Fourth, we have made several technical improvements to our laser and hollow-core-fiber-based HHG apparatus to enable future work on: THz-based molecular orientation; the generation of few femtosecond UV and VUV pulses to initiate molecular electron/hole dynamics; and coherent enhancement of high-harmonic yields from low density molecular gases.

Strong-Field Molecular Ionization Rate Anisotropies

The ability to predict and characterize electron/hole evolution initiated via strong-field ionization is an important capability for guiding and interpreting experiments seeking to follow such processes using high-harmonic spectroscopy. Because the angular dependence of the strong-field ionization rate depends critically on the relative contributions of different molecular orbitals, comparisons of experimental and theoretical ionization anisotropies can serve as an important test of the accuracy and predictive power of the TDDFT calculations which members of the LSU team will rely upon for calculating charge-migration dynamics. Accordingly, we have begun a series of measurements employing transient laser-alignment to extract angular-dependent strong-field ionization rates for different molecules. Following [Kumarappan 2015] we record the ionization yield as a function of the delay between a non-ionizing alignment pulse and the ionizing laser. Using the known rotational constants of the molecule, the experimental ionization rate anisotropies (angularly symmetrized versions for symmetric tops) can be determined from fits to the time-dependent yield and compared directly to calculations. Our initial experiments have focused on OCS, a molecule whose angular-dependent ionization has been studied in detail previously, but for which the agreement between theory and experiment is relatively poor [Hansen 2012]. We seek to compare our experimental results against previous measurements and calculations [Hansen 2012], as well as those currently being performed by Lopata and co-workers at the LSU node. We plan to soon begin measurement on several different methyl-halide species, moving from linear molecules to symmetric and asymmetric tops. Our goal is to use the results of these measurements to benchmark calculations of angular-dependent

strong-field ionization rates in systems predicted by the LSU team to exhibit robust femtosecond electron dynamics (see discussion on TDDFT in LSU node).

Probing Atomic Potentials with Near Threshold Attosecond Photoelectrons

The UVa and OSU nodes have been working together for several years, exploring the use of near threshold photo-electrons as time-resolved probes of the effective binding potential through which electrons escape from molecules. The UVa participation in that project was initially supported by Jones' DOE individual PI grant (DE-FG02-00ER15053). However, as of December 1, 2016, that grant has been placed on a no-cost-extension with insufficient funds to support the effort. Because the work is relevant to the exploration of attosecond and femtosecond electron dynamics and strengthens the connection between the UVa and OSU groups, UVa's participation now continues with funding from this collaborative grant.

In the experiments, which are performed at OSU, attosecond pulse trains are used to photoionize noble gas atoms near threshold in the presence of a moderately intense, infrared dressing laser. As in the standard RABITT technique, which is typically used to reconstruct the field in attosecond pulse trains [Paul 2001], we monitor the phase of interference modulations in photoelectron sidebands as a function of the delay between the dressing laser and the attosecond pulse train. These sidebands are produced via energy transfer between the dressing field and the photoelectrons produced directly by the XUV harmonic radiation. We add another dimension to the measurement by considering the information that can be extracted from the sideband amplitudes, in addition to the phase of the interference modulations. By comparing the amplitudes and phases of the low-energy sidebands for Ar, Ne, and He we can extract time-resolved information regarding the average depth and gradient of the He+ and Ne+ binding potentials experienced by the photoelectrons during the first 1 fs or so following their birth. Preliminary comparisons indicate reasonable agreement between the data and previous theoretical results from the LSU group [Mauritsson 2005]. In principal, a variant of these measurements might provide time-resolved information on changes in an atomic/molecular potential due to an external stimulus. A manuscript describing this work is in preparation.

THz Field-Enhancement Near Nano-Structured Metals

Intense THz pulses can be used to induce transient orientation in molecules [Fleischer 2011, Kitano 2013, Egodapitiya 2014]. While orientation techniques involving two-color laser fields are typically easier to implement [De 2009, Znakovskaya 2014], electronic excitation and ionization are negligible with direct, THz-based rotational excitation, even in large molecules with low ionization potentials. The primary limitation of THz-based methods is obtaining sufficient field strength to create the needed rotational coherences at non-zero temperatures.

To counter this issue, we have been exploring the use of nano- and micro-structured metals for THz field enhancement (and as sources of short, high energy electron bursts through THz-induced electron field emission). As with the low energy RABITT work just described, this project was initiated with funding from Jones' individual PI grant. However, the component that is relevant THz field enhancement and its application to transient orientation and quasi-static field modification of laser-based electron rescattering, is continuing with support from this collaborative grant.

We have obtained THz field-enhancements of approximately 3000 near tungsten nano-tips with radii of ~20 nm, corresponding to peak THz fields of 1 GV/cm. Unfortunately, the volume of the enhanced field region is far too small to be useful for affecting the gas sample throughout a laser focus. We are, therefore, considering other structures which might provide smaller enhancements, but over a much larger volume. We have achieved enhancements of roughly 50x near tips with radii of 1 micron. This might be useful for exploring THz orientation or the effects of quasi-static fields on electron recollisions in a tightly focused laser, but not for HHG applications where a larger focal volume is needed to obtain sufficient signal. We are, therefore, now exploring the use of micro-tip arrays or blade edges that might enhance the THz field over a considerably larger volume. Our work on THz field enhancement near, and electron field emission from, nano- and micro-tipped wires is described in a manuscript that was recently accepted for publication by Nature Communications [Li 2016].

Facilities and Apparatus Improvements

Several important technical improvements have been made over the past year which will facilitate our future work on this project. For example, we have redesigned our hollow-core-fiber based harmonic source in an attempt to increase reliability and reproducibility and enhance the UV/XUV yield. This upgrade will

be critical as we explore the use of coherent enhancement of weak harmonic signals in mixed gases in the next year. In addition, we commissioned a high-power amplifier extension to our kHz Ti:Sapphire amplifier. The increase in output energy to the 3-4 mJ level will enable experiments which require high pulse energies, e.g. THz induced molecular orientation. Just as importantly, splitting the beam into two or more components will allow us to work on different tasks in parallel, e.g. measurements of molecular ionization rate anisotropies and the generation of sub-3fs UV pulses to initiate and/or probe correlated electron dynamics.

Future Plans

With a full contingent of researchers now on the project, we plan to make significant progress on multiple fronts in the coming year. First, in close collaboration with K. Lopata at LSU, we will first extend our current work on strong-field ionization rate anisotropies in OCS to the methyl-halides for benchmarking purposes, and then to other species which calculations suggest should exhibit charge-migration triggered by strong field ionization.

Second, given that the planned high harmonic spectroscopy measurements will greatly benefit from the use of oriented molecular samples, we will initiate experiments aimed at demonstrating THz orientation of halogenated methanes or other symmetric top molecules of similar size and complexity. As noted above, field-free THz orientation may be preferable to 2-color orientation methods for larger molecules. As with the continuing angular-dependent ionization rate measurements, we will measure strong-field ionization rate anisotropies, now with the head vs. tail ambiguity removed, as a test of theory. We will continue to explore methods for THz field enhancements near micro-structured metals in an attempt to improve the degree of achievable orientation.

Third, we will initiate our efforts to develop a sub-3fs UV source as an alternative to strong field ionization for triggering charge migration dynamics. Our plan is to adapt, to the generation of lower order harmonics, the basic concepts behind the recently demonstrated “attosecond lighthouse” scheme [Kim 2013, Hammond 2016, Auguste 2016] for producing isolated attosecond XUV pulses. In essence, we will exploit ultrafast wavefront rotation in a few-cycle 800 nm beam to produce UV harmonic radiation with emission time mapped to propagation angle. Appropriate aperturing of the UV beam should confine the radiation to a sub-3fs burst.

Fourth, given the difficulties anticipated in producing sufficiently dense gas-phase samples to implement high-harmonic spectroscopy with larger molecules, we intend to study HHG from mixed gas samples in a hollow-core fiber to explore the possibility for exploiting coherent addition of the harmonic fields to enhance the signal from a low-density, minority component in the gas mixture. Working with the team at LSU, we hope to quantitatively assess phase-matching as a tool for coherently enhancing the observability of weak signals via interference.

Fifth, a graduate student (Sanjay Khatri) and postdoc (Peter Sandor) will visit LSU in October to prepare for the analysis of their OCS ionization rate anisotropy data, both comparing experimental and calculated rates and learning about the computational techniques used. The pair will visit the OSU laboratories for several weeks later in the year to prepare for future collaborative experiments involving the mid-infrared lasers and attosecond beamline there.

UVa Node Publications

[Li 2016] S. Li et al., “High-Energy Electron Emission from Metallic Nano-tips Driven by Intense Single-Cycle Terahertz Pulses”, Nat. Comm. To appear (2016).

The Ohio State University Node

Two-Source Two-Color Sub-Cycle Interferometry

In our project charge migration will be studied using high harmonic spectroscopy (HHS) of aligned/oriented molecules using the well-established RABBITT method. In the frequency domain picture, an atom ionized by the odd-order (2q+1) harmonic frequency comb produces an electron energy spectrum that is a replica of the comb’s amplitude. The electron spectrum, composed of peaks separated by $2\hbar\omega_f$, is simply the product of the harmonic comb amplitude and the detector atom’s photoionization cross-section. In RABBITT, a weak phased-locked fundamental field, ω_f, is imposed on the atom in the presence of the harmonic frequency comb resulting in the production of sidebands in the dressed electron spectrum which

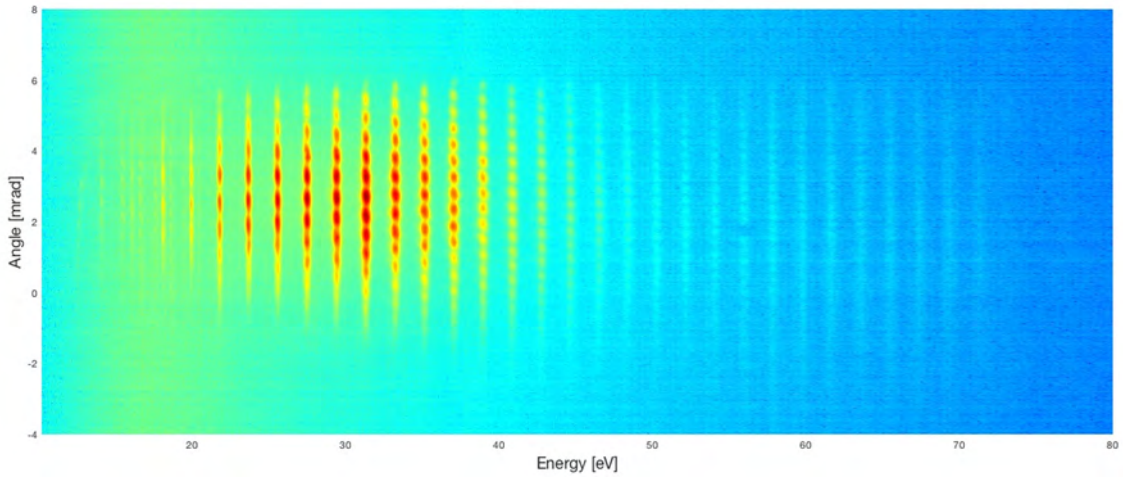

Figure 6: Two high harmonic source interference from argon atoms pumped at 1.35 μm using the new OSU HHG beamline. The XUV light was incident on a 1200 lines/mm VLS grating which preserved the divergence along the vertical direction and spectrally resolved along the horizontal direction. The spectrally resolved light was collected by an MCP/phosphor detector and imaged by a CMOS camera.

correspond to the absorption and emission of a fundamental photon at $(2q+1) \pm 1$. The sidebands from adjacent harmonics are degenerate in energy and therefore interfere. In the time domain, the sideband amplitude is modulated at $2\omega_f$ as the delay is varied between the fundamental and harmonic fields. Within the perturbative limit, the group delay is defined as the change in phase as a function of frequency. The measurement must carefully account for the contributions from the generator gas and the detection gas. For HHS the harmonic generator gas is the quantity of interest, thus the ideal detector would have a flat response in amplitude and phase, which is unrealistic. In addition, independent RABBITT scans of phase at different molecular alignment angles are not a priori connected. This limitation can be circumvented by studying the interference in the far-field of the emission from two independent but identical HHG sources. Additionally, the two-source method should provide a higher degree of sensitivity by acting as a two-arm interferometer particularly when dynamics are induced, e.g. UV pumped, in one source relative to the other.

In our laboratory, we create the two arm attosecond interferometer by mode conversion from a Transverse Electromagnetic Mode TEM00 (Gaussian) towards a TEM01 using a binary phase plate [Camper 2014, Camper 2015]. A 0-π spatial phase shaper is used to convert the spatial Gaussian into a TEM01 mode. We have procured phase plates at 0.8, 1.3 and 1.8 μm which are target wavelengths for our molecular studies. Under our typical operating conditions, the two equal intensity sources at focus are separated by approximately 50 μm and transverse to the molecular jet axis. Consequently, the two sources sample a constant molecular density and identical phase matching conditions. The techniques were first demonstrated by our collaborator, Dr. Salières (CEA-Saclay, France) and his former student, Dr. Antoine Camper. Currently, Dr. Camper is a post-doctoral researcher in our group working on our DOE supported attosecond program but has provided valuable guidance to this project.

Over the past year a new harmonic beamline was developed to implement the two-source interferometer. Briefly, the fundamental beam passes through a 0-π phase plate and then focused by a 0.5-0.4 meter lens into a supersonic gas jet. The waist of the two sources are transverse to the jet axis. The generated harmonics propagate down the beamline and are spectrally and spatially filtered. The HHG is focused by a demagnifying ellipsoidal mirror into the entrance slit of a XUV imaging spectrometer. A CCD captures the image from a phosphor screen in which the spatial information is encoded transverse to the dispersive direction. Figure 6 shows an image of the two-source interference from harmonic generated from an argon jet using a 1.35 μm fundamental beam. Clearly, two source interference fringes at high fidelity are observed in the harmonic spectrum extending to the Al filter cutoff (70 eV). In the near future, an existing magnetic bottle electron energy spectrometer will be installed at the focus of the ellipsoidal mirror allowing concurrent RABBITT and two-source interferometry measurements in our new beamline.

Molecular Phase Measurements

Early molecular HHS studies on this project have begun and focus on methane (CH_4), ethane (C_2H_6), and methyl chloride (CH_3Cl), as well as carbon monoxide (CO), carbon dioxide (CO_2) and nitrogen (N_2) for alignment calibrations. Measurements thus far have focused on the RABBITT technique. The RABBITT interference signal reveals the phase of a given harmonic relative to its neighbors, and allows us to create a phase map of the harmonic spectrum. Phase features in the spectrum then allow for the identification of dynamic behaviors in the generation process. The choice of CH_4/CH_3Cl was the result of a concerted discussion between the theoretical and experimental nodes, and was selected for their relative simplicity while offering perspectives for charge migration. In the future, as we move towards more complex molecular systems, we will keep relying on the expertise from the three nodes of the ATTO-CM team (perspectives for charge migration, for alignment, to get HHG signal …) to make these choices.

To date, reproducible features in the phase and amplitude have been observed, particularly as a function of intensity in CH_3Cl. The identification and characterization in terms of dynamic behaviors is under way and will benefit from the theoretical node input. To this end, the OSU and UVa experimental groups will visit their LSU collaborators over the first week of October 2016. We expect this time to be fruitful in discussions and contribute to shape the future of the project. In this perspective, formal presentations from all of the three nodes, as well as an exit meeting at the end of the week, have been scheduled. Between visits to the partners, LSU and OSU also maintain monthly Skype meetings to share advances on each side and make the efforts of both theorists and experimentalists converge.

Characterization of Phase Structures in Detection Gases

While the grant's objective is to measure the group delays resulting from harmonic generation in molecules, we have discovered several interesting features in the XUV spectrum of our detection gases, namely argon and krypton, by stepping the wavelength of the generating pulse to scan across the gaps in the frequency comb. Although these results are not the desired target of our charge migration experiments, they are an interesting by-product of these studies, and represent previously unobserved phase structures of XUV resonances in atomic ionization. Furthermore, complete characterization of our "detector gases" are a vital prerequisite for performing HHS so that the detector response can be deconvolved from the signal of interest.

With argon as a detection gas, we observe several structures in the group delay which are indicative of XUV autoionization resonances. Autoionizing states are manifested in the RABBITT phase when an odd-order harmonic comes into resonance with the 1-photon transition. Consequently, the resonance produces a change in the sidebands amplitude representative of the absorption and emission of a dressing fundamental photon. Likewise, since the sidebands are π out-of-phase, the resonance structure appears as mirror images separated by $2\hbar\omega_f$ about the actual resonance frequency.

Figure 7 shows several RABBITT phase measurements at incremental fundamental wavelengths using an argon generator and an argon detector. By varying the generator and detection gases, the source of the structures has been unequivocally identified as originating from argon atoms used as the detection gas. The most prominent structure observed in argon is centered near 26.7 eV (blue line) and confirms a recent measurement [Kotur 2016] of the $3s^2 4p^6 \rightarrow 3s^1 3p^6 4p^1$ autoionizing Fano resonance. The Kotur measurement was conducted with a 0.8 μm fundamental field, and our longer wavelength

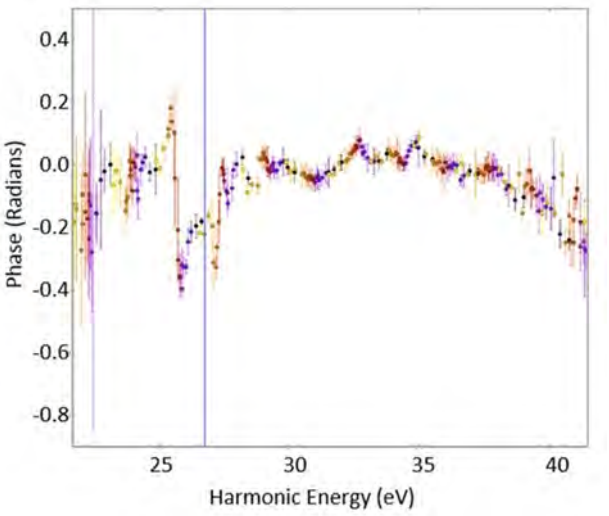

Figure 7: An overlaid series of RABBITT scans from 1.4-1.5 μm in driving wavelength in 0.01 μm steps. A phase structure centered at 26.7 eV (blue line) is observed consistent with the $3s^1 3p^6 4p^1$ autoionizing Fano resonance. In addition, another structure centered near 34 eV is observed but not yet identified.

driver results confirm their observation. In addition, we observe an additional phase structure in argon at higher energy (~34 eV), which is previously unreported. This energy is indicative of doubly excited states although its representative transition has not been identified at this time. Another Fano profile is also identified in krypton, consistent with the $4s^2 4p^6 \rightarrow 4s^1 4p^5 5p^1$ autoionization resonance, whose phase profile is also unreported.

These measurements provide us with newly-observed XUV ionization phase structures, and important calibrations of detection gases; these features will not be mistakenly attributed to molecular behavior in harmonic generation, and can instead be understood as atomic interactions in harmonic detection.

OSU Node Publications

None yet from the OSU node.

References

[Abanador 2016] P.M. Abanador et al., "Semiclassical modeling of high-order harmonic generation driven by an elliptically polarized laser field: the role of recolliding periodic orbits", submitted to J. Phys B (2016)

[Auguste 2016] T. Auguste et al., Phys. Rev. A 93, 033825 (2016)

[Becke 1990] A. D. Becke et al., J. Chem. Phys. 92, 5397-5403 (1990)

[Bruner 2016] A. Bruner et al., J. Chem. Theory Comput. 12, 3741 (2016)

[Burnus 2005] T. Burnus et al., Phys. Rev. A 71 010501 (2005)

[Camper 2014] A. Camper et al., Phys. Rev. A 89, 043843 (2014)

[Camper 2015] A. Camper et al., Nat. Photonics 2, 2010184 (2015)

[De 2009] S. De et al., Phys. Rev. Lett. 103, 153002 (2009)

[Egodapitiya 2014] K. Egodapitiya et al., Phys. Rev. Lett. 112, 103002 (2014)

[Eshuis 2009] H. Eshuis et al., Phys. Chem. Chem. Phys. 11, 10293-10298 (2009)

[Fleischer] S. Fleischer et al., Phys. Rev. Lett. 107, 163603 (2011)

[Fuks 2015] J. Fuks et al., Phys. Rev. Lett. 114, 183002 (2015)

[Hammond 2016] T.J. Hammond et al., Nature Photonics 10, 171 (2016)

[Hansen 2012] J.L. Hansen et al., J. Phys. B 45, 015101 (2012)

[Johansen 2016] R. Johansen et al., to appear (2016)

[Kim 2013] K.T. Kim et al., Nature Photonics 7, 651 (2013)

[Kitano 2013] K. Kitano et al., Phys. Rev. A 88, 061405(R), (2013)

[Kotur 2016] M. Kotur et al., Nat. Comm. 7, 10566 (2016)

[Kumarappan 2015] V. Kumarappan et al., Bulletin of the American Physical Society, DAMOP 2015

[Li 2016] S. Li et al., Nat. Comm. To appear (2016)

[Machholm 2001] M. Machholm et al., Phys. Rev. Lett. 87, 193001 (2001)

[Mairesse 2010] Mairesse et al., PRL 104, 213601 (2010)

[Mauger 2016] F. Mauger et al., Phys. Rev. A 93, 043815 (2016)

[Mauritsson 2005] J. Mauritsson et al., Phys. Rev. A 72, 013401 (2005)

[Paul 2001] P.M. Paul et al., Science 292, 1689 (2001)

[Penka Fowe 2011] E. Penka Fowe et al., Phys. Rev. A 84 035402 (2011)

[Rappoport 2004] D. Rappoport et al., J. Am. Chem. Soc. 126, 1277-1284 (2004)

[Sissay 2016] A. Sissay et al., J. Chem. Phys. 145, 094105 (2016)

[Znakovskaya 2014] I. Znakovskaya et al., Phys. Rev. Lett. 112, 113005 (2014)

Page is intentionally blank.

Tamar Seideman
Department of Chemistry, Northwestern University
2145 Sheridan Road, Evanston, IL 60208-3113
t-seideman@northwestern.edu

Strong-Field Control in Complex Systems

1. Program Scope

Our AMOS-supported research can be broadly categorized into two related topics: (1)the design and control of complex material system using strong field concepts that were developed in our earlier AMOS work, including alignment, 3D alignment, torsional alignment and molecular focusing; and (2)the physics, theory, and potential applications of high harmonics generated from aligned molecules. Whereas the first topic is a generalization of the thrust of our original AMOS-supported research, the second has been motivated by the intense interest of the AMOS Program in attosecond science and rescattering electrons physics, and has been carried out in collaboration with AMOS experimentalists colleagues.

Our AMOS-supported research during the past year has focused primarily on the former problem, as summarized in Secs. 2.1–2.7, and includes a theory development project, four collaborative research projects with different experimental laboratories, and two concept development projects. Research in the next year on the problem of strong field coherent control in complex molecular and material systems is discussed in Sec. 3.1. Within the second part of our AMOS-supported research during the past year (2.8), we continued earlier research in collaboration with experimental AMOS colleagues on the problem of ellipticity in harmonic signals. Our plans for further research in the area of attosecond physics and high harmonic generation (HHG) during the next year is outlined in Sec. 3.2. Citations refer to the list of AMOS-supported publications from the Sept. 2013–Aug. 2015 period, Sec. 4.

2. Progress during the past year

2.1 Alignment and Orientation of Semiconductor Nanorods with the Combination of Static and Laser Fields

Semiconductor nanorods have a broad range of interesting applications, including catalysis and solar energy conversion. Most of these applications rely on orientational order. In a recent publication, we present the results of molecular dynamics simulations of semiconductor nanorods aligning and orienting under the combined influence of static electric and laser fields. The transformation of the isotropic ensemble into an orientationally ordered assembly is a slow (microseconds) process, but in sharp contrast to previously oriented systems yields high levels of both alignment and orientation at elevated temperatures (300 K) and rather low fields (1.4 GWcm^{-2} laser intensity and 24 Vμm^{-1} static field amplitude). The resulting long range orientational order could serve to control the electric, magnetic and mechanical properties of the nanorods assembly and hence assist several of its applications. An article was submitted for publication.[1]

2.2 Alignment Thresholds of Molecules

Nonadiabatic alignment has been the topic of numerous studies, but the adiabatic case is equally interestingly and barely studied. We illustrated and studied the physical origin of a previously unexplored phenomenon in the adiabatic alignment dynamics of molecules, which is fundamentally interesting and has an important practical implication. Namely, the intensity dependence of the degree of adiabatic alignment exhibits a threshold behavior, below which molecules are isotropically distributed rotationally and above which the alignment rapidly reaches a plateau. Furthermore, we show that both the intensity and the temperature dependencies

of the alignment of all linear molecules exhibit universal curves and derived analytical forms to describe these dependencies. Finally, we illustrate that the alignment threshold occurs very generally at a lower intensity than the off-resonance ionization threshold, a numerical observation that is readily explained. This finding illustrates the generality of nonresonant alignment. The threshold behavior is attributed to a tunneling mechanism that rapidly switches off at the threshold intensity, where tunneling between the potential wells corresponding to the two orientations of the aligned molecules becomes forbidden. The universal threshold behavior of molecular alignment is a simple phenomenon, but one that was not reported before and can be readily tested experimentally. An article was submitted.[2]

2.3 Torsionally Gated Electron Transfer

Torsional alignment control of the torsion angle between two repeated units of a molecule was proposed in our 2007 AMOS-supported work and was recently confirmed in several laboratories. In recent research we use this concept to propose a way of enhancing desired forward electron transfer events from a photoexcited donor to an acceptor while suppressing undesired back transfer and recombination. By controlling the angle between molecular subunits we can modulate the electronic coupling between the subunits, thereby enhancing the forward transfer on short timescales and reducing the back transfer on longer timescales. This may be a useful method to reduce electron-hole recombination in applications such as solar cells and catalysis. An article is was submitted for publication.[3]

2.4 Dynamics from Noisy Data with Extreme Timing Uncertainty

Imperfect knowledge of the times at which snapshots of a system are recorded degrades our ability to recover dynamical information, and can scramble the sequence of events. In X-ray free-electron lasers, for example, the uncertaintythe so-called timing jitterbetween the arrival of an optical trigger (pump) pulse and a probing X-ray pulse can exceed the length of the X-ray pulse by up to two orders of magnitude, marring the otherwise precise time-resolution capabilities of this class of instruments. In recent work in collaboration with AMOS colleague Abbas Oumazd and a Hamburg group, we combine alignment with a data-analytical approach, based on singular-value decomposition and nonlinear Laplacian spectral analysis, which can recover the history and dynamics of a system from a dense collection of noisy snapshots spanning a sufficiently large multiple of the timing uncertainty. The power of the algorithm is demonstrated by extracting the underlying dynamics on the few-femtosecond timescale from noisy experimental X-ray free-electron laser data recorded with 300-femtosecond timing uncertainty. Using a noisy dataset from a pump-probe experiment on the Coulomb explosion of nitrogen molecules, our analysis reveals vibrational wave-packets consisting of components with periods as short as 15 femtoseconds, as well as more rapid changes, which have yet to be fully explored. Our approach can potentially be applied whenever dynamical or historical information is tainted by timing uncertainty. An article appeared in Nature.[4]

2.5 Collisional Decoherence and Rotational Quasi-Revivals in Asymmetric-Top Molecules

Whereas the revival pattern of linear molecules is simple and extensively studied, that of asymmetric tops contains new fundamental information and is relevant for applications. In collaboration with AMOS colleague Phil Bucksbaum and his group, we demonstrated the observation of quasi-periodic revivals out to 27 ps in an impulsively-aligned asymmetric-top molecule, sulfur dioxide (SO2), at high sample temperature and density (295 K, 0.5 bar). We found that the asymmetric top exhibits a strong correlation between population alignment and population lifetime (r = 0:97), in accordance with trends observed in linear molecules. We used a linear birefringence measurement fit to a full quantum simulation of the asymmetric rotor,

and were able to separately measure both the population (T1) and coherence (T2) lifetimes of the rotational wavepacket. Additionally, we observed a high rate of elastic decoherence (T2 = 9.6 ps), and attributed this to long-range interactions mediated by the permanent dipole of the SO2 molecule. We proposed the use of birefringence measurements to study intermolecular interactions in a coherent ensemble, as a step toward using field-free alignment to investigate reaction dynamics. An article was published in Phys. Rev. A.[5]

2.6 Time-Dependent, Optically-Controlled Dielectric Function

Plasmon resonances associated with metal nano-constructs, with their vast variety of applications, are sensitive to the dielectric function of the medium. In 6 we suggest optical modulation of the refractive index of a molecular monolayer adsorbed on a metal surface as a potential means of controlling plasmon resonance phenomena. The refractive index is altered using a laser pulse of moderate intensity and linear polarization to align the constituent molecules. Time-dependent, optically-controlled dielectric function is illustrated by molecular dynamics calculations.

2.7 Wigner Representation of the Rotational Dynamics of Rigid Tops

The broad rotational wavepackets associated with aligned molecules become increasingly difficult to compute quantum mechanically as the system complexity grows. Semiclassical methods make an attractive alternative that can also yield useful insight. In 7 we propose a methodology to design Wigner representations in phase spaces with nontrivial topology having evolution equations with desired mathematical properties. As an illustration, two representations of molecular rotations are developed to facilitate the analysis of laser-assisted molecular alignment, diagnostics of reaction dynamics, studies of scattering and dissipative processes.

2.8 Ultrafast Elliptical Dichroism in High-Order Harmonics as A Potential Probe of Molecular Structure and Electron Dynamics

Molecules illuminated by an elliptically polarized, high intensity laser field emit elliptically polarized high-order harmonics. In collaborative research with AMOS colleagues Margaret Murnane and Henry Kapteyn we found, surprisingly, ultrafast elliptical dichroism in the harmonic emission as the ellipticity of the driving field and the molecular alignment are scanned. We explained these observations by a simple model in which both the collision angle of the continuum electron with the molecule and the interference between recombination at multiple charge centers play a role. Our analysis ties the observed elliptical dichroism to the journey of the continuum electron in the field and the underlying bound state of the molecular ion. These results show how to use molecular structure and alignment to manipulate the polarization state of high-order harmonics, and also present a potential new attosecond probe of the underlying molecular system. Specifically, information about the bound state orbital structure and the continuum electron dynamics is contained in the variation of the dichroism with the laser ellipticity, the molecular alignment with respect to the field polarization, and the harmonic order. An article was submitted.[8]

3. Future Plans

3.1 Strong Field Coherent Control in Complex Material and Molecular Systems

1. We have initiated joint research with the groups of Stelios Tzortzakis and Maria Vamvakaki in Greece. These groups currently pursue an experimental realization of an ultrafast, nanoscale electron switch based on laser orientation of an organic molecule adsorbed onto a silicon surface and subject to a metal tip, which was proposed in our earlier AMOS-supported work. In numerical research we carry out calculations to assist the design of the molecule and the interpretation of the results. This work will be continued during the next year and will be hopefully brought to completion.

2. In collaboration with the group of AMOS colleague Phil Bucksbaum, we will explore the orientation of water molecules by half-cycle pulses. This work will continue our (already fruit bearing) collaborative efforts to unravel the quantum dynamics of the asymmetric top and their correlation to its classically unstable motion.

3.2 The Physics, Numerical Methodology and Applications of High Harmonics from Aligned Molecules

In unpublished work during the past several years we developed an approach for accurate modeling of the continuum electronic wavefunction underlying harmonic signals and combined it with our rotational theory of high harmonic generation. Our approach is based on time-dependent density functional theory and was tested by application to linear systems. My main interest, and the topic of future research, is the case of 3D aligned (e.g., by means of an elliptically polarized field) asymmetric top molecules as targets for the recolliding continuum electron. These I expect to allow both a new view of the electronic structure and dynamics in complex polyatomic molecules and a new and interesting approach to probe the (classically unstable) rotations of asymmetric tops in the fully quantum domain.

4. Publications from DOE-AMOS Sponsored Research(9/13–8/16, in citation order)

1. M. Artamonov and T. Seideman, *Alignment and Orientation of Semiconductor Nanorods with a Combination of Static and Laser Fields*, submitted for publication.
2. J. E. Szekely and T. Seideman, *Alignment Thresholds of Molecules*, submitted for publication.
3. B. A. Ashwell, A. M. Rasmussen, E. A. Weiss and T. Seideman, *Torsionally-Gated Electron Transfer*, submitted for publication.
4. R. Fung, S. Ramakrishna, T. Seideman, R. Santra and A. Ourmazd, *Accurate Dynamical Histories From Data with Extreme Timing Uncertainty*, Nature **532**, 471 (2016).
5. I. F. Tenney, M. Artamonov, T. Seideman and P. H. Bucksbaum, *Collisional Decoherence and Rotational Quasi-Revivals in Asymmetric-Top Molecules*, Phys. Rev. A **93**, 013421 (2016).
6. M. Artamonov and T. Seideman, *Time-Dependent, Optically-Controlled Dielectric Function*, J. Phys. Chem. Lett. **6**, 320-325 (2015).
7. D. V. Zhdanov and T. Seideman, *Wigner Representation of the Rotational Dynamics of Rigid Tops*, Phys. Rev. A. **92**, 012129, (2015).
8. P. A. J. Sherratt, R. M. Lock, X. Zhou, H. C. Kapteyn, M. M. Murnane, and T. Seideman, *Ultrafast Elliptical Dichroism in High-Order Harmonics as a Probe of Molecular Structure and Electron Dynamics*, submitted for publication in Phys. Rev. Lett.
9. J. E. Szekely, F. K. Amankona-Diawuo, and T. Seideman, *Laser-Driven, Surface-Mounted Unidirectional Rotor*, J. Phys. Chem. C, in press.
10. B. A. Ashwell, S. Ramakrishna, and T. Seideman, *Strong Field Coherent Control of Molecular Torsions - Analytical Models*, J. Chem. Phys. **143**, 064307, (2015).
11. S. M. Parker, M. Smeu, I. Franco, M. A. Ratner, and T. Seideman, *Molecular Junctions: Can Pulling Infuence Optical Controllability?*, NanoLett. **14**, 4587 (2014).
12. L. S. Spector, M. Artamonov, S. Miyabe, Todd Martinez, T. Seideman, M. Guehr, and P. H. Bucksbaum, *Axis-dependence of molecular high harmonic emission in three dimensions*, Nature Communications **5**, 3190 (2013).
13. J. Wu, X. Gong, M. Kunitski, L. Ph. H. Schmidt, T. Jahnke, A. Czasch, T. Seideman, and R. Dorner, *Sequencing Strong Field Multiple Ionization of a Multicenter Multibond Molecular System*, *Phys. Rev. Lett.* **111**. 083003 (2013)
14. B. Ashwell, S. Ramakrishna and T. Seideman, *Laser-Driven Torsional Coherences*, *J. Chem. Phys.* **138**, 044310 (2013).
15. B. Ashwell, S. Ramakrishna and T. Seideman, *Dissipative Dynamics of Laser-Induced Torsional Coherences* , Special Issue of J. Phys. Chem. C **117**, 22391 (2013) (**invited**).
16. S. Ramakrishna and T. Seideman, *Rotational Wave Packet Imaging of Molecules*, Phys. Rev. A **87**, 023411 (2013).
17. B. Ashwell, S. Ramakrishna and T. Seideman, *Laser-Driven Torsional Coherences*, J. Chem. Phys. **138**, 044310 (2013).

Inelastic X-ray Scattering Under Extreme and Transitional Conditions

Gerald T. Seidler, seidler@uw.edu,
Department of Physics
University of Washington
Seattle, WA 98195-1560

Program Scope

The goal of this program is to expand the scope and scientific potential of advanced x-ray spectroscopies, including x-ray absorption fine structure (XAFS), x-ray emission spectroscopy (XES), and time-resolved inelastic x-ray scattering (IXS). Notable accomplishments include: a rejuvenation of laboratory-based XAFS and XES; measurements of the branch ratios for double-photoionization channels in Ni; new theoretical and experimental methods for the study of dense plasmas, such as in the transitional, 'warm dense matter' regime; combined measurement and theory aimed at establishing a new protocol for RoHS compliance testing for Cr(VI); improved instrumentation and resulting strong collaborations focused on the time- dynamics of energy transfer in photosynthetic proteins and on the f-electron physics of lanthanide elements and compounds at high pressures.

Selected Recent Progress and Future Directions

I. A Rejuvenation of Laboratory-based High-Resolution X-ray Spectroscopies

In October 2013 we commissioned a new type of inexpensive lab-based spectrometer for high-resolution x-ray studies, including x-ray absorption fine structure (XAFS) and x-ray emission spectroscopy (XES). The startling performance of this modest instrument has garnered significant interest focused on DOE-priority research issues and that does not have the character of competition with synchrotron facilities. In addition to providing a true introductory capability that can help attract and educated entire new user communities, laboratory-based XAFS enables measurements that, for reasons of long duration, sample preparation complexity, chemical hazards, or radioisotope hazards, cannot be performed with regularity or certainty at synchrotron light sources.

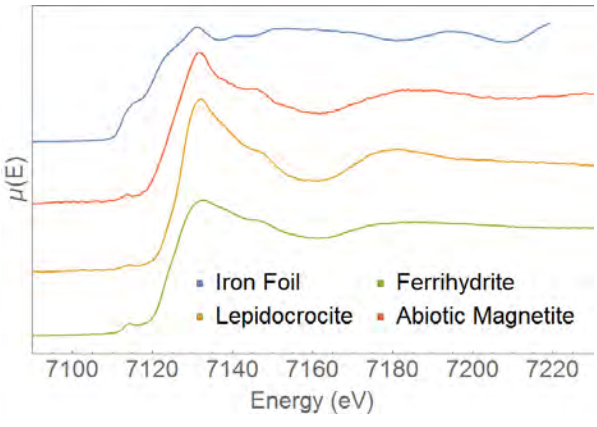

Figure 1: Fe K-edge XAFS of Fe foil and standard reference minerals. The data was collected 1 hr per scan on the CEIXANES lab XAFS user facility.

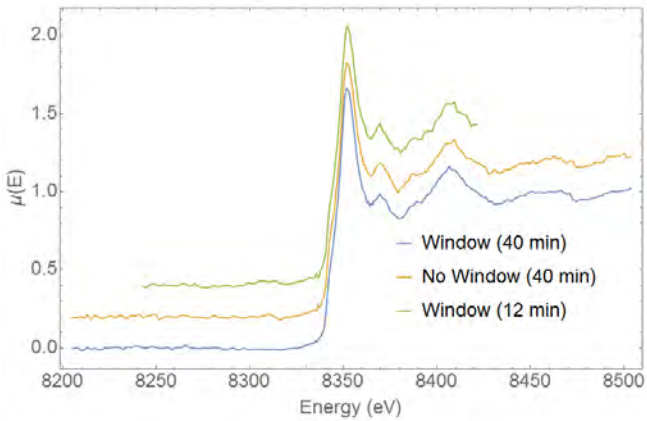

Figure 2: Ni K-edge XANES of a Ni-Mn-Co Li-ion pouch cell battery. With new x-ray window methods developed with PNNL, users can now perform *in operando* studies at the same charge rates used at synchrotron beamlines.

Representative data on mineral reference materials and on pouch cell batteries is shown in Figures 1 and 2. The 'window' data in Fig. 2 shows improved performance thanks to an ongoing collaboration with PNNL scientists that has developed a new formulation for x-ray windows on pouch-cell batteries, now capable of sustaining hundreds of cycles without contamination and capacity fade due to window materials and adhesives. This holds high potential to accelerate Li-ion battery research and development.

The technology developed under this award has now been licensed to *easyXAFS LLC* and has entered active manufacturing.

II. Quantification of Cr(VI) for RoHS Compliance via XES and Atomic Multiplet Calculation

Cr(VI) is a well-known carcinogen with high mobility in the ecosystem. For this reason Reduction of Hazardous Substances (RoHS) regulations in the European Union and elsewhere strongly constrain the Cr(VI) content to be, e.g., less than 100ppm by mass in each identifiable subcomponent of consumer electronics. For many plastic components, liquid extraction methods have proven unreliable and consequently the ASTM has had difficulty certifying broadly-applicable testing procedures for compliance.

In this project, we have demonstrated that laboratory-based high-resolution XES may help address this issue, bringing advanced core-shell atomic spectroscopy into a new role for environmental compliance in an industrial context. The data in Figures 3 and 4 show, respectively, reference spectra for Cr Kα XES in different oxidation states and then the XES from a NIST Standard Reference Material and its linear decomposition onto a superposition of Cr(III) and Cr(VI) states. The energy resolution of all data is strictly core-hole limited.

We are completing a survey of Cr(III) and Cr(VI) ions in different local environments and chemistries to determine the variability of the deep, atomic-like Cr Kα signatures in these nominal classical oxidation states. This is being complemented with perturbed, charge-transfer multiplet calculations to further validate the determined range of variation of, especially, Cr(VI) signatures. A manuscript is in preparation on this new approach in analytical chemistry. The relevant ASTM committee has been approached and, based on the results of the complete study, we will initiate a discussion of possible certification of high-resolution Cr Kα XES as a method for RoHS compliance for Cr(VI) composition.

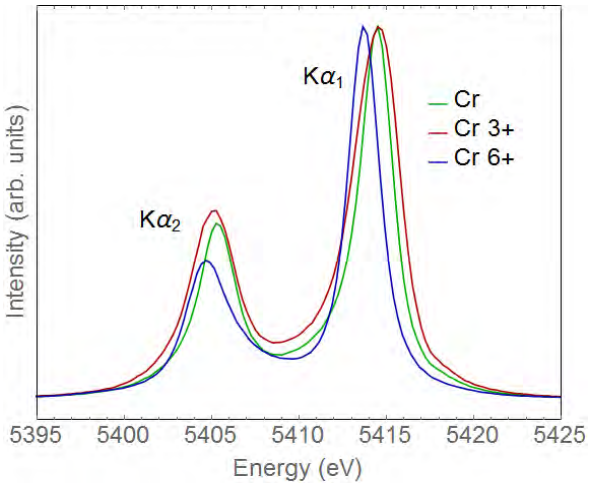

Figure 3: Cr Kα x-ray emission data for Cr metal and for two reference compounds having Cr(III) or Cr(VI) classical oxidation states.

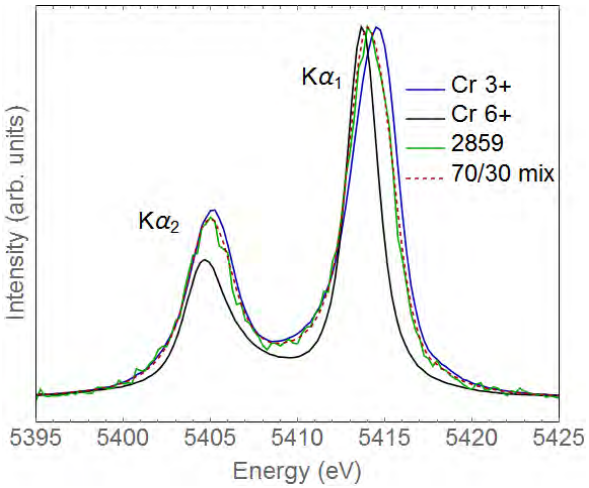

Figure 4: Analysis of Cr oxidation state in NIST SRM 2859 via linear decomposition of measured Cr Kα x-ray emission onto that of reference materials.

III. Multielectron Excitations, Branch Ratios and Absolute Cross-sections in XES

Due especially to many-body effects, x-ray interactions with matter are often quite incompletely described with single-electron treatments. A case in point is provided by double photoionization of core and semicore levels by hard x rays. In this research thrust, we use laboratory-based XES to quantify the absolute cross-sections and relative branch ratios for KL and KM double ionization in Ni in the adiabatic limit. The [1s2s] part of the KL double ionization XES, for example, has a net branch ratio less than 10^{-4} that of the single-ionization Kα XES, requiring ultra-low backgrounds. In addition, since the double-ionization XES is above the single-particle Fermi level, the intensities of these emission channels requires careful correction for absorption effects that in turn demand precise placement of the measured XES onto the same absolute energy scales as a measurement of the XANES. The interesting ability of the lab-based spectrometer to place both XES and XANES on the same energy scale has allowed exactly such a complete study, and the interim results are shown in Figure 5, together with a labeling of three double-ionization XES lines, labeled under the Z+1 approximation. After normalization to the Kβ intensity (at ~50 eV lower energy than shown in the figure) and careful consideration of resonant Raman and other contributions to the above-E_F background under the KL and KM XES lines, we will be able to quantify their branch ratios for the first time, and compare to atomic-level theory.

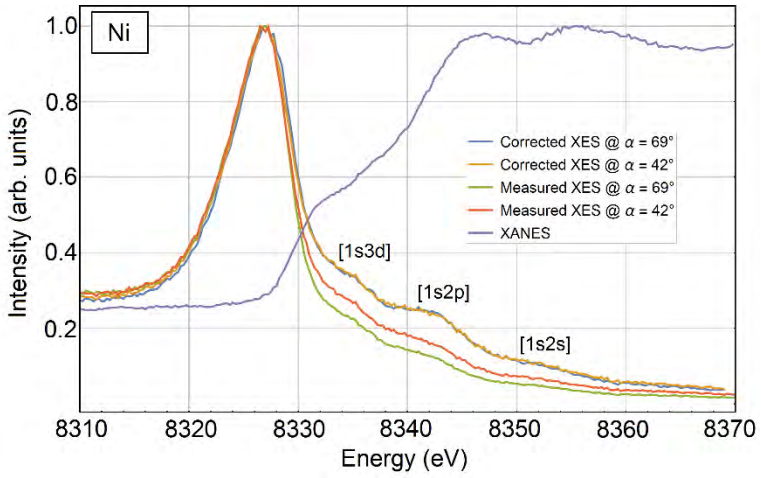

Figure 5: Valence-level and double-ionization-shifted XES from Ni metal. The ability to place the XANES (blue) and XES on the same absolute energy scale using the lab-based spectrometer allows for absorption-effect corrections. With these results, we are able to extract absolute cross-sections and also branch ratios for the different double-ionization channels.

IV. X-ray Heating Studies at LCLS/MEC

The recent LK20 campaign at LCLS/MEC was led by the PI. This beamrun emphasized the further development and application of two-color, x-ray pump / x-ray probe methods using wide-angle x-ray diffraction. While data analysis is ongoing, it is clear that an improved methodology for wide-angle XRD was demonstrated and that several scientific goals were met, including especially a careful determination of the dependence of Bragg peak intensities in crystalline MgO on x-ray heating conditions, allowing an interrogation of valence-level screening effects at finite T reaching as much as 50 eV.

Manuscripts and Publications in the Last 3 Years of this Award

1. E. Jahrman, J. Seiber, G.T. Seidler, "Direct Sensitivity to Hexavalent Cr via Very High Resolution Wavelength Dispersive X-ray Fluoresence," *in preparation*, Analytical Chemistry (2016).
2. R.A. Valenza, E. Jahrman, G.T. Seidler, "Absolute cross-sections for multi-electron excitation in Ni," *in preparation*, Phys. Rev. B (2016).
3. O. R. Hoidn, R.A. Valenza, et al., "X-ray Diffraction and Charge Reorganization in X-ray Heated MgO," *in preparation,* Phys. Rev. Letters (2016).
4. D.R. Mortensen, G.T. Seidler, et al., "Valence-to-Core X-ray Emission Spectroscopy for Inorganic Materials: A Critical Comparison to Different Theoretical Approaches," *in prepration*, Phys. Rev. B (2016).
5. D.R. Mortensen and G.T. Seidler, "Robust optic alignment in a tilt-free implementation of the Rowland circle spectrometer," *submitted*, Journal of Electron Spectroscopy and Related Phenomena (2016).
6. Katherine M. Davis, Brendan T. Sullivan, Mark Palenik, Lifen Yan, Vatsal Purohit, Gregory Robison, Irina Kosheleva, Robert W. Henning, Gerald T. Seidler, Yulia Pushkar, "Rapid Evolution of the Photosystem II Electronic Structure during Water Splitting," *submitted,* Science (2015).
7. G.T. Seidler, D.R. Mortensen, A. Ditter, N. Ball, and A. Remesnik, "A Modern Laboratory XAFS Cookbook," Journal of Physics: Conference Series **712,** 012015 (2016).
8. D.R. Mortensen, G.T. Seidler, A.S. Ditter, P. Glatzel, "Benchtop Nonresonant X-ray Emission Spectroscopy: Coming Soon to Laboratories and Beamlines Near You," Journal of Physics: Conference Series **712,** 012036 (2016).
9. K.M. Davis, M. Palenik, Lifen Yan, P.F. Smith, G.T. Seidler, G.C. Dismukes, Y. Pushkar, "X-ray emission spectroscopy of Mn coordination complexes towards interpreting the electronic structure of the Oxygen Evolving Complex of Photosystem II," Journal of Physical Chemistry C **120,** 3326 (2016).
10. M.J. Lipp, J.R. Jeffries, J.-H. Park Klepies, W.J. Evans, D.R. Mortensen, G.T. Seidler, Y. Xiao, and P. Chow, "4f-electron behavior in the cerium oxides Ce_2O_3 and CeO_2 under pressure," Phys. Rev. B **93**, 064106 (2015).
11. Oliver R. Hoidn and Gerald T. Seidler, "A Tender X-ray Camera Based on Mass Produced CMOS Sensors and Single-Board Computers," Review of Scientific Instruments **86**, 086107 (2015).
12. G.T. Seidler, D.R. Mortensen, A.J. Remesnik, J.I. Pacold, N.A. Ball, N. Barry, M. Styczinski, O.R. Hoidn, "A Laboratory-based Hard X-ray Monochromator for High-Resolution X-ray Emission Spectroscopy and X-ray Absorption Near Edge Structure Measurements," Review of Scientific Instruments **85**, 113906 (2014).
13. Joseph I. Pacold, David S. Tatum, Gerald T. Seidler, Kenneth N. Raymond, Xiaoyi Zhang, Andrew B. Stickrath, and Devon R. Mortensen, "Direct Observation of 4f Intrashell Excitation in Luminescent Lanthanide Complexes by Time-Resolved X-ray Absorption Near Edge Spectroscopy," Journal of the American Chemical Society **136**, 4186 (2014).
14. K.M. Davis, I. Kosheleva, R.W. Henning, G.T. Seidler, Y. Pushkar, "Kinetic Modeling of the X-ray-induced Damage to a Metalloprotein," Journal of Physical Chemistry B **117**, 9161 (2013). (DOI: 10.1021/jp403654n).
15. Stefan G. Minasian, et al., "Covalency in Metal–Oxygen Multiple Bonds Evaluated Using Oxygen K-edge Spectroscopy and Electronic Structure Theory", Journal of the American Chemical Society **135,** 1864 (2013).

DYNAMICS OF FEW-BODY ATOMIC PROCESSES

Anthony F. Starace, P.I.
The University of Nebraska, Department of Physics and Astronomy
855 North 16th Street, 208 Jorgensen Hall, Lincoln, NE 68588-0299
Email: astarace1@unl.edu

PROGRAM SCOPE

The goals of this project are to understand, describe, control, and image processes involving energy transfers from intense electromagnetic radiation to matter as well as the time-dependent dynamics of interacting few-body, quantum systems. Investigations of current interest are in the areas of strong field (intense laser) physics, attosecond physics, high energy density physics, and multiphoton ionization processes. Nearly all proposed projects require large-scale numerical computations, involving, e.g., the direct solution of the full-dimensional time-dependent or time-independent Schrödinger equation for two-electron (or multi-electron) systems interacting with electromagnetic radiation. In some cases our studies are supportive of and/or have been stimulated by experimental work carried out by other investigators funded by the DOE AMOS physics program. Principal benefits and outcomes of this research are improved understanding of how to control atomic processes with electromagnetic radiation and how to transfer energy optimally from electromagnetic radiation to matter.

RECENT PROGRESS

A. Carrier-Envelope-Phase-Induced Asymmetries in Double Photoionization of He by an Intense Few-Cycle XUV Pulse

The carrier-envelope-phase (CEP) dependence of electron angular distributions in double ionization of He by an arbitrarily-polarized, few-cycle, intense XUV pulse is formulated using perturbation theory in the pulse amplitude. Owing to the broad pulse bandwidth, interference of first and second order perturbation amplitudes produces asymmetric angular distributions that are sensitive to the CEP. Our perturbation theory parametrization is shown to be valid by comparing with results of solutions of the full-dimensional, two-electron time-dependent Schrödinger equation for the case of linear polarization. (*See reference [2] in the publication list below*.)

B. High-Order Harmonic Generation of Be in the Multiphoton Regime

The high-order harmonic generation (HHG) spectrum of Be was investigated in the multiphoton regime by solving the full-dimensional, two-active-electron, time-dependent Schrödinger equation in an intense (10^{13}W/cm^2), 30-cycle laser field. As the laser frequency ω_L varies from 1.7 to 1.8 eV (which is in the tunable range of a Ti:sapphire laser), the 7th harmonic becomes resonant sequentially with the transition between the ground state and two doubly-excited autoionizing states while the 3rd harmonic becomes resonant with the 2s2p(^{1}P) singly-excited state. At each resonant frequency, the HHG power spectrum increases by an order of magnitude over a range of harmonics that form a plateau, extending from the resonant harmonic up to a cutoff at the 25th harmonic. In contrast to the well-known rescattering plateau cutoff law appropriate in the tunneling

regime (which predicts a cutoff at the 5th or 7th harmonic), the multiphoton regime plateau we find for Be originates from atomic resonance effects. Off-resonance, the Be HHG spectrum decreases monotonically with harmonic order. By taking the ratio of the integrated harmonic power of the 7th harmonic to that of the 5th harmonic, one can isolate the resonant effects of the two doubly-excited states in the HHG spectrum from those of singly-excited resonance states. These ratios exhibit resonance profiles for driving laser pulse durations much longer than the lifetimes of these autoionizing states. The energy widths of these resonance features are comparable to the widths of the laser pulse and are much smaller than the autoionizing state widths. These results demonstrate an important role for electron correlations in enhancing harmonic generation rates in the multiphoton regime. (*See reference [3] below*.)

C. ***Potential Barrier Features in Three-Photon Ionization Processes in Atoms***

Resonance-like enhancements of generalized three-photon cross sections for XUV ionization of Ar, Kr, and Xe have been demonstrated and analyzed within a single-active-electron, central-potential model. The resonant-like behavior is shown to originate from the potential barriers experienced by intermediate- and final-state photoelectron wave packets corresponding to absorption of one, two, or three photons. The resonance-like profiles in the generalized three-photon ionization cross sections are shown to be similar to those found in the generalized two-photon ionization cross sections [*Phys. Rev. A* **82**, 053414 (2010)]. The complexity of Cooper minima in multiphoton ionization processes is also discussed. Owing to the similar resonance-like profiles found in both two- and three-photon generalized cross sections, we expect such potential barrier effects to be general features of multiphoton ionization processes in most atoms with occupied *p*- and *d*-subshells. (*See reference [4] in the publication list below*.)

D. ***Nonlinear dichroism in back-to-back double ionization of He by an intense elliptically-polarized few-cycle XUV pulse***

We have predicted a new dynamical effect observable in double photoionization of the He atom by an elliptically-polarized, ultrashort laser pulse: nonlinear dichroism (ND). The ND effect is exquisitely sensitive not only to electron correlations, but also to the temporal duration, the polarization, and the carrier-envelope phase (CEP) of a laser pulse. This new effect thus permits one to explore electron correlations on their natural time scale (in the case of attosecond XUV pulses), providing both dynamical and phase information on the double photoionization amplitudes involved. It also provides a new means for experiment to characterize the duration, the polarization, and the CEP of ultrashort (attosecond) XUV pulses. Measurement of this predicted ND effect requires more intense attosecond pulses than are available currently, but great strides are being made to increase the intensity of attosecond pulses. Finally, our predictions have required us to develop theoretical tools to solve the full six-dimensional problem of the interaction of the fundamental two-electron He atom with an ultrashort, elliptically-polarized attosecond pulse. (*See reference [5] in the publication list below*.)

E. ***Electron Vortices in Photoionization by Circularly-Polarized Attosecond Pulses***

Single ionization of He by two oppositely circularly-polarized, time-delayed attosecond pulses is shown to produce photoelectron momentum distributions in the polarization plane having helical vortex structures sensitive to the time-delay between the pulses, their relative phase, and their

handedness. The matter-wave vortex patterns we predict have a counterpart in optics, in which similar vortex patterns have been produced by interference of particular kinds of laser beams. However, such vortices have never before been either observed or predicted by interference of electron matter waves. *We thus have here a dramatic example of wave-particle duality*. Results are obtained by both *ab initio* numerical solution of the two-electron time-dependent Schrödinger equation and by a lowest-order perturbation theory analysis. The energy, bandwidth, and temporal duration of attosecond pulses are ideal for observing these vortex patterns. In particular, attosecond pulse durations are required to observe the momentum space vortex patterns we predict. Our results indicate the exquisite sensitivity of the spiral vortex patterns to both the properties of the two laser pulses and the time-delay between them, thus indicating (i) that this is a new means to control electron motion with laser pulses and (ii) that this process provides a new diagnostic tool for characterizing the laser pulses and for determining the delay between them. (*See reference [6] in the publication list below*.)

F. *Favorable target positions for intense laser acceleration of electrons in hydrogen-like, highly-charged ions*

Classical relativistic Monte Carlo simulations of petawatt laser acceleration of electrons bound initially in hydrogen-like, highly-charged ions show that both the angles and energies of the laser-accelerated electrons depend on the initial ion positions with respect to the laser focus. Electrons bound in ions located after the laser focus generally acquire higher (≈ GeV) energies and are ejected at smaller angles with respect to the laser beam. Our simulations assume a tightly-focused linearly-polarized laser pulse with intensity of $\approx 10^{22}$ W/cm^2. Up to fifth order corrections to the paraxial approximation of the laser field in the focal region are taken into account. In addition to the laser intensity, the Rayleigh length in the focal region is shown to play a significant role in maximizing the final energy of the accelerated electrons. Results are presented for both Ne^{9+} and Ar^{17+} target ions. (*See reference [7] in the publication list below*.)

G. *Multi-start Spiral Electron Vortices in Ionization by Circularly Polarized UV Pulses*

Multi-start spiral vortex patterns have been predicted for the electron momentum distributions in the polarization plane following ionization of the He atom by two time-delayed circularly polarized ultrashort laser pulses. For two ultraviolet (UV) pulses having the same frequency (such that two photons are required for ionization), single-color two-photon interferometry with co-rotating or counter-rotating time-delayed pulses was found to lead respectively to zero-start or four-start spiral vortex patterns in the ionized electron momentum distributions in the polarization plane. In contrast, two-color one-photon plus two-photon interferometry with time-delayed co-rotating or counter-rotating UV pulses was found to lead respectively to one-start or three-start spiral vortex patterns. These predicted multi-start electron vortex patterns were found to be sensitive to the carrier frequencies, handedness, time delay, and relative phase of the two pulses. Our numerical predictions are obtained by solving the six-dimensional two-electron time dependent Schrödinger equation (TDSE). They are explained analytically using perturbation theory (PT). Comparison of our TDSE and PT results for single-color two-photon processes probes the role played by the time-delay-dependent ionization cross channels in which one photon is absorbed from each pulse. These cross channels can be controlled by means of the parameters of the fields and the ionized electron detection geometries. (*See reference [8] in the publication list below*.

FUTURE PLANS

Our group is currently carrying out research on the following additional projects:

• We are investigating kinematical vortices in double photoionization of He by elliptically polarized attosecond pulses for a variety of experimental configurations.

• We are investigating the description of electromagnetic fields of vortex laser beams carrying orbital angular momentum beyond the paraxial approximation.

• We are investigating the use of vortex laser beams carrying orbital angular momentum to accelerate electrons bound in highly-charged ions to GeV energies.

• We are investigating resonant harmonic generation with chirped laser pulses, using the chirp as a means to be on resonance with doubly-excited states of two-electron atoms such as He and Be.

PUBLICATIONS STEMMING FROM DOE-SPONSORED RESEARCH (2013 – 2016)

[1] J.M. Ngoko Djiokap, S.X. Hu, W.-C. Jiang, L.-Y. Peng, and A.F. Starace, "Asymmetries in Production of $He^+(n=2)$ with an Intense Few-Cycle Attosecond Pulse," *Phys. Rev. A* **88**, 011401(R) (2013).

[2] J.M. Ngoko Djiokap, N.L. Manakov, A.V. Meremianin, and A.F. Starace, "Carrier-Envelope-Phase-Induced Asymmetries in Double Photoionization of He by an Intense Few-Cycle XUV Pulse," Phys. Rev. A **88**, 053411 (2013).

[3] J.M. Ngoko Djiokap and A.F. Starace, "Resonant Enhancement of the Harmonic Generation Spectrum of Beryllium," Phys. Rev. A **88**, 053412 (2013).

[4] L.-W. Pi and A.F. Starace, "Potential Barrier Effects in Three-Photon Ionization Processes," Phys. Rev. A **90**, 023403 (2014).

[5] J.M. Ngoko Djiokap, N.L. Manakov, A.V. Meremianin, S.X. Hu, L.B. Madsen, and A.F. Starace, "Nonlinear dichroism in back-to-back double ionization of He by an intense elliptically-polarized few-cycle XUV pulse," Phys. Rev. Lett. **113**, 223002 (2014). *This Letter was featured in the February 2015 issue of Photonics Spectra (p. 32); the online version appears here*: http://www.photonics.com/Article.aspx?PID=5&VID=125&IID=801&Tag=Tech+Pulse&AID=56939

[6] J.M. Ngoko Djiokap, S.X. Hu, L.B. Madsen, N.L. Manakov, A.V. Meremianin, and A.F. Starace, "Electron Vortices in Photoionization by Circularly Polarized Attosecond Pulses," Phys. Rev. Lett. **115**, 113004 (2015). *This work was featured on the cover of the 11 September 2015 issue of Physical Review Letters. It is also a Research Highlight in Nature Physics **11**, 800 (October 2015).*

[7] L.-W. Pi, S.X. Hu, and A.F. Starace, "Favorable Target Positions for Intense Laser Acceleration of Electrons in Hydrogen-Like, Highly-Charged Ions," Phys. Plasmas **22**, 093111 (2015).

[8] J.M. Ngoko Djiokap, A.V. Meremianin, N.L. Manakov, S.X. Hu, L.B. Madsen, and A.F. Starace, "Multistart Spiral Electron Vortices in Ionization by Circularly Polarized UV Pulses," Phys. Rev. A **94**, 013408 (2016).

FEMTOSECOND AND ATTOSECOND LASER-PULSE ENERGY TRANSFORMATION AND CONCENTRATION IN NANOSTRUCTURED SYSTEMS

DOE Grant No. DE-FG02-01ER15213

Mark I. Stockman, PI

Department of Physics and Astronomy, Georgia State University, Atlanta, GA 30303

E-mail: mstockman@gsu.edu, URL: http://www.phy-astr.gsu.edu/stockman

Current Year Grant Period of 2015-2016 (Publications 2014-2016)

1 Program Scope

The program is aimed at theoretical investigations of a wide range of phenomena induced by ultrafast laser-light excitation of nanostructured or nanosize systems, in particular, metal/semiconductor/dielectric nanocomposites and nanoclusters. Among the primary phenomena are processes of energy transformation, generation, transfer, and localization on the nanoscale and coherent control of such phenomena.

2 Recent Progress and Publications

Publications resulting from the grant during the period of 2014-2016 are: [1-19]. During the current grant period of 2015-2016, the following articles with this DOE support have been published: [4, 14-19]. The following articles received, as acknowledged, supplementary support of this grant during 2015-2016: [10-13, 17, 20] . Below we highlight selected articles that we consider most significant.

2.1 Semimetallization of dielectrics in strong optical fields [19]

At the heart of ever growing demands for faster signal processing is ultrafast charge transport and control by electromagnetic fields in semiconductors. Intense optical fields have opened fascinating avenues for new phenomena and applications in solids. Because the period of optical fields is on the order of a femtosecond, the current switching and its control by an optical field may pave a way to petahertz optoelectronic devices. Lately, a reversible semimetallization in fused silica on a femtosecond time scale by using a few-cycle strong field (~1 V/Å) is manifested. The strong Wannier-Stark localization and Zener-type tunneling were expected to drive this ultrafast semimetallization. Wider spread of this technology demands better understanding of whether the strong field behavior is universally similar for different dielectrics. In this publication [19] we develop theory of the universal semimetallization; experimentally, we employ a carrier-envelope-phase stabilized, few-cycle strong optical field to drive the semimetallization in sapphire, calcium fluoride and quartz and to compare this phenomenon and show its remarkable similarity between them. The similarity in response of these materials, despite the distinguishable differences in their physical properties, suggests the universality of the physical picture explained by the localization of Wannier-Stark states. Our results elucidate fundamental limit on optical field-induced processes in solids and may blaze a trail to PHz-rate optoelectronics.

2.2 Attosecond nanoscale near-field sampling [17]

The promise of ultrafast light-field-driven electronic nanocircuits has stimulated the development of the new research field of attosecond nanophysics. An essential prerequisite for advancing this new area is the ability to characterize optical near fields from light interaction with nanostructures, with sub-cycle resolution. Here we experimentally demonstrate attosecond near-field retrieval for a tapered gold nanowire. By comparison of the results to those obtained from noble gas experiments and trajectory simulations, the spectral response of the nanotaper near field arising from laser excitation can be extracted. Attosecond nanoscale near-field sampling (ANNS), proposed by us in 2007 and extensively

studied theoretically, has been shown to provide sub-cycle resolution of optical near-field dynamics in nanostructured materials, but has not yet been implemented experimentally. ANNS relies on the emission of photoelectrons with high initial momentum by an attosecond extreme ultraviolet (XUV) pulse, and subsequent acceleration of the photoelectrons in the near fields. In this publication, we perform ANNS measurements on a nanotaper at near-infrared (NIR) intensities well below the onset of non-linear effects. Using the gold nanotaper sample geometry, we show that through careful analysis of field homogeneity and streaking electron trajectories, a meaningful attosecond characterization of near fields can be performed in spite of the inherent challenges associated with the large emission area.

2.3 Strong-Field and Attosecond Physics in Solids [2]

In this article, we consider the status of strong-field and attosecond processes in bulk transparent solids near the Keldysh tunneling limit. For high enough fields and low-frequency excitations, the optical and electronic properties of dielectrics can be transiently and reversibly (adiabatically) modified within the applied pulse. One of the phenomena considered is high harmonic generation (HHG) from solids. We conclude that the solid-state HHG is significantly different from that in gases due to structural periodicity inherent in crystals. One of the consequences is that the cutoff harmonic frequency is linearly proportional to the field, instead of quadratic dependence in gases. This can be interpreted as a result of adiabatic Wannier-Stark localization and Bloch oscillations of electrons in the presence of the strong field. Other class of the considered phenomena is reversible semi-metallization of dielectric n the strong fields, which causes appearance of ultrafast electrical currents controlled by the carrier-envelope phase of the pulse.

2.4 Strong-Field Perspective on High-Harmonic Radiation from Bulk Solids [3]

In this article, mechanisms of HHG from crystals are described by treating the electric field of a laser as a quasistatic strong field. Under the quasistatic electric field, electrons in periodic potentials form dressed states, known as Wannier-Stark states. The energy differences between the dressed states, which is the Bloch frequency $\omega_B = eaF/\hbar$, where e is unit charge, a is lattice constant, and F is the electric field, determine the frequencies of the radiation. The radiation yield is determined by the magnitudes of the interband and intraband current matrix elements between the dressed states. The generation of attosecond pulses from solids is predicted. Ramifications for strong-field physics are discussed. In particular, HHG from solids may provide a pathway to creation of a nanosource of VUV and XUV radiation with pronounced application potential.

2.5 Graphene in Ultrafast and Superstrong Laser Fields [4]

For graphene interacting with a few-fs intense optical pulse, we predict unique and rich behavior dramatically different from three-dimensional solids. Quantum electron dynamics is shown to be coherent but highly nonadiabatic and effectively irreversible due to strong dephasing. This dephasing is due to the absence of the bandgap – graphene is a semimetal. Electron distribution in reciprocal space exhibits hot spots at the Dirac points and oscillations whose period is determined by nonlocality of electron response and whose number is proportional to the field amplitude. The optical pulse causes net charge transfer in the plane of graphene in the direction of the instantaneous field maximum at relatively low fields and in the opposite direction at high fields. This behavior of graphene is related to peculiarities of the Wannier-Stark states of electrons in strong fields [6]. The phenomena described in this article [4] promise ultrafast optoelectronic applications with petahertz bandwidth.

2.6 Ultrafast Field Control of Symmetry, Reciprocity, and Reversibility in Buckled Graphene-Like Materials [11]

In this article, we theoretically show that buckled two-dimensional graphene-like materials (silicene and germanene) subjected to a femtosecond strong optical pulse can be controlled by the optical field component normal to their plane. In such strong fields, these materials are predicted to exhibit nonreciprocal reflection, optical rectification, and generation of electric currents both parallel and normal

to the in-plane field direction. Reversibility of the conduction band population is also field- and carrier-envelope phase controllable. There is a net charge transfer along the material plane that is also dependent on the normal field component. Thus a graphene-like buckled material behaves analogously to a field-effect transistor controlled and driven by the electric field of light with subcycle (femtosecond) speed.

3 Directions of Work for the Next Period

We will develop the present success in the optics of ultrastrong and ultrafast fields on the nanoscale. We will extend the existing theory to other systems focusing on modern two-dimensional solids such as graphene, transitional metal dichalcogenides, boron nitride, and surfaces of topological insulators. We will extend theory to describe photoelectron emission caused by the strong ultrashort pulses and probe attosecond XUV pulses in in the two-dimensional materials. In particular, we will theoretically describe ultrafast angular-resolved photoelectron emission spectroscopy (ARPES) from the two-dimensional materials and the topological properties of these solids revealed by it. A case of particular interest to study will be effects of the topological (Berry) phase in superlatticies and Moiré stacks of the two-dimensional solids. Finally, we will turn to theory of topological insulators in strong fields and effects of spin-polarized ARPES.

4 *References*

1. H. K. Kelardeh, V. Apalkov, and M. I. Stockman, *Interaction of Graphene Monolayer with Ultrashort Laser Pulse*, arXiv:1401.5786 [cond-mat.mes-hall], 1-11 (2014).
2. S. Ghimire, G. Ndabashimiye, A. D. DiChiara, E. Sistrunk, M. I. Stockman, P. Agostini, L. F. DiMauro, and D. A. Reis, *Strong-Field and Attosecond Physics in Solids*, Journal of Physics B: Atomic, Molecular and Optical Physics **47**, 204030-1-10 (2014).
3. T. Higuchi, M. I. Stockman, and P. Hommelhoff, *Strong-Field Perspective on High-Harmonic Radiation from Bulk Solids*, Phys. Rev. Lett. **113**, 213901-1-5 (2014).
4. H. K. Kelardeh, V. Apalkov, and M. I. Stockman, *Graphene in Ultrafast and Superstrong Laser Fields*, Phys. Rev. B **91**, 0454391-8 (2015).
5. V. S. Yakovlev, S. Y. Kruchinin, T. Paasch-Colberg, M. I. Stockman, and F. Krausz, *Ultrafast Control of Strong-Field Electron Dynamics in Solids* arXiv:1502.02180, 1-21 (2015).
6. H. K. Kelardeh, V. Apalkov, and M. I. Stockman, *Wannier-Stark States of Graphene in Strong Electric Field*, Phys. Rev. B **90**, 085313-1-11 (2014).
7. F. Krausz and M. I. Stockman, *Attosecond Metrology: From Electron Capture to Future Signal Processing*, Nat. Phot. **8**, 205-213 (2014).
8. V. Apalkov and M. I. Stockman, *Proposed Graphene Nanospaser*, Light-Sci Appl **3**, e191-1-6 (2014).
9. Y.-J. Lu, C.-Y. Wang, J. Kim, H.-Y. Chen, M.-Y. Lu, Y.-C. Chen, W.-H. Chang, L.-J. Chen, M. I. Stockman, C.-K. Shih, and S. Gwo, *All-Color Plasmonic Nanolasers with Ultralow Thresholds: Autotuning Mechanism for Single-Mode Lasing*, Nano Lett. **14**, 4381–4388 (2014).
10. E. I. Galanzha, R. Weingold, D. A. Nedosekin, M. Sarimollaoglu, A. S. Kuchyanov, R. G. Parkhomenko, A. I. Plekhanov, M. I. Stockman, and V. P. Zharov, *Spaser as Novel Versatile Biomedical Tool*, arXiv:1501.00342, 1-33 (2015).
11. H. K. Kelardeh, V. Apalkov, and M. I. Stockman, *Ultrafast Field Control of Symmetry, Reciprocity, and Reversibility in Buckled Graphene-Like Materials*, Phys. Rev. B **92**, 045413-1-9 (2015).

12. M. I. Stockman, *Nanoplasmonics: Fundamentals and Applications*, in *Nano-Structures for Optics and Photonics*, edited by B. diBartolo and e. al. (Springer Netherlands, 2015), p. 3-102.
13. M. I. Stockman, *Quantum Nanoplasmonics*, in *Photonics, Volume Ii: Scientific Foundations, Technology and Applications*, edited by D. L. Andrews (John Wiley & Sons, Inc., Hoboken, NJ, USA. , 2015), p. 85-132.
14. B. Förg, J. Schoetz, F. Suessmann, M. Foerster, M. Krueger, B.-N. Ahn, K. Wintersperger, S. Zherebtsov, A. Guggenmos, V. Pervak, A. Kessel, S. Trushin, A. Azzeer, M. Stockman, D.-E. Kim, F. Krausz, P. Hommelhoff, and M. Kling, *Attosecond Nanoscale near-Field Sampling*, arXiv:1508.05611 [physics.optics] (2015).
15. V. S. Yakovlev, M. I. Stockman, F. Krausz, and P. Baum, *Atomic-Scale Diffractive Imaging of Sub-Cycle Electron Dynamics in Condensed Matter*, Sci. Rep, **5**, 145811-1-13 (2015).
16. Y. Abate, D. Seidlitz, A. Fali, S. Gamage, V. E. Babicheva, V. S. Yakovlev, M. I. Stockman, R. Collazo, D. E. Alden, and N. Dietz, *Nanoscopy of Phase Separation in Inxga1-Xn Alloys*, ACS Appl Mater Inter (2016).
17. B. Förg, J. Schötz, F. Süßmann, M. Förster, M. Krüger, B. Ahn, W. Okell, K. Wintersperger, S. Zherebtsov, A. Guggenmos, V. Pervak, A. Kessel, S. Trushin, A. Azzeer, M. Stockman, D. E. Kim, F. Krausz, P. Hommelhoff, and M. Kling, *Attosecond Nanoscale near-Field Sampling*, Nature Communications **7**, 11717-1-7 (2016).
18. M. H. Javani and M. I. Stockman, *Real and Imaginary Properties of Epsilon-near-Zero Materials*, Phys. Rev. Lett. **117**, 107404 (2016).
19. O. Kwon, T. Paasch-Colberg, V. Apalkov, B.-K. Kim, J.-J. Kim, M. I. Stockman, and D. E. Kim, *Semimetallization of Dielectrics in Strong Optical Fields*, Sci. Rep, **6**, 21272-1-9 (2016).
20. H. K. Kelardeh, V. Apalkov, and M. I. Stockman, *Attosecond Strong-Field Interferometry in Graphene: Chirality, Singularity, and Berry Phase*, Phys. Rev. B **93**, 155434-1-7 (2016).

Laser-Produced Coherent X-Ray Sources

Donald Umstadter
Physics and Astronomy Department
University of Nebraska, Lincoln, NE 68588-0207
donald.umstadter@unl.edu

Program Scope

The development of ultra-short pulsed x-ray light sources has led to rapid advancement in ultrafast x-ray science. As part of this project, we developed a new compact source of bright femtosecond x-rays. The new light source is based on inverse Compton (Thomson) back-scattering driven by two intense light pulses, each of which is amplified by a single high-power laser system. One laser pulse rapidly accelerates electrons (~3 GeV/cm) by means of the laser-wakefield mechanism; and the other laser pulse backscatters from the relativistic electrons. The scattered light is relativistically Doppler upshifted to high photon energy. We have demonstrated that these x-ray beams have several other unique features: narrow spectral bandwidth ($\Delta E/E \sim 25\%$), large energy-tuning range (50 keV $\leq h\nu \leq$ 10 MeV), and small angular divergence (10 mrad).

These features are enabling the development of a test-bed for the study of atomic and optical physics with extreme light. An exceptionally large x-ray-energy tuning range can facilitate the probing of almost any element's inner-shell atomic structure. Femtosecond x-ray pulse duration, coupled to high photon energy, can enable ultrafast time-resolved studies with atomic-scale spatial and temporal resolutions. Synchronization with ultra-high-intensity laser light pulses ($\leq 10^{22}$ W/cm^2, $a_0 \sim 100$) can merge ultrafast science with ultra-high-field science to study extreme conditions of matter.

Recent Progress

Research during the last funding cycle has led to a substantial increase in both the average and peak x-ray brightness (now comparable to that of third-generation synchrotron light source). Also, first ever measurements were made of the evolution of free electrons under extreme conditions: of high space-charge density [1] and, separately, of high photon density [2]. Our progress also involved improvement, characterization, and increased control, of the component systems, including: (1) the high peak power laser, (2) the laser-driven electron accelerator, and (3) the laser-driven Thomson x-ray source.

High peak power laser

The DIOCLES laser has an all-solid-state architecture, based on the technique of chirped-pulse amplification, broadband amplification medium (titanium sapphire), and an oscillator with Kerr-lens mode-locking. For the experiments described here, 3-J, 35-fs, 805-nm laser pulses were produced at 10-Hz repetition rate. Fourier-transform-limited light pulses were obtained at the focus of a 100-TW peak-power laser in vacuum. The spectral-phase distortion induced by the dispersion mismatching between the stretcher, compressor, and dispersive materials was fully compensated by means of an adaptive closed-loop [3, 4]. Wavefront correction of terawatt-peak-power laser beams at two distinct and well-separated wavelengths (fundamental and second harmonic) has allowed simultaneous near diffraction-limited focusing, and thus higher x-ray energy to be reached

without increasing the electron beam energy. This also enables two-color experiments at relativistic intensities [5].

Laser-driven electron accelerator

A key technology enabling our narrow-bandwidth and tunable x-ray source is the laser-wakefield electron accelerator. By implementing a staged device, based on a double-jet gas target, independent injection and acceleration was achieved [6-9]. This independent control over both the injection and acceleration processes enabled independent control over the charge and energy of the accelerated electron beam, while preserving the quasi-monoenergetic character of the beam. The charge and energy were varied in the ranges of 2–45 pC, and 50–450 MeV, respectively.

Laser-driven Thomson x-ray source [6, 8, 10-12]

Two separate counter-propagating laser beams are generated by means of beam-splitting a single beam. One beam is spatially overlapped with the electron beam that was accelerated by the other. The interaction occurs in vacuum outside the plasma. By varying the electron energy (from 50 MeV to 300 MeV), the x-ray photon energy could be tuned over a range extending from 50 keV to 10 MeV. This is the first all-laser-driven hard x-ray source with a peaked photon-number spectral density spectrum. It is also the widest tuning range of an x-ray source of any type.

Pump and probe measurements of the evolution of electrons under extreme conditions

All-laser-driven inverse-Compton scattering is itself a pump-probe experiment, using precisely synchronized optical pump and probe pulses, both of which are femtosecond in duration and focused to ultra-high intensity levels. The pump pulse produced a femtosecond-duration electron pulse, which was probed by another synchronized laser pulse. The evolution of the electrons was measured via the Thomson scattered x-rays. In one experiment, the evolution of the electrons was measured under conditions of extreme space charge field strength (ultra-high electron density) [1]. In another, the evolution of the electrons was measured under conditions of extreme EM field strength (ultra-high photon density) [2].

Extreme space charge (electron density)

When the electron charge density in free space is extremely high, the repulsive force of the space charge tends to blow the electron beam apart. In our experiment, we were able to observe the evolution of this process. Evolution of the electrons under these conditions was measured via single-shot spectroscopic imaging of the Thomson scattered x-rays, as well as measurements of the electron beam.

Through this study, we obtained a value for the transverse emittance of the electron beam of $\varepsilon_{\mathrm{nt}} = 0.15 \pm 0.06\,\pi$ mm mrad (after propagation in free space of 1.5 mm), which to the best of our knowledge, this is the lowest measured so far for an LWFA electron beam. We also experimentally measured the evolution of electron bunch transverse emittance to infer its duration. The result, 10 fs, matched known predictions on the duration of a typical laser-wakefield-accelerated electron bunch, as well as experimentally measured values [1].

Extreme EM field strength (photon density)

In another, the evolution of the electrons was measured under conditions of extreme EM field strength (ultra-high photon density). X-rays produced by highly nonlinear scattering of electrons by an ultra-intense electromagnetic field ($I = 7\times10^{20}$ W-cm^{-2}, $a_0 \sim 15$) were studied experimentally

and compared with simulations. Highly multi-photon scattering was observed (> 1,000 photons), producing a continuum of harmonics (> 1,000th order) [2].

Future Plans

We propose to increase the x-ray source brightness and coherence even further, through implementation of several theoretically predicted, but as-yet-untested, concepts. These include travelling wave enhancement, predicted to increase the x-ray brightness by a factor of ten [25, 26], and coherent backscattering [27, 28], predicted to produce bright sub-100-attosecond-duration hard x-ray pulses.

We will also benchmark our newly developed capabilities against previous conventional ones in a proof-of-concept ultrafast time-resolved pump-probe experiment on the dynamics of the atomic lattice under extreme conditions [29].

Publications supported in part by this DOE grant (published within last three years)

1. G. Golovin, S. Banerjee, C. Liu, S. Chen, J. Zhang, B. Zhao, P. Zhang, M. Veale, M. Wilson, P. Seller, and D. Umstadter, "Intrinsic beam emittance of laser-accelerated electrons measured by x-ray spectroscopic imaging," Sci. Rep. **6,** 24622 (2016). doi:10.1038/srep24622
2. W. Yan, G. Golovin, D. Haden, C. Fruhling, P. Zhang, J. Zhang, B. Zhao, C. Liu, S. Chen, and S. Banerjee, "Highly Nonlinear Inverse Compton Scattering," in High-Brightness Sources and Light-Driven Interactions, OSA Technical Digest (online) (Optical Society of America, 2016), paper HM3B.3. doi:10.1364/HILAS.2016.HM3B.3
3. C. Liu, J. Zhang, G. Golovin, S. Chen, S. Banerjee, B. Zhao, N. Powers, I. Ghebregziabher, and D. P. Umstadter, "Adaptive spectral-phase control for laser wakefield electron acceleration," in *CLEO: Science and Innovations,* (Optical Society of America, 2014), pp. JTh4L. 3.
4. C. Liu, J. Zhang, S. Chen, G. Golovin, S. Banerjee, B. Zhao, N. Powers, I. Ghebregziabher, and D. Umstadter, "Adaptive-feedback spectral-phase control for interactions with transform-limited ultrashort high-power laser pulses," Opt. Lett. **39,** 80-83 (2014).
5. B. Zhao, J. Zhang, S. Chen, C. Liu, G. Golovin, S. Banerjee, K. Brown, J. Mills, C. Petersen, and D. Umstadter, "Wavefront-correction for nearly diffraction-limited focusing of dual-color laser beams to high intensities," Optics express **22,** 26947-26955 (2014).
6. G. Golovin, S. Chen, N. Powers, C. Liu, S. Banerjee, J. Zhang, M. Zeng, Z. Sheng, and D. Umstadter, "Independent control of laser wakefield-accelerated electron-beam parameters," Proc. SPIE 9514, Laser Acceleration of Electrons, Protons, and Ions III; and Medical Applications of Laser-Generated Beams of Particles III, 951405 (May 14, 2015); doi:10.1117/12.2182707.
7. G. Golovin, S. Banerjee, J. Zhang, S. Chen, C. Liu, B. Zhao, J. Mills, K. Brown, C. Petersen, and D. Umstadter, "Tomographic imaging of nonsymmetric multicomponent tailored supersonic flows from structured gas nozzles," Appl. Opt. **54,** 3491-3497 (2015).
8. G. Golovin, S. Chen, N. Powers, C. Liu, S. Banerjee, J. Zhang, M. Zeng, Z. Sheng, and D. Umstadter, "Tunable monoenergetic electron beams from independently controllable laser-wakefield acceleration and injection," Phys. Rev. STAB **18,** 011301 (2015).
9. G. Golovin, S. Banerjee, S. Chen, N. Powers, C. Liu, W. Yan, J. Zhang, P. Zhang, B. Zhao, and D. Umstadter, "Control and optimization of a staged laser-wakefield accelerator," Nuclear Instruments and Methods in Physics Research Section A 830, 375-380 (2016). doi:10.1016/j.nima.2016.06.022
10. S. Banerjee, S. Chen, N. Powers, D. Haden, C. Liu, G. Golovin, J. Zhang, B. Zhao, S. Clarke, and S. Pozzi, "Compact source of narrowband and tunable X-rays for radiography," Nuclear Instruments and Methods in Physics Research Section B: **350,** 106-111 (2015).
11. G. Golovin, S. Chen, N. Powers, C. Liu, S. Banerjee, J. Zhang, M. Zeng, Z. Sheng, and D. Umstadter, "Laser-wakefield electron accelerator with independent beam-parameter control," in *2014 IEEE 41st International Conference on Plasma Sciences (ICOPS)*, pp. 1 (2014).

12. D. P. Umstadter, "All-laser-driven Thomson X-ray sources," Contemporary Physics **56,** 417-431 (2015).
13. G. Golovin, S. Banerjee, C. Liu, S. Chen, J. Zhang, B. Zhao, P. Zhang, M. Veale, M. Wilson, P. Seller, and D. P. Umstadter, "Laser-Driven Electron Beams With Ultra-Low Emittance Measured Via Inverse-Compton-Scattered X-Rays," in ***High-Brightness Sources and Light-Driven Interactions***, OSA Technical Digest (online) (Optical Society of America, 2016), paper HM3B.4.
14. D. Umstadter, "All-laser-driven Compton x-ray light source," in High-Brightness Sources and Light-Driven Interactions, OSA technical Digest (online) (Optical Society of America, 2016), paper ET2A.2.
15. S. Chen, G. Golovin, C. Miller, D. Haden, S. Banerjee, P. Zhang, C. Liu, J. Zhang, B. Zhao, S. Clarke, S. Pozzi, and D. Umstadter, "Shielded radiography with a laser-driven MeV-energy X-ray source, " Nuclear Instruments and Methods in Physics Research Section B **366**, 217-223 (2016).
16. D. Umstadter, "Hard x-rays from a tabletop all-laser-driven synchrotron light source," Proc. SPIE **9590**, Advances in Laboratory-based X-Ray Sources, Optics, and Applications IV, 959002 (August 26, 2015);
17. D. Umstadter, "Narrow bandwidth and tunable hard x-rays from an all-laser-driven Thomson light source," Proc. SPIE **9509**, Relativistic Plasma Waves and Particle Beams as Coherent and Incoherent Radiation Sources, 95090A (May 12, 2015); doi:10.1117/12.2182696.
18. S. Banerjee, G. Golovin, P. Zhang et al., "Photonuclear and radiography applications of narrowband, multi-MeV all-optical Thomson x-ray source," Proc. SPIE **9515**, Research Using Extreme Light: Entering New Frontiers with Petawatt-Class Lasers II, 95151C (May 1, 2015);
19. C. Liu, G. Golovin, S. Chen et al., "Generation of 9-MeV γ-rays by all-laser-driven Compton scattering with second-harmonic laser light," Opt. Lett. **39**, 14, 4132-4135 (2014).
20. N. D. Powers, I. Ghebregziabher, G. Golovin et al., "Tunable and quasi-monoenergetic x-rays from a laser-driven Compton light source," Nat. Photonics **8**, 28-31 (2014).
21. S. Chen, N. D. Powers, I. Ghebregziabher et al., "MeV-energy x-rays from inverse Compton scattering with laser-wakefield accelerated electrons," Phys. Rev. Lett. **110**, 155003 (2013).
22. S. Banerjee, S. Y. Kalmykov, N. D. Powers et al., "Stable, tunable, quasi-monoenergetic electron beams produced in a laser wakefield near the threshold for self-injection," Phys. Rev. ST Accel. Beams **16**, 031302 (2013).
23. I. Ghebregziabher, B. A. Shadwick and D. Umstadter, "Spectral bandwidth reduction of Thomson scattered light by pulse chirping," Rev. ST Accel. Beams **16**, 030705 (2013).
24. J. Silano S. Clarke, S. Pozzi et al., "Selective activation with all-laser-driven Thomson γ-rays," Proceedings of the 2013 *IEEE* International Conference on Technologies for Homeland Security, 429 - 434 (Waltham, MA, 2013).

References

25. A. D. Debus, M. Bussmann, M. Siebold, A. Jochmann, U. Schramm, T. E. Cowan, and R. Sauerbrey, "Traveling-wave Thomson scattering and optical undulators forÂ high-yield EUV and X-ray sources," Applied Physics B **100,** 61-76 (2010).
26. K. Steiniger, M. Bussmann, R. Pausch, T. Cowan, A. Irman, A. Jochmann, R. Sauerbrey, U. Schramm, and A. Debus, "Optical free-electron lasers with Traveling-Wave Thomson-Scattering," Journal of Physics B: Atomic, Molecular and Optical Physics **47,** 234011 (2014).
27. F. Li, Z. Sheng, Y. Liu, J. Meyer-ter-Vehn, W. Mori, W. Lu, and J. Zhang, "Dense attosecond electron sheets from laser wakefields using an up-ramp density transition," Phys. Rev. Lett. **110,** 135002 (2013).
28. F. Li, Z. Sheng, M. Chen, H. Wu, Y. Liu, J. Meyer-ter-Vehn, W. Mori, and J. Zhang, "Coherent kilo-electron-volt backscattering from plasma-wave boosted relativistic electron mirrors," Appl. Phys. Lett. **105,** 161102 (2014).
29. K. Gaffney, A. Lindenberg, J. Larsson, K. Sokolowski-Tinten, C. Blome, O. Synnergren, J. Sheppard, C. Caleman, A. MacPhee, and D. Weinstein, "Observation of structural anisotropy and the onset of liquidlike motion during the nonthermal melting of InSb," Phys. Rev. Lett. **95,** 125701 (2005).

Combining High Level *Ab Initio* Calculations with Laser Control of Molecular Dynamics

Thomas Weinacht
Department of Physics and Astronomy
Stony Brook University
Stony Brook, NY
thomas.weinacht@stonybrook.edu

and

Spiridoula Matsika
Department of Chemistry
Temple University
Philadelphia, PA
smatsika@temple.edu

1 Program Scope

We use intense, shaped, ultrafast laser pulses to follow and control molecular dynamics and high level *ab initio* calculations to interpret the dynamics and guide the control.

2 Recent Progress

There have been two experimental foci in the past year: Developing experiments which probe excited state dynamics using VUV ionization, and studying strong field molecular double ionization in order to understand correlated electron dynamics in strong laser fields. A focus of the theoretical part of this project for the past year has been understanding better the dynamics of radical cations formed during strong field ionization, and how they proceed to fragmentation. Ionization processes can lead to the formation of radical cations with population in several ionic states. An important question is whether fragmentation occurs on the excited ionic states, or very fast relaxation to the ground ionic state occurs first followed by fragmentation.

In the past year we have made significant progress along the following fronts:

2.1 UV pump VUV probe measurements of excited state dynamics

In our UV pump VUV probe experiments we solved a number of technical problems which kept us from being able to make frequent measurements. One of these was the buildup of residue on VUV optics in our vacuum chamber, which resulted in decreased reflectivity and a loss of VUV signal. Another was the difficulty of routinely finding spatial and temporal overlap between our UV and VUV beams. We also improved our time resolution significantly and are currently working on improving it further such that we can achieve sub 100 fs time resolution. We are in the process of implementing both solid state samples and velocity map imaging detection of ions and electrons created by the UV and VUV pulses. Scientifically, we made pump-probe measurements on a number of molecules, including CH_2I_2, 1-3 cyclohexadiene and pyrrole. Figure 1 illustrates the signal to noise achievable with our apparatus, showing a pump probe measurement together with a single exponential fit to the data. We are in the process of interpreting these measurements, which highlight internal conversion, hot ground state dynamics, and dissociation.

2.2 Molecular double ionization

In our strong field molecular double ionization experiment, we have studied a series of molecules and established that the enhanced double ionization occurs for conjugated molecules, but not for unconjugated ones. Figure 2 illustrates the momentum resolved measurement of fragment ion pairs from the double ionization. We also characterized the ellipticity, intensity and pulse duration dependence. Furthermore, we carried out a quadruple coincidence measurement, where we measured the velocities of two electrons and two ionic fragments in coincidence from each molecule that we double ionized. These coincidence measurements show that the electrons emitted from double ionization of CHD have a propensity to come out in the same direction.

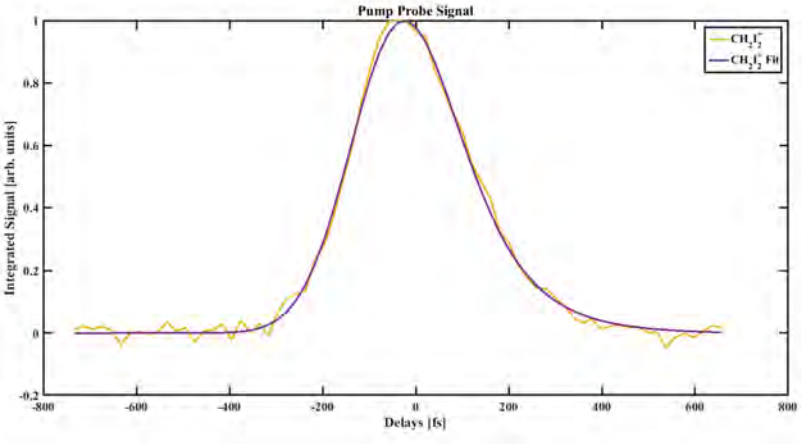

Figure 1: *UV pump VUV probe measurements of internal conversion and dissociation in CH_2I_2.*

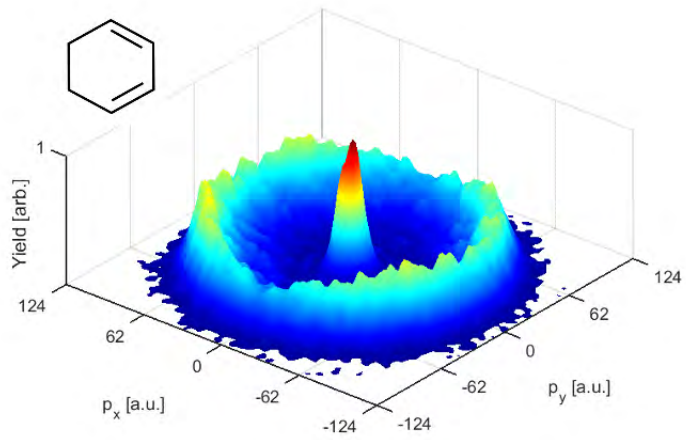

Figure 2: *Coincidence momentum resolved measurement of fragments from double ionization of 1-3 Cyclohexadiene using sub 10 fs laser pulses.*

2.3 Surface hopping investigation of the relaxation dynamics in radical cations

A focus of the theoretical part of this project for the past years has been understanding better the dynamics of radical cations formed either during strong field or weak field (one photon) ionization, and how they may proceed to fragmentation. Ionization processes can lead to the formation of radical cations with population in several ionic states. An important question is whether fragmentation occurs on the excited ionic states, or very fast relaxation to the ground ionic state occurs first, followed by fragmentation. In a recent study, we examined the dynamics of three radical cations starting from an excited ionic state using trajectory surface hopping dynamics in combination with multiconfigurational electronic structure methods. The competition between relaxation to the ground state and fragmentation was examined. The results on CHD, hexatriene (HT) and uracil indicate that relaxation to the ground ionic state is very fast in these systems, while fragmentation before relaxation is rare. Figure 3 shows the adiabatic state populations of the three radicals starting from the second excited state D_2 and decaying to the ground D_0 state. All radicals decay fast, although there are differences in their decay times. Ultrafast relaxation is facilitated by the close proximity of electronic states and the presence of two- and three-state conical intersections. Examining the properties of the systems in the Franck-Condon (FC) region can give some insight the subsequent dynamics. Figure 4 shows how many trajectories in the simulations break or form

a C-C bond to isomerize between CHD and HT, and it is obvious that a very small fraction of trajectories is reactive.

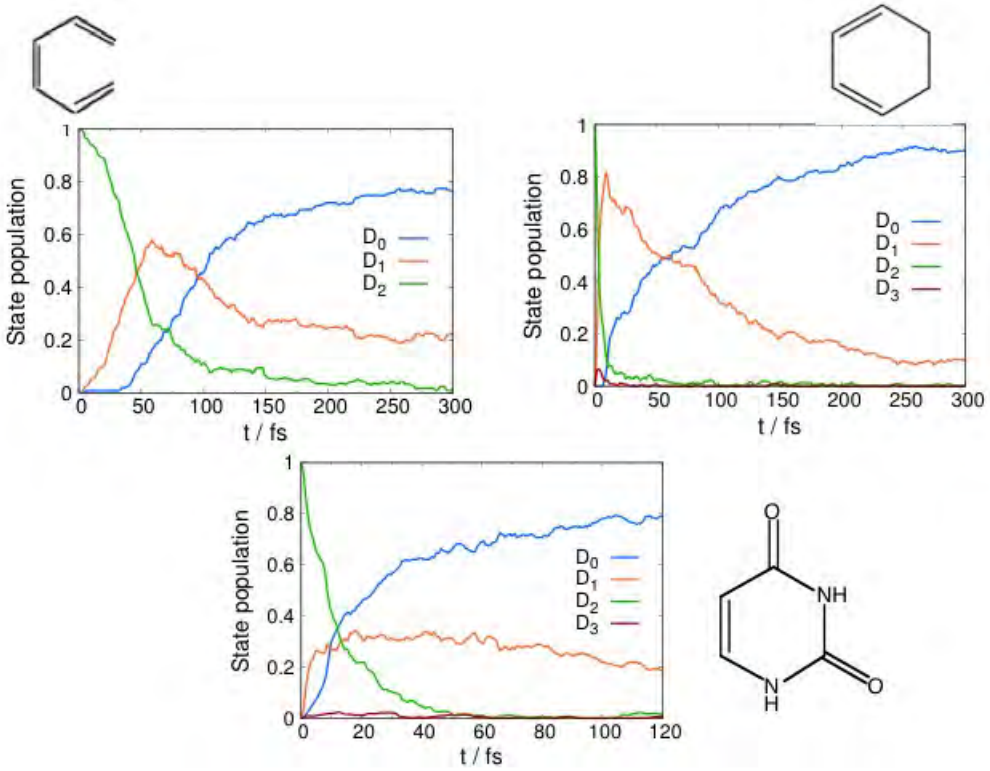

Figure 3: *Adiabatic state populations of HT, CHD, and uracil starting from the D_2 state.*

2.4 Using optimal control theory to achieve control of excited state wavepackets

We have been interested in excited state dynamics of nucleobases because of their relevance to UV damage in nucleic acids. We have collaborated with Regina de Vivie-Riedle in order to examine whether shaped lasers can be used to control the excited state dynamics in these systems. By using a reduced dimensionality surface of uracil and UV light in the form of shaped laser pulses, we show that it is possible to influence the ultrafast relaxation process after photoexcitation in uracil. In our theoretical study, we perform wave packet dynamics of the excitation and relaxation process on a reduced-dimensional potential energy surface. By designing shaped laser pulses with Optimal Control Theory, we are able to achieve two opposite control aims: The relaxation process can be accelerated as well as delayed significantly through alteration of the excitation laser pulse. The optimized laser pulses are feasible to generate experimentally.

3 Future Plans

We have several goals for the immediate future:

1. We plan on further improving the time resolution in our UV/VUV experiments, implementing VMI detection and working with solid state samples.

2. We plan on interpreting the quadrupole coincidence measurements for the molecular double ionization work.

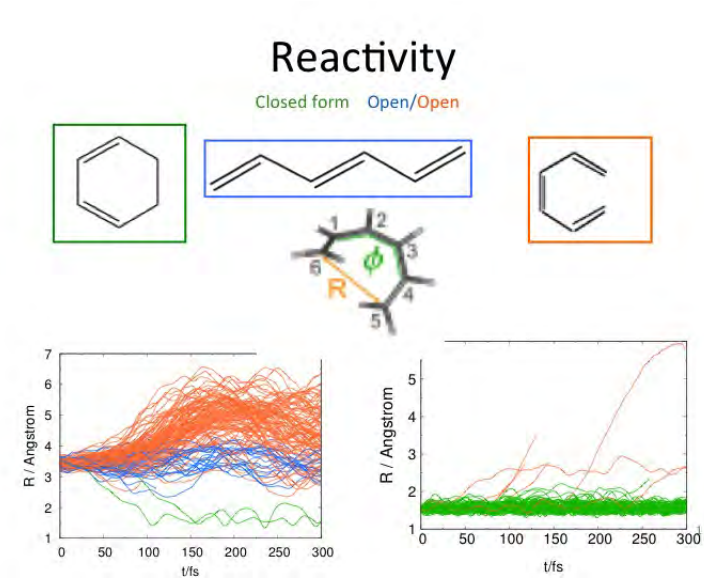

Figure 4: *Evolution of the distance R with time. On the left panel are trajectories starting from HT, while on the right panel are trajectories starting from CHD. Trajectories that isomerize to ctc-HT are colored orange, those in which the ring closes are green and those corresponding to ccc-HT are blue.*

3. We will work further to understand better strong field double ionization. In particular, we will examine whether particular features on the potential energy surfaces of the neutral and ionic systems (such as conical intersections) play a role in double ionization.

4. We will implement the calculation of Dyson orbitals using multiconfigurational (MCSCF) electronic structure methods and use them to interpret and understand better the VUV experiments.

4 Publications of DOE Sponsored Research (11/15/2014-9/14/2016)

- "Surface hopping investigation of the relaxation dynamics in radical cations", Mariana Assmann, Thomas Weinacht, and Spiridoula Matsika, *J. Chem. Phys.*, **144**, 034301 (2016)
- "Molecular Double Ionization using Strong Field Few Cycle Laser Pulses", Arthur Zhao, Péter Sándor, Vincent Tagliamonti, Thomas Weinacht, and Spiridoula Matsika, *J. Phys. Chem. A*, **120**, pp 3233 - 3240, (2016)
- "Field Dressed Orbitals in Strong Field Molecular Ionization", Robert Siemering, Oumarou Njoya, Thomas Weinacht, Regina de Vivie-Riedle, *Phys. Rev. A*, **92**, 042515, (2015)
- "Photoelectron spectrum and dynamics of the uracil cation", Mariana Assmann, Horst Köppel and Spiridoula Matsika, *J. Phys. Chem. A*, **119**, 866-875, (2015)
- "Modified Nucleobases', S. Matsika, "Topics in Current Chemistry - Photoinduced Phenomena in Nucleic Acids" **355**, 209-243, (2015)

List of Participants

Page is intentionally blank.

Atomic, Molecular, and Optical Sciences Research PI Meeting (AMOS)
October 23-26, 2016

Participant List

Thomas Allison
Stony Brook University
thomas.allison@stonybrook.edu

Andreas Becker
JILA, University of Colorado
andreas.becker@colorado.edu

Ali Belkacem
Lawrence Berkeley National Laboratory
abelkacem@lbl.gov

Itzhak Ben-Itzhak
J.R. Macdonald Laboratory, Kansas State Univ.
ibi@phys.ksu.edu

Nora Berrah
University of Connecticut
nora.berrah@uconn.edu

Christoph Bostedt
Argonne National Laboratory
cbostedt@anl.gov

Philip Bucksbaum
SLAC/Stanford University
phb@slac.stanford.edu

Martin Centurion
University of Nebraska
martin.centurion@unl.edu

Shih-I Chu
University of Kansas
sichu@ku.edu

Amy Cordones-Hahn
SLAC National Accelerator Laboratory
acordon@slac.stanford.edu

James Cryan
SLAC National Accelerator Laboratory
jcryan@slac.stanford.edu

Steven Cundiff
SLAC National Accelerator Laboratory
cundiff@umich.edu

Marcos Dantus
Michigan State University
dantus@msu.edu

Louis DiMauro
The Ohio State University
dimauro.6@osu.edu

Gilles Doumy
Argonne National Laboratory
gdoumy@aps.anl.gov

Joseph Eberly
Univeristy of Rochester
eberly@pas.rochester.edu

Veit Elser
Cornell University
ve10@cornell.edu

Brett Esry
J.R. Macdonald Laboratory, Kansas State Univ.
esry@phys.ksu.edu

Roger Falcone
University of California, LBNL
rwf@berkeley.edu

Jim Feagin
California State University, Fullerton
jfeagin@fullerton.edu

Chris Fecko
US DOE/Basic Energy Sciences
Christopher.Fecko@science.doe.gov

Gregory Fiechtner
US DOE/Basic Energy Sciences (CPIMS)
gregory.fiechtner@science.doe.gov

Atomic, Molecular, and Optical Sciences Research PI Meeting (AMOS)
October 23-26, 2016

Participant List

Matthias Fuchs
University of Nebraska, Lincoln
mfuchs@unl.edu

Kelly Gaffney
PULSE Institute
kgaffney@slac.stanford.edu

Thomas Gallagher
University of Virginia
tfg@virginia.edu

Oliver Gessner
Lawrence Berkeley National Laboratory
ogessner@lbl.gov

Shambhu Ghimire
SLAC National Accelerator Laboratory
shambhu@slac.stanford.edu

Chris Greene
Purdue University
chgreene@purdue.edu

Tony Heinz
SLAC National Accelerator Laboratory
tony.heinz@stanford.edu

Phay Ho
Argonne National Laboratory
pho@anl.gov

Robert Jones
University of Virginia
bjones@virginia.edu

Henry Kapteyn
JILA/University of Colorado
kapteyn@jila.colorado.edu

Victor Klimov
Los Alamos National Laboratory
klimov@lanl.gov

Jeffrey Krause
US DOE/Basic Energy Sciences
Jeff.Krause@science.doe.gov

Vinod Kumarappan
Kansas State University
vinod@phys.ksu.edu

Anh-Thu Le
Kansas State University
atle@phys.ksu.edu

Stephen Leone
LBNL/University of California, Berkeley
srl@berkeley.edu

Raphael Levine
University of California, Los Angeles
rafi@chem.ucla.edu

Wen Li
Wayne State University
wli@chem.wayne.edu

Chii-Dong Lin
Kansas State University
cdlin@phys.ksu.edu

Kenneth Lopata
Louisiana State University
klopata@lsu.edu

Robert Lucchese
Texas A&M University
lucchese@mail.chem.tamu.edu

Steven Manson
Georgia State University
smanson@gsu.edu

Diane Marceau
US DOE/Basic Energy Sciences
Diane.Marceau@science.doe.gov

Atomic, Molecular, and Optical Sciences Research PI Meeting (AMOS)
October 23-26, 2016

Participant List

Anne Marie March
Argonne National Laboratory
amarch@anl.gov

Todd Martinez
SLAC National Accelerator Laboratory
toddjmartinez@gmail.com

Spiridoula Matsika
Temple University
smatsika@temple.edu

William McCurdy
Lawrence Berkeley National Laboratory
cwmccurdy@lbl.gov

Alfred Msezane
Clark Atlanta University
amsezane@cau.edu

Shaul Mukamel
University of California, Irvine
smukamel@uci.edu

Margaret Murnane
JILA/University of Colorado
murnane@jila.colorado.edu

Adi Natan
SLAC National Accelerator Laboratory
natan@slac.stanford.edu

Keith Nelson
Massachusetts Institute of Technolgy
kanelson@mit.edu

Daniel Neumark
Lawrence Berkeley National Laboratory
dneumark@berkeley.edu

Thomas Orlando
Georgia Institute of Technology
thomas.orlando@chemistry.gatech.edu

Abbas Ourmazd
University of Wisconsin, Milwaukee
ourmazd@uwm.edu

Enrique Parra
Air Force Office of Scientific Research
enrique.parra@us.af.mil

Herschel Rabitz
Princeton University
hrabitz@princeton.edu

David Reis
Stanford PULSE Institute/SLAC
dreis@stanford.edu

Françoise Remacle
University of Liege
fremacle@ulg.ac.be

Thomas Rescigno
Lawrence Berkeley National Laboratory
tnrescigno@lbl.gov

Francis Robicheaux
Purdue University
robichf@purdue.edu

Jorge Rocca
Colorado State University
wrightan@rams.colostate.edu

Daniel Rolles
J.R. Macdonald Laboratory, Kansas State Univ.
rolles@phys.ksu.edu

Christoph Rose-Petruck
Brown University
crosepet@brown.edu

Artem Rudenko
Kansas State University
rudenko@phys.ksu.edu

Atomic, Molecular, and Optical Sciences Research PI Meeting (AMOS)
October 23-26, 2016

Participant List

Kenneth Schafer
Louisiana State University
schafer@phys.lsu.edu

H. Bernhard Schlegel
Wayne State University
hbs@chem.wayne.edu

Tamar Seideman
Northwestern University
t-seideman@northwestern.edu

Tom Settersten
US DOE/Basic Energy Sciences
thomas.settersten@science.doe.gov

Daniel Slaughter
Lawrence Berkeley National Laboratory
DSSlaughter@lbl.gov

Stephen Southworth
Argonne National Laboratory
southworth@anl.gov

Anthony F. Starace
University of Nebraska
astarace1@unl.edu

Mark Stockman
Georgia State University
mstockman@gsu.edu

Carlos Trallero
James R. Macdonald Laboratory
trallero@phys.ksu.edu

Donald Umstadter
University of Nebraska, Lincoln
donald.umstadter@unl.edu

Thorsten Weber
Lawrence Berkeley National Laboratory
TWeber@lbl.gov

Thomas Weinacht
Stony Brook University
thomas.weinacht@stonybrook.edu

Philip Wilk
US DOE/Basic Energy Sciences
philip.wilk@science.doe.gov

Thomas Wolf
SLAC National Accelerator Laboratory
tw2809@slac.stanford.edu

Linda Young
Argonne National Laboratory
young@anl.gov